SEDIMENTATION ON THE CONTINENTAL MARGIN OFF THE ORANGE RIVER AND THE NAMIB DESERT

J. ROGERS

Thesis submitted in fulfilment of the
requirements for the degree of
Doctor of Philosophy in the
Faculty of Science at the
University of Cape Town

April, 1977

ABSTRACT

This study is the first detailed reconnaissance survey of the bathymetry, bedrock geology and the superficial sediments of the continental margin off the Orange River and the Namib Desert. The study area is bounded by latitudes 25° and 30°S.

The Orange shelf is up to 100 km wide and 200 m deep, and the Walvis shelf off Lüderitz is up to 80 km wide and 400 m deep. The inner shelf is underlain by Precambrian bedrock and is usually less than 10 km wide and shallower than 100 m. Tripp Seamount penetrates the upper slope in a depth of 1000 m and rises to within 150 m of sea level, the level of the Orange Banks on the outer Orange shelf.

South of the Orange River unfossiliferous ferruginous sandstones and mudstones crop out as seaward-dipping scarps on the middle shelf. North of the Orange River, similar scarps are composed of quartzose lime wackestones, identical to a Palaeogene suite on the Agulhas Bank. The shallow outer Orange shelf is underlain in places by Upper Middle Miocene nummulitic limestones, which are overlain by glauconitic conglomeratic phosphorites. Quartz-free algal limestones are found both on the Orange Banks and on the tip of Tripp Seamount.

Authigenic pyrite and gypsum were found in two samples of semi-consolidated Neogene clay on the slope off Lüderitz. Pyrite is formed by combining terrigenous adsorbed iron with sulphur released by anaerobic reduction of sea-water sulphate. The dissolution of planktonic foraminiferal tests provides calcium ions which combine with sulphate to form gypsum, once the calcium/sulphate solubility product is exceeded.

On the Walvis shelf off Lüderitz residual glauconite was reworked from older Neogene sediments, particularly on Lüderitz Bank. North of latitude 26°S residual phosphorite pellets were probably formed in Neogene diatomaceous oozes and then concentrated during a Late-Tertiary regression. Erosion of semi-consolidated Neogene clays and ?Palaeogene quartzose limestones on the middle and outer Walvis shelf led to deposition of very fine residual quartz sand south of Lüderitz. Coarse quartz sand was reworked from littoral sandstones on the middle shelf south of the Orange River.

The effect on sedimentation in the hinterland of poleward shifts of climatic belts during Quaternary interglacials and the reverse movement during glacials is assessed.

Recent terrigenous sediments are derived by erosion of poorly consolidated Karoo sediments in the catchment of the Upper Orange. Erratic but powerful floods transport the sediments to the coast in suspension each summer. At the mouth in-

tense wave action dominates the submarine delta of the Orange River and fractionates the sediment load. Sand is transported equatorwards by littoral drift and is blown off beaches towards the Namib Sand Sea during violent Trade-Wind gales each summer. In contrast, silt and clay are transported polewards by a countercurrent, particularly during westerly winter storms.

Recent biogenic sedimentation is controlled by upwelling in the Benguela Current System, which is most intense off the wind-dominated Sperrgebiet, south of Lüderitz. Weaker upwelling off the Orange River allows oceanic planktonic foraminifera to penetrate to the middle shelf, whereas on the Walvis shelf in the study area they only reach the outer shelf. Towards latitude 25°S the Benguela Current System decays and interacts with poleward-flowing warm oxygen-poor water. Periodic mass mortalities of oxygen-starved phytoplankton lead to some of the most organic-rich sediments in the world.

ACKNOWLEDGEMENTS

Initially the funding of this project was undertaken by the South African National Committee for Oceanographic Research (SANCOR), whose Marine Geology Programme was run by Professor E.S.W. Simpson. Administrative assistance was supplied by the Council for Scientific and Industrial Research (CSIR) and the Programme's activities were reviewed periodically by an advisory commission headed by Dr. W.P. De Kock. On 1st April, 1972 SANCOR, who had initiated the overall programme in January, 1967, transferred financial responsibility to the Geological Survey of South Africa. The programme was then renamed the Joint Geological Survey/University of Cape Town Marine Geology Programme. During 1975 a Marine Geoscience Group was formed at the University of Cape Town with Professor R.V. Dingle as Director. The Joint Geological Survey/University of Cape Town Marine Geoscience Unit, run by Mr. A. Du Plessis and Professor Dingle, provides the bulk of both the finance and the personnel to the group as a whole.

The samples utilized in this study were taken between latitudes 25° and 30°S off the west coast of southern Africa, during the period February, 1971 to May, 1974. The project is designed to be integrated with parallel studies farther south (Birch, 1975: (30°-35°S) and farther north (Bremner, in preparation: (17°-25°S)).

I gratefully acknowledge the opportunity to participate fully in the Programme from its inception in 1967. Without the financial backing involved in obtaining ship's time, running the Unit, purchasing equipment and paying my salary this project would not have been viable.

Since May, 1975, the writer has been employed by the Geological Survey and based in the Cape Town branch office. The opportunity is taken to thank the Directorate of the Geological Survey for permission to process the data obtained, to work towards a thesis with the data and, finally, to submit the thesis to the University of Cape Town for Ph.D. purposes. The writer is grateful for encouragement from the Director and from my immediate superior, Dr. J.N. Theron, to bring the project to a satisfactory conclusion.

Professors E.S.W. Simpson, A.M. Reid, L.H. Ahrens and J.K. Mallory are thanked for making the technical facilities of the Geology, Geochemistry and Oceanography Departments available. Messrs. T.G.J. Pistorius, V.E. Viljoen and D. De Jager are also thanked for arranging all P_2O_5 and K_2O analyses at Phosphate Development Corporation laboratory in Phalaborwa, Transvaal.

Professor Mallory, Captains W.H. Eggert and A.J. Childs and through them the officers and crew are thanked for their friendly cooperation during many sampling cruises aboard R.V. "Thomas B. Davie" during the past decade.

I should like to thank my supervisor, Professor A.O. Fuller for guidance and encouragement, particularly at critical stages both in my research and in the preparation of this manuscript. He also paid particular attention to Chapter VII (Terrigenous). Professor Dingle is thanked for constructive criticism over the years and for examining Chapters I and II (Introduction and Bathymetry). Dr. W.G. Siesser reviewed Chapters III (Petrography), IV (Gypsum and Pyrite) and VIII (Biogenic). Dr. G.F. Birch scrutinized Chapter V (Residual) and Dr. A.J. Tankard perused Chapter VI (Palaeoclimate). Mr. J.M. Bremner checked sections of the Appendix for me.

The following persons deserve special mention for their contributions at various stages of the research programme and in the preparation of this manuscript: Drs. M.J. Orren and G.A. Eagle for supervision of atomic absorption analyses; Mrs. G. Pomplun, Mr. A. Veldtkamp, Mrs. K. Trotter, Mrs. J.A. Woodford and Miss S.N. Wheeler for performing hundreds of routine chemical and textural analyses; Drs. A.R. Duncan and M. Lasserre, Messrs. J.M. Bremner, C.J. Hartnady and H. Fortuin and Mrs. S.M.L. Sayers for computing assistance; Mr. J. Williams for preparation of thin-sections; Mr. F. Coley, Mrs. S.M.L. Sayers, Miss S.N. Wheeler and Mrs. J.A. Woodford for meticulous draughting of numerous diagrams; Mr. K. Behr of the Cartography Unit in the Geography Department and Mr. N. Dolley of the Printing Department for photographic reductions; Dr. A.J. Tankard for assistance with photomicrography; Mr. P. Forsythe for photographic assistance; Mr. R.H. Cross, Ms L. Cadle and Dr. Tankard for help with scanning electron microscopy and Mr. J. Appollis for reproducing the entire thesis very efficiently.

Throughout the study detailed discussions have been held with colleagues in the Marine Geoscience Group and in the Oceanography Department, in particular Mr. J.M. Bremner, Dr. G.F. Birch, Mr. B.W. Flemming, Drs. W.G. Siesser and N.D. Bang, Mr. A. Du Plessis and Professors Dingle and T.F.W. Harris. The personnel of the Marine Diamond Corporation, namely Messrs K. Joynt, D. O'C. O'Shea, R.W. Foster and A. Hockney, were also very helpful with detailed information from their intensive work on the inner shelf north of the Orange River. More long-range discussions were also held with colleagues both in South Africa and abroad who corresponded willingly and provided much useful literature.

This thesis was typed in draft form by Mrs. E.G. Krummeck and Mrs. J. Abbott, and the final copy was typed, with dedication, speed and accuracy by Mrs. Krummeck. A special word of appreciation is expressed to her for performing this particular task so well.

Finally, I thank my family and my friends, but particularly my wife, Phil, for her support and encouragement throughout my post-graduate career.

LIST OF CONTENTS

LIST OF FIGURES

LIST OF PLATES

LIST OF TABLES

CHAPTER I. INTRODUCTION

A. SEDIMENTOLOGIC FEATURES OF THE STUDY AREA

The shelf and the upper slope off southwestern Africa, between latitudes 25° and 30°S, are of particular interest to sedimentologists for several reasons. 1) The sole source of fluviatile terrigenous sediment is the Orange River, one of the major rivers on the African continent. 2) Powerful winds and swells are highly effective in dispersing terrigenous sand along the coast and have helped emplace subeconomic deposits of gem-quality diamonds on the inner shelf and the coastal plain, particularly north of the Orange River. 3) The powerful winds between the Orange River and Lüderitz trigger off upwelling on a large scale in the Benguela Current System, which in turn controls the aridity of the little-studied Namib Desert. 4) The shelf off Lüderitz is one of the deepest in the world.

B. PREVIOUS INVESTIGATIONS

The first bottom sediments from the study area were collected by marine biologists involved in the development of a trawling industry between the world wars. The samples were briefly described but not studied in any detail (Marchand, 1928). Brief mention is also made of sediments off the Orange and north of Lüderitz by Copenhagen (1953) in an oft-quoted discussion of the causes of mass mortalities off Walvis Bay.

A decade later, in 1961, diamonds were discovered on the inner shelf and the Marine Diamond Corporation then undertook a detailed study of bedrock topography and sediment distribution to pinpoint potential orebodies (Wright, 1964; Hoyt, Smith and Oostdam, 1965a, 1965b; Ahmed, 1968; Hoyt, Oostdam and Smith, 1969; Murray, 1969; Murray et al., 1971; O'Shea, 1971; Joynt et al., 1972).

Again in 1961, Russian oceanographers of the Research Institute of Oceanology and of Marine Fisheries and Oceanography initiated a regional survey of the west African shelf. Morphological features of the continental margin and adjacent sea floor were described by Ilyin (1971) and by Bogorov et al. (1971). Regional sedimentological trends were discussed by Senin (1969), Emilianov and Senin (1969) and Baturin (1971, 1972), and Baturin et al. (1972) reported important research on phosphatic sediments from the northern part of the area.

In 1968 the Scripps Institution of Oceanography organized a cruise of R.V. "Argo" to the Walvis shelf between latitudes 20° and 26°S. Van Andel and Calvert (1971) have interpreted the morphological and geophysical results. Sedimentological and geochemical data are presented by Calvert and Price (1970; 1971a; 1971b), Price and Calvert (1973) and by Veeh, Calvert and Price (1974).

The Joint University of Cape Town/Geological Survey Marine Geoscience Group was formed in 1975 by amalgamating geoscientists from three pre-existing groups. Geophysical and bathymetric results from the study area are presented by Simpson (1966, 1968, 1971), Simpson and Needham (1967), Simpson and Du Plessis (1968), Simpson and Purser (1974), Bryan and Simpson (1971), Du Plessis et al. (1972), Rogers and Bremner (1973), Dingle (1973a, 1973b, 1973c), Scrutton (1973), Dingle and Scrutton (1974), Siesser et al. (1974) and Scrutton and Dingle (1975). Regional sedimentological trends based on samples collected systematically between 1971 and 1974 are reported by Rogers et al. (1972), Birch and Rogers (1973), Rogers (1972, 1973, 1974, 1975a, 1975b), Siesser et al. (1974) and Birch et al. (1976). Rogers and Tankard (1974), Rogers (1975c) and Rogers and Krinsley (in prep.) discuss surface textures on quartz grains from the coast and the inner shelf. Summerhayes et al. (1973) describe the distribution of phosphate in the sediments, and Davey and Rogers (1975) published results of a preliminary study of marine palynomorphs. Martin (1974) presented preliminary results on the distribution of benthonic foraminifera in the study area.

During 1972, powerful seismic gear was brought to the area aboard R.V. "Atlantis" of the Woods Hole Oceanographic Institution, and up to 7 000 m of sediment were penetrated in the Orange Basin (Emery, 1971, 1972; Emery et al., 1975). Underway measurements of water properties (including suspended matter) and of seabird distribution are reported by Emery et al. (1973) and by Summerhayes et al. (1974), respectively.

Where appropriate, details from the above papers will be discussed in the following chapters.

C. PURPOSE OF THE PRESENT INVESTIGATION

The chief purpose of the investigation is to study the interaction of the oceanographic and atmospheric environments on the production, dispersal and deposition of Recent sediments. In addition, attention is paid to the effect of Pleistocene fluctuations of climate on local sedimentation patterns, and the depositional history of Tertiary and Cretaceous sediments is also discussed.

The investigation represents the first attempt to make a detailed survey of the shelf and the upper slope between latitudes 25° and 30°S off southwestern Africa. It forms part of a reconnaissance exploration of the southern African continental margin by the Joint Geological Survey/University of Cape Town Marine Geoscience Group.

D. LIMITS OF THE INVESTIGATION

The investigation was of a preliminary nature in various aspects because of

limitations both in the nature of the equipment available both at sea and in the laboratory, and to the nature of the material available for study. The accuracy of the bathymetric chart could now be improved with the satellite navigation system recently installed on the "Thomas B. Davie". Rock sampling could now be better controlled and structures determined using the side-scan sonar now available. The planned construction of a vibrocorer opens up the possibility of obtaining closely spaced, pinpointed, bedrock samples. Sedimentary sequences could also be determined and estimates of available tonnages of potentially economic minerals made with more confidence than is the case at present. A combination of presently operating waverider buoys, proposed bottom-current meters, planned satellite-tracked surface buoys and available side-scan sonar equipment makes it feasible to study sediment dispersal processes in greater detail.

Relatively little attention has been paid to the mineralogical and geochemical aspects of the sediments, both consolidated and unconsolidated, in contrast to studies in adjacent areas by Birch (1975) and Bremner (in prep.). In addition only superficial attention has been paid to the numerous types of biogenic material available for study, each group requiring intensive study by trained specialists.

Within these limits emphasis has been placed on the dispersal and deposition of terrigenous sediment from the Orange River. Sufficient data on the mineralogical, geochemical and biogenic aspects has nevertheless been presented to facilitate a greater understanding of the marine geology of the entire continental margin off southwestern Africa.

CHAPTER II

MORPHOLOGY OF THE SHELF AND THE UPPER SLOPE

A. PREVIOUS INVESTIGATIONS

Simpson (1966, 1968, 1971) was the first to describe the morphology of the study area in any detail. He presented 10 bathymetric profiles from between 25° and 30°S taken by H.M.S. HECLA in 1966. At the same time Van Andel and Calvert (1971) and Calvert and Price (1971a) produced a bathymetric map of the margin north of 26°S (Saddle Hill) between the 100 m and 600 m isobaths, based on profiling done from R.V. ARGO in 1968. Two of the accompanying bathymetric profiles were from the study area.

Subsequently, the work of the Marine Geoscience Group aboard R.V. THOMAS B. DAVIE between 1967 and 1972 was reported by Dingle (1973a) and by Rogers and Bremner (1973). Dingle discussed the morphology of the area south of Lüderitz (26°30'S). Five profiles of the margin and 7 shelf-break profiles north of 30°S accompanied a bathymetric map extending seawards to the 1000 m isobath (Dingle, 1973a, Figs.2-5). Rogers and Bremner presented a bathymetric map of the margin shallower than 1500 m, north of 27°45'S (Baker Bay) to 23°S (Walvis Bay), as well as a series of 30 bathymetric profiles between 25° and 30°S. Regional variations in microrelief were also illustrated (Rogers and Bremner, 1973, Figs. III-1, III-2, III-3).

On a larger scale, the morphology of the Orange River's submarine delta has been outlined by Hoyt, Oostdam and Smith (1969). Details of submerged surf-cut platforms on the Precambrian platform near the coast are discussed by Hoyt, Smith and Oostdam (1965a), Murray, Joynt, O'Shea, Foster and Kleinjan (1971) and O'Shea (1971).

The aim of this chapter is to collate previous work, both published and unpublished, and to present the results of a more intensive study of the region. After discussing regional aspects, the various morphological zones will be dealt with, beginning with the upper slope and moving towards the inner shelf.

B. BATHYMETRY

1. Introduction

Shepard (1973, p.259) described parts of this shelf as "... perhaps the deepest in the world ..." excluding the ice-deepened shelf of Antarctica. He also mentioned the difficulty of determining the exact depth of the shelf break and the sparseness of soundings. These broad conclusions are confirmed and all available soundings have been compiled to form a bathymetric map at a scale of 1:1 000 000 (Fig. II-1). Five additional maps (Figs. II-17-21) depict some of the detail on the inner shelf shallower than 130 m. Most data were from records

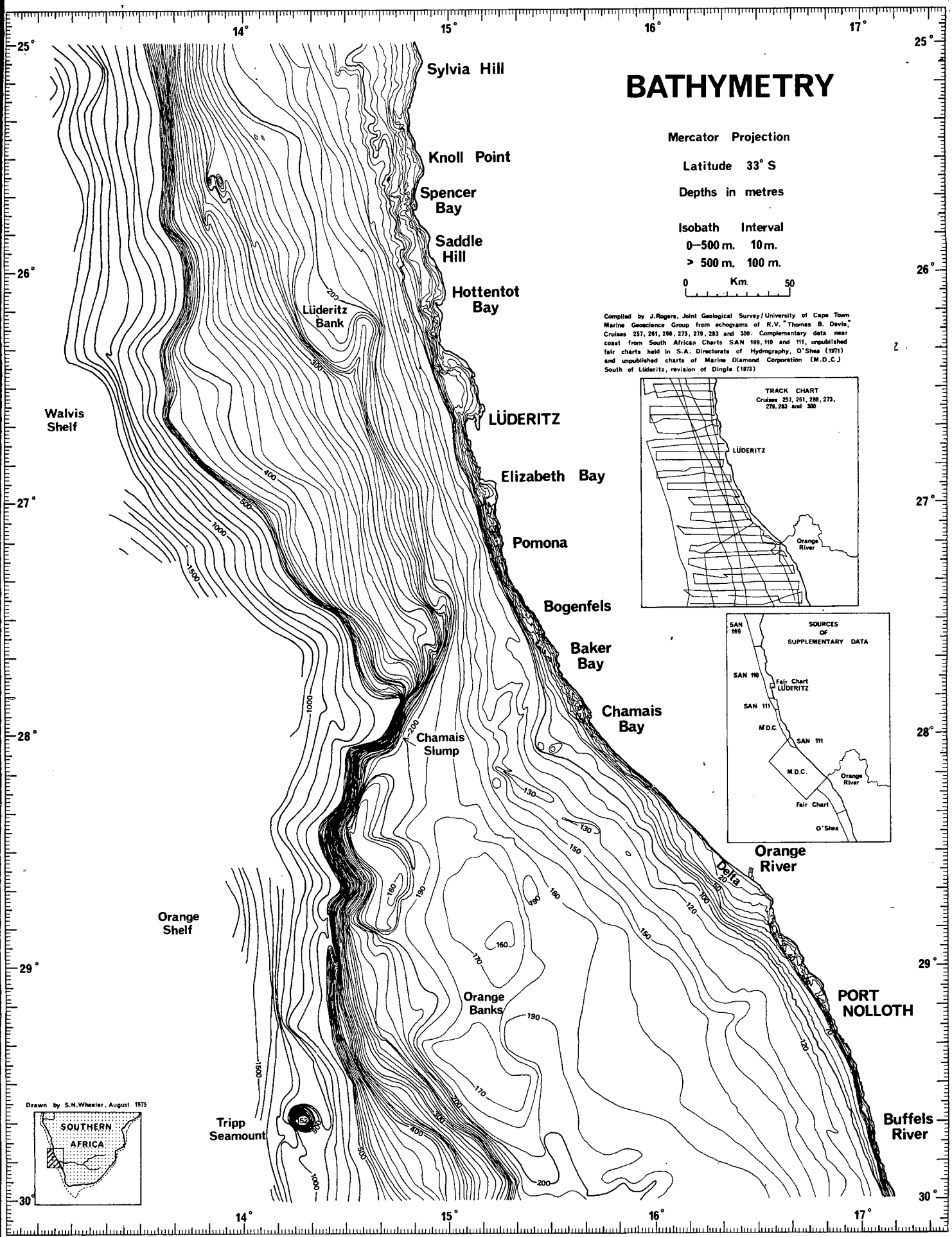
BATHYMETRY
Mercator Projection
Latitude 33° S
Depths in metres
Isobath Interval
0–500 m. 10 m.
> 500 m. 100 m.
0 Km. 50
Compiled by J.Rogers, Joint Geological Survey / University of Cape Town Marine Geoscience Group from echograms of R.V. "Thomas B. Davie," Cruises 257, 261, 268, 273, 279, 283 and 300. Complementary data near coast from South African Charts SAN 109, 110 and 111, unpublished fair charts held in S.A. Directorate of Hydrography, O'Shea (1971) and unpublished charts of Marine Diamond Corporation (M.D.C.) South of Lüderitz, revision of Dingle (1973)
TRACK CHART
Cruises 257, 261, 268, 273, 279, 283 and 300
LÜDERITZ
Orange River
SOURCES OF SUPPLEMENTARY DATA
SAN 109
SAN 110
Fair Chart LÜDERITZ
SAN 111
M.D.C.
SAN 111
M.D.C.
Orange River
Fair Chart
O'Shea
Sylvia Hill
Knoll Point
Spencer Bay
Saddle Hill
Hottentot Bay
Lüderitz Bank
Walvis Shelf
LÜDERITZ
Elizabeth Bay
Pomona
Bogenfels
Baker Bay
Chamais Bay
Chamais Slump
Orange River Delta
Orange Shelf
Orange Banks
PORT NOLLOTH
Tripp Seamount
Buffels River
Drawn by S.N.Wheeler, August 1975
SOUTHERN AFRICA
14°
15°
16°
17°
25°
26°
27°
28°
29°
30°

Fig.II-1

obtained aboard R.V. "THOMAS B. DAVIE" by the UCT Marine Geoscience Group, and processed as described in the Appendix. Additional data near the coast were supplied by the Marine Diamond Corporation and the South African Directorate of Hydrography.

2. Regional trends

The continental shelf can be subdivided into three parts: the Orange shelf (28-30°S), the Walvis shelf north of Lüderitz (27°S), and a transitional section off Chamais Bay, where the shelf is at its narrowest (Figs. II-1 and II-2).

The Orange shelf is characterised by its greater width, well-defined shallow shelf breaks, shallow outer shelf (the Orange Banks), and the Recent delta of the Orange River. The Walvis Shelf has a more constant, narrower width, deeper and more poorly defined shelf breaks and, overall, a more subdued morphology.

3. Shelf width

The shelf off the Orange (Figs. II-1 and II-2) is wider, shallower and flatter than the shelf farther north. The width varies from 230 km (125 n.m.) near Tripp Seamount (30°S) to 90 km (50 n.m.) off Chamais Bay (28°S) at the shelf's narrowest point. The shelf then widens to 130 km (70 n.m.) off Lüderitz (26°40'S) and varies between 100 and 130 km (55-70 n.m.) northwards to Sylvia Hill (25°S).

4. Depth of shelf break

Except for the slump-generated shelf break between the Orange River and Chamais Bay, a gently convex shelf break of sedimentary origin is typical of the study area. Where the sedimentary shelf break is deep, as off the Buffels River, and off Lüderitz, there is an inner shelf break separating the middle and outer shelves. It is therefore understandable that the plot of the depth of the shelf break versus latitude is complex (Fig. II-3).

In the southern section of the Orange shelf (Fig. II-2), there are clearly defined inner and outer shelf breaks. The inner shelf break (Fig. II-3) shoals northwards from 210 m to 170 m and then peters out. The outer shelf break rises from 480 m to 210 m, progressing northwards from an unusally deep position to the shallow, slump-generated, well-defined shelf break characteristic of the Orange Shelf. The northward continuation of this shelf break is difficult to define with certainty with the data available. The writer's interpretation is that it swings coastwards and forms a poorly defined inner shelf break between Chamais Bay and Lüderitz. It then follows the well-defined outer edge of the Lüderitz Bank, which will be discussed further in Section II-C-5c. Between Lüderitz Bank and Sylvia Hill no inner shelf break was detected.

Off Chamais Bay, where the Orange shelf break becomes less well defined, the southern end of the sediment-draped Walvis shelf break lies at a depth of 490 m. The shelf break remains deep at between 400 and 500 m as far north as Saddle Hill

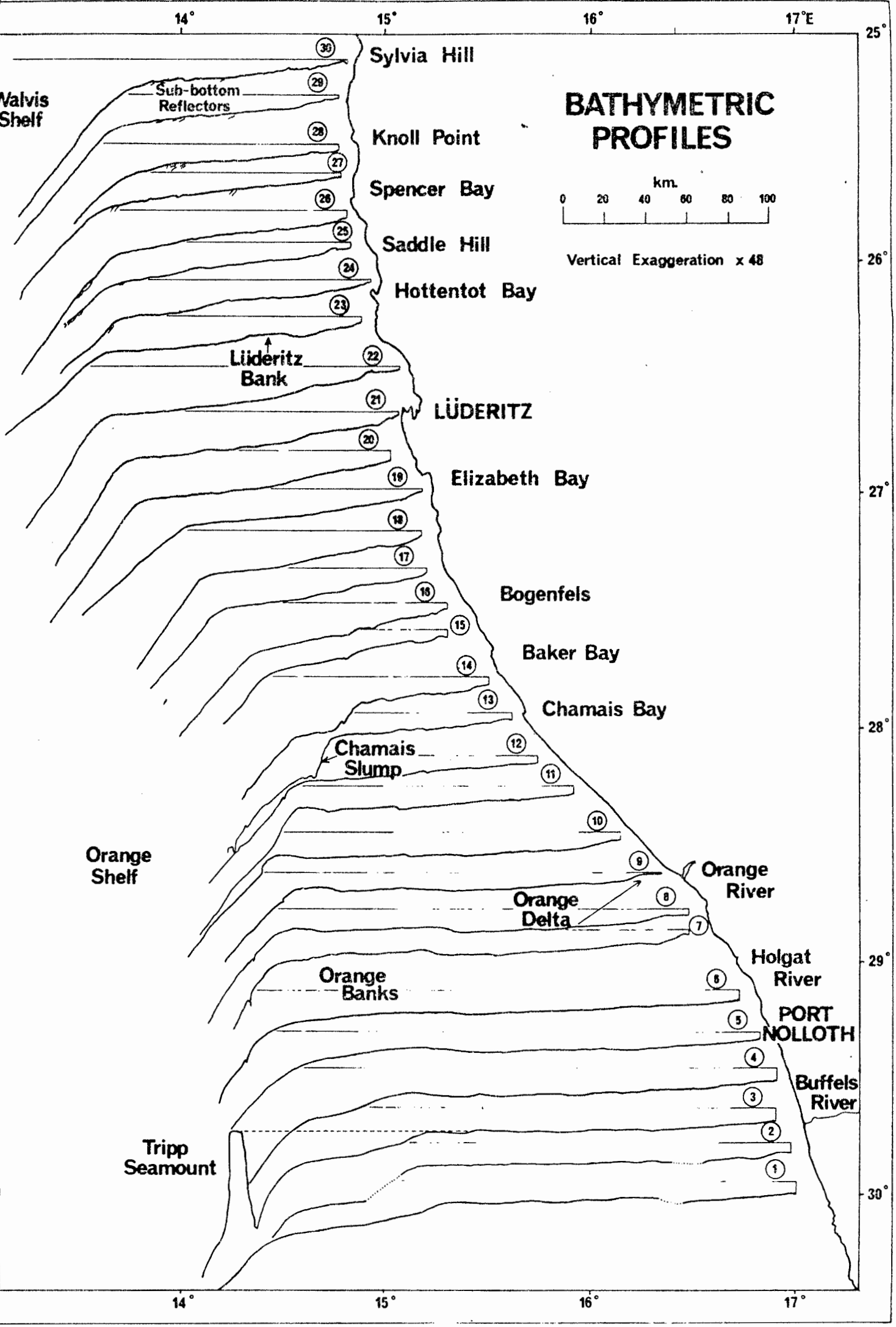
14°
15°
16°
17°E
25°
26°
27°
28°
29°
30°
Walvis Shelf
Sub-bottom Reflectors
Sylvia Hill
Knoll Point
Spencer Bay
Saddle Hill
Hottentot Bay
Lüderitz Bank
LÜDERITZ
Elizabeth Bay
Bogenfels
Baker Bay
Chamais Bay
Chamais Slump
Orange Shelf
Orange River
Orange Delta
Holgat River
Orange Banks
PORT NOLLOTH
Buffels River
Tripp Seamount
BATHYMETRIC PROFILES
km.
0 20 40 60 80 100
Vertical Exaggeration x 48

Fig. II-2

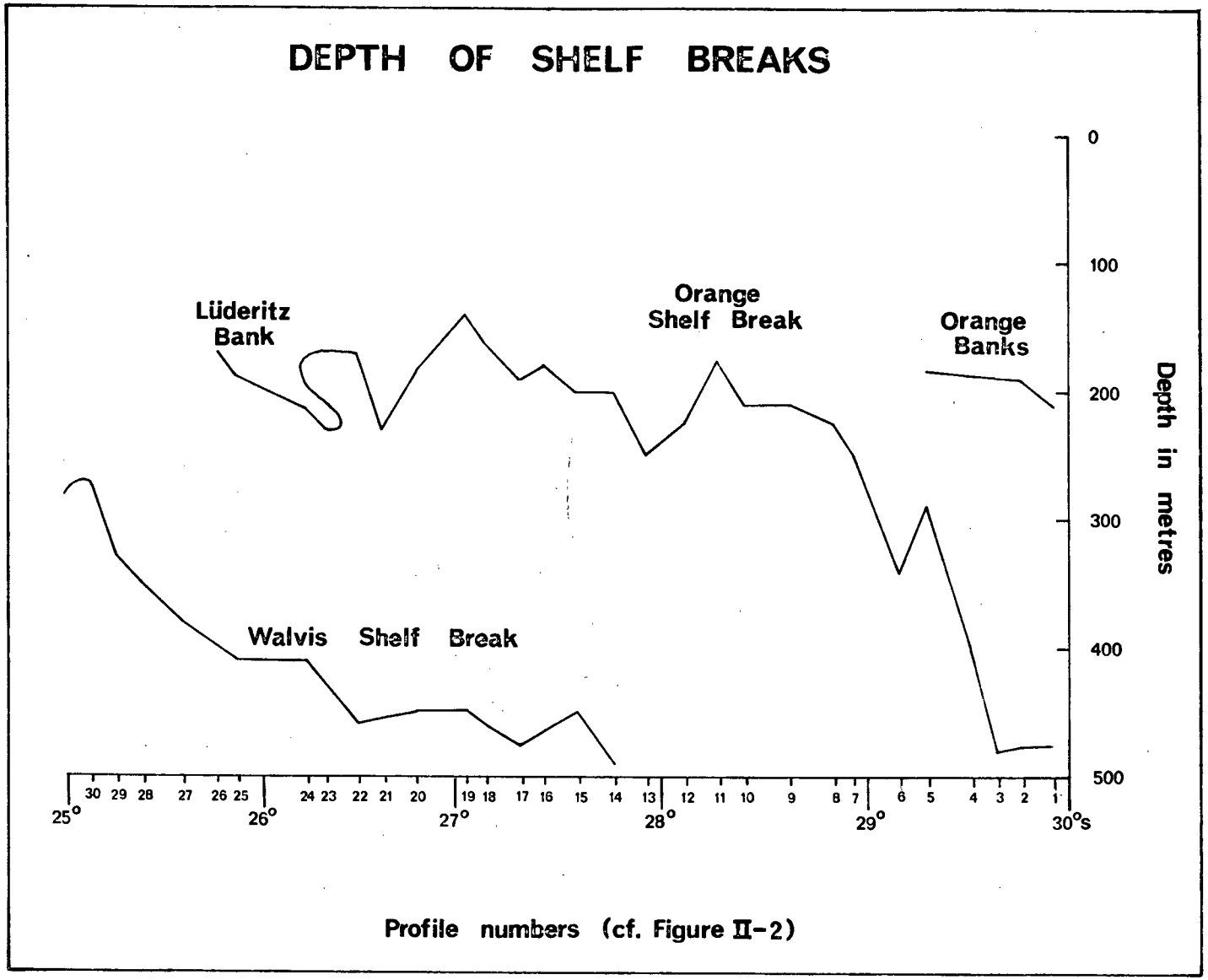
DEPTH OF SHELF BREAKS
Lüderitz Bank
Orange Shelf Break
Orange Banks
Walvis Shelf Break
0
100
200
300
400
500
Depth in metres
30 29 28 27 26 25 24 23 22 21 20 19 18 17 16 15 14 13 12 11 10 9 8 7 6 5 4 3 2 1
25°
26°
27°
28°
29°
30°s
Profile numbers (cf. Figure II-2)

Fig.II-3

(26°S) and then shoals rapidly northwards to a depth of 275 m off Sylvia Hill.

5. Shelf and slope gradients

The shelf gradient, between the deepest shelf break and the coastline, is consistently more gentle on the Orange Shelf than on the Walvis Shelf (Fig. II-4). The Orange Shelf has an average gradient of 0,1° or 1,75 m/km. Off Chamais Bay the gradient steepens sharply to 0,32° or 5,6 m/km and then decreases to 0,20° or 3,5 m/km off Elizabeth Bay. The average gradient northwards between Elizabeth Bay and Knoll Point is 0,2°, twice that of the Orange Shelf.

The gradient of the upper slope (Fig. II-4) is steeper and more variable than that of the shelf. No clear trend is apparent beyond the contrast between the shelf gradients (0,1-0,3°) and the slope gradients (0,8-1,8°) and the lowering of slope gradient as shelf gradient increases off Chamais Bay. This convergent trend is linked with the Chamais Slump, which will be described and discussed in Section II-C-2. The average slope gradient is a gentle 1,2° or 21 m/km.

6. Microrelief

Echograms have been examined in an attempt to classify and to map various types of microrelief on the sea floor. Four types are distinguished. 1) An irregular surface with relief of up to 15 m and often with several multiple reflections that indicates bedrock outcrop with negligible sediment cover. 2) A gently undulating surface, where the undulations usually have amplitudes of approximately 0,5 m, that indicates a thin veneer of sediment overlying relatively subdued bedrock topography. 3) A smooth surface with a single clear reflection indicates a firm bottom composed of sandy sediment. 4) A smooth bottom underlain by acoustically transparent sediment, allowing the measurement of sediment thickness above bedrock, that indicates a soft bottom of muddy sediment.

Similar types of microrelief were recognised by King (1967), who conducted a detailed comparison on the Nova Scotia shelf between lithofacies maps obtained both by the interpretation of echograms and by conventional textural analyses of grab samples. The efficacy of this technique can be judged by comparing microrelief and sediment texture maps for the continental margin between Lüderitz and Port Elizabeth (Birch and Rogers, 1973). These maps were used to plan an intensive rock-dredging programme on the Agulhas Bank. It was found that dredging need not be restricted to areas of irregular microrelief, because the veneer of sediment in the "undulating" and "smooth but firm" categories is often only centimetres thick. In contrast, areas of soft bottom usually represent mud layers several metres thick, and dredging is effectively prevented. The search for drowned diamondiferous beaches north of the Orange River is restricted by "smooth but soft" deltaic sediments up to 60 m thick, which are too thick for the vibrocoring and suction sampling gear operated by the Marine Diamond Corporation (Joynt, 1976, personal communication).

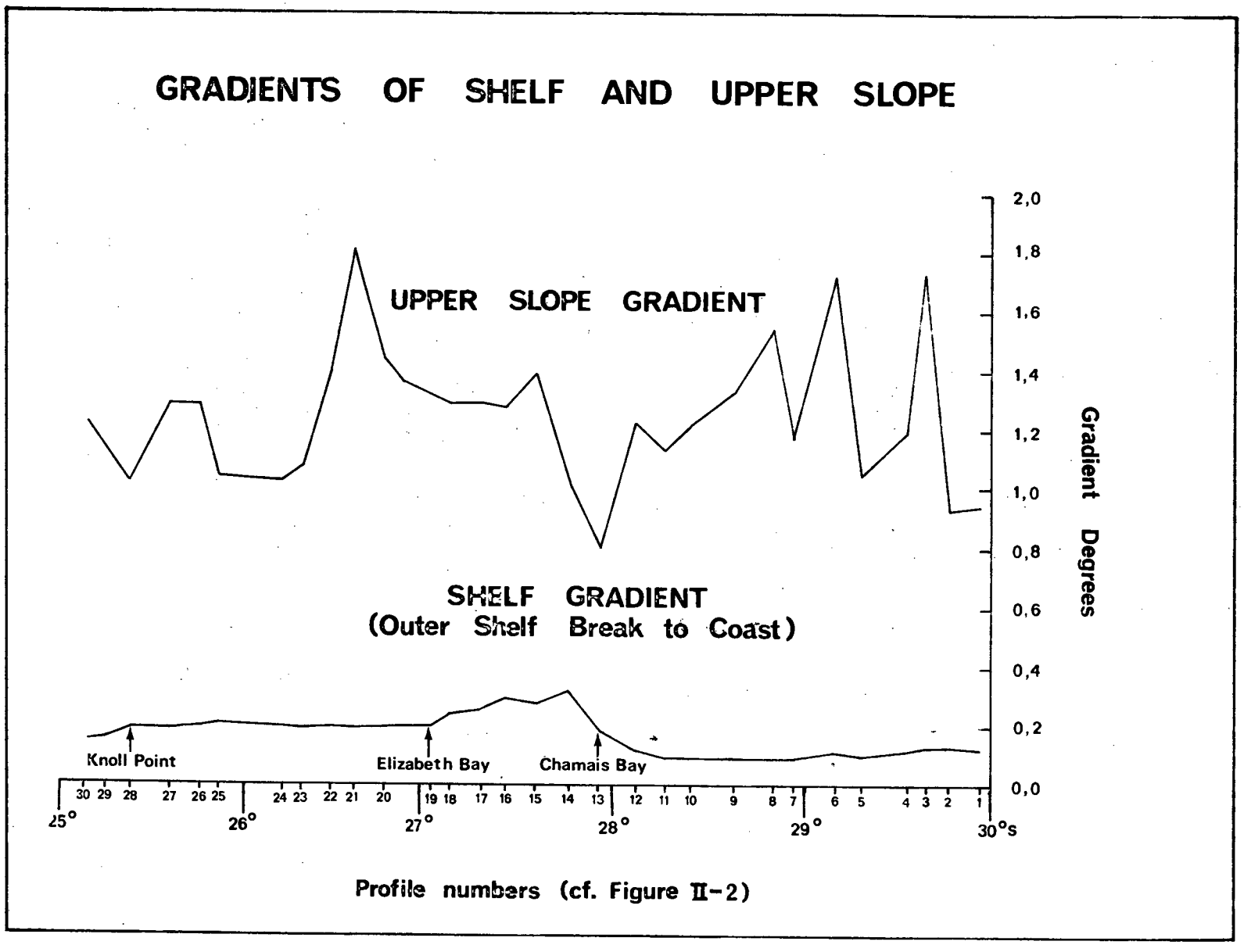
GRADIENTS OF SHELF AND UPPER SLOPE
UPPER SLOPE GRADIENT
SHELF GRADIENT
(Outer Shelf Break to Coast)
Gradient Degrees
2,0
1,8
1,6
1,4
1,2
1,0
0,8
0,6
0,4
0,2
0,0
Knoll Point
Elizabeth Bay
Chamais Bay
30 29 28 27 26 25 24 23 22 21 20 19 18 17 16 15 14 13 12 11 10 9 8 7 6 5 4 3 2 1
25°
26°
27°
28°
29°
30°S
Profile numbers (cf. Figure II-2)

Fig.II-4

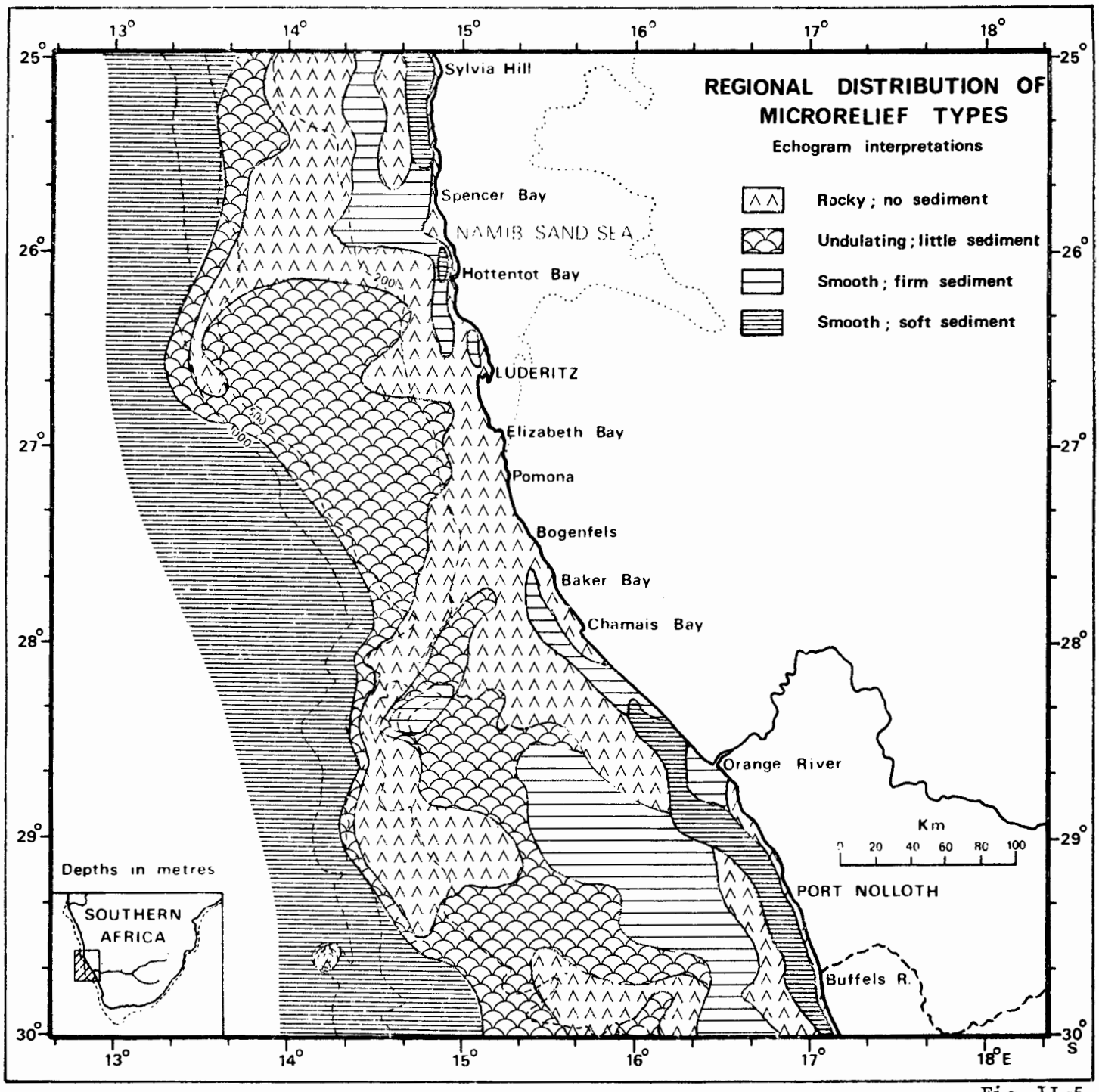
REGIONAL DISTRIBUTION OF MICRORELIEF TYPES
Echogram interpretations
Rocky ; no sediment
Undulating ; little sediment
Smooth ; firm sediment
Smooth ; soft sediment
Sylvia Hill
Spencer Bay
NAMIB SAND SEA
Hottentot Bay
LUDERITZ
Elizabeth Bay
Pomona
Bogenfels
Baker Bay
Chamais Bay
Orange River
PORT NOLLOTH
Buffels R.
Km
0 20 40 60 80 100
Depths in metres
200
500
1000
SOUTHERN AFRICA
13°
14°
15°
16°
17°
18°E
25°
26°
27°
28°
29°
30°S

Fig. II-5

Figure II-5 shows that most of the shelf has relatively little sediment cover, in contrast with the slope which is draped by soft sediment. Sediments related to the Orange River are found both north and south of the mouth. Firm sediment is found on the delta front, whereas soft sediment characterises the prodelta farther seaward as well as its narrow extension to the south. The prodelta off the mouth of the Orange grades into an extensive belt of smooth firm sediment, which farther north and south is separated from the prodelta mud belt by elongate bands of rock outcrop (discussed further in Section II-C-5). The Orange Banks have subdued relief but little sediment cover.

On the Walvis Shelf smooth surfaces on the middle shelf north of Lüderitz represent southerly extensions of the organic-rich diatomaceous muds best developed off Walvis Bay (Calvert and Price, 1971a; Bremner, 1975b). In addition sand is eroded from cliffs of dune sand north of Hottentot Bay and transported seawards to the inner shelf (Figs. II-20 and II-21) where they give rise to a microrelief of smooth firm sediment.

Between Chamais Bay and Lüderitz both the inner and middle shelves have little sediment cover and consequently the bulk of the dredged rock samples come from this region. North of Hottentot Bay the outer shelf is rocky and truncated reflectors crop out on the sea floor (Van Andel and Calvert, 1971; Section II-C-4c). In contrast the deeper outer shelf off Lüderitz is underlain by flat-lying strata (Dingle, 1973a), and the topography is correspondingly subdued.

C. MORPHOLOGICAL ZONES

The areal distribution of the morphological zones in the study area is mapped in Figure II-6. The zones will be discussed in sequence, beginning at the slope and ending at the coast. The information available increases coastwards, so that more attention will be paid to the shallower zones.

1. Upper slope

The initial formation of the continental margin on the west coast of Southern Africa was by tension-rifting (Dingle and Scrutton, 1974). Sediment draping the continental slope has been deposited at an average gradient of only $1{,}2^{o}$. Du Plessis *et al.* (1972, p.77) present seismic profiles showing a smooth merging with the continental rise below about 3000 m. Microrelief, as can be seen in Fig. II-5, is smooth and generally featureless. The slope is clearly a depositional feature (Fig. II-7, profile 228).

Despite the low gradient, a slump has been mapped just below the shelf break off Lüderitz. Similar slumps on similarly low gradients have been mapped by Lewis (1971) on the slope off the east coast of New Zealand, and two large slumps were located by Summerhayes (1974, pers.comm. in Bremner, 1975b, p.7) off Conception Bay and Swakopmund north of the study area. Bremner (1975b, p.7), also noted

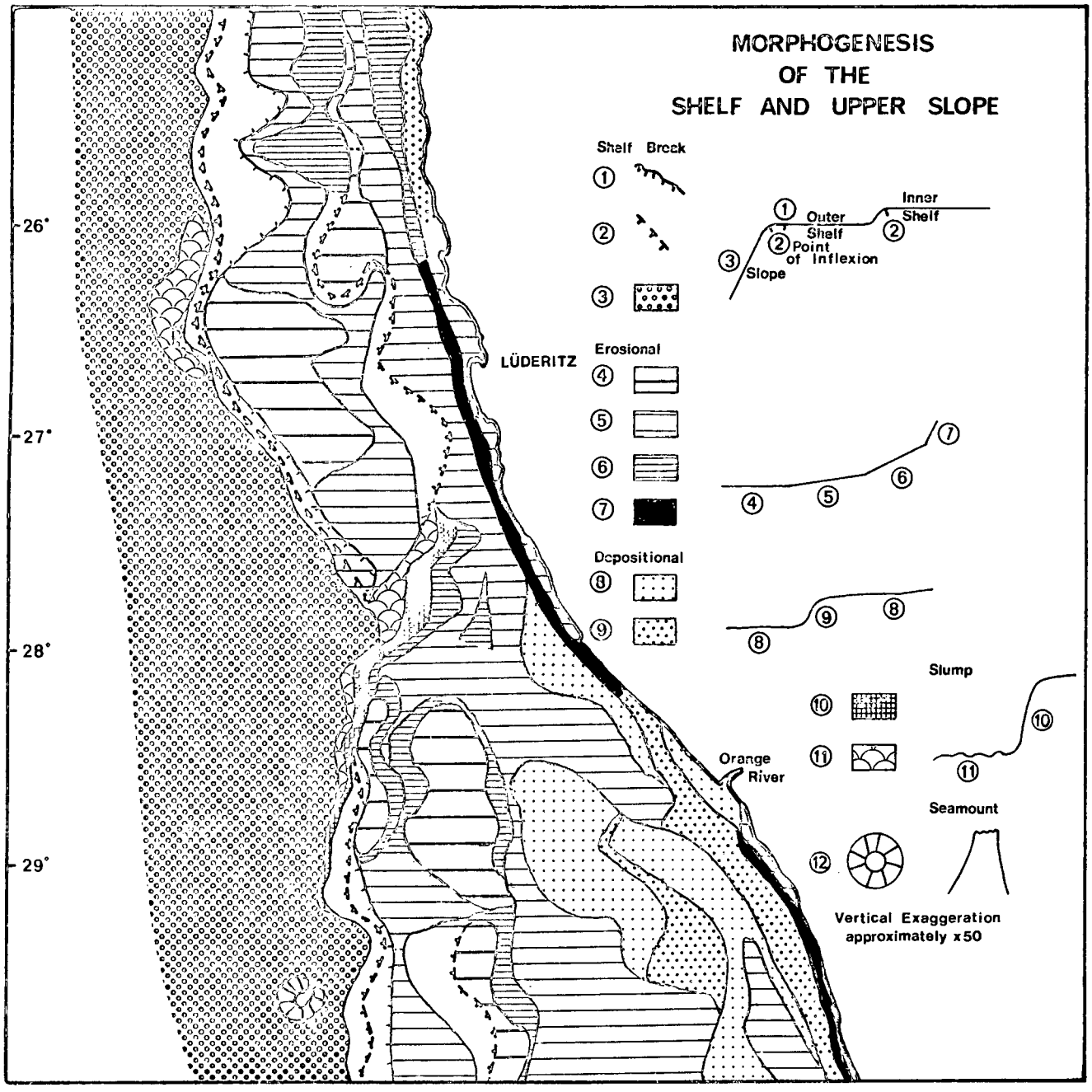
MORPHOGENESIS
OF THE
SHELF AND UPPER SLOPE
Shelf Break
Inner Shelf
Outer Shelf
Point of Inflexion
Slope
Erosional
Depositional
Slump
Seamount
Vertical Exaggeration approximately x50
LÜDERITZ
Orange River
26°
27°
28°
29°

Fig.II-6

SEISMIC PROFILES OF THE SHELF-BREAK ZONE
(After Dingle, 1973)

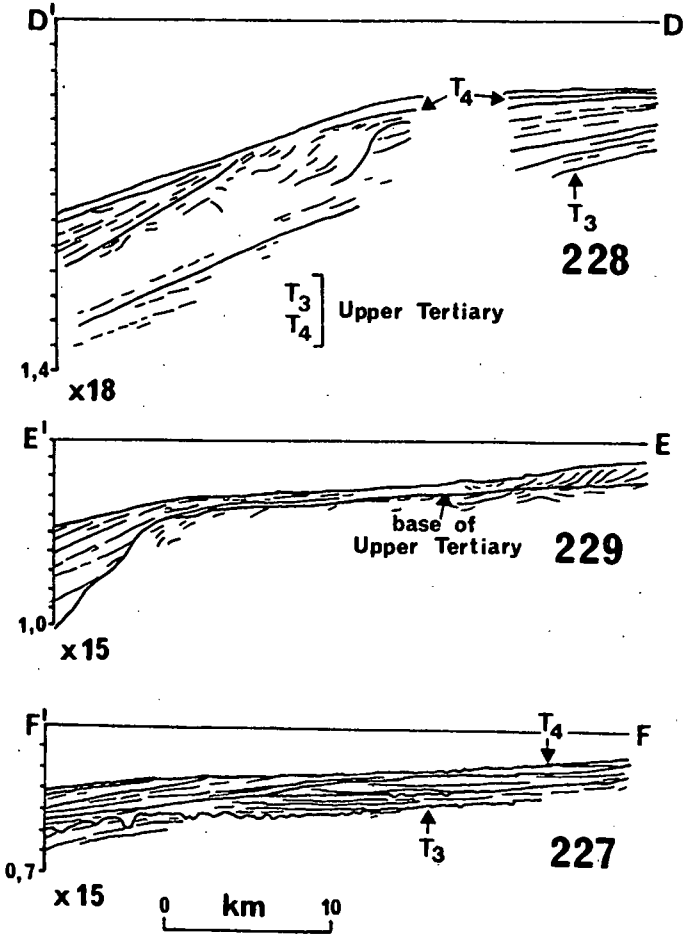

Vertical scale in seconds, one way

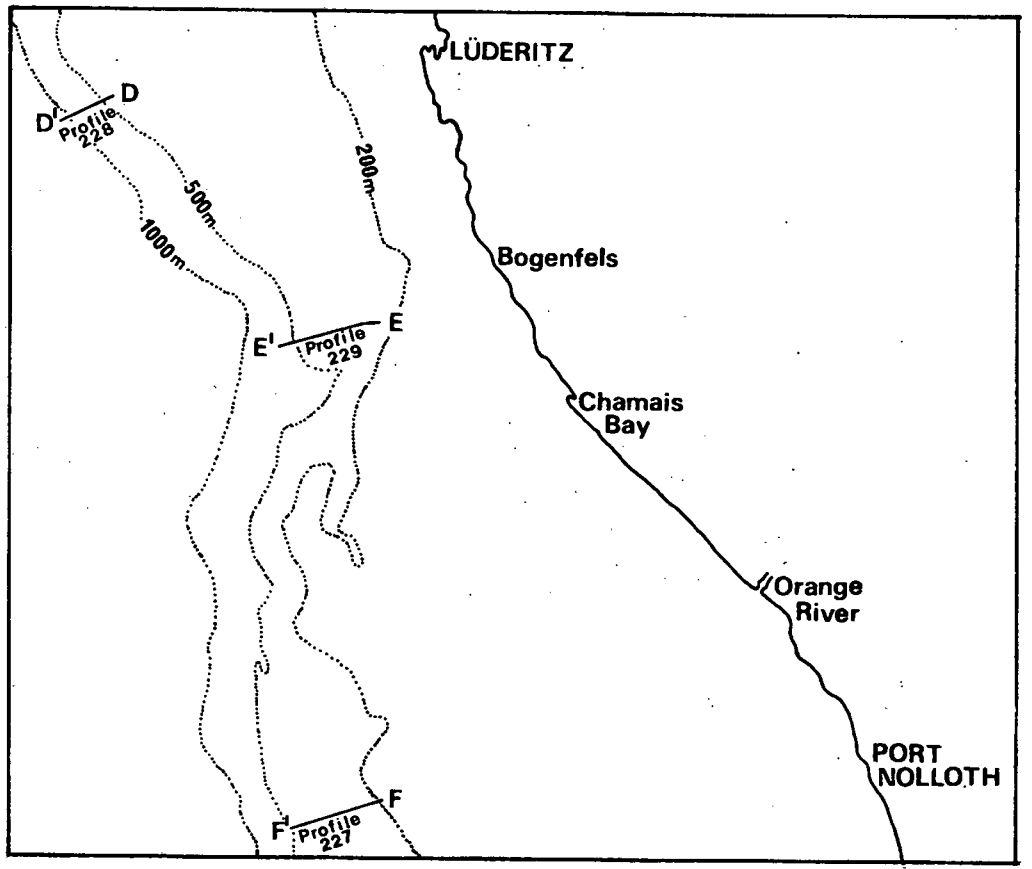

Fig. II-7

a decrease in slope gradient opposite these slumps.

Isolated small submarine canyons have been found off Chamais Bay but they are not a characteristic feature of the slope.

The isolated Tripp seamount (Fig. II-8), as yet undated, rises above the upper slope in a depth of about 1000 m just north of 30°S. It has an uneven surface of limestone (proved by dredging) filling in the crater of the original volcano (Du Plessis et al., 1972, Fig. 3; Emery et al., 1975, Fig. 22). The shallowest peak lies at a depth of 152 m, but the average depth of the relatively flat top is 160 m, similar to that of the Orange Banks (Fig. II-2). The seamount possesses the steepest gradient (17,4° or 313 m/km) of all the features studied on the continental margin.

2. Chamais Slump

Dingle (1973a, Fig. 6) mapped a slump scarp, which truncates the edge of the shelf off Chamais Bay, but peters out southwards towards Tripp Seamount. The slump has been mapped in more detail (Fig. II-9) and a slump toe distinguished below the scarp. It is here named the Chamais Slump, because of its greater significance and extent off that locality. The slump is 220 km (120 n.m.) long and up to 30 km (17 n.m.) wide. The scarp is at its steepest off Chamais Bay itself where it drops 270 m, from 240 m to 510 m, at an apparent angle of 2,6° (Fig. II-9). The Walvis Shelf rises northwards from a trough at the foot of the scarp to a level of 335 m, 145 m below the level of the Orange Shelf at 190 m.

Kaiser (1926, pp.432-433) postulated a warp-hinge at Bogenfels (27°30'S) to account for Lower Miocene marine sediments at a height of over 160 m east of Bogenfels, and non-marine sediments of the same age near sea level at Elizabeth Bay. Kaiser's warp-hinge coincides closely with the marginal offset near latitude 27°30'S first postulated by Francheteau and Le Pichon (1972, p.1004), and possibly linked to a Precambrian line of weakness along the Orange River (Fuller, 1972, p.164). Marsh (1973, p.321) has associated Early Cretaceous alkaline igneous complexes in Uruguay and at Pomona (27°13'S), just north of Bogenfels (Fig. II-8) with Francheteau and Le Pichon's marginal offset. Scrutton and Dingle (1973, p.258) also refer to the same offset as a boundary separating bathymetric and sedimentation provinces. It is suggested that the Chamais Slump (27°30'S-29°00'S) is one of the more recent manifestations associated with tectonic instability along the marginal offset.

Modern seismicity onshore is concentrated in the Escarpment region associated with ".... a very slow upwarping, a movement which to some extent makes use of existing (post-Karoo) faults" (Korn and Martin, 1951a, p.87). Perhaps similar seismicity associated with downwarping of the shelf break, the Escarpment's offshore equivalent, triggered the Chamais Slump.

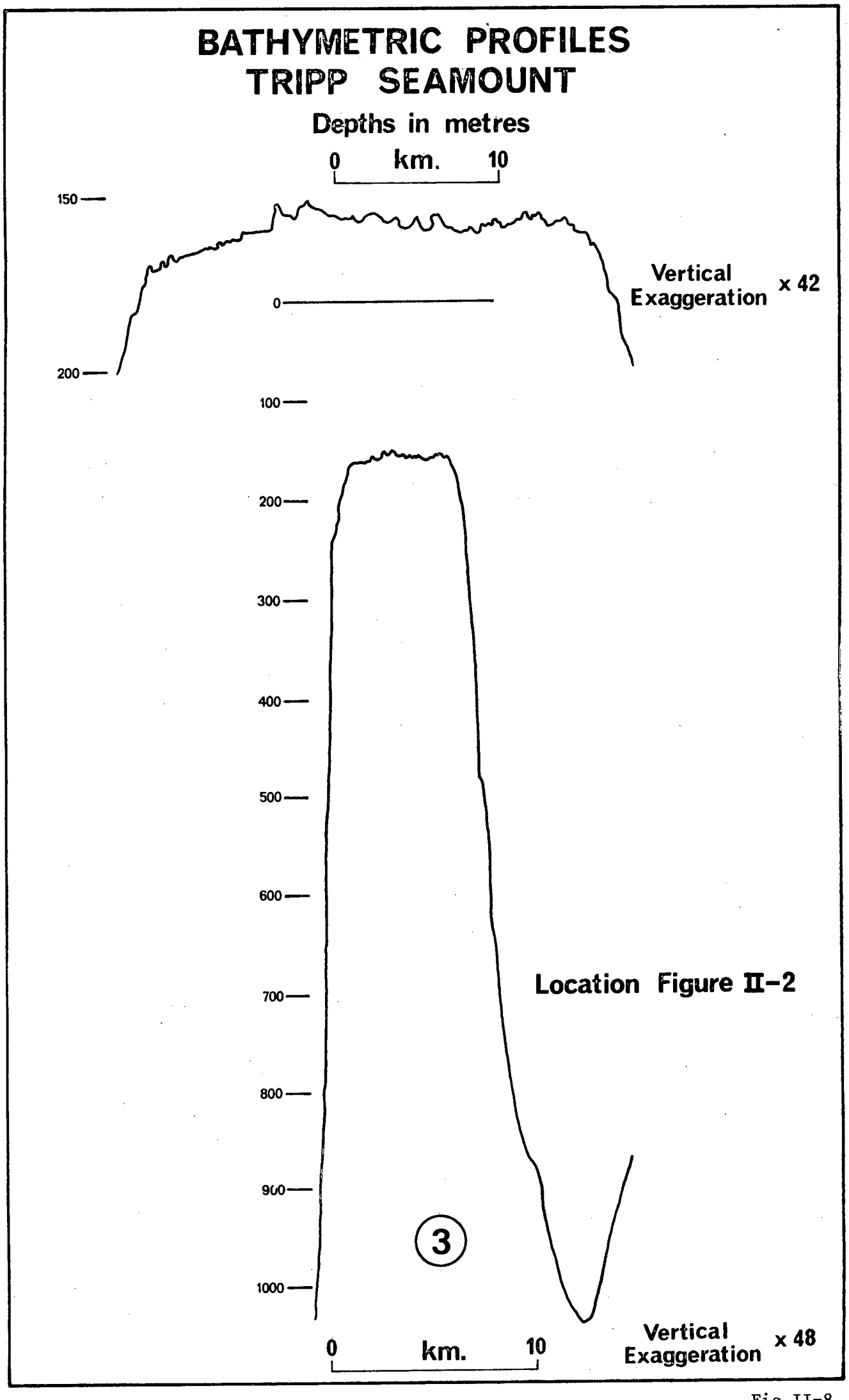
BATHYMETRIC PROFILES
TRIPP SEAMOUNT
Depths in metres
0 km. 10
150
0
200
Vertical Exaggeration x 42
100
200
300
400
500
600
700
800
900
1000
Location Figure II-2
3
0 km. 10
Vertical Exaggeration x 48

Fig. II-8

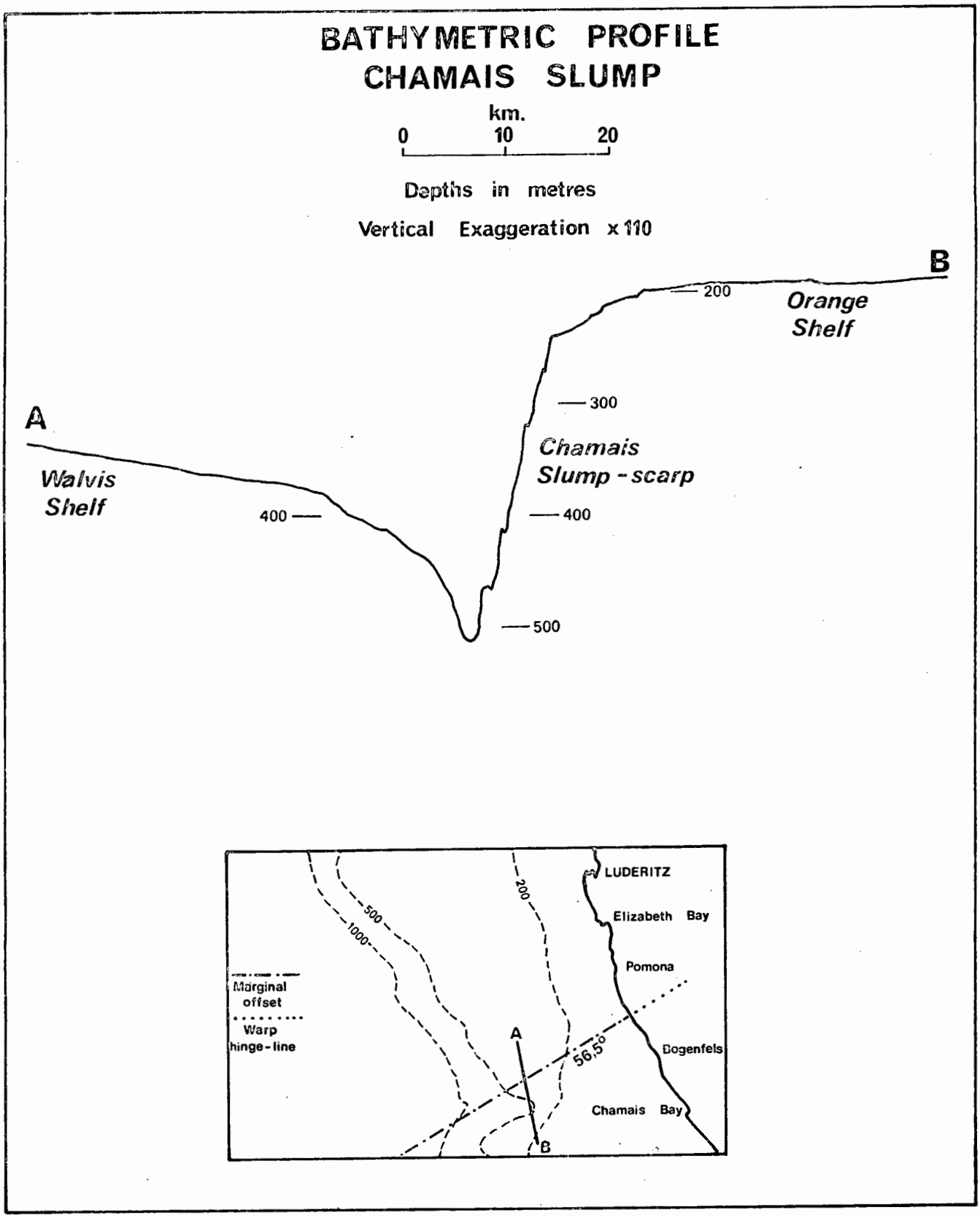
BATHYMETRIC PROFILE
CHAMAIS SLUMP
km.
0
10
20
Depths in metres
Vertical Exaggeration x 110
A
B
Walvis Shelf
Chamais Slump - scarp
Orange Shelf
200
300
400
400
500
LUDERITZ
Elizabeth Bay
Pomona
Bogenfels
Chamais Bay
Marginal offset
Warp hinge-line
500
1000
200
56,5°
A
B

Fig.II-9

3. Shelf breaks

The shelf break has been mapped (Fig. II-6) as a zone separating the shelf from the upper slope, and a point of inflexion has been selected on each profile where its gradient steepens rapidly towards the slope. The zone is narrowest (9 km or 5 n.m.), and the shelf break therefore best defined, between the Chamais Slump (27°30'S) and Lüderitz (26°40'S). It broadens to 22 km (12 n.m.) near Tripp Seamount (29°40'S) and to 44 km (24 n.m.) north of Hottentot Bay (26°10'S). North of Hottentot Bay, within the broad shelf-break zone, the point of inflexion lies much nearer to the upper edge of the slope than to the outer edge of the shelf. The style of this section of the shelf break is illustrated in Fig. II-13.

The effect of the Chamais Slump on the morphological style of the Orange shelf break is depicted in Fig. II-10. On profile 11 the slump clearly truncates the edge of the shelf, but in other profiles farther south the slump is found at ever-increasing depths, until it peters out below the 500 m isobath.

Double shelf breaks are a feature of the study area. Near Tripp Seamount, Dingle (1973a) (Fig. II-7, profile 227) has shown that the outer shelf break is underlain by sub-parallel beds, which are truncated between the inner and outer shelf-breaks. The inner shelf-break marks the seaward edge of an outlier of Tertiary sediment which caps the Orange Banks. Dingle (1973a, p.359) postulates that a double shelf break has characterised this area since at least the end of Lower Tertiary times. He suggested that the origin of the feature was either deposition on a step-shaped feature eroded in post-Cretaceous times or deposition on an irregular surface related to basement topography. More closely spaced seismic lines with greater penetration would shed more light on this issue, as would publication of drilling records from SEDCO 135, which drilled to over 4000 m below the outer edge of the Orange Shelf.

The origin of the inner shelf break on the Walvis Shelf is less problematical. According to Du Plessis et al. (1972, profile 7) and Dingle (1973a) (Fig. II-7, profile 229) off Bogenfels (27°30'S) where the inner shelf break is best defined, Tertiary sediments with relatively steep seaward dips merge into a thinner sequence of more flat-lying beds above the same unconformity. The Walvis middle shelf appears to owe its origin to more rapid upbuilding than outbuilding near the coast. The dominant lithofacies in this part of the shelf is a quartzose limestone (Fig. II-11) (see Chapter III) containing few fossils. Drilling of the upper few hundred metres would establish whether there are major lithofacies variations within the Tertiary layers above the unconformity. Micropalaeontological work on such core material would help to resolve ambiguities such as the dating of the sediments below the upper unconformity in the four seismic profiles within the study area. Du Plessis et al. (1972) considered them to be Cretaceous, whereas Dingle (1973a) chose a Lower Tertiary age.

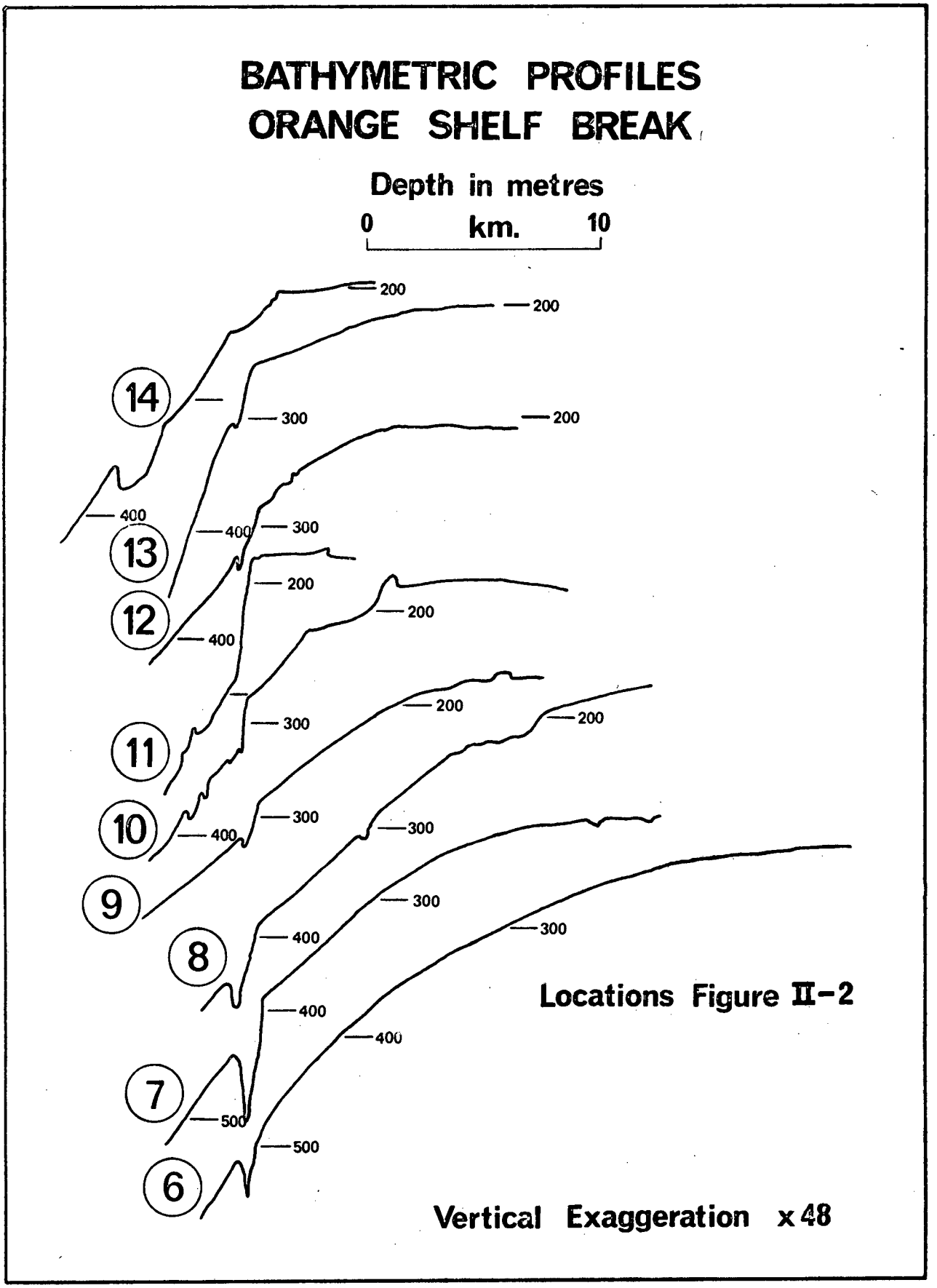
BATHYMETRIC PROFILES
ORANGE SHELF BREAK
Depth in metres
0
km.
10
14
13
12
11
10
9
8
7
6
200
300
400
500
Locations Figure II-2
Vertical Exaggeration x48

Fig.II-10

SEISMIC PROFILES FROM THE INNER SHELF TO THE MIDDLE SHELF

(After Dingle, 1973)

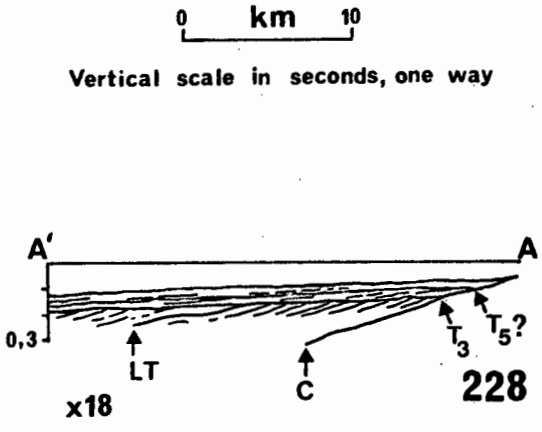

T_5 / T_3 Upper Tertiary

LT Lower Tertiary

C Cretaceous

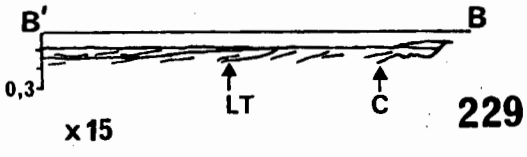

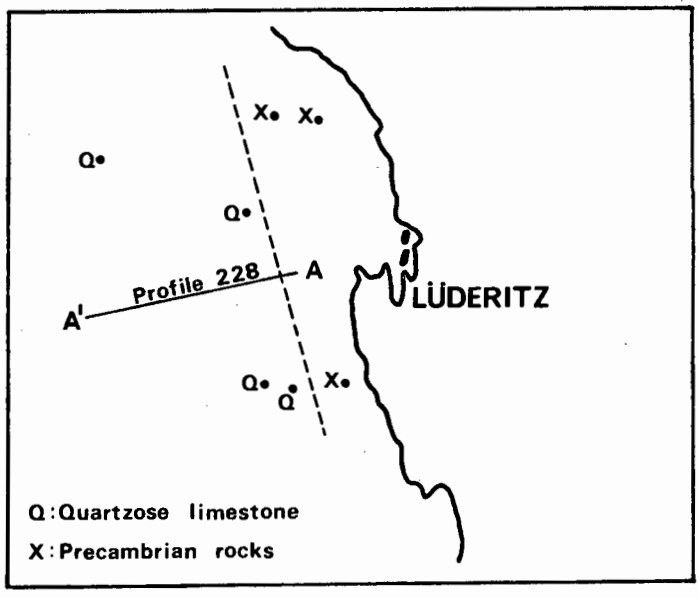

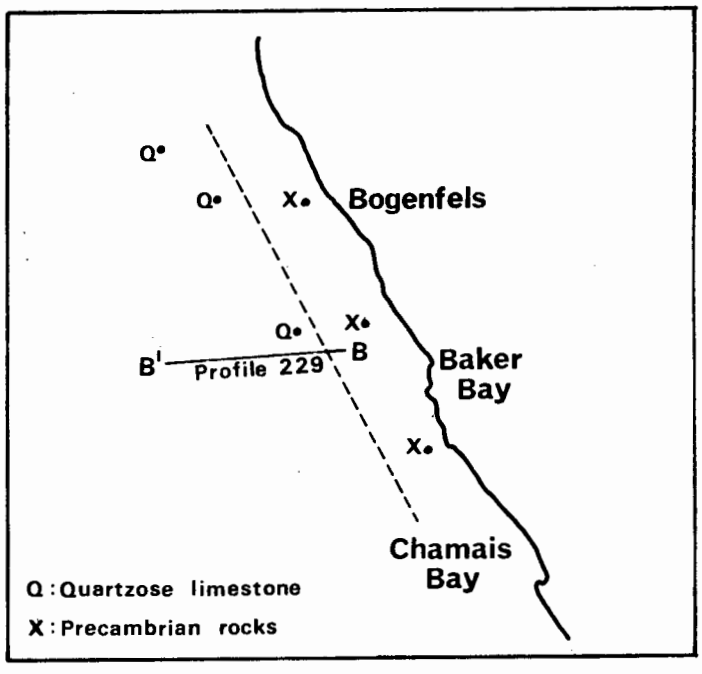

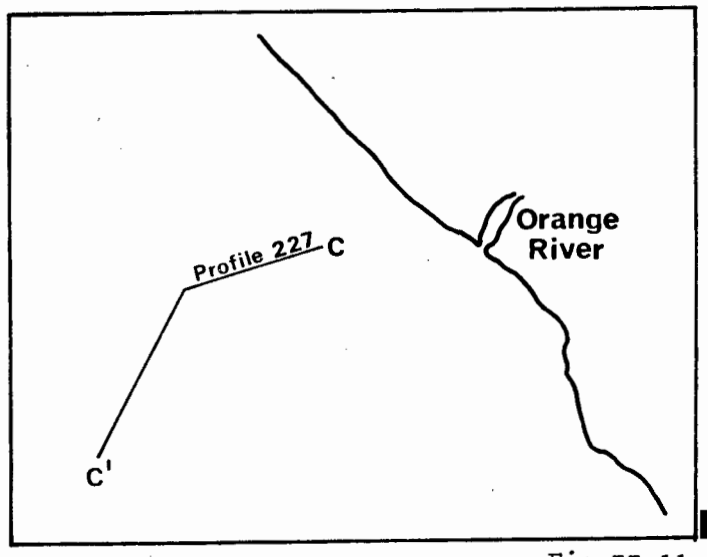

Fig.II-11

4. Outer shelf

a. Orange Banks

Dingle (1973a, p.341) recognised that the outer part of the Orange Shelf was shallower than parts of its middle shelf. He further outlined "three distinct banks" which he termed the Orange Shoals. As their average depth is 160 m they are not navigational hazards and they have subsequently been referred to as the Orange Banks (Rogers, 1974, p.24; Siesser, Scrutton and Simpson, 1974, p.641). The most westerly bank (Figs. II-1 and II-12) lies along the Orange shelf break separated from the largest bank by a shallow valley leading north to the Chamais Slump. The western edge of the most southerly bank forms an inner shelf break.

In Figures II-5 and II-12 the microrelief is depicted as rocky to undulating, and although few dredging operations have been attempted, two samples of Miocene Nummulitic limestone have been recovered (see Chapter III). Dingle (1973a, profile 227) has traced an outlier of his "T4" sediments on the Orange Banks. No internal structures were recognised, although a similar outlier capping Childs Bank showed a rich variety of structure, interpreted by Dingle as evidence of rapidly changing shallow-water conditions. The abundance of coralline algae in some of the rocks from the Orange Banks at least indicates deposition within the euphotic zone, but the total absence of terrigenous components implies deposition far from the coast.

The individual banks are often delineated by small scarps about 10 m high, particularly along their eastern edges (Fig. II-12, profile B'-B). As on Childs Bank, slumps have removed parts of the seaward edge of the westernmost bank.

b. Outer shelf off Lüderitz

Semi-consolidated Neogene clays (Siesser, 1975) underlie this featureless portion of a concave section of the Walvis Shelf. Seismic profiles (Fig. II-7, profile 228) reveal truncated, seaward-dipping strata on the outer shelf overstepping older beds dipping more steeply seawards (Du Plessis *et al.*, 1972). It is probable that the lack of consolidation of the substrate facilitated erosion. The steeper dip of the underlying strata implies outward tilting before deposition of the younger strata. This abnormally deep outer shelf is ascribed, then, to seaward tilting of the seaward-thickening sedimentary pile, coupled with differential erosion and followed by downwarping towards the north (cf. Knetsch, 1973, p.196; Kaiser, 1926, p.432).

c. Sub-bottom reflectors, Spencer Bay to Sylvia Hill

Van Andel and Calvert (1971, p.586, Figs. 2-3) obtained 60 m penetration during their survey of the outer shelf north of 26°S using a 3,5 kHz high-resolution seismic profiler. They found seaward-dipping sub-bottom reflectors truncated at the sea floor, and they postulated a major regression to account for such erosion. The same sub-bottom reflectors were recorded on the 12 kHz ELAC echo sounder

BATHYMETRIC AND SEISMIC PROFILES OF THE ORANGE BANKS

(After Dingle, 1973)

Depths in metres

0 km. 10

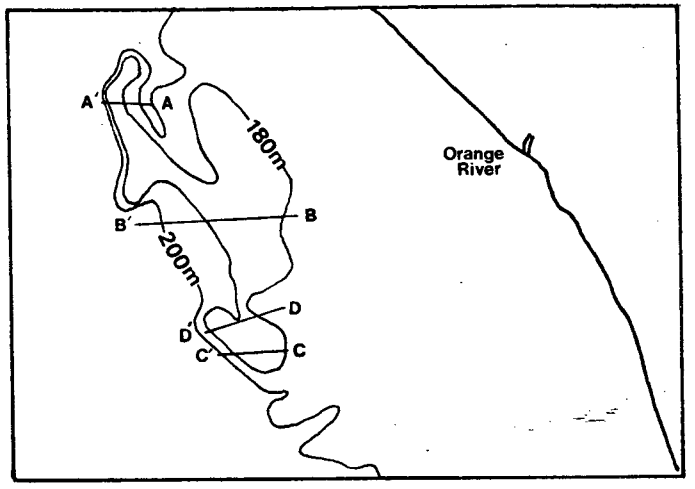

West

Vertical Exaggeration x48

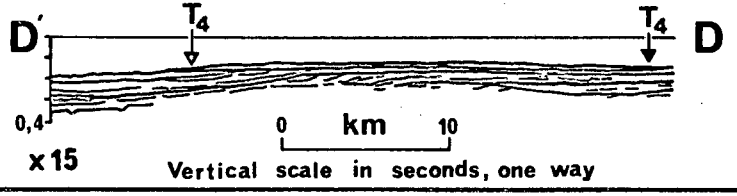

Fig. II-12

aboard R.V. THOMAS B. DAVIE and a penetration of 50 m was achieved (Fig. II-13). As the echo sounder, with its high frequency, is not designed to penetrate bedrock such penetration was unexpected. An extensive deposit of residual sand rich in pelletal phosphorite has been sampled on this part of the outer shelf and at station 3232 pelletal phosphorite rock was obtained (Fig. II-13) (Summerhayes et al., 1973). Well-consolidated lime mudstone was recovered at the same station, so that the lithology of the reflectors is as yet unproven. Dredging and rock-drilling is required to establish their lithology.

The overall shelf gradient in this part of the shelf varies between $0,15^{o}$ and $0,19^{o}$. The sub-bottom reflectors have true dips of $0,78^{o}$ due west (270^{o}). Sub-bottom reflectors detected along a longitudinal traverse had a maximum northward apparent dip of $0,33^{o}$. Because the strata become horizontal northwards the writer concludes that the sub-bottom reflectors form a basin north of Lüderitz Bank and west of the middle shelf.

5. Middle shelf

The middle shelf in the study area is best delimited by defining the outer and inner shelves either side of it. The outer shelf on the Orange Shelf extends from the shelf break to the landward edge of the Orange Banks; on the Walvis Shelf it is bounded in most places by the inner shelf-break. The inner shelf is defined for the study area as the zone, beside the coast, which is underlain by "acoustic basement". Because this "acoustic basement" crops out within 5 km of a coast composed entirely of Precambrian rocks, the outcrop forming the inner shelf is assumed to be Precambrian. Limited dredging at the coastal ends of some traverses invariably recovered schists and gneisses similar to those found onshore. A simple definition of the middle shelf, then, is that it lies immediately seaward of the Precambrian outcrop.

a. Post-Palaeozoic outcrops south of the Orange River

Du Plessis et al. (1972) and Dingle (1973a) interpreted two seismic profiles over the Orange Shelf. One profile extended from Hondeklip Bay to Childs Bank just south of the study area, and the other ran from the mouth of the Orange River to Tripp Seamount (Profile 227, Figs. II-7, II-11). Acoustic basement (Precambrian outcrop) near the coast is overlain with a marked unconformity by seaward-dipping sediments which are truncated at the sea floor. These relatively steeply dipping layers are themselves overlain by more flat-lying layers (Fig. II-11, profile 227). In both papers the sediments overlying acoustic basement are assumed to be Cretaceous in age. Figure II-14 illustrates the seaward-dipping scarps with relief of up to 10 m over the "Cretaceous" outcrop and the positions of unfossiliferous ferruginous sandstones and mudstones dredged from the outcrop. (The rock samples are discussed in Chapter III). The outcrop is flanked by areas of

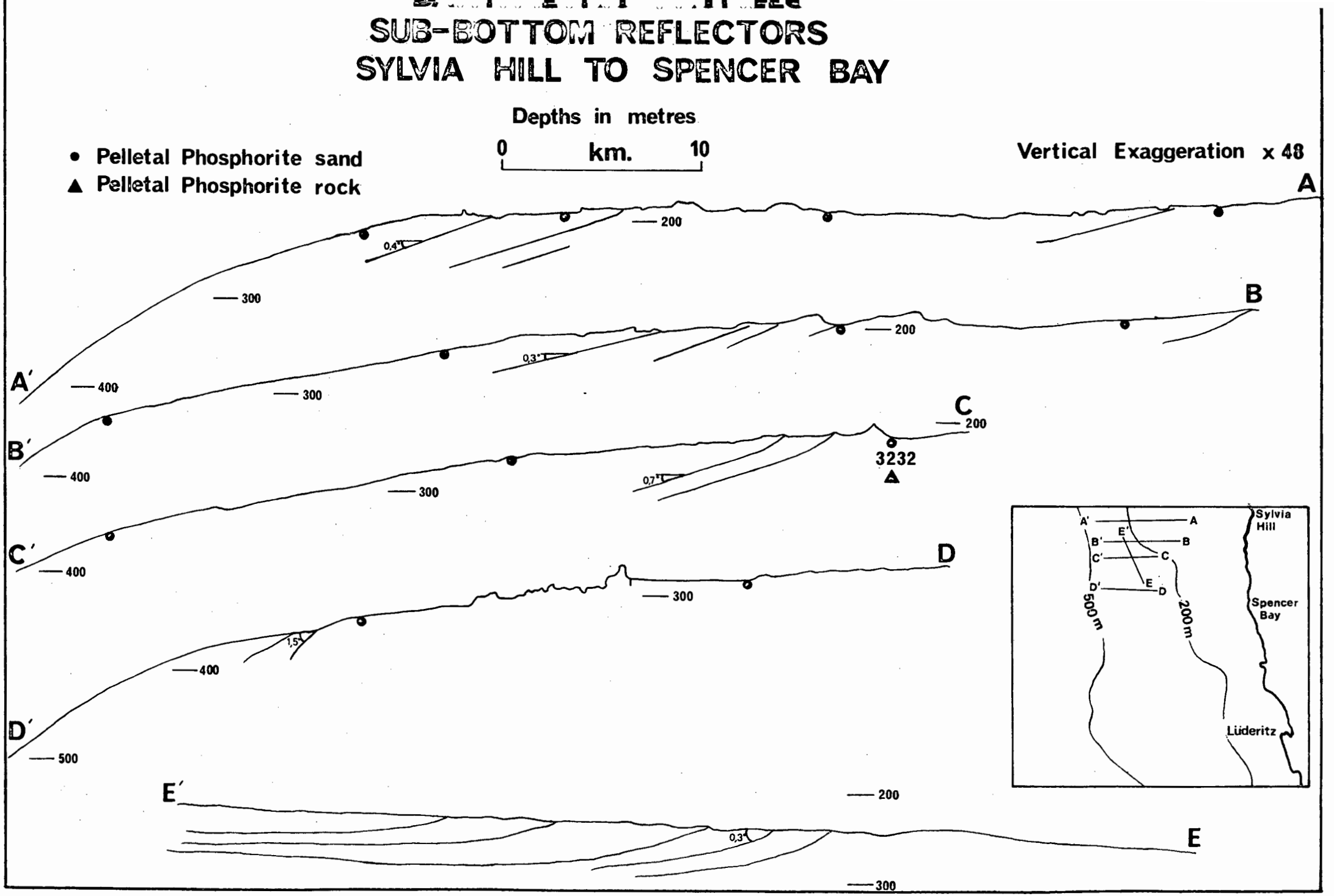
SUB-BOTTOM REFLECTORS
SYLVIA HILL TO SPENCER BAY
Depths in metres
0 km. 10
Vertical Exaggeration x 48
• Pelletal Phosphorite sand
▲ Pelletal Phosphorite rock
A
B
C
D
E
A'
B'
C'
D'
E'
200
300
400
500
0,4°
0,3°
0,7°
1,5°
3232
Sylvia Hill
Spencer Bay
Lüderitz
500 m
200 m

Fig.II-13

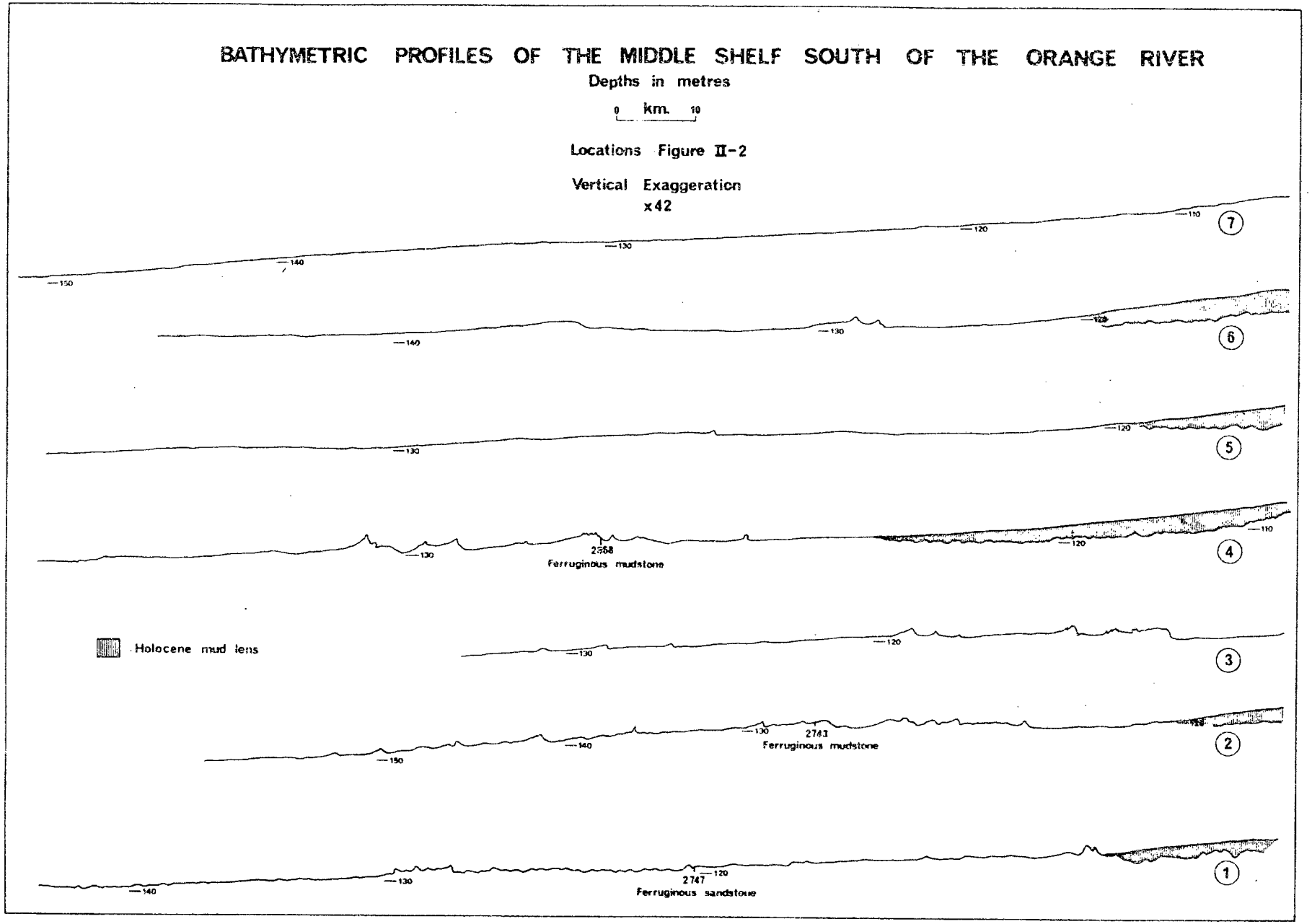
BATHYMETRIC PROFILES OF THE MIDDLE SHELF SOUTH OF THE ORANGE RIVER
Depths in metres
0 km. 10
Locations Figure II-2
Vertical Exaggeration
x42
7
6
5
4
3
2
1
Holocene mud lens
2568
Ferruginous mudstone
2783
Ferruginous mudstone
2747
Ferruginous sandstone

Fig. II-14

smooth sediment both landwards and seawards (Fig. II-5).

b. Post-Palaeozoic outcrops north of the Orange River

Extensive outcrops of seaward-dipping strata with relief of up to 15 m (Figs. II-5 and II-15) are found north of the Orange River, particularly off Chamais Bay. The widely scattered dredge samples are chiefly unfossiliferous ?Tertiary quartzose limestones (Fig. II-11, profiles 228 and 229) and no ferruginous sediments were recovered. The writer therefore favours Du Plessis et al's (1972) interpretation of the seismic profile off Bogenfels. Unlike Dingle (1973a) who showed Cretaceous strata cropping out on the middle shelf, Du Plessis et al. (1972) extended the overlying Tertiary layer to the Precambrian outcrop. They found similar relationships as far north as Spencer Bay (25°36'S), north of Lüderitz. In Chapter III it will be shown that quartzose limestones are characteristic of the middle shelf from the Orange River to Spencer Bay, thus supporting Du Plessis et al's (1972) interpretation.

c. Lüderitz Bank

A smooth, flat-topped elevation (Fig. II-16) dominates the middle shelf northwest of Lüderitz (Fig. II-1). It is a bench-like extension of the middle shelf due west of Hottentot Bay (26°10'S). The elevation is 37 km (20 n.m.) wide and rises from a depth of 290 m on the outer shelf to 205 m at its crest, which forms part of the inner shelf break on the Walvis Shelf. Its steepest slope is to the southwest. To the southeast a valley separates it from the rest of the middle shelf. The feature was named the Lüderitz Shoal by Rogers and Bremner (1973, p.8). Like the Orange Banks, the feature poses no threat to navigation, and it is now referred to as the Lüderitz Bank (Rogers, 1974, p.26). The bank is the locus of a rich deposit of glauconitic sand.

6. Inner shelf

For the purposes of this thesis, the inner shelf is defined as the zone underlain by Precambrian rocks beside the coast. South of latitude 32°S, where Palaeozoic sediments crop out along the coast, this zone is termed "Pre-Mesozoic basement" (Dingle, Gerrard, Gentle and Simpson, 1971, p.203; Dingle, 1973a, p.344). Because only Precambrian rocks crop out on the coast between latitudes 25 and 30°S, and because one of the Precambrian subdivisions will itself be termed "Basement", the term "Precambrian bedrock" is preferred to "Pre-Mesozoic basement".

a. Precambrian bedrock

i) Seaward boundary

South of Hottentot Bay (26°S) the Precambrian bedrock forms a relatively steep-sided, narrow, rocky platform beside the coast (Figs. II-17 to II-22). North of Hottentot Bay an uneven rocky zone slopes more gently down to the middle shelf. The edge of the Precambrian bedrock has been traced from latitude 20°S

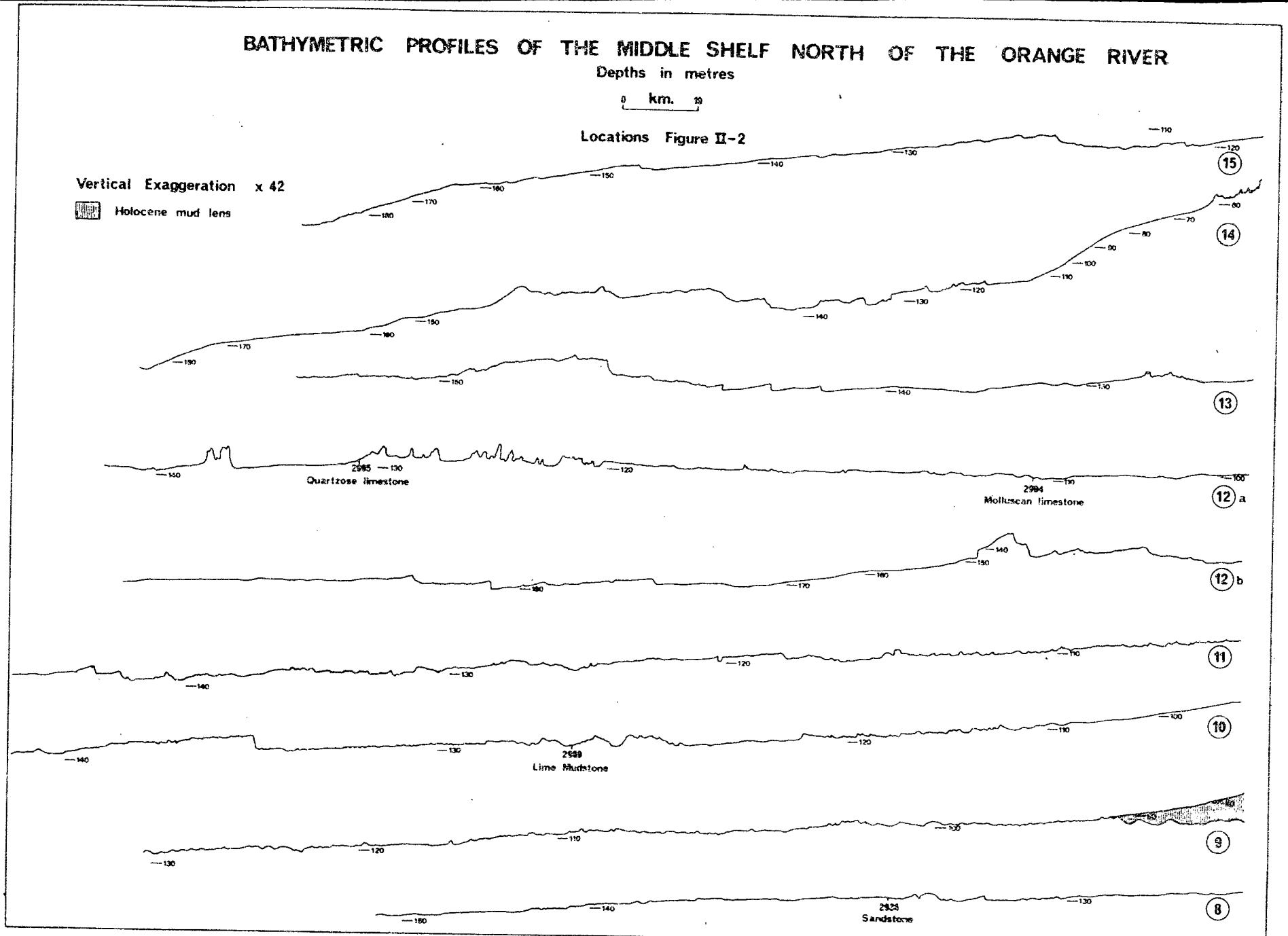
BATHYMETRIC PROFILES OF THE MIDDLE SHELF NORTH OF THE ORANGE RIVER
Depths in metres
0 km. 10
Locations Figure II-2
Vertical Exaggeration x 42
Holocene mud lens
15
14
13
2985
Quartzose limestone
2984
Molluscan limestone
12 a
12 b
11
10
2989
Lime Mudstone
9
2928
Sandstone
8

Fig. II-15

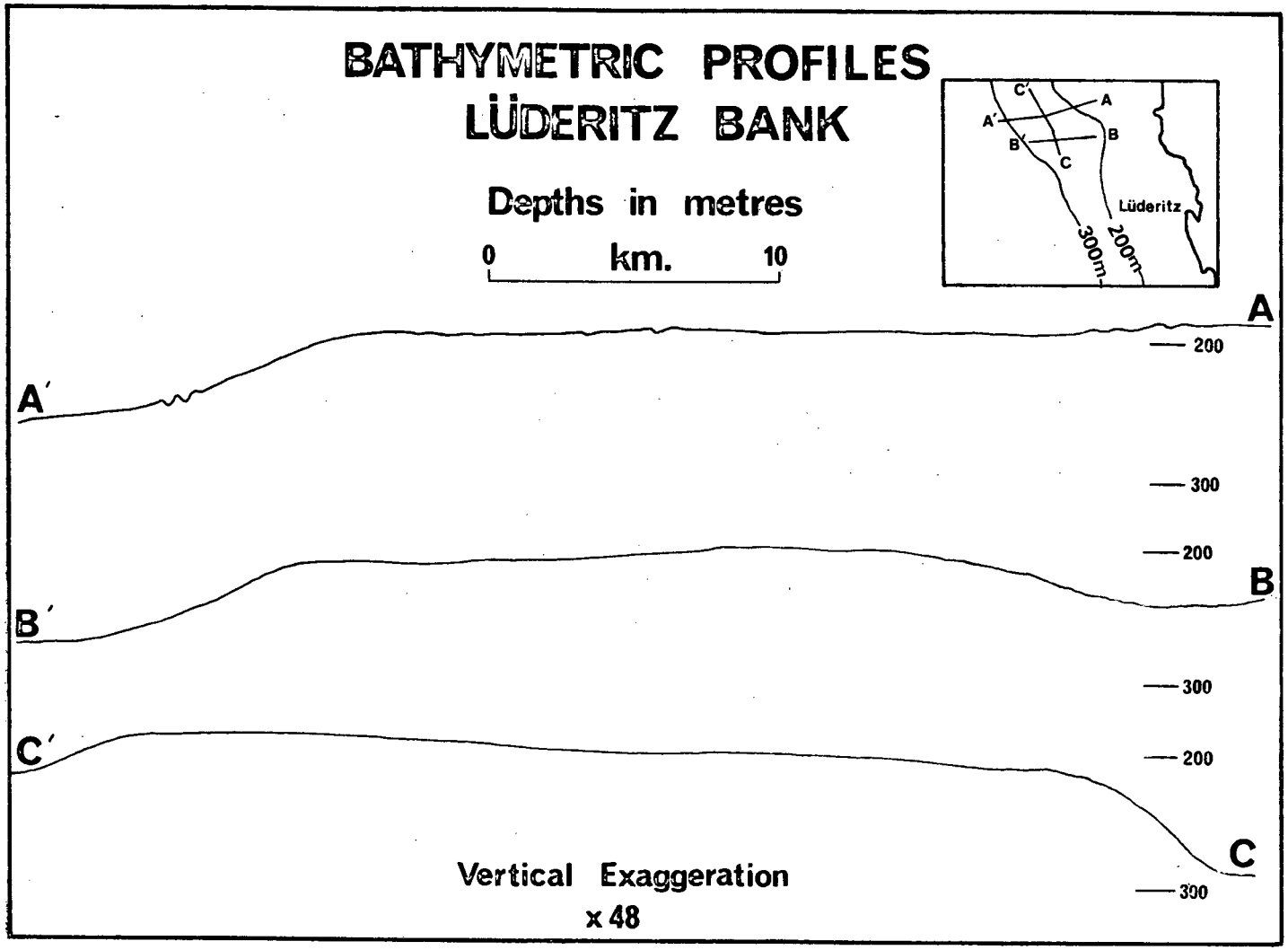
BATHYMETRIC PROFILES
LÜDERITZ BANK
Depths in metres
0 km. 10
C'
A
A'
B
B'
C
Lüderitz
300m
200m
A
A'
200
300
200
B
B'
300
200
C
C'
300
Vertical Exaggeration
x 48

Fig. II-16

BATHYMETRIC PROFILES OF INNER SHELF

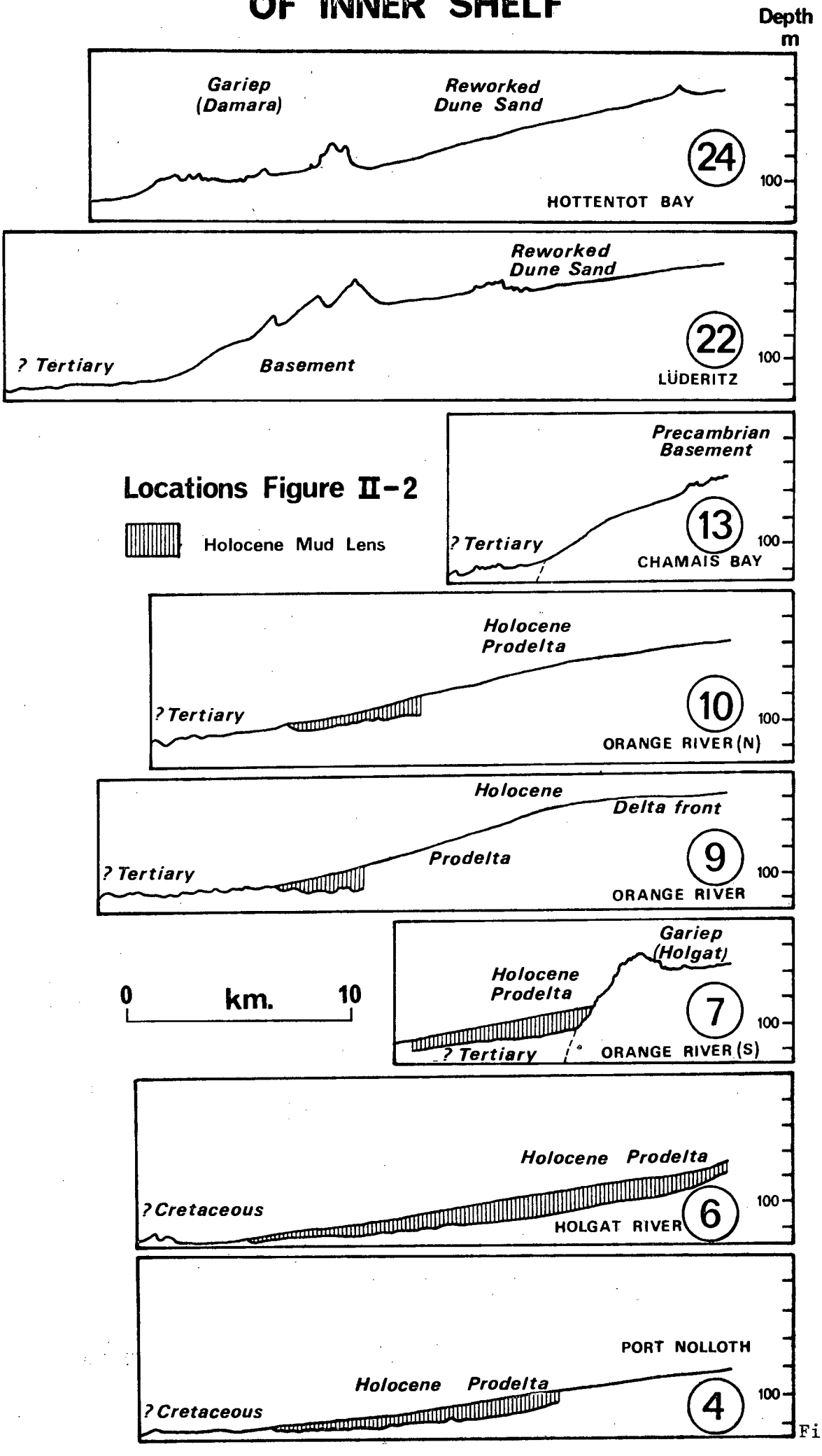

Fig.II-17

(north of Walvis Bay) to 26°S (Hottentot Bay) by Van Andel and Calvert (1971, p.589) who write: "The most widespread (erosion-cut notch) is a low but sharp escarpment at 110 m, which, in many profiles, forms the seaward limit of a nearshore zone of rugged small-scale relief, while in others it is covered with more recent acoustically transparent deposits". Calvert and Price (1970, p.177) and Bremner (1975b, Plate XI-1) have shown that the acoustically transparent deposits between these latitudes are diatomaceous oozes, and Van Andel and Calvert (1971, p.589) conclude that the sea regressed to a depth of 110 m during the last Pleistocene glacial. This depth corresponds closely with that associated with the drowned delta off the Orange (section II-C-5c).

Farther south the edge of the outcrop remains at approximately 110 m as far as Chamais Bay (28°S) (Fig. II-20). Beyond this point the edge of the Precambrian bedrock is blanketed by a lens of deltaic mud, which pinches out seawards in a depth of 120 m (Fig. II-19). Where the lens is thinner than about 10 m, sub-bottom reflections have been obtained from the bedrock, which confirm that the edge of the Precambrian bedrock persists at 110 m. The constant depth of this geological boundary is thus confirmed between 20° and 30°S, and implies that the shelf has not been warped between these latitudes since the last Pleistocene glacial 15 to 20 000 years ago (Curray, 1961; Milliman and Emery, 1968). Hoyt, Smith and Oostdam (1965b, p.227) related this constant depth to a sea-level regression of about 100 m. Off Cape Town, Dingle (1973a, p.346) reports that the boundary lies at 180 m, which implies downwarping of 70 m to the south.

ii) South of Port Nolloth

The bathymetric style of the Precambrian bedrock and the configuration of the associated coastline are intimately connected with variations in lithology and structure of Precambrian formations. The outcrop is narrowest (2-3 km) off Namaqualand south of Port Nolloth (Fig. II-18) and drops steadily from the coast to the middle shelf at an angle of 1,8° or 31,8 m/km. From latitude 30°S to just south of the Buffels River, the narrow inner shelf is constructed of Basement gneiss, quartzite and schist (Rogers, 1915a, p.84; Joubert and Kröner, 1971, p.50). Despite the geological boundary near the Buffels River, the bathymetric style of the inner shelf remains constant as far north as Port Nolloth.

Joubert (1975, p.339) reports an increasing predominance of quartzite and schist towards the coast within the Basement complex. Within the Stinkfontein Formation of the Gariep Group, which overlies the Basement north of the Buffels River, the lithology changes northwards from basal boulder conglomerate near the river to orthoquartzite of the Lower Stinkfontein Formation. Feldspathic quartzite as well as arkose crop out midway between the Buffels River and Port Nolloth but are granitised into "... gneisses ... virtually indistinguishable from some Basement-rocks." according to Joubert and Kröner (1971, p.48). South of Port

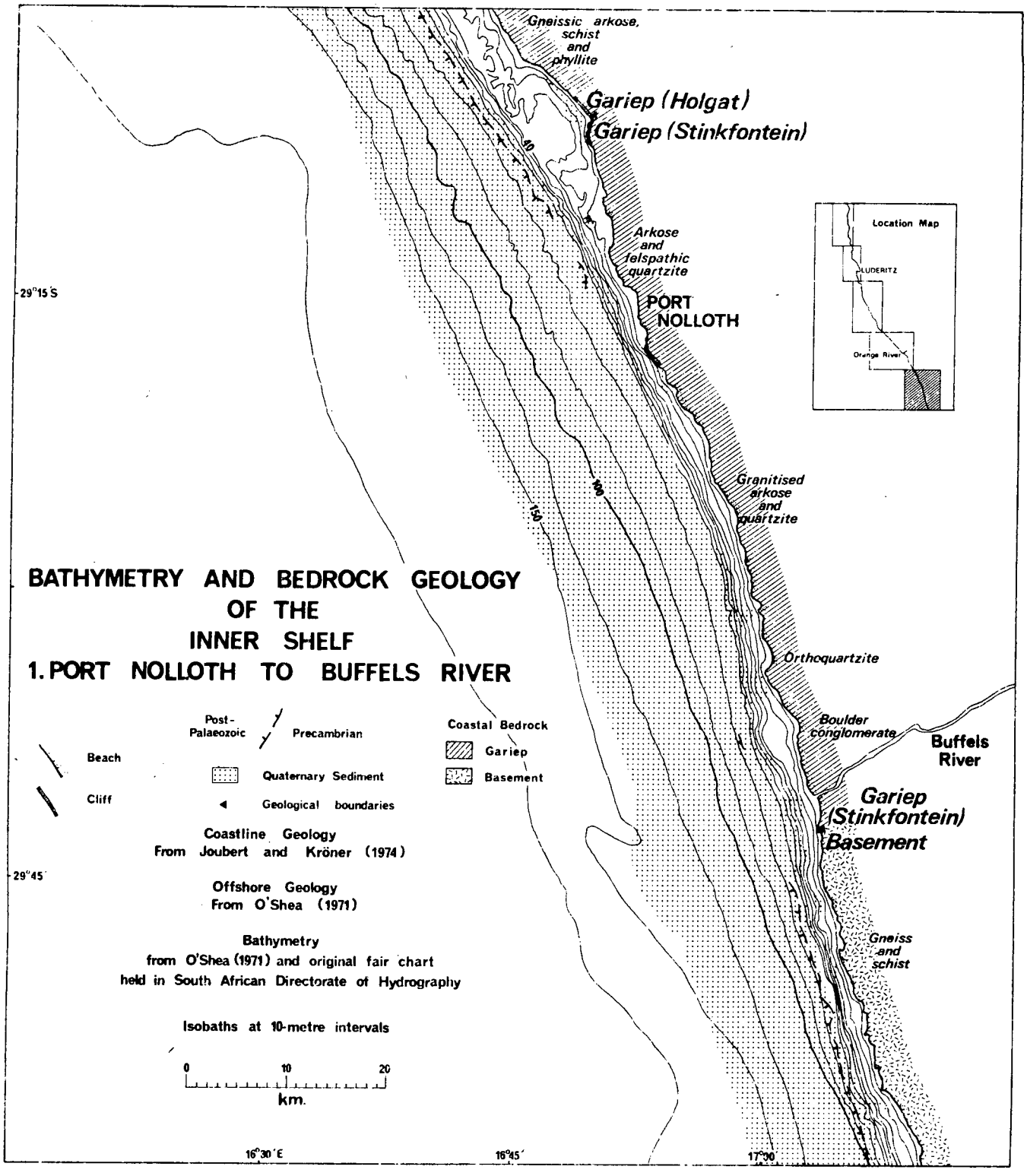
Gneissic arkose, schist and phyllite
Gariep (Holgat)
Gariep (Stinkfontein)
Arkose and felspathic quartzite
PORT NOLLOTH
Granitised arkose and quartzite
Orthoquartzite
Boulder conglomerate
Buffels River
Gariep (Stinkfontein) Basement
Gneiss and schist
Location Map
LUDERITZ
Orange River
29°15'S
29°45'
16°30'E
16°45'
17°00'
BATHYMETRY AND BEDROCK GEOLOGY OF THE INNER SHELF
1. PORT NOLLOTH TO BUFFELS RIVER
Post-Palaeozoic
Precambrian
Beach
Cliff
Quaternary Sediment
Geological boundaries
Coastal Bedrock
Gariep
Basement
Coastline Geology
From Joubert and Kröner (1974)
Offshore Geology
From O'Shea (1971)
Bathymetry
from O'Shea (1971) and original fair chart
held in South African Directorate of Hydrography
Isobaths at 10-metre intervals
0
10
20
km.

Fig.II-18

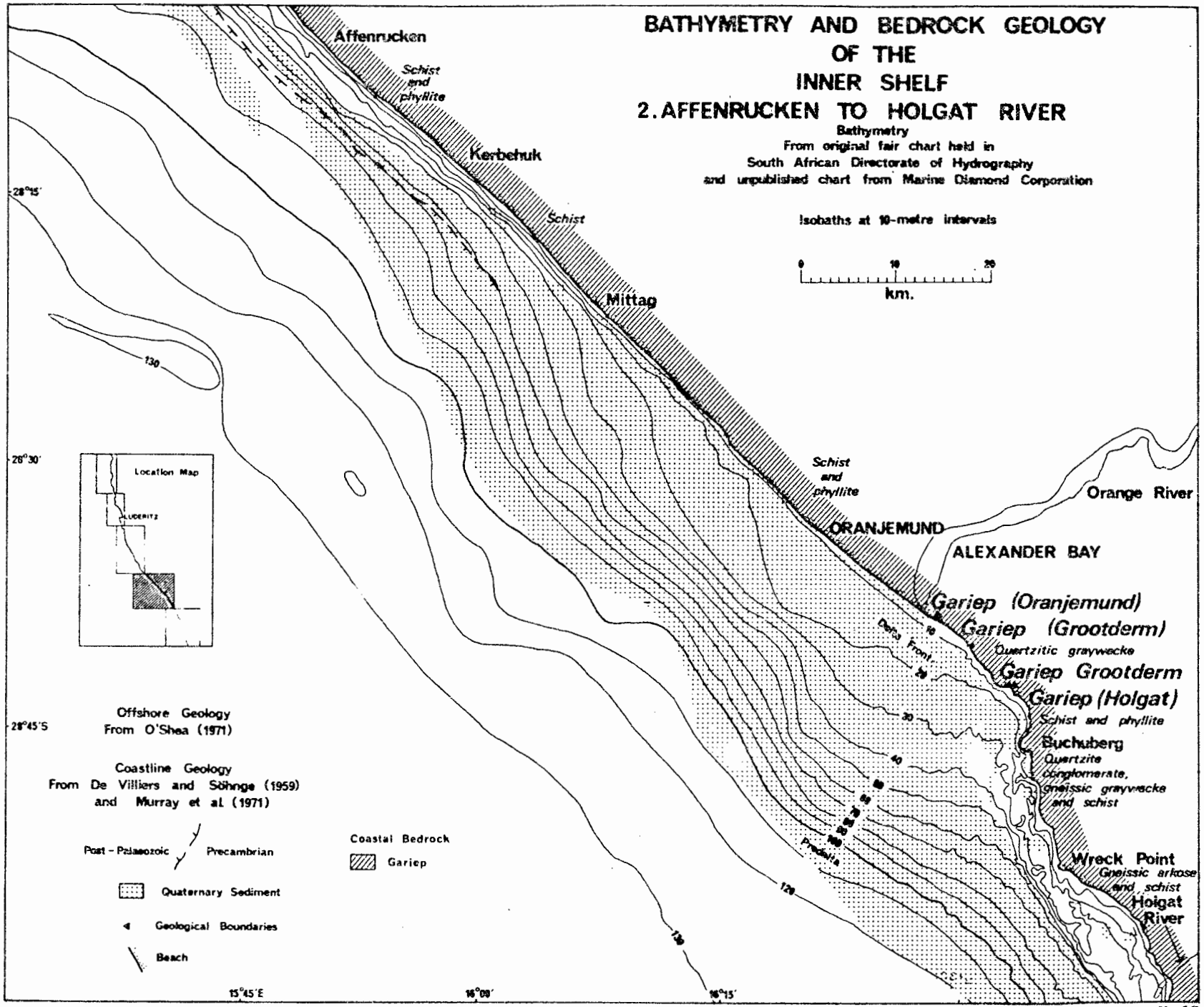
BATHYMETRY AND BEDROCK GEOLOGY
OF THE
INNER SHELF
2. AFFENRUCKEN TO HOLGAT RIVER
Bathymetry
From original fair chart held in
South African Directorate of Hydrography
and unpublished chart from Marine Diamond Corporation
Isobaths at 10-metre intervals
0
10
20
km.
Affenrucken
Schist and phyllite
Kerbehuk
Schist
Mittag
Schist and phyllite
ORANJEMUND
Orange River
ALEXANDER BAY
Gariep (Oranjemund)
Gariep (Grootderm)
Quartzitic greywacke
Gariep Grootderm
Gariep (Holgat)
Schist and phyllite
Buchuberg
Quartzite conglomerate, gneissic greywacke and schist
Wreck Point
Gneissic arkose and schist
Holgat River
Depth Front
Prodelta
130
28°15'
28°30'
28°45'S
15°45'E
16°00'
16°15'
Location Map
LUDERITZ
Offshore Geology
From O'Shea (1971)
Coastline Geology
From De Villiers and Söhnge (1959)
and Murray et al (1971)
Post - Palaeozoic
Precambrian
Quaternary Sediment
Geological Boundaries
Beach
Coastal Bedrock
Gariep

Fig. II-19

Nolloth, then, the narrowness and steepness of the inner shelf is due to resistant granitised quartzite, orthoquartzite, and boulder conglomerate of the Stinkfontein Formation and gneiss, quartzite and schist of the Basement complex.

North of Port Nolloth (Figs. II-18 and II-19) the bathymetric style of the inner shelf alters from a narrow, uniformly steep slope to a wider platform up to 6 km wide, bounded by the northern continuation of the same steep slope below the 40 m isobath. The platform persists northwards to the Orange River where it is buried by the river's Recent delta. The coastline has been cut back by heavy surf action driven by persistent southwesterly swells. Data collected by Marine Diamond Corporation during prospecting operations along the coast are summarised by Murray et al. (1971, p.123): "The coast is exposed to swells generated in the South Atlantic, and throughout the summer, swells with a significant height in excess of 3 m are experienced for about 8 days in the month, increasing to 14 days a month in winter". Any weaknesses in the lithology are etched out by the surf and it will be shown that the rocks north of Port Nolloth are of less resistant lithologies than those to the south.

iii) Port Nolloth to Cliff Point

Between Port Nolloth and Cliff Point ungranitised arkose and feldspathic quartzite of the Stinkfontein Formation are exposed. At Cliff Point the Stinkfontein Formation grades into the Holgat Formation, also of the Gariep Group (Joubert and Kröner, 1971, p.48). The coastline at this point is distinguished by a line of cliffs up to 18 m high, capped by Middle Terrace gravels containing warm-water molluscs (Keyser, 1972, pp.4 and 10) probably of Pleistocene age. The inner shelf widens towards these high cliffs that truncate Pleistocene raised beaches, overlying Precambrian bedrock that is clearly less resistant to surf erosion than the formations south of Port Nolloth.

iv) Cliff Point to the Orange River

The Holgat Formation crops out between Cliff Point and Cape Voltas (Figs. II-18 and II-19) and its variable lithology is reflected in the irregularity of the coastline. The coast was first mapped in detail by De Villiers and Söhnge (1959, pp.56-63) north of latitude 29°S. The geology of the area has recently been reviewed by Kröner (1975, pp.394-398). The Holgat Formation consists of relatively weak schist, phyllite and gneissic arkose between Cliff Point and Wreck Point either side of the mouth of the Holgat River. The inner shelf is consequently widest between these points. North of Wreck Point the Holgat Formation becomes more arenaceous and quartzite becomes dominant at Buchuberg. Softer phyllite and schist between Buchuberg and Cape Voltas have been eroded to form a shallow embayment.

At Cape Voltas the Grootderm Formation succeeds the Holgat Formation (De Villiers and Söhnge, 1959, p.59) and is composed of sheared quartzitic graywacke between Cape Voltas and Alexander Bay (De Villiers and Söhnge, 1959, p.62).

v) Orange River to Chamais Bay

At the Orange River the Grootderm Formation gives way to the Oranjemund Formation (Kröner, 1975, p.398), which continues north along the coast to Chamais Bay.

At the mouth of the Orange and for about 40 km to the north the Precambrian bedrock is buried by the river's Recent delta, which merges with a beach extending continuously along the coast towards Chamais Bay for just over 100 km. The bedrock has been surveyed offshore by seismic profiling and has been exposed onshore by diamond-mining operations.

In the area immediately north of the deltaic sediments (Fig. II-19) the Precambrian bedrock slopes seaward with no equivalent of the flatter platform inshore of the 40 m isobath noted south of the Orange. However it has a shallower gradient than off Namaqualand south of Port Nolloth, chiefly because it is composed of soft, fissile, schist and phyllite of the Oranjemund Formation. Murray et al. (1971, p.130) traced a 2 m-high drowned cliff in this region at the head of a surf-cut gullied platform in a depth of 20 m. The platform is best developed in the Oranjemund Formation, but is confined to softer strata in the Grootderm Formation north of Chamais Bay. Between Bogenfels and Lüderitz no surf-cut platforms were found in the resistant Basement gneiss of that section (Fig. II-20).

A practical result of the Oranjemund Formation's susceptibility to erosion was pointed out by Knetsch (1937, p.202). He correlated high concentrations of diamonds on the southern bank of the Orange with a steep, narrow platform 30-50 m wide, cut by heavy surf action in relatively resistant rocks of the Grootderm Formation. He drew a contrast with lower concentrations on the northern bank deposited on platforms as wide as 600-900 m cut in the less resistant Oranjemund Formation. He argued that the same numbers of diamonds were spread over a wider platform, which absorbed more of the energy of the breakers and thus weakened the concentration process.

The remarkably straight coastline between the mouth of the Orange River and Chamais Bay has an average orientation of 315°. This is related to fracture zones accompanied by heavy jointing reported by Murray et al. (1971, p.130) and by Kröner (1975, p.424) to have orientations between 320 and 340°. Kröner ascribes the structures to deformation at the close of the Pan-African Orogeny in Late Precambrian to Early Pleistocene times. The relative weakness and homogeneity of the Oranjemund Formation also played important roles in the straightness of the coastline.

vi) Chamais Bay to Bogenfels

The complex geology of the region between Chamais Bay (27°55'S) and Bogenfels (27°30'S) (Fig. II-20) is being studied by Kröner (1975, personal communication). He has found a highly deformed sequence in which the dominant Grootderm

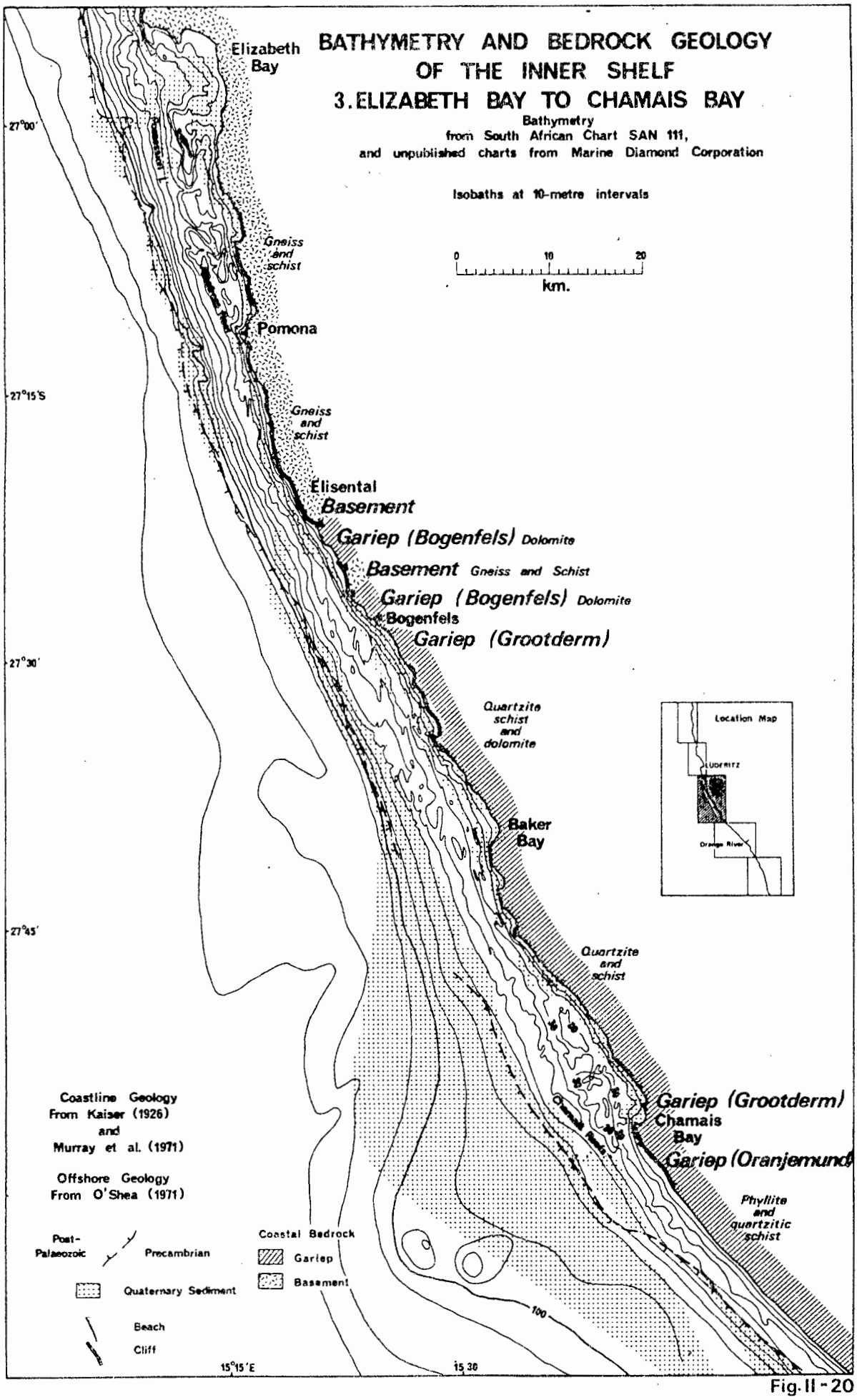
BATHYMETRY AND BEDROCK GEOLOGY
OF THE INNER SHELF
3. ELIZABETH BAY TO CHAMAIS BAY
Bathymetry
from South African Chart SAN 111,
and unpublished charts from Marine Diamond Corporation
Isobaths at 10-metre intervals
0
10
20
km.
Elizabeth Bay
27°00'
Gneiss and schist
Pomona
27°15'S
Gneiss and schist
Elisental
Basement
Gariep (Bogenfels) Dolomite
Basement Gneiss and Schist
Gariep (Bogenfels) Dolomite
Bogenfels
Gariep (Grootderm)
27°30'
Quartzite schist and dolomite
Location Map
Baker Bay
27°45'
Quartzite and schist
Gariep (Grootderm)
Chamais Bay
Gariep (Oranjemund)
Phyllite and quartzitic schist
Coastline Geology
From Kaiser (1926)
and
Murray et al. (1971)
Offshore Geology
From O'Shea (1971)
Post-Palaeozoic
Precambrian
Quaternary Sediment
Beach
Cliff
Coastal Bedrock
Gariep
Basement
100
15°15'E
15 30

Fig. II - 20

lavas have been intruded by a suite of mafic gabbroic bodies (Kröner, 1975, pp. 399 and 402). In general the area is now characterised by north-south striking softer schist and resistant massive quartzite. "These have been differentially weathered by sheet flood erosion and wind deflation, resulting on land in a north-south ridge and valley topography which continues out to sea where there are subdued submarine ridges, islands, exposed rocks and also numerous rocky headlands with north-facing bays." (Murray et al., 1971, p.128). The most important submarine ridges are the Chamais Reefs (Fig. II-20). Whereas the coastline between Chamais Bay and the Orange River is directly related to the structure of the Oranjemund Formation, Beetz and Kaiser (1926, p.142) point out that north of Chamais Bay the trend of the coastline (330°), is oblique to the north-south strike of the rocks. The morphological consequence of this obliquity is the formation of a series of log-spiral beaches in small bays cut in soft schist between headlands of resistant quartzite. The significance of these bays in the dispersal of coastal sediments will be discussed in Chapter VII.

vii) Bogenfels to Elisental

North of Bogenfels, itself a 55 m-high arch cut through a fold of eastward-dipping massive dolomite, a series of cliffs is cut in resistant massive dolomite of the Bogenfels Formation (Martin, 1965, p.80; Kaiser, 1926). The lithological change to dolomite is expressed on the inner shelf by a steepening and narrowing of the inner shelf and the disappearance of the irregular platform best developed off Chamais Bay. The Bogenfels headland appears to continue seaward due south, cutting obliquely across the inner shelf (Fig. II-20). The dolomite gives way not far north of Bogenfels to a narrow strip of Basement gneiss forming cliffs, south of a bay cut in dolomite and leading to a narrow valley called Elisental (27°25-S) (Fig. II-20).

viii) Elisental to Hottentot Bay

Between Elisental and Hottentot Bay (26°10'S) (Figs. II-20 and II-21) the inner shelf consists of Basement gneiss, granite and schist flanked to the west by reworked Basement in the form of highly micaceous quartzitic schists grading into pseudo-boulder conglomerates in places (Kröner and Jackson, 1974, pp.91-92). A steep cliff up to 50 km long, characterises the coast between Elisental and Prinzenbucht (27°05'S), south of the Namib Sand Sea. The coastal hinterland was named the "Wannen" or Trough Namib by Kaiser (1926, p.33). It was formed by powerful aeolian erosion of north-south striking schist within the more resistant gneiss. Stocken (1962, p.6) describes the region as follows: "Reaching a maximum width of about 12 miles (20 km), the Trough Namib presents a marked ridge and valley topography with a relief of some hundreds of feet. Strongly controlled by underlying rock type and structure the Trough Namib presents a series of roughly parallel north-south trending closed valleys or basins following more or less closely upon

BATHYMETRY AND BEDROCK GEOLOGY OF THE INNER SHELF 4. HOTTENTOT BAY TO LÜDERITZ

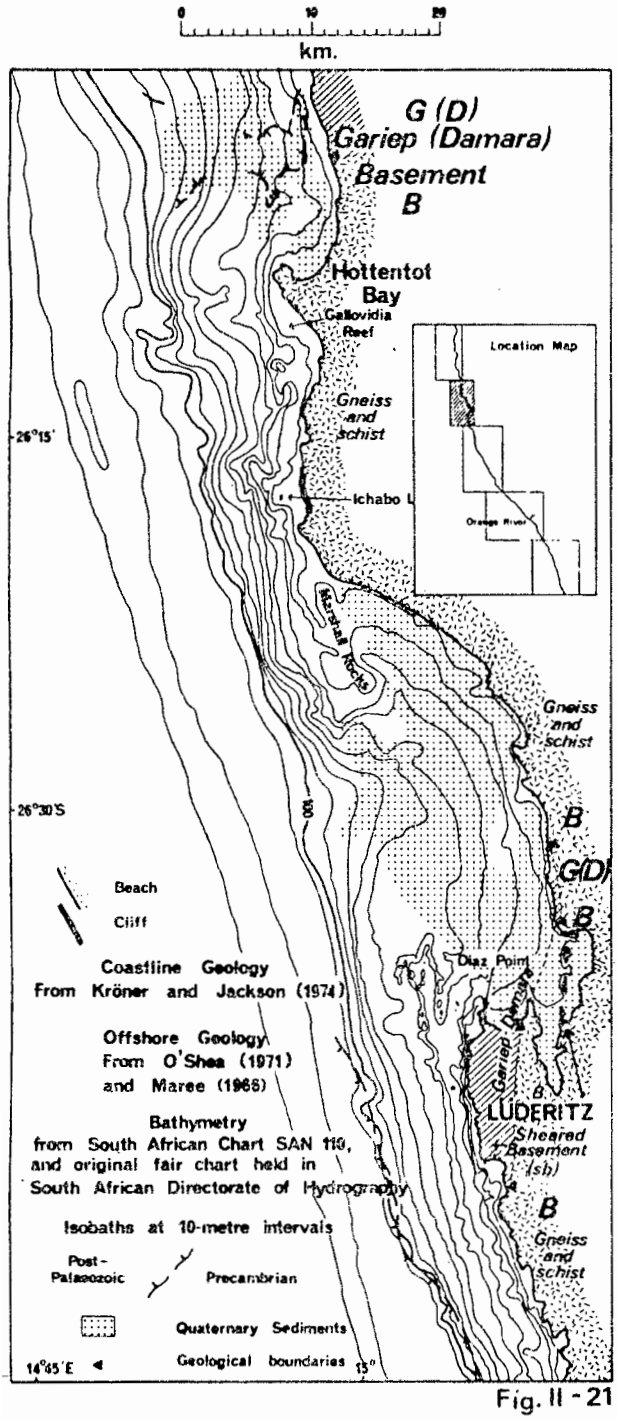

Fig. II - 21

BATHYMETRY AND BEDROCK GEOLOGY OF THE INNER SHELF 5. SYLVIA HILL TO SADDLE HILL

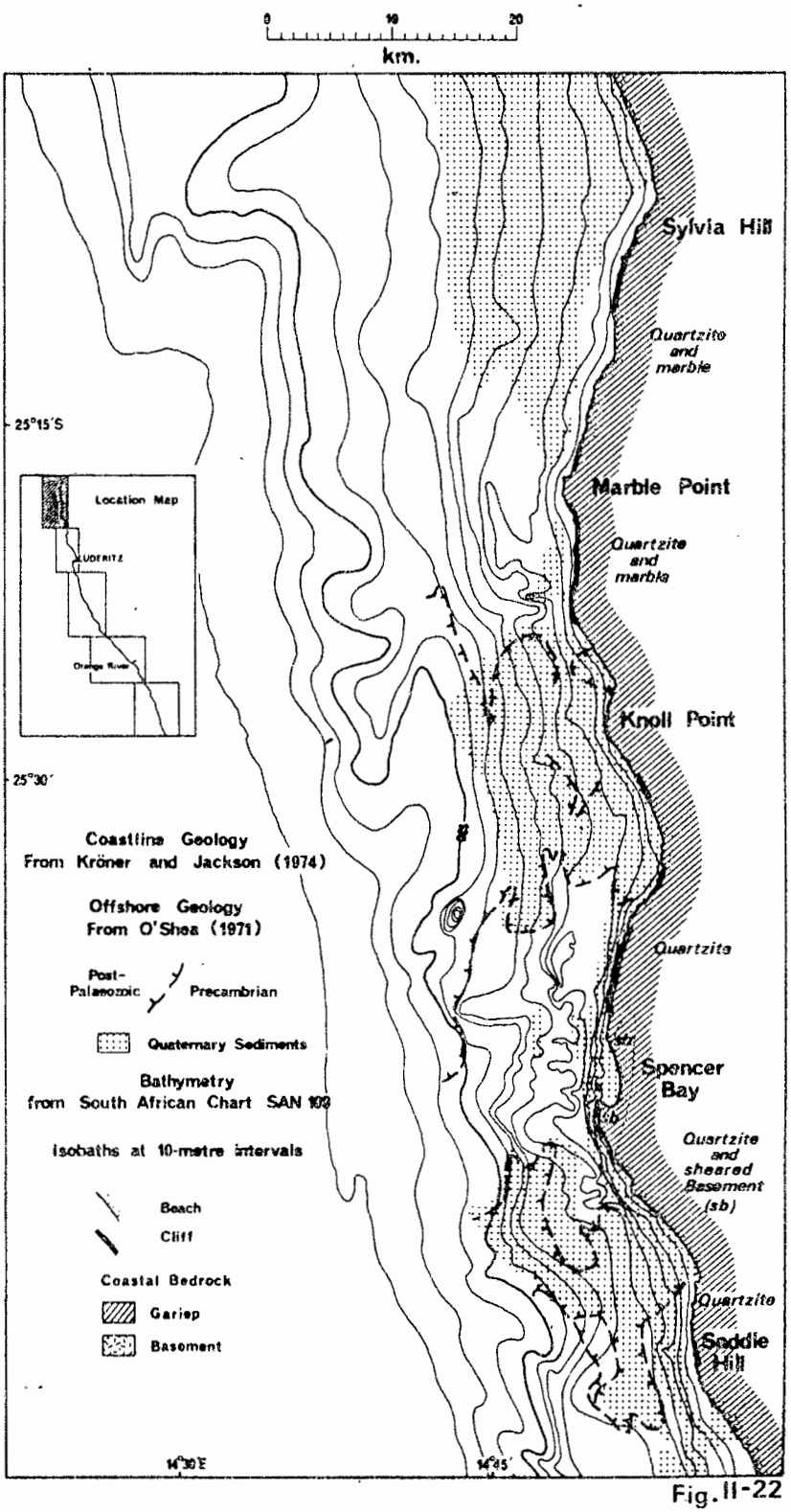

Fig. II-22

synclinal structures. Individual troughs vary greatly in size but the larger ones such as the Idatal may be as much as 14,5 kilometres long, 1,25 kilometres wide and 125 m deep". This distinctive topography is reflected offshore in a series of north-south striking ridges and islands on the inner shelf (Figs. II-20 and II-21). Three of the islands are now joined to the coast by salt pans on their lee sides; one lies north of Prinzenbucht, 3 km from Possession Island, which, with its submerged reef is 10 km long. Two other former islands mark the western edge of a 25 km long salt pan south of Hottentot Bay. Their submerged southerly extensions are named Gallovidia Reef and Marshall Rocks (Fig. II-21). A series of islands belonging to the Republic of South Africa and providing a rich source of bird guano (Watson, 1930) includes Pomona Island, Halifax Island near Diaz Point, Shark, Penguin, Seal and Flamingo Islands just north of Lüderitz and Ichabo Island south of Hottentot Bay (see Figs. II-20 and II-21).

The islands mark the crests of ridges in a drowned portion of the Trough Namib. A drowned trough is represented by the valley to the north of Elizabeth Bay. It is partially filled with Tertiary sandstones (Greenman, 1969), whose aeolian deflation caused the concentration of diamonds (Merensky, 1909, p.19).

The embayment north of Diaz Point and Lüderitz is the largest in the study area and provides the sole harbour north of the Orange River. The inner shelf is over 15 km wide and was cut back into schistose reworked Basement (Fig. II-21) (Kröner and Jackson, 1974, p.92). The preservation of its drowned aspect, namely the highly irregular coastline and the unattached islands, is due to diversion of the coastal sediment-dispersal system inland from Elizabeth Bay past Lüderitz to reach the coast north of the cluster of guano islands.

ix) Hottentot Bay to Sylvia Hill

North of Hottentot Bay, as previously mentioned, the Precambrian outcrop loses its steeper westward slope (Fig. II-22). The Basement rocks at the coast are overlain by Late Precambrian metasediments correlated recently with the Gariep and Damara Groups (Kröner and Jackson, 1974). Seaward-dipping quartzite of the Spencer Bay Formation crops out in a series of cliff-girt headlands separated from one another by sand cliffs up to 150 m high and undercut by the surf. At Marble Point and Sylvia Hill the quartzite is intercalated with marble of the Marble Point Formation. The Spencer Bay Formation resembles the Stinkfontein Formation and the Marble Point Formation is similar to the Bogenfels Formation according to Kröner and Jackson (1974, pp.94-95). North of Marble Point, the NNW structural trend of the Gariep, which roughly parallels the coastline, changes to NE indicating a correlation of the coastal rocks with Damara outcrops towards the inner edge of the Namib Sand Sea (Kröner and Jackson, 1974, p.95.).

In the isolated log-spiral Spencer Bay, selective surf erosion has cut into a zone of schistose reworked Basement caused by eastward overthrusting (Kröner and

Jackson, 1974, p.92) (Fig. II-22).

Like the Precambrian bedrock, the edge of the post-Palaeozoic outcrop is distinctive north of Hottentot Bay (O'Shea, 1971). Instead of lying near the 110 m isobath the post-Palaeozoic sediments have filled in valleys crossing the inner shelf and leading to indentations in the coast, which are often characterised by zones of reworked Basement (Kröner and Jackson, 1974, p.92) (Fig. II-22).

b. Recent delta and mud lens

Off the Orange River the Precambrian bedrock is buried by the river's aerofoil-shaped submarine Recent delta (Fig. II-19), which attains a maximum thickness of over 60 m (Hoyt, Oostdam and Smith, 1969, Figs. 3-5). The prodelta has a seaward slope of $0,1^{o}$ (1,8 m/km) and pinches out on the middle shelf at a depth of 120 m. The effect of deltaic sedimentation has been to shift the 120 m isobath some 25 km seawards to a distance of 33 km offshore, whereas the same isobath is only 8 km offshore off Pomona, where the outer edge of the Precambrian bedrock is virtually sediment free.

Deltaic sediment obscures the Precambrian bedrock beside the coast up to 45 km north of the mouth, near Mittag, and pinches out altogether 95 km north of the mouth at Affrenrucken (Hoyt et al., 1969, Figs. 3 and 5; Murray et al., 1971, Fig. 1). The prodelta sediments continue southwards as a mud lens between the 70 and 120 km isobaths, masking the westward limit of the Precambrian bedrock (Figs. II-18 and II-19). The lens extends southwards for 380 km to St. Helena Bay (O'Shea, 1971; Birch and Rogers, 1973) probably receiving minor contributions from the Olifants and Berg Rivers en route.

c. Pleistocene delta of the Orange River

Although this feature is located on the middle shelf it is preferable to discuss it along with its better-defined Recent analogue. West of the Orange River mouth several traverses cross a delta-like feature (Figs. II-6 and II-23). The gradient steepens at about 150 km and flattens again at about 170 km. The surface samples inshore of 150 m contain substantial amounts of very fine quartz, the sediment type characteristic of the Recent delta front. Seaward of 170 m only minor amounts of very fine quartz sand were observed. In order to correlate these facts it is instructive to compare the middle-shelf delta with the Recent delta at the mouth of the Orange.

The low gradient of the Holocene delta front steepens at about 50 m and then flattens again onto the middle shelf at 110-120 m (Fig. II-22). Taking the outer depth of the drowned delta front (150 m) as analogous to the same feature on the Recent delta front (50 m) the delta on the middle shelf is covered by 100 m more water than when it was formed, presumably during the last Pleistocene glacial. The 20 m difference in depth between the crest and the base of the drowned delta

BATHYMETRIC PROFILES OF THE HOLOCENE AND PLEISTOCENE DELTAS OF THE ORANGE RIVER

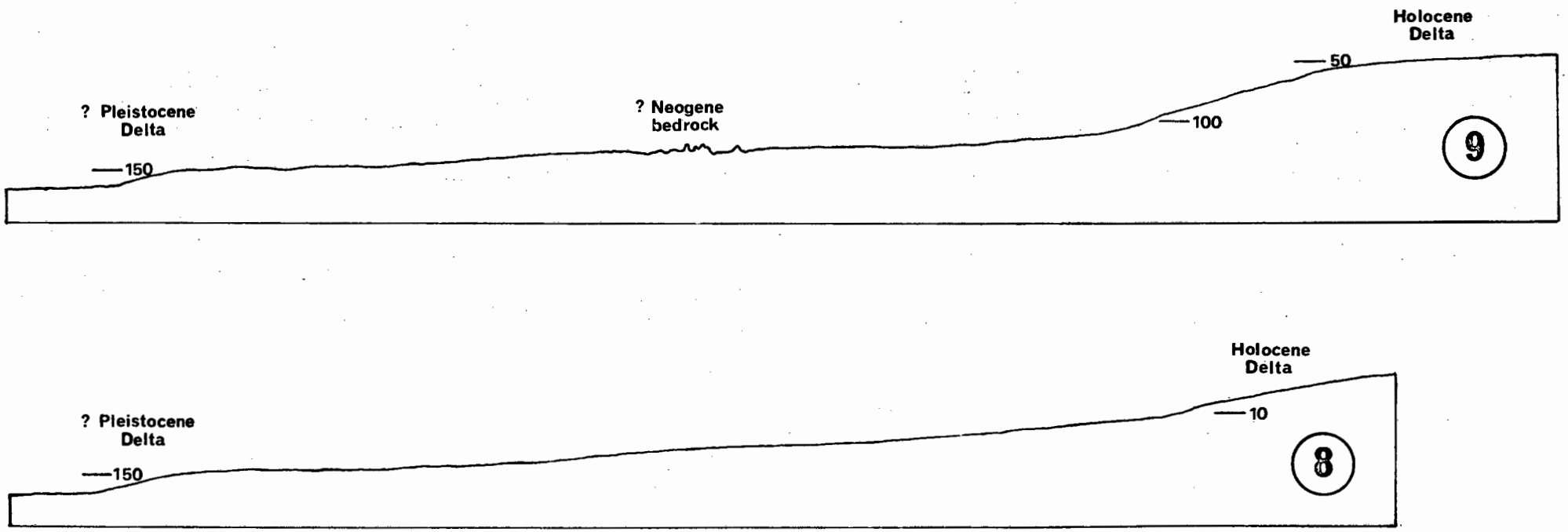

Locations Figure II-2

Vertical Exaggeration x 48

Fig.II-23

contrasts with the 70 m difference of the Recent delta. This is attributed to deposition onto a shallow shelf in the Pleistocene, compared with deposition onto a deep, drowned shelf in the Holocene. Study of a suite of vibrocores from the mouth of the Orange to the foot of the drowned delta is warranted to verify the above conclusions.

d. Recent nearshore sand prism

The nearshore zone of littoral drift along the coast of Namaqualand is starved of sediment because its dune-covered arid hinterland readily absorbs the scanty runoff (Figs. II-18 and II-19). The Holgat River, for instance, last flowed in 1925 (Keyser, 1972, p.4). However, had the exotic Orange River never reached the West Coast, the nearshore zone of South West Africa would have been as sediment-starved as that of Namaqualand.

There is a practically continuous nearshore sand prism between the Orange River and Elizabeth Bay. Because the sand bypasses Lüderitz, the nearshore zone between Elizabeth Bay and Diaz Point is in fact as sediment-starved as the coast of Namaqualand.

A rock zone lies between Diaz Point and Marshall Rocks (Fig. II-21) inshore of which is an extensive sand prism (Maree, 1966, p.153). The sand is derived from surf erosion of the Namib Sand Sea where its western edge coincides with the coast (Fig. II-21). This process is increasingly important north of Hottentot Bay, and especially beyond Sylvia Hill, where the first "Lange Wand" or dune wall provides so much sand that the irregular topography of the Precambrian bedrock is completely blanketed (Fig. II-22).

CHAPTER III

CONSOLIDATED POST-PALAEOZOIC ROCKS

A. INTRODUCTION

The geological history of the study area has been interpreted by several authors (Du Plessis et al., 1972; Dingle, 1973a; Dingle and Scrutton, 1974; Scrutton and Dingle, 1975; Emery et al., 1975), who used a combination of seismic and bathymetric profiles. To date no record of the petrology of the outcropping strata has appeared. In this chapter the results of a preliminary petrographic study of 91 rock samples from 47 locations is reported (Figs. III-1 and III-2; Table III-1). The rocks have been divided into seven main groups; terrigenous sandstones and mudstones, quartzose limestones, lime mudstones, foraminiferal limestones, algal limestones, phosphorites and molluscan limestones as well as into 21 sub-groups. The area therefore displays a great variety of sedimentary rock-types and would repay detailed sampling in certain areas to clarify stratigraphical relationships.

TABLE III-1. LITHOFACIES OF CONSOLIDATED ROCKS

Lithofacies	Age	Stations
Molluscan limestones	?Pliocene	5
Phosphorites	?Late Miocene to Pliocene	6
Algal limestones	Early to Middle Miocene	5
Foraminiferal limestones	Early to Middle Miocene	4
Lime mudstones	?Palaeocene to Eocene	7
Quartzose limestones	?Palaeocene to Eocene	20
Terrigenous sandstones and mudstones	?Late Cretaceous	13
Schists and gneisses	Precambrian	13

B. CLASSIFICATION

1. Terrigenous sandstones and mudstones

The classification devised by Folk (1968, p.123) was selected to describe the terrigenous sandstones and mudstones from the study area (Fig. III-2). The system is modified from earlier classifications devised by Folk (1954) and by McBride (1963) amongst others. Each rock description has three parts: grain-size, textural maturity and mineral composition. The rock's grain size is determined using grain-size triangles depicted in Folk (1954, Figs. 1a and 1b). Textural maturity is determined by the abundance of clay matrix and the degree of rounding of the grains (Folk, 1954, p.344). The mineral composition of the rock is found using Folk's (1968, p.124) triangle

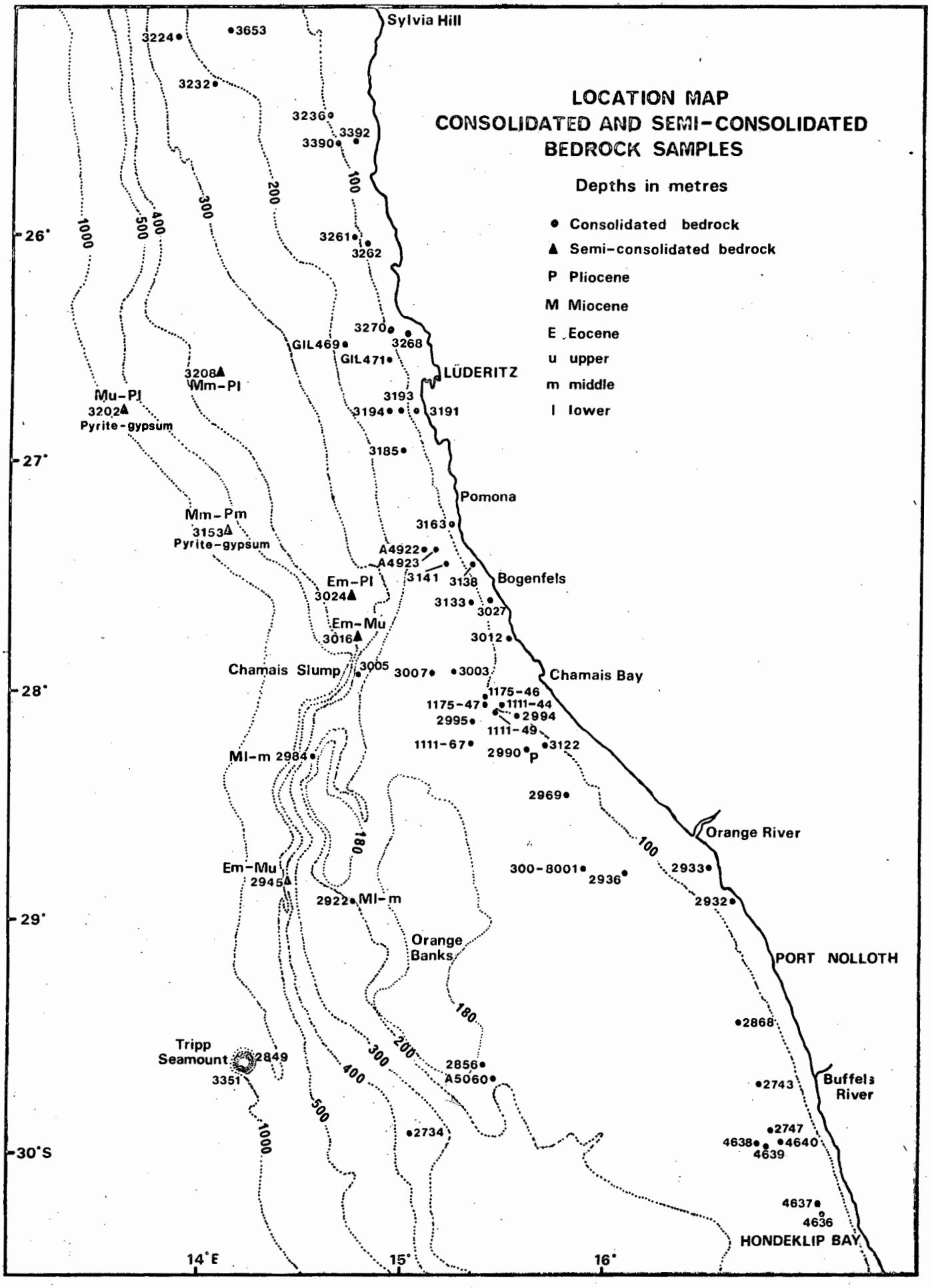
LOCATION MAP
CONSOLIDATED AND SEMI-CONSOLIDATED
BEDROCK SAMPLES
Depths in metres
● Consolidated bedrock
▲ Semi-consolidated bedrock
P Pliocene
M Miocene
E Eocene
u upper
m middle
l lower
Sylvia Hill
LÜDERITZ
Pomona
Bogenfels
Chamais Bay
Orange River
PORT NOLLOTH
Buffels River
HONDEKLIP BAY
Orange Banks
Tripp Seamount
Chamais Slump
Mu-Pl
Mm-Pl
Mm-Pm
Em-Pl
Em-Mu
Ml-m
Pyrite-gypsum
26°
27°
28°
29°
30°S
14°E
15°
16°

Fig.III-1

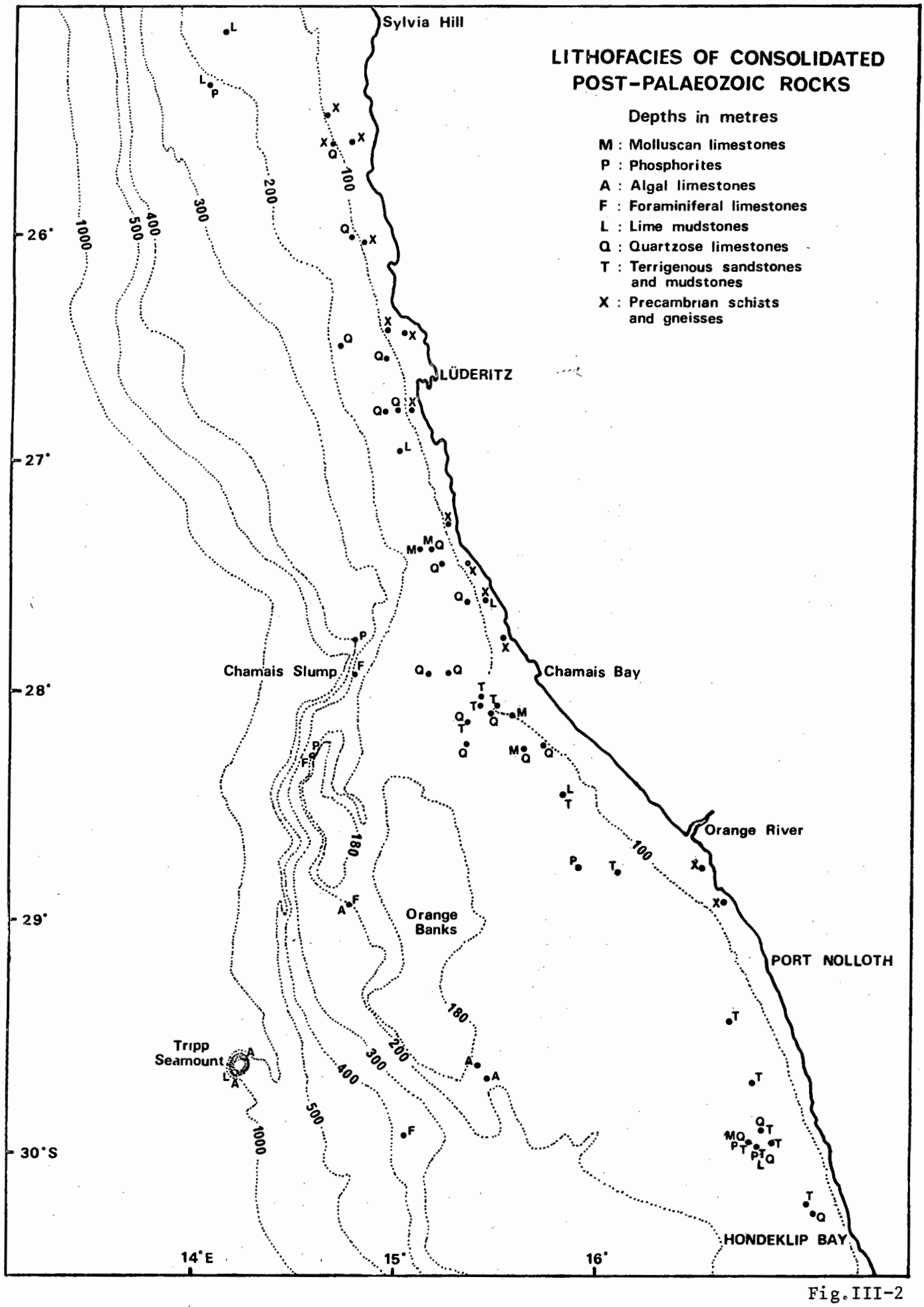
LITHOFACIES OF CONSOLIDATED POST-PALAEOZOIC ROCKS
Depths in metres
M : Molluscan limestones
P : Phosphorites
A : Algal limestones
F : Foraminiferal limestones
L : Lime mudstones
Q : Quartzose limestones
T : Terrigenous sandstones and mudstones
X : Precambrian schists and gneisses
Sylvia Hill
LÜDERITZ
Chamais Slump
Chamais Bay
Orange River
Orange Banks
PORT NOLLOTH
Tripp Seamount
HONDEKLIP BAY
26°
27°
28°
29°
30°S
14°E
15°
16°
100
200
300
400
500
1000
180

Fig.III-2

in which quartz and metaquartzite constitute the Q-pole and all other rock fragments constitute the RF-pole. Clay matrix, mica, cements, glauconite, heavy minerals, and biogenic grains are ignored. Following McBride (1963), Folk substituted "quartzarenite" for "orthoquartzite" to describe rocks containing more than 95% quartz plus metaquartzite. Blatt, Middleton and Murray (1972, p.316) decried the rejection of the term "orthoquartzite" and recommended that it be retained. This appears logical because the composition of the rock can be based on the composition of not only sand-size but also of silt-size grains (Folk, 1968, p.142). In other words one can speak of both an orthoquartzite sandstone and of an orthoquartzite siltstone. The writer follows Folk's (1968, p.125) suggestion that where an identifiable rock fragment is dominant over other rock fragments the term "litharenite" should be replaced by terms like "chert-arenite" or "sedarenite".

2. Limestones and phosphorites

The classification system devised by Dunham (1962) has been applied successfully to limestones and their phosphatized counterparts both on the Agulhas Bank (Siesser, 1972a; Parker and Siesser, 1972; Parker, 1975) and on the shelf off the southwestern Cape (Birch, 1975). In order to be consistent, Dunham's classification has been applied to rocks from the study area. Lithofacies identical to those found elsewhere on the South African continental margin have been identified in this way.

The Dunham classification was originally designed to classify limestones. According to this scheme, limestones containing less than 10% grains set in a lime mud matrix are termed "lime mudstones"; those containing more than 10% grains are termed "lime wackestones" or "lime packstones". In a "lime wackestone" the grains are supported by the matrix, whereas in a "lime packstone" the grains support one another. In the present study, Dunham's scheme is extended to phosphorites, which contain more than 50% apatite (18% P_2O_5) according to the definition of Bushinsky (1966, in Parker, 1975). In such rocks the term "phosphate" is substituted for the term "lime". Thus a standardized description such as "glauconitic calclithic phosphate packstone" (Sample 2984B) can be substituted for "glauco-conglomeratic phosphorite" (Parker, 1975) when describing the abundant conglomerates from the Agulhas Bank and elsewhere.

Addition of a grain-size modifier allows greater precision in description (Folk, 1959, p.15; Siesser, 1971, p.67). The limestone terms "calcirudite", "calcarenite" and "calcilutite" are replaced by new phosphorite terms, namely "phosphorudite", "phospharenite" and "phospholutite". Thus a more

detailed description of conglomeratic phosphorite is "Fine sandy phosphorudite: glauconitic calclithic phosphate packstone". In applying a more "complicated" classification to the complex rock-type, phosphorite, the writer is following principles laid down by Folk (1954, p.346) who wrote "... if a classification is ever to become a precision tool, it must have some degree of 'complication' - ie., a sufficient number of subdivisions to be precise, with consistency in usage insured by a few simple rules".

On the Agulhas Bank the limestones were studied by Siesser (1971) and "phosphorites" by Parker (1971). In a subsequent joint paper Parker and Siesser (1972) referred to "unphosphatized limestones" and "phosphatized limestones" because most of the rocks contained less than 18% P_2O_5. The boundary separating unphosphatized from phosphatized limestones, arbitrarily set at 5% P_2O_5 by Siesser (1971, p.83), has subsequently been applied by Birch(1974, p.17) and will be applied in this study. The term, "phosphatic" is preferred to "phosphatized" because the term is purely descriptive.

3. Component proportions

In order to describe component proportions the following rules were followed:

More than 50%	: Rock name e.g. lime, phosphate.
25-50%	: Major component.
10-25%	: Suffix "-rich" added to component name.
2-10%	: Suffix "-bearing" added to component name.
Less than 2%	: "Trace" added after component name.

The components in excess of 2% are listed from left to right in order of increasing abundance. Trace components are listed after the main sediment name. Thus a ferruginous muddy sandstone (2747A) is described as a "Muddy fine sandstone: immature chert-bearing calcitic and ferruginous chert-arenite. Feldspar and mica traces.". An algal limestone (2849B-4) is described as a "Medium calcarenite: Benthonic and planktonic foraminifer- and bryozoa-bearing coralline algae-rich lime wackestone. Echinoderm traces".

C. LITHOFACIES

1. Terrigenous sandstones and mudstones

a. Location.

A suite of ferruginous terrigenous sandstones and mudstones was dredged from the middle shelf between Hondeklip Bay and Port Nolloth (Fig. III-2). The rocks have been recovered from a relatively narrow depth-range between 130 and 160 m in a belt of irregular topography described in the previous chapter (Fig. II- 5). The inshore edge of the outcrop is blanketed by a lens of Rec-

ent terrigenous mud at the foot of the Precambrian outcrop; seawards the outcrop is covered with foraminiferal sediment. For comparison, a sample of ferruginous conglomerate was obtained from cliffs near The Point just north of the Olifants River.

A suite of non-ferruginous terrigenous sandstones and mudstones is located on the middle shelf between Port Nolloth and Chamais Bay; most samples lie north of the Orange River in a region noted in the previous chapter for irregular topography (Fig. II- 5). The depth range is 90-130 m. The outcrops lie seaward of the Precambrian outcrop and the Recent delta, as well as north of the Pleistocene delta of the Orange River.

b. Petrography.

The ferruginous rocks range in hue from 10R through 5YR to 10YR. Moderate reddish brown (10R4/6) and dark yellowish brown (10YR4/2) are the commonest colours. In contrast with the reddish-brown hues of the ferruginous rocks, the non-ferruginous rocks are generally gray (N7), yellowish gray (5Y8/2) or yellowish brown (10YR5/4).

The ferruginous rocks are classified into three main subgroups: ferruginous muddy sandstones, phosphatic ferruginous muddy sandstones and ferruginous mudstones. The first two groups are separated from one another by a boundary of 5% P_2O_5, and both are considerably coarser-grained than the ferruginous mudstones. All the offshore samples contain substantial amounts of ferruginous matrix and are therefore texturally immature. The grains of the muddy sandstones are commonly poorly sorted and range from angular very fine sand grains to rounded fine pebbles. The presence of chert grains as the dominant rock fragment in some samples has led to several samples being classified as chert arenites, and only one of the muddy sandstones is not a litharenite or sublitharenite. Jasper, agate and chalcedony grains are rarer but nevertheless characteristic components of these rocks. One sample contained bryozoan fragments but otherwise the suite is devoid of biogenic grains. Coarse weathered feldspar grains are a distinctive feature of some samples (Plate III-1a).

The ferruginous mudstones are classified as immature, micaceous, orthoquartzite mudstones in Folk's (1968, p.152) classification, whereas in his earlier classification (Folk, 1954), which included mica, the same rocks are classified as graywackes. Laminae and flame structures are observed, the laminae being marked by angular quartz silt and by mica flakes.

Three subgroups are recognized in the non-ferruginous suite; sandy mudstones, sandstones and micaceous mudstones. The sandstones are unusual in being texturally mature, whereas all other rocks described in this chapter are

Plate III-1. Petrography of post-Palaeozoic rocks

III-1a. Slightly altered feldspar grain in immature ferruginous quartzose chert-arenite from the middle shelf (138 m) off the Buffels River. Note poor degree of sorting and wide range in angularity in this rapidly deposited ?fluviatile muddy fine sandstone. (Sample 2747B4).(X20).

III-1b. Vein of phosphorite penetrating immature ferruginous chert-arentie. (Sample 2747B5).(X20).

III-1c. Cavity in immature, ferruginous very fine sandy claystone filled with glauconitic phosphorite. (Sample 2747B3).(X20).

III-1d. Mould of molluscan shell in quartzose lime wackestone from the middle shelf (108 m), south of Chamais Bay. Texturally the rock is a very fine calcarenite. Note benthonic foraminifer to right of photomicrograph. (Sample 3122).(X20).

III-1e. Sections of large benthonic foraminifera in phosphatic nummulitic lime packstone from the Orange Banks (190 m). (Sample 2922).(X20).

III-1f. Phosphatized foraminiferal infillings in planktonic foraminiferal lime wackestone from the outer shelf (312 m) south-east of Tripp Seamount. (Sample 2734).(X20).

III-1g. Glauconite grains in glauconitic calclithic phosphate packstone from the Orange shelf break (250 m) south west of Chamais Bay. Birch (1975) found that the lighter centres were an admixture of carbonate-apatite and glauconite and that the proportion of glauconite increased towards the darker rims. (Sample 2984B). (X70).

III-1h. Fish vertebrae in a phosphate mudstone, tentatively identified as a coprolite, from the outer shelf (215 m) west of Sylvia Hill. (Sample 3224). (X70).

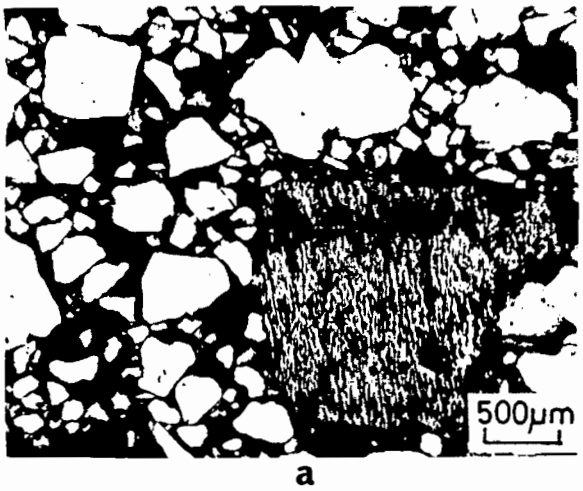

a

b

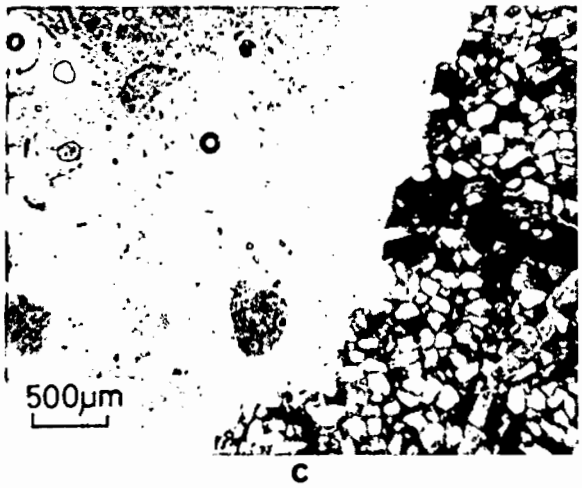

c

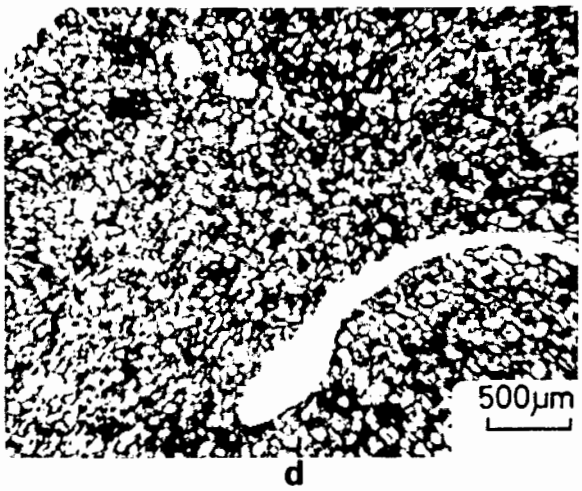

d

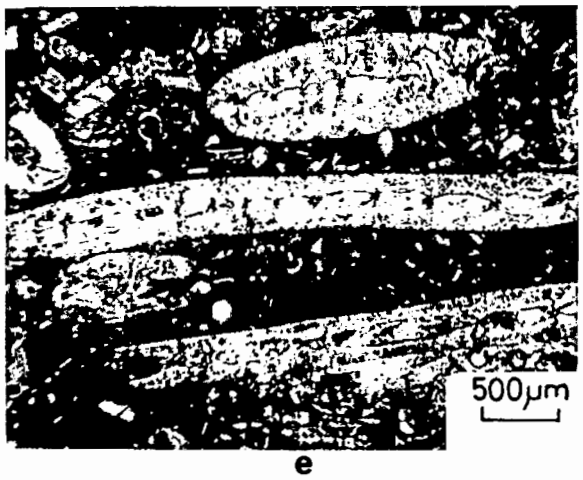

e

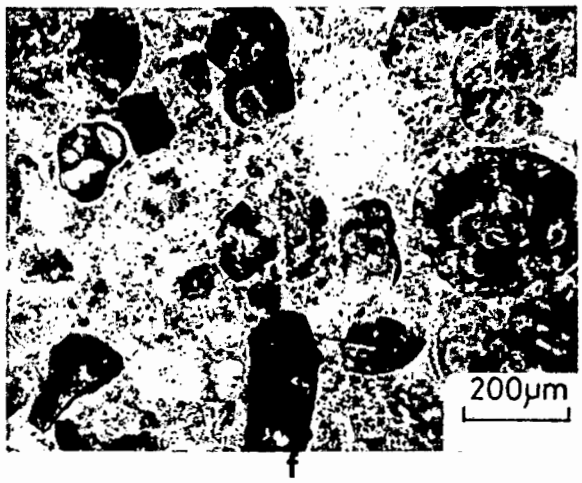

f

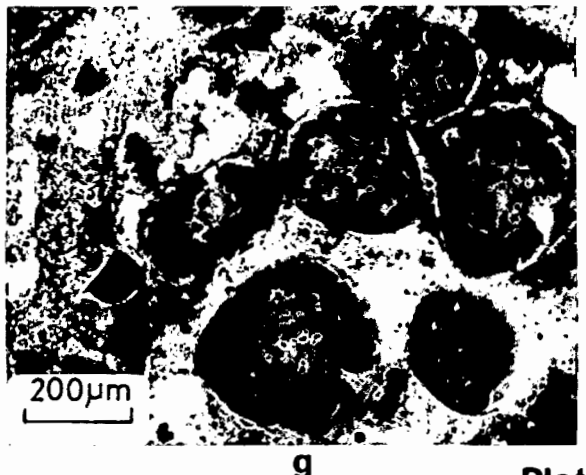

g

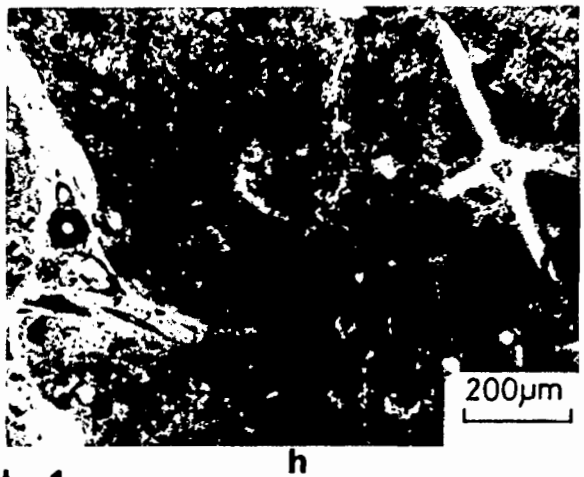

h

Plate III - 1

texturally immature.

The sandy mudstones contain angular fine to very fine quartz grains set in a terrigenous matrix. Sparry calcite is present in some samples and veins one sample extensively. Feldspar is a minor component in some samples and fragments of a porphyritic volcanic rock were noted in sample 2995C. This sample lies several kilometres east of sample 1111-49 (Fig. III-1), which is a quartzose lime wackestone containing similar rock fragments The rocks are classified either as arkoses or litharenites.

The micaceous mudstones occur at two locations and are both silty claystones; they are classified as orthoquartzites or as graywackes in the same manner as the ferruginous mudstones. Angular quartz silt and mica flakes are set in a terrigenous matrix.

The mature sandstones may well be aliens from the Orange River, but as many of the other dredged samples have not actually been physically broken from the outcrop and yet are undoubtedly of marine origin, rounded phosphorite cobbles for instance, they are included for completeness. The rocks are characterized by their quartzitic appearance in hand specimen, gray colour and low matrix content. Angular to subrounded medium to very fine quartz grains are predominant. The varying amounts of fresh microcline and plagioclase feldspar and of chert classify the rocks as orthoquartzites and subarkoses. Traces of micaceous matrix are found in two samples, whereas up to 20% sparry calcite cement, often concentrically banded, characterizes sample 1175-47.

c. Provenance.

The Orange River catchment is a likely source area for the ferruginous suite of rocks. Distinctive pebbles of jasper are to this day characteristic of the Orange River gravels. Hallam (1964, p.705) considers the Griquatown Series in the Prieska area to be the prime source of such pebbles. Reuning (1931, p.213) mentions rare typical Orange River boulders in the Olifants River conglomerate. An important alternative source for the chalcedony and agate grains is the silicified land surface underlying the Pomona beds (Kaiser, 1926). The presence of ferruginous friable mudstones of Karoo age (Burgersdorp and Elliot Formations) in the modern catchment of the Orange will be invoked in Chapter VII to explain the high iron content of modern Orange River clay. It is likely that these same formations were the source of much of the ferruginous material in the suite under study. In fact at this earlier stage of pediplanation it is probable that these formations cropped out more extensively within the catchment than they do today.

From the preliminary data available little can be inferred about the provenance of the non-ferruginous rocks. The distinctive chalcedony, agate and

jasper grains typical of the previous suite were not observed implying a differing provenance. Rare metamorphic and volcanic rock fragments amongst an abundance of angular and rounded quartz and feldspar grains indicate that both sedimentary and granitic rocks are important in the catchment area, with minor contributions from metamorphic and volcanic sources. The large catchment of the Orange contains extensive outcrops of Karoo sediments and Basement granitic rocks as well as a wealth of both metamorphic and volcanic rocks.

d. Depositional environment.

The immature ferruginous sediments were mostly deposited in a low-energy subaerial environment. The abundance of matrix, the poor degree of sorting and the angularity of many of the grains implies a low-energy environment. The laminated micaceous mudstones were deposited in an even quieter environment. In contrast, the mature iron-cemented conglomerate at The Point was deposited in a relatively high-energy environment.

The reddish-brown hues of these rocks indicate that hematite is the dominant ferruginous mineral, although this has not been confirmed experimentally. Hematite is only stable under oxidizing conditions, which immediately excludes the reducing marine environment (Blatt et al., 1972, p.367). The rare bryozoan grains nevertheless signify that the sea was not far distant. Such marine grains may have been blown off coastal dunes or transported into an estuary from the sea.

The depositional environment of the non-ferruginous rocks was continental because there are no traces of marine biogenic grains. The energy of the depositional regime rises from the mudstones through the muddy sandstones to the sandstones. Without access to field relationships and to sedimentary structures the depositional regime can only be suggested tentatively. Fluviatile environments of varying energy levels are most likely.

e. Age.

A Late Cretaceous age is postulated for the ferruginous rocks. Seismic profiling in the vicinity of the outcrop, immediately seaward of the Precambrian outcrop, has revealed strata dipping at angles of 2-3^{o} seawards (Hoyt, Oostdam, and Smith, 1969, Fig. 4). Dingle (1973a,p.346) suggests an Early Cretaceous age derived from the date of rifting between South America and Southern Africa as 125-130 Ma B.P. (Larson and Ladd, 1973, p.209).

The Pomona beds exposed onshore between the Olifants River (Reuning, 1931) and Pomona (Kaiser, 1926) are commonly ferruginous. They occur near the coast either as cliffs as at The Point or in the form of mesa cappings dipping seawards near the coast, as at Tafelberg, south of Chamais Bay, and

in the Pomona region itself. The underlying silicified land surface drops from a height of 190 m east of Pomona to 15 m at Jammerbucht on the coast just south of Pomona (Beetz, in Kaiser, 1926, Vol.II, p. 9). The silicified rocks are all Precambrian in age and it has been shown in the previous chapter that the Precambrian outcrop on the inner shelf is only a few kilometres wide near Pomona (Fig. II-20). It is therefore suggested that the continuation of the old land surface crops out along the seaward edge of the Precambrian outcrop offshore. The age of sediment overlying the surface varies from place to place due to erosion and deposition during regressions and transgressions. Thus Dingle (1973, Fig. 7) finds both Cretaceous and Tertiary beds overlying Precambrian bedrock off Lüderitz (Profile 228) but only Cretaceous beds off Bogenfels (Profile 229). It is suggested, on the basis of lithologic similarity, that the ferruginous rocks described in this section may be correlated with the Pomona beds which crop out onshore both north and south of the offshore exposures. A comparative petrographic study of the Pomona beds may help to verify this suggestion.

Having suggested the possibility that the Pomona beds may be onshore correlates of the rocks under study, on broad lithologic grounds, what evidence is there to establish the age of the formations more precisely? The offshore rocks contain no dateable marine fossils and it is unlikely that the oxidizing conditions necessary for the formation and preservation of hematite allowed the preservation of terrigenous palynomorphs. A minimum age for the onshore Pomona beds is available, however. At Swartkop in the Sperrgebiet an outlier of phonolite lava overlies the Pomona beds (Stocken, 1962, p.5). The lava has been dated radiometrically as 37 Ma., i.e. at the Eocene-Oligocene boundary (personal communication from J. de Villiers in Greenman, 1969). The beds therefore have a minimum age of earliest Oligocene. They are unfortunately not in contact with the foyaite intrusion of Granitberg (Stocken, 1962, p. 7) which has an Early Cretaceous age of 130 Ma (Stocken, personal communication in Marsh, 1973). However Beetz (in Kaiser, 1926, Voll.II, p. 9) records that the old silicified land surface rises over Granitberg. Therefore the Pomona beds lying upon that surface have a maximum Early Cretaceous age of 130 Ma. A Late Cretaceous age midway between the Early Cretaceous maximum and the Early Tertiary minimum has already been suggested by Stocken (1962, p. 7). Little additional evidence is available from the Olifants River outcrop, although the Pomona equivalent contains and overlies marine fossils. No age is assigned to the distinctive assemblage of molluscs and fish teeth found there (Reuning, 1931; Haughton, 1931).

There is no information on the age of the non-ferruginous rocks.

f. Diagenesis.

The original matrix in the ferruginous suite offshore probably contained an abundance of iron in the lattices of minerals like montmorillonite, biotite, amphiboles, pyroxenes, ilmenite and magnetite. Walker and Honea (1969, p.329) found that only 0,1% extractable iron was present in one bright-red sample from the Saharan Desert and postulated post-depositional intrastratal alteration of iron-bearing minerals under oxidizing conditions to account for the hematite stain in red beds. It has already been suggested that the hematite may originate in the Elliot Formation (Red Beds) of the Karoo Supergroup, which today are a prime source for Orange River sediment. In the Cretaceous the outcrop of this formation would have been much more extensive than today and may have played a more important role than it does today.

The common occurrence of a later generation of apatite and calcite cement in many of the muddy sandstones is interpreted as evidence that the rocks were subsequently covered by sea water. In several samples yellow apatite cement appears to have replaced parts of the original ferruginous matrix. In addition, sample 2747B-5 is unusual in having ferruginous cement rather than matrix. Pores are filled by light reddish-brown crystals, probably of goethite, which coalesce towards the centre of the pore. Veins, which in places are apatite and in others calcite, penetrate the rock, cutting across the cement and often separating the cement from the grains (Plate III-1b). The later date of the phosphatization episode is best illustrated by infilling of mollusc borings with glauconitic phosphorite (Plate III-1c). The conglomerate from The Point has similar aspects; its dark brown ferruginous cement giving way in places to a yellow, presumably phosphatic, cement (Reuning, 1931, p.208).

Little is known of the diagenetic history of the non-ferruginous rocks, but one of the sandstones was subsequently cemented by sparry calcite.

2. Quartzose limestones and lime mudstones

a. Location.

Quartzose limestones and lime mudstones are found on the middle shelf throughout the study area, although most samples were recovered between the Orange River and Lüderitz (Fig. III-2). The depth range is from 50 m to 200 m.

b. Petrography.

Grayish hues (N5 for example) are characteristic of this petrographically homogeneous and widespread suite of limestones. The rocks have been classified into quartzose lime wackestones, pyritic lime wackestones and lime mudstones and they have been distinguished from their phosphatic equivalents

using a 5% P_2O_5 boundary. The subgroups are described together because they are found interlaminated and form a continuum texturally and compositionally.

Texturally, the limestones range from calcilutites to medium calcarenites; very fine calcarenites dominate the quartzose lime wackestones. The matrix is usually an intermixture of micrite and microspar in varying amounts. In a minority of samples the matrix has been phosphatized or lime mud has recrystallized to pseudospar.

Angular very fine quartz grains are the most common and the most characteristic allochems in this suite of limestones. Finer silt and coarser sand grains occur but very fine quartz sand is by far the most abundant. Fresh angular very fine grains of microcline and plagioclase feldspar are present in minor amounts in some samples. Heavy minerals, chert, jasper and volcanic rock fragments are rare but distinctive components in others. Calcitic pseudomorphs after ?olivine in the form of dipyramidal orthorhombic prisms set in a matrix rich in laths of altered ?feldspar are distinctive components of sample 1111-49. As mentioned earlier, similar rock fragments are found in sample 2995C, a few kilometres to the west.

Silt- and very fine sand-size aggregates of pyrite characterize the pyritic lime wackestone subgroup. In the quartzose lime wackestones, minor amounts of fine sand-size glauconite and trace amounts of coarse phosphorite fragments are distinctive but not ubiquitous authigenic components. Glauconite occurs only as discrete grains and not as infillings.

The biogenic content of the suite is low. Molluscs, bryozoans, echinoderms, cirripeds, benthonic foraminifera, planktonic foraminifera and faecal pellets are present in trace to minor amounts. Moulds of dissolved mollusc shells characterize some samples (Plate III-1d) but several samples contain no biogenic grains at all.

c. Provenance.

The suite contains a variety of terrigenous, marine authigenic and marine biogenic grains set in a lime mud matrix. Both terrigenous and marine sources are therefore required to explain the origin of the grains. The presence of volcanic rock fragments, fresh feldspar, heavy minerals and abundant quartz is compatible with input from an arid hinterland. The fineness and angularity of the quartz grains suggest that Orange River sediment is the source, because the sediment on the river bed, on the delta front and along the coast on the inner shelf is today dominated by similar angular, fine to very fine quartz sand (see Chapter VII).

d. Depositional environment.

The common presence of reworked glauconite and phosphorite grains, as

well as the marine biogenic grains and the occasional mollusc moulds, confirms that the environment of deposition was undoubtedly marine. Quiet-water conditions are implied by the abundance of lime-mud matrix. However the association of very fine quartz sand, randomly distributed and floating in the matrix is anomalous. Such a textural inversion may be explained by bioturbation, and the occurrence of unbroken valves of a molluscan (bivalve) infauna supports this contention. Siesser (1972a,p.86) came to the same conclusion for a similar suite of quartzose limestones on the eastern Agulhas Bank.

Let us consider two possible quiet-water marine environments conducive to the formation of carbonate mud; the deep sea and a lagoon. The abundance of terrigenous components, sometimes quite coarse, and the rarity of planktonic foraminifera favours the nearshore lagoonal environment. In addition if the hinterland were arid, as inferred from the freshness of the feldspars, then evaporation of sea water in lagoons is a distinct probability. The modern analogues of such lagoons are common along the Namib Desert coast, immediately east of the shelf outcrop. Salt pans have formed in these lagoons which are at or near sea level. They are normally cut off from the sea by beach berms, but during spring tides the sea breaks through and replenishes the supply of sea water (Hallam, 1964, p.679). The sediments of the above lagoons have not been investigated mineralogically in order to substantiate the proposed hypothesis for the formation of carbonate mud. However inorganic precipitation of calcium carbonate has been reported from both salinity extremes. Blatt et al. (1972, p.452) reported such precipitation in the supersaline Dead Sea, as well as the freshwater lakes of Minnesota and Wisconsin. It is therefore not unlikely that calcium carbonate could be precipitated in Namib Desert lagoons. Surf-zone abrasion of calcareous material is less likely to be an important source, because the modern beach sediments north of the Orange contain negligible quantities of carbonate (see Chapter VII). This may be due to a combination of dilution by terrigenous material from the Orange and inhibition of shell formation in the cold upwelled coastal waters of the Benguela Current.

e. Age.

Petrographically these quartzose lime wackestones are almost identical to Siesser's (1972a,p.84) "lagoonal-quartzose lime wackestone lithofacies" from the middle shelf between Cape St. Blaize and Cape Seal on the Agulhas Bank, which have been dated as Palaeocene-Eocene on the basis of ostracods from associated marls (Dingle, 1971, p.186). No palaeontological evidence is available to determine the date of the suite under discussion.

f. Diagenesis.

The diagenetic history of this suite of limestones is similar to that described for the Agulhas Bank quartzose lime wackestones (Siesser, 1972a, p.89). Carbonate mud has neomorphosed, often to microspar and occasionally to pseudospar. Unlike the Agulhas Bank suite, where microspar predominates (Siesser, 1972a,p.85), subequal amounts of micrite and microspar are characteristic of the West Coast suite. A further point of difference is that mollusc moulds occur more frequently, implying dissolution of the original metastable aragonite by meteoric waters during subaerial exposure. On the Agulhas Bank the aragonite was neomorphosed to stable, low-Mg calcite in the form of pseudospar (Siesser, 1972a,p.90).

In the pyritic lime wackestone subgroup one has evidence of reducing conditions during diagenesis of carbonate muds to lime mudstone; the absence of pyrite in Agulhas Bank limestones was commented upon by Siesser (1972a, p.88).

A final difference from the Agulhas Bank suite is that the calcitic matrix in a few samples, especially towards the north of the outcrop has been phosphatized to a greater or lesser degree. Sample 3390E, for example, contains 15,8% P_2O_5 and is classified as a phosphatic quartzose lime wackestone.

3. Foraminiferal limestones

a. Location.

Two subgroups of foraminiferal limestones have been identified, one characterized by large benthonic (nummulitic) foraminifera and the other by planktonic foraminifera.

The distinctive and age-diagnostic nummulitic limestones have been recovered from two localities in the study area (Fig. III-2) and from one locality in the area studied by Birch (1974, p.19). The largest sample (2922) (Fig. III-1) comes from a depth of 190 m on the Orange Banks, due west of the Orange River. In addition, a layer less than 1 cm thick was found attached to a sample of glauconitic phosphorite (2984) from the shelf break forming the edge of the Orange Banks, southwest of Chamais Bay in a depth of 250 m.

The more important (sample 2734) of the two samples of planktonic-foraminiferal limestone originates from the outer shelf near the Tripp Seamount, between the two shelf breaks in a depth of 312 m. The second sample (3005), which is tentatively correlated with sample 2734, is from the outer shelf due west of Chamais Bay in a depth of 244 m (Figs. III-1 and III-2).

b. Petrography.

The angular cobble-size fragment of phosphatic nummulitic limestone from station 2922 initially drew attention because of its content of large benthonic foraminifera up to 1 cm in diameter. These are clearly visible in the hand specimen, usually in cross section, but occasionally revealing the detailed spiral ornamentation on the external surface (Plate III-1e).

Sample 2734 consists of poorly consolidated lumps of planktonic-foraminiferal limestone observed within a sample of unconsolidated sediment recovered with a grab at that station. Sample 3005, likewise was found as part of a grab sample of unconsolidated sediment. Sample 2734 is grayish yellow (5Y8/2) and sample 3005 is very pale orange (10YR8/2).

Both samples of nummulitic limestone are classified as calcirudites and as phosphatic nummulitic lime packstones. The designations "rudite" and "nummulitic" are drawn from the pebble-size foraminifera, one species of which has been identified as Nummulites. A value of 13,6% P_2O_5 has been obtained for sample 2922, but no separate value was obtained for the thin nummulitic layer of sample 2984. Collophane is the major matrix component (30%) and predominates over micrite and microspar.

Like the algal limestones the samples are devoid of both terrigenous and authigenic grains. The large benthonic foraminifera are the major biogenic components (50%). Sample 2922 contains minor amounts of planktonic foraminifera and a trace of ostracods. Both samples contain traces of molluscs, bryozoans, echinoderms and coralline algae.

Texturally both samples of planktonic foraminiferal limestone are fine calcarenites; 2734 is a wackestone and 3005 is a packstone. Terrigenous grains are completely absent. Authigenic grains in the form of glauconitic and phosphatic foraminiferal infillings are found in trace amounts in sample 3005, but comprise up to 10% and are characteristic components of sample 2734 (Plate III-1f). In addition, the predominantly micritic matrix is phosphatized along the outer margins of the lumps of sample 2734. The same phosphatization process of pebble margins of planktonic-foraminiferal limestones from the Agulhas Bank has been reported by Parker and Siesser (1972, p.473) and by Siesser (1972a,p.93).

The chief biogenic components are planktonic foraminifera (20-35%) and benthonic foraminifera (5-15%). Both types are usually filled with yellow "apatite" or green "glauconite", the different types often occurring in neighbouring grains. Birch (1975, p.77) has made a detailed microprobe study of similar grains from Childs Bank on the outer shelf just south of the study area. He found that the infillings are intimate mixtures of both glauconite and apatite phases, and that colour is an imprecise criterion of their mineralogy.

c. Depositional environment.

A quiet mid-shelf environment is suggested to account for the presence of micrite matrix and the absence of terrigenous material in the nummulitic limestones. Most of the large benthonic foraminifera are unbroken, as are the thin-walled planktonic foraminifera, where present. The writer therefore postulates a mid-shelf environment too far offshore to receive terrigenous sediment and yet not within the main zone of planktonic foraminiferal sedimentation on the outer shelf and the slope. The environment is quiet enough to allow the deposition of planktonic foraminifera. Without further information on the mineralogy and morphology of the micrite matrix, little can be said concerning its origin. A biogenic origin as coccolith debris is possible, the benthonic foraminfera living at the sediment-water interface as epifauna and being incorporated in the sediment at death.

The abundance of micrite matrix and of planktonic foraminifera and the absence of terrigenous grains clearly indicate an outer shelf-upper slope environment for the planktonic-foraminiferal limestones. The Agulhas Bank analogue is Siesser's (1972a,p.91) "pelagic-foraminiferal lime packstone lithofacies".

d. Age.

Subsamples from both samples of nummulitic limestone were sent to Dr. D.D. Bayliss of Robertson Research International Limited who identified the foraminiferal species in thin section and determined the age of the assemblage. Dr. Bayliss reported as follows:

"Evidence for a Neogene age (Miocene) involves the presence of the following planktonic foraminiferal taxa in the rocks

Orbulina universa d'Orbigny

Orbulina suturalis Bronnimann

Globigerinoides spp.

These have ranges which extend from the base of the Middle Miocene to Recent.

Associated with these planktonics are abundant larger foraminifera including : very abundant Operculina complanata (Defrance) and rare Heterostegina cf. complanata Meneghini.

Species of these genera (Operculina and Heterostegina) occur in present seas, but have been recorded from the Miocene and various parts of West Africa including Angola and Nigeria, e.g. Dartevelle and Roger 1954 (Angola) Operculina benevidea - H. heterostegina, Fayose 1970 (Nigeria) Heterostegina panamaensis.

The genus Sherbornina sp. is also present in one sample (2922) which has a restricted range from Late Eocene to Miocene.

The overlapping ranges of the genera Sherbornina (Late Eocene to Miocene) and the planktonic species Globigerinoides (Early Miocene to Recent) and Orbulina (Middle Miocene to Recent), together with the abundant operculine/heterostegine assemblage generally regarded as of Early Miocene (Aquitanian-Burdigalian) age in the West African area suggest an Early Neogene, Early to Middle Miocene age for these rocks." (Bayliss, personal communication, 1973).

According to the Treatise on Invertebrate Palaeontology (Loeblich and Tappan, 1964, p.C643) the generic name Operculina gives way to Nummulites, hence the group designation "nummulitic limestone".

Dingle (1973a,p.354) assigned an "Upper Upper Tertiary (T4)" label to an outlier of unstructured sediment on the Orange Banks, which he correlated with similar outliers farther south, all "... erosional remnants of a presumably once extensive deposit ...". It now appears that the Orange Banks outlier, at least, is Early to Middle Miocene, and not Pliocene as suggested by Dingle (1973a,p.358) before dates became available. His underlying "Lower Upper Tertiary (T3)" may therefore be Lower Tertiary (probably Eocene) if the unconformity separating "T3" and "T4" beds coincides with an Oligocene regression invoked by Dingle and Scrutton (1974, p.1472) to explain the stratigraphy of the Southern African margin.

Siesser obtained an Early Miocene date for four samples and an Upper Miocene date for three samples of "pelagic foraminiferal lime packstone" on the Agulhas Bank. Sample 2734 was recovered from the outer shelf, morphologically and stratigraphically below the Orange Banks outliers from which the Early to Middle Miocene nummulitic limestones just described were recovered. Although as yet undated, a minimum date for the planktonic-foraminiferal limestones is Middle Miocene. A detailed seismic profile from the area between the two shelf breaks near station 2734 presented by Dingle (1973a,Fig.13) reveals a succession, interpreted as Late Tertiary overlying an irregular erosion surface cut into Early Tertiary sediments. The unconsolidated sediments are thin in this region and the limestones are poorly consolidated so that a series of cores would provide much useful material with which to clarify the stratigraphy on the outer Orange shelf.

e. Diagenesis.

Some of the original lime mud neomorphosed to microspar in the nummulitic limestones, but the chief diagenetic event has been the phosphatization of much of the calcitic, chiefly micrite, matrix to collophane.

Micrite in the planktonic-foraminiferal limestones is assumed to be derived from coccolith debris, because it is associated with abundant planktonic foraminiferal tests. Siesser (1972a,Fig.5, and 1975) detected coccoliths in

in the micrite fraction of his foraminiferal limestones. In Chapter VIII the writer demonstrates the association of coccoliths and planktonic foraminifera in Recent sediments on the outer shelf and the slope of the study area. In the key sample, 2734, micrite is dominant over a small amount of collophane. Microspar is absent as in the Agulhas Bank suite (Siesser, 1972a, p.98) and therefore the same *in situ* submarine lithification process by solution and reprecipitation of calcium carbonate is invoked.

4. Algal limestones

a. Location.

In contrast to the previous rock types, which crop out on the middle shelf, the algal limestones have all been recovered from the Orange Banks on the outer shelf or from the tip of the Tripp Seamount (Fig.III-2). Despite their strikingly different morphological positions, the depth ranges are similar. On the Orange Banks the two samples occur close together in a depth range of 180 to 200 m and the summit of the Tripp Seamount lies mainly between 150 and 170 m. It is difficult to determine the maximum possible depth of the dredged samples when some dredging operations were at times commenced as deep as 800 m, well down the side of the seamount.

A seismic profile across Tripp Seamount appears as Figure 22 in Emery *et al.* (1975, p.30) who wrote: "A seismic profile made across Tripp Seamount ... suggests that this peak is capped by well-stratified sediments probably of carbonate composition and about 0,2 sec thick ...". This suggestion has been proved by dredging of algal limestones, which are described here for the first time.

b. Petrography.

The phosphate content of the Tripp Seamount limestones varies from 0,7 to 8,6% P_2O_5, whereas the Orange Banks limestones contain 14,0 and 18,1% P_2O_5. The last-mentioned sample is, strictly speaking, a phosphorite. It was included because it was on the 18% P_2O_5 boundary separating phosphorites from phosphatic limestones, and because of its petrographic similarity to the rest of the group.

These limestones are difficult to describe because of their heterogeneity, which often prevented a representative thin-section being included within the compass of a standard slide.

Texturally the rocks range from fine calcarenites to calcirudites and phosphorudites. Equal numbers are classified as wackestones and packstones.

The suite is characterized by an absence of both terrigenous and authigenic grains. (A trace of glauconite was noted in the Orange Banks phosphorite).

Coralline algae and bryozoans are important biogenic constituents, often amounting to 50% of the rock. Other biogenic components are benthonic foraminifera, planktonic foraminifera, molluscs and echinoderms. In sample 2849B-4 unusual triangular fossils have been interpreted as benthonic foraminifera sectioned perpendicular to their axes.

The matrix usually contains more micrite than microspar, but some samples contain goethite and pseudospar; others are rich in collophane.

c. Depositional environment.

Siesser (1971, p.58 and Plate IV-A) has described algal nodules (rhodolites) from the Tripp Seamount. The coralline algae of the nodules and the limestones, although providing evidence of formation in the euphotic zone, are not indicative of a specific depth. The lack of terrigenous material also indicates distance from the turbid waters generally found towards the coast. The clear oceanic water expected in the depositional environment leads to a thicker euphotic zone making depth determinations less precise. However the rounded shape of the nodules implies wave or current action able to, at least periodically, roll the nodules over. Because even a Late Pleistocene lowering of sea level to -140 m would bring the tip of the seamount within the zone of wave action it is possible that the nodules grew through several successive regressions.

Both the Orange Banks and the Tripp Seamount are elevated topographically which also helps to explain the lack of terrigenous components. Any terrigenous sediment emanating from the Orange would have been deposited on the middle shelf inshore of both the seamount and the shallower Banks.

The abundance of micrite in the suite may be due to settling of coccolith and foraminiferal debris similar to that which today constitutes the clay and silt fraction of modern sediments on the outer shelf (Chapter VIII). However the relatively low amounts of planktonic foraminifera argue against this possibility. Inorganic precipitation is unlikely in an offshore environment. Therefore the mechanical breakdown of skeletal carbonate either by marine organisms or by wave action is suggested as a likely origin of the micrite.

d. Age.

Dingle (1973a,p.354) has labelled the deposits on the Orange Banks as "Upper Upper Tertiary (T4)" on seismic evidence. The nummulitic limestones from the Orange Banks somewhat farther north have been dated as Early to Middle Miocene and a small portion of sample 2922 is composed of algal limestone, indicating a similar age for the algal limestones. Despite several attempts, no igneous rock has been dredged from the Tripp Seamount thus discounting the possibility of determining a maximum age for its limestone capping. On the

basis of seismic evidence Du Plessis et al. (1972, p.84) consider the seamount to be "older than the oldest visible sediments", which in that area are probably Neogene.

e. Diagenesis.

This suite of limestones has the highest proportion of micrite in its matrix and also contains samples with more collophane than the suites described in previous sections. Siesser (1972a,pp.98 and 106) emphasized the abundance of micrite and the dearth of microspar in his "infralittoral-skeletal lime packstone lithofacies" and his "pelagic-foraminiferal lime packstone lithofacies" on the Agulhas Bank. The reverse applied to his "lagoonal-quartzose lime wackestone lithofacies" where microspar greatly predominated over micrite (Siesser, 1972a,p.85). Therefore the abundance of micrite supports the evidence of the biogenic grains that the rocks were deposited, subsequently lithified and in some cases later phosphatized, by replacement of calcium carbonate, in a relatively shallow shelf environment at some distance from the coast.

5. Phosphorites

a. Location.

Unlike the Agulhas Bank (Parker, 1975) and the West Coast shelf south of latitude 30°S (Birch, 1975), conglomeratic phosphorite has been recovered from very few localities within the study area. The largest dredge-haul came from station 2984 at the shelf break off Chamais Bay from a depth of 250 m. Sample 3016, a small pebble, came from the Chamais Slump from a depth range of 360 to 390 m. Sample 4638 was found as an encrustation on silicified wood from the middle shelf (160 m) on latitude 30°S. Sample 4639, on the other hand, is an infilling of a boring in a sample of quartzose lime wackestone from the same latitude in a depth of 152 m (Figs. II-1 and II-2).

During vibrocoring operations off the Orange River the Marine Diamond Corporation penetrated several metres of unconsolidated sediment and sampled bedrock at a depth of 157 m. Their sample (300-8001), although characterized more by its goethite content than by its glauconite content, has been placed in this group for purposes of description.

One sample (3232C) of pelletal (intraclastic) phosphorite has been recovered from a depth of 210 m on the outer shelf off Sylvia Hill (Figs. III-1 and III-2). It was dredged from an area of uneven topography, where echograms show seaward-dipping sub-bottom reflectors within the upper 50 m of the shelf (Fig. II-13). The recovery of the sample was reported by Summerhayes et al. (1973, p.1510). This rock-type will be described further in Chapter V in the discussion on the origin of unconsolidated pelletal-phosphorite sand.

b. Petrography.

In hand specimen the samples of conglomeratic phosphorite vary in size from pebbles to cobbles, are well consolidated and frequently display surfaces heavily bored by marine organisms. Yellowish gray (5Y8/1) is the commonest colour, but the goethite-rich sample, 300-8001, is moderate yellowish orange (10YR6/4).

Texturally the rocks are phospharenites or sandy phosphorudites and are further described as glauconitic calclithic phosphate packstones. Pebbles in sample 2984 are composed of planktonic-foraminiferal lime wackestone and coralline-algal lime packstone, two rock-types already described in this chapter. The pebbles in sample 300-8001 are mainly goethite-rich lime wackestones containing varying amounts of molluscs, benthonic foraminifera, bryozoa and very fine quartz sand.

The grains of sample 2984 are dominated by fine-sand-size glauconite grains (25-40%) which usually have lighter centres (Plate III-1g). Birch (1975, p.75) has studied similar grains from phosphorites south of latitude 30°S. He found a mixture of glauconite and apatite in the light centres grading into more glauconitic darker material towards the rims. A pellicle of pure apatite was often noted and was first described by Parker (1971, p.24). Angular grains of very fine quartz sand occur in small amounts (5%) along with phosphorite fragments, rare phosphorite pellets, fish debris, sponge spicules, planktonic foraminifera and benthonic foraminifera. The intergranular matrix is a mixture of collophane and micrite.

c. Depositional environment.

The same signs of textural inversion noted by Parker (1975, p.238) are present in these phosphorites. Clay-size micrite and collophane are mixed with very fine quartz sand, fine planktonic-foraminiferal sand, fine glauconitic sand and pebbles of limestone. Parker (1975, p.238) postulated a triple-facies initial phase: foraminiferal sand, quartz silt and lime mud on the outer shelf and the upper slope, glauconitic sands on the middle shelf, and quartzose sand on the inner shelf. A transgression then allowed the outer-shelf environment to reach glauconitic and quartzose sediment on the former middle and inner shelves. Carbonate mud and fragile foraminiferal tests were deposited and then mixed by bioturbation into the underlying hydrodynamically coarser sediment. Submarine lithification then began to alter carbonate mud to micrite in the former outer-shelf environment.

The process of conglomerate formation was explained by invoking a regression which brought the high-energy intertidal zone onto the original outer shelf. The effect was two-fold. Firstly the weakly lithified carbonate mud

was eroded into hydro-plastic clasts. Secondly the bioturbated mixture of lime mud, quartz and glauconite was transported to the original outer shelf. Parker then suggested that the regression proceeded farther leaving the clasts and the transported sediment to settle and to lithify in lagoonal/estuarine conditions landward of the high-energy intertidal zone.

d. Age.

At station 2984 an unconformity was observed between a thin layer of nummulitic limestone and overlying conglomeratic phosphorite. The relationship was confirmed in thin section, where truncated tests of Nummulites are overlain by phosphorite. A maximum age for this key sample is therefore Early to Middle Miocene, the age of the nummulitic limestone.

Kolodny and Kaplan (1970) found that the Agulhas Bank phosphorites were older than 0,8 Ma because the uranium isotopes they studied had reached equilibrium. Siesser (1972a, p.96) showed that several of the planktonic-foraminiferal limestones he studied were Early Miocene to Upper Middle Miocene in age. Therefore because pebbles of these limestones are incorporated in the conglomerates a maximum age of Early to Middle Miocene is also proposed for the Agulhas Bank phosphorites.

e. Diagenesis.

The writer follows Parker (1975, p.239) concerning the diagenetic history of these phosphorites. Phosphatization occurs by replacement of calcitic mud by phosphate carried by interstitial waters originating in phosphate-rich bottom waters associated with the Benguela Current. Parker (1975, p.240) links the presence of goethite to terrigenous iron deposited in an estuarine environment.

6. Molluscan limestones

a. Location.

Poorly consolidated molluscan limestones were recovered from the middle shelf off Bogenfels, south of Chamais Bay and south of the Buffels River between 110 and 160 m (Fig. III-2).

b. Petrography.

The samples are distinguished macroscopically by their abundance of recrystallized, fragile mollusc shells set in a soft matrix. Two of the five samples were not thin-sectioned due to the softness of the material. Colours range from light gray (N7) to light olive gray (5Y6/1) and pale greenish yellow (10Y8/2).

Texturally all the samples are calcirudites and all are mollusc-rich limewackestones. Matrix comprises 60-80% and, unlike the previous group, biogenic

components predominate amongst the grains with an average of 20%. In order of decreasing abundance are molluscs, benthonic foraminifera, bryozoans, cirripeds, echinoderms and planktonic foraminifera. Aragonitic mollusc shells have often recrystallized to a pseudospar mosaic. Angular grains of very fine quartz sand occur in varying amounts from trace to 20% and traces of glauconite and pyrite are noted. Matrix is composed of varying proportions of micrite, microspar and pseudospar.

c. Depositional environment and age.

Several kilograms of molluscan limestone fragments were dredged from station 2990 in 120 m southwest of Chamais Bay. This sample was too friable to thin-section, but this drawback was offset by the possibility of examining the constituent fossils palaeontologically. Identifications were made by Dr. A.J. Tankard and Mr. A.J. Carrington of the South African Museum and Anglo American Corporation, respectively. The high degree of recrystallization and the resultant overall poor degree of preservation hindered the task of identification considerably. Often only internal moulds were available so that external ornamentation and hinge details were non-existent. The following molluscs were nevertheless identified.

Lamellibranchs	Gastropods
Glycymeris cf. borgesi (Cox)	Conus gradatulis (Weinkauf)
Venerupis senegalensis Gmelin	Patella granatina (Linn.)
Arca sp.	Turritella declivis (Adams and Reeves)
Calyptraea sp.	Clavatula sp.
Ostrea sp.	

Among the fossils identified by Dr. Tankard were Patella granatina (Linn.), Venerupis senegalensis Gmelin and Ostrea sp. P. granatina inhabits the mid-tidal zone and both V. senegalensis and Ostrea are thought to be subtidal. P. granatina and V. senegalensis are today found along the coast south of Lüderitz as far east as Cape Agulhas and Port Elizabeth, respectively.

The most abundant moulds were identified by Mr. Carrington as Glycymeris cf. borgesi (Cox). This species of Glycymeris is only known from the Neogene in South Africa. Bearing in mind the poor state of preservation of the fossils Mr. Carrington felt that the assemblage as a whole resembled Pliocene assemblages he has studied on the coast of Namaqualand. He therefore suggested that the molluscs in the limestone at station 2990 were deposited during the Pliocene in a nearshore subtidal to intertidal environment. The abundance of carbonate matrix suggests quiet water similar to that invoked for the quartzose limestones, but the greater abundance of marine organisms and the smaller amounts

of quartz indicate greater distance from the coast. A deeper-water environment is suggested by the presence of coccoliths of Palaeogene age (Siesser, 1976, personal communication).

In sample 4638, inclusion of a lithoclast of ferruginous muddy sandstone, similar to the ferruginous muddy sandstone from the same locality is evidence of the greater age of the ferruginous suite.

The lithofacies resembles the "infralittoral-skeletal lime packstone lithofacies" from the eastern Agulhas Bank which was described by Siesser (1972a,p.98). The microfauna from this lithofacies extended from the Holocene to the Pliocene or Miocene and most of the macrofossils were of extant species. Siesser (1972a,p.105) concluded that the age of the lithofacies was Pleistocene, probably Last Interglacial (Riss-Würm) between 75 000 and 113 000 years B.P. He also postulated a transgressing sea to account for the initial deposition of coarse molluscan fragments in the turbulent nearshore zone and the subsequent deposition of micrite in the succeeding quieter environment as water depth increased. The same depositional process may apply to this West Coast suite in which case the carbonate mud could be a mixture of disintegrated skeletal material from the surf-zone and coccolith debris deposited with the planktonic foraminifera.

d. Diagenesis.

Unlike the Agulhas Bank lithofacies, the few samples in the West Coast suite do contain microspar as well as micrite. Siesser (1972a,p.106) obtained electron photomicrographs of the micrite that dominated the Agulhas Bank suite. He interpreted the lack of sorting and the "ragged" appearance of the individual crystals as evidence of abrasion and biologic breakdown of skeletal material in the turbulent nearshore zone. He found no evidence of inorganic precipitation, but did not dismiss the possibility. Without similar detailed work the origin of the micrite remains indeterminate.

The original matrix of carbonate mud partly lithified to micrite and partly neomorphosed to microspar. Most of the mollusc shells neomorphosed to pseudospar. As in the Agulhas Bank suite (Siesser, 1972a,p.100) no sparry calcite was observed, indicating that the effect of subaerial exposure was negligible, due to reduced permeability caused by earlier submarine lithification (cf. Siesser, 1972a,p.107).

7. Miscellaneous.

a. Location.

Two samples of silicified wood and one of a coprolite of phosphate mudstone are discussed in this section. The wood samples were dredged from the middle shelf from depths of 150-160 m on latitude 30°S between the Buffels River and Hondeklip Bay, and the coprolite from a depth of 215 m off Sylvia Hill (25° 08'S).

b. Petrography.

The wood is medium gray (N5) in colour and clearly shows its original woody features such as grain and knots. Its colour and its density immediately indicates that it has been silicified and this fact is confirmed in thin section. Individual silicification units include several tracheids of the wood, which have been veined by yellow carbonate-apatite subsequent to silicification.

The coprolite sample is cylindrical in shape and dark yellowish brown (10YR4/2) in colour. In thin section it is composed of pseudo-isotropic collophane with organic matter disseminated throughout the matrix. Fish vertebrae (Plate III-1h) are minor but characteristic components. The sample is classified as a phospholutite: bone-bearing phosphate mudstone.

c. Identification, depositional environment and age.

Thin sections of the wood have been examined by Dr. T. Erasmus (personal communication, 1975), who described the samples as araucarioid coniferous wood of the form genera Dadoxylon ENDL. and Dammaroxylon SCH.-M. Dr. E.P. Plumstead (personal communication, 1975) warns that "the term (Dadoxylon) is applied (by geologists) to all southern-hemisphere silicified wood and is not a true genus. In recent years there has been a tendency to call the Palaeozoic specimens Dadoxylon and the Mesozoic ones Araucarioxylon. The (wood) is found at every (Karoo) horizon up to the Drakensberg lavas and ... in the Wood Beds". Because of this wide age range, because the wood was distributed widely throughout Gondwanaland, and because cobbles and boulders of silicified wood are durable and able to withstand transport over long distances, Dr. Plumstead is sceptical of the value of the wood as a zone fossil.

Araucarioid conifers are not indigenous to South Africa today, because the southern tip of Africa does not extend into the temperate latitudes required for its survival. The name, Araucaria, comes from the Chilean province of Arauco (latitude 37°S) on the boundary between the Mediterranean and temperate climatic zones. Annual rainfall is about 1300 mm, well above the minimum of 750 mm required for tree growth. One South American araucarioid, the Chile pine or monkey puzzle, grows along the tree line on the slopes of the Andes.

Although the available evidence is not conclusive, it is significant that the only samples of silicified wood were dredged from two localities only 4 km apart in a region characterized by the distinctive ferruginous bedrock already described. It has been suggested that the ferruginous rocks can be correlated with Late Cretaceous Pomona beds onshore. It is likely that the wood was silicified and then eroded from older formations before being deposited

in the ferruginous beds. The evidence suggests that during the wood's original growth period, South Africa lay farther south in cooler and moister temperate latitudes.

The coprolite was excreted by a fish-eating seal in the highly productive waters off Sylvia Hill in Recent times. Lithification occurred by precipitation of carbonate-apatite within the organic-rich coprolite to form microsphorite.

d. Diagenesis.

According to Blatt et al. (1972, p.250) no satisfactory mechanism has been proposed to explain the silicification of wood tissue. The subsequent phosphatization episode is analogous to that noted in ferruginous sediment from the same location. It is likewise ascribed to the action of phosphate-rich seawater, which became abundant after the onset of upwelling in the Oligocene (Van Zinderen Bakker, 1975).

The coprolite probably lithified by the in situ precipitation of microsphorite (microcrystalline phosphate mud) (Riggs and Freas, 1965, p.10) in interstitial solutions within the coprolite.

CHAPTER IV

PYRITE-GYPSUM ASSOCIATION IN NEOGENE CLAYS

A. INTRODUCTION

In two samples (3153 and 3202) from the upper slope of Lüderitz (Fig. III-1) an unusual association of authigenic pyrite and authigenic gypsum was detected (Siesser and Rogers, 1976). In a joint study, Siesser identified the nannofossils and microfossils in the samples, arranged X-ray diffraction and microprobe analyses of pyrite and gypsum, and conducted an extensive literature survey. The writer undertook petrographic analyses of the samples and co-authored the paper. The petrographic section of the paper is now extracted and the other sections summarized.

B. PETROGRAPHY

The sediments containing the pyrite and gypsum grains are olive grey (5Y3/2) to olive black (5Y2/1) silty clays. The sand-size fraction (5% of 3153 and 8% of 3202) is mostly composed of subangular quartz, glauconite, benthonic and planktonic foraminifera, gypsum and pyrite. Faecal pellets, diatoms and echinoid spines are present, but are rare. Sample 3153 contains relatively more pyrite and gypsum than 3202, as well as more diverse morphological forms of these grains.

1. Pyrite

In sample 3153, pyrite (Plate IV-1-a,b,e and g) occurs as 1) irregular granular masses (0,25-1,0 mm in diameter), 2) straight to slightly curved "worm" tubes (up to 5 mm in length), 3) foraminiferal infillings, and 4) framboids (0,06-0,10 mm in diameter). These morphological forms are listed in approximate order of decreasing abundance. Second-order spheroids (Hein and Griggs, 1972) are present on some of the granular masses and "worm" tubes. Pyrite occurs only as granular masses in sample 3202.

The reason for the variety of different morphological forms of pyrite seems largely to be related to the presence and localization of organic matter. Hein and Griggs (1972) felt that the organic binding or film along burrow walls acts as the initial locus for pyritic "worm" tube formation. Protoplasm remaining in a foraminifer test would create similar conditions. Berner (1970) proved that concentration gradients in sediments favoured the migration of dissolved iron and sulphur towards an organic mass. The irregular granular masses were considered to be derived from irregularly shaped concentrations of organic matter, i.e., where organic matter is concentrated but not in a discrete shape such as provided by a burrow or foraminifer test.

Plate IV-1. Association of gypsum and pyrite in Neogene clays

IV-1a. Granular mass of pyrite.

IV-1b. Hollow "worm" tube of pyrite.

IV-1c. Gypsum (selenite) crystal with lenticular shape owing to rounding of the pinacoids.

IV-1d. Gypsum (selenite) diametral prisms forming interpenetration twins.

IV-1e. Gypsum (selenite) diametral prisms with vicinal forms on their surfaces. Note the partially enclosed hollow "worm" tube of pyrite.

IV-1f. Swallowtail contact twins and clusters of bladed crystals of gypsum (selenite).

IV-1g. Gypsum (selenite) diametral prism partially enclosing a tube of pyrite.

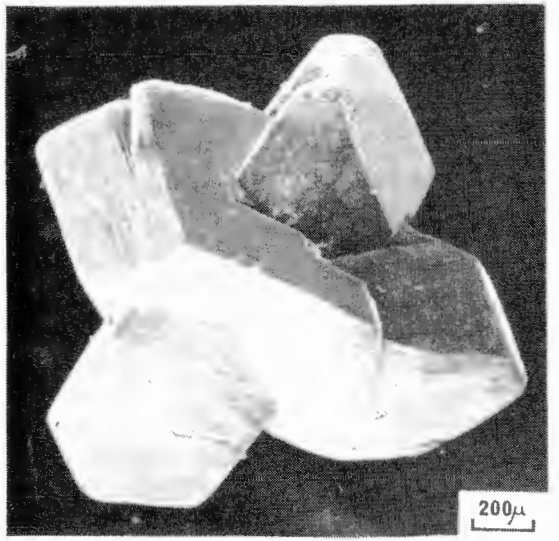

d

f

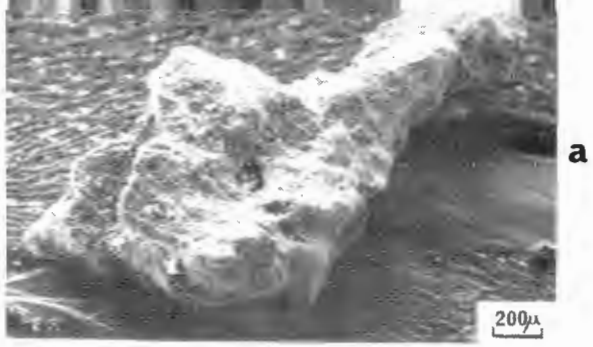

a

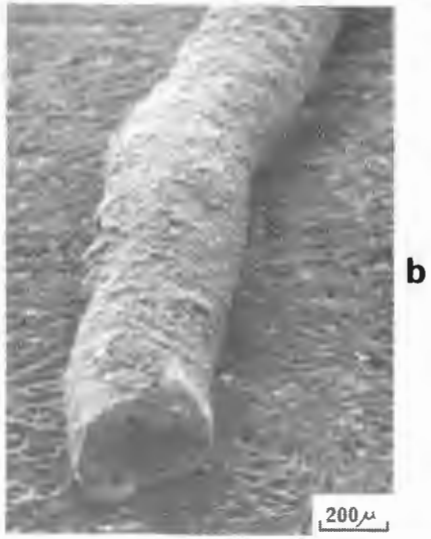

b

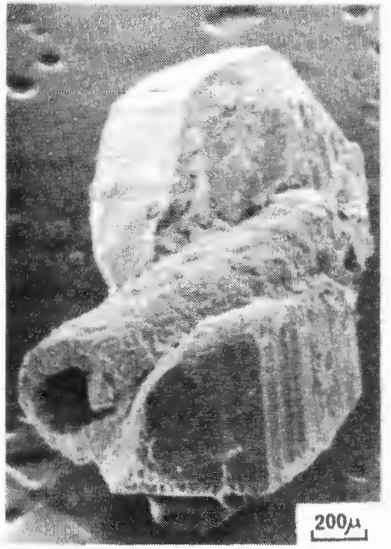

e

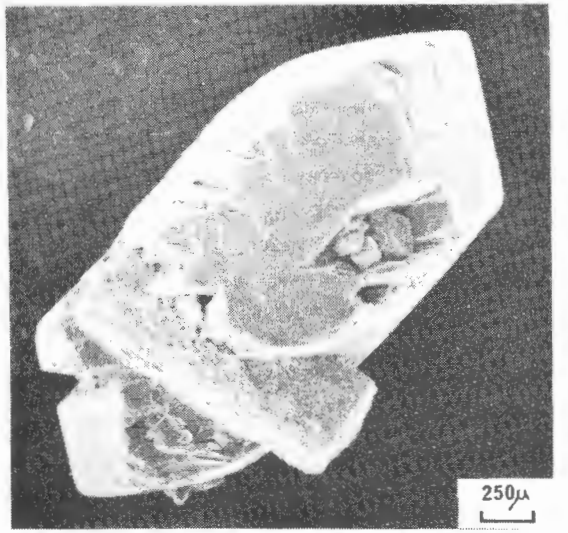

g

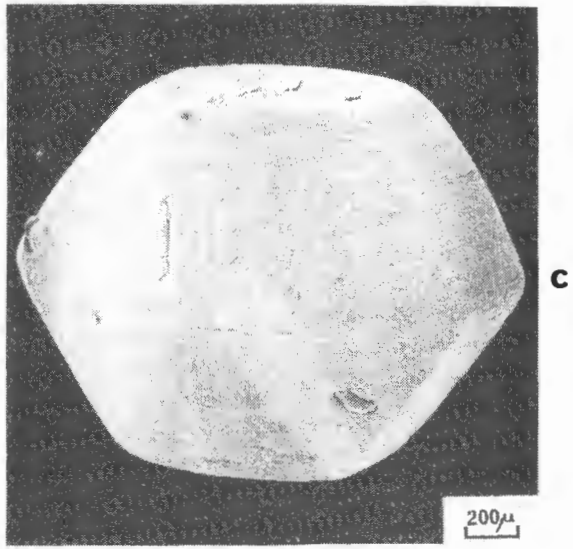

c

Plate IV-1

Earlier ideas of sedimentary framboid formation also stressed biogenic involvement. Aggregates of organic cells (Love, 1965) or organic globules (Rickard, 1970) were believed to be replaced. However, laboratory syntheses of framboids have shown that organic cells or globules are not necessary (Goldhaber and Kaplan, 1974). Instead, the initial iron sulphide precipitate develops a spherical form when it transforms to greigite (Fe_3S_4). This spherical form is either retained or changed to a framboid when greigite changes to pyrite (Goldhaber and Kaplan, 1974).

2. Gypsum

Gypsum occurs as euhedral crystals of selenite (the vitreous, colourless, transparent to translucent variety of gypsum). Crystals vary in length from 0,06 to 5,0 mm. Most of the larger crystals, which form the coarsest fraction of both samples, develop a lenticular habit by rounding of the pinacoids (111) and ($\bar{1}03$) (Plate IV-1-c). Irregular grooves occur on the crystal faces and the edges are rarely sharp. Some crystals are diametral prisms composed of the basal pinacoid (001), the orthopinacoid (100), and the clinopinacoid (010) (Plate IV-1-d). Vicinal forms are noted on the surface of some of the less perfect crystals (Plate IV-1-f). Cruciform interpenetration twins (Plate IV-1-d) of diametral prisms are present, but are relatively rare. In the finer sediment fraction (0,1-0,3 mm), swallowtail contact twins of delicate, tabular selenite are associated with radiating clusters of bladed and/or acicular crystals (Plate IV-1-f); (100) is the twin plane.

Pyritized "worm" tubes and foraminiferal infillings are sometimes enclosed partially or completely by gypsum (Plate IV-1-e and -g), thus illustrating the sequence of their formation (Siesser and Rogers, 1976).

C. GEOCHEMISTRY

The visual identification of pyrite and gypsum was confirmed by X-ray diffraction of picked grains. Microprobe analyses showed pyrite to contain normal amounts of sulphur (53%) and iron (43-44%), but unexpectedly high concentrations (0,4%) of manganese. Gypsum contained expected values of 28% calcium and 23% sulphur.

D. AGE

The planktonic foraminifer, Globigerina nepenthes, was found in sample 3153 and an Upper Middle Miocene to Middle Pliocene age was assigned to the sample. Sample 3202 contained diagnostic calcareous nannofossils and was dated as Upper Miocene to Lower Pliocene (Siesser, 1975).

E. ORIGIN

The presence of pyrite is not unexpected because an anaeorobic, H_2S-rich environment conducive to its formation exists off Walvis Bay today (Copenhagen, 1934, 1953; Calvert and Price, 1970, 1971a; Veeh, Calvert and Price, 1974). World-wide oceanographic conditions are thought to have remained the same from Neogene times onwards (Hay, 1974). Active upwelling of nutrient-rich water promotes extremely high productivity of phytoplankton in the euphotic zone, which is subject to high levels of solar radiation. Although zooplankton and fish graze the phytoplankton continually, vast amounts of organic detritus sink through the water column to the sea floor. In the better-oxygenated upper layers of the water column, aerobic bacteria decompose the organic debris. In so doing they consume dissolved oxygen and in the lower layers there is so little oxygen that anaerobic conditions prevail. The task of decomposing the residual organic debris falls on a population of the sulphate-reducing anaerobic bacterium Desulphovibrio desulphuricans (Butlin, personal communication, in Copenhagen,1953, p.11) both in the bottom waters and in the interstitial waters of the sediments.

Berner (1970) concludes that undecomposed metabolizable organic matter, (present to excess in the bottom sediments off Walvis Bay), acts as an energy source for anaerobic bacteria. These bacteria liberate a certain amount of sulphur from organic matter, but most of the sulphur they produce (in the form of hydrogen sulphide) is reduced from sulphate dissolved in sea water (Berner, 1970, p.2). Constant diffusion of sulphate into the anaerobic zone from the surrounding sea water means that sulphate is not a limiting factor in the production of either pyrite or gypsum.

The only likely limiting factor in the production of pyrite in this region is the availability and reactivity of iron-bearing terrigenous material. It has been found that the modern organic-rich muds off Walvis Bay are depleted in iron, but that both the Orange and the Kunene Rivers are major sources of the element (see Chapter VII and Bremner, in prep.). Therefore the anaerobic sediments off the Namib Desert today have ample local supplies of organic matter, sulphate, anaerobic bacteria and hydrogen sulphide, but distant sources of iron.

Berner (1970) showed that the most likely reactions leading to the formation of pyrite are:

$$Fe^{++} + H_2S \rightarrow \text{"FeS"} + 2H^+$$

$$\text{"FeS"} + S^o \rightarrow FeS_2$$

The black, very fine-grained "FeS" is actually a mixture of non-crystalline FeS, of mackinawite ($Fe_{1,05}S$) and of greigite (Fe_3S_4). Elemental sulphur

(S^o) is required to oxidize "FeS" to pyrite (FeS_2). Berner (1970, p.20) stated that elemental sulphur can be introduced into anaerobic sediments by the gradual build-up and then upward diffusion of excess H_2S into the aerobic water overlying the anaerobic interstitial and/or bottom water. In reacting with the dissolved oxygen the H_2S further increases the extent of the anaerobic zone, while liberating elemental sulphur particles. These particles then settle back into the sediment and react with "FeS" to form pyrite. Part of the process has been observed in the Walvis Bay region by Copenhagen (1953, p.13): "The sulphur in the sea water runs the gamut of changes from sulphate to complete reduction, and then again to complete oxidation $\rightarrow SO_4 \rightarrow H_2S \rightarrow S \rightarrow SO_4$. It should be noted that during the oxidation of sulphuretted hydrogen back to sulphate, a considerable amount of dissolved oxygen is removed from sea water. The 'milky' sea water often observed in the sea in and around Walvis Bay may be due to colloidal sulphur formed by the oxidation of sulphuretted hydrogen."

Berner (1970, p.22) estimated that several years are required for the complete transformation of "FeS" to FeS_2 in the presence of abundant H_2S and elemental sulphur. Stable conditions are thus essential. Similarly, the size of the gypsum crystals surrounding the pyrite indicate conditions of slow growth.

Baturin (1972) recorded pH values as low as 7,26 in the modern anaerobic muds, with an average value of 7,56. Because $CaCO_3$ has a tendency to dissolve below a pH of 7,8 (Mason, 1966, p.173) any calcareous detritus such as foraminiferal tests or coccoliths would dissolve and increase the concentration of calcium ions. Although severely depleted, sulphate ions can still be present under pyrite-producing anaerobic conditions (Berner, 1970). As soon as the product of the concentrations of calcium and sulphate ions exceeds the solubility product of calcium sulphate, then gypsum is precipitated. As long as the pH stays low enough for calcareous detritus to dissolve, the gypsum crystals continue to grow.

The two samples containing pyrite and gypsum both occur in Neogene clays on the upper slope, whereas the modern anaerobic environment discussed above is situated on the middle shelf. However, Dingle and Scrutton (1974) postulated an Upper Miocene-Lower Pliocene regression, which would have shifted any Neogene analogue of the anaerobic zone towards the slope, while simultaneously lowering sea level. The introduction of anaerobic conditions to the upper slope then led to this unusual association of pyrite enclosed by gypsum in a non-evaporitic environment.

CHAPTER V

UNCONSOLIDATED RESIDUAL SEDIMENTS

A. INTRODUCTION

This is the first of four chapters on the unconsolidated sediments of the study area. (See Fig.V-1 for sample locations). The sediments have been subdivided into 1) residual sediments reworked from bedrock, probably during a late-Pliocene regression, 2) sediments relict of Pleistocene regressions, 3) Recent terrigenous sediments, and 4) Recent biogenic sediments. The authigenic components, glauconite and phosphorite are readily identified as residual; calcium carbonate and organic matter include the bulk of the biogenic components and the remaining components are assumed to be of terrigenous material. Sponge spicules, diatom frustules and radiolaria contribute biogenic silica to the "terrigenous fraction" of some samples, usually to a negligible extent. This terrigenous fraction comprises Recent, Pleistocene and residual components, the material generally increasing in age from the inner shelf seawards.

Figures V-2 and V-3 summarize the broad compositional and textural trends of the sediments. Recent terrigenous sand characterizes the inner shelf along the entire coastline. This coastal sand is flanked by Recent terrigenous mud north and south of the Orange River, the chief source of terrigenous sediment in the region. The terrigenous mudbelt grades seawards to coarse relict terrigenous sand diluted with mud. Most of the Orange shelf is blanketed by foraminiferal biogenic sediment; mud values are lowest along the outer shelf and highest on the slope. The foraminiferal biogenic mud on the Walvis slope merges with terrigenous, glauconitic and phosphatic sand on the outer and middle Walvis shelf.

Detailed geophysical and vibrocoring traverses between the Orange River and Lüderitz (Joynt, 1975, personal communication) show that the residual and biogenic components overlie strata which dip very gently seawards. The residual and biogenic sediment is usually less than 1 m thick, but is flanked on its landward side by a lens of terrigenous sediment, which reaches a thickness of over 70 m off the Orange River (Hoyt et al., 1969).

Figure V-3 complements Figure V-2 by showing the variation in the composition and texture of the surficial sediments along six selected profiles, whereas Figures V-4 to V-9 illustrate, in greater detail, the variations in texture and in coarse-fraction components along the same six profiles.

In this chapter the residual authigenic components, glauconite and phosphorite, are first discussed, emphasizing the depositional history of an important pelletal phosphorite source-rock. A short section is devoted to a lag deposit of coarse quartzose sand on the Orange middle shelf.

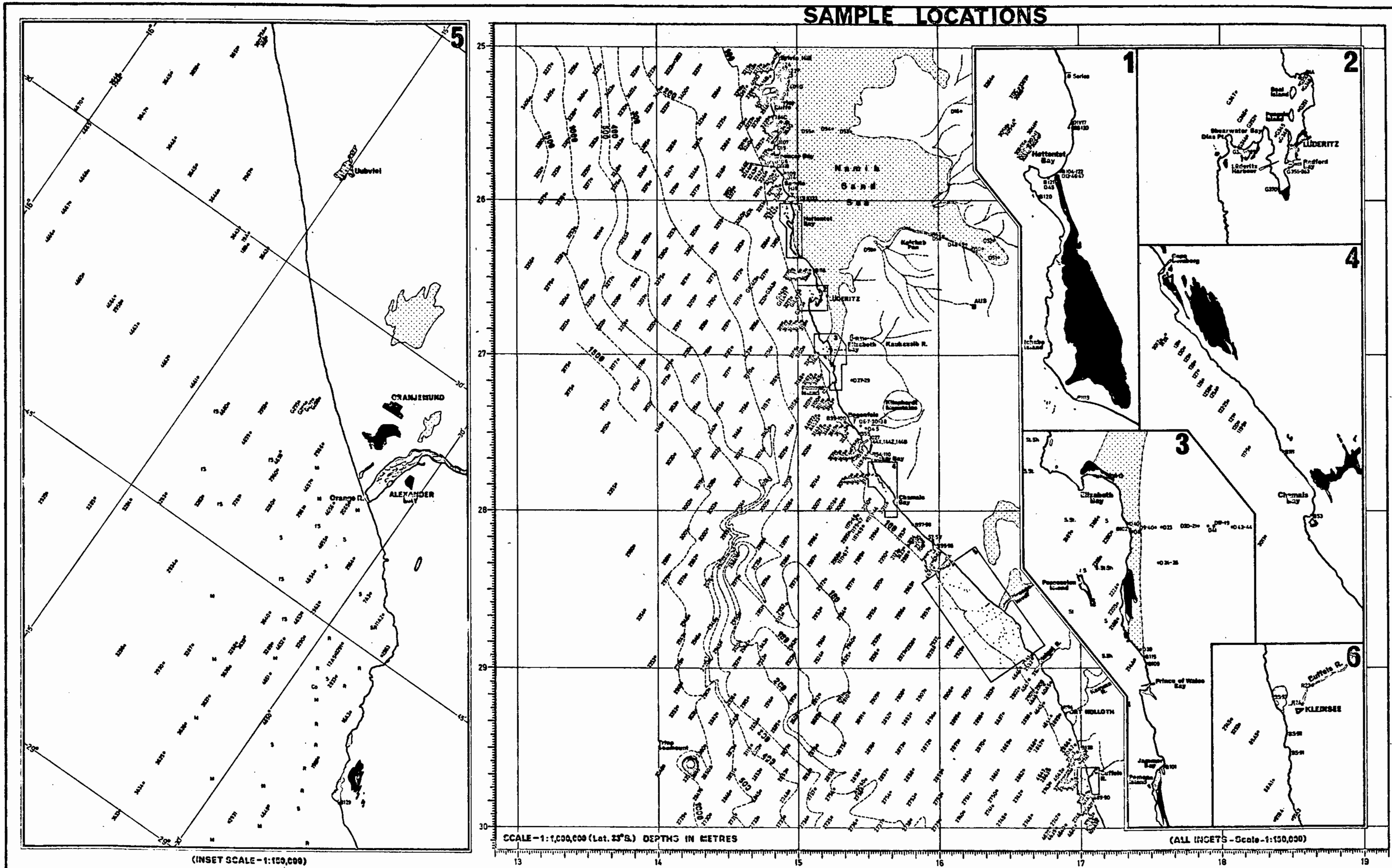
SAMPLE LOCATIONS
SCALE-1:1,000,000 (Lat. 33°S.) DEPTHS IN METRES
(ALL INSETS-Scale-1:150,000)
(INSET SCALE-1:150,000)
Namib Sand Sea
LÜDERITZ
Hottentot Bay
Elizabeth Bay
Chamais Bay
Prince of Wales Bay
HOLLOTH
KLEINSEE
Buffels R.
Orange R.
ALEXANDER Bay
ORANJEMUND
Uubvlei
AUS
Kaukausib R.
Possession Island
Shearwater Bay
Lüderitz Harbour
Dias Pt.
Radford Bay
Seal Island
Tripp Seamount
Jammer Bay

Fig.V-1

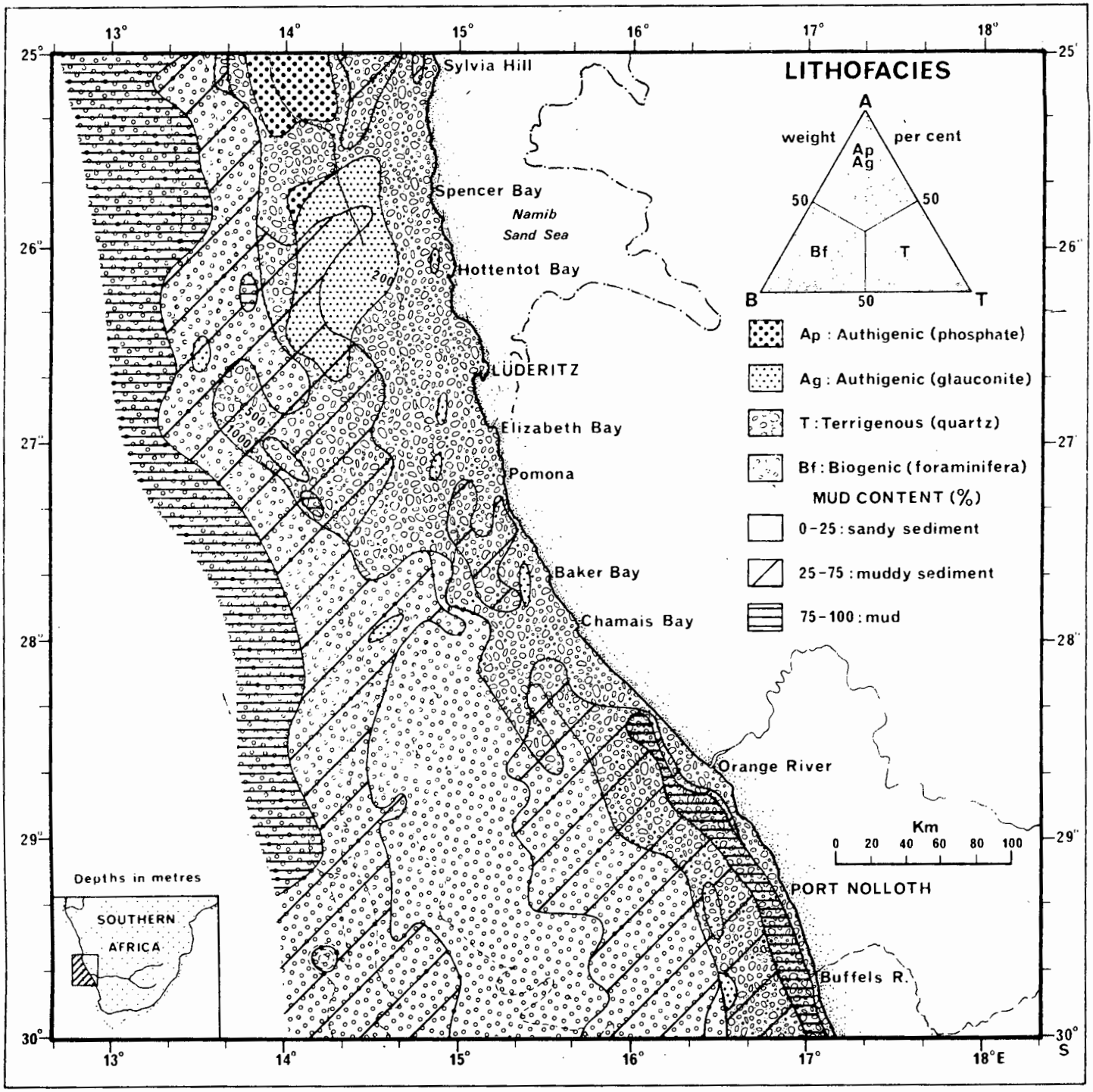
LITHOFACIES
A
weight per cent
Ap
Ag
50
50
Bf
T
B
50
T
Ap : Authigenic (phosphate)
Ag : Authigenic (glauconite)
T : Terrigenous (quartz)
Bf : Biogenic (foraminifera)
MUD CONTENT (%)
0-25 : sandy sediment
25-75 : muddy sediment
75-100 : mud
Sylvia Hill
Spencer Bay
Namib
Sand Sea
Hottentot Bay
LÜDERITZ
Elizabeth Bay
Pomona
Baker Bay
Chamais Bay
Orange River
PORT NOLLOTH
Buffels R.
Km
0 20 40 60 80 100
Depths in metres
SOUTHERN
AFRICA
13°
14°
15°
16°
17°
18°
18°E
25°
26°
27°
28°
29°
30°
S

Fig.V-2

COMPOSITIONAL, TEXTURAL AND BATHYMETRIC PROFILES

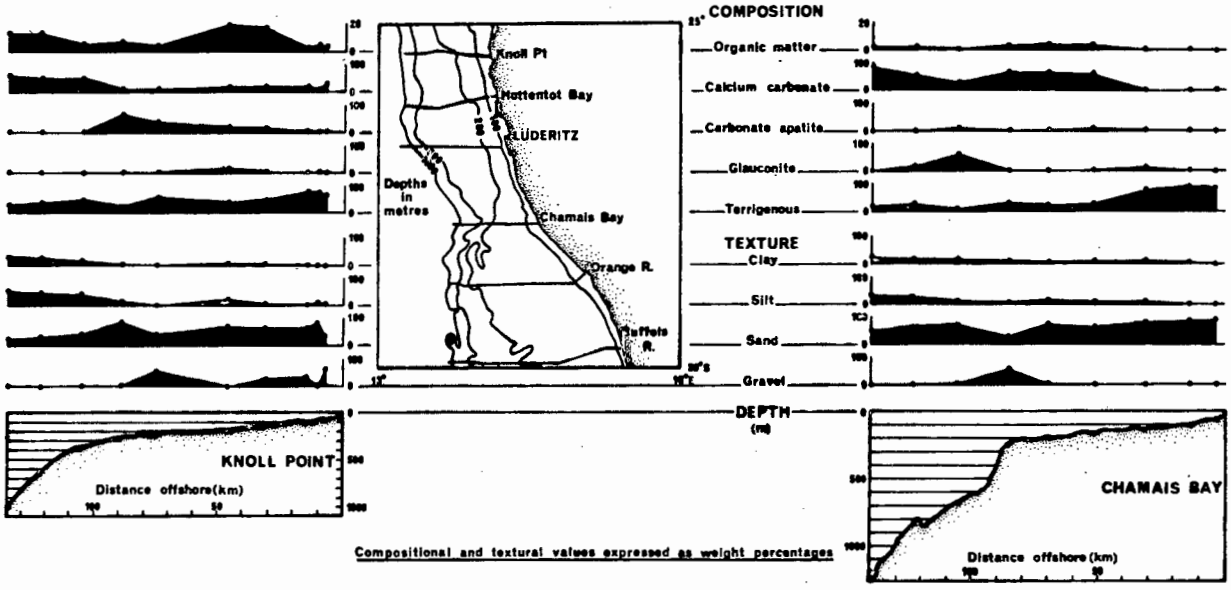

Compositional and textural values expressed as weight percentages

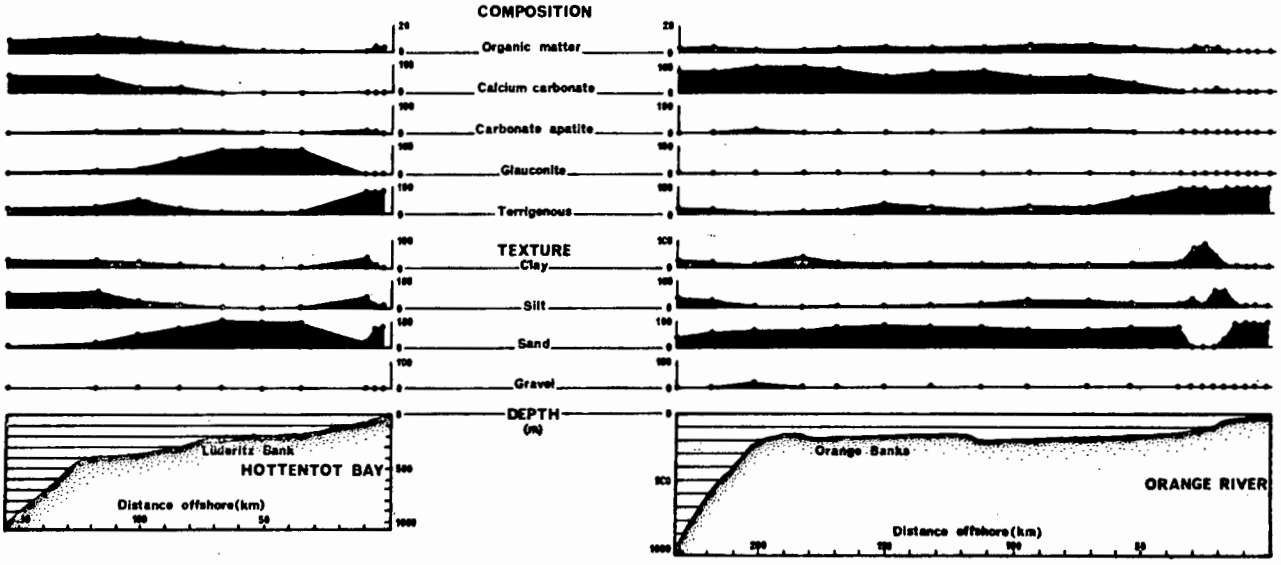

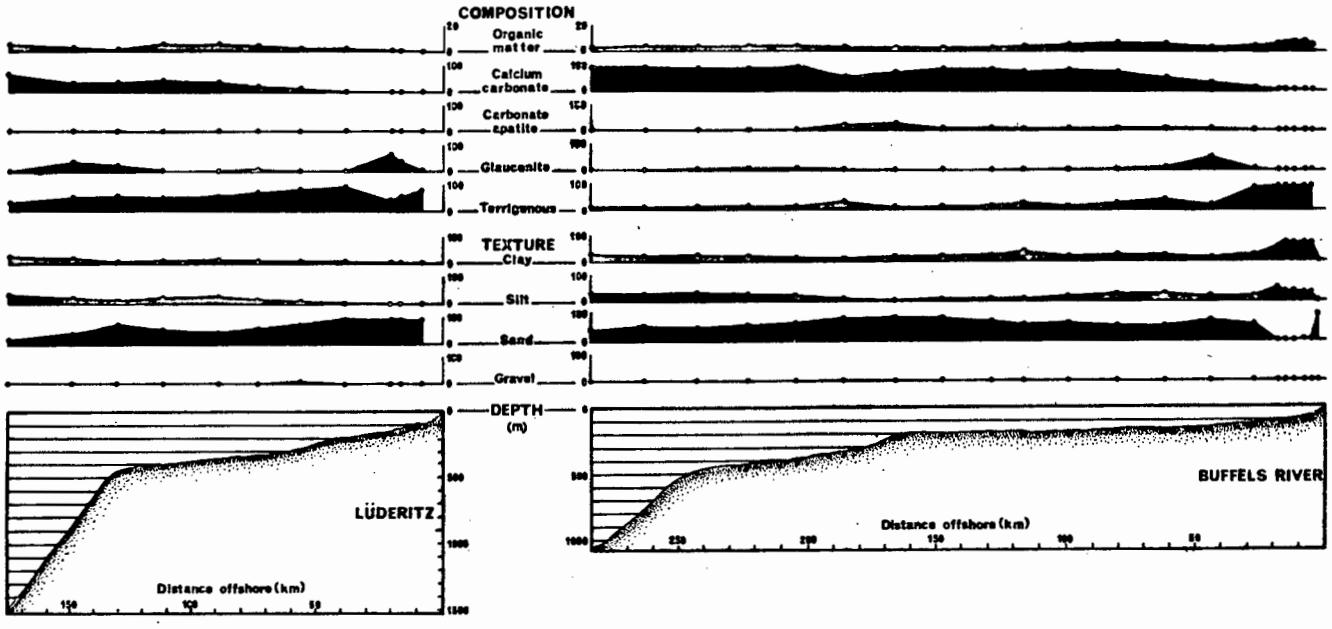

Fig.V-3

COARSE-FRACTION-COMPONENT AND TEXTURAL VARIATION OFF BUFFELS RIVER

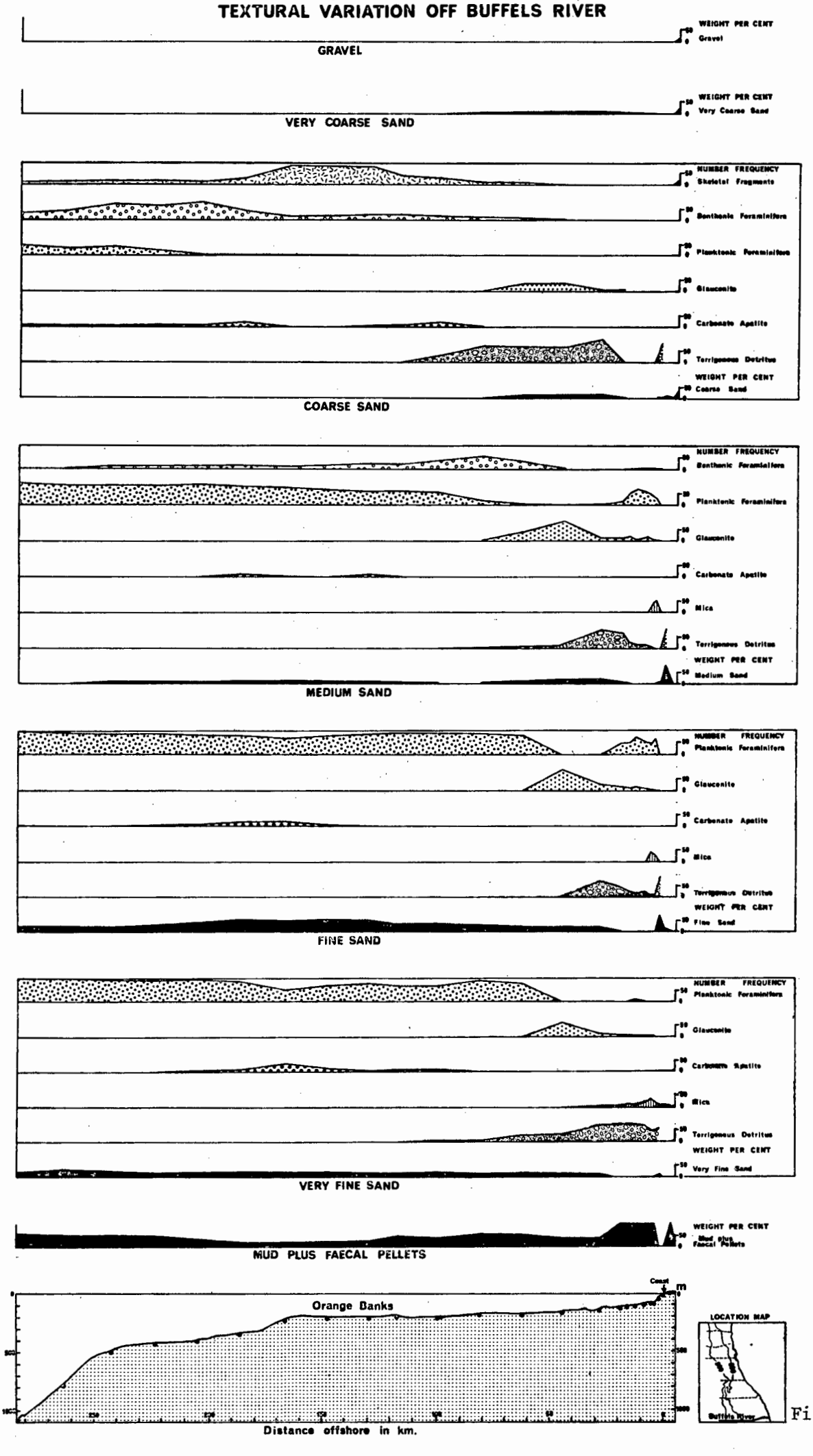

Fig.V-4

COARSE-FRACTION COMPONENT AND TEXTURAL VARIATION OFF ORANGE RIVER

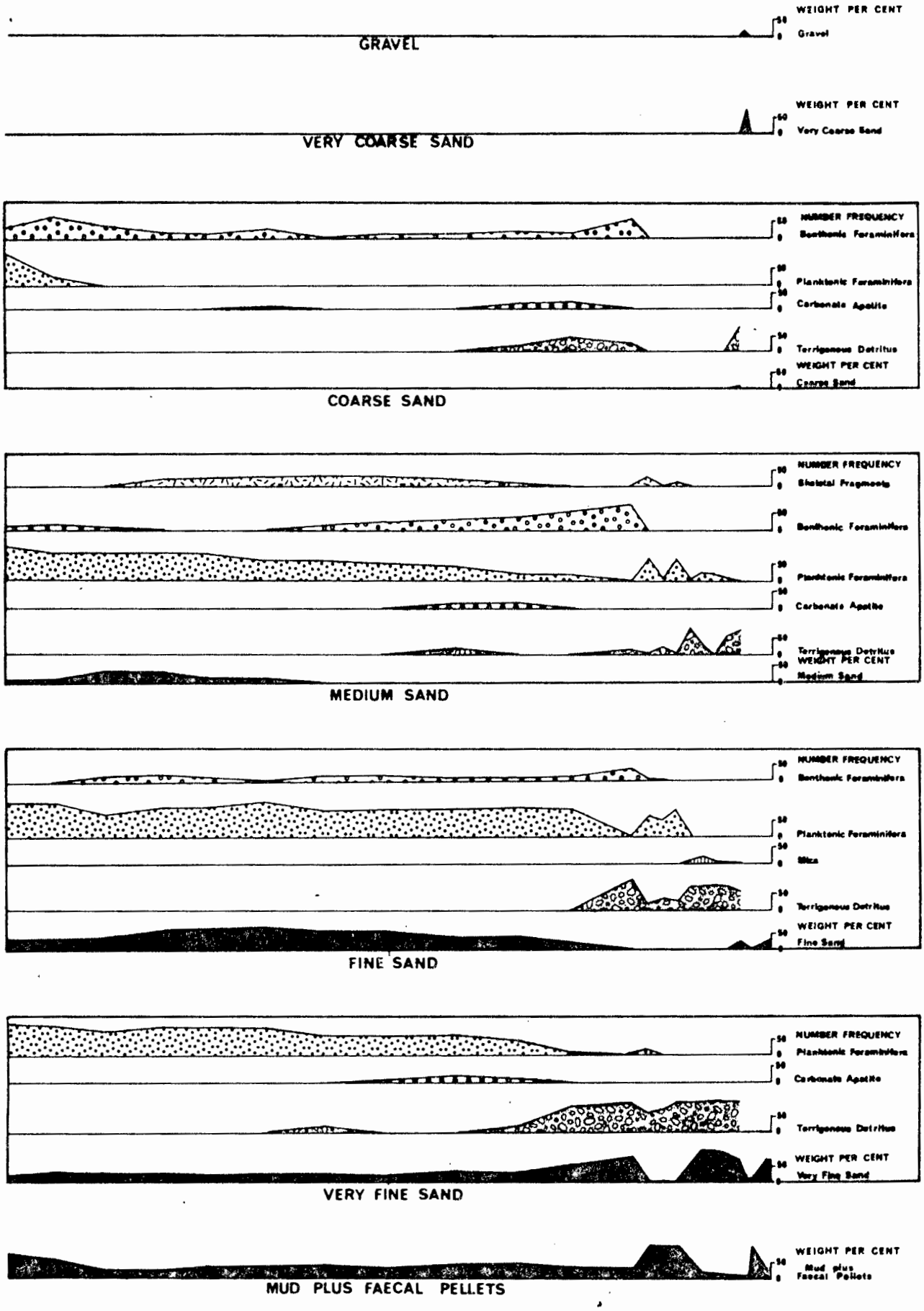

Fig. V-5

COARSE-FRACTION-COMPONENT AND TEXTURAL VARIATION OFF CHAMAIS BAY

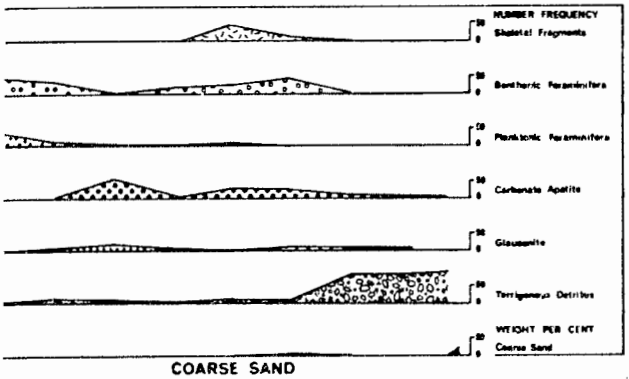

COARSE SAND

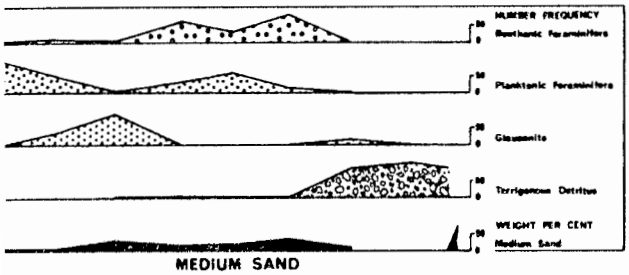

MEDIUM SAND

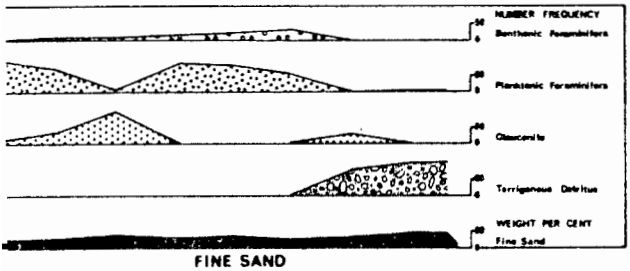

FINE SAND

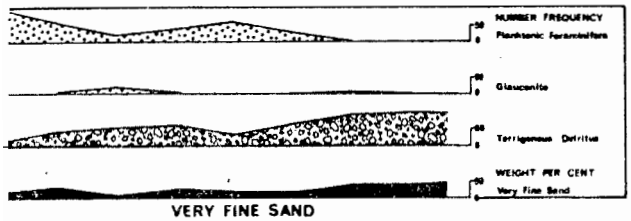

VERY FINE SAND

MUD PLUS FAECAL PELLETS

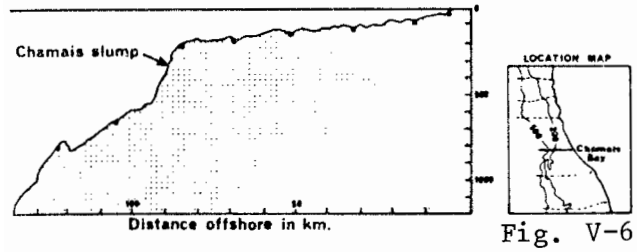

Fig. V-6

COARSE-FRACTION-COMPONENT AND TEXTURAL VARIATION OFF LÜDERITZ

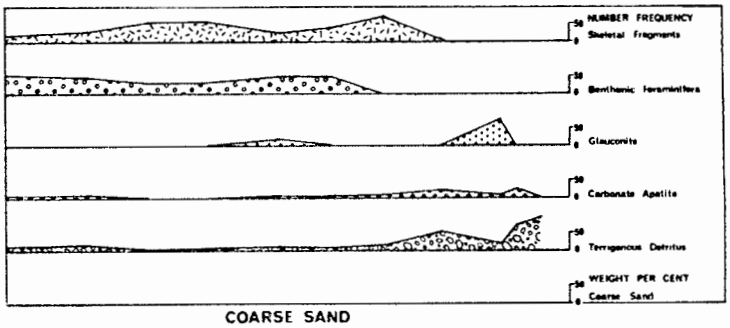

COARSE SAND

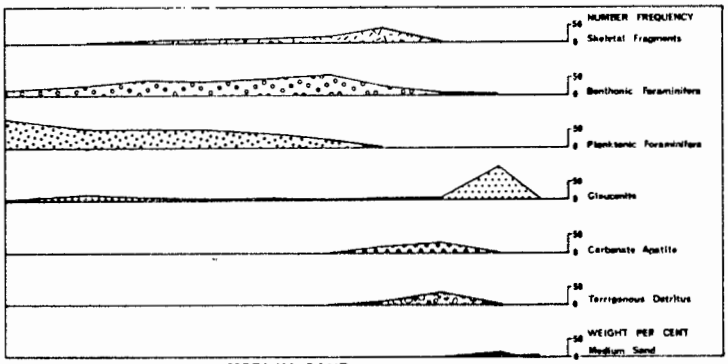

MEDIUM SAND

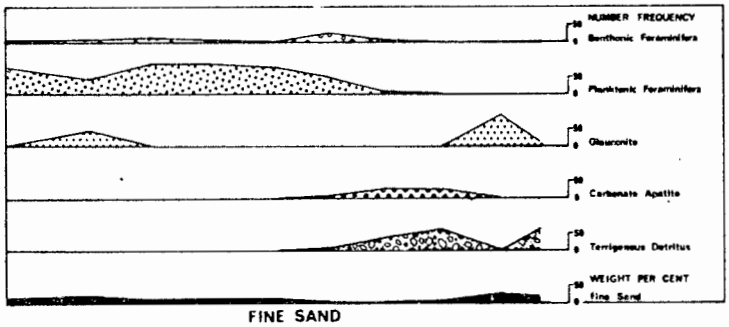

FINE SAND

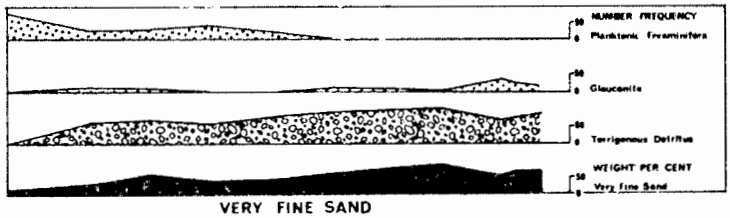

VERY FINE SAND

MUD PLUS FAECAL PELLETS

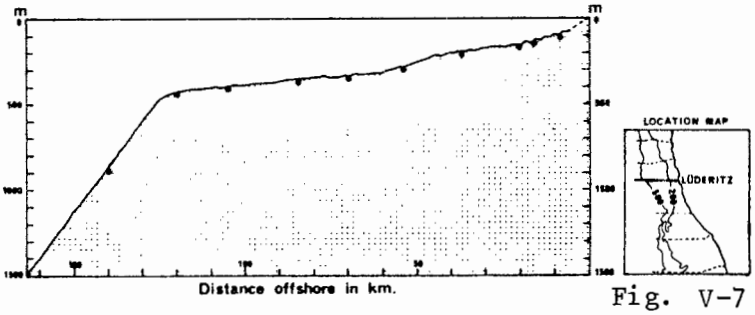

Fig. V-7

COARSE-FRACTION-COMPONENT AND TEXTURAL VARIATION OFF HOTTENTOT BAY

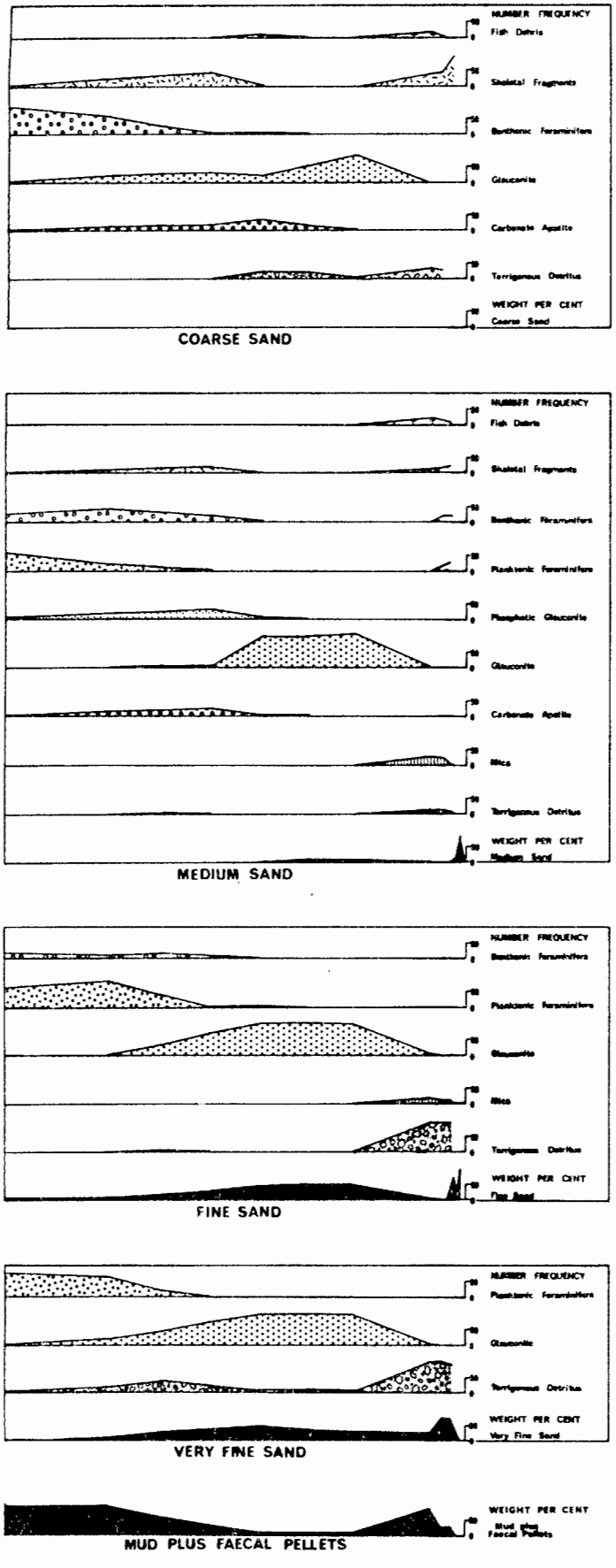

Fig. V-8

COARSE-FRACTION-COMPONENT AND TEXTURAL VARIATION OFF KNOLL POINT

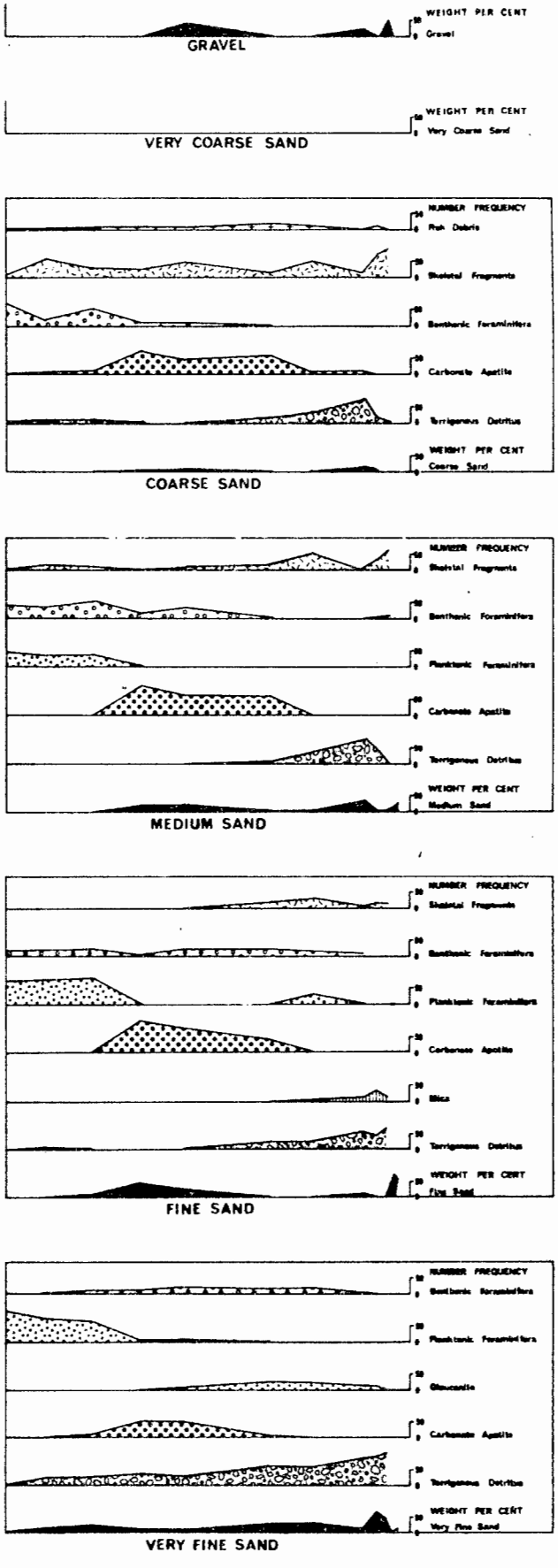

Fig. V-9

B. GLAUCONITE

1. Regional distribution

Most of the sediments contain at least a trace of glauconite (Fig. V-10). The only glauconite-free sediments are terrigenous muds off the Orange and biogenic muds on the slope. Four deposits contain more than 5% glauconite, three on the Walvis shelf and one on the Orange shelf. The southernmost belt extends from Hondeklip Bay (Birch, 1975, Fig. II-11) to Port Nolloth. Birch (1975) related this deposit to outcrops, which Dingle (1973a) presumes to be Cretaceous and Palaeogene in age. To date few samples of this glauconitic rock have been sampled and none has been dated.

The glauconite belts on the Walvis shelf each transgress the margin from the middle shelf southwestwards towards the upper slope. The belts are wider and richer towards the north. Rare granules of purely glauconitic sandstone were detected in superficial sediments from the Lüderitz Bank indicating a probable source-rock for the glauconite off Hottentot Bay. Glauconite-rich conglomeratic phosphorite of post Middle-Miocene age was recovered from the southern tip of the middle belt off Chamais Bay. Glauconite decreases in abundance shorewards in the belt off Baker Bay. A vibrocore operated by the Marine Diamond Corporation near the bay penetrated 9,5 m of very fine terrigenous sand and then 1 m of almost pure glauconite sand before reaching bedrock, composed of glauconitic phosphorite (O'Shea, 1973, personal communication). The glauconite deposit on the middle shelf off Baker Bay therefore persists shorewards but becomes buried beneath a lens of terrigenous sand.

2. Relationship of K_2O to glauconite

The 1,5% K_2O isopleth on the Walvis shelf (Fig. V-11) outlines the three glauconite deposits described above. On the Orange shelf the K_2O derived from glauconite on the middle shelf merges landwards with the K_2O derived from the glauconite-free terrigenous muds (Figs. V-10, and V-11). Thus, where blanketing or dilution of residual glauconite is at a minimum, as on the Lüderitz Bank (Fig. V-12), there is a direct relationship between the concentrations of glauconite and of K_2O. This is further demonstrated by the bivariate plot of glauconite versus K_2O (Fig. V-13). Despite the independent trend caused by terrigenous sediments there is a clear positive relationship between the two variables with a correlation coefficient of 0,773.

The distribution of K_2O in the mud fraction (Fig. V-14) parallels the distribution of K_2O in the total sample and is similarly related to glauconite on the Walvis shelf and to terrigenous mud on the Orange shelf. This implies that glauconite contributes K_2O to the mud fraction, particularly on the Lüderitz Bank.

3. Relationship of glauconite to shelf morphology and to sediment texture

Glauconite is present along each of the six selected profiles, except that

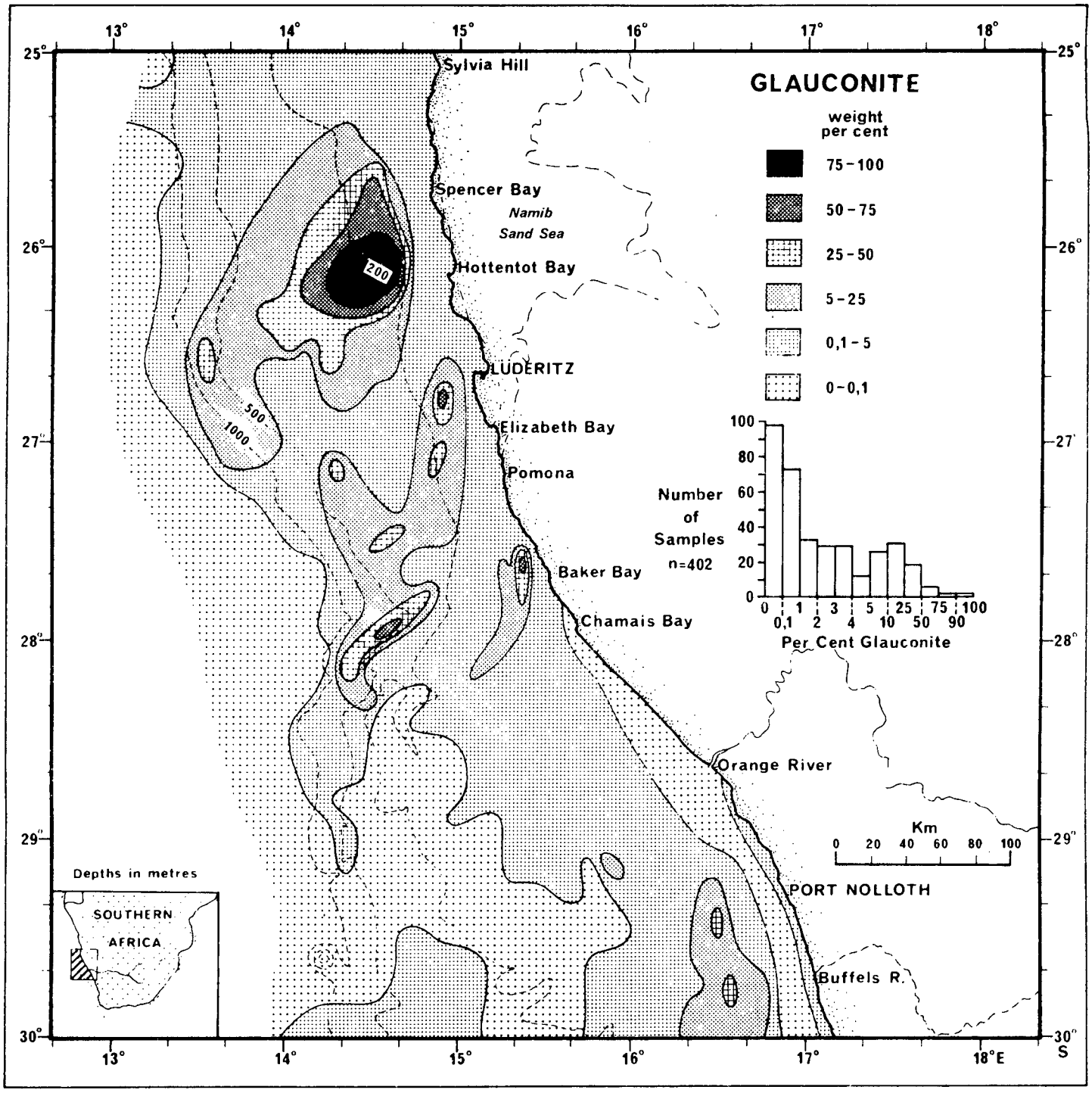
GLAUCONITE
weight per cent
75 - 100
50 - 75
25 - 50
5 - 25
0,1 - 5
0 - 0,1
Sylvia Hill
Spencer Bay
Namib
Sand Sea
Hottentot Bay
LUDERITZ
Elizabeth Bay
Pomona
Baker Bay
Chamais Bay
Orange River
PORT NOLLOTH
Buffels R.
200
500
1000
Number of Samples n=402
Per Cent Glauconite
0 1 3 5 25 75 100
0,1 2 4 10 50 90
Km
0 20 40 60 80 100
Depths in metres
SOUTHERN AFRICA
13° 14° 15° 16° 17° 18°E
25° 26° 27° 28° 29° 30° S

Fig.V-10

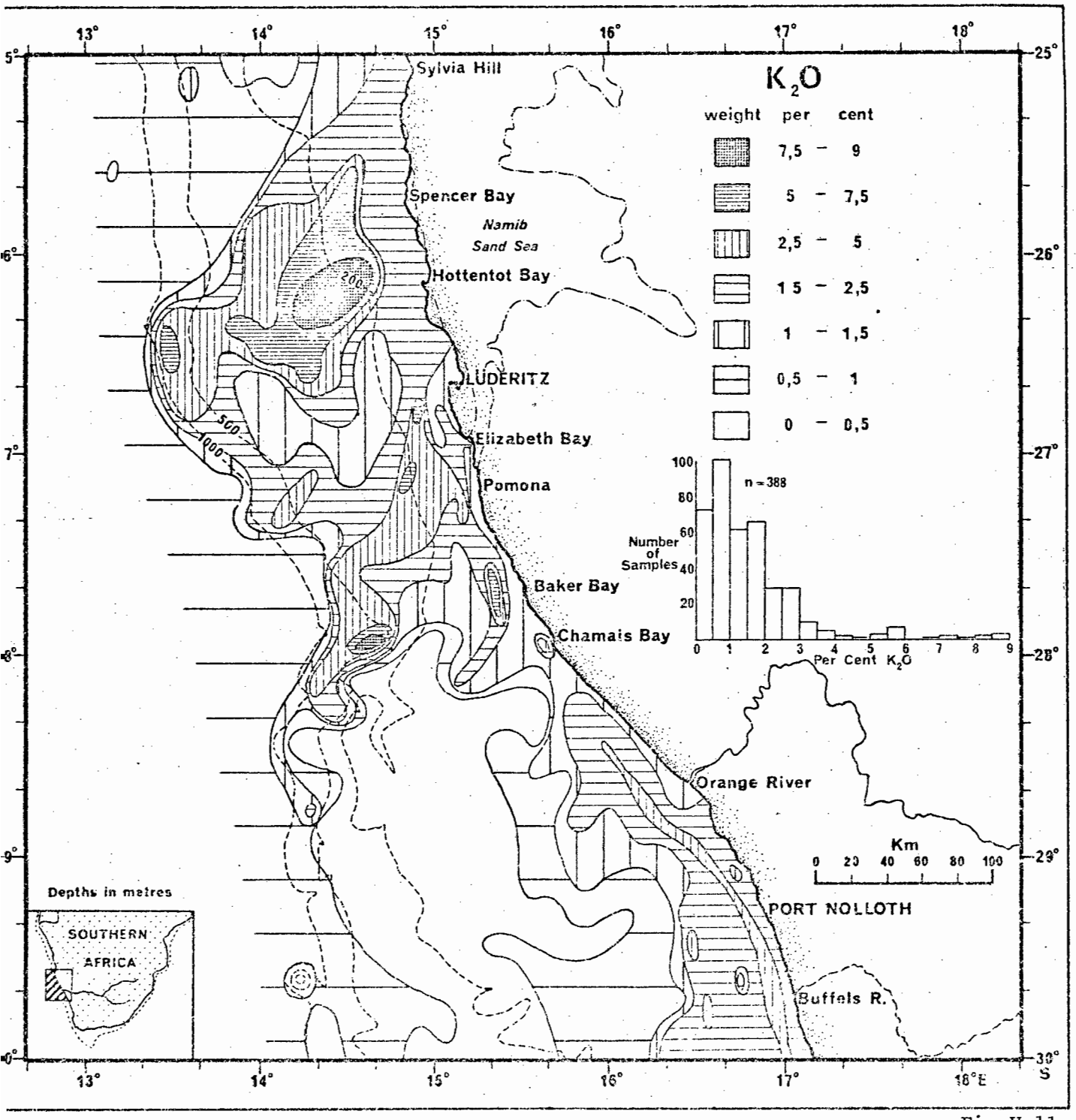
13°
14°
15°
16°
17°
18°
25°
26°
27°
28°
29°
30° S
18°E
Sylvia Hill
Spencer Bay
Namib
Sand Sea
Hottentot Bay
LÜDERITZ
Elizabeth Bay
Pomona
Baker Bay
Chamais Bay
Orange River
PORT NOLLOTH
Buffels R.
200
500
1000
K2O
weight per cent
7,5 – 9
5 – 7,5
2,5 – 5
1 5 – 2,5
1 – 1,5
0,5 – 1
0 – 0,5
n = 388
Number of Samples
Per Cent K2O
Km
0 20 40 60 80 100
Depths in metres
SOUTHERN AFRICA

Fig.V-11

RELATIONSHIP BETWEEN K_2O, GLAUCONITE, TERRIGENOUS DETRITUS AND TEXTURE

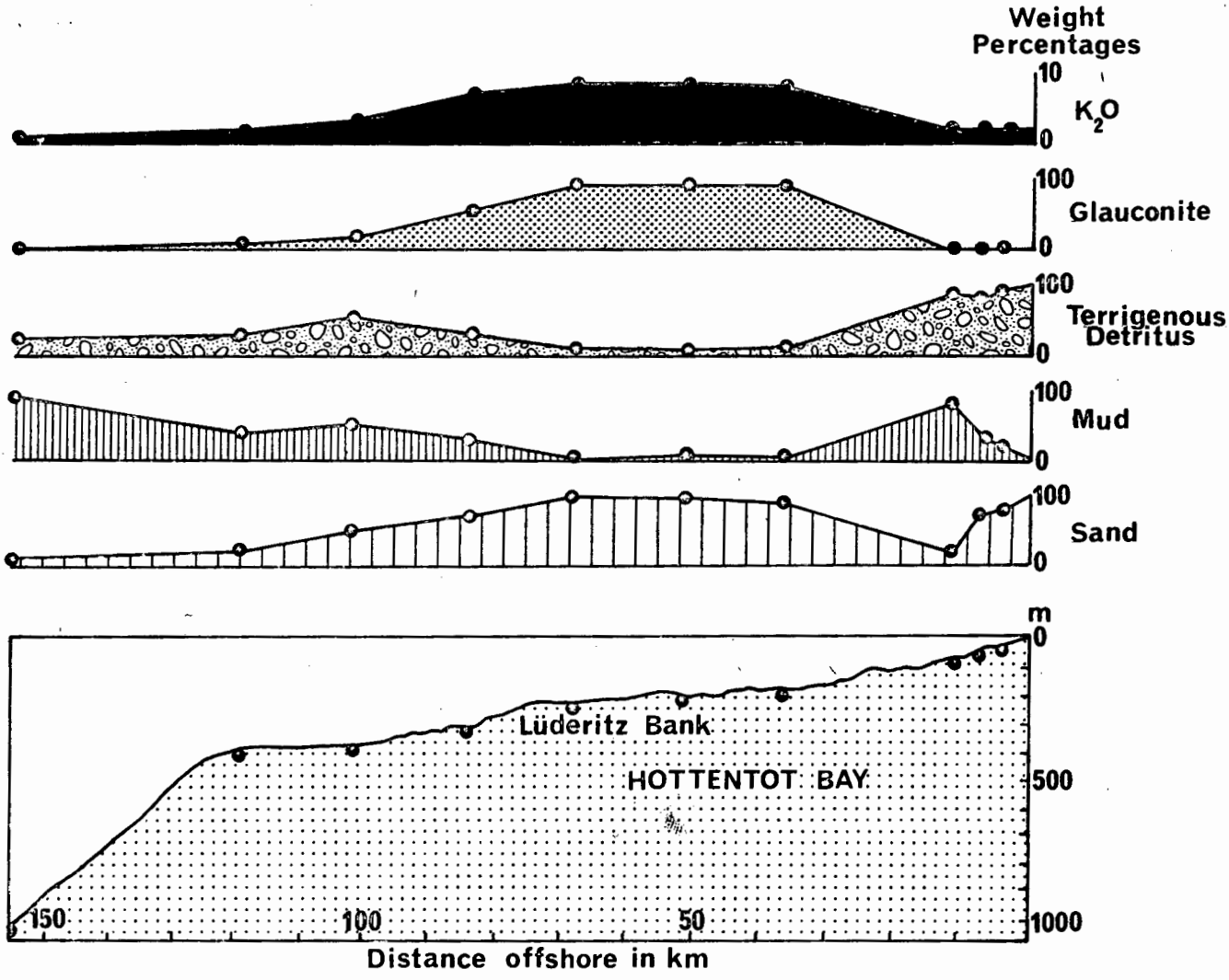

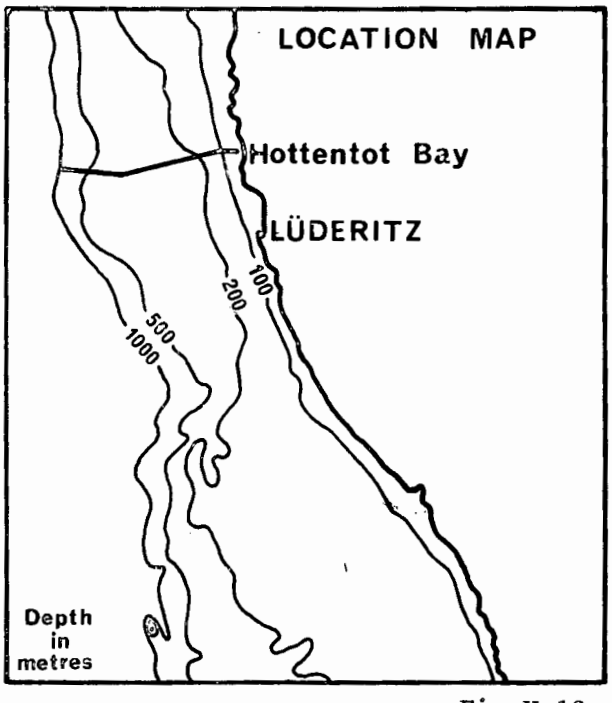

Fig.V-12

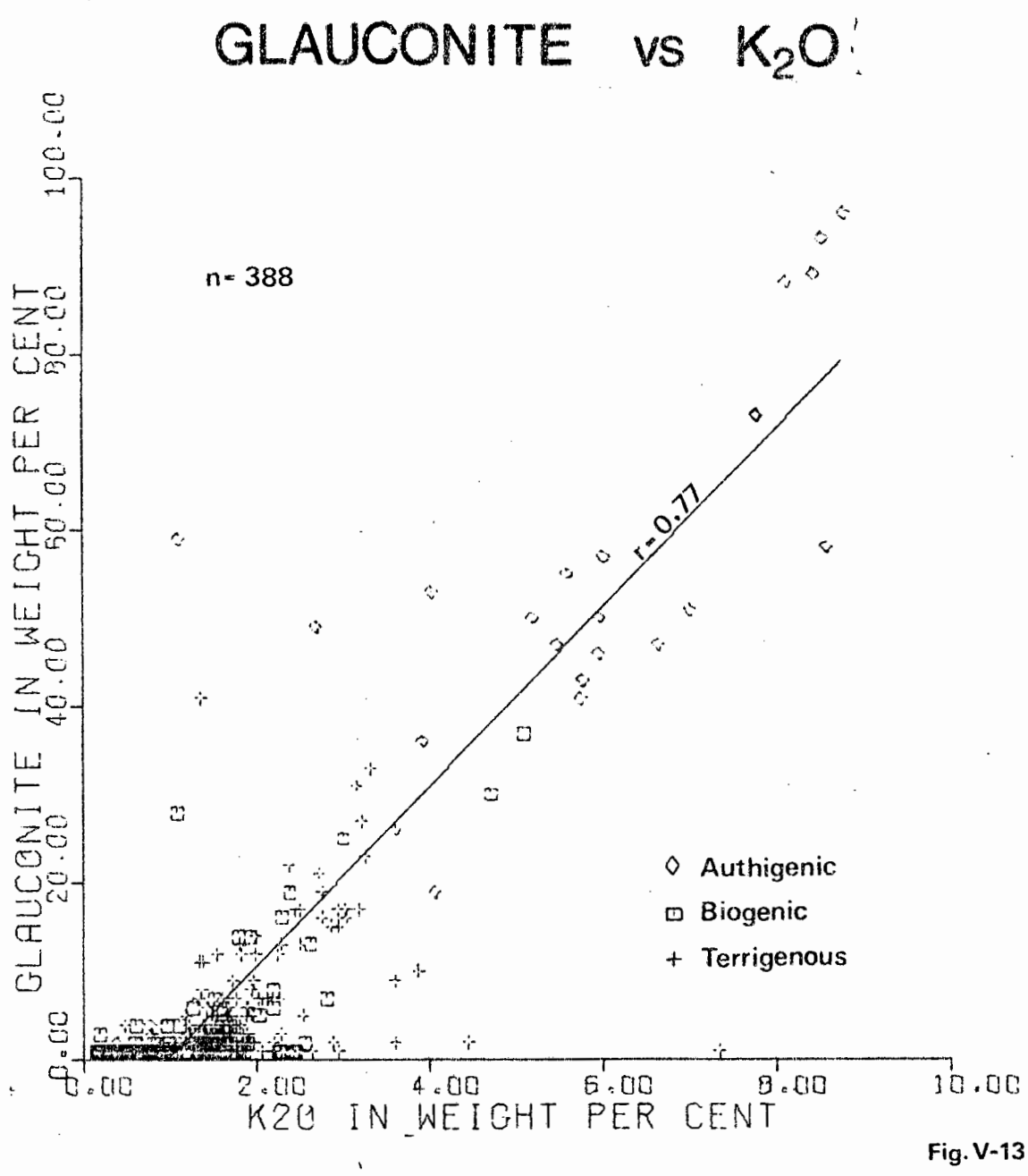
GLAUCONITE vs K_2O
n= 388
r=0.77
◇ Authigenic
□ Biogenic
+ Terrigenous
GLAUCONITE IN WEIGHT PER CENT
0.00
20.00
40.00
60.00
80.00
100.00
0.00
2.00
4.00
6.00
8.00
10.00
K20 IN WEIGHT PER CENT

Fig. V-13

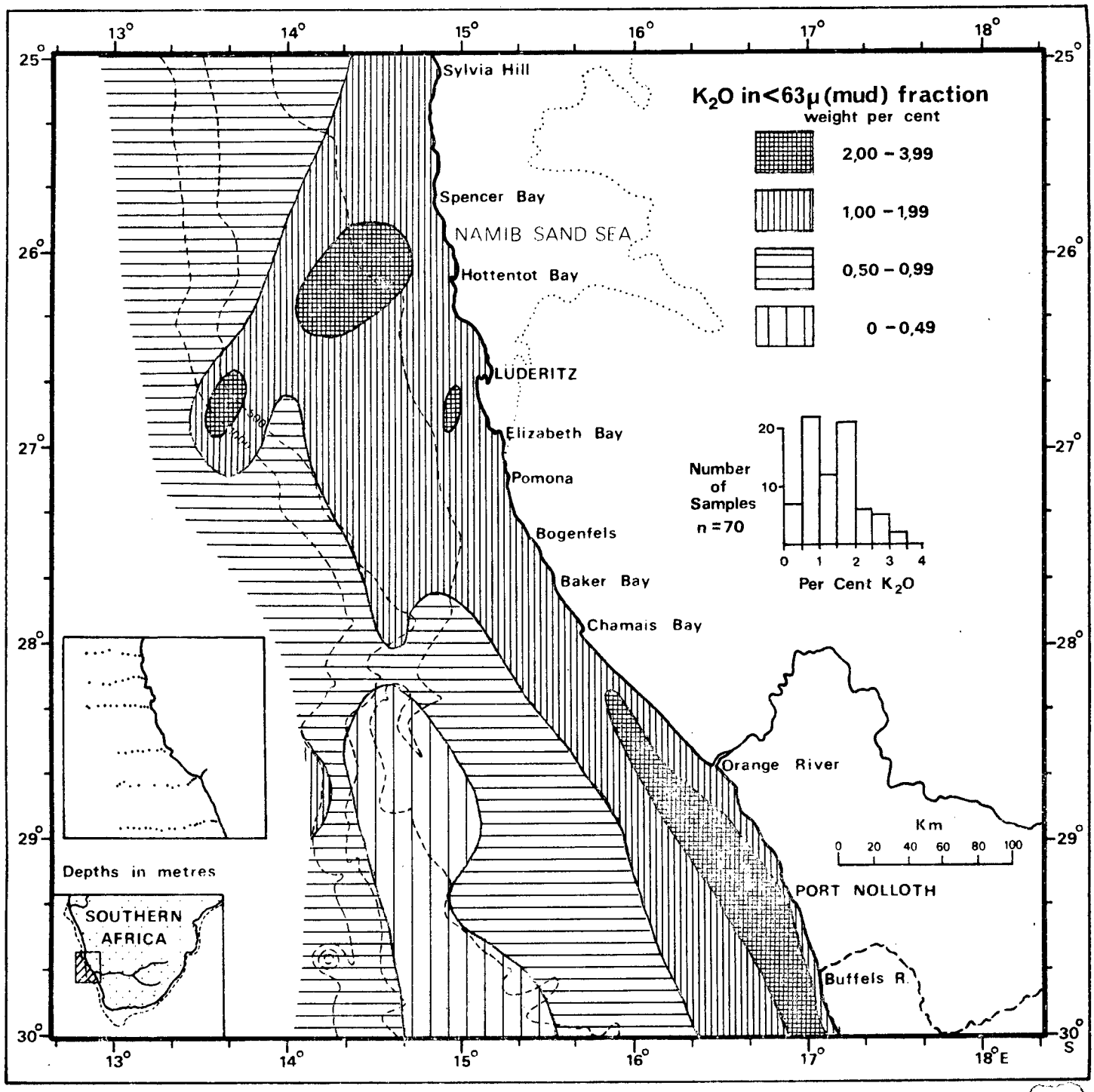
13°
14°
15°
16°
17°
18°
25°
26°
27°
28°
29°
30°
Sylvia Hill
Spencer Bay
NAMIB SAND SEA
Hottentot Bay
LUDERITZ
Elizabeth Bay
Pomona
Bogenfels
Baker Bay
Chamais Bay
Orange River
PORT NOLLOTH
Buffels R.
K_2O in<63μ (mud) fraction
weight per cent
2,00 - 3,99
1,00 - 1,99
0,50 - 0,99
0 - 0,49
Number of Samples n = 70
20
10
0 1 2 3 4
Per Cent K_2O
Km
0 20 40 60 80 100
Depths in metres
SOUTHERN AFRICA
18°E
S

Fig. V-14

off the Orange River (Figs. V-3 to V-9). Off Knoll Point (Fig. V-9) glauconite is confined to the very fine sand fraction and is located on the middle shelf. Off Hottentot Bay, Lüderitz, Chamais Bay and the Buffels River (Figs. V-8, V-7, V-6 and V-4) glauconite ranges from very fine to coarse sand-size. Off the Buffels River (Fig. V-4) glauconite is exposed on the middle shelf, midway between terrigenous sediment beside the inner shelf and foraminiferal sediment on the outer shelf. Off Chamais Bay (Fig. V-6) glauconite concentrations occur both on the middle shelf and at the foot of the Chamais Slump; glauconitic phosphorite was dredged from the slumped shelf break to the south of the profile. Glauconite also occurs on both the shelf and the slope off Lüderitz (Fig. V-7) but the shelf concentration becomes dominant as the Lüderitz Bank is approached off Hottentot Bay (Fig. V-8). There is a striking correlation between the morphological feature of Lüderitz Bank and the abundance of glauconite. Concentrations of up to 98% have been obtained, making parts of this deposit the richest found thus far on the continental margin of southern Africa. The grains are chiefly concentrated in the fine and very fine sand fractions. They are typically the well-rounded, polished and unsutured black to dark green variety reported by Birch (1971 and 1975) to be the dominant variety on the Agulhas Bank and on the shelf south of the study area.

C. PHOSPHORITE

1. Nomenclature

Several terms used in the following discussion of the phosphatic components of the sediment are defined first.

Phosphorite Bushinsky (1966) defined phosphorite as a marine sedimentary rock containing more than 18% P_2O_5. Sand-size pellets will also be referred to as phosphorite in this chapter, because they are considered to be intraclasts formed from phosphorite material.

Microsphorite Riggs and Freas (1965, p.10) originally defined microsphorite as "... a microcrystalline mud ... which is precipitated within the basin of deposition and shows little or no evidence of transportation. It occurs disseminated as a cement or binder to the terrigenous diluents; as discreet laminae and beds; and in organically controlled structures such as burrows, fossil molds, algae structures, and faecal pellets.".

Carbonate fluorapatite The mineral characteristic of phosphorites (Gulbrandsen, 1969; Tooms, Summerhayes and Cronan, 1969; Rooney and Kerr, 1967).

Francolite The fluorine-rich variety of carbonate fluorapatite.

Intraclast Folk (1962, p.63) first defined the term, but only applied it to carbonate sediments. Riggs and Freas (1965, p.12), in describing the phosphorites of Florida, used the word in the same sense as Folk, but applied it to microsphorite: "Intraclasts are particles of contemporaneous microsphorite beds, which were periodically torn up during periods of high energy, transported as clastic grains, and deposited within the basin as sands and gravels". Folk (1962, p.63) spoke of a wide size range from very fine sand to boulders, of variable forms from equant to highly discoidal, and of a high degree of rounding.

Pellet In several papers, (for example, Rooney and Kerr, 1967; D'Anglejan, 1967; Tankard, 1974a) the term "pellet" describes grains which are identical to the organic-rich phosphorite pellets discussed below. The terms "pelletal phosphorite rock" and "phosphorite pellet" avoid genetic implications and already enjoy wide acceptance in the literature. However, the terms "intraclastic phosphorite rock" and "microsphorite intraclast" are perhaps more precise if the model proposed by Baturin (1971, p.375) for the formation of such particles is correct. At this early stage of research into the South West African phosphorites and diatomaceous muds, it is premature to use the more precise terms for two reasons. Firstly, there is as yet little direct evidence to link microsphorite formation in diatomaceous muds and the formation of microsphorite intraclasts derived by disruption of microsphorite layers or concretions. Secondly, the term "microsphorite", although coined over ten years ago, as a term parallel to "micrite", and despite its potential, has not gained general acceptance. This may be due to a combination of two factors; the clumsiness of the word itself, and publication of the term in relatively inaccessible sources (Riggs and Freas, 1965; Freas and Riggs, 1968; Trueman, 1971). The term "pellet" is nevertheless unsatisfactory and should be replaced by "intraclast" as soon as it is justified by future research. In fact, pellets, as defined by Folk (1959, p.7) have a size range of 0,03 to 0,15 mm (coarse silt and very fine sand), whereas the phosphorite "pellets" generally have diameters between 0,125 and 0,5 mm (fine and medium sand). In addition, Folk (1959, p.7) considers the pellets to be faecal pellets in most cases, whereas the "pellets" under discussion are probably intraclasts.

2. Regional distribution

As in the case of glauconite, most of the sediments contain some phosphorite, with the general exception of inner-shelf terrigenous sediments and upper-slope biogenic muds (Fig. V-15). Pellets occur on the middle shelf off the Buffels River to Lüderitz and P_2O_5 values do not exceed 10% (Fig. V-15). Phosphorite-poor sediments on the inner and outer shelves have background values of less than 0,5% P_2O_5. North of Hottentot Bay, north of the Lüderitz Bank, a very rich deposit of phosphorite pellets is exposed on the outer shelf. Sands containing up to 26,4% P_2O_5 are blanketed by younger phosphorite-poor calcareous sediment on the upper slope and by younger organic-rich muds on the middle shelf. This residual deposit of phosphorite extends north towards Walvis Bay (Bremner, 1975a) where organic-rich diatomaceous muds cover the middle shelf (Calvert and Price, 1971a). The source of the phosphorite pellets is possibly pelletal-phosphorite bedrock, which has been sampled at station 3232 (25°22,0'S, 14°05,0'E) in a depth of 210 m (Summerhayes et al., 1973). The petrography and depositional history of this rock-type will be discussed in Section V-C-6. Its occurrence in association with seaward-dipping sub-bottom reflectors is discussed in Section II-4c (Fig. II-13).

Phosphatized foraminiferal infillings characterize the area between the inner and outer shelf breaks off the Buffels River. They are derived from a planktonic-foraminiferal limestone, friable fragments of which have been noted within samples of unconsolidated sediment. Texturally, the foraminiferal infillings are confined to fine and very fine sand (Fig. V-16), the fractions which normally contain the bulk of planktonic-foraminiferal sediments (Fig. V-4). Phosphorite pellets range in size from coarse to very fine sand (Figs. V-16 and V-9), reflecting their residual rather than biogenic origin.

Seawards of the Lüderitz Bank (Fig. V-8) unsutured black phosphorite is partially replaced in the medium-sand fraction by a highly sutured, orange-coloured variety, which has been mapped and analyzed by Bremner (in prep.) on the Walvis and Kunene shelves north of 25°S. He has shown by microprobe analyses that a nucleus of organic-carbon-rich, unsutured phosphorite is surrounded by a pellicle of highly sutured, orange-brown, slightly glauconitized phosphorite (Bremner, 1975, personal communication).

3. Carbon dioxide content

Most South African research on phosphorites has been concentrated on the abundant Agulhas Bank deposits (Parker, 1971; 1975; Parker and Siesser, 1972; Dingle, 1975). One feature of the francolite in the Agulhas Bank phosphorite rocks is a relatively high CO_2 content, which ranges from 5,3 to 5,9% with a mean value of 5,5% CO_2 (Parker, 1971). This is in sharp contrast to the Phosphoria Formation in the western United States of America (Gulbrandsen, 1970), where val-

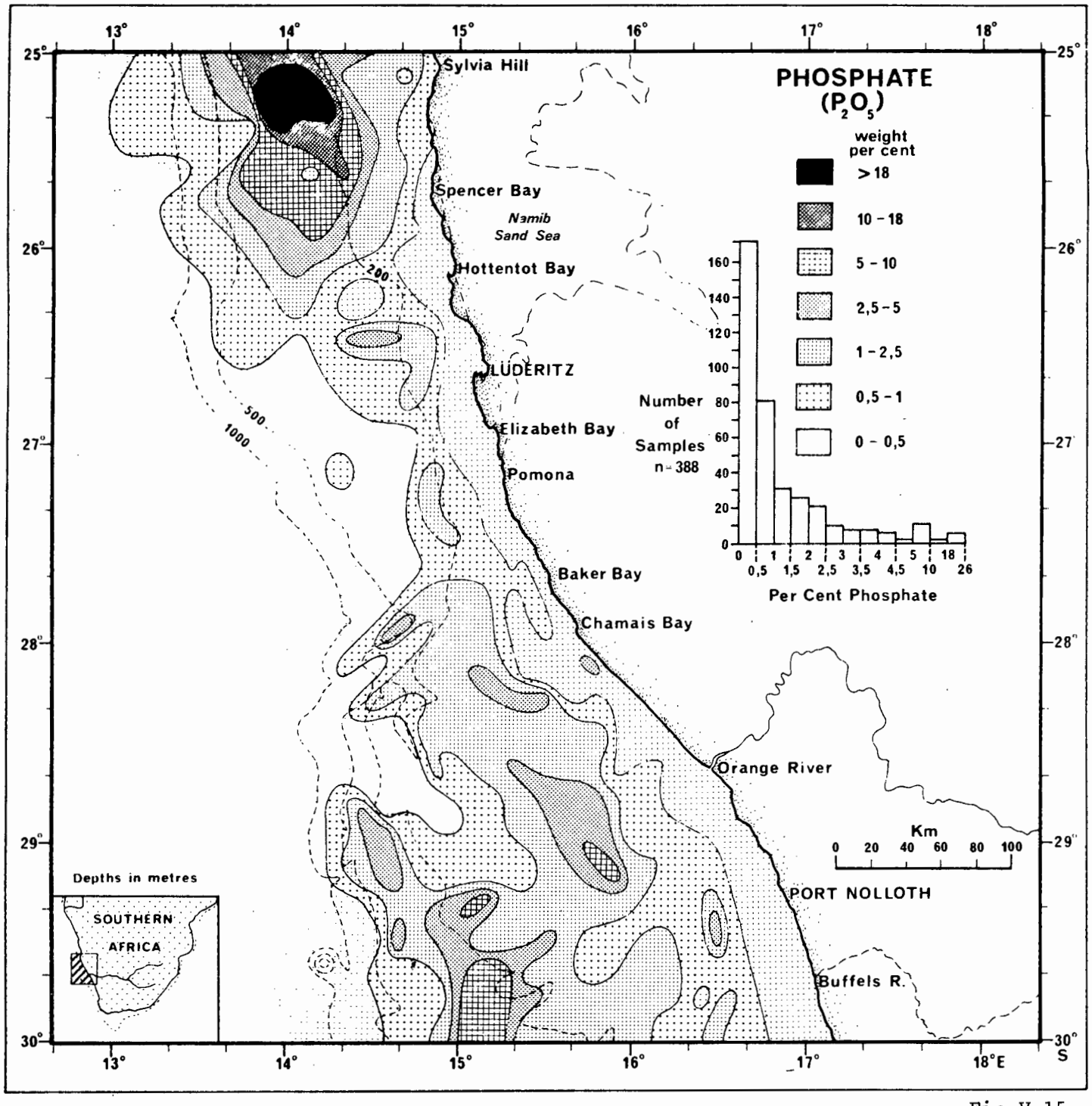
PHOSPHATE
(P_2O_5)
weight per cent
> 18
10 - 18
5 - 10
2,5 - 5
1 - 2,5
0,5 - 1
0 - 0,5
Number of Samples n = 388
Per Cent Phosphate
Sylvia Hill
Spencer Bay
Namib Sand Sea
Hottentot Bay
LÜDERITZ
Elizabeth Bay
Pomona
Baker Bay
Chamais Bay
Orange River
PORT NOLLOTH
Buffels R.
200
500
1000
Km
Depths in metres
SOUTHERN AFRICA
13°
14°
15°
16°
17°
18°
18°E
25°
26°
27°
28°
29°
30°
S

Fig. V-15

WEIGHT PER CENT CARBONATE-APATITE IN ONE-PHI SAND-SIZE FRACTIONS

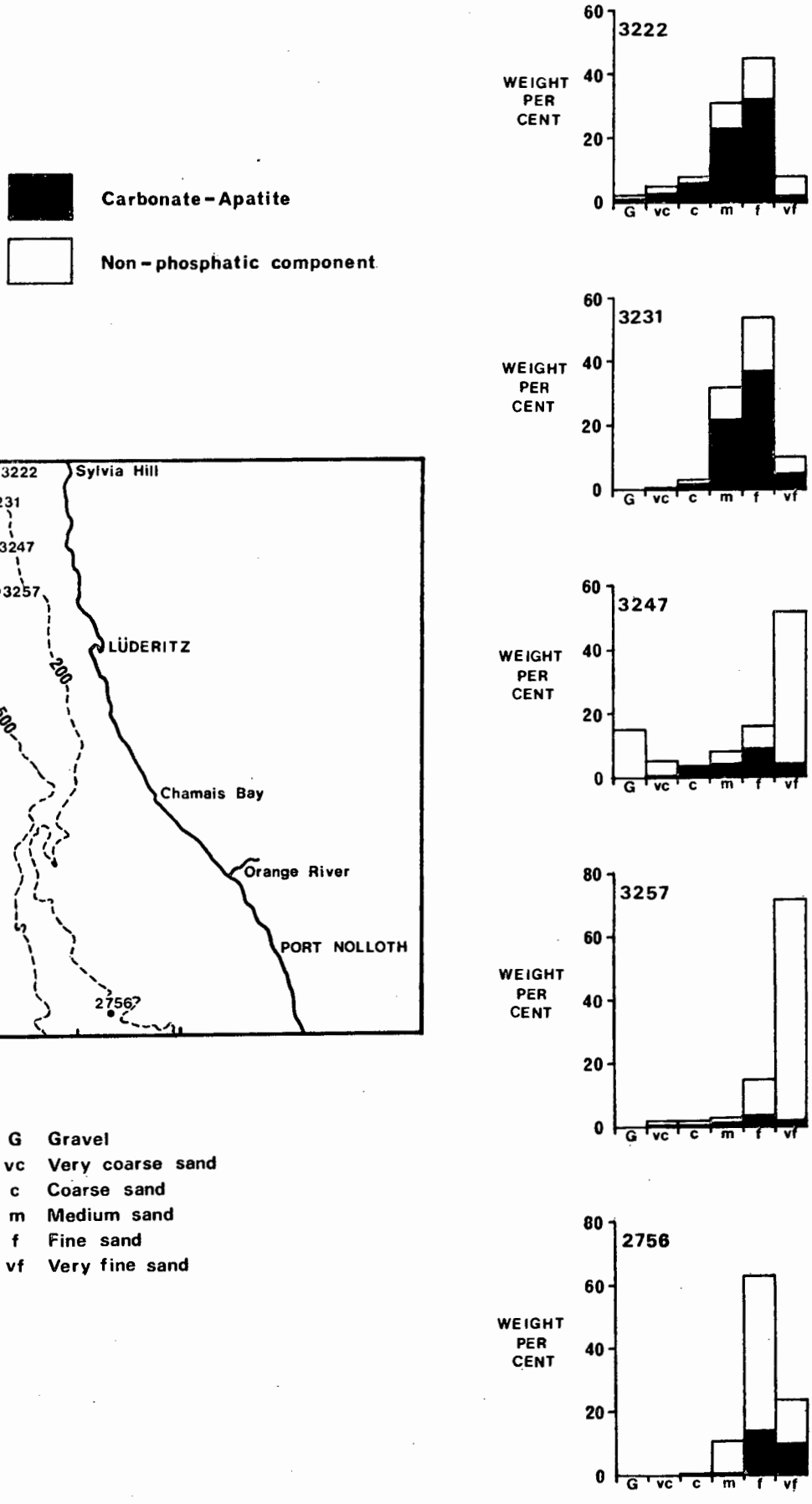

Fig. V-16

ues range from 0,5 to 2,7% CO_2 with a mean value of 1,8% CO_2. Bremner (1975a) analyzed 7 samples of phosphorite pellets from the Walvis shelf north of 25°S. Using the peak-pair method (Gulbrandsen, 1970) employed by Parker (1971) he obtained values ranging from 3,0 to 4,1% CO_2 with a mean value of 3,3% CO_2 midway between the Agulhas Bank and the Phosphoria results. Three samples of phosphorite pellets and one sample of phosphatized foraminiferal infillings have been analyzed by the writer (Fig. V-17). Phosphorite pellets exhibit a wide range from 4,3 to 5,8% CO_2 with a mean value of 5,1% CO_2. The highest vlaue was for sample 3232 from the station where pelletal-phosphorite rock was dredged. This value is surprisingly high, because the phosphorite rock represents the source for the pellets analyzed by Bremner (1975a), who obtained consistently lower values of CO_2.

4. Relationship of P_2O_5 to other variables

Senin (1969) has discussed the occurrence of phosphorite pellets in bottom sediments of the shelf between St Helena Bay (33°S) and the Kunene River (17°S), based on analyses of 140 samples. He described the interrelationships between phosphorus and mud, clay, median diameter, calcium carbonate and organic carbon. A negative relationship was observed with both mud and with clay and the highest concentrations of phosphorus were associated with fine and medium sands (cf. Fig. V-16). No trend was observed in the P versus $CaCO_3$ plot, nor in the P versus organic carbon plot. However the latter plot was based on only 28 samples and therefore Senin (1969) queried its validity.

The present writer's data, based on analyses of approximately 400 samples, likewise show no clear trend between either P_2O_5 and $CaCO_3$, or between P_2O_5 and organic carbon. An indication of a positive relationship between P_2O_5 and organic carbon (Fig. V-18) is noted in samples containing more than 6% organic carbon, from the middle shelf and the upper slope north of Lüderitz (Chapter VIII). However no comparable trend is seen in the diatomaceous oozes on the middle shelf off Walvis Bay (Bremner, 1976, personal communication), which is attributed to rapid recycling of phosphate back into the sea water after the death of planktonic organisms.

Like Senin (1969) the writer found negative relationships between P_2O_5 and mud as well as clay; conversely there was a weak positive relationship between P_2O_5 and sand. In contrast, the P_2O_5-content of a small suite of mud samples (Fig. V-19) was markedly low (less than 1% P_2O_5). Nevertheless the P_2O_5-content increases steadily northwards towards both the P_2O_5-rich residual sands on the outer shelf and the organic-rich muds on the middle shelf, again stressing the importance of phosphate, both residual and modern north of Lüderitz.

CARBON DIOXIDE CONTENT OF PHOSPHORITE TYPES

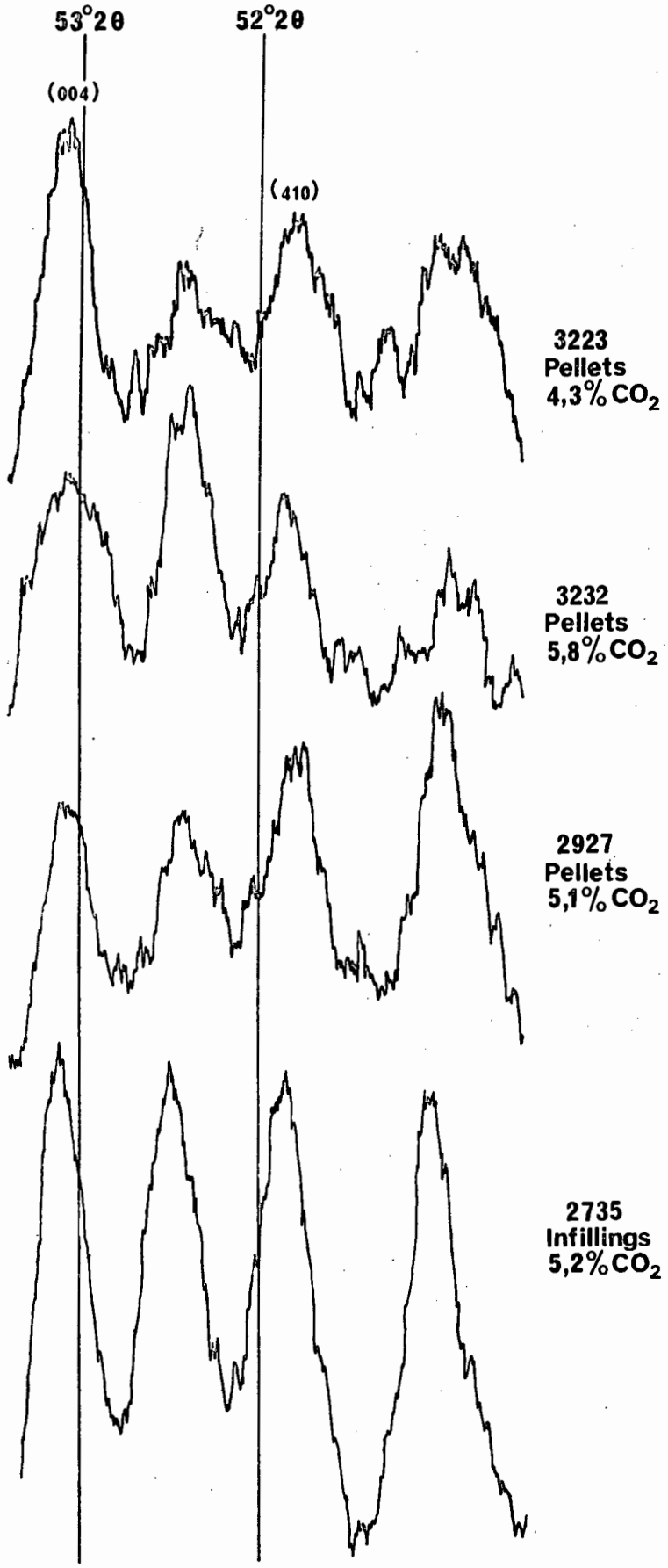

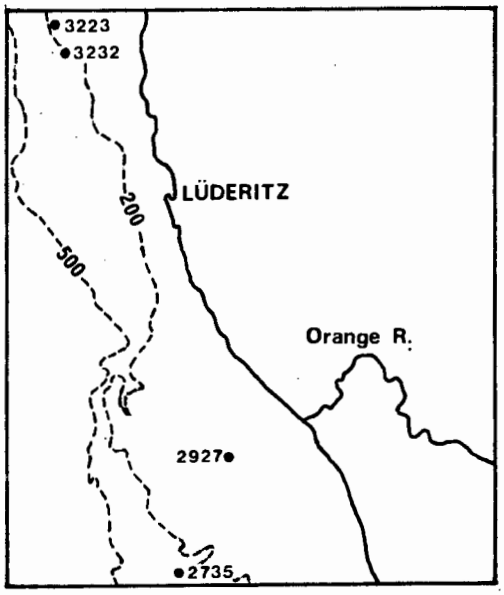

Fig.V-17

P_2O_5 vs ORGANIC CARBON

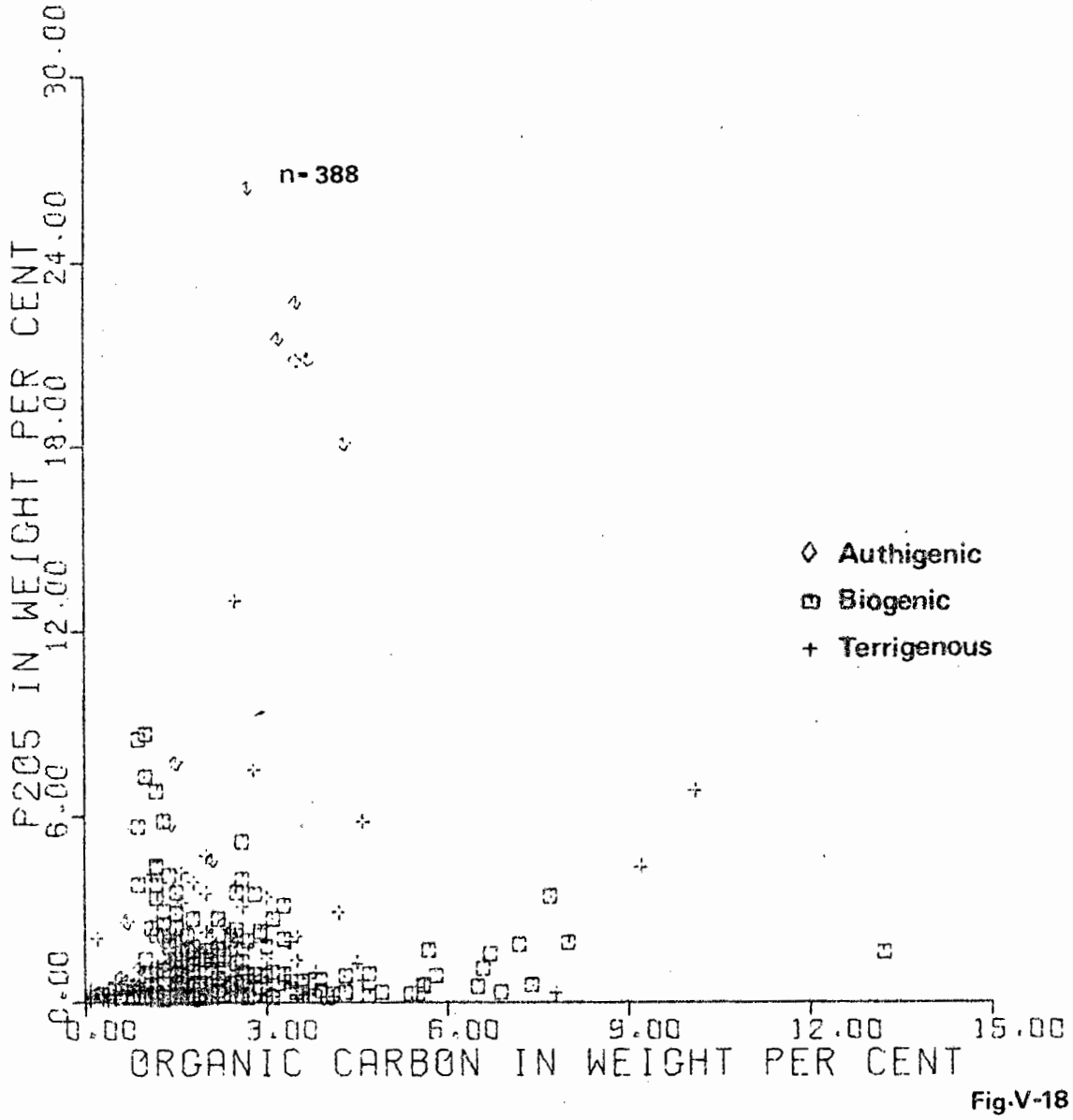

Fig.V-18

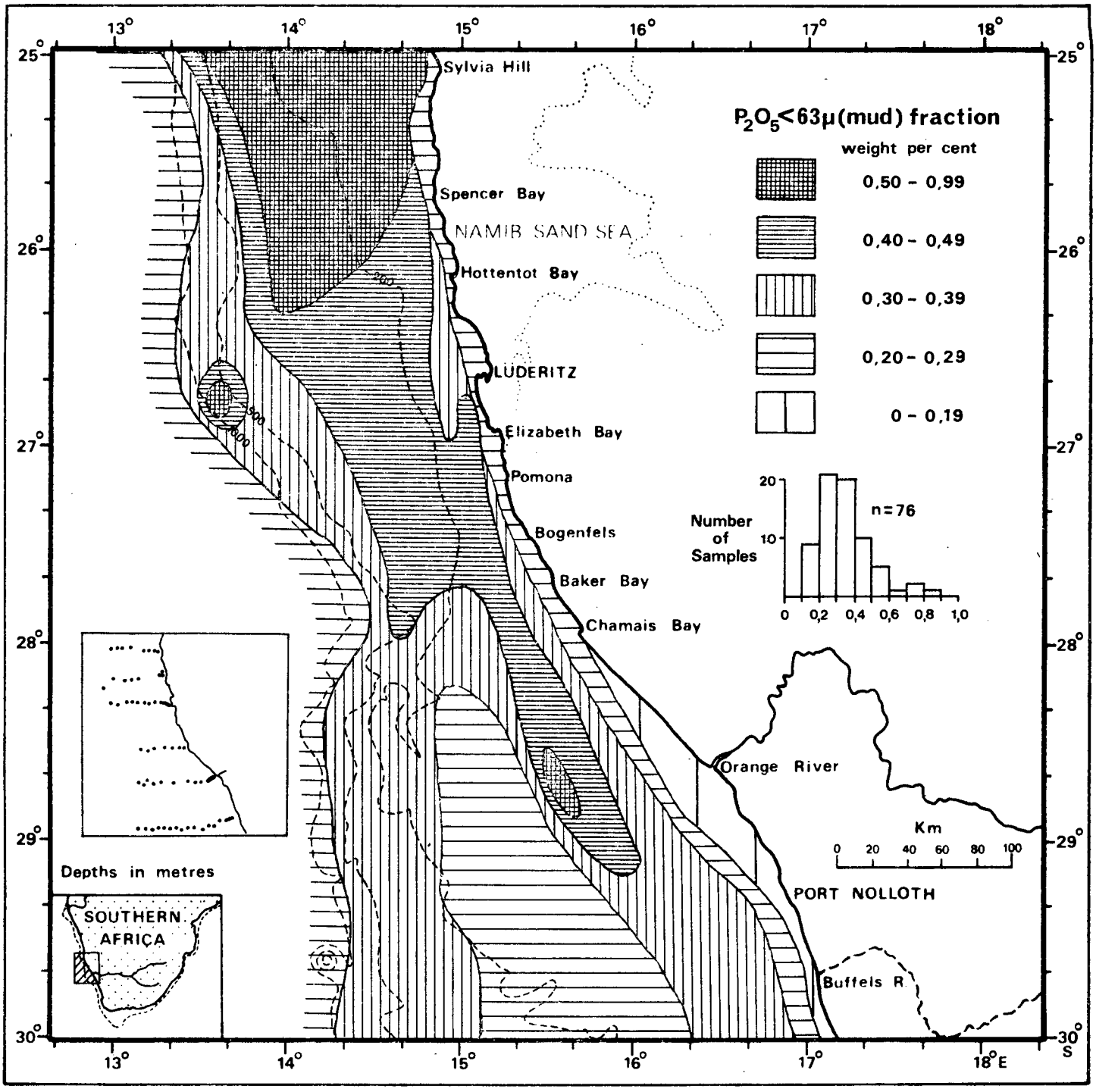
13°
14°
15°
16°
17°
18°
25°
26°
27°
28°
29°
30°
Sylvia Hill
Spencer Bay
NAMIB SAND SEA
Hottentot Bay
LUDERITZ
Elizabeth Bay
Pomona
Bogenfels
Baker Bay
Chamais Bay
Orange River
PORT NOLLOTH
Buffels R.
P_2O_5<63μ(mud) fraction
weight per cent
0,50 - 0,99
0,40 - 0,49
0,30 - 0,39
0,20 - 0,29
0 - 0,19
Number of Samples
n=76
0 0,2 0,4 0,6 0,8 1,0
Km
0 20 40 60 80 100
Depths in metres
SOUTHERN AFRICA
18°E
S

Fig. V-19

5. Relationship of phosphorite to shelf morphology and to sediment texture

The textural variations of the phosphorite pellets were discussed in Section C.1. Figure V-4 demonstrates the localization of phosphatized foraminiferal infillings, over the inner shelf break off the Buffels River. Off the Orange River, Chamais Bay and Lüderitz (Figs. V-5 to V-7) phosphorite is found on the middle shelf. Its presence on the middle shelf off Lüderitz beside the inner shelf-break and seaward of a glauconite concentration, also on the middle shelf, is significant because these residual components were probably derived from Neogene phosphorite rocks and Palaeogene quartzose limestones, respectively. The seismic profile from this region across the middle shelf was interpreted as a Tertiary sequence by Du Plessis et al. (1972) and as a Quaternary deltaic sequence by Dingle (1973a). The sedimentological evidence favours the former interpretation, because the Recent deltaic sediments off the Orange River are typically phosphorite-deficient.

The profiles in Figures V-4 to V-9 illustrate that phosphorite maxima are usually found adjacent to glauconite maxima. This characteristic is brought out in Figure V-20. Glauconite maxima on the Orange shelf occur on the flanks of a broader phosphatic zone. It is suggested that the phosphorite is derived from both the Miocene phosphatic limestones capping the Orange Banks (Fig. II-7) as well as from the underlying strata, which crop out on the middle shelf. Glauconite on the landward side of the broad middle shelf is probably derived from yet older (probably Palaeogene) strata (Dingle, 1973a) but on the outer shelf it is derived from Dingle's (1973a) T3 sediments between the inner and outer shelf breaks.

On the Walvis shelf, the two belts of glauconitic sediment between Chamais Bay and Lüderitz may be related to the same horizon. Off Chamais Bay (Fig. V-6) the seaward maximum occurs at the foot of the Chamais Slump. It is suggested that glauconite is derived from a horizon cropping out on the middle shelf off Baker Bay, which is re-exposed by the Chamais Slump. Similarly the extensive deposit on the Lüderitz Bank may be linked to the glauconite maximum on the upper slope by slumping and exposure of a continuous glauconitic horizon underlying the outer shelf (cf. Fig. II-6 for location of slumping on the upper slope).

In contrast to the Orange shelf, where a weak antipathetic relationship was observed between glauconite and phosphorite, there is a marked antipathetic relationship between the two components on the Walvis shelf (Fig. V-20). This is in contrast with the shelf south of latitude 30°S (Birch, 1975) and to the Agulhas Bank (Birch, 1971) where both glauconite and phosphorite are typically closely associated.

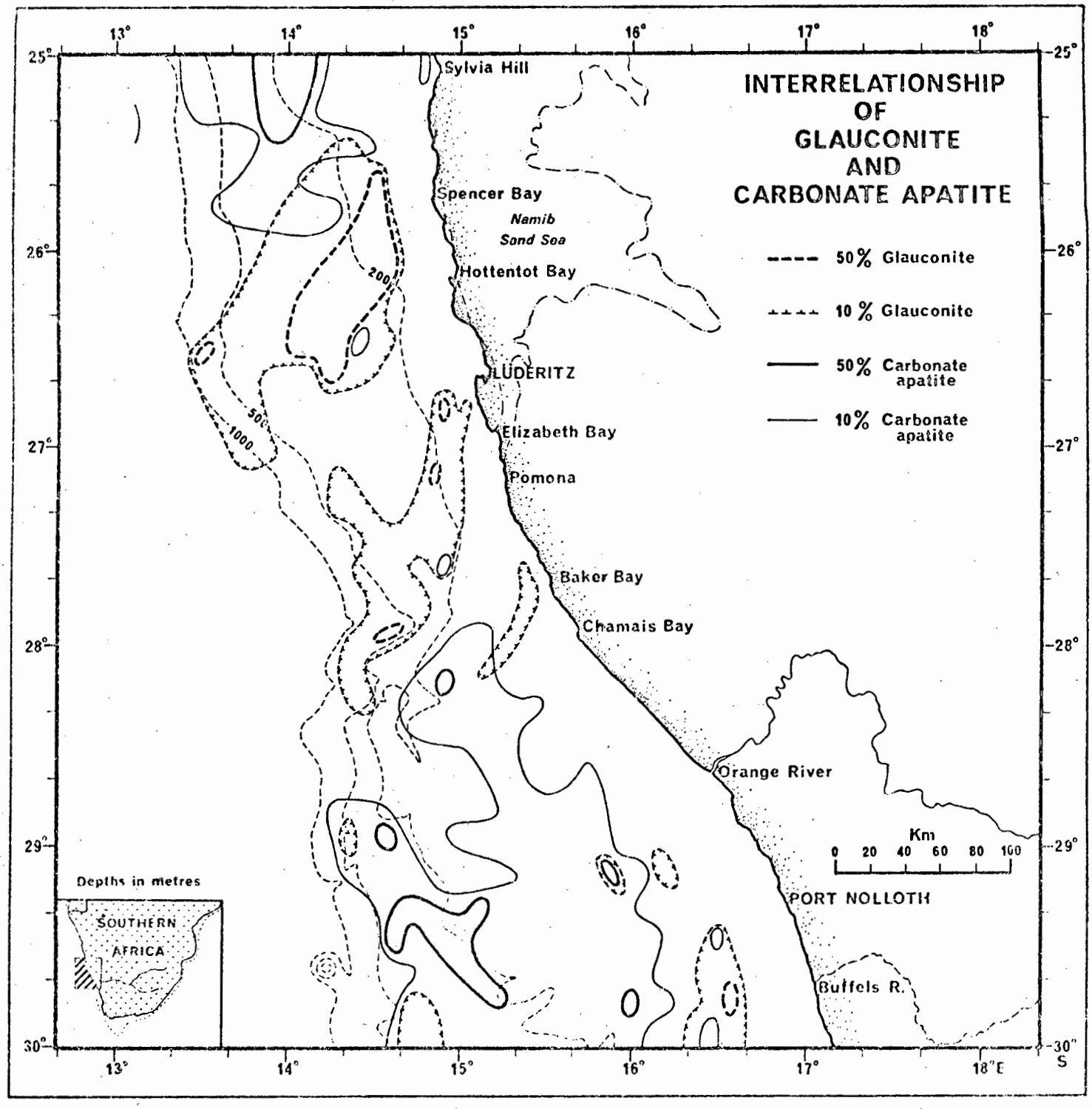
INTERRELATIONSHIP
OF
GLAUCONITE
AND
CARBONATE APATITE
50% Glauconite
10 % Glauconite
50% Carbonate apatite
10% Carbonate apatite
Sylvia Hill
Spencer Bay
Namib
Sand Sea
Hottentot Bay
LUDERITZ
Elizabeth Bay
Pomona
Baker Bay
Chamais Bay
Orange River
PORT NOLLOTH
Buffels R.
Km
0 20 40 60 80 100
Depths in metres
SOUTHERN
AFRICA
200
500
1000
13°
14°
15°
16°
17°
18°E
25°
26°
27°
28°
29°
30°S

Fig.V-20

6. Pelletal phosphorite source-rock

a. Location

The rock was dredged from a depth of 210 m on the outer shelf off Knoll Point at station 3232 (25°22,0'S, 14°05,0'E).

b. Petrography

The sample consists of several angular pebble-size fragments of pale greenish yellow (10Y7/2) phosphorite, containing dark brown lithoclasts (Plate V-1a) and an occasional molluscan cast. The phosphate value (26,2% P_2O_5, or 72,8% carbonate-apatite) is amongst the highest obtained thus far for any rock on the southern African continental margin.

The phosphorite is classified as slightly pebbly fine to medium phosparenite:quartz-rich pelletal phosphate wackestone. Intergranular fabric is composed of a mixture of 20% collophane and 20% micrite. Biogenic grains are restricted to small amounts (2%) of fish bones (Plate V-16) and traces of benthonic foraminifera. Angular very fine quartz sand constitutes 20% of the rock.

The lithofacies differs from all the lithofacies described in Chapter III, because authigenic grains are the dominant components. Phosphorite pellets constitute 30% of the rock. The pellets are very fine to medium sand-size, are chiefly spheroidal, and are rounded to well rounded (Plate V-1c). The few elongate ellipsoidal pellets usually display elongate nuclei, often of fish bones (Plate V-1d) and some have a poorly defined concentric structure (Plate V-1e). Most pellets have transparent, anisotropic rims around an opaque centre (Plates V-1c to V-1e). Bremner (personal communication, 1975) has analyzed pellets from this rock sample as part of a detailed microprobe study of unconsolidated residual phosphorite pellets on the Walvis shelf. He finds that both the pellets and the intergranular fabric of the rock sample are rich in carbonate-apatite, but that the transparent rims of some of the pellets are slightly glauconitized. The opaque centres of the pellets are rich in pyrite, probably formed by the processes described in Chapter IV. Birch (1975, p.79, Plate IV-21) obtained similar results for phosphorite pellets from the shelf south of 30°S.

c. Depositional environment and diagenesis

Several of the petrographic characteristics of this rock can be explained by invoking a depositional process similar to that invoked for the conglomeratic phosphorite rocks described in Chapter III. Both the pellets and the lithoclasts have been reworked from an older formation under high-energy conditions. I suggest that the original environment of deposition of the reworked material was within highly reducing, organic-rich diatomaceous muds like those off Walvis Bay today. Veeh et al. (1974, p.190) reported: "Thin unconsolidated laminae and lenses of phosphatized muds, presumably 'incipient' phosphorite, made visible by

Plate V-1. Petrography of pelletal phosphorite and surface texture of residual quartz grains

V-1a. Fragment of older phosphorite containing fish debris within pelletal phosphorite (Sample 3232C).(X20).

V-1b. Pellets and fish debris in pelletal phosphorite. (Sample 3232C).(X20).

V-1c. Spheroidal pellets rich in opaque material, chiefly organic matter, set in organic-free matrix. Note transparent pellicle around most pellets. (Sample 3232C).(X70).

V-1d. Two ellipsoidal pellets with nuclei of fish debris. (Sample 3232C).(X70).

V-1e. Faint indications of concentric structure in spheroidal pellet. (Sample 3232C).(X70).

V-1f. Well-rounded quartz grain from relict, residual deposit on middle Orange shelf. (Sample 2743).(X20).

V-1g. Impact pits on quartz grain relict from Neogene regression, stringers of reprecipitated silica from prolonged burial in sea water. (Sample 2743).(X2500).

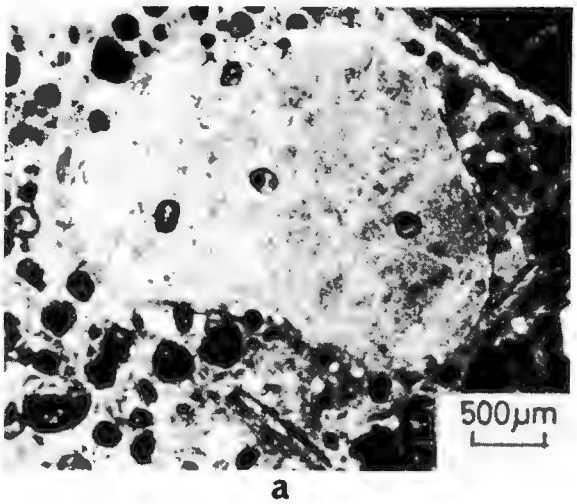

a

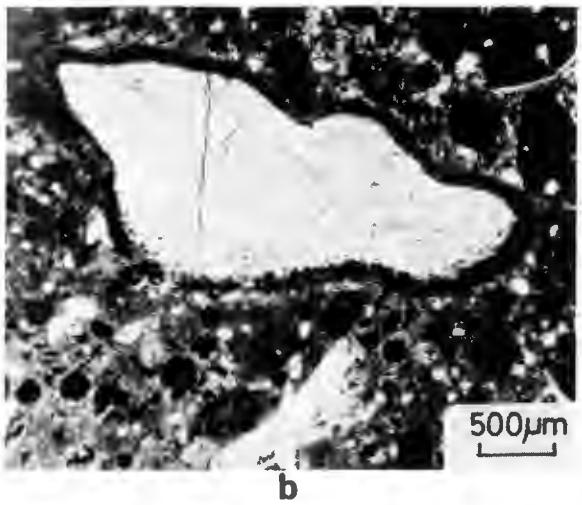

b

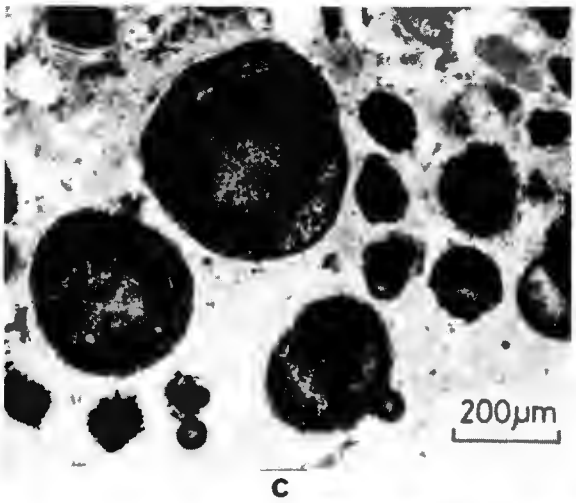

c

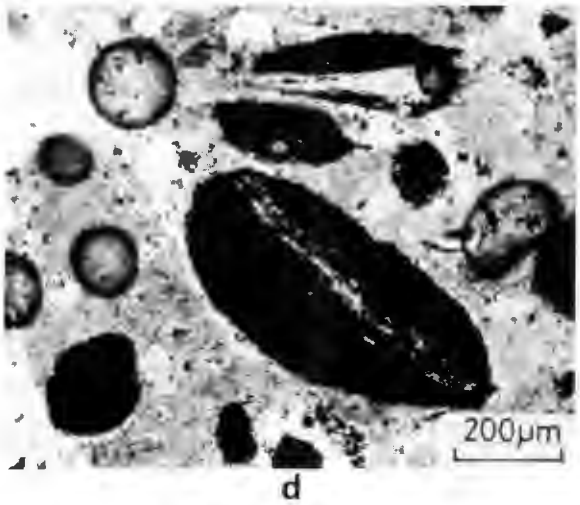

d

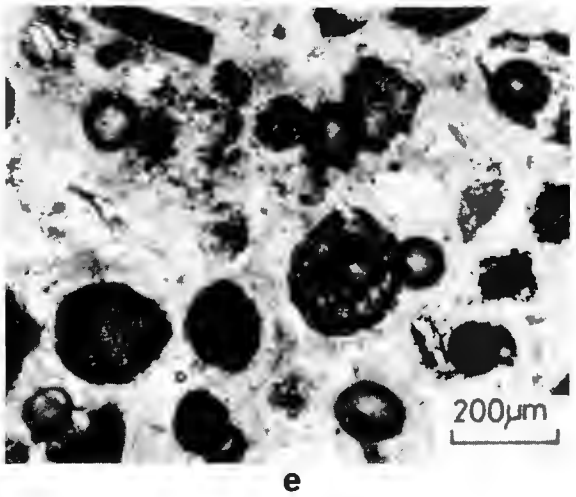

e

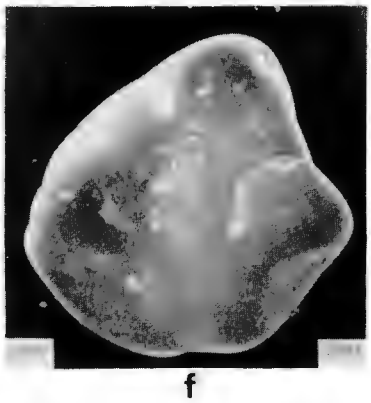

f

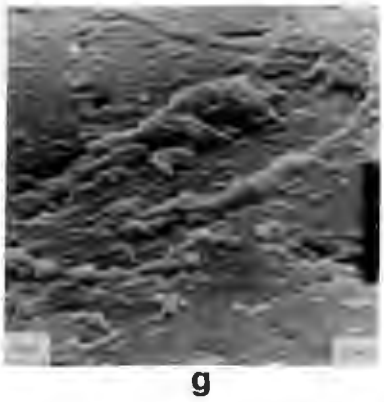

g

Plate V-1

X-ray radiography (Fig. 2) ..." within the diatomaceous muds. Such laminae and lenses fall within the definition of microsphorite as do Recent phosphatic concretions discovered off Peru (Veeh et al., 1973). Baturin (1972, p.85) favours in situ precipitation of carbonate-apatite from interstitial solutions supersaturated with phosphate. His model has also been adopted by Burnett (1974, p.150) to explain the formation of Peruvian phosphorite rock.

Baturin (1971, p.375) has proposed a sedimentation model to account for the presence of phosphorite pellets on the outer shelf off South West Africa. He invokes lowering of sea level to wash out diatomaceous fines, to disrupt the microsphorite laminae and lenses, and to sort and round the resultant intraclasts in the surf zone. Repetition of this cycle would lead to a substantial deposit of phosphorite pellets.

The discovery of the pelletal phosphorite rock under discussion adds a further stage to the history of the deposit. Assuming that the organic-rich pellets in sample 3232C are intraclasts, one must account for the fact that the intergranular fabric is a mixture of both collophane and micrite with little or no organic matter. Had the sea risen to its former level, this intergranular fabric would have been as rich in organic matter as the intraclasts. The small amounts of organic matter and the presence of micrite indicate that the sea rose to a higher level than previously, so that the intraclasts became buried by both phosphate- and carbonate-rich debris along the oceanward edge of the diatomaceous mud belt. The overlying waters were not as poorly saline or as cold as the water upwelling beside the coast, permitting coccolithophorids to intrude from the open ocean. At the same time, the greater depth of water, coupled with smaller amounts of organic matter allowed bacteria greater opportunity to decompose organic matter before it reached the sea floor. The resultant sediment locally became lithified to form phosphorite bedrock.

The mixture of micrite and collophane in the intergranular material may indicate that an original matrix of carbonate mud was partially replaced by carbonate-apatite (Ames, 1959; D'Anglejan, 1968). This would be in contrast to the direct-precipitation process postulated for the organic-rich pellets or intraclasts as proposed by Burnett (1974).

d. Age

It is probable that the original intraclasts were washed out of their original diatomaceous muds during the Late Miocene-Early Pliocene regression proposed by Dingle and Scrutton (1974). No direct palaeontological information is available on the age of the phosphorite.

e. Comparable deposits

Similar deposits of phosphorite pellets of Neogene age are found near Sal-

danha, 150 km north of Cape Town, in Florida, North Carolina, and on the continental shelf off Baja California. The petrology and origin of Pliocene phosphorite pellets in the Varswater Formation near Saldanha have been described by Tankard (1974a). The pellets were reworked from the well-consolidated Saldanha Formation, a quartzose phosphorite rock tentatively dated as Miocene (Tankard, 1975a) by correlation with a similar lithology, bearing Miocene penguin bones near Cape Town (Simpson, 1973). A similar sequence of events in Florida led to the deposition in the Miocene of the Noralyn Member of the Bone Valley Formation, which was reworked in the Pliocene during the deposition of the overlying Homeland Member (Freas and Riggs, 1968). Rooney and Kerr (1967) describe a similar deposit of phosphorite pellets in North Carolina, focussing on the pellets' mineralogy. Finally, D'Anglejan (1967) described a residual shelf deposit off Baja California between latitudes similar to those of the study area. No source-rock was detected on the shelf but the study is solely devoted to pellets completely analogous to those which are studied only as a section of both this study and that of Bremner (1975a).

D. QUARTZ

1. Regional distribution and relationship to shelf morphology

Muddy sediment containing coarse quartz grains overlies the belt of rocky topography on the middle shelf south of the Orange River (Figs. V-21 and V-4). This anomalously coarse terrigenous sediment lies seaward of Recent terrigenous muds, and presumably forms a lag deposit beneath the mud. Sediment immediately seaward of the most quartzose samples is rich in glauconite, as well as in well-rounded, granule-size, quartzose and glauconitic phosphorite lithoclasts. A seaward change in bedrock lithology is indicated. Farther seawards foraminiferal sediment covers the sea floor. The quartzose sediment is therefore fortuitously exposed between zones of biogenic and terrigenous Recent sediments.

Off Lüderitz (Figs. V-21 and V-7) quartz is found across the entire shelf and on the upper slope. It is chiefly restricted to the very fine sand fraction, unlike the coarser material just described.

2. Depositional history

A detailed study of surface textures of quartz grains in the coarse sand fraction (Rogers and Krinsley, in prep.) indicates that the grains are well rounded, polished, pitted and grooved (Plates V-1f and V-1g) in a similar fashion to grains studied from a beach on the exposed west coast of Namaqualand (Plates VII-a to VII-c). Granules within the sediment, however, contain similar well-rounded and pitted grains indicating a local source of grains that have already undergone at least one cycle of littoral modification. The writer suggests that, like the

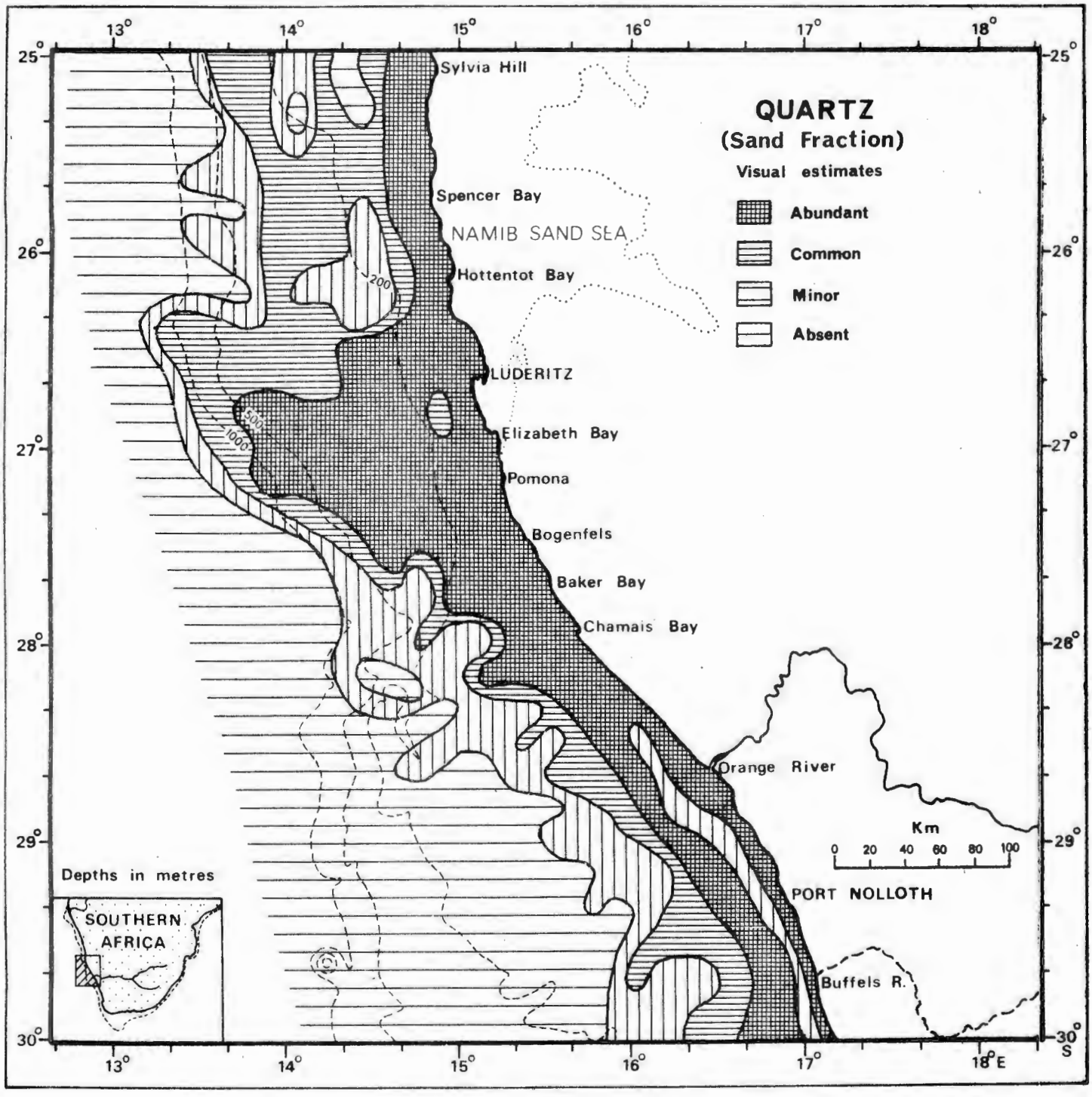
QUARTZ
(Sand Fraction)
Visual estimates
Abundant
Common
Minor
Absent
Sylvia Hill
Spencer Bay
NAMIB SAND SEA
Hottentot Bay
LUDERITZ
Elizabeth Bay
Pomona
Bogenfels
Baker Bay
Chamais Bay
Orange River
PORT NOLLOTH
Buffels R.
Km
0 20 40 60 80 100
Depths in metres
SOUTHERN AFRICA
200
500
1000
13°
14°
15°
16°
17°
18°
18°E
25°
26°
27°
28°
29°
30°
30°S

Fig. V-21

phosphorite pellets, the original sandstone was deposited during a Late Miocene Early Pliocene regression (Dingle and Scrutton, 1974). The present deposit of coarse quartz sand was produced during a Late Pliocene-Early Pleistocene regression (Dingle, 1973a).

Off Lüderitz the outer shelf and the upper slope are underlain by semi-consolidated Neogene clays (cf. Chapter IV). The coarse fraction of these clays is dominated by very fine quartz sand, which was reworked and winnowed during the Late Pliocene regression mentioned above.

E. CONCLUSIONS

Residual sediments in the form of glauconite and phosphorite pellets are easily identified in middle-shelf to upper-slope sediments in the study area. Texturally anomalous deposits of both coarse and fine residual quartz sands are also recognized, seaward of Recent deposits of terrigenous mud. Both types of quartzose deposit contain residual grains of glauconite and of phosphorite. These residual sediments were probably derived from Tertiary sediments underlying the margin.

Pelletal phosphorite rock from the outer shelf north of Lüderitz may be a source-rock for the distinctive deposit of phosphorite pellets extending north past Walvis Bay (Bremner, 1975a). The pellets were probably formed in Miocene, organic-rich, diatomaceous oozes and reworked during a Late Miocene-Early Pliocene regression. They were then buried after the succeeding transgression and locally became consolidated as pelletal phosphorite rock.

CHAPTER VI

THE EFFECT OF PLEISTOCENE CLIMATIC VARIATION ON WEST-COAST SEDIMENTATION

A. MODEL FOR CLIMATIC CHANGE

I do not propose to discuss the ultimate causes of Pleistocene climatic fluctuations because these are treated in detail elsewhere (cf. Flint, 1971, Chapter 30). I will restrict myself to the effects of such changes on continental-shelf sedimentation and on the catchment areas of rivers draining towards the west coast, particularly between latitudes 25° and 30°S.

Penck (1914) proposed a simple model to explain the climatic fluctuations occurring through glacial-interglacial cycles. He proposed that during glacials the climatic belts shifted equatorward, by about 5° of latitude, and vice versa during interglacials. Van Zinderen Bakker (1967, 1975, 1976) applied this basic model to the Quaternary history of Africa. The model has subsequently been applied in a discussion of palynological data derived from Upper Quaternary cores near Cape Town (Schalke, 1973), to the distribution of Late Pleistocene molluscs in the southwestern Cape (Tankard, 1975b) and to evidence of climatic change in the Sahel region, south of the Sahara (Burke et al., 1971).

A discussion of modern seasonal fluctuations of climate is presented as a key to understanding both equatorward and poleward shifts of climate in the Pleistocene. The great significance of these drastic climatic changes on the discharge of terrigenous sediment onto the continental shelf is stressed.

B. THE MODERN CLIMATE OF SOUTHERN AFRICA

1. Introduction

The following summary of the complex climate of southern Africa is taken from descriptions supplied by Schulze (1965), by the Meteorological Services of the Royal Navy and the South African Air Force (1944) and by Van Zinderen Bakker (1976). The patterns detected by meteorologists after years of observations enable one to speculate on possible palaeoclimatic patterns. In Figure VI-1b and 1d the changing seasons of today's interglacial climate are simplified by Van Zinderen Bakker (1976).

2. Atmospheric controls

A subtropical belt of high pressure over the South Atlantic and Indian Oceans is flanked by low-pressure belts over the equator and over the Southern Ocean (Schulze, 1965). In the subtropical zone the stable South Atlantic anticyclone usually lies relatively close to the west coast, but shifts equatorward in winter and poleward in summer (Fig. VI-1). It is generally centred over latitude 30°S, but in summer a subsidiary anticyclone frequently lies south of Cape Agulhas

ATMOSPHERIC AND OCEANOGRAPHIC CIRCULATION DURING GLACIAL AND INTERGLACIAL TIMES

(From Van Zinderen Bakker, 1976)

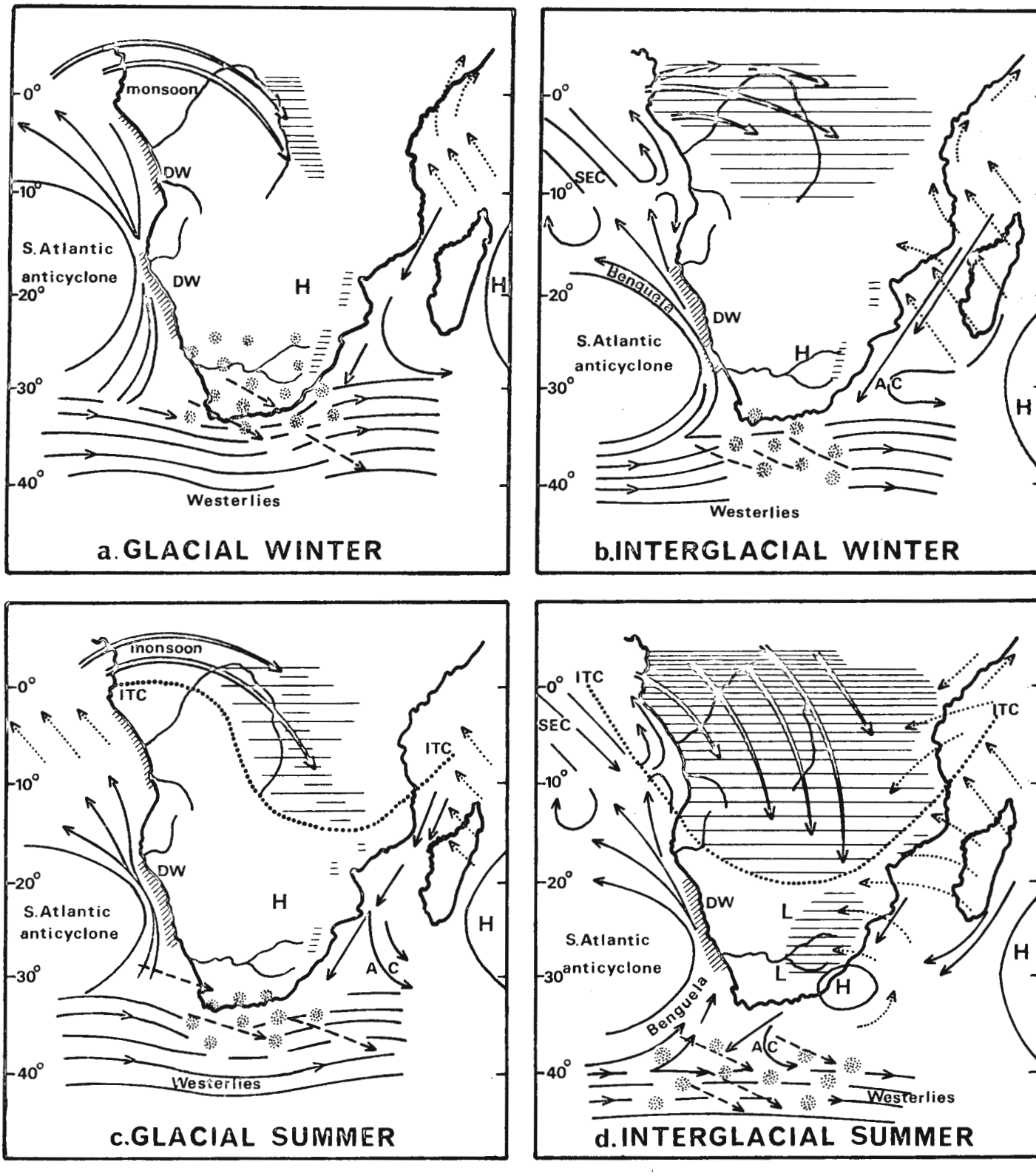

ITC *Intertropical Convergence*

DW *Dry Westerlies*

AC *Agulhas Current*

SEC *South Equatorial Countercurrent*

H *High pressure*

L *Low pressure*

Cyclonic rain

Upwelling

Intensity of precipitation

Moist 'monsoon'

Maritime air and SE Trades

Ocean currents

Trajectories of depressions

Fig.VI-1

($35^{o}S$) causing the sequence of southerly gales, upwelling, fog and aridity along the west coast as far north as Walvis Bay ($23^{o}S$) and beyond. The presence of a low-pressure cell travelling south over the west coast during summer increases the pressure gradient at the coast and powerful gales result (Van Zinderen Bakker, 1976, p.6). (The effects of these gales on sedimentary processes will be discussed in Chapters VII and VIII).

The Indian-Ocean anticyclone lies well to the east of southern Africa during summer, permitting moist maritime air to penetrate beyond the Drakensberg, where orographic rain precipitates over the headwaters of the Vaal and the Orange rivers (Fig. VI-1d. However if the anticyclone maintains a stable westward position beside the east coast in summer, the rain-bearing winds cannot reach the interior and droughts result.

In winter the high-pressure belt is found at the surface over both the oceans and the continent, leading to dry conditions inland. At the same time, equatorward shifting of the westerlies brings the southwestern and southern coasts into the path of the storm track of the Southern Ocean's westerlies (Fig. VI-1b. This cyclonic winter rain is precipitated orographically on the Western Cape mountains and on the Great Escarpment as far north as the Orange River, where it falls as a gentle drizzle (De Villiers and Söhnge, 1959, p.18).

Tropical convectional rain moves southward in summer as the Inter-Tropical Convergence shifts south with the sun. Rain is brought in this way to the catchments of the north-bank tributaries of the Orange River and to the intermittent rivers of South West Africa draining into the Namib Desert. The erosional effect of a rare summer thunderstorm as far south as Vioolsdrif on the Lower Orange River is vividly described by De Villiers and Söhnge (1959, p.18): "In summer thunder conditions may arise in the interior as a result of which restricted areas may receive more rain in an hour than they usually receive in a year or more. The authors were privileged to witness one such summer thunderstorm at Vioolsdrif, towards the end of November, 1943. The storm approached from the northwest and was heralded by a wind of gale force that swept sand and dust to a height judged to be at least 2,000 feet. This dust-storm swirled and eddied down all the tributary gorges into the Orange River and beyond to the sandy plains, and was followed by a deluge of rain swept along almost horizontally by the wind. So much rain fell that the shallow drainage-channels on the level portions of the Neint Nababeep Plateau were unable to accommodate the waters, which fell as roaring cataracts over the edge of the escarpment and formed a magnificent waterfall, miles long and as much as 700 feet high. All the tributaries to the Orange River were raging torrents, and water flowed where it had not been known to flow for years, transporting enormous quantities of sand and rubble .... Old alluvial fans were deeply incised ... and a new fan, containing gigantic boulders the size of a room, was

deposited at the edge of the old. This one storm gave some idea of the amount of transportation and deposition that can take place over a long period of time, even in deserts, as the result of water-action following sudden thunderstorms."

3. Oceanic controls

The atmospheric climatic controls are reinforced by the equally important oceanic controls. Moist maritime air crossing the cold upwelled water of the Benguela Current is condensed to form low cloud banks and fog along the arid west coast (Meteorological Services of the Royal Navy and the South African Air Force, 1944). The cloud cover simultaneously accentuates and alleviates the aridity of the west coast. By preventing rain from falling over the land it is a major cause of desert conditions. Any shift in the mean position of the Benguela Current and its associated cloud cover thus implies a shift in the mean position of the Namib Desert. At the same time a daily precipitation of dew and "mist-rain" accumulates to double the amount received from unreliable and rare showers in any one year (Meteorological Services of the Royal Navy and the South African Air Force, 1944). Succulents rely on this minimal but reliable source of moisture and can therefore play a role in sedimentary processes, particularly in Namaqualand where coastal fog is most prevalent (Meteorological Services ...., 1944). The dew also supports an abundant population of snails (mainly Trigonephrus spp.), whose shells are such a distinctive feature of Quaternary sediments on the west coast (Rogers, 1917).

Along the east coast the warm Agulhas Current facilitates evaporation leading to high relative humidity in the overlying atmosphere. In summer the uncommon but significant situation of a series of anticyclones, moving along the east coast from the south coast, causes the moist air over the Current to be drawn up to the Drakensberg Mountains (Fig. VI-1d. In contrast with the Namib Desert's mist rain and the winter showers of the southwestern Cape, the rain over the Drakensberg frequently occurs during thunderstorms and sometimes during hailstorms (Schulze, 1965, p.295). This intense orographic rain sometimes continues for more than two weeks causing catastrophic floods in the Vaal and in the Upper Orange Rivers (Schulze, 1965, p.7).

C. CLIMATIC CHANGE DURING PLEISTOCENE GLACIALS

1. Introduction

The seasonal cycle of climatic variation today reflects an equatorward shift during winter and a poleward shift during summer. In essence, the Penck-Van Zinderen Bakker model envisages Pleistocene glacials as extreme winters and interglacials to have climates similar to those prevailing today. We shall first examine the effect of climatic change during glacials when the southern part of

southern Africa experienced cooler and wetter conditions, while the northern region became cooler and more arid. During the same period sea level was lowered substantially. We shall then evaluate evidence of the reversal of these trends during interglacials. Tentative evidence of a steady equatorward shift of the interglacial position of the Benguela Current System is correlated with indications of reduced precipitation during the later Pleistocene interglacials.

2. Equatorward extension of the climatic belts

Evidence of a cooler and wetter climate would be expected during a glacial in the southwestern part of southern Africa. Butzer (1973a) and Tankard and Schweitzer (1974) have reported frost-shattered (cryoclastic) debris within coastal caves at Die Kelders, west of Cape Agulhas, and at Plettenberg Bay on the south coast. This led Butzer (1973b) to postulate a 10°C lowering in temperature at these sites during glacials. Schalke (1973) examined a core from the Cape Flats near Cape Town and found abundant (40%) Podocarpus pollen in peat with a Würm Interstadial date of $41\,500^{+2\,100}_{-1\,800}$ B.P. He pointed out that the tree is today restricted to the Knysna region, which receives a mean annual rainfall of 860 mm with no seasonal maximum. Today Cape Town receives 625 mm annually but with a pronounced winter maximum and a drought in summer.

On the west coast, Van Zinderen Bakker (1976, p. 31) estimates that winter rainfall reached as far north as Walvis Bay (23°S), which today receives a small amount of rain in summer. This is probable because Lüderitz, almost 4 degrees of latitude farther south, receives its meagre rainfall in winter (Meteorological Services ..., 1944). A steady poleward increase in the amount of winter rainfall reaching the Great Escarpment south of Walvis Bay would have rejuvenated most of the rivers of the Sperrgebiet and Namaqualand (Fig. VI-2). Today the most northerly perennial river is the Olifants River (32°S) and it lies north of the Sand Leegte, a dry river course which has not flowed in living memory (Visser and Toerien, 1971). A northward shift by 4° latitude of the winter rainfall belt would probably have resulted in perennial river flow as far north as latitude 28°S, north of the Orange River. Today the Uguchab River is found near latitude 28°S, but it is dammed by the Obib Dunes, which are blown northward from the Orange River during the dry season, some 45 km inland. During Pleistocene glacials it may have reached the sea at Chamais Bay, where there are clear traces of an old river course. South of the Orange River, in Namaqualand and in the southwestern Cape, all the rivers would have been perennial with a maximum discharge in winter. Today, the Holgat River (29°S), just south of the Orange River, is the most northerly winter-rainfall intermittent river that reaches the coast. Since it last flowed in 1925 it is obviously contributing little sediment to the shelf. An equatorward shift of 4° latitude during a glacial may have allowed the Tsauchab River near latitude 25°S to reach the sea, whereas it is today dammed by 300-m

WEST-COAST DRAINAGE DURING QUATERNARY GLACIALS AND INTERGLACIALS

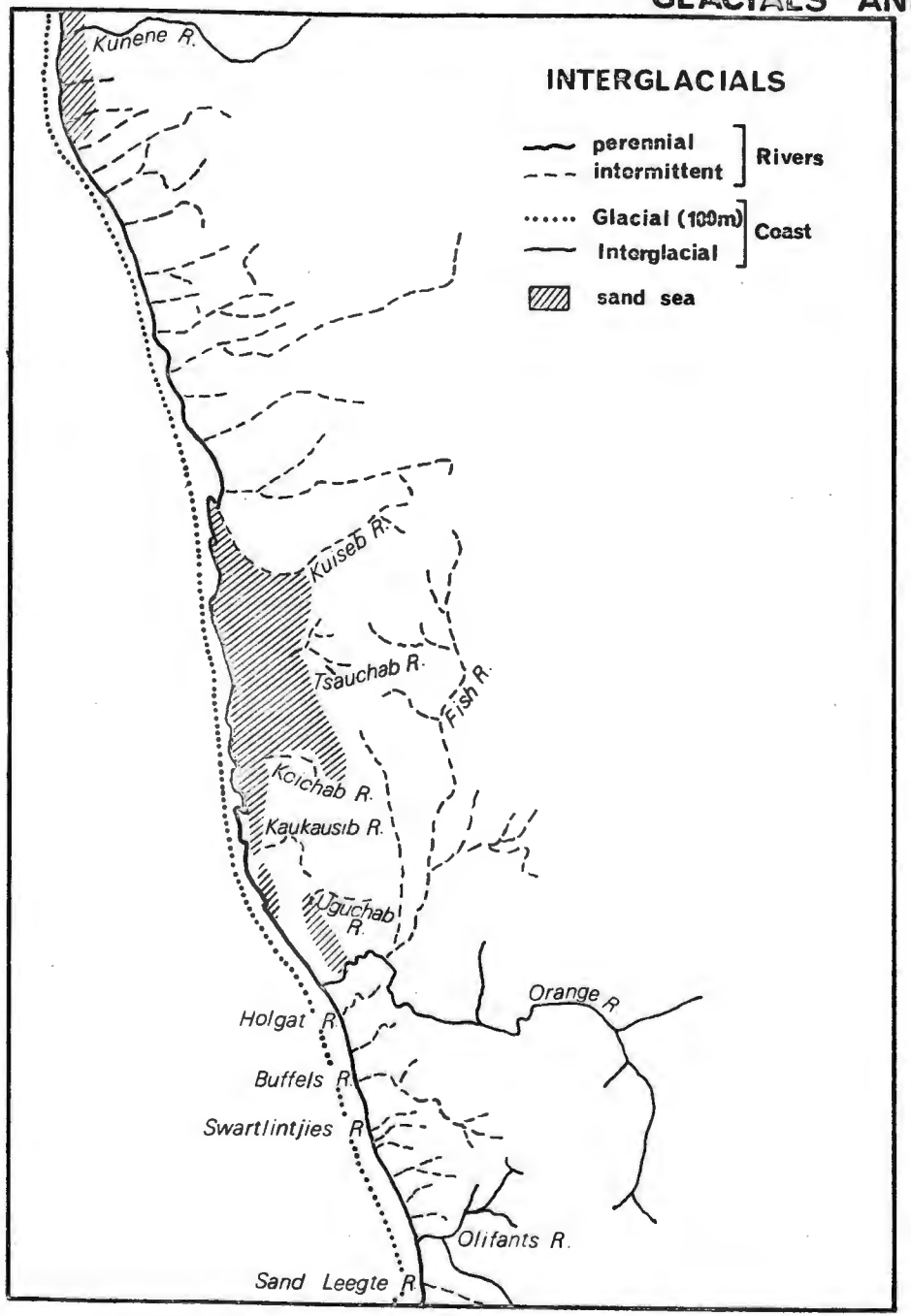

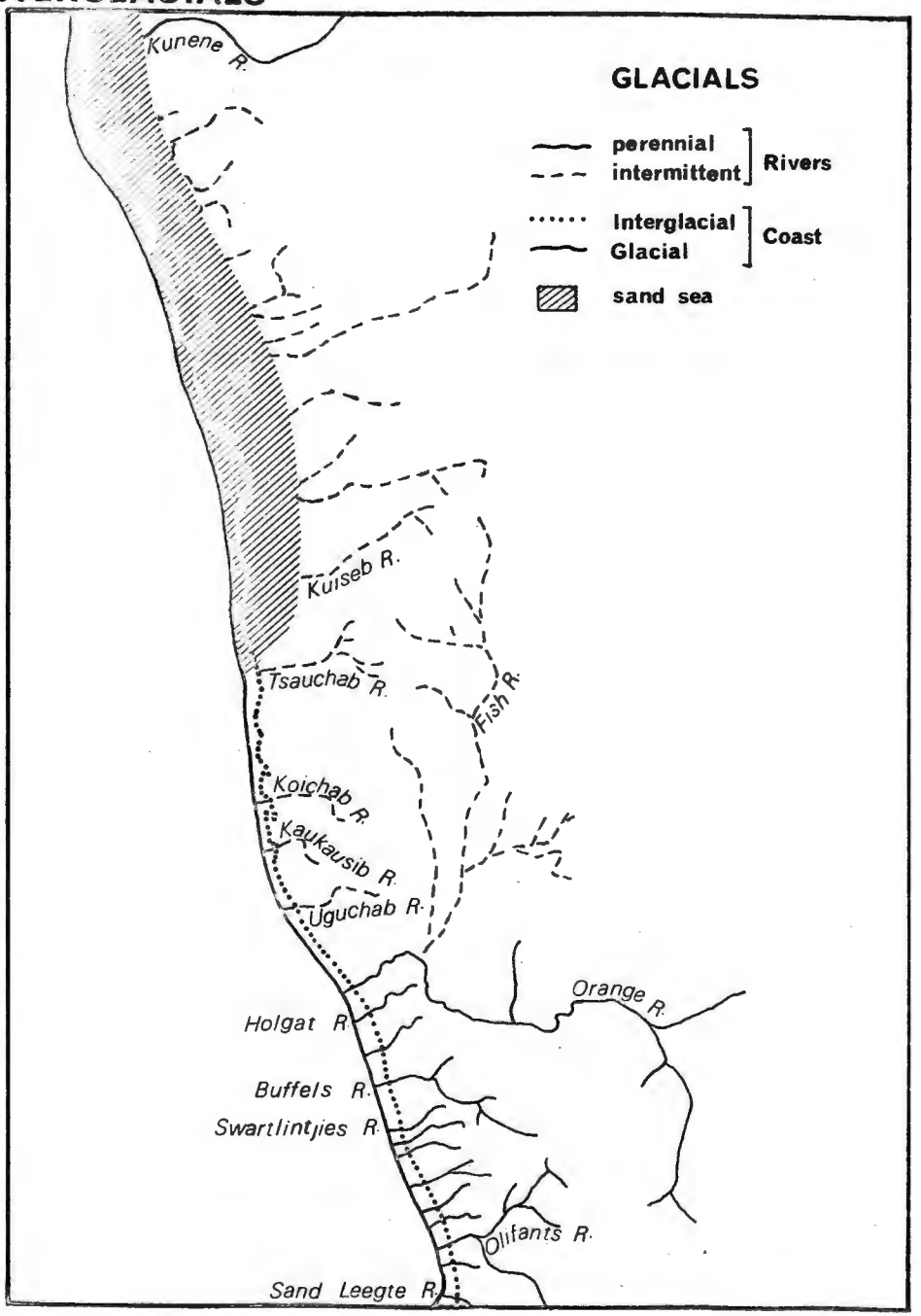

Fig.VI-2

high dunes at Sossus Vlei, in the heart of the Namib Sand Sea. Biogeographic evidence of moister conditions in Namaqualand is provided by Rourke (1972, p.187). He noted the isolation of four subspecies of Leucospermum proteas on four separate highlands from the Kamiesberge in Namaqualand to the Cold Bokkeveld mountains farther south. He remarked: "Climatic conditions prevailing today are such that migration between the four centres ... is impossible. It seems reasonable to assume that during a hypothermal (glacial) period, a single variable complex was distributed over this range. Subsequently, during periods of greater aridity populations survived only on the higher peaks such as the Kamiesberge ..."

3. The Orange River during glacial periods

a. The Vaal-Upper Orange catchment

Gevers et al. (1937) record that most of the scanty winter rainfall of Namaqualand today falls on the west-facing slopes of the Great Escarpment, and that very little winter rainfall crosses this watershed into the catchment of the Orange River. During glacials, however, Van Zinderen Bakker (1976) envisages deep eastward penetration of cyclonic winter rains into the interior (Fig. VI-1a). Supporting evidence for this may come from the palaeo-lake at Alexandersfontein, near Kimberley between the Vaal and the Upper Orange, where Butzer, Rock et al. (1973) found an abandoned shoreline 19 m above the lake floor. The authors postulated a 6°C drop in temperature and a doubling of the prevailing rainfall in order to fill the lake, but it could not be determined whether the wet season was in summer or in winter. Corroborating evidence of lower temperature and higher rainfall is given by Van Zinderen Bakker and Butzer (1973, p.238) who describe a marked decrease in Karoo under-shrub pollen (Compositae) and an increase in grass pollen from the Würm Interstadial to the Würm Upper Pleniglacial in a profile from Florisbad, east of Alexandersfontein, indicating "... a lower temperature, or ... a considerable increase in precipitation, or both." The Florisbad profile is complemented by a younger sequence at Aliwal North, beside the Upper Orange, where Coetzee (1967) found an abundance of grass pollen at the bottom of the profile, which has been dated as 12 000 to 13 200 years B.P. near the Holocene boundary of the Würm Upper Pleniglacial. The author commented: "The site was much wetter ... and was surrounded by pure grassveld in which Stoebe plumosa indicates cooler conditions similar to those now prevailing at higher altitudes." The effect of these cooler and moister climatic conditions during the Würm Upper Pleniglacial in the Vaal River catchment was to initiate deposition of gravels and silty sands in Member III of the Riverton Formation (Butzer, Helgren et al., 1973). The authors dated shells of the freshwater snail, Achatina zebra abesa, as about 17 200 years B.P. at the top of Member III. Butzer, Helgren et al. (1973) rejected all other dates on suspicion of contamination by younger material, so that the ages of

Members IV and V are undetermined. The evidence suggests that Würm Upper Pleniglacial conditions favoured the formation of a protective mat of grassy vegetation in the Vaal's upper and middle catchment, leading to reduced runoff, increased percolation, a high water table and alluviation of fine sediment (Butzer, 1971a, p.45).

b. The Kalahari

Having discussed the possible effect of glacials on the Vaal-Upper Orange catchment, what of the Molopo-Nossop system draining the southern Kalahari? No discharge reaches the Orange today via either the Molopo or the Nossop. The Molopo flowed as far as Pepani Laagte, 500 km upstream from the Orange-Molopo confluence, in 1893 (Grove, 1969). This inability of the Molopo to reach the Orange may be due to insufficient precipitation, to seepage into the Kalahari Sand, to tapping of underground reservoirs in dolomite bedrock, recently exposed from beneath a cover of impervious Karoo sediments by Bushveld rivers (Wellington, 1955), or to a combination of all three factors. The Nossop drains the highlands near Windhoek in South West Africa, but its flow only travels as far as Witputs, some 150 km upstream from the Orange-Molopo confluence. At Witputs a modern barchan dune diverts any discharge out of the river bed to pans at Abiquas Puts (Lewis, 1936). As a result, the Molopo downstream from Witputs is a fossil channel today.

During glacials the situation was probably very different, particularly in winter when cyclonic rains swept across the interior from the west coast. Signs of increased discharge are clear. The most dramatic are the dry Riemvasmaak Falls, 13 km upstream from the Orange-Molopo confluence. Haughton (1927) has linked the falls with the upstream regression, during King's (1968) Miocene to Recent, Victoria Falls cycle, of the nickpoint responsible for carving the Fish River Canyon (Simpson and Davies, 1957) and the precipitous gorge of the Lower Orange below the Aughrabies Falls (Gevers et al., 1937; Von Backström and De Villiers, 1972). Incision of a 30-m deep channel in quartzite near Khuis, midway between Pepani Laagte and the Molopo-Nossop confluence, and the cutting of a gorge through banded ironstone west of Mafeking, are further evidence of increased flow in the past (Grove, 1969).

The northern half of the Kalahari would have been more arid than today at the height of the glacial period, when the Kalahari sands that are vegetated today were redistributed by aeolian action as far north as Zaire (Van Zinderen Bakker, 1975). Bearing in mind that the arid zone oscillated between the northern Kalahari and the Karoo, how was sediment distributed in the Kalahari during glacials? Grove (1969) mapped dune patterns and noted that the predominant longitudinal dunes were aligned in a broad arc, concave to the east. He interpreted this pattern as evidence of their formation around an anticyclone centred over the Transvaal, presumably during a glacial period. Similar evidence of aridity in

the tropical areas of the world has been collated by Williams (1975).

e. The tributaries of the Lower Orange

According to Rogers (1915b; 1922), the sand-choked tributaries of the Lower Orange have contributed no sediment to the master stream since the end of the Cretaceous. This opinion has been generally accepted by several authors (Gevers et al., 1937; De Villiers and Söhnge, 1959; Von Backström, 1964; Von Backström and De Villiers, 1972) but was queried by Haughton (1927). Rogers (1915b) interpreted the discovery of Late-Cretaceous dinosaur bones at the bottom of a well in a tributary of the Henkries Valley as evidence of a climate humid enough until the end of the Cretaceous to both support herbivorous dinosaurs and to excavate the valley. However it is probable that the Henkries Valley, one of the largest south-bank tributaries of the Lower Orange, was repeatedly re-excavated during Pleistocene glacials by abundant winter rains. The present infilled nature of the valley is doubtless due to accumulation of aeolian sand and sheetwash debris during the past 10 000 years. This suggestion agrees with the observation by De Villiers and Söhnge (1959, p.18) who wrote: "In spite of the low rainfall, the drainage-pattern of the area is remarkably well established and integrated, and obviously owes its inception and development to much wetter conditions." It also offers an explanation for the lack of hanging valleys in the tributaries, which would be expected were the tributaries to have ceased to flow at the end of the Cretaceous.

4. Glacio-eustatic lowering of sea level

a. Worldwide estimates of the Würm Upper Pleniglacial sea level

Numerous estimates have been made of the lowering of sea level during Pleistocene glacial periods. In his review Guilcher (1969, p.83) concluded: "The greater part of the recent findings point to one or two lowerings of more than 100 m". Butzer (1971b, p.217) came to a similar conclusion: "It should be realized that precise estimates are impossible at present, and a general estimate of -100 to -150 m is quite sufficient for all practical purposes". In the same vein Flint (1971, p.321) wrote: "In view of the uncertainties, we can still improve little on the round value of -100 m quoted by several researchers during the last half century".

Recent work on oxygen-isotope and palaeomagnetic variations in a deep-sea core from the equatorial Pacific by Shackleton and Opdyke (1973) suggests that a maximum lowering of -120 m occurred during the Würm Upper Pleniglacial about 17 000 B.P. They stressed that this figure is independent of any isostatic effects. Walcott (1972) and Chappell (1974) have estimated these isostatic effects caused both by unloading of ice from the land masses in the northern hemisphere and by loading of the sea floor by the meltwater. Neglecting ice unloading

in unglaciated southern Africa, the effect of water loading depends on the geometry of the shelf and the structure of the underlying mantle. In the study area a deep or "box" shelf is up to 100 km wide off the Orange River (See Chapter II). Chappell (1974) estimates overdeepening of less than 5 m for such a shelf. He also selected the consistent data of Curray (1960) from the Texas shelf and of Emery and Garrison (1967) from the northeast U.S. shelf and applied corrections for isostatic corrections for isostatic deformation. He concluded that sea level dropped to around -135 m and compared his value with the value of -132 m obtained by Flint (1971, p.318) from ice-volume calculations.

Paterson (1972, in Chappell, 1974) recalculated ice volumes and estimated that sea level dropped to -115 m. This figure correlates well with measurements in the Adriatic Sea (Van Straaten, 1965) where sea level was probably lowered to -110 m. Chappell (1974, p.421) summarizes the present position as follows: "Whether or not the 10-15 m discrepancy is significant, between Paterson's upper estimate of ice volume and either Flint's estimate or the estimate made here of 130-135 m lowering, is left as an open question.".

b. Local evidence of lowered sea level

In Chapter II the depth of the contact between post-Palaeozoic and Precambrian outcrops was related to a lowering of sea level during a Pleistocene glacial. Hoyt, Smith and Oostdam (1965b), allowing 10 to 15 m as the effective depth of surf abrasion, calculated that sea level dropped about 100 m during Pleistocene glacials. The same break in slope was traced by Van Andel and Calvert (1971) on the shelf north of Lüderitz to beyond Walvis Bay, and they also suggested a glacio-eustatic origin.

The clearest indication of a lowered sea level is provided by the discovery of two gravel beaches in the vicinity of the -75 m and the -100 m bedrock contours, between the mouth of the Orange River (29°S) and Pomona (27°S). They were sampled during an intensive vibro-coring operation by the Marine Diamond Corporation (Foster, 1974). The shallower beach coincides with a break in slope at -75 m and possibly also with the base level of the shorter of two incised channels off the Orange River (Murray et al., 1971). The deeper beach lies in the vicinity of the Precambrian/Post-Palaeozoic contact and probably reflects deposition of Orange River gravel during the Würm Upper Pleniglacial.

Hoyt et al. (1969), Murray et al. (1971) and O'Shea (1971) presented geophysical evidence of river valleys which extended seawards across the present inner shelf to the Pleniglacial shoreline, deepening their beds in response to the lowered base level. In between Possession Island and Elizabeth Bay, Murray et al. (1971) report a submerged river channel, which is incised into Precambrian Basement bedrock to an apparent base level of -130 m. The valley bifurcates towards the

present shoreline, one valley leading to the N-S trending valley north of Elizabeth Bay, the other leading to the E-W trending valley of Grillental. Thick accumulations of modern dune sand mask the inland portion of the Elizabeth Bay valley, but it is possible that it was carved by the Koichab River during Pleistocene glacials, before its path to the sea was blocked at Koichab Pan, some 40 km from the modern coast. Grillental, on the other hand, was almost certainly linked to the Kaukausib River from which it is separated by a low rise, causing the river to discharge its rare floodwaters into a small pan, 14 km inland. Both valleys are floored by sediments of the Miocene Elizabeth Bay Formation (Greenman, 1969) and it is probable that the valleys reflect Tertiary drainage lines (Kaiser, 1926, p.41).

The incised valley of the Orange River underlies the present coast about one kilometre north of the present mouth (Murray et al., 1971). The valley bifurcates seawards; one valley reaches its base level at about -70 m and the other a level of at least -80 m before it is buried beneath acoustically impervious Recent deltaic mud. The two channels were probably cut during two separate regressions (Hoyt et al., 1969). Murray et al. (1971) report that the Orange River can be followed inland from the present coastline into a meandering channel, about one kilometre wide, filled with fluviatile gravels (Hallam, 1964, p.705). Both Stocken (1962) and Hallam (1964) describe channels filled with fluviatile sediments cut through the various raised abrasion platforms north of the Orange. These channels are cited as clear evidence of regression following platform abrasion.

Similar river channels, today buried beneath dune sand, have been detected on the coast between the Orange River and Port Nolloth (Keyser, 1972). The rivers played a major role in the distribution of diamonds during Pleistocene glacials. Increased winter rainfall in the upper catchments of these rivers changed their character from intermittent to perennial, but there is little evidence of bedrock dissection below sea level near the present coastline. In contrast, the buried Orange River channel is incised over 30 m below present sea level (Murray et al., 1971).

In Chapter II a drowned Pleistocene delta of the Orange River was identified on bathymetric and sedimentological evidence. The drowned delta resembles the Recent delta in morphology (Fig. II-15) and very fine quartzose sand on its delta front is identical to that found on the modern delta front. The break in slope marking the boundary between the modern delta front and the prodelta is in the vicinity of -40 m. The equivalent feature on the Pleistocene delta occurs at -150 m, implying a lowering of sea level to -110 m. Such a depth is compatible with the evidence of a beach at -100 m, which was described earlier.

c. Wave action during Pleistocene glacials

The present state of knowledge on the modern wave regime on the west coast is limited and the effect of wave-driven currents on sedimentation has received little attention. One can therefore merely speculate on the probable wave regime during Pleistocene glacials. However three trends are probable. Firstly, Flemming (1965) suggests that the drop in air temperature during glacials, and the enhanced temperature difference between the air and the sea would increase wave height. This in turn would increase wave energy. Secondly, the equatorward shift of the westerlies would tend to increase the frequency of storms. Thirdly, lowering of sea level by 110 m would alter the present deep shelf to a relatively shallow shelf, most of it shallower than the wave base ($L_o/2$) of the most frequent wave period (11 seconds) recorded today at Lüderitz (Van Ieperen, 1975) (Fig. VI-3) (L_o - deepwater wave-length).

A wave-controlled sand-mud boundary on the Orange Delta lies today in the vicinity of the 40-m isobath. Due to higher energy levels, this boundary probably lay at deeper levels, perhaps at 50 m. This would bring the zone of significant wave action to near the 160 m isobath during glacials (Fig. VI-3).

Wave action above wave-base therefore probably affected the entire Orange shelf, the summit of the Tripp Seamount and the middle Walvis shelf. Storms probably disturbed upper slope sediments off the Orange shelf, initiating such features as the Chamais Slump. Wave action powerful enough to keep fines in suspension affected the Orange middle shelf, the Orange Banks and the summit of the Tripp Seamount (Fig. VI-3).

D. CLIMATIC CHANGE DURING QUATERNARY INTERGLACIALS

1. Poleward movement of the climatic belts

a. Equatorward shift of climatic belts during the Quaternary

Detailed work on Cenozoic molluscan assemblages in marine sediments of the southwestern Cape and Namaqualand led Tankard (1976a) to postulate a steady equatorward drift of the Benguela Current System accompanied by Pleistocene glacial-interglacial oscillations. He correlated the distribution of warm-water molluscs with the southern limit of the Angola Current, which under favourable circumstances today penetrates as far south as 25°S, inshore of the Benguela Current (Moroshkin et al., 1970). During the Pliocene when the Varswater Formation was deposited in the Saldanha area (33°S) Tankard (1974b) reports that several warm-water molluscs were included in the assemblages. He coupled this fact with Hendey's (1974) identification of tree-browsing giraffids and grazers such as Hipparion to conclude that the northern end of the Benguela Current lay off Saldanha and that the Inter-Tropical Convergence Zone was able to bring convectional rain to the area in summer.

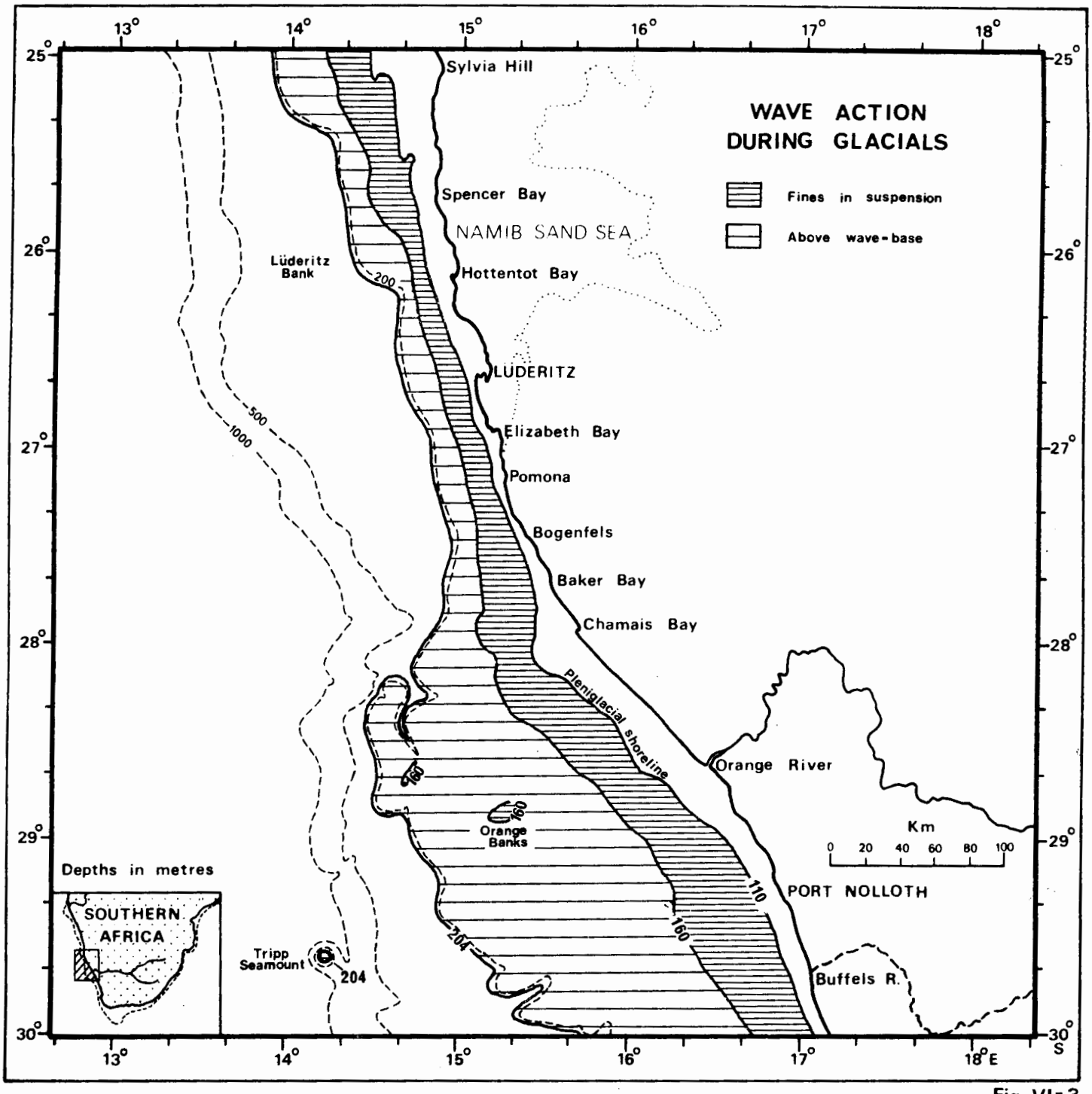
WAVE ACTION
DURING GLACIALS
Fines in suspension
Above wave-base
Sylvia Hill
Spencer Bay
NAMIB SAND SEA
Hottentot Bay
Lüderitz Bank
LUDERITZ
Elizabeth Bay
Pomona
Bogenfels
Baker Bay
Chamais Bay
Pleniglacial shoreline
Orange River
Orange Banks
PORT NOLLOTH
Buffels R.
Tripp Seamount
204
Depths in metres
SOUTHERN AFRICA
Km
0 20 40 60 80 100
13° 14° 15° 16° 17° 18°
25° 26° 27° 28° 29° 30° S

Fig. VI-3

If this hypothesis should be confirmed, the implications for the drainage history of the Orange River are profound. It would mean that the Orange River would receive its rainfall in summer like it does today, with the difference that the discharge would have been considerably higher. Perhaps this concept helps to explain an apparent decline in discharge in both the Vaal and the rivers of South West Africa at the end of the Middle Pleistocene. Cooke (1947) and more recently Butzer, Helgren et al., (1973) contrasted the deposition of cobbles and boulders in the Early to Middle Pleistocene, Older and Younger Gravels of the Vaal with deposition of clay, silt and sand in the Late Pleistocene Riverton Formation. They particularly emphasized that the gravels lie in channels with gradients less than that of the modern river, which today deposits negligible quantities of gravel. Similarly Korn and Martin (1951b, p.21) summarized their conclusions on the Pleistocene of South West Africa: "The whole sequence seems to show, right through the Pleistocene, a decline of the rainfall on which the pluvial and interpluvial fluctuations are superimposed." Possibly aggradation of the Late-Pleistocene Riverton Formation took place under a wetter climate caused by low-intensity winter rains, whereas the gravels were deposited after floods caused by convectional cloudbursts in summer.

b. Poleward movement of the Namib Desert

Van Zinderen Bakker (1967, p.135) has compared modern conditions to the latter half of an interglacial. Conditions at the height of an interglacial are thus different only in degree from the conditions prevailing today. Evidence of the Hypsithermal Interval when more extreme interglacial conditions prevailed in the Early Holocene (9 000 - 2 500 B.P.) is given by Seely and Sandelowsky (1974). They obtained a provisional date of 10 000 $\pm$2 000 years B.P. from the freshwater snails Lymnaea natalensis and Biomphaleria pfeifferi which require a permanent water body for survival. The snails were found west of Tsondab Vlei, the present limit of the Tsondab River, within the Namib Sand Sea. More extreme interglacial conditions would have brought an increase in summer rainfall in the river's headwaters in the Naukluft Mountains to provide the discharge to erode a 50-m deep river channel and to deposit dolomite cobbles west of Tsondab Vlei (Seely and Sandelowsky, 1974, p.63).

2. The Orange River during interglacials

a. The Vaal-Upper Orange catchment

According to Van Zinderen Bakker (1976a) two trends would be accentuated during an interglacial. Firstly semi-arid Karoo conditions would invade the Highveld, pushing the zone of grassland to cooler and moister altitudes (cf. Coetzee, 1967). Secondly, the Indian-Ocean anticyclone would tend to maintain a position well east of the east coast, encouraging the inflow of maritime air towards the Drakensberg, as described in Section VI-B. This combination of increas-

ed rainfall in the headwaters of the Vaal and the Orange Rivers and reduced vegetal cover in the middle and lower catchment would create a situation conducive to accelerated erosion. Assuming such erosion were characteristic of the Hypsithermal Interval in the Early Holocene it may account for the 15 metres of dissection into the Würm Upper Pleniglacial Member III of the Riverton Formation (Butzer, Helgren et al., 1973). Bad veld management leading to decreased vegetal cover has a similar effect and is the direct cause of extensive erosion in many parts of the catchment today.

If, as postulated at the beginning of this section, the entire climatic system has shifted equatorward during the Quaternary, then abundant tropical rain would have characterized interglacials in the Early to Middle Pleistocene. Fine sediment would have been carried to the coast and coarse gravels and sands would have been deposited in the river channels. Glacials in the Early to Middle Pleistocene would have had erosive characteristics similar to the Late Quaternary interglacials just described. Erosion was more intense, however, because bedrock dissection is typical of the erosive phases of the Vaal cycle (Butzer, Helgren et al., 1973).

b. The Kalahari and the tributaries of the Lower Orange

Clear evidence of both wetter and drier climates exist side by side in the Kalahari, although little chronological information has yet emerged. The landforms described by Grove (1969) are best discussed through a complete cycle from the Last (Eem) Interglacial through the Würm Glacial to the Hypsithermal Interval and on to the present. The fluctuations in climate in the Kalahari are of particular significance to sediment discharge into the Lower Orange, because discharge is liable to vary from abundant in both glacials and interglacials to nothing in the periods in between.

An attempt is made to interpret the presence of vegetated barchan dunes within Ntwetwe Pan, itself in the centre of palaeo-Lake Makarikari in the northern Kalahari (Grove, 1969, p.205). Nearer the Orange River is the dessicated Molopo-Nossop drainage network, in places cutting perpendicularly through belts of vegetated longitudinal dunes.

During the Last (Eem) Interglacial, the Inter-Tropical Convergence Zone would have penetrated south to about latitude 20°S in summer (Fig. VI-1d) bringing increased precipitation to palaeo-Lake Makarikari between latitudes 20 and 21°S. At present, rainfall is so inadequate in the Molopo-Nossop catchment and in the Lower Orange that aeolian and sheetwash processes of aggradation are dominant. More southerly penetration of high-intensity convectional rain would have increased runoff considerably.

During the Würm glacial the arid zone moved equatorward causing palaeo-Lake Makarikari to dry up and a belt of westward-facing barchan dunes was formed

on the floor of the lake by easterly winds. As the glacial drew to a close the arid zone moved south again and formed dunes across the Molopo-Nossop drainage network. With the onset of the Hypsithermal Interval convectional rain again moved poleward and rejuvenated the Molopo-Nossop Rivers, which in places cut a course perpendicular to the dunes. At the same time the longitudinal dunes were probably degraded by the high rainfall and they became vegetated. During this period Lake Dow and Ntwetwe Pan were formed on the floor of Lake Makarikari, partially drowning the barchan dunes which had been stabilized by vegetation. An equatorward retreat of the summer position of the Inter-Tropical-Convergence Zone since the Hypsithermal Interval is denoted by traces of higher lake levels on the flanks of the barchans and by the meagre flow of water in the river channels of the Molopo and Nossop rivers. The prevailing arid conditions have allowed the Witputs dune to block the Molopo, thus depriving the Lower Orange of any sediment from the Kalahari Basin under modern conditions.

3. Glacio-eustatic rise of sea level

a. Infilling of incised river channels

During the eustatic rise of sea level the discharge characteristics of the local rivers not only had to adjust to the rising base-level, but also to changes of climate in their catchments. In the first place, those rivers which received enough discharge to incise their beds during glacials filled these incised channels with sediment during interglacials. However, those rivers whose lower reaches were dammed by coastal dunes were prevented from incising their beds at all during glacials.

b. Development of coastal dune plumes in Namaqualand

At the mouths of several of the intermittent rivers of Namaqualand are distinctive plumes of coastal dunes. The best-defined plume lies north of the mouth of the Swartlintjies River, which is adjacent to a narrow part of the inner shelf, only 5 km wide (Fig. VI-4). The plume has three main elements: 1) Pre-Flandrian dunes; 2) Flandrian dunes (Episode I); 3) Flandrian dunes (Episode II). The nomenclature is derived from Cooper (1967) who described coastal dunes from similar latitudes on the Californian west coast of America. The dune patterns of southern California and of Namaqualand are identical (cf. Cooper, 1967, Plate 12).

The Pre-Flandrian dunes were formed during earlier rises of sea level from previous interglacials to the Würm Interstadial. These dunes exhibit the same parabolic outlines as the Flandrian (Episode I) dunes which override them (Fig. VI-4). The outlines of the Pre-Flandrian dunes are softened due to degradation in a moister climate during glacials. Both sets of parabolic dunes are stabilized by vegetation, and both sets display the extremely long and narrow "hairpin" shape that Cooper (1967) found to be characteristic of the southern Californian dunes.

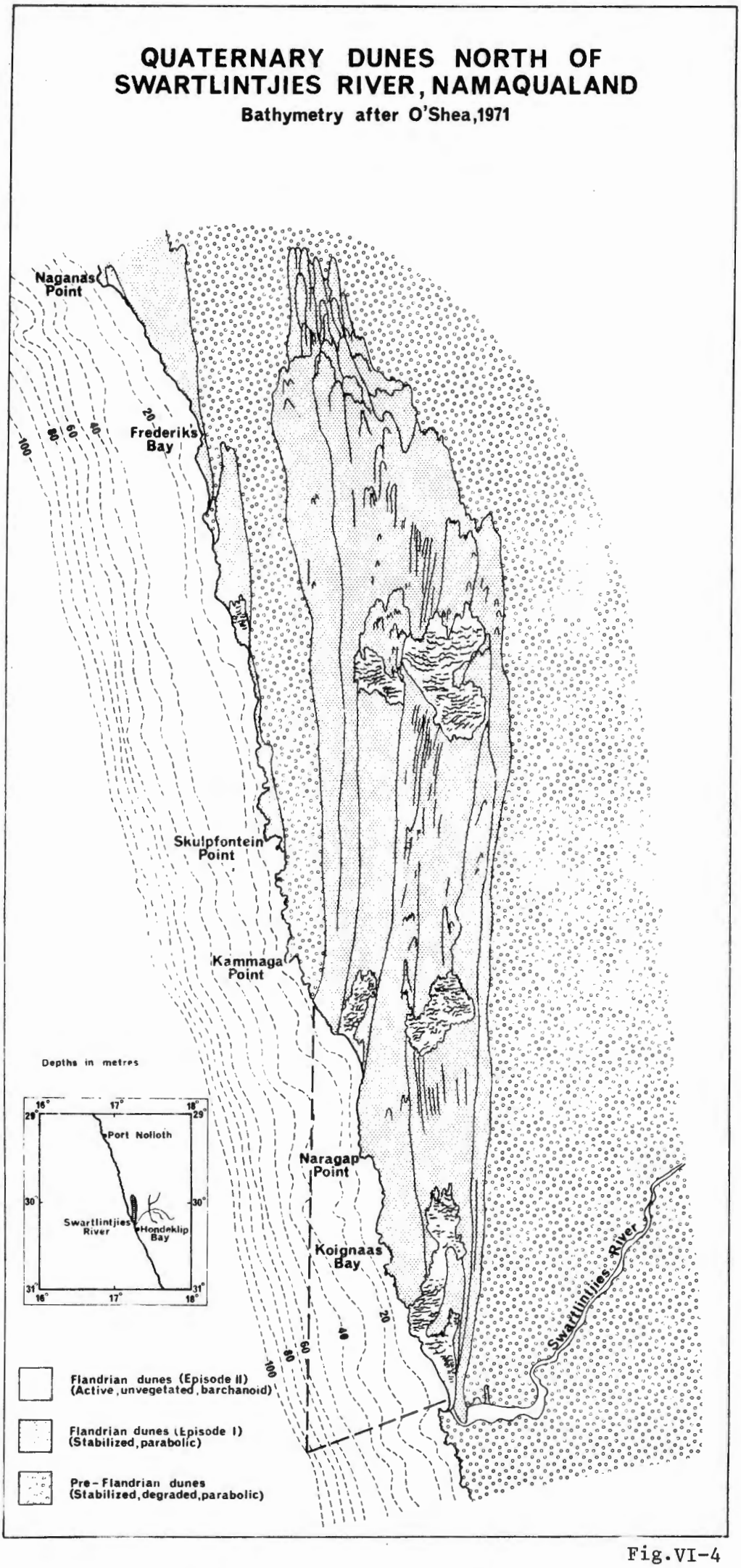
QUATERNARY DUNES NORTH OF
SWARTLINTJIES RIVER, NAMAQUALAND
Bathymetry after O'Shea, 1971
Naganas Point
Frederiks Bay
Skulpfontein Point
Kammaga Point
Naragap Point
Koignaas Bay
Swartlintjies River
Depths in metres
Port Nolloth
Swartlintjies River
Hondeklip Bay
Flandrian dunes (Episode II)
(Active, unvegetated, barchanoid)
Flandrian dunes (Episode I)
(Stabilized, parabolic)
Pre-Flandrian dunes
(Stabilized, degraded, parabolic)

Fig.VI-4

Overriding the vegetated, parabolic, Episode I dunes are discrete masses of shifting, unvegetated, barchanoid Episode II dunes. The leading edge of each mass has a lobate form, which is preserved when the mass loses too much material and becomes stabilized by vegetation.

The patterns of the southern Californian and the Namaqualand dunes are so similar that it is appropriate to quote Cooper's (1967, p.85) model for their formation:

"The greatest effectiveness in invasion of older masses or new territory, determined by the 'effective wind' is straight ahead; burial of vegetation is easy at the front of the mass. A trough develops behind the advancing front, which becomes a path for a concentrated forward air current. Drag due to the containing walls retards air velocity along the sides, deflecting the flow lines to right and left. Sand is dropped building lateral ridges. As the active mass moves on, these, and the floor of the trough as well, are occupied by vegetation and gradually stabilized .... Loss of material left behind in the flanking ridges, not fully compensated by what is picked up from older deposits, results in decrease in the mass of mobile sand.. The trough narrows; movement ceases when the lateral ridges meet."

The Flandrian dunes of Episode I north of the Swartlintjies River were formed during the Flandrian transgression at the close of the Würm II glacial from sand originally supplied to the lowered glacial mouth of the river by increased winter runoff. Strong unidirectional southerly winds blew the sand off the beach in summer, initially from beaches formed at the mouth of the river. Assuming that sea level was lowered to -110 m, it is seen in Figure VI-4 that the seaward projection of the river's course intercepts the seaward projection of the western edge of the dune plume on the 110-m bedrock contour (O'Shea, 1971). Thus at the height of the glacial the equatorward movement of the winter rainfall zone had converted the Swartlintjies River from an intermittent to a perennial river delivering sediment to a mouth 5 km west of the present mouth and 110 m lower than present sea level.

Onshore the Episode I dunes were rapidly stabilized in parabolic forms by vegetation supported by the winter rains, which supported Leucospermum (Rourke, 1972) well north of its modern habitat. During the retreat of the river mouth in response to a rising sea level, winter runoff gradually declined as the belt of westerlies gradually shifted polewards bringing more arid conditions to the river's catchment. The diminishing supply of sand at the river mouth was rapidly augmented by surf-erosion and remobilization of stabilized Flandrian (Episode I) and pre-Flandrian dunes. The length of the beach created in this way steadily increased as sea level rose, so that the point-source at the glacial river mouth was gradually replaced by a linear source, the beach. The older stabilized Episode I dunes are

thus invaded by active masses of unvegetated barchanoid dunes of Episode II.

A beach sand from this vicinity was examined under a scanning electron microscope (Rogers and Krinsley, in prep.). Grains from the coarse-sand fraction (0,5-1,0 mm) were found to have well-rounded shapes inherited from earlier aeolian cycles, as well as distinctive boat-shaped (scaphoid) grooves (Plate VII-1a and VII-1c) attributed to mechanical impact in the high-energy surf, which continuously pounds the Namaqualand coast. It is not surprising to find such grains on a coastal platform where sand is repeatedly recycled from a beach to a dune and back to a beach again.

c. Worldwide estimates of raised sea level

There is a voluminous literature on raised sea levels, a subject that has continually been a source of controversy. The subject has recently been reviewed by Tankard (1976b), who examined the many factors complicating the study of these features. Shackleton and Opdyke (1973) studied oxygen-isotope variations in deep-sea sediments and predicted sea levels at 6 m (120 000 B.P.) and at -13 m (100 000 and 80 000 B.P.) during the Last (Eem) Interglacial. These peaks correlated well with sea levels measured on Barbados by Broecker et al. (1968) and in New Guinea by Veeh and Chappell (1970).

d. Local evidence of raised sea levels

Although the diamondiferous raised beaches of Namaqualand and southern South West Africa were discovered fifty years ago (Hallam, 1964, p.726) and although they have been mined ever since, the final word remains to be said on the age and correlation of the various terraces.

Of the older references Wagner and Merensky (1928), Haughton (1931) and Knetsch (1937) are the most useful. Hallam (1964) gives the most comprehensive survey of all aspects of the raised beaches between latitudes 18°S in the Kaokoveld of South West Africa and 32°S at the Olifants River in Namaqualand.

Stocken (1962) gives a concise account of the raised beaches immediately north of the Orange River. Terrace D (9,25 m) is the highest reported terrace, followed at lower levels by Terraces C (6-8 m), B (3-5 m) and A (1-2 m). As mentioned previously, each transgression was followed by a regression. Terraces D and C contain warm-water molluscs, whereas Terraces B and A contain only cold-water molluscs. South of the Orange River Keyser (1972) reports a sequence of four terraces which, in descending order, are termed the Grobler Terrace (64-84 m), the Upper Terrace (34-47 m), the Middle Terrace (17-26 m) and the Lower Terrace (0-9 m). The three highest terraces all contain warm-water molluscs. Farther south along the coast of Namaqualand, Carrington and Kensley (1969) identified molluscs from a series of raised beaches at the mouth and north of the Swartlintjies River (30°S). The lowest beach in which warm-water molluscs were found was the Early Pleistocene

45-50 m transgression complex. Tankard (1976c) correlated a 10-m beach at Saldanha (33°S) with the 45-50 m beach at the Swartlintjies River by comparing the mollusc fauna. He postulated a warp axis linking the Tertiary volcanics of the Alphard Banks to those of the Klinghardt Mountains. Westward downwarping about this axis explains the discrepancy in altitude, because Saldanha lies west of the axis which lies at the coast beside the Swartlintjies River beaches.

Carrington and Kensley (1969) also report an unfossiliferous beach at 75-90 m and two Middle Pleistocene beaches at 29-34 m and at 17-21 m, two Late Pleistocene beaches at 7-8 m and at 5 m, and a Holocene beach at 2-7 m. A detailed study of the mollusc fauna of the Namaqualand beaches by Carrington (in prep.) may allow correlation of the various terraces and detection of local warping.

e. Poleward movement of the Polar Front

Meriodional movements of the atmospheric and oceanic circulations over and beside southern Africa have already been described. Synchronous movements of the Antarctic Polar Front in the Southern Ocean are reflected in radiolarian assemblages in deep-sea cores. Hays et al. (1974a) estimate that since the Würm Upper Pleniglacial the Polar Front has moved poleward by 5-6° latitude. The ocean temperature seems to have reached a maximum at 10 000 years B.P. during the Hypsithermal Interval after which temperatures declined (Hays et al., 1974b).

CHAPTER VII

UNCONSOLIDATED RECENT TERRIGENOUS SEDIMENTS

A. INTRODUCTION

In Chapter VI attention was paid to the possible effects of Pleistocene climatic fluctuations on sedimentary processes in the hinterland of the west coast. In this chapter the writer examines sedimentary processes occurring today "... in the latter half of an interglacial" (Van Zinderen Bakker, 1967, p.135). Thus, data on the sediment load of the Orange River reflect the climatic conditions prevailing in the catchment today. However, even these data are inaccurate because the catchment had already been severely affected by man's agricultural activities before proper measurements were taken. Therefore no data exist for prehistoric Recent times and those for historic times do not reflect undisturbed Recent processes. The present is thus an imperfect key to the past in this case.

Furthermore, if it is shown that the climate of the Orange catchment was considerably wetter during its most active period of erosion in the Cretaceous, and that its depositional basin was subject neither to vigorous wave action not to violent wind action, then the process-response model to be developed in this chapter may be strictly applicable only to the Late Cenozoic.

B. SEDIMENT DISCHARGE FROM THE ORANGE RIVER SYSTEM

1. Introduction

The Orange River is the only major river to receive its rainfall on the east side of a continent and to have its delta sited on the poleward side of one of the major coastal deserts of the world. To that extent the Orange River is unique. Like other subtropical rivers it has a highly erratic discharge fed by summer rainfall. Like the Kunene and the Senegal Rivers on the equatorwide sides of the Namib and the Sahara, respectively, its lower reaches receive negligible runoff from the arid and semi-arid surroundings (Midgley and Pitman, 1969); the Orange River is therefore autochthonous upstream and allochthonous downstream.

Wellington (1933) divided the river into the Upper Orange, above the Vaal confluence, the Middle Orange between this confluence and the Aughrabies Falls, and the Lower Orange between the Falls and the sea. The reader is referred to Wellington (1955) for a thorough description of the entire potential catchment of the Orange River system.

2. The Recent regime of the Orange River

a. Data sources

The meteorological processes affecting the catchment of the Orange River

System have been discussed in broad terms in Chapter VI. The available data on the effects of these processes in terms of water and sediment discharge will now be examined. Data are chiefly extracted from Rooseboom and Maas (1974), who critically analysed data collected since 1928 by the Department of Water Affairs. The Rooseboom and Maas study is complemented by that of Keulder (1973, 1974) who studied the hydro-chemistry of the Upper Orange catchment.

b. Effective catchment

Kokot (1965) and Kriel (1972) have listed the areas of the various subcatchments of the Orange River system (Fig. VII-1) (Table VII-1). Significant runoff is restricted to an area of 294 000 km^2, only 35% of the potential catchment area of 829 000 km^2 (Midgley and Pitman, 1969). Even then some of this runoff is trapped in the pans of the Sak River system, on the southern bank of the Middle Orange. According to Rooseboom and Maas (1974, p.B3), practically the entire sediment load of the Orange River is derived from the catchment of the Hendrik Verwoerd Dam on the Upper Orange. This area of 70 000 km^2 comprises only 8,5% of the potential catchment area of the system. The areas of the individual subcatchments are summarised in Table VII-1:

TABLE VII-1

Areas of the subcatchments of the Orange River System (Kokot, 1965; Kriel, 1972)

Subcatchment		Area km^2	Percentage of total catchment area %
Catchment of the Hendrik Verwoerd Dam	Upper Orange	35 290	4,3
	Caledon	21 600	2,6
	Kraai	9 300	1,1
	Stormberg	4 200	0,5
	Vaal	194 250	23,4
	Lower and Middle Orange	139 860	16,9
	Molopo-Nossop	233 100	28,1
	Fish	108 780	13,1
	Balance	82 880	10,00
	Total	829 260	

c. Water and sediment discharge

The highly variable nature of the Orange River is illustrated in Figure VII-2, which depicts monthly discharge at Vioolsdrif, the sampling point closest to the mouth of the river. The rainy summer season produces one or more floods each

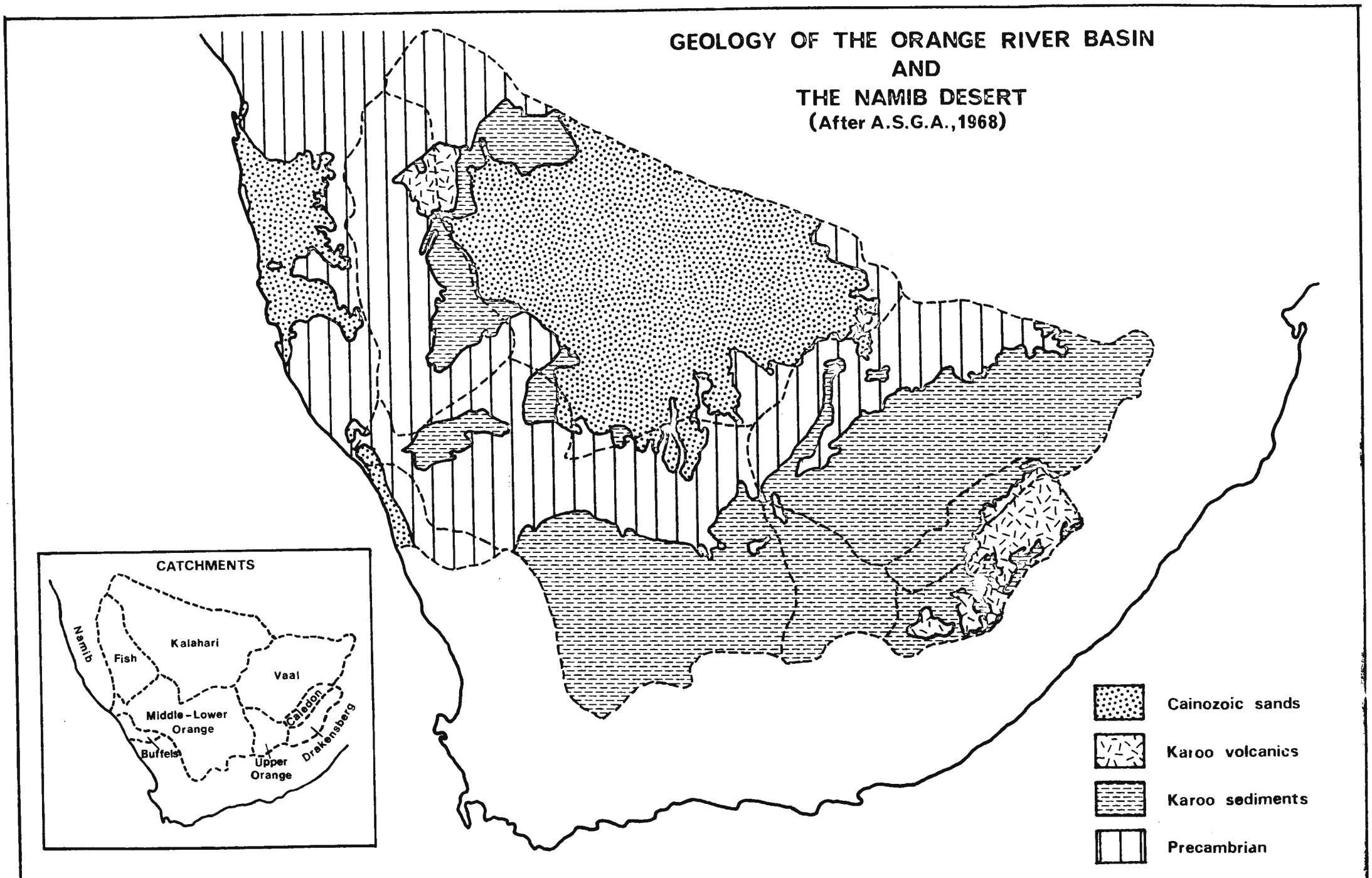
GEOLOGY OF THE ORANGE RIVER BASIN
AND
THE NAMIB DESERT
(After A.S.G.A., 1968)
CATCHMENTS
Namib
Kalahari
Fish
Vaal
Middle-Lower
Orange
Caledon
Buffels
Upper
Orange
Drakensberg
Cainozoic sands
Karoo volcanics
Karoo sediments
Precambrian

Fig.VII-1

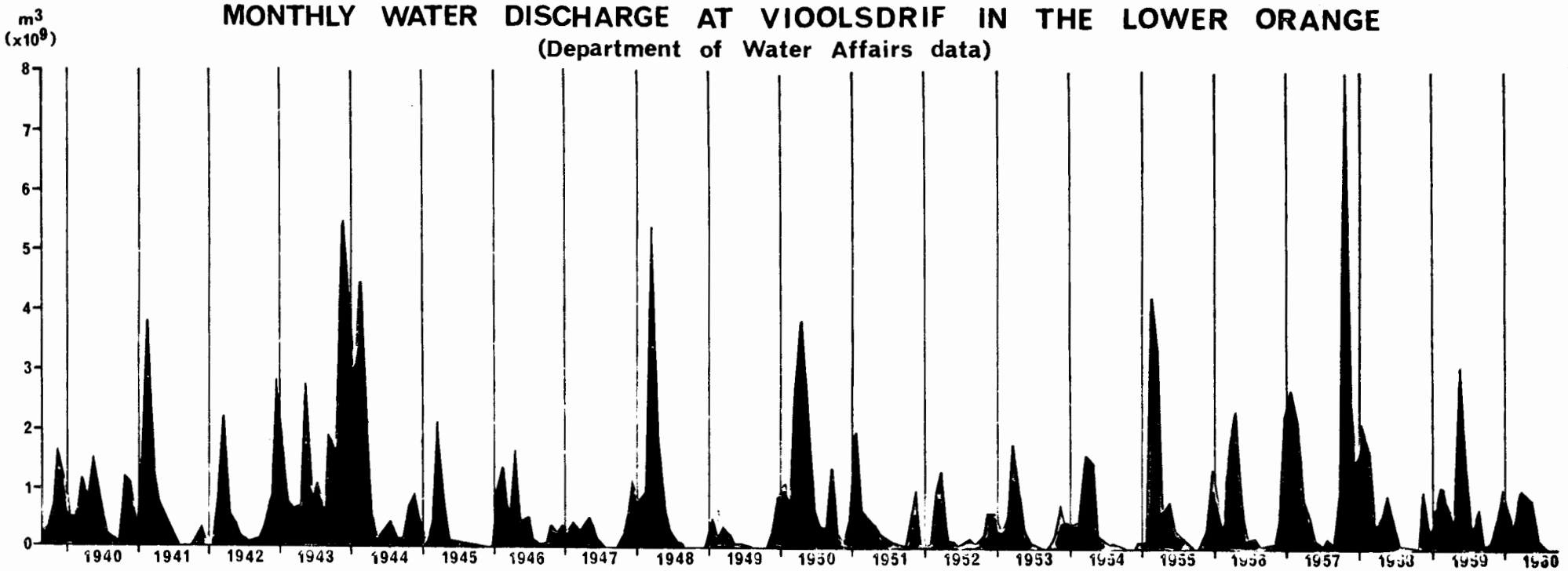
MONTHLY WATER DISCHARGE AT VIOOLSDRIF IN THE LOWER ORANGE
(Department of Water Affairs data)
m3 (x10^9)
0
1
2
3
4
5
6
7
8
1940
1941
1942
1943
1944
1945
1946
1947
1948
1949
1950
1951
1952
1953
1954
1955
1956
1957
1958
1959
1960

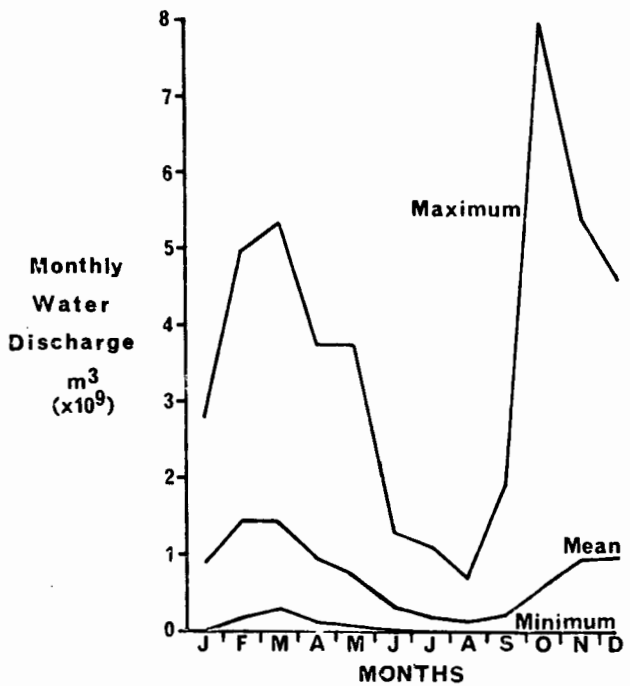
Monthly Water Discharge m3 (x10^9)
Maximum
Mean
Minimum
J F M A M J J A S O N D
MONTHS

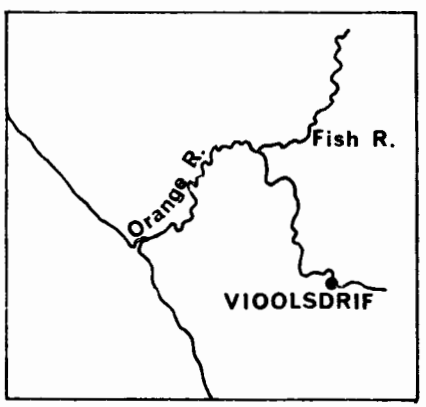
Fish R.
Orange R.
VIOOLSDRIF

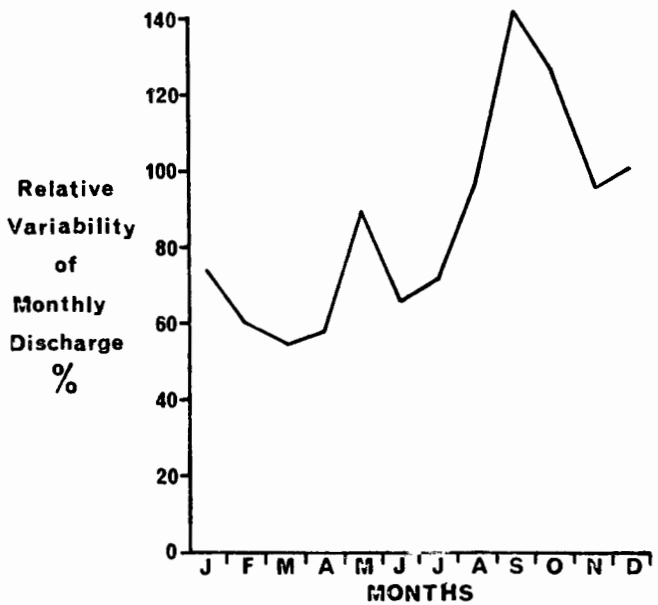
Relative Variability of Monthly Discharge %
J F M A M J J A S O N D
MONTHS

Fig.VII-2

year; the maximum discharge was 8 x 10^9 m^3 for the month October, 1957. However, during several months no discharge at all was recorded. Van Warmelo (1922, p.172) quoted evidence that the river stopped flowing in 1862-63, 1903 (for two months) and 1912, which disqualifies the Orange as a truly perennial river. The driest month appears to be August, with a mean monthly discharge of 0,14 x 10^9 m^3. March has the highest mean monthly discharge (1,45 x 10^9 m^3), closely followed by February (1,44 x 10^9 m^3). The mean annual discharge is 9,30 x 10^9 m^3, with a relative variability of 49,4%. However, this value for relative variability is exceeded in all months, from 58,7% during March floods to 130,8% during September at the end of the dry season. Summary statistics are listed in Table VII-2:

TABLE VII-2

Water discharge at Vioolsdrif on the Lower Orange River for the period 1939-1960 (Department of Water Affairs)

Month	Years of Observation	Mean Discharge $m^3 \times 10^9$	Maximum Discharge $m^3 \times 10^9$	Minimum Discharge m^3	Relative Variability %
January	24	0,89	2,84	478 768	74,3
February	24	1,44	4,97	182 093 164	72,9
March	24	1,45	5,35	285 660 570	58,7
April	24	0,96	3,74	114 456 776	60,9
May	24	0,77	3,74	46 352 028	85,5
June	22	0,35	1,28	28 424 248	75,6
July	22	0,19	1,13	1 215 134	74,1
August	24	0,14	0,69	0	95,7
September	24	0,23	1,92	0	130,8
October	23	0,63	7,99	0	123,6
November	24	0,96	5,42	0	89,5
December	24	0,99	4,66	0	90,6
Year	21	9,30	22,85	979 005 102	49,4

Rooseboom and Maas (1974) have demonstrated that the Upper Orange River is far more important than the Vaal River, in terms of annual water and sediment discharge. Overlapping data exist for the years 1928 to 1943, during which period the mean annual water discharge of the Upper Orange was 7,75 x 10^9 m^3 compared with 2,26 x 10^9 m^3 for the Vaal (Fig. VII-3). The individual years varied widely from 1,38 x 10^9 m^3 to 14,77 x 10^9 m^3 in the case of the Upper Orange, and from 0,37 x 10^9 m^3 to 4,97 x 10^9 m^3 in the case of the Vaal (Table VII-3).

A similar but accentuated relationship applies to sediment discharge from the two rivers, for the overlapping period 1931 to 1943 (Fig. VII-2). The mean annual sediment discharges of the Upper Orange and the Vaal were 6,65 x 10^6 and

ANNUAL WATER AND SEDIMENT DISCHARGE OF THE VAAL, UPPER ORANGE AND MIDDLE ORANGE

(After Rooseboom, 1974)

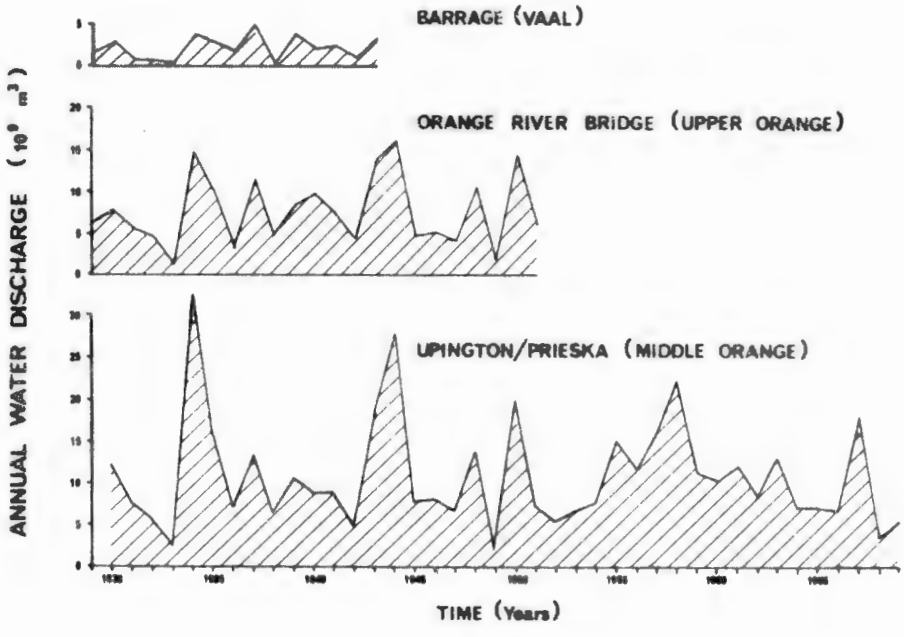

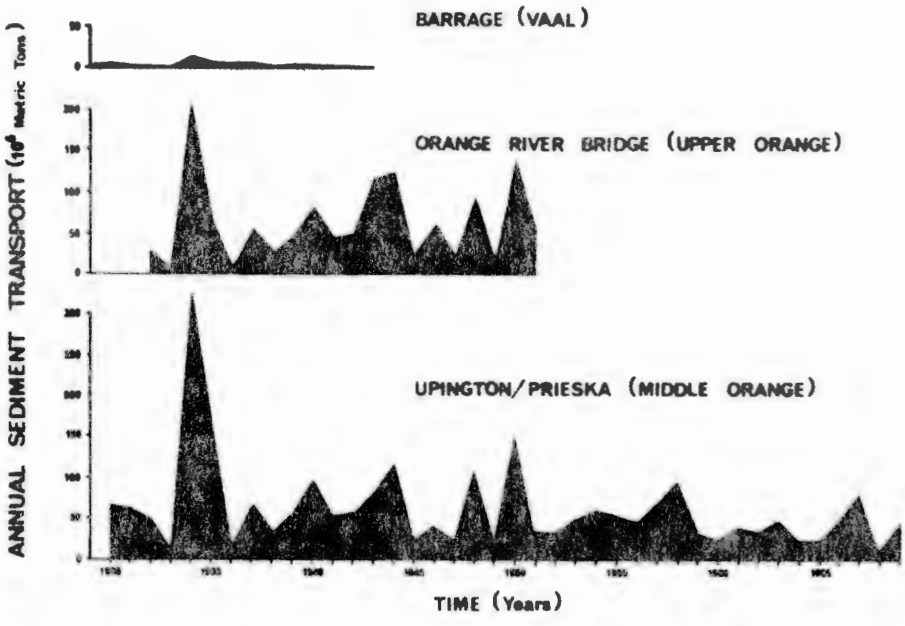

ANNUAL SEDIMENT DISCHARGE

(10-Year Moving Average)

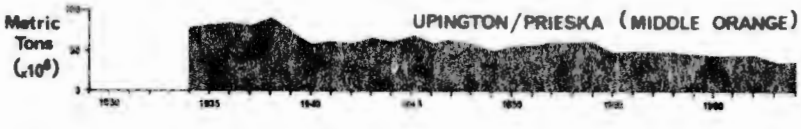

Fig.VII-3

3,04 x 10^6 tons respectively. The Upper Orange values ranged from 6,1 x 10^6 to 204,6 x 10^6 tons, and those of the Vaal ranged from 0,1 x 10^6 to 12,7 x 10^6 tons (Table VII-3).

Mean values are perhaps less significant than cumulative values in a system as erratic as that of the Orange River. Thus the mean annual water discharge of the Upper Orange was three and a half times that of the Vaal. The cumulative totals, however, differ by a factor of five. Van Warmelo (1922, p.175) in discussing the greater flow of the Upper Orange, pointed to the much higher rainfall and runoff in the Maluti Mountains drained by the headwaters of the Upper Orange, as well as the Caledon "running parallel to the Maluti like a moat round a castle". Most of the Eastern Vaal River tributaries except the Wilge thus receive little runoff from the mountains. Wellington (1955, p.346) pointed out that the result of this aggressive river capture by the Caledon is that the Caledon is perennial, whereas the Vaal's left-bank tributaries are intermittent. In the case of sediment discharge, the mean annual discharge and the cumulative totals of the Upper Orange are both twenty times that of the Vaal. Rooseboom and Maas (1974, p.83) are thus justified in identifying the Upper Orange as the most important subcatchment in terms of sediment production. The relevant data for the two subcatchments are presented in Table VII-3. The Upper Orange was sampled at Orange River Bridge relatively near the Orange-Vaal confluence, whereas the Vaal was sampled at the Barrage near the Reef. However, the Vaal receives relatively little runoff downstream from the Barrage (Midgley and Pitman, 1969) and although the discharge imbalance between the two rivers may be exaggerated slightly, the basic pattern remains.

TABLE VII-3

Water and sediment discharge in the Upper Orange and the Vaal Rivers (Department of Water Affairs)

Water Year		Water Discharge $m^3 \times 10^9$		Sediment Discharge tons $\times 10^6$	
October	September	Orange River Bridge	Vaal Barrage	Orange River Bridge	Vaal Barrage
1928	1929	6,79	1,87		
1929	1930	7,84	2,95		
1930	1931	5,97	0,78		
1931	1932	4,67	0,70	28,6	1,0
1932	1933	1,38	0,44	6,1	0,4
1933	1934	14,77	3,96	204,6	12,7
1934	1935	10,46	2,81	66,4	6,5
1935	1936	3,03	1,82	9,4	4,2
1936	1937	11,43	4,97	55,3	6,3
1937	1938	5,00	0,37	28,7	0,1
1938	1939	8,65	3,91	47,2	1,9
1939	1940	9,99	2,18	83,6	0,7
1940	1941	7,59	2,67	45,2	1,1
1941	1942	4,55	1,06	48,9	0,2
1942	1943	14,06	3,45	116,1	1,3
Cumulative total		116,18	33,93	740,1	36,4
Annual Mean		7,75	2,26	61,71	3,0

Rooseboom (1974) found it necessary to apply a correction factor of 1,3 to the sediment data supplied by the Department of Water Affairs. A comparative study at Bethulie, just below the Caledon-Orange confluence, showed that a sophisticated measuring device called the Turbidisonde produced results 25% higher than those produced using the traditional sampling bottle. An additional allowance of only 5% was made for bedload, because textural analyses of sediment in the catchment and in the river bed showed that little sediment is coarse enough to be transported as bedload. The annual sediment discharge values were thus obtained by multiplying the daily sediment concentration values by their respective water discharge values, summing the daily sediment discharge values thus obtained for each hydrological year (1 October to 30 September) and then multiplying by 1,3. This approach was modified in the case of the combined Prieska-Upington data from the

Middle Orange because in some years higher values were obtained in the Upper Orange than in the Middle Orange. Suspecting that some sediment was settling out in deep pools along the Middle Orange, causing the surface samples to be unusually inaccurate, Rooseboom and Maas (1974) applied a correction factor of 1,5 to the combined Prieska-Upington data. (Fig. VII-3).

d. Accuracy of modern sediment discharge data

The validity of modern sediment discharge data as an accurate response to normal Recent processes is seriously questioned. If a ten-year moving average is applied to the combined Prieska-Upington data, which are taken to represent the total sediment discharge of the river, a steady downward trend is revealed (Fig. VII-3) (cf. Rooseboom and Maas, 1974). Values of 80-90 x 10^6 tons per year in the 1930's declined to 30-40 x 10^6 tons per year in the 1960's. Some of the decline is due to the construction of dams, which accounted for the mean annual storage of 1,86 x 10^6 tons between 1946 and 1973, according to data from the Department of Agricultural Technical Services quoted by Rooseboom and Maas (1974). Because the mean annual sediment discharge was 60,4 x 10^6 tons and the values ranged from 8,2 x 10^6 to 325,8 x 10^6 tons, the construction of dams before September 1970 cannot be the cause of the decline. After this date, however, the Hendrik Verwoerd Dam can be expected to trap an average of 46,8 x 10^6 tons annually (Rooseboom and Maas 1974).

The higher values obtained at the end of the 1930's were probably due to severe soil erosion which commenced in the 1880's after the discovery of gold and diamonds attracted large numbers of immigrants to South Africa. Agriculture was stimulated but led to overstocking and burning of the grassveld. The resultant soil erosion caused the topsoil to be stripped off, exposing bedrock or calcrete, which then halted soil erosion, particularly in areas of thin soil cover. Rooseboom and Maas (1974) invoked this permanent removal of topsoil as the chief mechanism to explain the decline in sediment discharge in the past few decades.

Meade (1969) has stressed that modern data on sediment discharge should not be used indiscriminately to extrapolate rates of erosion or deposition into even the Recent geological past. He cites the particularly severe erosion caused by bad farming practices in the Southern Piedmont of America (Meade and Trimble, 1974). Trimble (1973) quoted numerous examples of streams flowing deep and crystal clear, even when in flood, before bad farming practices damaged their catchments and caused extensive soil erosion.

Comparable descriptions of the Orange River in its undisturbed state are unfortunately scanty. Burchell (1922, p.322) crossed the river in mid-September 1811, before the first floods, and described the water as " ... quite transparent". Late in October of the same year he witnessed a flood of the Upper Orange (Nu-

gariep) where it joins the Vaal to become the Middle Orange (Great River). "... I beheld the mouth of the Nu-gariep rolling into the Great River, a rapid and agitated tide of muddy water, swelled to a terrific height, overwhelming the trees on its own banks, and thrown into waves by the force of its own impetuous current ..." (Burchell 1822, p.390). By this vivid account the Upper Orange in pre-agricultural times was clearly subject to powerful floods capable of transporting large volumes of water and sediment to the sea. The duration of the floods appears to have been longer in the past according to Germond (1967, pp.36 and 59, in Jacot Guillarmod, 1972a, p.93).

Butzer (1971a, p.45) visualized the undisturbed Recent Orange River near the Orange-Vaal confluence as grassveld or grass savanna, providing excellent soil protection, slowing down surface runoff and indirectly smoothing out discharge maxima. Relatively fine sediment was deposited in vegetation-choked channels containing perennial pools, linked to a high water table in the river banks. According to Butzer (1971a), the modern disturbed catchment is characterised by the replacement of grass with shrubs of the False Karoo (Acocks, 1953; Edwards, 1974). Rapid runoff, widespread sheet erosion of topsoil and donga formation are common and stream discharge is erratic. The intensity of downcutting and headward erosion noted today in most tributaries was not equalled during earlier erosive phases. The present erosive phase, which brought the natural accumulation of the Younger Fill to an end, commenced in the late 19th and early 20th centuries with the arrival of immigrants requiring intensive agricultural support.

The modern figures for sediment discharge are therefore probably unnaturally high. However, during a full Late-Pleistocene interglacial the Karoo vegetation would normally invade the catchment of the Orange as far as the False Karoo does today (Coetzee, 1967). The modern data are thus probably more indicative of sediment discharge during Late-Pleistocene interglacials than of modern conditions. With the advance of a glacial the grassveld would replace the Karoo flora, leading to aggradation in the river channel above lithologically controlled base levels down to the Aughrabies Falls. Reduced sediment discharge in the Lower Orange would be partially compensated by lowering of the river channel in response to a eustatically lowered sea level.

3. Provenance of sediment

The geology of the potential catchment area of the Orange River system is shown along with the individual subcatchments in Figure VII-1. However, it has been shown that the Upper Orange delivers most of the sediment. The varying lithology of the bedrock of this critical subcatchment plays an important role in making sediment available for erosion.

Basalt of the Drakensberg Formation (Johnson et al., in press) caps the

highest mountains of Lesotho (Figs. VII-1 and VII-4). The mountains receive over 2 000 mm of rain each year and are sometimes snowcapped in winter. Most of the streams originate in springs surrounded by bogs, which both regulate water discharge and filter sediment from the water (Jacot-Guillarmod, 1962, 1963, 1969, 1972b). Keulder (1973) selected the Bell River to represent the clear mountain streams. He found very low concentrations of suspended sediment and attributed this to the mechanically resistant basalt over which it flows (Bruce and Kruger, 1970, in Keulder, 1974) (Fig. VII-4).

Underlying the basalt of the Drakensberg Formation, in sequence, are first the Clarens Formation (Cave Sandstone), then the Elliot Formation (Red Beds), the Molteno Formation and the Burgersdorp Formation (Upper Beaufort) (Johnson et al., in press). Wellington (1955, p.344) describes the Khubedu and Sinqu headwaters of the Orange, which flow for the first 75 km over glutinous, montmorillonitic soils overlying basalt. On reaching the Clarens Formation (Cave Sandstone) the river receives "a heavy load of fine sand". Size analyses by Beukes (1969, 1970) showed that the massive, thick beds typical of the Clarens Formation are composed chiefly of very fine sand or coarse silt. Caves are formed when the matrix is calcitic, but a silicic outer crust can prevent erosion (Beukes, 1970). The Clarens Formation clearly releases more sediment than does the basalt of the Drakensberg Formation, and the fineness of the sand fraction ensures that it is transported rapidly in suspension rather than as bedload. By forming scarps the Clarens Formation is equally more resistant to erosion than the underlying mudstones of the Elliot Formation (Red Beds) (Harmse, 1974, Fig. 3). Silica-cemented sandstones of the Molteno Formation (Turner, 1970, 1972, 1975), in turn, form scarps above the less resistant shales and sandstones of the Burgersdorp Formation (Upper Beaufort) (Harmse, 1974, Fig. 4).

The outcrop of the Elliot Formation is much less extensive than that of the equally friable Burgersdorp Formation, which has been pinpointed as the chief source of the sediment carried to the sea today by the Orange River (Keulder, 1973; 1974). This is brought home by the rapid increase in sediment concentration once the various tributaries reach the outcrop of the Burgersdorp Formation (Fig. VII-4). Theron (1970, 1973) found that the mean grain size of this formation's sandstones lies in the fine to very fine sand range, which, like the sand released by the Clarens Formation, is readily transported in suspension.

Sediment discharge data (Rooseboom and Maas, 1974) are available for three of the eight stations occupied by Keulder (1973): at Aliwal North below the Orange-Kraai confluence; at Wepener half-way down the Caledon River; and at Bethulie below the Orange-Caledon confluence (Fig. VII-4). Above Aliwal North the mean annual sediment production for the years 1932-1939 (Rooseboom and Maas, 1974) was 444 ton/km^2, reflecting sediment released from a catchment underlain chiefly by resist-

SUSPENDED SEDIMENT LOAD IN THE UPPER ORANGE CATCHMENT

(After Keulder, 1973)

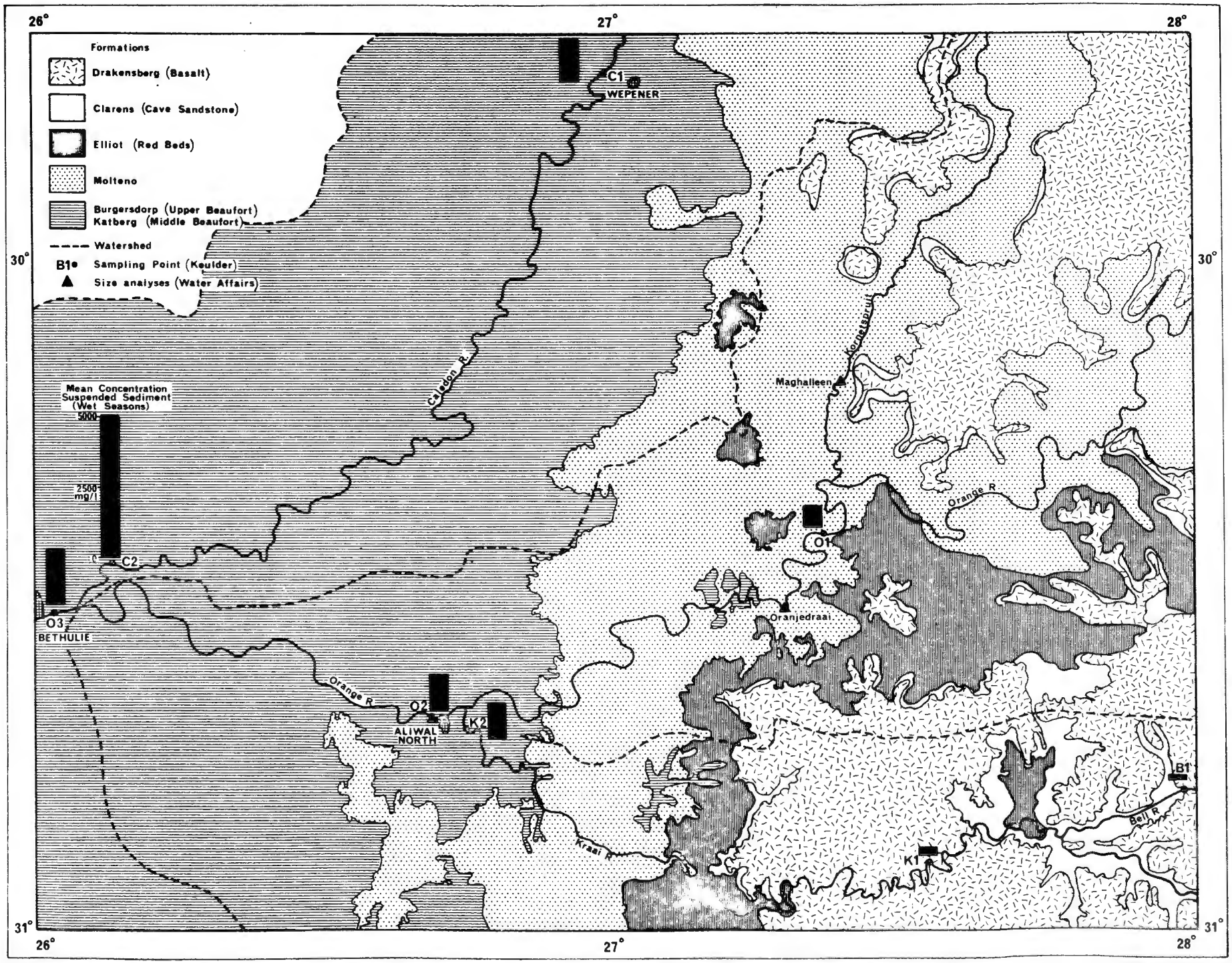

Fig. VII

ant basalt and sandstone. In contrast, the corresponding figures are 1089 tons/km^2 for the area above Wepener in the Caledon catchment, and 1005 tons/km^2 for the area above Wepener in the Caledon catchment, and 1005 tons/km^2 for the area between Bethulie and the other two sampling points. Erosion of Burgersdorp Formation sediments is responsible for the two and a half-fold increase in sediment production. Despite these differences in erosion potential, the mean annual sediment discharges from the individual sections are comparable due to varying catchment areas; the values all lie between 13,6 and 16,5 x 10^6 tons (Rooseboom and Maas, 1974).

4. Fluviatile transport of sediment

Beukes (1970), Turner (1970) and Theron (1970) have shown that the coarse fractions of the sandstones in the Clarens, Molteno and Burgersdorp Formations chiefly comprise medium to very fine sand. Such material travels in suspension if the stream velocity exceeds 100 cm/sec (Allen, 1965, Fig. 10). The writer has located no data on stream velocities during Orange River floods, but it is probable that this threshold velocity is exceeded by several orders of magnitude. The flooding river is probably competent to transport the available sand fraction in suspension along with the silt and clay from the mudstones of the Elliot, Molteno and Burgersdorp Formations.

Data on the size distribution of suspended sediment have been supplied to the author by the Department of Water Affairs (Fig. VII-5); silt predominates over both clay and sand. Harmse (1974) pointed to the Elliot and the Burgersdorp Formations as the source of the readily erodible silt. Although subordinate in amount, the sand fraction ranges from medium to very fine sand, the latter size fraction always being most abundant. It will be shown that the size fractions dominant in the river's suspended load are dominant on the river's submarine delta.

The coarse fractions of 43 samples of river sediment have been sieved at half-phi intervals. The samples were collected at various points adjacent to road bridges in the Upper, Middle and Lower Orange, as well as in the Fish River, and generally represent topstratum deposits deposited from suspension after floods. Plotting mean size versus standard deviation (Fig. VII-6) we find a suite ranging from very well sorted to poorly sorted, with mean sizes chiefly in the fine and the very fine sand categories.

5. Summary

Hydrological and sedimentological data characterise the Orange River as a highly erratic, seasonal river, which transports an average of 60 million tons of sediment to the sea each year. The effective catchment of the Orange is restricted to the subcatchments of the predominant Upper Orange and the subordinate Vaal, which are chiefly underlain by fine-grained sedimentary formations of the Karoo

SIZE DISTRIBUTION OF SUSPENDED SEDIMENT IN THE ORANGE RIVER

(From data supplied by Department of Water Affairs)

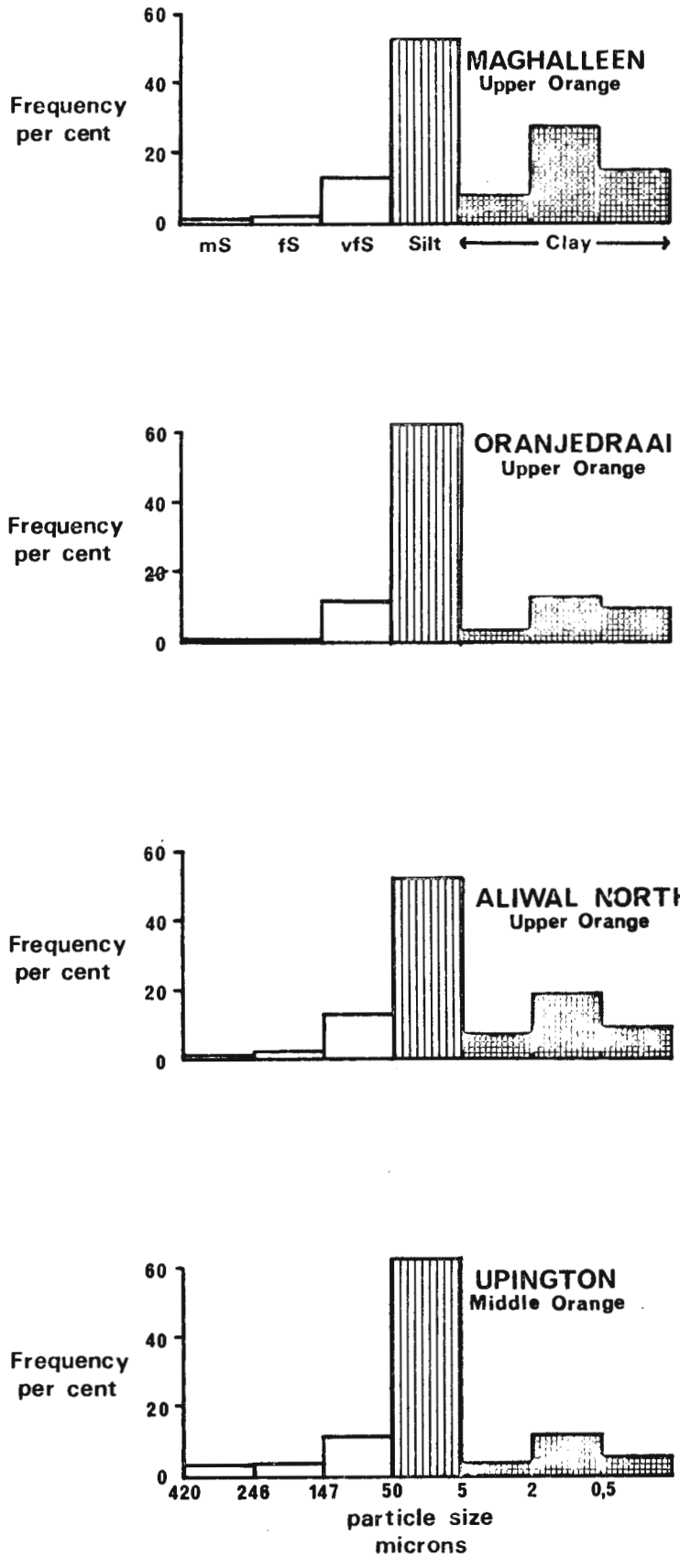

For Locations see Fig. VII-5

Fig.VII-5

MEAN VERSUS STANDARD DEVIATION (MOMENT MEASURES) FOR SEDIMENTS FROM THE NAMIB HINTERLAND AND COASTAL ZONE

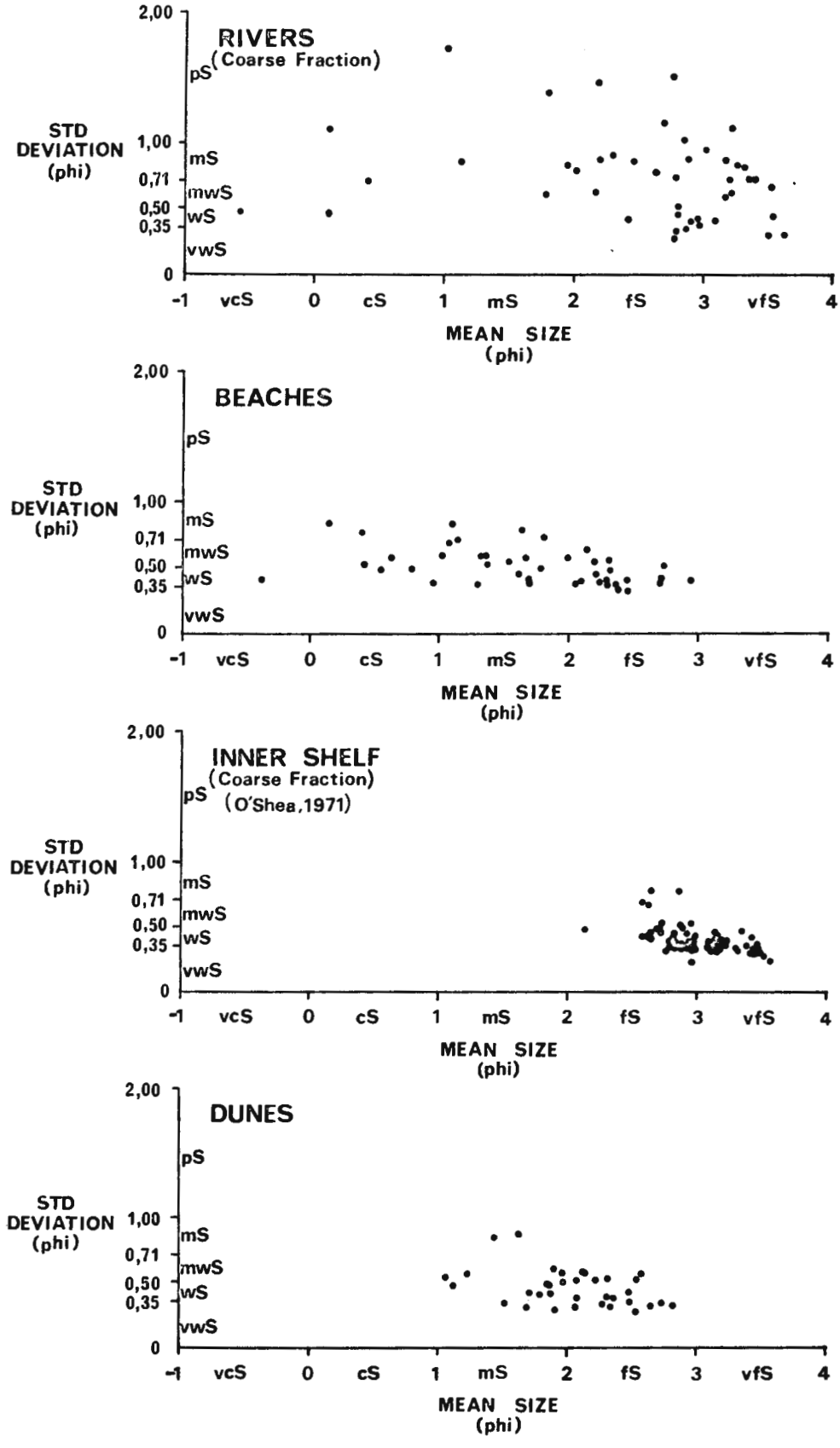

Fig.VII-6

Supergroup. As a result clay, silt, very fine sand and fine sand are eroded and transported rapidly in suspension to the mouth during powerful seasonal floods.

C. DISPERSAL AND DEPOSITION OF TERRIGENOUS SEDIMENT

1. Introduction

At the mouth of the Orange River coarse sediment is trapped in the littoral zone and transported northwards to the Namib Sand Sea, modifying the morphology of the coastline en route. Fine sediment is dispersed southwards by geostrophic counter currents, particularly in winter when cyclonic storms accelerate southerly drift and storm waves increase bottom turbulence.

In discussing this basic model the Namib Desert will first be placed in regional perspective, and then the interrelated effects of pressure systems, waves, winds and currents on the dispersal and deposition of Orange River Sediment will be delineated.

2. The Namib Desert

a. Worldwide setting

The Namib Desert is one of five west-coast deserts, each of which has both shared and unique characteristics (Meigs, 1966). These deserts are found in Western Australia, Baja California (Inman et al., 1966), Northwest Africa (Wilson, 1971; Sarnthein and Walger, 1974), Chile-Peru (Rich, 1942) and South West Africa (Kaiser, 1926; Logan, 1960).

Each desert lies on the western side of a continent in subtropical latitudes and, with the exception of Western Australia (Meigs, 1966), the aridity of each desert is intensified by coastal upwelling. Due to its lack of offshore upwelling, Western Australia lacks an extreme-arid core and grades from a winter-rainfall semi-desert in the south to a summer-rainfall semi-desert in the north (Meigs, 1966). Northwest Africa (Meigs, 1966; Wilson, 1971; Sarnthein and Walger, 1974) is similar to the Namib in most respects, but it is also part of the Sahara Desert, which stretches right across the African continent. Sandflow (Wilson, 1971) is primarily perpendicular towards the coast, whereas in the Namib sandflow is chiefly parallel to the coast. In Baja California (Inman et al., 1966), the desert is situated along a narrow, tectonically hyperactive peninsula west of a spreading centre along the Gulf of California. The desert is therefore very restricted in surface area.

The Atacama Desert of northern Chile and its extension in southern Peru are confined to a narrow, tectonically active coastal plain west of the Andes Mountains (Rich, 1942). The mountains were formed by the American plate spreading westwards and overriding the eastward-spreading Nazca plate. Due to the narrowness of the coastal plain, the South American desert lacks the older, less-mobile sections that

characterise the eastern edges of the two African deserts, but parallels the high-energy coastal section of the Namib Desert. The region has been subjected to meticulous scientific study for many years (e.g. Bowman, 1924; Finkel, 1959; Hastenrath, 1967; Grolier et al., 1974) and by direct analogy, conclusions reached in South America will be applied to the relatively unstudied Namib Desert.

b. Subdivisions of the Namib Desert

Climatically the Namib Desert can be subdivided into an arid to extreme-arid core in South West Africa, a summer-rainfall desert in Angola north of the Kunene River, and a winter-rainfall desert in Namaqualand south of the Orange River. The northern limit of the desert is the Coroca River (15°S) in Angola, the southern limit is the Oliphants River (32°S) in Namaqualand, and the eastern limit is the Great Escarpment (Wellington, 1955).

The desert has been subdivided geomorphologically by a succession of authors (Kaiser, 1926; Wellington, 1955; Logan, 1972; Barnard, 1973; Kayser, 1973; Breed et al., in McKee, in press). Each classification can be criticised as being too detailed, too generalized or too restricted geographically. The writer suggests the following subdivisions, moving from south to north:

i) Namaqualand Sandy Namib
ii) Sperrgebiet Sandy Namib
iii) Sperrgebiet Trough Namib
iv) Sperrgebiet Pediplain
v) Coastal outgrowths
vi) Namib Sand Sea
vii) Namib Rocky Platform
viii) Skeleton Coast
ix) Kaokoveld
x) Kunene Sand Sea.

The Namaqualand Sandy Namib (Fig. VII-7) is a Mediterranean desert receiving rain in winter. The combination of rain in winter (Table VII-4) and daily fog provides enough moisture to support vegetation which stabilises the sand that blows onshore during summer droughts. As detailed in Chapter VI most of the sand was probably brought to the coast by local rivers during a wetter glacial period. Relatively little sediment is being supplied to the coast today.

The Sperrgebiet Sandy Namib (Fig. VII-8) lies north of the Orange River to the Koichab River east of Lüderitz, and derives most of its sand from sand banks in the Orange River during the dry season. Sediment is thus replenished annually during summer floods from the interior of the subcontinent. Kaiser's (1926, p.32) "Die Flächennamib" or "Plains Namib" is not favoured, a) because the plain was probably formed under different climatic conditions during the Tertiary (King, 1951), and b) because a "plain" can be either rocky or sandy.

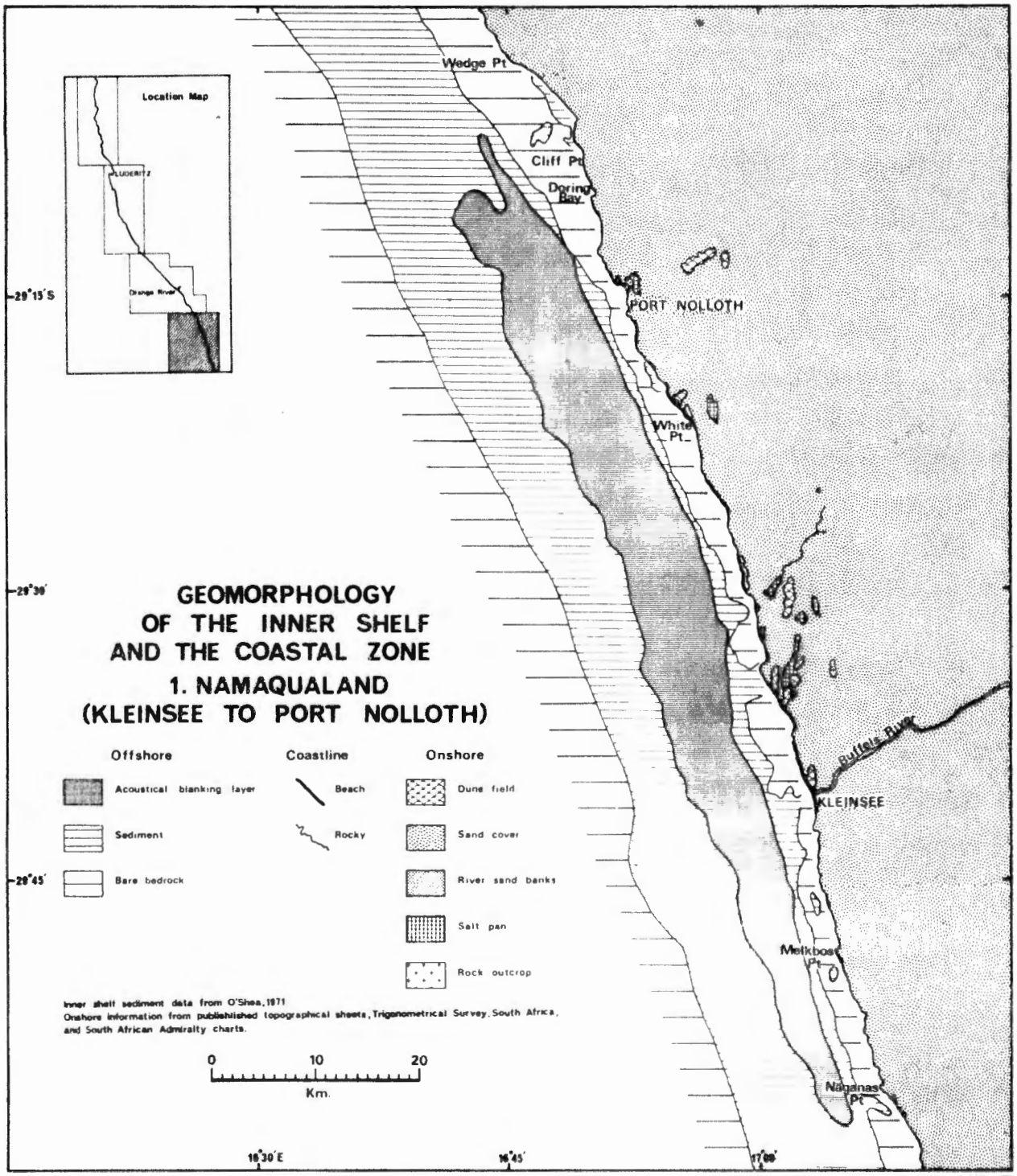
Location Map
LUDERITZ
Orange River
Wedge Pt
Cliff Pt
Doring Bay
PORT NOLLOTH
White Pt
Buffels River
KLEINSEE
Melkbos Pt
Nagenas Pt
29°15'S
29°30'
29°45'
16°30'E
16°45'
17°00'
GEOMORPHOLOGY
OF THE INNER SHELF
AND THE COASTAL ZONE
1. NAMAQUALAND
(KLEINSEE TO PORT NOLLOTH)
Offshore
Acoustical blanking layer
Sediment
Bare bedrock
Coastline
Beach
Rocky
Onshore
Dune field
Sand cover
River sand banks
Salt pan
Rock outcrop
Inner shelf sediment data from O'Shea, 1971
Onshore information from publishlished topographical sheets, Trigonometrical Survey, South Africa, and South African Admiralty charts.
0
10
20
Km.

Fig. VII-7

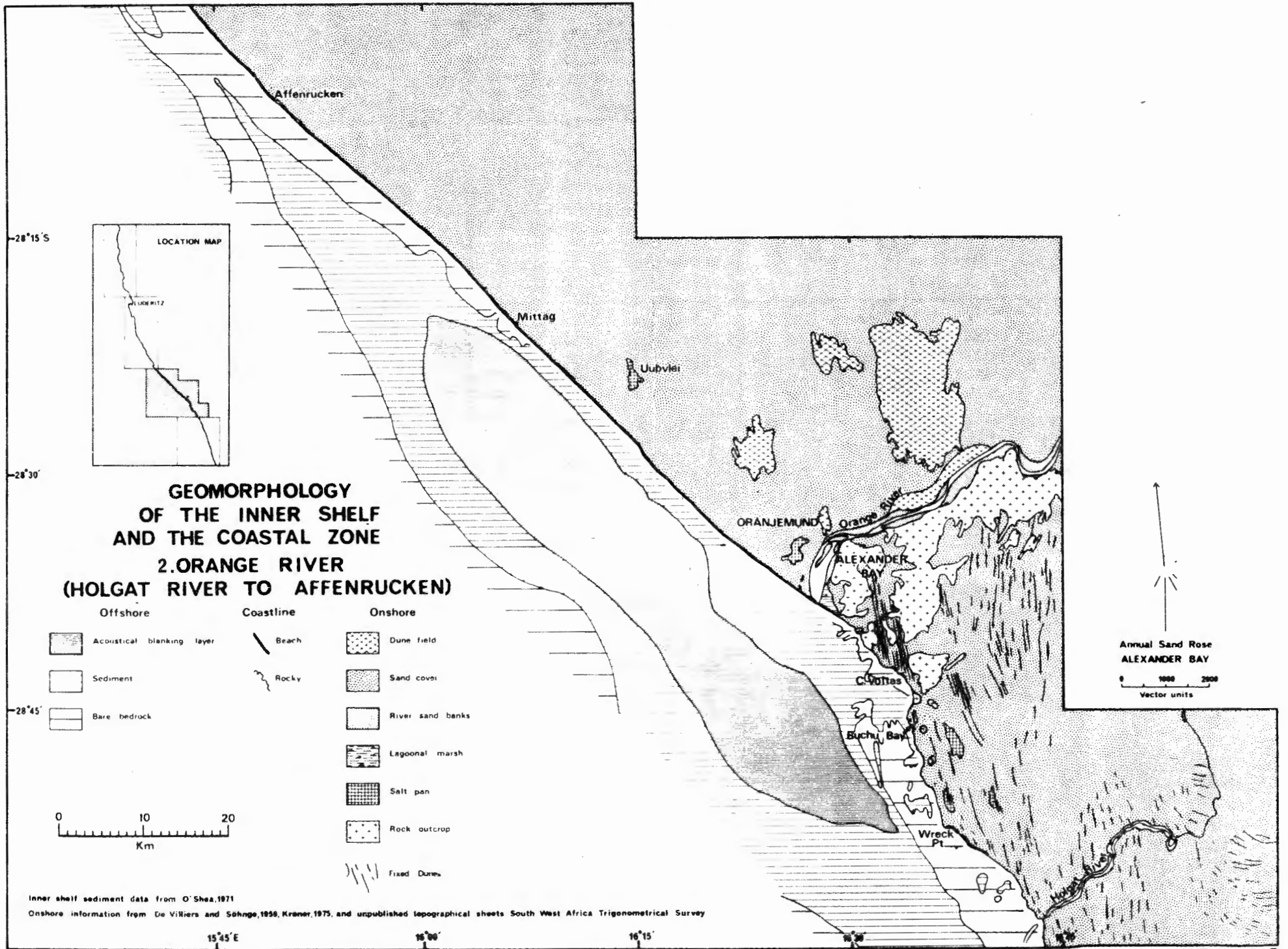
Affenrucken
Mittag
Uubvlei
ORANJEMUND
Orange River
ALEXANDER BAY
C. Voltas
Buchu Bay
Wreck Pt
Hotaz River
LOCATION MAP
LUDERITZ
28°15'S
28°30'
28°45'
15°45'E
16°00'
16°15'
GEOMORPHOLOGY
OF THE INNER SHELF
AND THE COASTAL ZONE
2.ORANGE RIVER
(HOLGAT RIVER TO AFFENRUCKEN)
Offshore
Acoustical blanking layer
Sediment
Bare bedrock
Coastline
Beach
Rocky
Onshore
Dune field
Sand cover
River sand banks
Lagoonal marsh
Salt pan
Rock outcrop
Fixed Dunes
0 10 20
Km
Annual Sand Rose
ALEXANDER BAY
Vector units
Inner shelf sediment data from O'Shea,1971
Onshore information from De Villiers and Söhnge,1959, Kroner,1975, and unpublished topographical sheets South West Africa Trigonometrical Survey

Fig. VII - 8

TABLE VII-4

Mean rainfall (mm) along the west coast of southern Africa (from Tripp, 1975)

Period/ Station	Walvis Bay (Pelican Point)	Lüderitz (Diaz) Point)	Pomona	Alexander Bay (Weather office)	Port Nolloth	Cape Town (Wingfield)
January	2,0	1	0	1	1	14
February	0,2	2	15	3	2	10
March	3,1	3	0	4	4	16
April	0,6	2	0	3	6	54
May	0,4	3	0	8	9	78
June	0,5	2	15	7	9	83
July	0,0	2	0	5	8	92
August	0,3	1	0	8	6	70
September	0,1	1	0	2	4	44
October	0,2	0,2	0	2	3	30
November	1,1	0,4	0	2	2	21
December	0,1	1	0	8	2	10
YEAR	8,6	19	30	53	59	522
Period of Observation (years)	13	30	36	19	84	24

Kaiser (1926) confined most of his work to the "Wannennamib" or "Trough Namib", where the topography has been created by aeolian deflation and corrasion. The writer names this small but important area, the Sperrgebiet Trough Namib, which lies between Chamais Bay and Lüderitz, where aeolian deflation and corrasion almost obliterate any signs of fluvial processes. In practice, its interior boundary is marked by a conspicuous train of large barchan dunes, which leaves the coast at Chamais Bay and joins the Namib Sand Sea east of Lüderitz (Fig. VII-9).

The Sperrgebiet Pediplain lies below the Great Escarpment between the Orange and the Kuiseb Rivers. Under present climatic conditions little sediment is contributed from the Escarpment, but any climatic shifts either poleward or equatorward, would increase annual rainfall and consequently accelerate alluviation of the pediplain.

Coastal outgrowths occur on a small scale between Chamais Bay and Lüderitz, but south of Hottentot Bay (Fig. VII-10) and particularly from Meob Bay to Walvis Bay (Logan, 1960), the coast has clearly accreted extensively in historical times.

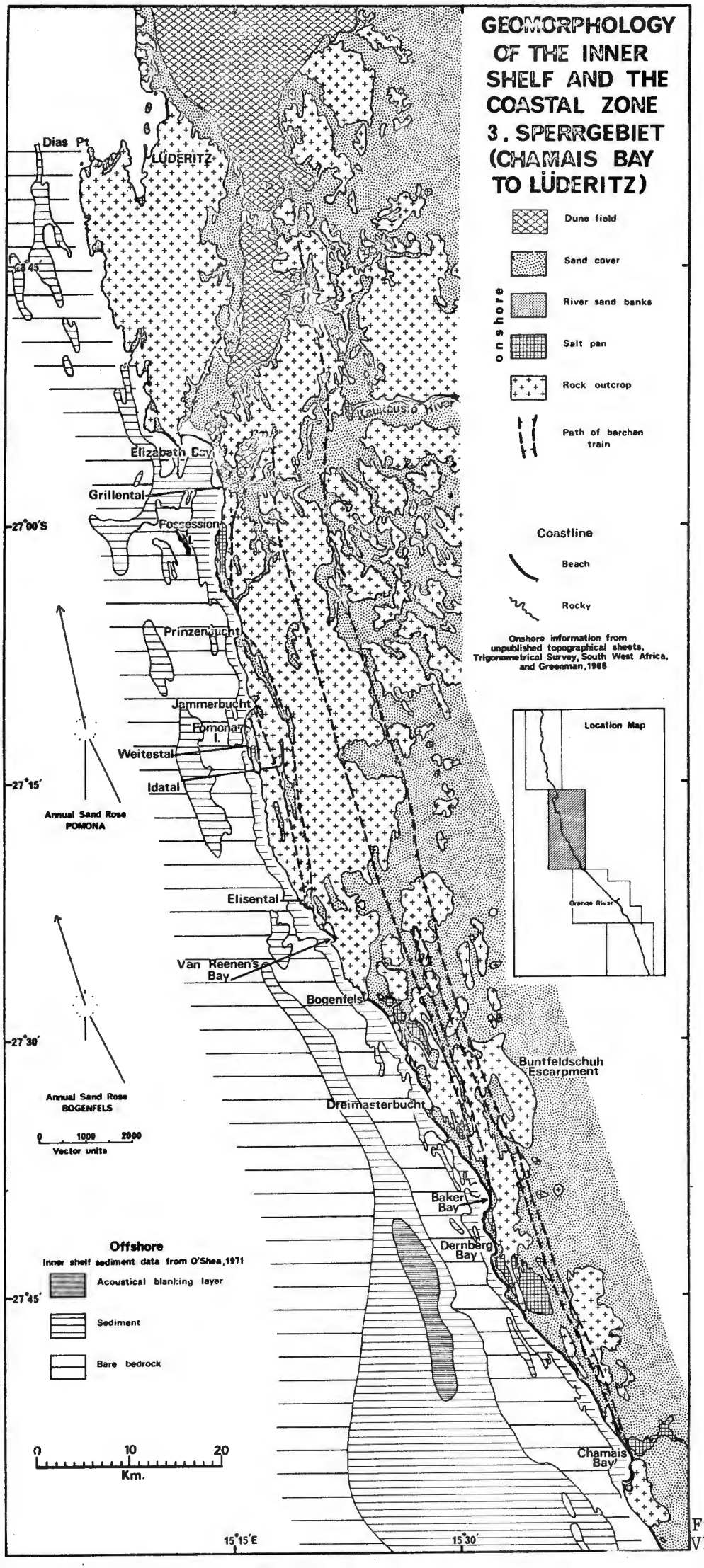
GEOMORPHOLOGY OF THE INNER SHELF AND THE COASTAL ZONE 3. SPERRGEBIET (CHAMAIS BAY TO LÜDERITZ)
Dune field
Sand cover
River sand banks
Salt pan
Rock outcrop
Path of barchan train
onshore
Coastline
Beach
Rocky
Onshore information from unpublished topographical sheets, Trigonometrical Survey, South West Africa, and Greenman, 1966
Location Map
Orange River
Dias Pt
LÜDERITZ
Elizabeth Bay
Grillental
Possession I.
Prinzenbucht
Jammerbucht
Pomona I.
Weitestal
Idatal
Elisental
Van Reenen's Bay
Bogenfels
Buntfeldschuh Escarpment
Dreimasterbucht
Baker Bay
Dernberg Bay
Chamais Bay
Kaukausib River
27°00'S
27°15'
27°30'
27°45'
15°15'E
15°30'
Annual Sand Rose POMONA
Annual Sand Rose BOGENFELS
0 1000 2000
Vector units
Offshore
Inner shelf sediment data from O'Shea, 1971
Acoustical blanking layer
Sediment
Bare bedrock
0 10 20
Km.

Fig. VII-9

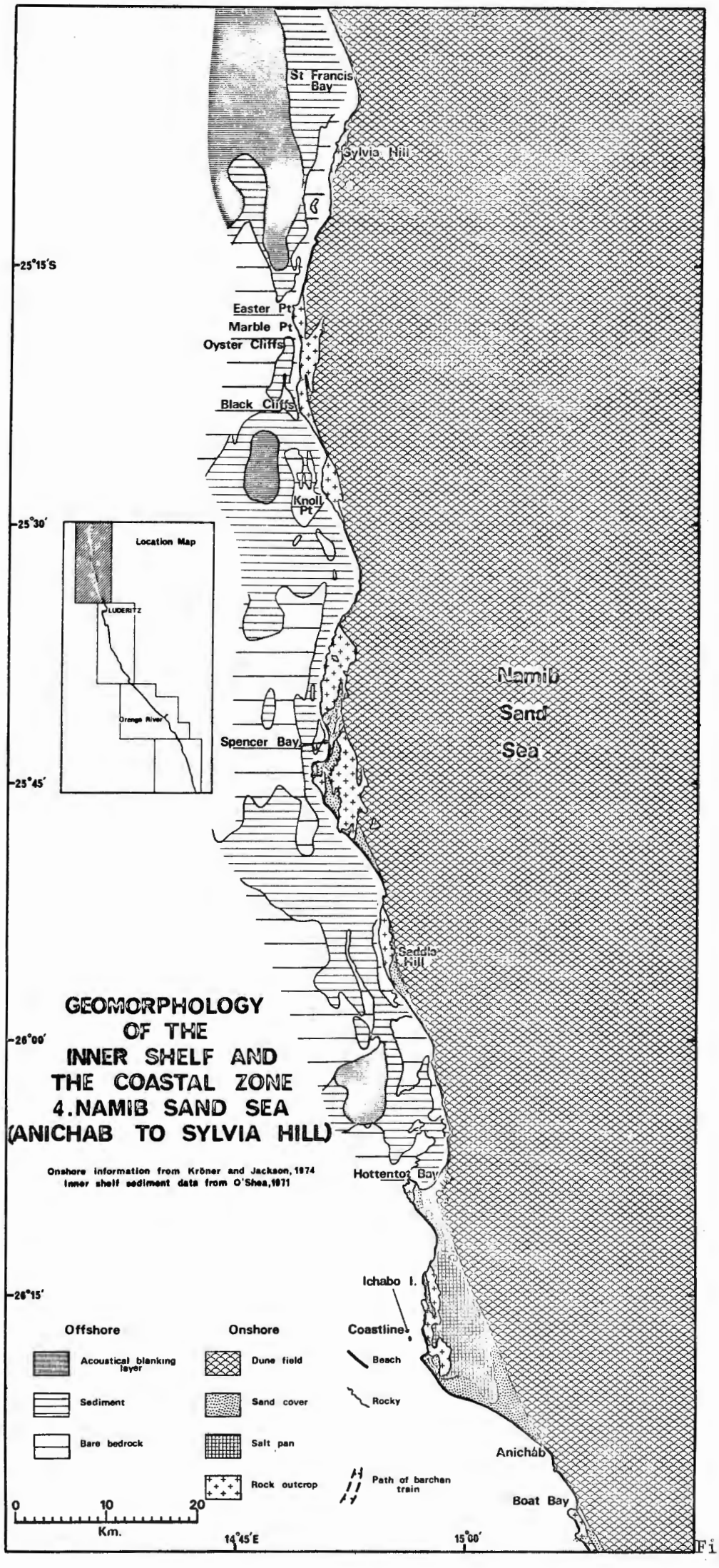
St Francis Bay
Sylvia Hill
25°15'S
Easter Pt
Marble Pt
Oyster Cliffs
Black Cliffs
Knoll Pt
25°30'
Location Map
LUDERITZ
Orange River
Spencer Bay
25°45'
Namib Sand Sea
Saddle Hill
GEOMORPHOLOGY OF THE INNER SHELF AND THE COASTAL ZONE 4.NAMIB SAND SEA (ANICHAB TO SYLVIA HILL)
26°00'
Onshore information from Kröner and Jackson, 1974
Inner shelf sediment data from O'Shea, 1971
Hottentot Bay
Ichabo I.
26°15'
Offshore
Acoustical blanking layer
Sediment
Bare bedrock
Onshore
Dune field
Sand cover
Salt pan
Rock outcrop
Coastline
Beach
Rocky
Path of barchan train
Anichab
Boat Bay
0
10
20
Km.
14°45'E
15°00'

Fig.VII-10

The Namib Sand Sea has three main sections. Near the coast, barchanoid dunes stretch from Elizabeth Bay (Fig. VII-9) to Swakopmund (Barnard, 1973; Breed et al., in McKee, in press). Farther inland are longitudinal dunes between the Koichab and the Kuiseb Rivers, and beside the Sperrgebiet Pediplain are unconsolidated star dunes, frequnetly overlying older consolidated dunes (Barnard, 1973).

Between the Kuiseb River and the Brandberg (Logan, 1972) is the seaward-sloping rocky plain called here the Namib Rocky Platform (cf. Logan, 1969). North of the Brandberg, the Great Escarpment becomes clearly defined and its pediplain is well known as the Kaokoveld. The coastal area has long been known as the Skeleton Coast (Logan, 1972). The small sand sea north and south of the Kunene River has recently been referred to as the Kunene Sand Sea (Bremner, 1976, personal communication), to distinguish it from the larger Namib Sand Sea farther south.

3. Pressure systems

In summer, when Orange River discharge is at a maximum, the subcontinent frequently is a low-pressure area, whereas the South Atlantic is constantly a high-pressure area. The belt of cyclones of the Southern Ocean is likewise a constant feature, but in summer it lies south of the subcontinent. Van Ieperen (1975) is of the opinion that the cyclones contribute relatively little energy to the wave spectrum during summer, particularly north of Lüderitz. He suggests that strong southerly gales generate the relatively short-period waves observed. These gales, in turn, are the result of the steep pressure gradient between the South Atlantic High, centred near latitude 32°S, and "coastal lows" (Van Zinderen Bakker, 1976).

In winter the pressure gradient over the west coast decreases markedly, because the subcontinent is a zone of high pressure like the adjacent ocean. Anticyclonic winds are thus greatly reduced in magnitude. South of Lüderitz, however, the cyclones of the Southern Ocean regularly cause stormy seas and high swells, during a period when Orange River discharge is at a minimum.

Therefore both wind and wave action are important in summer, whereas in winter wind activity declines and wave action is relatively more important.

4. Wave regime

Wave action plays an important role in the dispersal and deposition both of coarse sediment in the littoral zone and of fine sediment on the middle shelf. Van Ieperen (1976) presents spectral analyses of the waverider date from Saldanha Bay (33°S), Lüderitz (27°S) and from Walvis Bay (23°S). Maximum wave heights (H_{max}) at Saldanha Bay and at Lüderitz both centre around 2-4 m, compared with 1-3 m at Walvis Bay. (Using a conversion factor of 0,606, the corresponding figures for significant wave heights are 1,2-2,4 m and 0,6-1,8 m). Wave action clearly intensifies southwards. However, a closer inspection of the Lüderitz data suggests

that the wave-height histogram of Lüderitz is skewed towards higher waves, whereas that of Saldanha Bay is skewed towards lower waves. Unfortunately, the data are far from synoptic so that confirmation of this trend awaits further spectral analysis, which will hopefully also include data from a waverider installed off the mouth of the Orange River early in 1976 (Woodward, 1976, personal communication).

Van Schaik et al. (1970) present data on wave direction, height and period for Buchu Bay just south of the Orange River mouth. The data were collected three times per day using an onshore clinometer and an offshore buoy, moored in 23 m of water, between June 1969 and May 1970. No records were taken at weekends or, more significantly, during "bad weather", so that overall coverage was as low as 55%. The dominant wave direction proved to be SW from spring through summer to autumn, but from WSW and secondly from SW during winter. Local cyclonic storms are doubtless the cause of the winter trend.

Recorded wave heights for the year ranged from 0,5 to 4,0 m with 95% of the waves between 0,5 and 2,0 m. Maximum wave height at Buchu Bay ranged from 2,0 m in winter and in spring, to 3 m in summer, and to 4 m in autumn, just after the summer floods.

Wave periods at Buchu Bay varied from 9 to 17 seconds, over 50% of which were between 11 and 13 seconds, and 99% between 9 and 15 seconds. The longest wave periods were recorded in winter and in spring. Van Ieperen's (1975, 1976) more sophisticated analyses of the continuously recorded Lüderitz data (buoy moored in 108 m) showed that relatively little energy was contributed by waves with periods longer than 12,5 seconds. Most of the wave periods were between 8 and 12 seconds. The peak for both spring and summer (Van Ieperen, 1975) was 11 seconds, but the overall range was narrower and the peak more pronounced in spring. Seasonal variations in wave period therefore appear to be insignificant.

5. Wind regime

a. Data sources and data presentation

Parts of the west coast of Southern Africa are possibly the windiest in the world. Several approaches have been used to illustrate the area's wind regime. Firstly conventional eight-point wind-roses have been constructed for seven localities (Fig. VII-11). Both morning and afternpon data for both winter and summer are depicted to illustrate diurnal and seasonal trends.

Daily readings (summer only) from an offshore drilling rig were supplied by SOEKOR (De Winter, 1975, personal communication). Data for Port Nolloth, O'Okiep, Lüderitz and Aus were obtained from an official handbook entitled "Weather on the Coasts of Southern Africa" (Meteorological Services of the Royal Navy and the South African Air Force, 1944). Readings for Oranjemund, taken by the Marine Diamond Corporation, were supplied by Dr. M.K. Seely (1975, personal communication) of the Namib Desert Research Station at Gobabeb. The Bogenfels data were recorded by

WIND ROSES

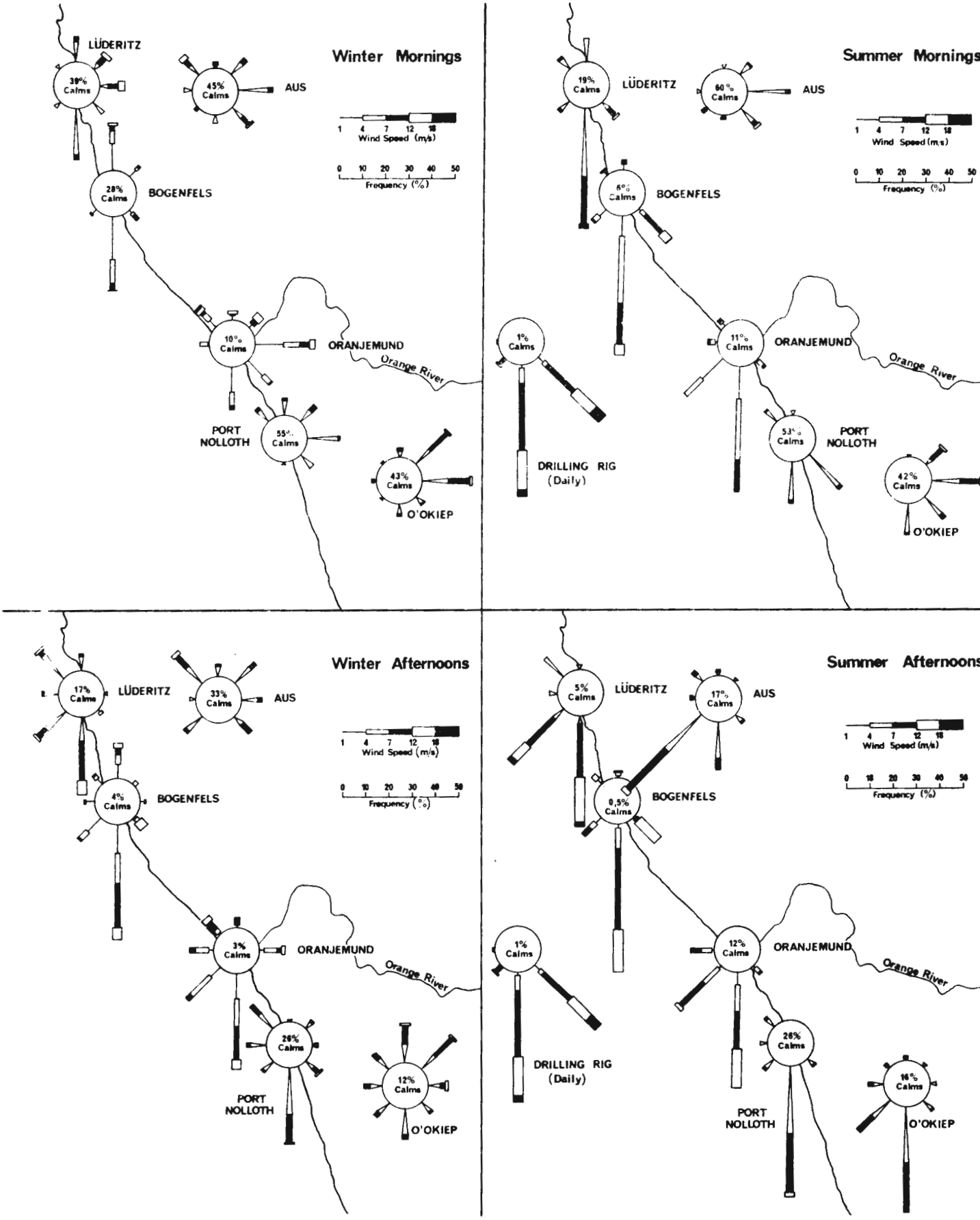

Fig.VII-11

German diamond-miners during the First World War and were discovered in an abandoned hut there within the last decade. They were kindly made available by the Marine Diamond Corporation (Hockney, 1975, personal communication).

A second approach was to use hourly data from Alexander Bay on the south bank of the Orange River (Schulze, 1965) to illustrate diurnal and seasonal variations (Fig. VII-12).

Thirdly, thrice-daily data for winter and summer at Oranjemund, on the north bank of the Orange River, and at Bogenfels in the Sperrgebiet Trough Namib were plotted to depict the frequency of gales capable of transporting sand (Fig. VII-13).

The fourth attack on the problem will be discussed more thoroughly, both because the technique is relatively new, and because the results were particularly meaningful. Data from Cape Town (Wingfield), and Walvis Bay (Pelican Point) (Meteorological Service of the Royal Navy and the South African Air Force, 1944), from Alexander Bay (Schulze, 1965), Bogenfels (Hockney, 1975, personal communication) and from Pomona (Kaiser, 1926) were used in wind-analysis procedures developed by the U.S. Geological Survey during a study of the sand seas of the world (Fryberger, in McKee, in press). In these procedures the equation for rate of aeolian sand transport (q) is generalised and related to wind velocity (V) (measured at the standard height of 10 m):

$$q \alpha V^2(V-V_t)$$

In this formula V_t is the impact threshold wind velocity at 10 m, or phrased differently, the minimum wind velocity (measured at 10 m) required to keep sand in motion (Fryberger, in McKee, in press). Fryberger chose 12 knots (6 m/s) as the threshold velocity for loose, dry, unvegetated quartz sand with a mean size of 0,25 mm (2 phi) and no bedforms larger than ripples. Weighting factors for the mean velocity of each velocity category above the threshold velocity are calculated by inserting the mean velocity as V into the formula

$$q \alpha V^2 (V-V_t)$$

The rate of sand transport (q), divided by 100 for convenience, for each velocity category in each direction, is multiplied by the frequency of occurrence (f) of each velocity category in each direction. By this procedure the amount of sand drift (Q) in vector units for each velocity category can be obtained for each direction, and then summed to obtain the drift potential (DP) for the period concerned. The DP for each direction is then resolved into x- and y-components to calculate the resultant. The resultant drift direction (RDD) is then calculated using the formula RDD arctan x/y. The resultant drift potential (RDP) is calculated from the formula RDP = $\sqrt{x^2+y^2}$. The RDP/DP ratio is also calculated, as a measure of the constancy of wind direction.

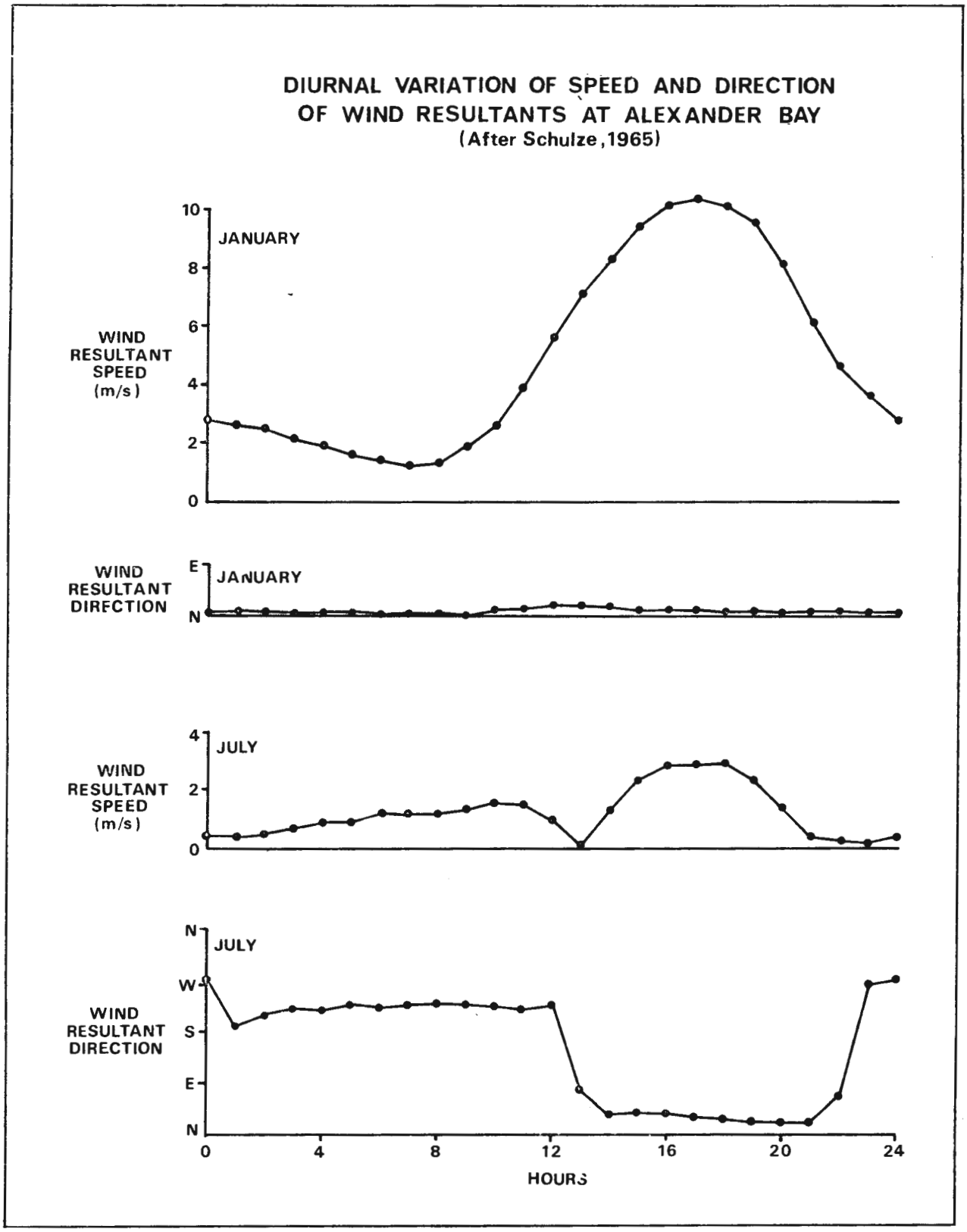
DIURNAL VARIATION OF SPEED AND DIRECTION
OF WIND RESULTANTS AT ALEXANDER BAY
(After Schulze,1965)
WIND RESULTANT SPEED (m/s)
JANUARY
10
8
6
4
2
0
WIND RESULTANT DIRECTION
JANUARY
E
N
WIND RESULTANT SPEED (m/s)
JULY
4
2
0
WIND RESULTANT DIRECTION
JULY
N
W
S
E
N
0
4
8
12
16
20
24
HOURS

Fig.VII-12

THRICE – DAILY WIND OBSERVATIONS AT BOGENFELS AND ORANJEMUND

(Marine Diamond Corporation)

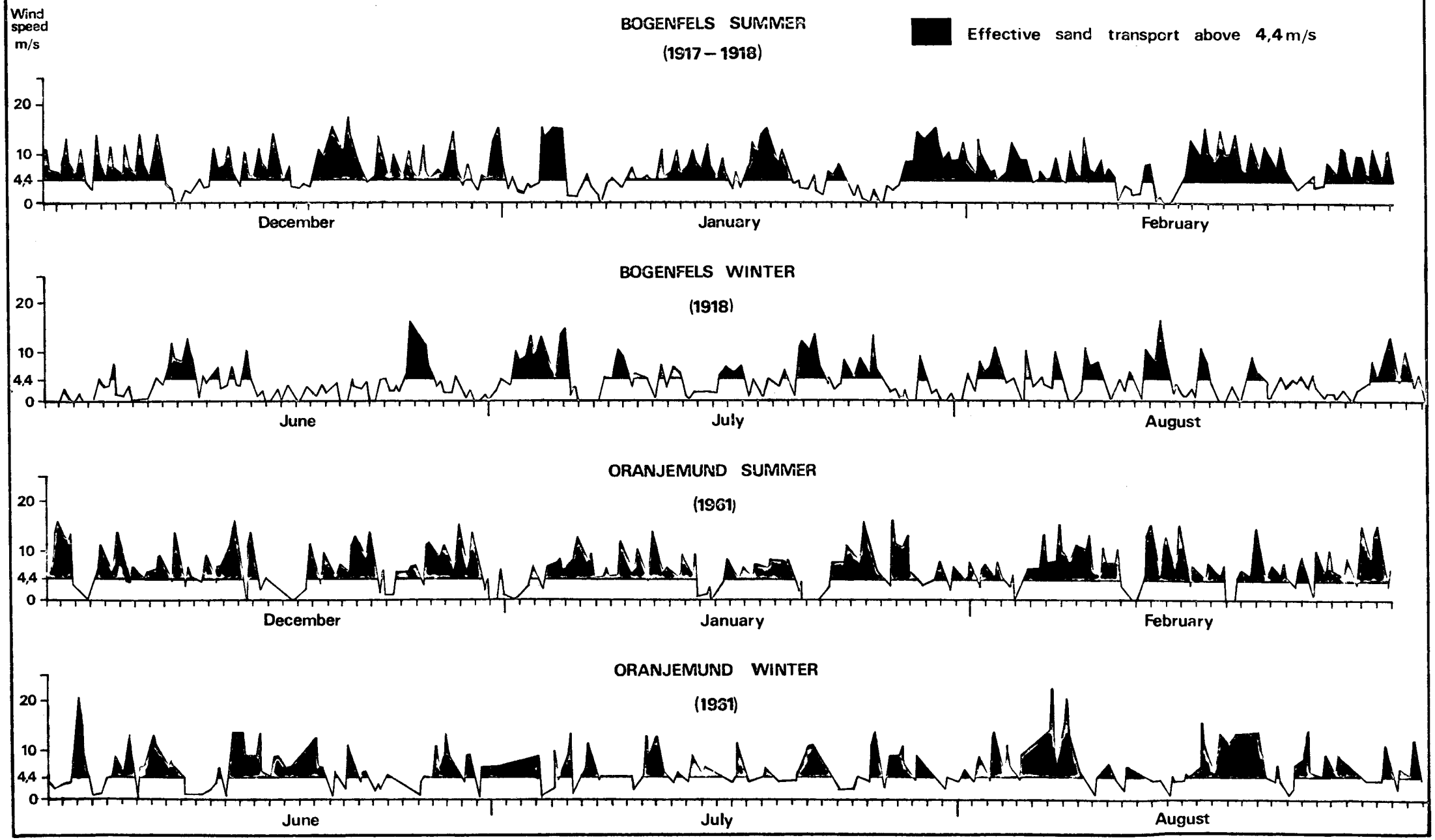

Fig.VII-13

The wind parameters for the west coast from Cape Town to Walvis Bay are listed in Table VII-5. The latitudinal variations in both annual RDP (Fig. VII-14) and in monthly RDP (Fig. VII-15) are illustrated. The annual drift potentials for each direction and the annual resultant drift potential were used at each locality to construct annual "sand roses" (Fig. VII-16) to illustrate the effective wind regime.

TABLE VII-5

Annual wind parameters along the west coast of southern Africa

Locality	Drift Potential (DP) vector units	Resultant Drift Potential (RDP) vector units	RDP/DP	Resultant Drift Direction (RDP)	Sand-rose Classification
Walvis Bay (Pelican Point)	492 (high energy)	456	0,93(Constant)	30,8°	Narrow unimodal
Pomona	2823 (high energy)	2731	0,97(Constant)	347,7°	Narrow unimodal
Bogenfels	2252 (high energy)	2065	0,92(Constant)	342,3°	Narrow unimodal
Alexander Bay	2346 (high energy)	1990	0,85(Constant)	355,2°	Wide unimodal
Cape Town (Wingfield) rain-bearing winds excluded	653 (high energy)	618	0,95(Constant)	1,1°	Narrow unimodal

b. Discussion of available wind data

Considerable attention is paid to the wind regime a) because it is vital to an understanding of sediment dispersal, b) because wind locally controls upwelling, and c) because much of the data have never been analysed scientifically.

Eight-point wind data are presented in the standard wind-rose format for seven localities, two inland, four on the coast, and one offshore (Fig. VII-11). The diurnal increase in wind velocity in the afternoon is clearly illustrated (cf. Fig. VII-12) and the stronger wind regime of summer is apparent. East winds are significant at all onshore stations except Bogenfels in the Sperrgebiet Trough Namib, particularly in the mornings. Offshore the drilling rig was situated in the South East Trade Winds. At Port Nolloth the winds are mainly from the south,

LATITUDINAL VARIATION IN ANNUAL RESULTANT DRIFT POTENTIAL CAPE TOWN TO WALVIS BAY

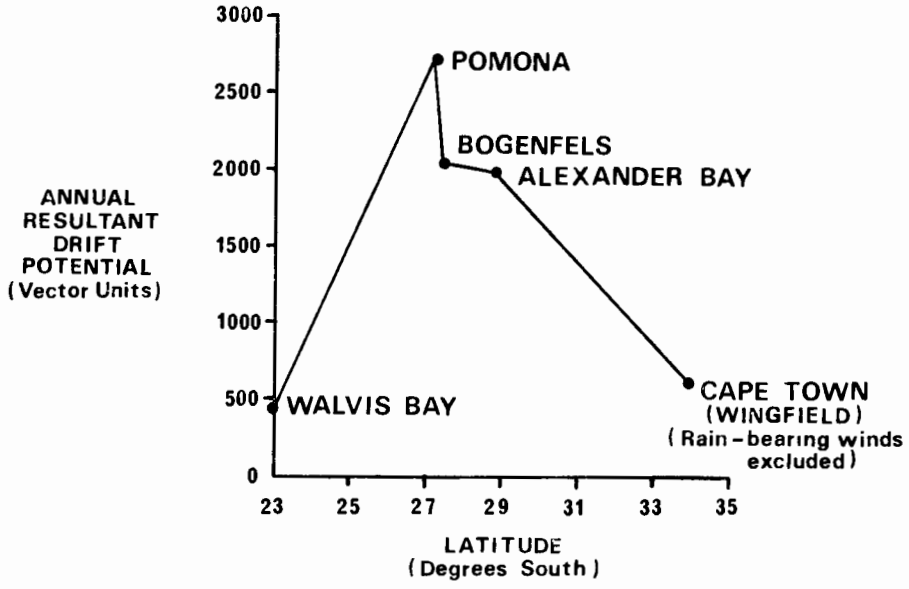

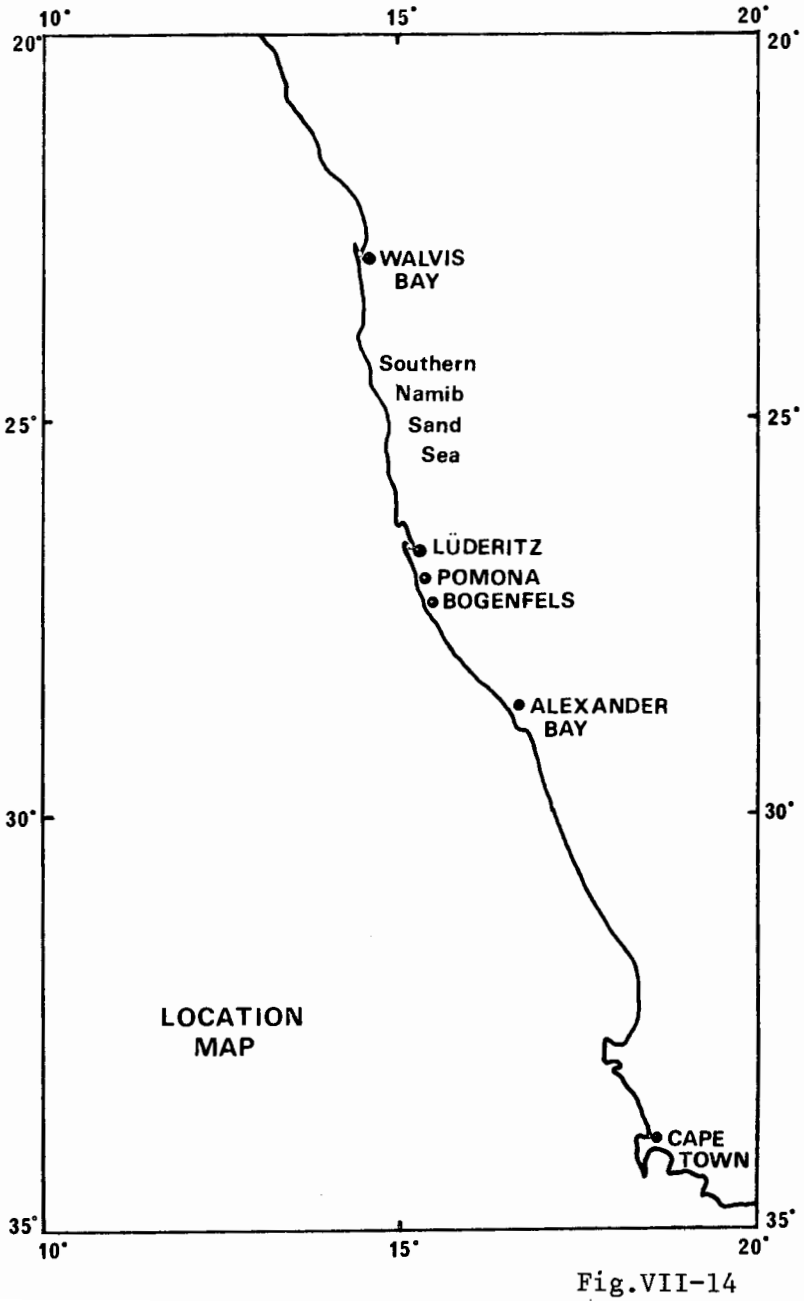

Fig.VII-14

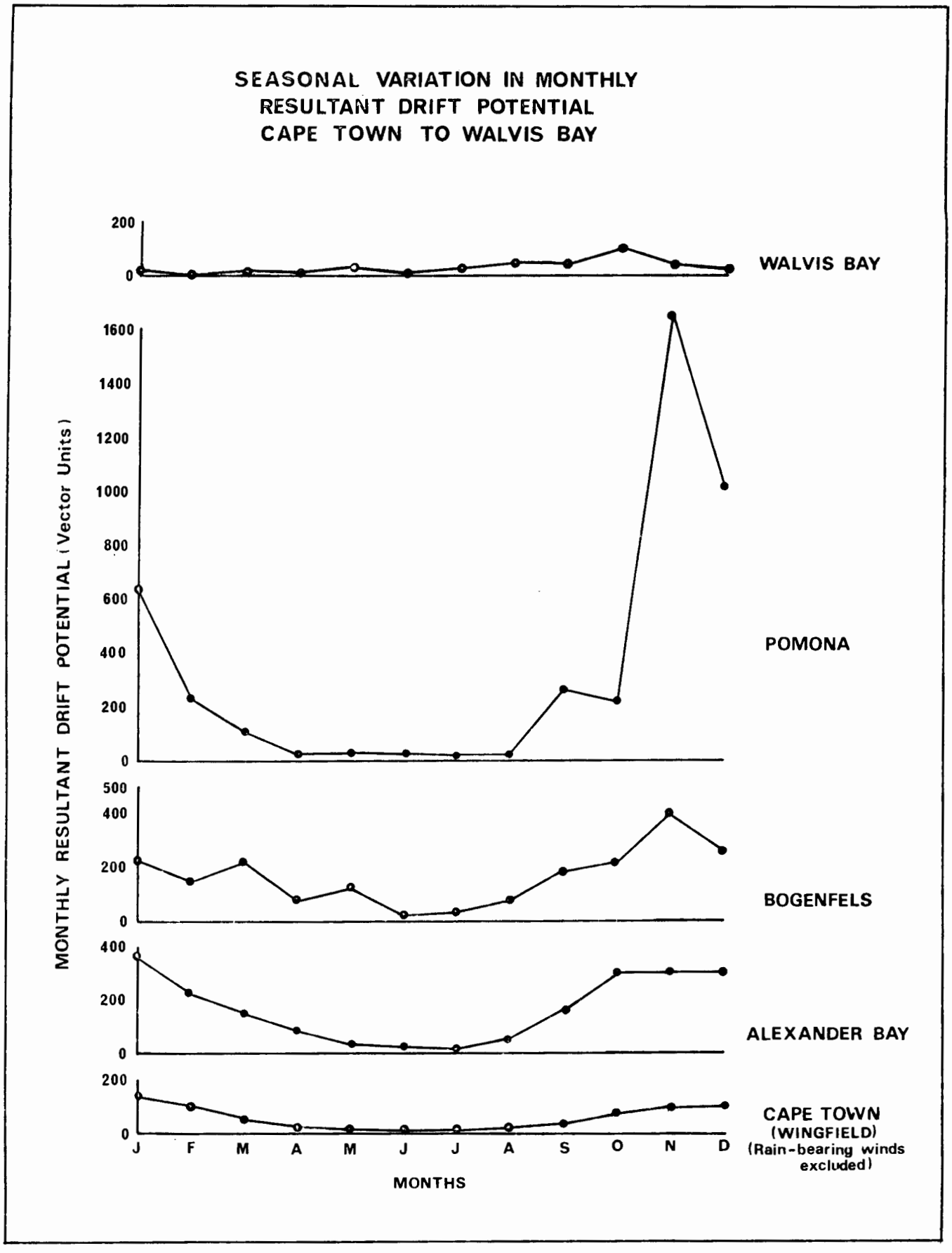
SEASONAL VARIATION IN MONTHLY
RESULTANT DRIFT POTENTIAL
CAPE TOWN TO WALVIS BAY
MONTHLY RESULTANT DRIFT POTENTIAL (Vector Units)
200
0
WALVIS BAY
1600
1400
1200
1000
800
600
400
200
0
POMONA
500
400
200
0
BOGENFELS
400
200
0
ALEXANDER BAY
200
0
CAPE TOWN
(WINGFIELD)
(Rain-bearing winds
excluded)
J F M A M J J A S O N D
MONTHS

Fig.VII-15

ANNUAL SAND ROSES
CAPE TOWN TO WALVIS BAY

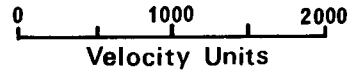

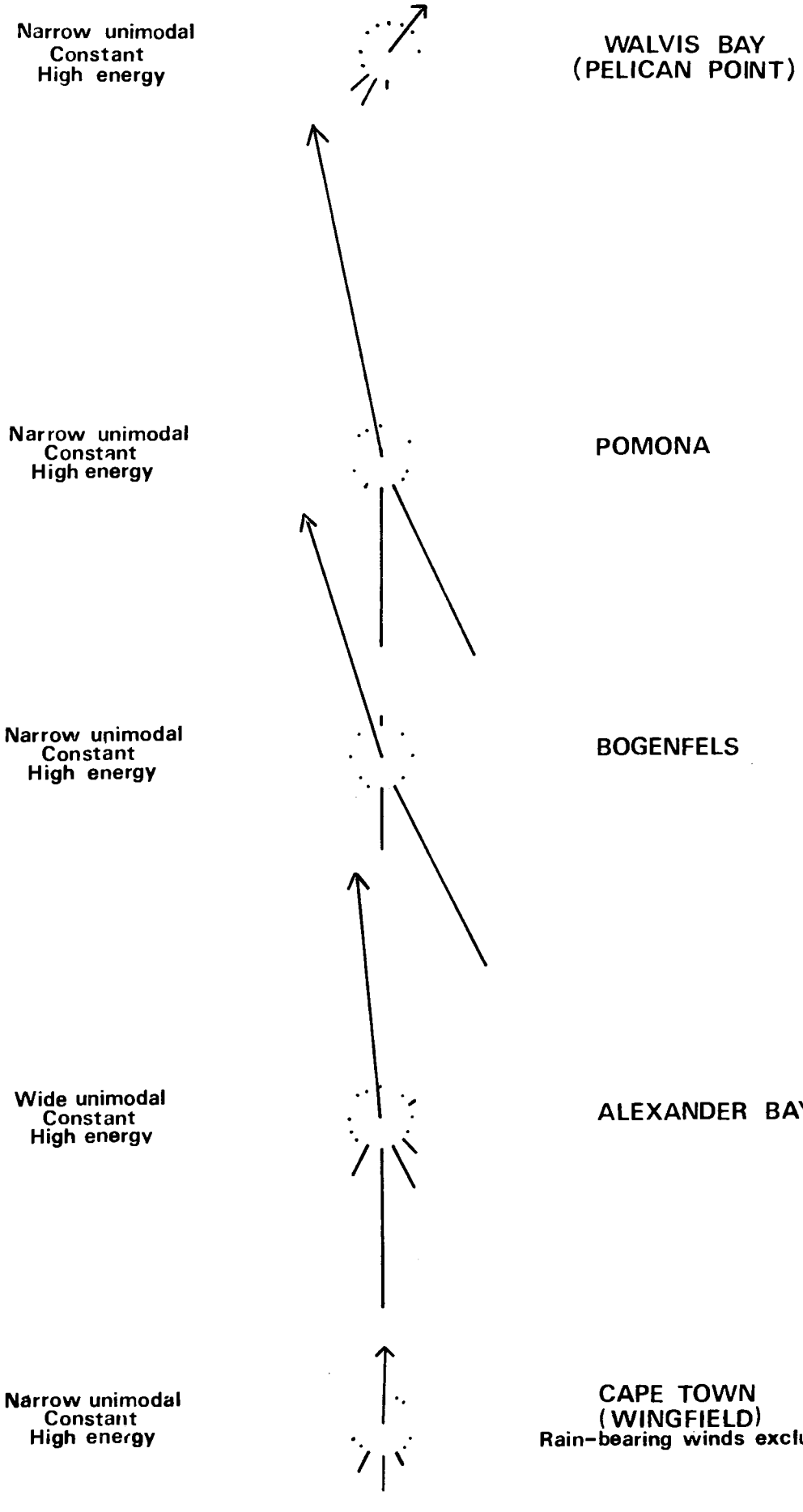

Fig.VII-16

whereas at O'Okiep in the interior of Namaqualand the wind veers to the southwest during summer afternoons. The trade winds are therefore deflected by about 90° landwards by warming of the interior during summer. During other periods the winds are chiefly offshore and flow seawards over the cold, heavy air near the coast. The same trend is noted at Aus, farther north, and has been measured in a traverse along the Kuiseb River towards Walvis Bay (Breed et al., in McKee, in press). Therefore at the coast there is a tendency for cold, moist air to blow northwards near the surface, while warm, dry winds blow westwards at higher levels.

The data from Bogenfels and from the drilling rig in the Trade Winds are similar in two respects. Firstly, both stations have high wind velocities, and secondly the dominant direction lies east of south. Both at Lüderitz to the north and Oranjemund to the south, the winds are weaker and from the southwest. Bogenfels therefore has a wind regime controlled more by oceanic than by land conditions.

These observations are supported by Hart and Currie (1960) and by Stander (1964), who analysed wind data to study their relationship to upwelling phenomena. These authors particularly stressed the constancy and strength of south-easterly winds offshore and the greater variability in both speed and direction of the coastal winds.

Figure VII-12 illustrates the marked diurnality of the wind regime at the mouth of the Orange River (Alexander Bay). The higher wind velocities in summer and in the afternoons of both seasons are clear. Summer winds blow steadily northwards, but in winter the morning winds blow westwards out to sea, and only the afternoon winds blow north. Due to the northwesterly trend of the coastline north of Alexander Bay (Fig. VII-11), the northward winds are effectively onshore winds.

Thrice-daily data for winter and summer from Oranjemund and Bogenfels in Figure VII-13 show that winds capable of transporting sand occur more frequently in summer than in winter, and that the diurnal rhythm is maintained throughout gales, which last as long as two weeks in the summer. Peak velocities fluctuate generally between 10 and 15 m/s, but velocities as high as 20 m/s have been recorded.

The Fryberger technique was used to analyse monthly and annual data for five coastal stations. Only regional trends will be discussed.

The annual resultant drift potential (RDP) reaches a maximum of 2731 vector units (v.u.) at Pomona just south of Lüderitz in the Sperrgebiet Trough Namib (Fig. VII-16), and decreases northwards to 456 v.u. at Walvis Bay and southwards to 618 v.u. at Cape Town, where rain-bearing cyclonic winds were excluded from the calculations. Fryberger (1975, personal communication) has encountered no station with RDP as high as that of Pomona. Each one of the five stations, however, falls into the high-energy category (>400 v.u.).

The seasonal variation of RDP as a fraction of the annual RDP (Fig. VII-15) shows that winter is the calmest season at all stations. It is here particularly relevant to stress that the data were recorded for varying periods, usually using different years, and therefore are not strictly comparable in fine detail. The broad trends are nonetheless considered valid. As in Figure VII-14, RDP increases from Cape Town to Pomona and then decreases rapidly towards Walvis Bay. Maximum RDP shifts from October at Walvis Bay to November at Pomona and Bogenfels, and to January at Alexander Bay and Cape Town, reflecting the poleward shift of the South Atlantic Anticyclone in summer.

The wind regimes along the west coast of southern Africa are of such high energy that the sand roses (Fig. VII-6) are plotted on a scale of 1 mm = 50 v.u. rather than the recommended 1 mm = 1 v.u. (Fryberger, in McKee, in press). The wind regimes vary in energy content as already described and are all constant (RDP/DP>0,8) in direction. The annual resultant drift direction swings from north (001°) at Cape Town to 12° west of north at Pomona, but swings back to 31° east of north at Walvis Bay. The lack of suitable data prevented the construction of a similar northeasterly trend observed at Lüderitz (Fig. VII-11) just north of Pomona. The different annual resultant drift directions may be due to strong Trade-Wind influence south of Lüderitz, east of the Anticyclone's central position. North of Lüderitz to Walvis Bay, farther away from the Anticyclone, the warming of the land during the day creates enough low pressure to divert the coastal winds onshore. Topography may influence the data available to some extent but are unlikely to alter the regional trends.

6. Wave-driven sand transport

No results of quantitative sand-transport studies on the coast of the study area have as yet been published. Kilner and Woodward (1976, personal communication) have directed preliminary studies on the 100 km-long beach between the Orange River and Chamais Bay, in connection with diamond-mining operations. Sand transport is reported to be vigorous, and longshore drift carried some of the workers northwards at the speed of a running man (Mennè, 1975, personal communication). Detailed data are now being accumulated from a waverider buoy, an anemometer and from a sledge-supported survey rod towed through the surf-zone (Woodward, 1976, personal communication). The helicopters stationed at Oranjemund for security purposes may be used to photograph the river mouth at fortnightly intervals (Moes, 1976, personal communication) to monitor changes in the mouth's configuration and effluent-dispersal patterns. A quantitative model of sand movement north of the Orange River thus appears to be within reach.

O'Shea (1971) interpreted his sedimentological data from the inner shelf as a reflection of the influence of the Orange River. He showed that south of the

river, carbonate values in inner-shelf sediments were relatively high (up to 30%), whereas north of the river the carbonate content, diluted by terrigenous sediment from the Orange River, dropped to below 10%. The writer's data on beach samples confirm this trend (Fig. VII-17). O'Shea also separated heavy components from his samples using bromoform. Again the influence of the river was plain in a marked increase of heavy components north of the river mouth. Values of less than 10% south of the mouth increased to as much as 60% at the mouth itself. The writer's data on beaches conform O'Shea's findings, but values were, on average, considerably lower. Although both data sets refer to the heavy components (rock fragments included) of the total sand fraction, the coarser mean size of most of the beach sediments led to truncation of the finer fractions, which are normally rich in heavy minerals.

O'Shea (1971, p.30) did not consider it worthwhile to plot his size statistics on a regional scale. As shown in Figure VII-17, the mean size of the inner shelf sands shows no regional trend, as forecast by O'Shea. However, it is informative to compare the mean-size trends of inner-shelf and beach sands along the coast. In general, mean size varies irregularly between 2 and 4 phi (fine to very fine sand) along the inner shelf and is, on average, considerably finer than on the adjacent beaches. This trend reflects the higher energy-levels generally associated with the beaches and the lower energy-levels on the inner shelf.

A suite of beach samples from the exposed edge of the spit partially closing the mouth of the Orange River, showed a steady northward increase in mean size from coarse sand to very coarse sand (in the actual channel) and back to coarse sand. Between the Orange River and Bogenfels the beaches are steep and narrow, reflecting mean sizes of medium to very coarse sand. Between Bogenfels and Jammerbucht the cliffs along the coastline (Figs. II-20 and VII-9) prevent any deposition of sediment on beaches. From Jammerbucht to Prinzenbucht and Elizabeth Bay (Fig. VII-9) along the coast of the Sperrgebiet Trough Namib, the beach sands are considerably finer. This is attributed to deposition in the lee of Possession Island, in the case of Elizabeth Bay's beaches, and to deposition in the lee of a former island north of Prinzenbucht (Fig. VII-10). Mean sizes of 2 to 4 phi (fine to very fine sand) are encountered on wide, gently-sloping beaches. (Seasonal variations in mean size, and therefore in beach slope and width, will not alter these trends observed during a field trip along the length of the Sperrgebiet). The erratic trends noted north of Hottentot Bay reflect the input of material of varying grain size along a coast composed of cliffs of unconsolidated dunes (Fig. VII-10), which are undercut by the waves at every high tide. It was also impossible to collect an adequate suite of samples along this virtually inaccessible stretch of coastline.

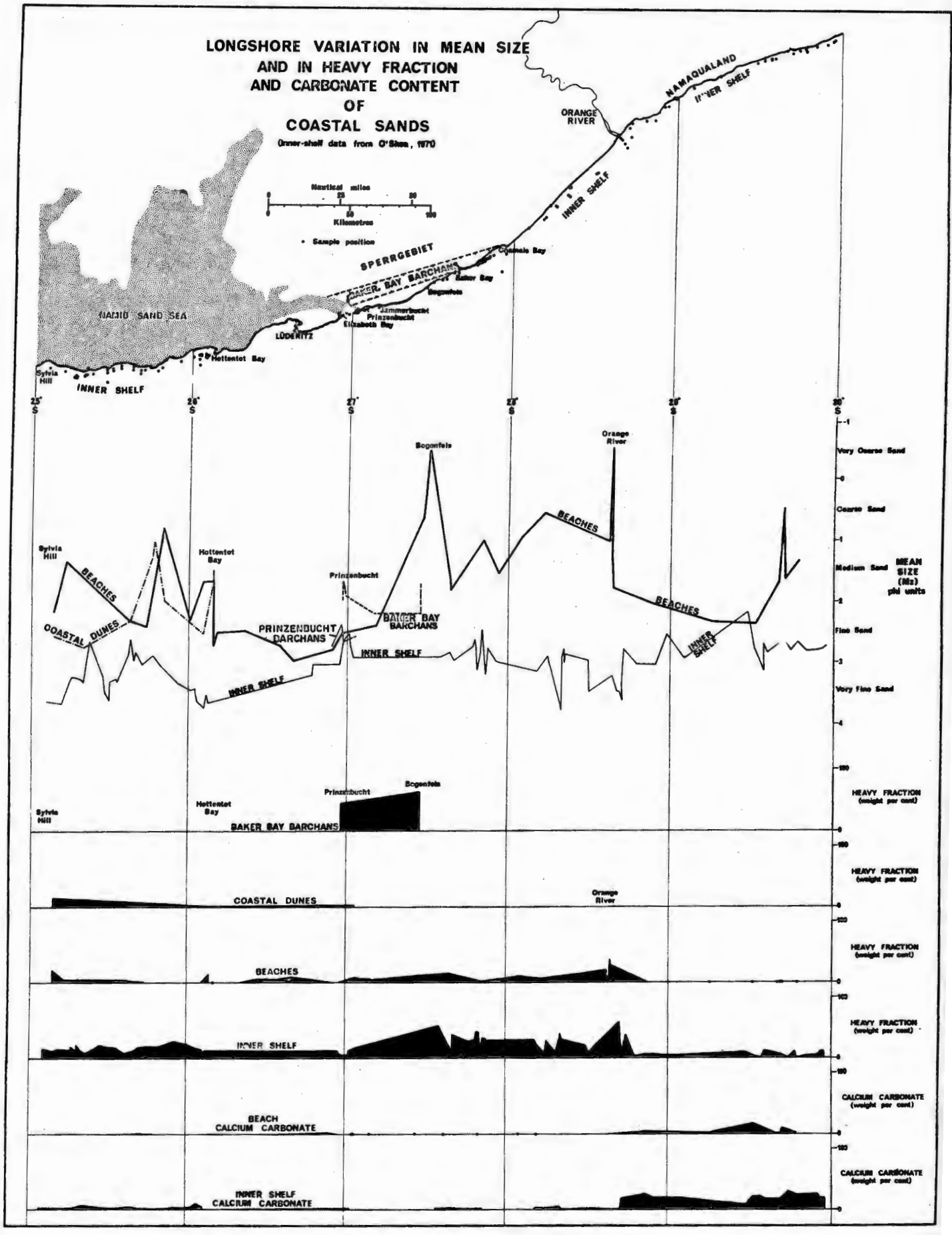
LONGSHORE VARIATION IN MEAN SIZE
AND IN HEAVY FRACTION
AND CARBONATE CONTENT
OF
COASTAL SANDS
Inner-shelf data from O'Shea, 1970
Nautical miles
Kilometres
Sample position
NAMIB SAND SEA
SPERRGEBIET
BAKER BAY BARCHANS
INNER SHELF
ORANGE RIVER
NAMAQUALAND
INNER SHELF
LÜDERITZ
Elizabeth Bay
Hottentot Bay
Sylvia Hill
Bogenfels
Prinzenbucht
Orange River
25° S
26° S
27° S
28° S
29° S
BEACHES
COASTAL DUNES
PRINZENBUCHT BARCHANS
BAKER BAY BARCHANS
INNER SHELF
Very Coarse Sand
Coarse Sand
Medium Sand
Fine Sand
Very Fine Sand
MEAN SIZE (Mz) phi units
HEAVY FRACTION (weight per cent)
COASTAL DUNES
BEACHES
INNER SHELF
BEACH CALCIUM CARBONATE
INNER SHELF CALCIUM CARBONATE
CALCIUM CARBONATE (weight per cent)

Fig.VII-17

7. Aeolian transport of sand

a. Introduction

The high-energy wind regime of the coastal zone was characterised in Section VII-C-5. The presented data have the advantage that calculations of drift potential and resultant drift direction can be made. It was pointed out that the data were recorded for varying periods during different years, and that topography may have affected the data. A case in point is Pomona, where the highest energies were recorded. The data were for only 18 months and the station lay in a long, narrow valley in the Sperrgebiet Trough Namib.

Wilson (1971) regarded the use of wind data as only one of three methods to estimate aeolian transport of sand. He stresses the lack of long-term wind data from widely spaced stations, which are often poorly sited with respect to local topography. He also mentioned that roughness calculations require wind measurements from two different heights and that these are rarely available. Finally he pointed out that actual sand transport rates correspond with potential rates only when sand is available to load the air-flow completely.

A second method is to record the duration and direction of sandstorms. Figure VII-13 is an attempt to portray at least the duration of such storms and Figure VII-16 proves that southerly winds are the predominant stormwinds.

A third method is the study of bedforms, which Wilson (1971) has divided into a four-stage hierarchy descending in size from ergs to draas, dunes and ballistic ripples. McKee and Breed (1974) have replaced the terms "erg" and "draa" with "sand sea" and "megadune", respectively, and these more explicit terms will be used in the following discussion. Besides Kaiser's (1926, p.366) 34-month observation of a 33 m high barchan near Bogenfels (48 m/year), no detailed long-term studies of aeolian sand movement comparable to those of Finkel (1959) and Hastenrath (1967) from Peru have been undertaken in the Namib Desert. The writer is therefore restricted to regional observations and the development of a broad model of sandflow through the southern half of the Namib.

b. Wind-created topography in the Namib Desert

In the Namaqualand Sandy Namib, the combination of strong, unidirectional summer winds and southward-increasing winter rainfall results in the formation of sets of nested parabolic dunes, anchored by vegetation (see Chapter VI). The active masses of unvegetated sand have the barchanoid form typical of unvegetated sand subjected to unidirectional winds (Bagnold, 1941, p.195; Fryberger, in McKee, in press).

Sand blown out of the Orange River bed into the Sperrgebiet Sandy Namib generally occurs as sand sheets near the coast and vegetation plays no part in stabilising it. North of Chamais Bay to Lüderitz in the Sperrgebiet Trough Namib,

trains of barchan dunes are the dominant bedforms. There, as has been demonstrated, the winds are extremely powerful, and northwards from Chamais Bay the area of windswept outcrop increases towards Lüderitz (Fig. VII-9). Kaiser (1926, Plates 1 to 4) and Harger (1913) have illustrated the corrasion of bedrock in the Trough Namib. Dolomite of the Bogenfels Formation is particularly susceptible, its windward surfaces being wind-fluted and fresh, whereas the lee surfaces are subject only to chemical weathering processes. The dominant wind direction can be determined at ground level by the direction of the fluting. In aerial photographs of the dolomite outcrop, windward escarpments can be seen as a series of yardangs, indicating the predominance of south-southeasterly winds (160^{o}) as eroding agents. Better-developed yardangs have been reported from the Peruvian desert by McCauley (1973) and by Grolier et al. (1974), but in Peru the eroded formations are uplifted, unconsolidated marine sediments, not well-consolidated, Precambrian dolomite, as in the Sperrgebiet Trough Namib. It is unfortunate that, for security reasons, the authorities were unable to grant permission to reproduce the relevant aerial photographs illustrating the power of the winds in the Sperrgebiet.

Between Chamais Bay and Prinzenbucht, four barchan trains lead inland from beaches at Chamais Bay, Baker Bay, Elisental and Weitestal (Fig. VII-9). The first two trains are the most important. They coalesce north of Bogenfels as a train of large barchan dunes, the largest about 30 m high, corresponding to the maximum height recorded by Bagnold (1941, p.214). Kaiser (1926, p.366) reported a height of 33 m and a dune, 26 m high, was carefully surveyed by O'Brien(1972) with modern equipment. When crossing light-coloured areas the dunes are distinguishable on LANDSAT images (e.g. 1184-08225). The coastal origin of the dunes is particularly clear at Chamais Bay, where a zone of northward-moving, highly mobile sand appears as a northward-broadening belt of darker tone, west of lighter-toned material, which is transported intermittently towards the coast by sheetwash processes via a network of channels perpendicular to the coast.

The resultant drift directions of the annual sand roses at both Bogenfels and Pomona (Fig. VII-9) coincide with the alignment of both the dolomite yardangs and the path of the barchan trains (seen on aerial photographs), and with the inner boundary of the darker-toned mobile zone beside the coast (visible both on aerial photographs and on LANDSAT images). In the writer's opinion these alignments are cumulative proof of a Trade-Wind-dominated, extremely high-energy wind regime in the Sperrgebiet Trough Namib.

The wind is not only powerful but is undersaturated with sand from the exposed beaches between Chamais Bay and Bogenfels. Barchans are the bedforms typical of undersaturated winds (Wilson, 1971). In Figure VII-17 it is shown that the mean size of samples from the crests of these dunes is greater (average 2,55 phi) than that of the much smaller dunes that leave the coast between Prinzenbucht and

Elizabeth Bay. The coarser, larger dunes are also richer in heavy components (up to 70%), which explains their striking dark appearance on both aerial photographs and LANDSAT images. Kaiser (1926, Plate 3) presents a ground-level view of a well-formed dark barchan dune moving across a pale surface in Grillental, east of Elizabeth Bay (Fig. VII-9).

The Prinzenbucht-Elizabeth Bay region has long been identified as the chief conduit for sand moving towards the Namib Sand Sea north of Lüderitz (Kaiser, 1926, p.370; Hallam, 1964, p.676). The finer grain size of the region's beaches has been discussed, but attention is now drawn to the similarity in mean size of the inner-shelf, beach and dune sediment (Fig. VII-17). Several factors have combined to form this major sandflow conduit. The structure and lithology of the Precambrian bedrock consists of relatively soft schist layers in north-south oriented synforms within resistant Archaean gneiss (Kaiser, 1926). This configuration led to aeolian erosion of the schist to form the north-south ridge-valley topography of the Trough Namib. The most westward ridge was isolated as Possession Island during the Flandrian transgression and today it absorbs most of the wave energy directed towards Elizabeth Bay (Fig. VII-9). A similarly elongate island lay much closer to the coast immediately north of Prinzenbucht, but the quiet water in its lee has been filled in by sediment. Today, terrigenous sand that entered the sea 200 km farther south at the mouth of the Orange River and travelled along the inner shelf past the exposed coast of the Sperrgebiet, is deposited on the beach north of Prinzenbucht, linking the former island to the main rocky coastline.

Because of its fine grain size (Fig. VII-17) the beach is wide and gently sloping. Therefore not only is the material easier to erode, but the area available for erosion is much more extensive than that of the steeper, coarser beaches farther south. The strong winds of the region lead to coastal upwelling and ensure that the hinterland is extremely arid. There is consequently little vegetation to hinder aeolian transport. The coldness and therefore the greater density of the air blowing across the upwelled water accelerates deflation of the beaches even further (Selby et al., 1974). Finally, the coastline includes a major south-facing re-entrant in Elizabeth Bay, which ensures that sediment is funnelled onshore along a major valley floored by Tertiary sediments (Greenman, 1969). Merensky (1909) visited the region when diamonds were first discovered and found the gems concentrated on the crests of ballistic ripples up to 40 cm high and composed of gravel. He interpreted the ripples as a lag deposit concentrated by the hurricane-force prevailing winds.

The dunes of Prinzenbucht and Elizabeth Bay are finer-grained (average mean size 3,00 phi) and therefore smaller (Wilson, 1972), than the Chamais Bay-Baker Bay dunes. They also contain a smaller proportion of heavy components (Fig. VII-17), and consequently are much lighter in colour. This tonal contrast enables one to

distinguish, on aerial photographs, the dark dunes from Chamais Bay and Baker Bay when they coalesce near Lüderitz with the volumetrically much more important dunes from Prinzenbucht and Elizabeth Bay (Fig. VII-9).

Whereas the dark dunes are typically barchans, the light dunes vary in form from coppice dunes behind the beach at Elizabeth Bay, to small barchans, and also to megadunes with barchanoid dunes on their windward slopes. The coppice dunes are evidence of active deflation of the beach zone (Cooke and Warren, 1973, p.318). The significance of the small, numerous barchans downwind of the beaches is that they move considerably faster than the larger, dark dunes according to Bagnold (1941, p.214) and Finkel (1959). The megadunes have formed in hollows in highly undulating gneissose terrain north of the Trough Namib in direct response to the increased hydrodynamic roughness of the surface (Bagnold, 1941, p.49).

North of Lüderitz the coast is flanked by the Namib Sand Sea at many points. Barchanoid megadunes dominate the coastal zone. Dunes on the windward slopes of the megadunes decrease in size towards the interdune hollows, where wind velocities are lower. On coastal outgrowths, such as the pan between Anichab and Hottentot Bay joining two former islands to the Sand Sea (Fig. VII-10), long trains of coppice dunes are a striking feature of aerial photographs. Cooper (1958, pp.31-33) discovered that the relatively small coppice dunes are dependable indicators of the direction of effective winds, whereas the more striking barchanoid megadunes tended to lie slightly oblique to the wind direction, rather than perpendicular to it. Hastenrath (1967, p.329) in addition found that "barchans act as extremely sensitive anemometers". In the absence of any wind data immediately north of Lüderitz, the evidence from coppice dunes and barchans on the pan is that the dominant effective wind comes from the south-south-east like the winds in the Sperregebiet Trough Namib. The steep westward edge of the barchanoid megadunes, some up to 30 m high (Barnard, 1973, personal communication), also lies parallel to this direction (Fig. VII-10), and is the largest-scale indicator of wind direction in the vicinity. In passing, both the barchans running towards the sea at Hottentot Bay and the barchanoid megadunes along the western edge of the Sand Sea disperse downward from their sources of supply in the manner explained and illustrated by Bagnold (1941, p.218).

c. Development of the Namib Sand Sea

Wilson (1971) developed a model for the development of sand seas and applied it to the Sahara Desert. He maintained that only when the sandflow is both saturated and either decelerating or converging can deposition occur. The presented wind data show that along the Namib coast the sandflow decelerates north of Lüderitz. He further demonstrated that any sand sea lies downwind of a source-area, where deflation and unsaturated sandflow are dominant. The Sperrgebiet Trough

Namib falls into this category as a well-defined zone of deflation and corrasion upwind of the Namib Sand Sea.

Although erosion of Tertiary sediments (Wagner, 1914) and Precambrian bedrock (Wagner, 1916) has been demonstrated, the chief source of supply of the coastal barchanoid megadunes are the beaches between Prinzenbucht and Elizabeth Bay, supplemented by material from the beaches between the Orange River and Bogenfels. A certain amount is also blown directly into the desert from sandbanks in the Orange River during the dry season (Knetsch, 1937, p.203; Hallam, 1964, p.676). Wilson (1971, p.188) emphasised that coastal dunes tend to form only on beaches subject to continual replenishment by littoral drift from a fluvial point-source. The writer maintains that although they lie 200 km north of the Orange River, the beaches between Prinzenbucht and Elizabeth Bay are continually replenished by fine sand transported from the river along the inner shelf to beaches sheltered by two islands from the swells of the open ocean. Geology and topography then combine with the highest velocities of the coastal wind regime to funnel sand onshore towards the Namib Sand Sea. The unidirectional wind regime and the arid climate then dictate a barchanoid dune form transverse to the wind direction. Such forms trap sand very effectively (Wilson, 1971, p.194) so that, combined with the rapid deceleration of wind velocity, sand is deposited rapidly downwind of the deflation zone.

The subdivisions of the Namib Desert north of 25°S do not concern this study and have been described, mainly near Walvis Bay, by Hallam (1964), Logan (1960, 1969, 1972) and Nagtegaal (1973).

8. Surface textures of quartz grains

The sandflow model proposed in the previous sections was tested on the microscopic scale by a study of the surface textures of quartz grains from fluvial, littoral and aeolian environments (Rogers and Tankard, 1974; Rogers, 1975c; Rogers and Krinsley, in prep.). A summary of our findings is now presented.

a. Methods

Coarse sand grains (0,5 to 1 mm) from one river sample, two dune samples and four beach samples were selected, washed in ether and coated with gold-palladium alloy. The grains were examined under a scanning electron microscope (JEOL JSM-U3) operated by Mr. R.H.M. Cross and Ms L. Cadle of the Electron Microscopy Unit at Rhodes University, Grahamstown.

b. Sample locations

Figure VII-18 shows the locations of the seven onshore samples studied. BS-90 comes from a pocket beach on a low, rocky coastline flanking the sediment-covered coastal plain of Namaqualand. RS-63 was taken from a bank 5 km upstream from the mouth of the Orange River, BS-52 from a steep beach 1 km north of the

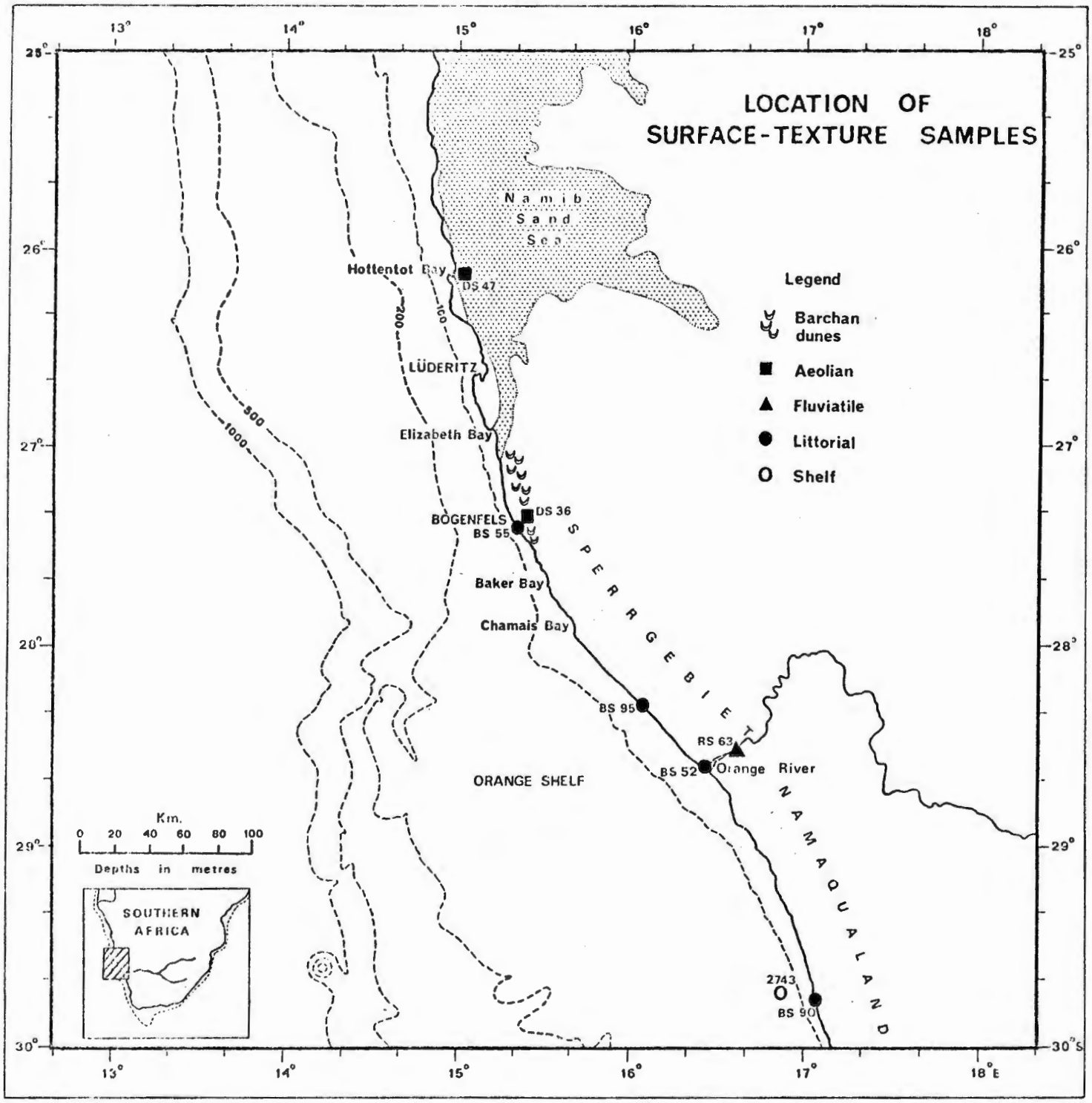
LOCATION OF
SURFACE-TEXTURE SAMPLES
Namib
Sand
Sea
Hottentot Bay
DS 47
LÜDERITZ
Elizabeth Bay
BOGENFELS
DS 36
BS 55
Baker Bay
Chamais Bay
SPERRGEBIET
BS 95
RS 63
BS 52
Orange River
NAMAQUALAND
ORANGE SHELF
2743
BS 90
200
500
1000
Legend
Barchan dunes
Aeolian
Fluviatile
Littorial
Shelf
Km.
0 20 40 60 80 100
Depths in metres
SOUTHERN AFRICA
13°
14°
15°
16°
17°
18°
25°
26°
27°
28°
29°
30°
18°E
30°S

Fig. VII--18

mouth and BS-95 was collected 60 km farther north along a continuous, steep straight beach. BS-55 comes from Bogenfels from the northernmost of the coarse-textured beaches referred to in Section VII-C-6, 165 km north of the Orange River's mouth. DS-36 was taken from the crest of a 10 m-high barchan several kilometres inland from Bogenfels, in the barchan train that originates at Baker Bay. DS-47 comes from the crest of a 30 m-high barchanoid megadune at Hottentot Bay.

c. Grain surfaces

A new surface feature is typical of the grains of BS-90, from a beach exposed to waves higher than 6 m at times (Van Ieperen, 1976). Grooves 80 to 300μm long, 30 to 100μm wide and 10 to 50μm deep were christened scaphoid (boat-shaped) grooves, and attributed to high-energy grain-to-grain impacts (Plate VII-1a). Krinsley (1975, personal communication) has observed such grooves from similar high-energy environments and has produced them experimentally by mechanical impact.

At high magnifications (X 5000), randomly oriented impact V's (Plate VII-1b) are abundant (up to 3V's per μm^2) and reflect the high energy of the environment according to Krinsley and Doornkamp (1973, Fig.1).

The grains are subrounded to well rounded (Plate VII-1c) and large, dish-shaped concavities are common. Krinsley (1975, personal communication) regards such features as relict of an earlier aeolian phase. This is probable because the coast is flanked by a plain blanketed in aeolian sand.

Subangular to subrounded grains of RS-63 from the Orange River are characterised by parallel fracture cleavages (Plate VII-1d) but abraded edges exhibit impact V's (Plate VII-1e). The grains appear to be first-cycle material weathered out of bedrock and are but slightly modified in the fluvial environment.

Knetsch (1937, p.191) graphically described the powerful floods of the Orange River, which transport gravel in protectively viscous muddy water. In contrast to the coast, where sand is continually swept up and down the beaches by the pounding surf, coarse sand grains in the river lie dormant for most of the year. Not only do floods occupy only a minor portion of the year, but they also, despite turbulence, carry their sediment mainly in one direction - downstream. Therefore, although both BS-90 and RS-63 come from subaqueous environments, their widely differing surface textures reflect the difference in energy of the two environments. Robinson (1976, personal communication), in studying surface textures of diamonds from the Transvaal alluvial diggings, also found that the fluvial subaqueous environment has little abrasional effect. Our combined findings conflict with the suggestion of De Villiers and Söhnge (1959, p.241) that the lack of abrasion on diamonds from raised beaches at Alexander Bay is proof that the diamonds have only been rolled on a boulder beach, rather than having been transported for 1500 km down the Orange River.

Plate VII-1. Surface texture of quartz grains from littoral, fluviatile and aeolian environments.

a. BS-90 (700 X). Scaphoid (boat-shaped) impact groove. Note smooth cleavage face on left, uneven surface across cleavage planes on right, and pointed ends. Groove is gouged out of a pitted, smooth surface in a high-energy littoral environment on the exposed coast of Namaqualand.

b. BS-90 (2500 X). Randomly orientated impact V's typical of subaqueous environment. Their density indicates a high-energy littoral environment. Note cleavage face.

c. BS-90 (40 X). Subrounded beach grain from Namaqualand, possibly relict from earlier aeolian environment.

d. RS-63 (40 X). Subangular river grain from the Orange River, characterized by sets of parallel fracture cleavages, probably caused during mechanical weathering from granitic rocks in semi-arid hinterland.

e. RS-63 (500 X). Subaqueously modified edges of cleavages. Note impact V's on edges.

f. BS-52 (20 X). Subangular grain from beach just north of the Orange River mouth.

g. BS-95 (20 X). Subrounded to subangular grain from beach 60 km north of the Orange River mouth.

h. BS-95 (200 X). Note rounding and pitting on protuberances and preservation of conchoidal and parallel fracture cleavages in depressions.

i. BS-55. (20 X). Subrounded beach grain from Bogenfels, 160 km north of the Orange River mouth. Rounding may be due to time spent either in the aeolian or the littoral environment. Note scaphoid impact groove near the top of the grain.

j. DS-36 (500 X). Upturned plates, a solution/reprecipitation phenomenon typical of desert grains, caused by the chemical action of desert dew on grains from the crest of a 10 m-high barchan dune near Bogenfels in the Sperrgebiet Trough Namib.

k. DS-47 (30 X). Subrounded grain with several dish-shaped depressions and a frosted surface, from the crest of a 30 m-high barchanoid megadune at Hottentot Bay in the Namib Sand Sea.

l. DS-47 (500 X). Frosted surface completely obliterating any mechanically formed features.

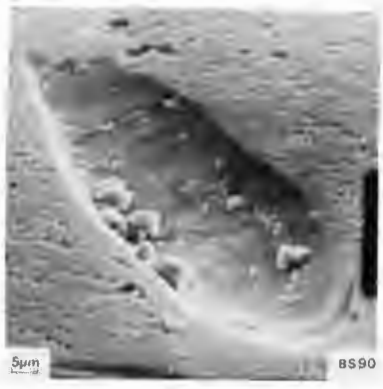

a

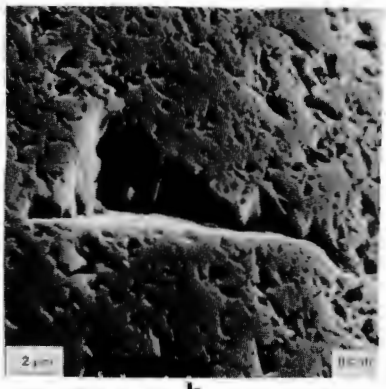

b

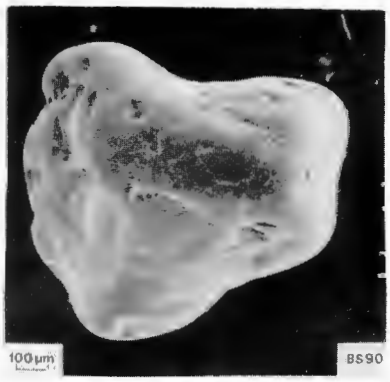

c

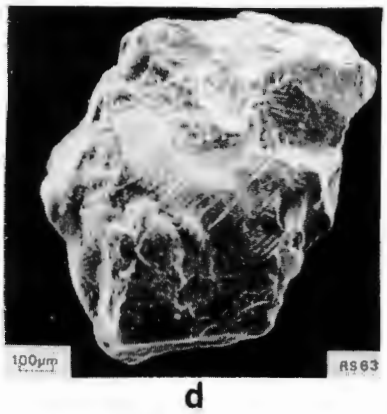

d

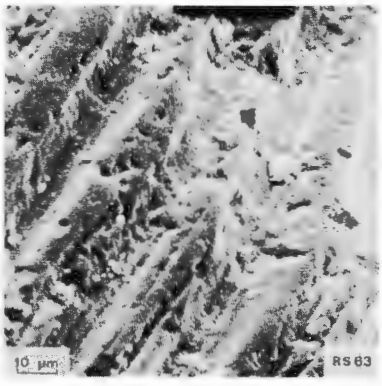

e

f

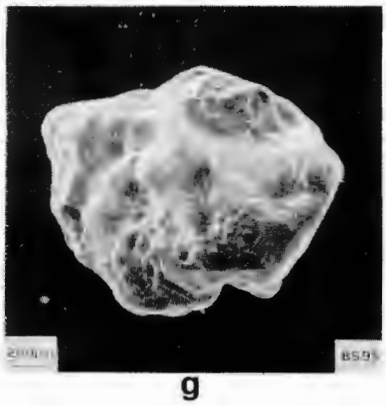

g

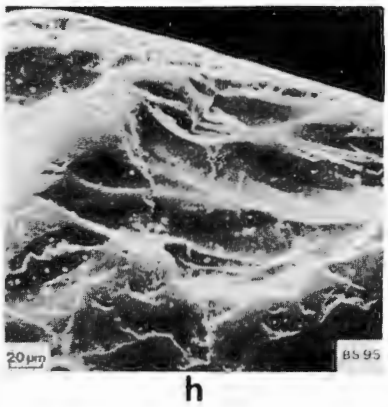

h

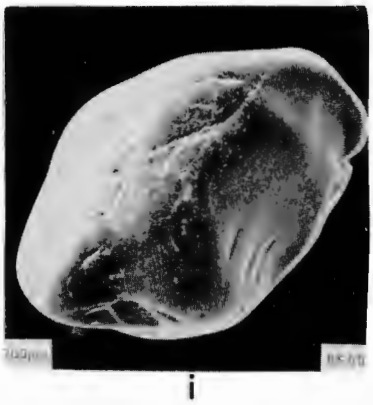

i

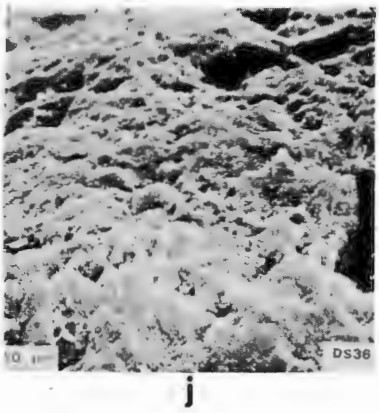

j

k

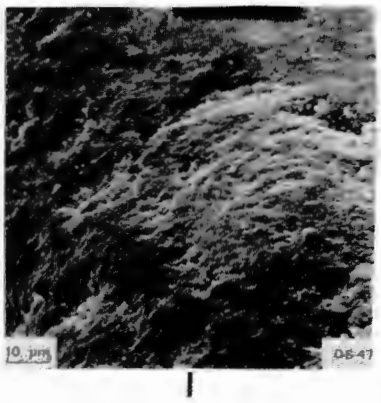

l

Plate VII - 1

The sequence from BS-52 at the mouth to BS-55 at Bogenfels illustrates the abrasion of fluvial grains in the littoral environment. BS-52 (Plate VII-1f) consists of unmodified subangular grains from the river, whereas BS-95 (Plates VII-1g and 1h) contains grains, which are already considerably modified by littoral abrasion. By the time the grains reach Bogenfels, they are as well rounded as those of BS-90 in Namaqualand (Plate VII-1i), and they exhibit scaphoid grooves and impact V's.

The dune sample, DS-36, from the barchan near Bogenfels was specifically chosen to search for evidence of earlier fluviatile and littoral surface features associated with modern aeolian features. However, only aeolian features such as upturned plates coated with reprecipitated silica were observed (Plate VII-1j) and they were superimposed on grains that had been recently released from bedrock, just like the fluvial grains. The evidence is compatible with the extremely arid, high-energy aeolian environment of the Sperrgebiet Trough Namib, where corrasion of bedrock has been amply demonstrated (section VII-C-7b).

More typical aeolian features were dominant in grains from DS-47, where the wind regime has been shown to be quieter and deposition dominates deflation. The grains are well rounded and have the typical concavities (Plate VII-1k) referred to earlier. The frosted surface of the grains is covered with re-precipitated silica (Plate VII-1l). Kuenen and Perdock (1962, p.651) ascribe this frosting to the action of desert dew, which is known to be abundant at night in the Namib (Logan, 1960, p.15). Salt spray carried onshore by the wind is deposited on the sand dunes, often forming a thin crust by lightly cementing the surface grains. At night the dew dissolves the salt and causes the pH of the dew to rise. A film of quartz on the grains then goes into solution, only to be reprecipitated when the dew evaporates in the course of the day.

d. Conclusions

The study characterised Orange River grains as relatively unmodified first-cycle grains, which dominate the beaches north of the river mouth and are rapidly abraded when carried northwards in the high-energy littoral environment. In contrast, the material from the Namaqualand coast is polycyclic and the Orange River clearly plays no part as a sediment source. The aeolian grains, while not reflecting a combined littoral and fluvial source, as expected, nevertheless confirmed that the Sperrgebiet Trough Namib is a higher-energy aeolian environment than the Namib Sand Sea downwind to the north.

9. Coastal currents

The hydrology of the Benguela Current System affects both terrigenous and biogenic sedimentation. The topic will be discussed more extensively in Chapter VIII in connection with the biogenic sediments that dominate the shelf areally.

The currents over the inner and middle shelves are of most relevance to the dispersal and deposition of terrigenous sediments.

Bang (1976) has bemoaned the dearth of direct current measurements in the study area, but nevertheless considers that the chief elements of the System have now been identified. He contrasted the present state of knowledge of the Benguela Current System with the volume of data being extracted from analogous systems off N.W. Africa and Oregon.

An examination of oxygen data from routine water-sampling stations off the south western Cape led to the discovery of a coastal poleward-flowing current named after the investigator, De Decker (1970). The Oregon analogue is the Davidson Current (Smith and Hopkins, 1972, p.161). In winter, storms reduce stratification in the water column and the Davidson Current flows poleward and, to a lesser degree, seaward along the bottom, in response to barotropic flow induced by cyclonic winds (Sternberg and McManus, 1972). Equatorward flow along the bottom develops in summer in response to barotropic flow induced by anticyclonic winds, but the flow is opposed by a stronger baroclinic flow polewards along the bottom. Therefore, off Oregon, the net flow along the bottom is poleward throughout the year, while the surface currents alter their direction of flow seasonally. However, bottom currents are reinforced by the wind-driven surface currents in winter and retarded in summer.

Off the west coast of southern Africa cyclonic winds are only effective in winter in accelerating the De Decker Current (Shannon, 1966), and they are most effective south of the Orange River (28^{o}S). Smith and Hopkins (1972) recorded highest bottom velocities off Oregon during winter, when stormwinds of 20 m/sec caused maximum bottom velocities of 54-58 cm/sec and maintained velocities in excess of 40 cm/sec for periods of up to 36 hours. The authors stressed that significant net sediment transport occurs when high bottom velocities are maintained for relatively long periods and with little variation in direction. Hopefully the necessary bottom-current data will shortly be obtained off the west coast of southern Africa, in order to check the relevance of the Oregon model locally.

10. Models of shelf sedimentation

The study of shelf sediments has passed through three stages, which can be broadly described as a) the qualitative, b) the quantitative and c) the dynamic stages.

a. Models based on qualitative studies

The earliest information on the sediments of most shelves is usally found in chart notations of nautical charts. In many areas the density of chart notations frequently still exceeds the density of bottom samples available for laboratory analysis. This greater density can be exploited, for example, south of the Orange

River, where numerous notations indicate muddy bottom. Such notations were used when delineating the extent of the terrigenous mud belt off the coast of Namaqualand

Shepard (1932) was the first geologist to use the worldwide network of chart notations by compiling a map of the shelf sediments of the world. He used his data to refute Johnson's (1919) theory that shelf sediments fine seawards across the continental shelf to the slope. Instead he found a mosaic of sediments reflecting the profound effects of Pleistocene low sea levels on sediment distribution.

Hayes (1967) continued to use chart notations because of the patchiness of bottom-sample nets. He pointed out the broad effects of the climatic belts on shelf sedimentation. Restricting himself to depths shallower than 60 m to minimise Pleistocene effects, he found sand characteristic of shelf sediment off arid coasts like the Namib Desert. He criticised one of his own assumptions, that the coastal climate of a region always represents the climate of the source area of the sediments. The Orange, along with the Nile, the Amazon and the Indus is one of many major rivers that cross several climatic zones en route to the coast. Hayes' trends are not invalidated, but his conclusions are devalued off coasts affected by such rivers.

b. Models based on quantitative studies

Emery (1968) produced a benchmark paper on shelf sediments after conducting regional surveys of bottom sediments in various parts of the world. He popularized the terms detrital for sediment derived from the land, biogenic for sediments of organic origin, authigenic for sediment precipitated chemically, relict for sediments out of equilibrium with their original environment of deposition and residual for sediment weathered from bedrock. (The term terrigenous (Lisitzin, 1972, p.25) is perferred to detrital in this text, because "detritus" may be either terrigenous or biogenic).

Hayes' (1967) contribution was updated by McManus (1970), who emphasised the role of extreme conditions in shelf sedimentation. For example, rivers such as the Orange deliver the bulk of their sediment during floods that occupy only a minor portion of the year. He also pointed out that much terrigenous mud is trapped in estuaries and that storm-driven currents can disperse mud deposited on shelves. He particularly emphasised the work of Gibbs (1967), who showed that the Amazon River delivers sediment characteristic of the Andes, and that only the shorter rivers deliver sediment characteristic of the tropical coastal climate. By analogy, the dominating influence of the catchment geology in the Upper Orange River on terrigenous sediment is readily appreciated.

c. Models based on dynamic studies

Swift (1970, p.9) reconciled modern data and concepts with Johnson's equili-

brium profile. He identified a nearshore modern sand prism as a "seaward thinning (and fining) wedge of nearshore sand" extending seawards from and including the mainland beach. The modern sand grades into the shelf modern mud blanket and both sediment bodies overlie and/or lie inshore of the shelf relict sand blanket. The relict sediment in turn overlies pre-Quaternary bedrock.

Johnson's seaward-fining concept is thus reinstated, but is restricted to the modern terrigenous sediments near the coast. Swift went on to distinguish autochthonous sedimentation off easily eroded coasts like the dune coast north of Lüderitz. Allochthonous sedimentation is exemplified by the Orange River delta. Finally, Swift et al. (1971, p.343) introduced the term palimpsest to describe any sediment "which exhibits petrographic attributes of an earlier depositional environment and, in addition, petrographic attributes of a later environment".

In both of the latter two papers, shelf sedimentation is depicted in terms of a stochastic process model, although it is not mentioned that the model refers only to terrigenous sediments. The coast is identified not only as the source of sediment delivered by rivers, wind and coastal erosion, but also as a reflector. (Loss of beach sand to coastal dunes, however, was recognised as a temporary store on the coastal plain). The zone of oscillatory wave motion beside the coast then gave way to a broad shelf zone, where rotary currents driven by passing storms were dominant. The slope below the shelf break was distinguished as a quiet zone acting as a store for any sediment that reached it.

Swift et al. (1971, p.325) have stated that "we will not be able to do little more than speculate about shelf sediment transport until geologists undertake to monitor shelf currents". Creager and Sternberg (1972, p.349) then stressed that quantitative data tend to be "ground into the classification scheme" and only then are dispersal patterns deduced, and then only by reasoning. They feared the creation of "a body of deceiving information", unconfirmed by direct current measurements.

Creager and Sternberg postulate the deposition in the Holocene of a basal transgressive sequence, overlain near the coast once sea level stabilised, by a nearshore modern sand prism and a shelf modern mud blanket. Farther out to sea the basal sequence is either relict or palimpsest. Curray (1965) restricted bedload transport to water shallower than 10 m in a nearshore zone. (See Section VII-C-6). Deeper than 10 m he regarded as the shelf zone, where suspended-load transport is dominant. Creager and Sternberg (1972, p.359) then emphasised the important role of wind-induced currents, such as the Davidson Current, in the shelf zone off Washington, "one of the most completely studied shelf areas in the world" and a direct west-coast analogue of the southwestern African shelf. They conclude with a plea for the simultaneous study of both processes and results, so that an increasing knowledge of modern environments will lead to more accurate interpreta-

tions of ancient environments.

An excellent example of an integrated study of both processes and results over a period of years is given by Drake et al. (1972), who monitored the dispersal and deposition of sediment from a major flood off southern California. Repeated measurements of both water properties and flood-sediment distribution showed that at least three years were required for the shelf to return to "normal". A similar long-term study of the Orange River delta was mooted by the writer at a workshop on shelf sedimentation (First interdisciplinary conference on marine and freshwater research in South Africa, Port Elizabeth, July 1976).

The most recent review of shelf dynamics was presented by Swift (1974) who would regard easily eroded coastlines, like that of the Namib Sand Sea, as shoreface "valves" releasing sediment from storage in the dunes. The Orange River would be regarded as a second "valve" bypassing sediment each flood from storage in river sandbanks and marginal mud flats. On the shelf, sediments may be stored under relatively quiet summer conditions and then dispersed farther by winter storms.

Taking a global view, southern Africa is seen as a "trailing-edge coast" facing a spreading centre, the mid-ocean ridge (Inman and Nordstrom, 1971). Such coasts are suited for allochthonous sedimentation off river mouths, but in sections of desert coast where rivers are dry, the coast is eroded and autochthonous sedimentation prevails.

11. The Orange River delta

a. Introduction

The Orange River delta, in comparison with other major deltas, is relatively unstudied. In contrast the deltas of the Mississippi (cf. Scruton, 1956; Gould, 1970; Wright and Coleman, 1974), the Po (Nelson, 1970), the Niger (Allen, 1964), the Rhone (Oomkens, 1970), the Amazon (Milliman et al., 1975) and the Orinoco (Van Andel, 1967) have been studied in detail. In these studies maps were compiled with the help of aerial photographs, surface samples and cores. Current velocities, suspended sediment concentrations, salinities, wave and wind parameters were measured to study the complex interaction between river and sea water at the river mouths.

Preliminary data on the Orange River delta have accumulated during the course of diamond mining operations along the west coast (Hoyt et al., 1969), and regional surveys of meteorology (Schulze, 1965), water resources (Rooseboom and Maas, 1974), and the geology of the continental margin (this study). These data will now be compiled and assessed and suggestions made concerning fruitful avenues of future research.

b. River-mouth processes

A model has been developed by Wright and Coleman (1974) for processes at the mouth of the Mississippi River. This model will be discussed in an attempt to explain preliminary observations of a major flood of the Orange River in the 1973-1974 water year. A series of oblique-angle photographs of the mouth of the river were taken by a number of observers, including the writer. The series extends from July, 1973 in the dry season, to June, 1974, after recording the impact of the flood. Low-water conditions were also recorded by the LANDSAT-1 (ERTS-1) satellite, which regrettably ceased functioning just before the flood. Had the satellite images been available, sediment-dispersal patterns would have been monitored at 18-day intervals. Standard aerial photographs of the river-mouth were also available and were used to map the subaerial sections of the delta in conjunction with 1: 50 000 topographical sheets. Unfortunately, permission to reproduce the photographs was not granted (Government Printer, 1976, personal communication).

The available images reveal a river meandering across a flat coastal plain after emerging from a deeply incised course within the Orange River Mountain Land (De Villiers and Söhnge, 1959). A sinuous thalweg, typical of straight channels (Allen, 1965, p.96) characterises most of the river's course during periods of low discharge. Pools between shallow riffles are locally called "zeekoegaten" or "hippo pools" and sediment settles in them at the end of the wet season. The first flood of the next wet season often contains more sediment than later floods due to scouring of these pools (Anonymous, 1922).

Between Upington and the Aughrabies Falls the river gradient increases substantially (Adamson, 1922) and the river channel consequently adopts a braided pattern (Wellington, 1955; Allen, 1965, Fig.3). Thirty kilometres from the river mouth the channel straightens, broadens and changes again to a braided pattern. However, this change is attributed to aggradation when the stream velocity is checked on approaching sea level. The river's competence is reduced and aggradation of excess sediment results. Four kilometres from the mouth the elongate sand banks of the braided channel diminish in size and number when the river reaches a final stretch of open water extending to the spit across the mouth. On the southern flank of this open stretch is a lagoonal marsh, which widens seawards to the river-mouth spit (Fig. VII-8).

At any river mouth the interface between fresh river water, however muddy, and denser sea water slopes from the surface downwards and upstream above a salt wedge. The oscillations of this wedge were briefly measured by Brown (1959) during July, 1956, when the river-mouth channel was some 30 m wide. At low water springs a salinity of 6,33°/oo was measured in the sea just outside the mouth, but at high water springs salinities of 34,7°/oo were measured on the upstream side of

the spit. Local inhabitants informed Brown (1959) that sometimes the mouth is completely closed for months and that at these times the water behind the spit can be used for drinking purposes. Green (1948,p.206) also records that the river mouth may be closed for months. He then relates an eye-witness account of the arrival of a flood and the explosive breaching of the spit.

During the flood that started in November, 1973, the width and configuration of the river-mouth channel varied considerably. In general the channel lay closest to the north bank. The bulk of the flow was confined to the main channel beside the lagoonal marsh. The spit was therefore subject to change only north of the marsh. During November, 1973, and May, 1974, a subsidiary spit was built southwards from the north bank, possibly caused by wave refraction around the lunate river-mouth bar.

Several of the features observed by Wright and Coleman (1974), on a much larger scale, at the mouth of the Mississippi River have been noted at the mouth of the Orange River. They divided the flow regime at the mouth into Regions I to IV, from the mouth seawards. The flow of the Orange into the sea can be neglected during the dry winter season when the mouth is frequently blocked. Therefore the flood situation will be described as more typical of the Orange River. In Region I, between the end of the river channel and the mouth, turbulent mixing of the effluent causes deceleration of river flow. This leads to transport of bedload in the main channel changing to deposition towards a shoaling river-mouth bar. At the same time the hydraulic head between the river water and the sea causes observed superelevation. This superelevation may account for the driftwood found by Brown (1959) 12 m above sea level in the dunes on the edge of the lagoonal marsh.

Region II is characterised by a zone of stationary surface waves near the seaward edge of the bar crest. This zone lay approximately 100 m seaward of the Orange River mouth. Wright and Coleman (1974) postulate intense turbulence and rapid deceleration in this region. Rapid deposition of bedload allows a lunate river-mouth bar to build up. In Region III the river water experiences an internal hydraulic jump, from supercritical densimetric Froude numbers with rapid flow in the river channel, to subcritical Froude numbers with tranquil flow in the sea. Region IV is the zone where wave, wind and tidal action mix the effluent with the ambient sea water. In both Regions III and IV the effluent carries suspended sediment in a buoyant layer above the denser sea water. The seaward edge of the effluent was clearly demarcated off the Orange River. The boundary was also seen on a radar screen aboard R.V. "Thomas B. Davie" as a distinct physical barrier by Bremner (1974, personal communication) who observed a thin line of foam, and a marked colour contrast between blue sea water and green effluent. There also appears to be a slight reduction in wave height in the effluent, which probably accounts for the boundary on the radar screen.

c. The Orange River delta within the deltaic spectrum

Wright and Coleman (1974) compared seven major deltas, which they placed in a spectrum from the river-dominated Mississippi delta to the wave-dominated Senegal delta. The Orange River delta belongs to the wave-dominated extreme of the spectrum. The subaerial portion of the delta does not protrude into the sea, the mouth being closed with a straight spit (Fig. VII-8); also the beaches near the mouth are deflated to form dune deposits along the coast (Fig. VII-8). Wright and Coleman (1973) fed monthly wave and discharge statistics into a computer programme which calculated the nearshore wave power, discharge intensity and the "discharge effectiveness index". This index is the ratio between the discharge per unit width of the river mouth and the wave power per unit width of wave crest near the coast. During floods the Orange River is at least partially effective, but during winter it is clearly ineffective. When the necessary data become available the relative position of the Orange River delta within the deltaic spectrum can be confirmed by calculating the mean annual discharge effectiveness index. This index varies from 5477,0 for the Mississippi delta to 0,3 for the Senegal delta (Wright and Coleman, 1973, Table 4).

d. Dispersal and deposition of suspended sediment

i) The immediate vicinity of the river mouth

According to Wright and Coleman (1974), the zone of maximum turbulence in Region II is the site of bedload deposition. In this way a lunate river-mouth bar is formed seaward of the mouth. In winter such a bar is eroded by longshore drift and the sediment is transported northwards along the beach towards Chamais Bay. The ultimate fate of the river's bedload was discussed in Section VII-C-6 and 7. Attention is now paid to the river's suspended load.

In the river itself the most common sediment sampled was fine to very fine sand of variable sorting (Fig. VII-6). Near the mouth (Fig. VII-19) the lagoonal marsh contains no sand, only silt and clay. This fine texture reflects the quiet depositional environment, protected from turbulent river flow in the main channel and surf-zone turbulence on the seaward side of the river-mouth spit. The high energy of the spit beaches, and particularly of the channel through the spit is apparent from the total absence of fines and the coarseness of the sand near the turbulent Region II. During an earlier major flood, Low (1967) sampled freshly deposited gravel with a mean size as coarse as 50 mm (very coarse pebbles) and a sand fraction rich in garnet and magnetite. Thus, as is typical in deltas, an extremely high-energy environment is situated close to an extremely low-energy environment. Offshore the textural gradations are less abrupt.

ii) Delta front

Like Wright and Coleman (1973, p.771), the writer was unable to sample the

GRAIN-SIZE TRENDS DOWN THE ORANGE RIVER AND ACROSS ITS HOLOCENE AND PLEISTOCENE DELTAS

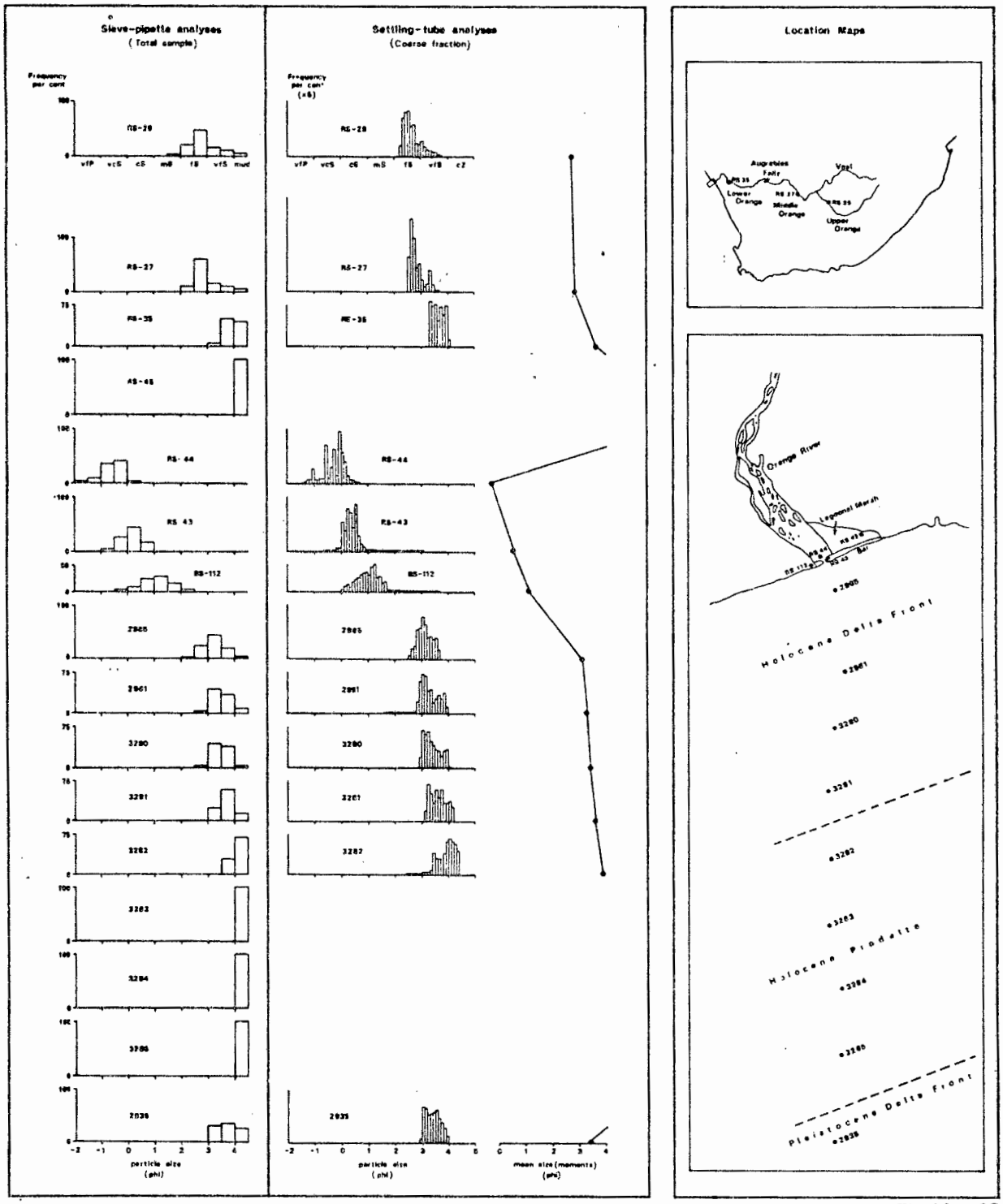

Fig. VII-19

river-mouth bar beneath the turbulent Region II. In other words the bar crest (Wright and Coleman, 1973, Fig. 14) has not been sampled. However, bottom samples from as shallow as 12 m seawards across the continental shelf can be used to follow textural trends in deeper water and to map the areal extent of the delta's lithofacies (Figs. VII-19 to VII-25). The offshore deltaic sediments fall into two main lithofacies. Slightly silty very fine sand on the delta front seaward of the river-mouth bar is succeeded below approximately the 40-m isobath by first clayey silts and then silty clays on the more steeply sloping prodelta (Fig. VII-21). This terminology is taken from Gould (1970), who reported clean sand on the bar crest of the Mississippi in depths of less than 10 m, and a sequence of silty sand and sandy silt on the delta front to a maximum depth of 120 feet (37 m).

In describing their deltaic spectrum, Wright and Coleman (1973) focussed their attention on the morphology and sedimentology of each delta's floodplain and coastline. No comparison of the subaqueous portions of each delta was made beyond the observation that river-dominated deltas have convex profiles, whereas wave-dominated deltas have concave profiles. The Orange delta, nevertheless has a convex profile due to deposition on a convex inner shelf of Precambrian rock. The primary control of the deposition of suspended sediment from the river, however, is quite clearly wave action.

Off the equally exposed west coast of Washington and Oregon, Smith and Hopkins (1972, p.163) found a band of very fine and fine sand, derived from the Columbia River, between the 0 and 40 m isobaths. They stressed the predominance of a 3,5Ø mode (very fine sand) in these sediments and a silt content of less than 10%. Examination of Figure VII-19 shows that such sediments also characterise the delta front between the 10 m and the 40 m isobaths off the Orange River. Settling-tube analyses of the sand fraction show a subtle but definite fining seawards of the very fine sand on the delta front. To what extent can this trend and the change to silt and clay near 40 m be ascribed to wave action?

iii) Boundary between delta-front sand and prodelta sand

Smith and Hopkins (1972, p.163) assumed that sediment transport by small-amplitude waves of moderate steepness begins when the depth (d) is approximately one quarter of the typical deep-water wavelength (L_o). For a typical (T = 10 seconds) swell off Washington, L_o equals 156 m ($L_o = 1{,}56\ T^2$). $L_o/4$ then equals 39 m, at the observed sediment boundary. In addition, bottom drifters released inside the 40 m isobath moved towards the beach under the influence of the shoaling waves, whereas drifters released between the 40 m and 90 m isobaths moved poleward parallel to the coast. Applying the same rule-of-thumb, the critical depth for the typical 11-second wave recorded at Lüderitz (Van Ieperen, 1975) is 47 m, relatively near the observed boundary between the delta front and the prodelta.

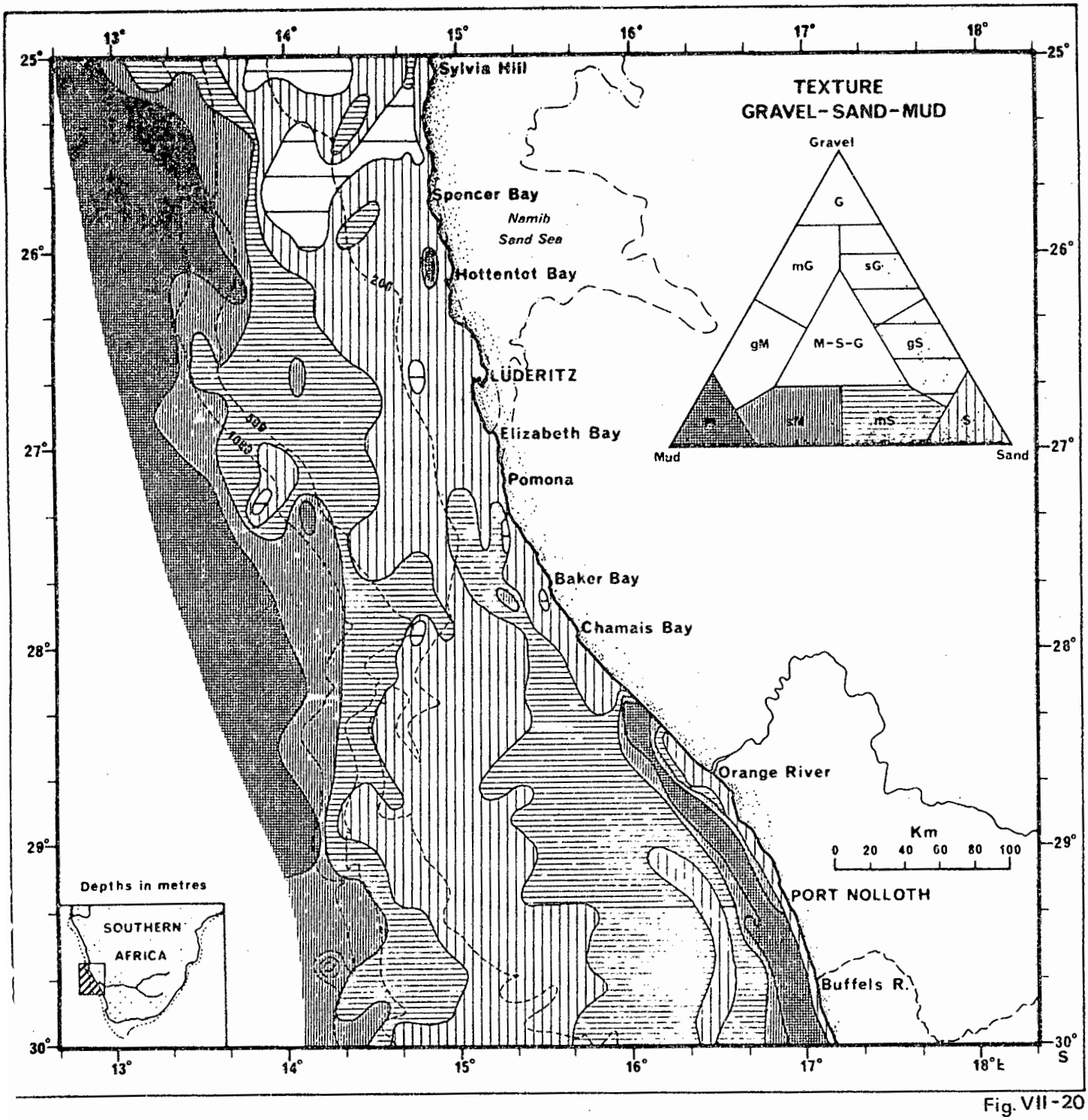
13°
14°
15°
16°
17°
18°
25°
26°
27°
28°
29°
30°
Sylvia Hill
Spencer Bay
Namib
Sand Sea
Hottentot Bay
LÜDERITZ
Elizabeth Bay
Pomona
Baker Bay
Chamais Bay
Orange River
PORT NOLLOTH
Buffels R.
200
1000
TEXTURE
GRAVEL-SAND-MUD
Gravel
G
mG
sG
gM
M-S-G
gS
mS
S
Mud
Sand
Km
0 20 40 60 80 100
Depths in metres
SOUTHERN
AFRICA
S
E

Fig. VII-20

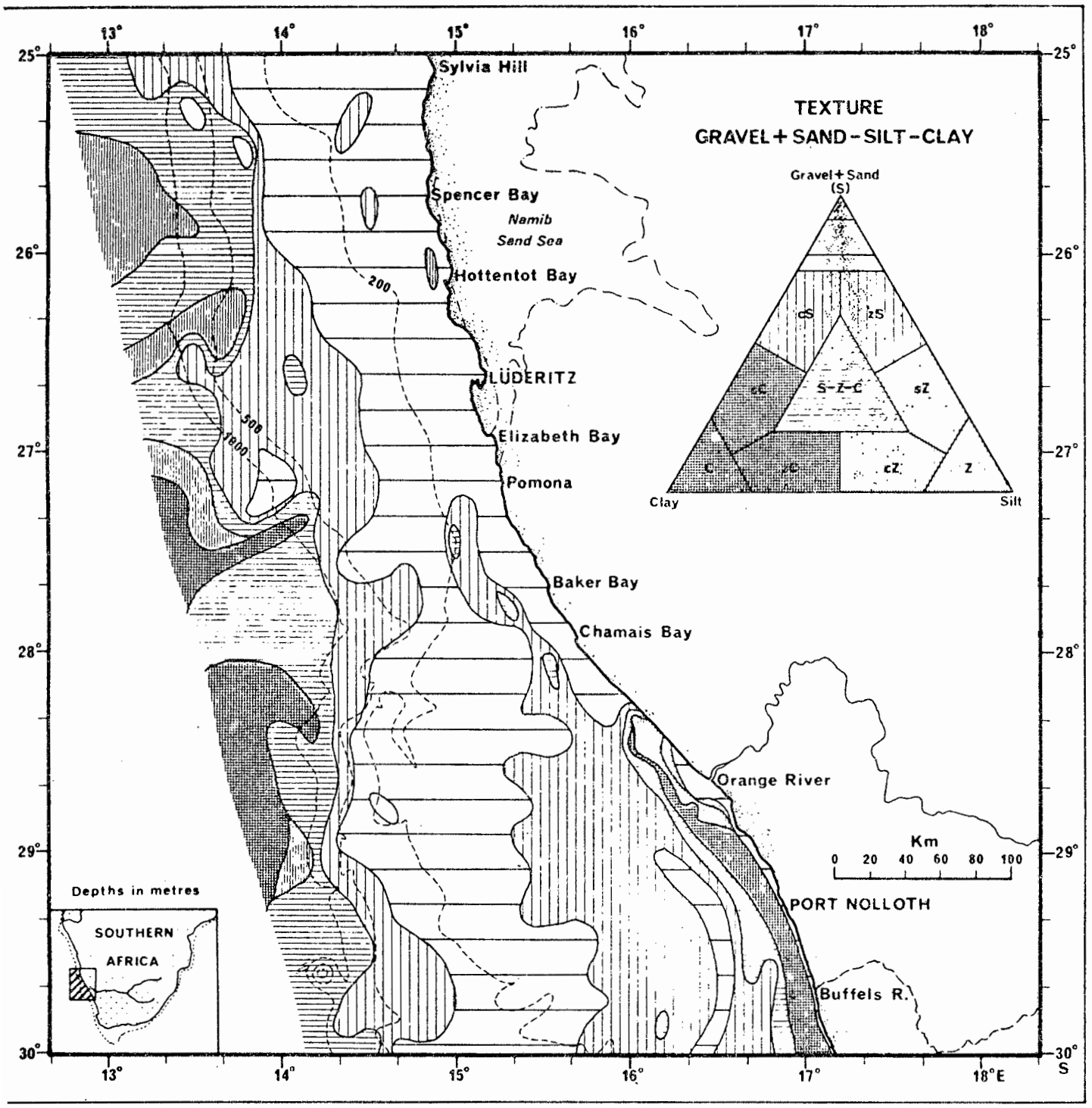
13°
14°
15°
16°
17°
18°
25°
26°
27°
28°
29°
30°
Sylvia Hill
Spencer Bay
Namib
Sand Sea
Hottentot Bay
LÜDERITZ
Elizabeth Bay
Pomona
Baker Bay
Chamais Bay
Orange River
PORT NOLLOTH
Buffels R.
200
500
1000
TEXTURE
GRAVEL + SAND - SILT - CLAY
Gravel + Sand
(S)
Clay
Silt
Km
0 20 40 60 80 100
Depths in metres
SOUTHERN
AFRICA
18°E
S

Fig. VII - 21

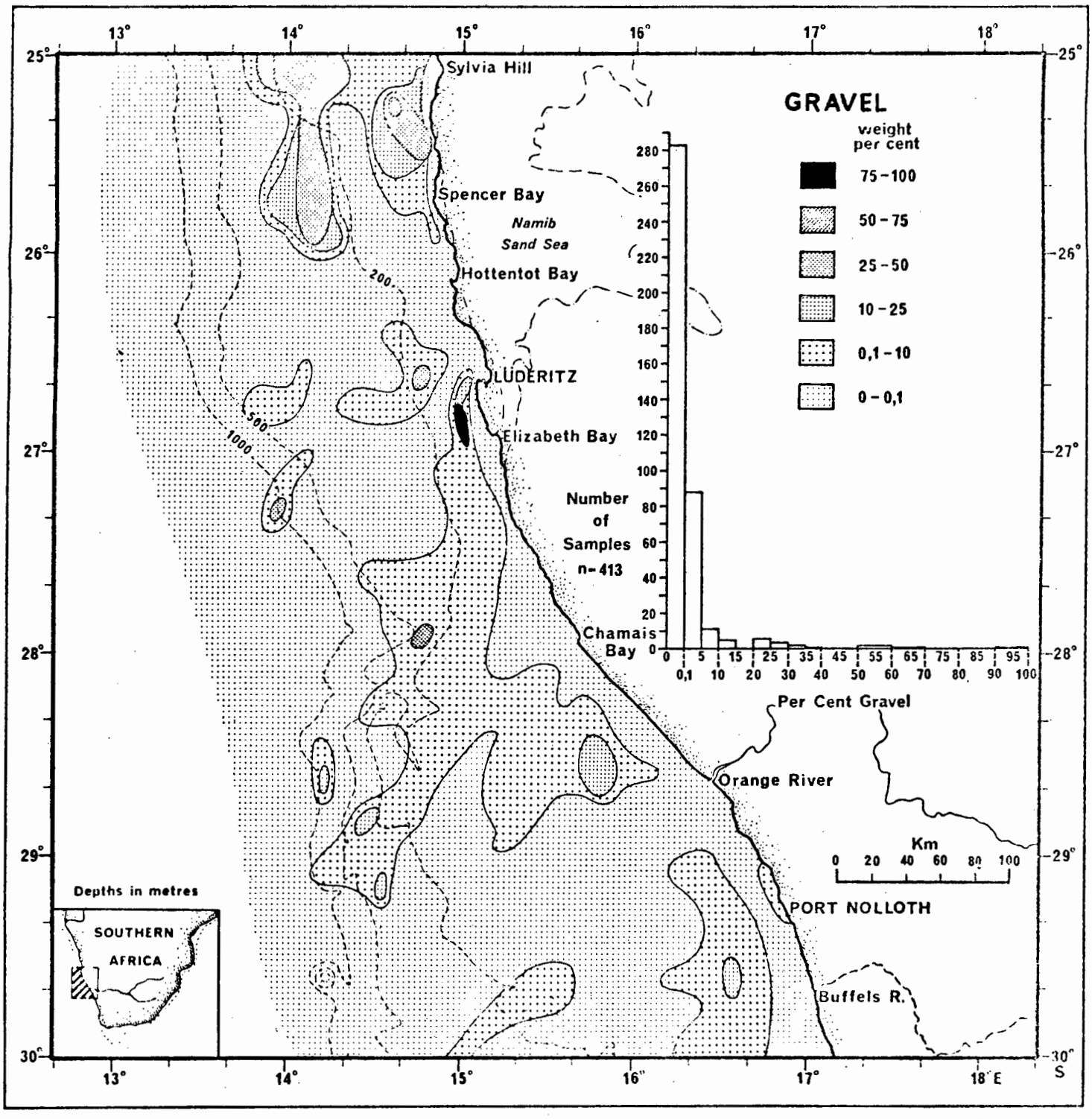
GRAVEL
weight per cent
75 - 100
50 - 75
25 - 50
10 - 25
0,1 - 10
0 - 0,1
Number of Samples n = 413
Per Cent Gravel
Sylvia Hill
Spencer Bay
Namib Sand Sea
Hottentot Bay
LÜDERITZ
Elizabeth Bay
Chamais Bay
Orange River
PORT NOLLOTH
Buffels R.
Km
Depths in metres
SOUTHERN AFRICA
200
500
1000
13°
14°
15°
16°
17°
18°
25°
26°
27°
28°
29°
30°
S
E

Fig.VII-22

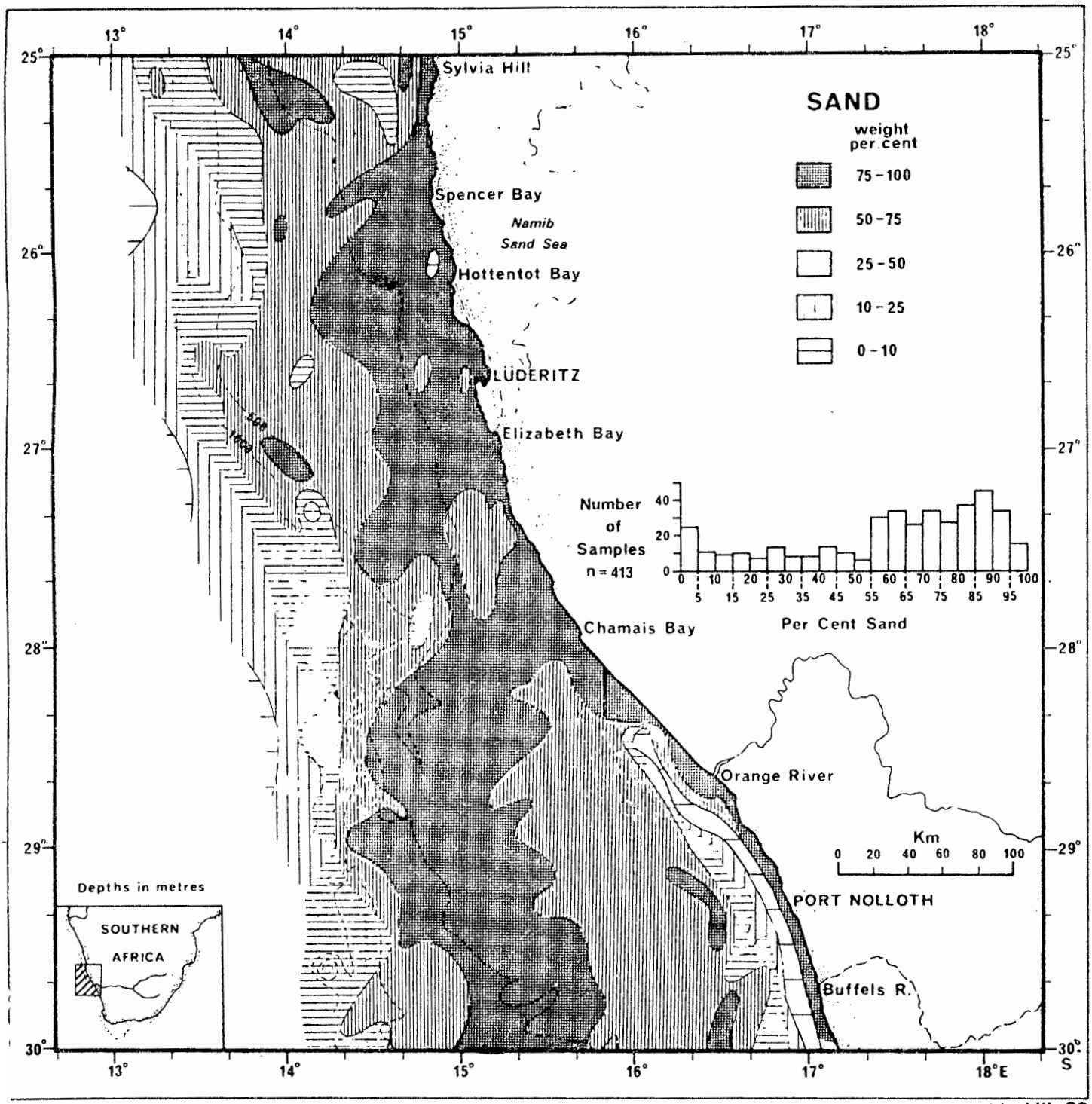
SAND
weight per cent
75 - 100
50 - 75
25 - 50
10 - 25
0 - 10
Sylvia Hill
Spencer Bay
Namib Sand Sea
Hottentot Bay
LÜDERITZ
Elizabeth Bay
Chamais Bay
Orange River
PORT NOLLOTH
Buffels R.
Number of Samples n = 413
Per Cent Sand
Km
0 20 40 60 80 100
Depths in metres
SOUTHERN AFRICA
13°
14°
15°
16°
17°
18°
18°E
25°
26°
27°
28°
29°
30°
30° S

Fig. VII-23

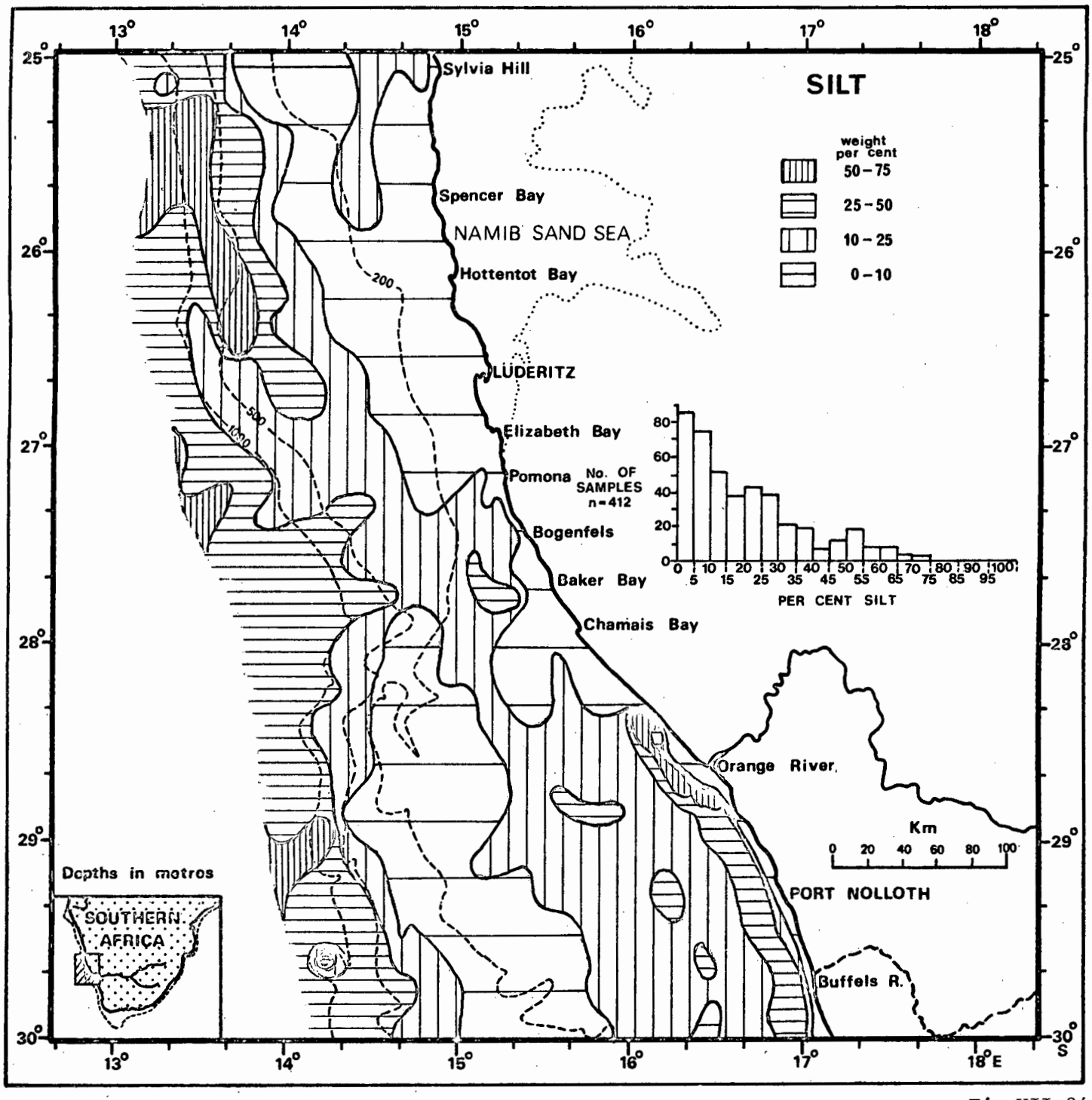
SILT
weight per cent
50 – 75
25 – 50
10 – 25
0 – 10
Sylvia Hill
Spencer Bay
NAMIB SAND SEA
Hottentot Bay
LÜDERITZ
Elizabeth Bay
Pomona
Bogenfels
Baker Bay
Chamais Bay
Orange River
PORT NOLLOTH
Buffels R.
200
500
1000
No. OF SAMPLES n=412
PER CENT SILT
Km
Depths in metres
SOUTHERN AFRICA
13°
14°
15°
16°
17°
18°E
25°
26°
27°
28°
29°
30°S

Fig.VII-24

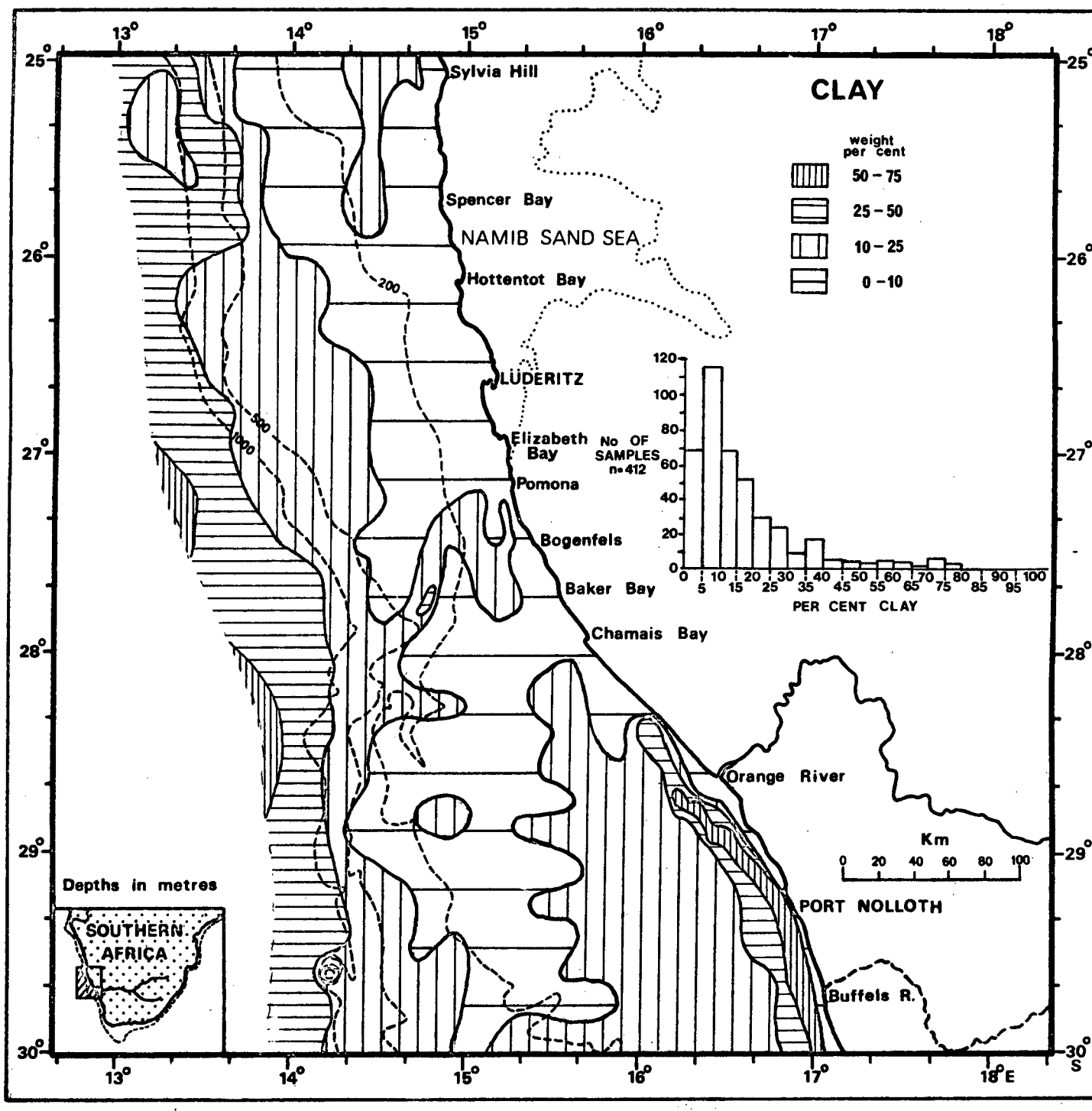
CLAY
weight per cent
50 – 75
25 – 50
10 – 25
0 – 10
Sylvia Hill
Spencer Bay
NAMIB SAND SEA
Hottentot Bay
LÜDERITZ
Elizabeth Bay
Pomona
Bogenfels
Baker Bay
Chamais Bay
Orange River
PORT NOLLOTH
Buffels R.
200
500
1000
No OF SAMPLES n=412
PER CENT CLAY
Km
Depths in metres
SOUTHERN AFRICA
13°
14°
15°
16°
17°
18°
25°
26°
27°
28°
29°
30°
S
18°E

Fig.VII-25

Another approach is to note the increase of orbital velocity at the bottom when waves leave deep water ($<L_o/2$) and enter water of intermediate depth ($L_o/2$ to $L_o/20$) (Allen, 1970, p.152). One can then observe at what depth the orbital velocity at the bottom exceeds the threshold velocity (10 cm/sec) of sediment at the delta-front/prodelta boundary (Allen, 1965, Fig. 10; Allen, 1970, Fig. 5.8).

Allen (1970, p.157) recommends that the mass transport velocity (U_m) be calculated using Stokesian theory, which applies to water depths greater than $L_o/10$. Values of U_m for the average wave at Lüderitz (Van Ieperen, 1975) can be obtained by inserting values for mean significant wave height (H_{mo}=1,8 m), mean wave period ($\overline{T}$ = 11 seconds), celerity (c), and wavelength (L) for various depths (d) in the following formula (Allen, 1970, equations 5.20 and 5.8):

$$U_m = \left(\frac{\pi H}{L}\right)\left(\frac{c}{2}\right)\frac{\cosh\ \frac{4\pi}{L}(d+z)}{\sinh^2\left(\frac{2\pi d}{L}\right)}\ \text{m/sec}$$

where $c = \sqrt{\frac{gL}{2}\tanh\frac{2\pi d}{L}}$ m/sec

and z = distance below sea level.

At the bottom $d + z = 0$ so that $\cosh\ \frac{4\pi}{L}(d+z) = 1$. The equation then simplifies to:

$$Um = \left(\frac{\pi H}{L}\right)\left(\frac{c}{2}\right)\frac{1}{\sinh^2\left(\frac{2\pi d}{L}\right)}\ \text{m/sec}$$

With the aid of standard tables (Wiegel, 1964) the following values were obtained (Table VII-6):

TABLE VII-6

Variation of mass transport velocity (U_m) with depth, using mean wave statistics from Lüderitz (Van Ieperen, 1975)

Water depth (d) m	Mass Transport Velocity (U_m) m/sec
20	23,2
25	16,0
30	11,3
35	8,2
40	6,7
45	4,4
50	3,2
55	2,4
60	1,7

Mean wave period ($\overline{T}$) = 11 secs. Mean significant wave height ($\overline{H}_{mo}$) = 1,8 m. Mean deepwater wavelength ($\overline{L}_o$) = 188,8 m.
$\overline{L}_o/2$ = 94,4 m. $\overline{L}_o/4$ = 42,2 m. $\overline{L}_o/10$ = 18,9 m.

The variation in mass transport velocity with depth is plotted against the variation in the proportions of sand, silt and clay across the Orange River delta (Figure VII-26). The threshold velocity is exceeded at 33 m for the mean data used and seaward of this depth deposition of silt and clay becomes important. Application of more sophisticated formulae to the waverider data now being collected off the mouth of the Orange River (Woodward, 1976, personal communication) may lead to more precise trends. These initial trends are nevertheless encouraging and confirm the dominance of wave action in determining the depth range of the delta front/prodelta boundary.

iv) Disequilibrium on the delta front

During May 1974, in the dying phase of the flood, a series of bottom samples across the prodelta to the delta front failed to detect the sharp boundary between the two zones near 40 m. Relatively high silt and clay values were found in delta-front sediments within the 40 m isobath. Similar results were obtained by Drake et al. (1972), who sampled the shelf off the mouth of the Santa Clara River in Southern California, after a major flood had deposited 50 x 10^6 tons of sediment. During an extended study involving periodic measurements of sediment thickness, sediment texture, suspended sediment concentration, currents, salinity and water temperature, Drake et al. (1972) traced the redistribution of the flood sediment from its initial locus within the 30-m isobath to its final resting place on the middle shelf below 100 m. An estimate of 3 years for the sediments to reach equilibrium was made.

v) Prodelta

Whereas the delta-front sand has a relatively restricted areal extent (Fig. VII-23) the silt and clay of the prodelta (Figs. VII-24 and 25) are found up to 100 km north of the mouth and as far south as St Helena Bay (33°S) (Birch, 1975). According to Hoyt et al. (1959) (Fig. VII-9), the delta front and the prodelta opposite the mouth reach a thickness of over 60 m. Only in such areas of high terrigenous input are unconsolidated sediments the sole control of the shelf's bathymetry (Fig. II-18). South of the mouth a lens of prodelta silty clay (Figs. VII-7 and VII-21) is clearly detected on detailed bathymetry charts (Figs. II-17 and II-18) as a zone of intermediate steepness between the 70 m and 120 m isobaths. However, the thickness of the lens is only of the order of 10 m (O'Shea, 1971).

Two textural trends are observed within the prodelta. Immediately opposite the river mouth and below the 40-m isobath a zone of clayey silt grades seawards into silty clay to a depth of 120 m (Fig. VII-21). In deeper water is a transgressive deposit of very fine sand (Fig. VII-19) deposited during the Flandrian

RELATIONSHIP BETWEEN WAVE-DRIVEN BOTTOM CURRENTS AND SEDIMENTS OF THE ORANGE RIVER DELTA

(Wave data after Van Ieperen, 1975)

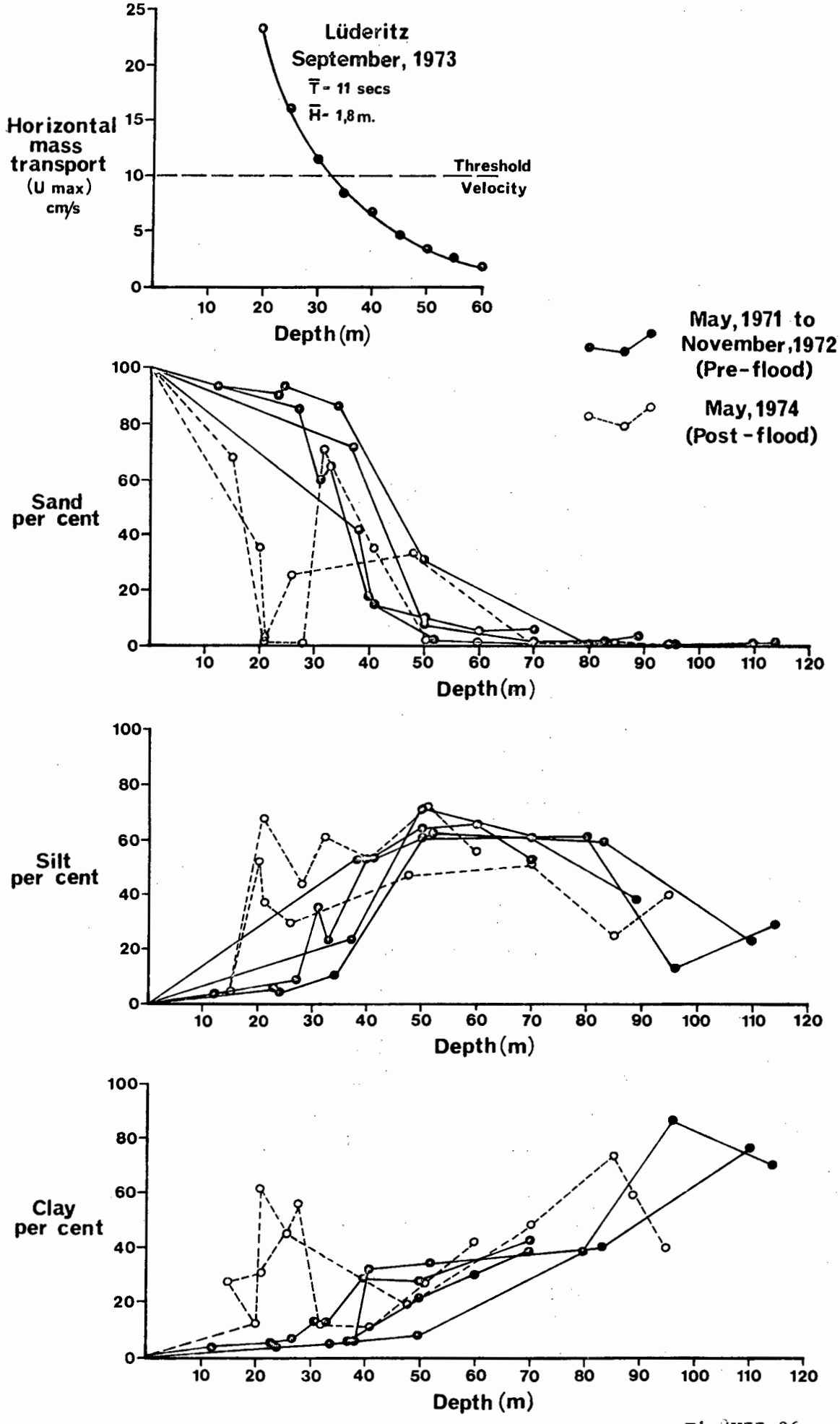

Fig. VII-26

transgression on the Early-Holocene delta front. Wave action is considered the prime control of this fining trend into deeper water. Despite an inadequate sampling grid a second trend was detected, from clayey silt at the northern tip of the prodelta to silty clay from the centre of the delta southwards (Fig. VII-21). This trend may have a more complex origin.

As shown on Fig. VI-3 the wave spectrum off the delta can affect the bottom out to the 175-m isobath, if wave base is assumed to be $L_o/2$ and the maximum wave period to be 15 seconds. The prodelta is therefore well within the zone of interaction with waves and the resultant agitation of the bottom waters probably both hinders deposition and causes resuspension of prodelta sediment.

During the 1973-1974 flood the turbid plume of effluent usually moved north of the mouth along the coast. One observer noted that during a morning flight this northward deflection was less marked and the boundary of the plume was less distinct. In contrast, during afternoon observations the plume was deflected sharply northwards and the plume's seaward boundary curved round to meet the coast only a kilometre or so south of the mouth. A similar pattern was observed by Low (1967) during the previous major flood. This oscillating pattern is probably caused by the marked diurnality of the west coast's wind system. Data from the first-order weather station at Alexander Bay show that the diurnality is more marked in summer, when floods can be expected, and that the southerly afternoon winds attain greater velocities in summer than in winter (Fig. VII-12). A northward wind-driven current of fluctuating velocity is postulated to account for deltaic deposition north of the mouth.

On certain of the LANDSAT-1 images taken before the 1973-1974 flood (e.g. 1183-08173) a dilute plume of effluent is seen beside the coast of Namaqualand, south of the delta, suggesting the presence of the poleward-flowing De Decker Current (De Decker, 1970; Bang. 1976). Regrettably few current measurements have been made of the De Decker Current. Foster (1973, personal communication) measured surface and mid-water currents with velocities of up to 1,5 m/sec flowing in various directions over the inner shelf. He noted a regular swing of the current to the south in the evenings when the wind abated. These observations were made aboard an anchored vessel, M.V. "Rockeater", during diamond-prospecting operations off the Orange River.

On a broader scale, Stander (1964) and De Decker (1970) observed that the De Decker Current normally reaches latitude 25°S on the northern edge of the study area, but in late summer and early autumn it penetrates as far south as the Orange River and sometimes as far as Cape Point south of Cape Town. The activity of this current during summer floods explains the discovery of driftwood from the Orange River and bean seeds from Angola on the Namaqualand coast as much as 400 km south of the delta (Wagner and Merensky, 1928). During summer floods the De Decker

Current is opposed on the surface by wind-driven equatorward currents, particularly in the afternoons. The mean position of the effluent plume will therefore tend to lie north of the mouth. This may explain the northward assymetry of the delta as a whole (Hoyt et al., 1969) and the deposition of the faster-settling very fine sand and coarser silt to the north (Fig. VII-24). Deposition of the finer silt and of the clay south of the mouth is attributed to transport by the De Decker Current, particularly at night and in the morning when wind velocities are at a minimum (Fig. VII-12).(Fig. VII-25).

Divers working off the west coast (Murray, 1969; Christie, 1975, personal communication) report extremely turbid conditions over the inner shelf. Similar conditions on the Agulhas Bank were studied by Zoutendyk (1973) who confirmed his own observations of zero visibility within a one-metre thick bottom layer, by measuring zero transmission near the bottom with a transmissometer. Poleward transport of clay and of silt therefore probably increases in winter, when storms both resuspend sediment and accelerate the De Decker Current (Shannon, 1966).

vi) Compositional tracers of sediment dispersal

The model proposed for the dispersal of effluent from the Orange River has been based, in the previous sections, on textural data. What evidence exists to substantiate or negate the model in the composition of the sediments?

In their study of clay minerals of the World Ocean, Griffin et al. (1968) noted that illite dominated deep-sea sediments off southern Africa. They attributed this distribution to drainage of illite-rich sediments from the more arid regions in the western catchment of the Orange River. A reconnaissance study of clay minerals in 44 marine samples and 7 river samples confirmed that illite is indeed the dominant clay mineral. It comprises 60-80% of most marine samples and also of the river samples from both the arid and temperate sections of the catchment (Fig. VII-27).

Montmorillonite is subordinate to illite in the river samples (Fig. VII-28), but there is a striking difference between samples from the mainstream of the Orange River (20-30%) and samples from rivers in the arid western part of the catchment (0-10%). On the inner shelf north and south of the Orange River mouth there is a concentration of montmorillonite (20-30%), but the highest values (30-60%) are concentrated on the upper slope. (Preliminary results from Chester and Elderfield (1975) indicate the absence of halmyrolysis of Orange River clays on entering sea water. They quote an average composition for their suite of river and delta samples of 50% montmorillonite, 40% illite, 10% kaolinite and less than 5% chlorite, but in the absence of further details this difference in dominant clay mineral cannot be assessed.) The Kunene River has been suggested as a likely source for montmorillonite; Bremner (1975c) found montmorillonite dominating kaolinite in the absence of illite in Kunene River sediment.

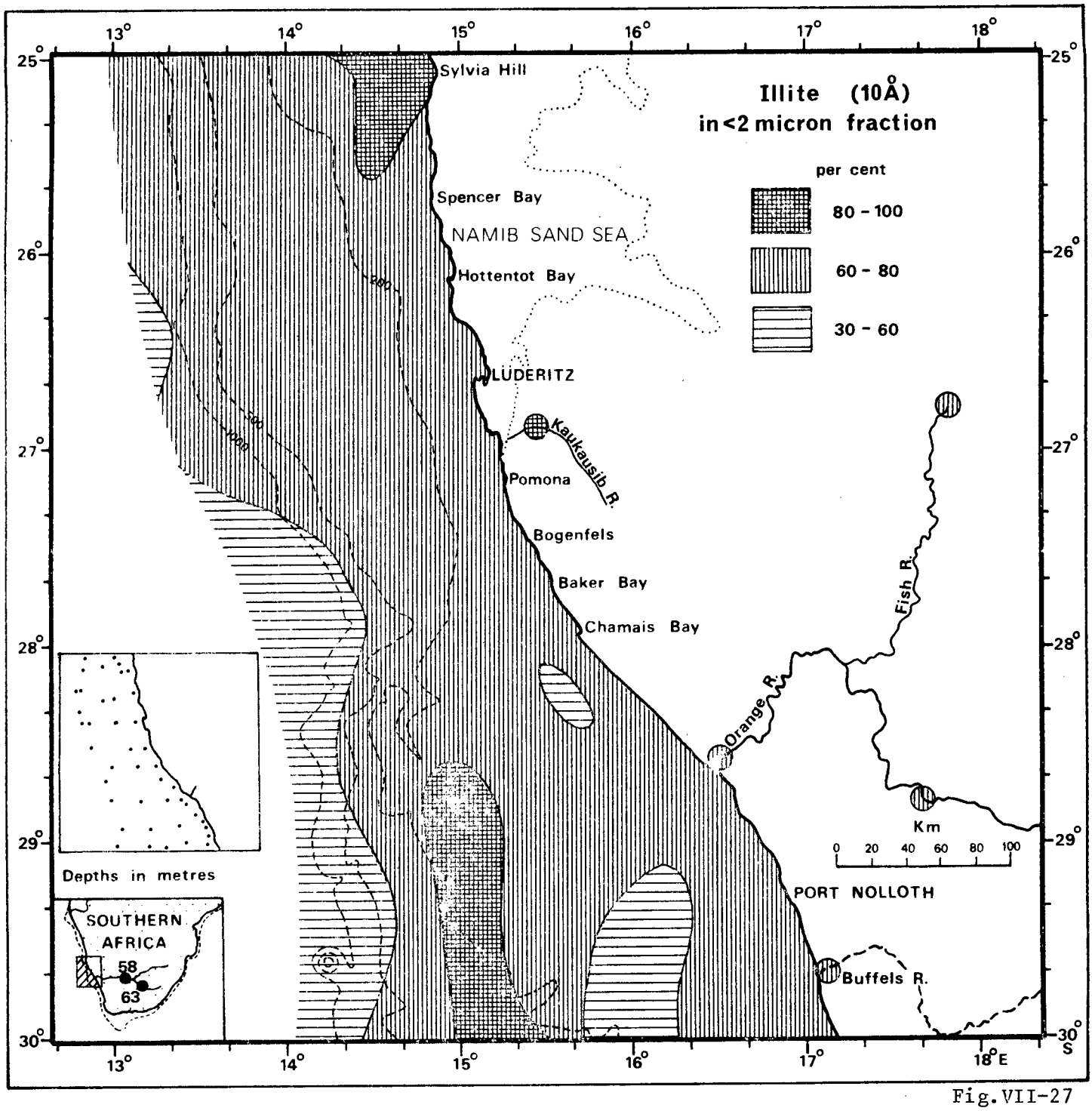
Illite (10Å)
in <2 micron fraction
per cent
80 - 100
60 - 80
30 - 60
Sylvia Hill
Spencer Bay
NAMIB SAND SEA
Hottentot Bay
LÜDERITZ
Kaukausib R.
Pomona
Bogenfels
Baker Bay
Chamais Bay
Fish R.
Orange R.
PORT NOLLOTH
Buffels R.
Km
0 20 40 60 80 100
Depths in metres
SOUTHERN AFRICA
58
63
13°
14°
15°
16°
17°
18°
18°E
25°
26°
27°
28°
29°
30°
S

Fig.VII-27

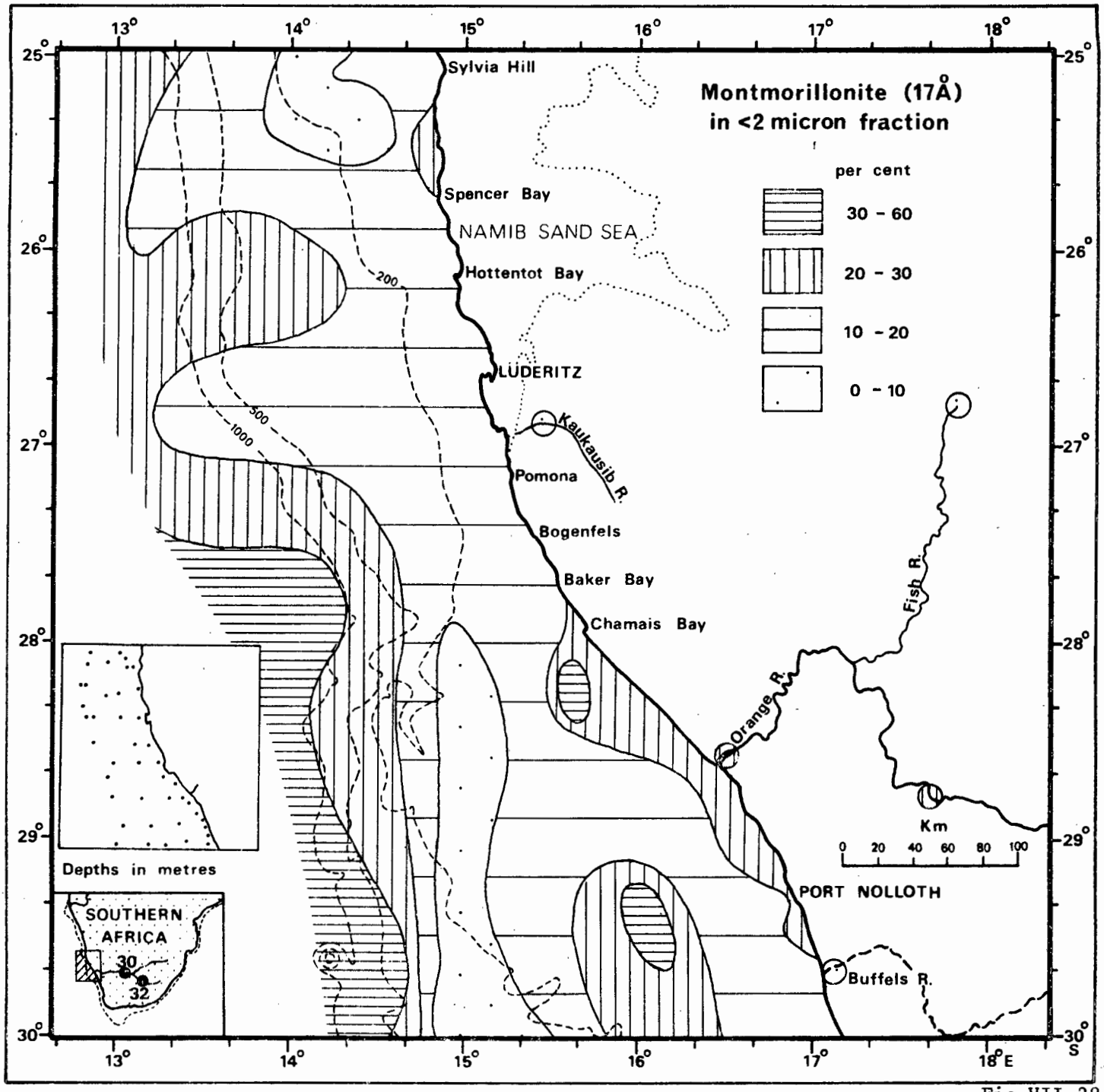
Montmorillonite (17Å)
in <2 micron fraction
per cent
30 - 60
20 - 30
10 - 20
0 - 10
Sylvia Hill
Spencer Bay
NAMIB SAND SEA
Hottentot Bay
LÜDERITZ
Kaukausib R.
Pomona
Bogenfels
Baker Bay
Chamais Bay
Orange R.
Fish R.
PORT NOLLOTH
Buffels R.
200
500
1000
Km
0 20 40 60 80 100
Depths in metres
SOUTHERN AFRICA
30
32
13°
14°
15°
16°
17°
18°E
25°
26°
27°
28°
29°
30°S

Fig.VII-28

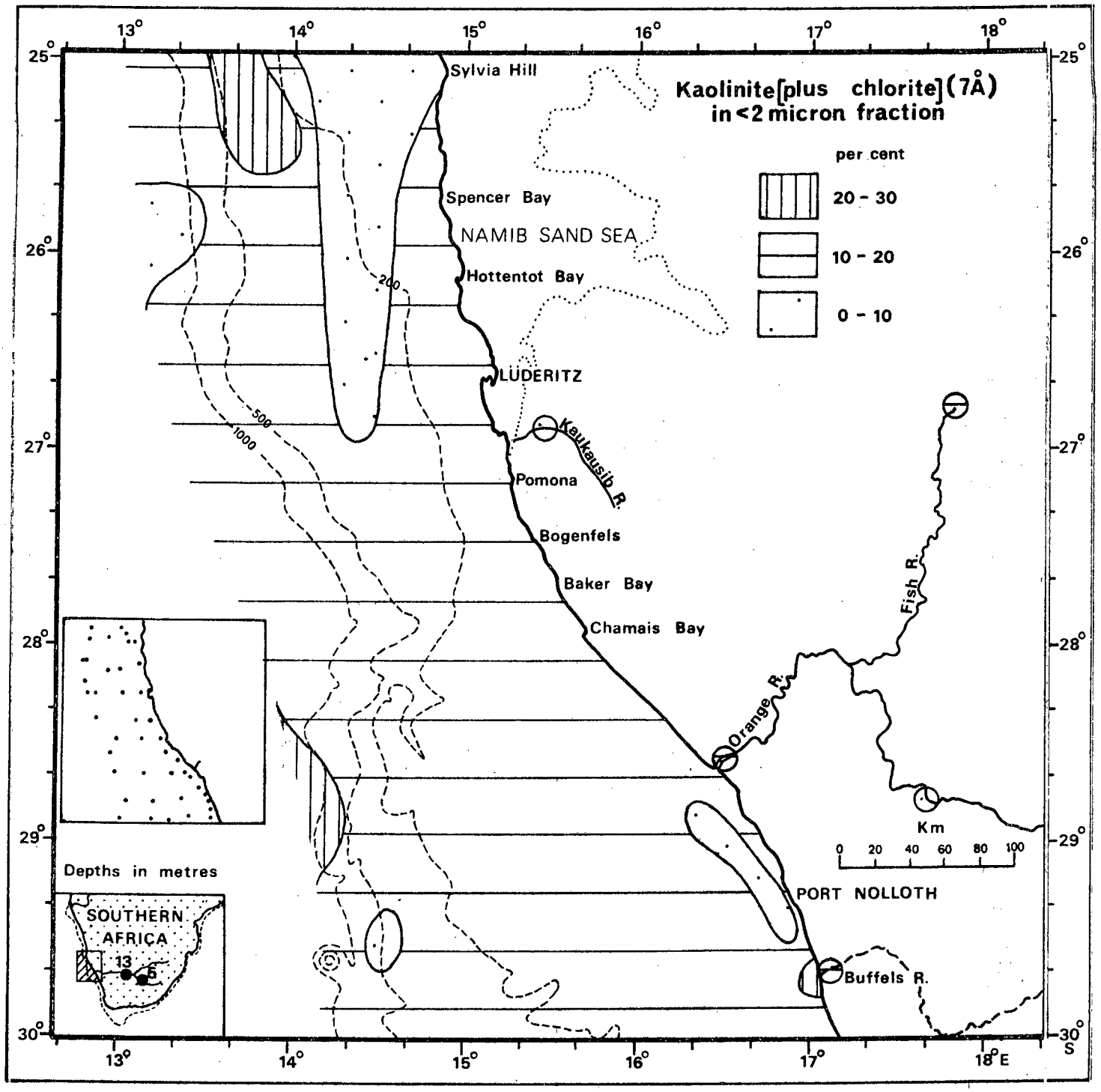
Kaolinite[plus chlorite](7Å)
in<2 micron fraction
per cent
20 - 30
10 - 20
0 - 10
Sylvia Hill
Spencer Bay
NAMIB SAND SEA
Hottentot Bay
LÜDERITZ
Kaukausib R.
Pomona
Bogenfels
Baker Bay
Chamais Bay
Orange R.
Fish R.
PORT NOLLOTH
Buffels R.
200
500
1000
Km
0 20 40 60 80 100
Depths in metres
SOUTHERN AFRICA
13
5
13°
14°
15°
16°
17°
18°E
25°
26°
27°
28°
29°
30°S

Fig.VII-29

Minerals with a 7Å peak, presumed to be dominantly kaolinite, have low abundances (Fig. VII-29). Values in excess of 20% are found on the slope and towards the north of the area and are probably due to poleward transport in the Deep Compensation Current (Hart and Currie, 1960) from the kaolinite-rich Congo River (Biscaye, 1965; Griffin et al., 1968; Bornhold, 1973). The current probably also entrains kaolinite from the Kunene River (Bremner, 1975c).

Van der Merwe and Heystek (1955a) show that montmorillonite dominates soils on weathered basalt in the Drakensberg Mountains and on weathered dolerite in the High Veld within the catchment of the Upper Orange. The same authors (1956) proved that the sedimentary rocks underlying the High Veld weather to illite-montmorillinoid mixed-layer minerals and then to illite and sometimes to soil kaolin. In the arid western half of the catchment, leaching is inhibited and bedrock is subjected chiefly to mechanical disintegration. Random mixed-layer illite-montmorillinoid minerals are typical of this region (Van der Merwe and Heystek, 1955b).

The predominance of illite in all the river samples and the greater concentration of montmorrillonite in the mainstream samples, confirms that the Upper Orange catchment, underlain by sediments of the Karoo Supergroup, is the chief source of suspended sediment in the Orange River. The clay-mineral distribution lends itself more to tracing sediment dispersal on an oceanic scale. Other approaches will therefore be used to trace the dispersal of Orange River sediment in finer detail.

The proportion of terrigenous detritus in the marine sediments has been calculated by adding the percentage of calcium carbonate, organic matter, glauconite, and carbonate apatite, and then assigning the residue to "terrigenous detritus". This indirect method is subject to an accumulation of experimental errors and the detritus includes biogenic silica in the form of diatom frustules, radiolarian tests and sponge spicules. However, all but one or two highly organic, diatom-rich samples from the middle shelf off Sylvia Hill (25°S) contain negligible proportions of such siliceous debris.

Near the coast, south of the Orange River (Fig. VII-30) the inner-shelf sediment is diluted by shell fragments, as previously noted in Fig. VII-17. North of the river, the inner-shelf sediment contains over 90% terrigenous detritus as far north as Hottentot Bay (26°S), where shell fragments become more important diluents again. South of the river, values in excess of 90% are confined to the narrow belt of silty clay extending south towards St Helena Bay (Birch, 1975). In general, sediment dominated by terrigenous detritus lies within 50 km of the land, due to dispersal processes parallel to the coast.

In a reconnaissance study of the clay fraction (<2 micron fraction), the

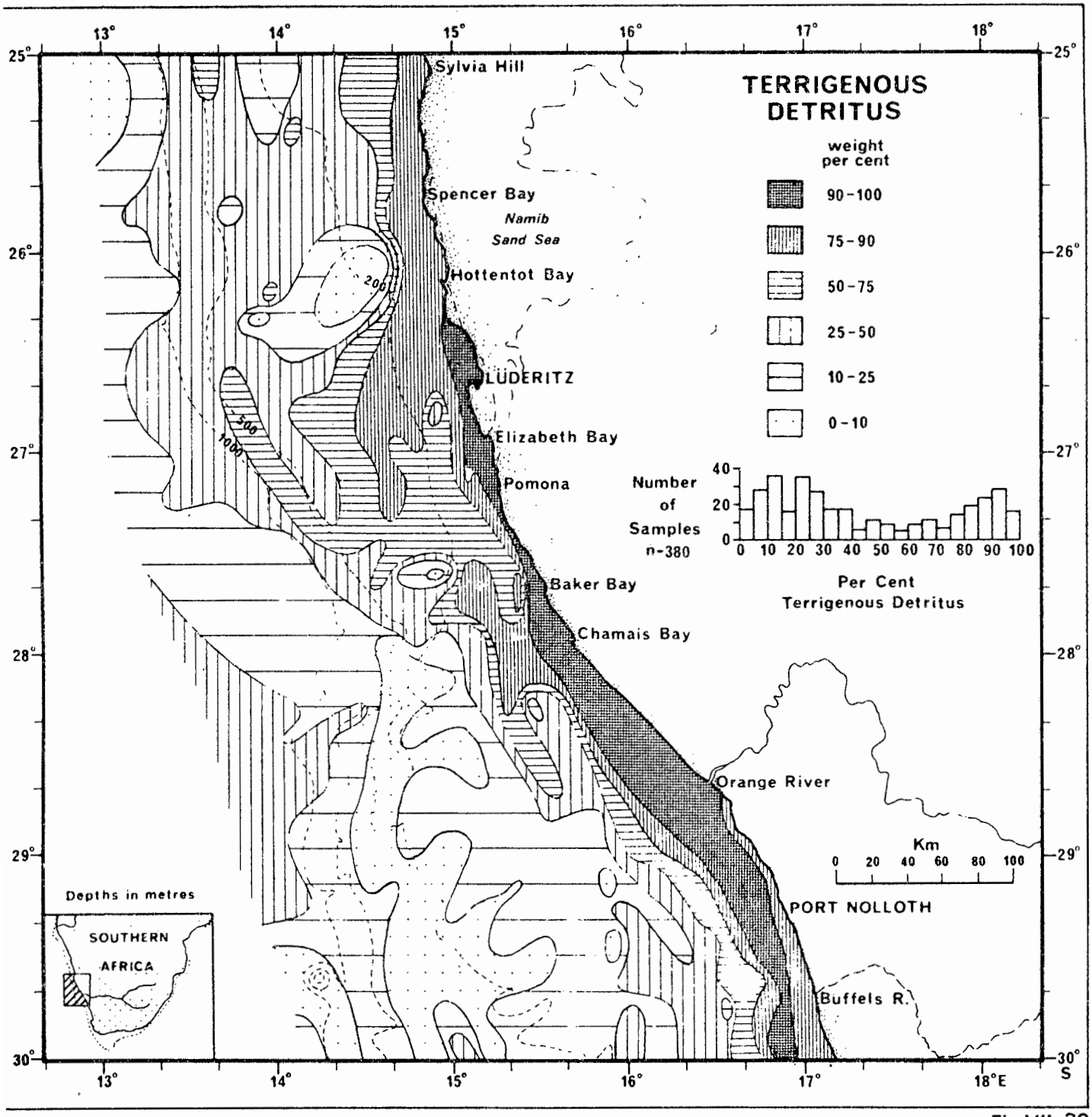
TERRIGENOUS DETRITUS
weight per cent
90-100
75-90
50-75
25-50
10-25
0-10
Number of Samples n-380
Per Cent Terrigenous Detritus
Sylvia Hill
Spencer Bay
Namib Sand Sea
Hottentot Bay
LÜDERITZ
Elizabeth Bay
Pomona
Baker Bay
Chamais Bay
Orange River
PORT NOLLOTH
Buffels R.
Km
Depths in metres
SOUTHERN AFRICA
13°
14°
15°
16°
17°
18°
18°E
25°
26°
27°
28°
29°
30°
S

Fig. VII-30

proportions of iron (Fig. VII-31) and of manganese (Fig. VII-32) were measured by atomic-absorption spectrophotometry. Both elements mimicked terrigenous detritus in their distribution, but the patterns were not as distorted seawards off Lüderitz, where residual quartz is common (Chapter V). River clay containing over 10% iron is dispersed northwards as far as Baker Bay (27°40'S) and south towards St Helena Bay (Fig. VII-31) (Birch, 1975). Seaward bulges of the regional trend off Lüderitz are attributed to terrigenous-poor, but iron-rich, glauconitic sediments (Chapter V). Low values (<4%) north of Spencer Bay (26°S) are probably due to dilution by organic matter (See Chapter VIII).

Manganese (Fig. VII-32) proved to be the least ambiguous tracer for the dispersal of Recent terrigenous clay. Values in excess of 400 p.p.m. were restricted to the rivers and the immediate vicinity of the Orange River mouth. Values in excess of 150 p.p.m. extended northwards along the inner and middle shelf to Spencer Bay (26°S) and southwards to St Helena Bay (33°S) (Birch, 1975).

The cumulative evidence of these compositional tracers confirms the bi-directional, coast-parallel dispersal and depositional model presented above. Seaward and northward dilution by biogenic sediment is the subject of Chapter VIII.

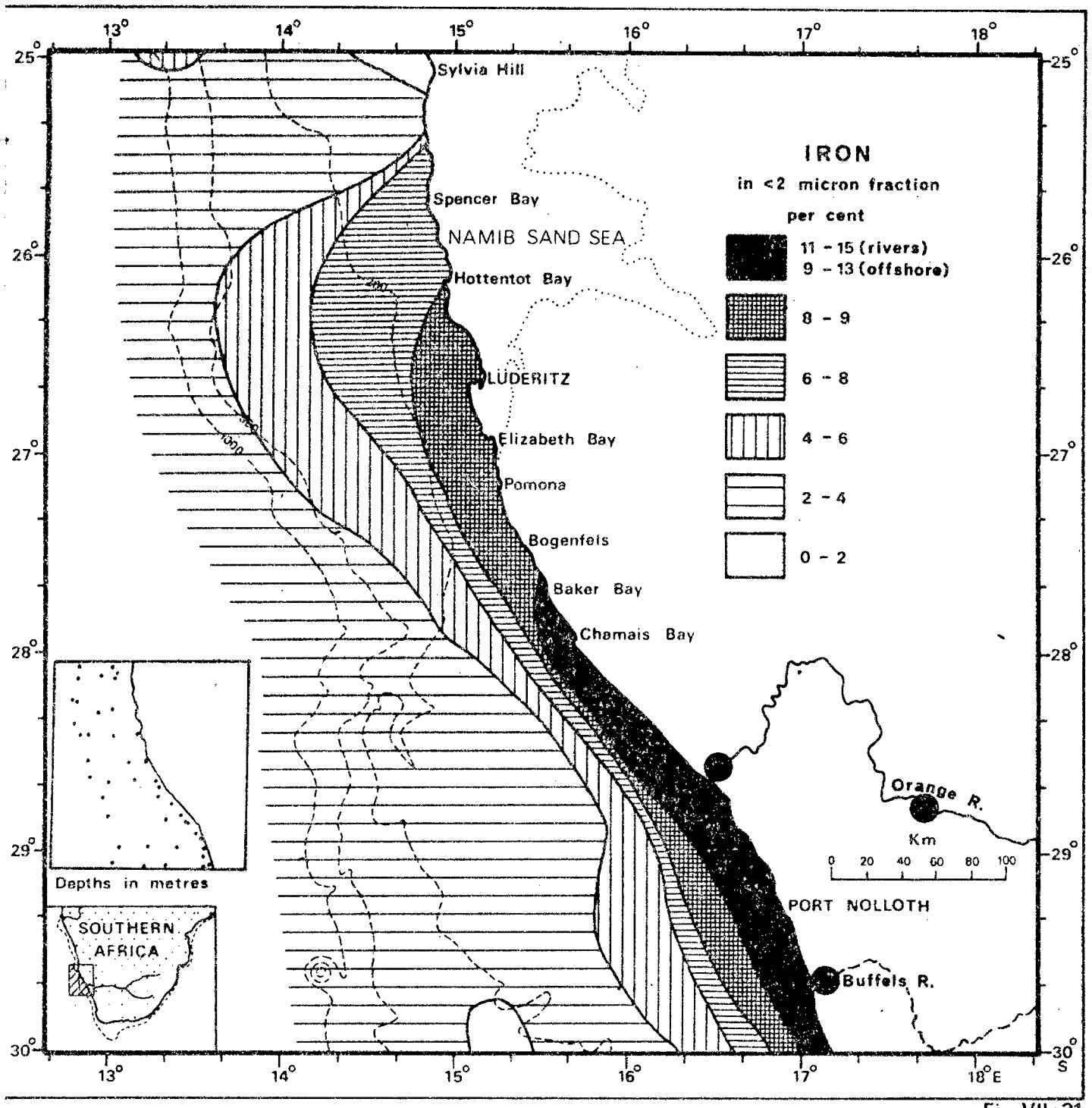
13°
14°
15°
16°
17°
18°
25°
26°
27°
28°
29°
30°
Sylvia Hill
Spencer Bay
NAMIB SAND SEA
Hottentot Bay
LÜDERITZ
Elizabeth Bay
Pomona
Bogenfels
Baker Bay
Chamais Bay
IRON
in <2 micron fraction
per cent
11 - 15 (rivers)
9 - 13 (offshore)
8 - 9
6 - 8
4 - 6
2 - 4
0 - 2
Orange R.
Km
0 20 40 60 80 100
PORT NOLLOTH
Buffels R.
Depths in metres
SOUTHERN AFRICA
13°
14°
15°
16°
17°
18°E
S

Fig. VII-31

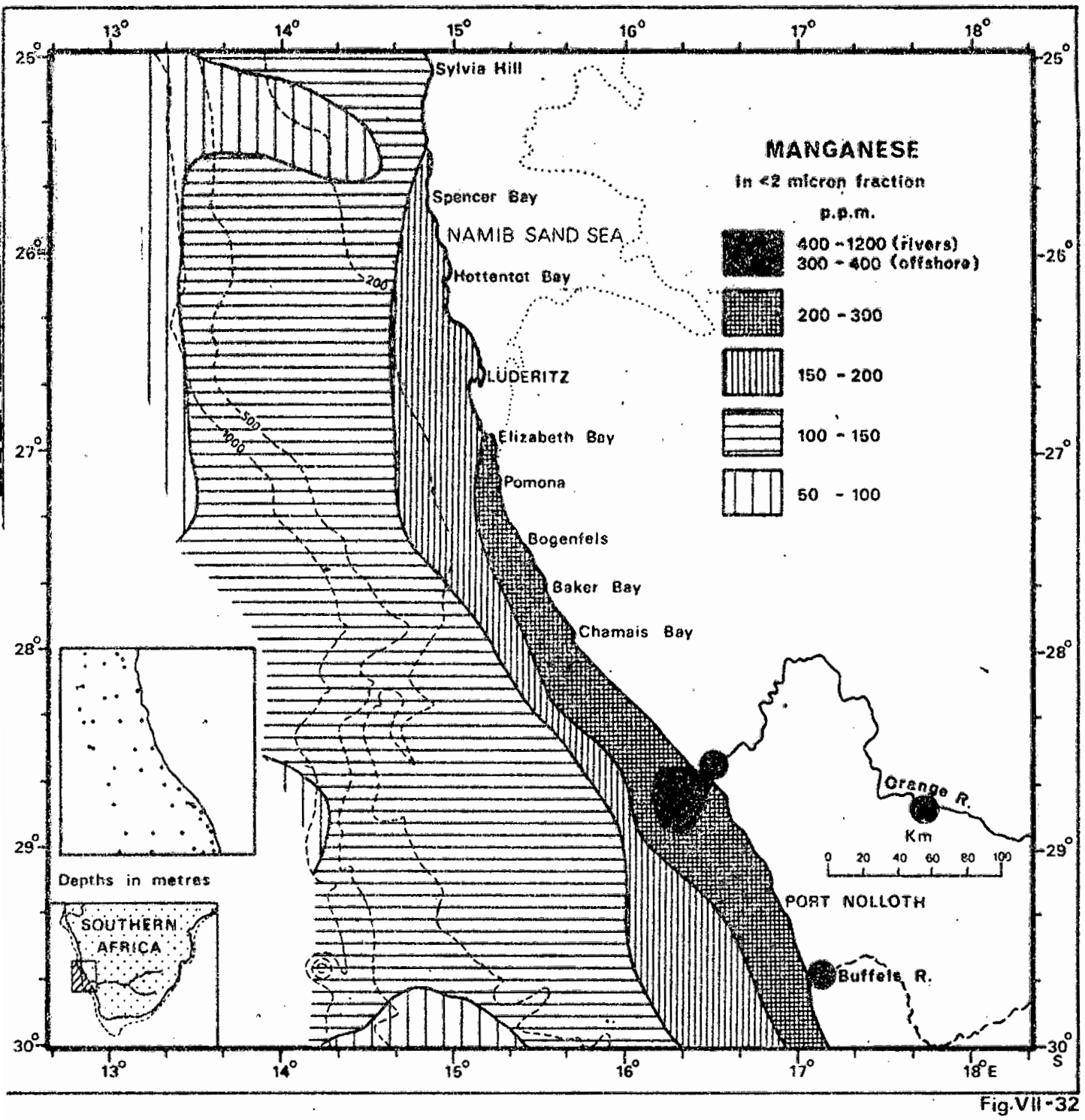
13°
14°
15°
16°
17°
18°
25°
26°
27°
28°
29°
30°
Sylvia Hill
Spencer Bay
NAMIB SAND SEA
Hottentot Bay
LÜDERITZ
Elizabeth Bay
Pomona
Bogenfels
Baker Bay
Chamais Bay
200
500
1000
MANGANESE
in <2 micron fraction
p.p.m.
400 - 1200 (rivers)
300 - 400 (offshore)
200 - 300
150 - 200
100 - 150
50 - 100
Orange R.
Km
0 20 40 60 80 100
PORT NOLLOTH
Buffels R.
Depths in metres
SOUTHERN AFRICA
18°E
S

Fig.VII-32

CHAPTER VIII

BIOGENIC SEDIMENTS

A. INTRODUCTION

The physical oceanography of the study area is characterized by variability within broadly defined patterns. Consequently, variability both in space (patchiness) and in time is characteristic of the distribution of the region's marine flora and fauna. Accepting that sea level reached its present average position some 6 000 years ago, the question should be asked "to what extent do the biogenic sediments in the area reflect 'average' conditions within the water column during the past 6 000 years?"

In this chapter the chief characteristics of the physical oceanography of the area are first described. Geochemical data, in the form of calcium-carbonate and organic-carbon distributions, are then discussed to assess their accuracy in reflecting conditions in the shelf waters. A series of reconnaissance studies of the biogenic components of the samples, divided into plankton, nekton and benthos are then presented as additional indicators of regional oceanographic trends.

B. PHYSICAL OCEANOGRAPHY

1. Regional setting

The study area lies at the centre of the Benguela Current System, one of the four major eastern-boundary currents in the world i.e. the Peru, California, Canary and Benguela Current Systems. The Benguela is bounded offshore by the South-East Atlantic Trade Wind Drift part of the gyral circulating anti-cyclonically around the South Atlantic Ocean (Hart and Currie, 1960). The Drift, of relatively warm, nutrient-poor oceanic water of normal salinity, is separated from the cool, nutrient-rich, low-salinity waters of the Benguela by an "offshore divergence belt" over the shelf break. Plumes of wind-induced upwelled water appear periodically beside the coast and are separated from the "divergence belt" by an intermediate zone of water upwelled in earlier phases (Bang, 1971).

Upwelling occurs frequently and is most intense between the Orange River and Lüderitz (Stander, 1964), north of a "pivot", such as that noted off Chamais Bay ($28^{o}S$) in late summer by Bang (1971, Fig. 15). Such a "pivot" tends to move equatorward in spring and again poleward in autumn (Stander, 1964) in harmony with the movement of the South Atlantic Anticyclone controlling the coastal winds (see Chapter VII).

2. Upwelling mechanism

Upwelling in the Benguela Current is caused primarily by the action of constant trade winds blowing equatorwards, combined with Coriolis force (the effect of

the earth's rotation). According to Ekman (1905, in Hart and Currie, 1960), such a combination of forces results in net offshore movement of the surface water to the left of the wind direction in the southern hemisphere. Hart and Currie (1960) concluded that South Atlantic Central Water is brought onto the shelf by this mechanism. However upwelling to the surface depends on the strength of coastal winds, which have already been discussed in some detail in Chapter VII. From the data available it can be predicted that upwelling will be strongest and most intense off the Sperrgebiet Trough Namib (27^{o}-28^{o}S). In addition, the season of most intense upwelling will vary from spring off Walvis Bay (cf. Stander, 1964, p.35) to summer off Cape Town (cf. Shannon, 1966, p.9).

Hart and Currie (1960, p.185) decided that all the water moved offshore by surface Ekman currents is replaced by upwelling across the shelf. Bang (1976, p.9) calculated that the rate of upwelling across the shelf is too slow to compensate for water moved rapidly offshore by surface Ekman currents. He suggested the probability of some compensatory movement equatorwards of the Good Hope Jet. This Jet is a bottom Ekman current, which attains velocities of up to 1,5 m/sec along the shelf break (Bang, 1973). It probably feeds directly into the upwelling system just north of the Chamais Slump, where the shelf is at its narrowest (Bang, 1971, Fig. 9; 1976, p.10).

3. Conservative properties

a. Introduction

Hart and Currie (1960) conducted an autumn survey off the Orange River ($28^{o}30'$S) and off Sylvia Hill (25^{o}S) during a period of quiescence subsequent to upwelling. They repeated their survey during spring, when upwelling was active and intense and correlated data on both conservative and non-conservative properties of sea water with microplankton studies.

b. Temperature

In autumn (Figs. VIII-1 and VIII-3) temperatures are higher and therefore temperature gradients greater due to solar heating of surface water. In spring (Figs. VIII-2 and VIII-3) gradients are correspondingly less pronounced despite the greater abundance of cold, upwelled water. Poleward flow off Sylvia Hill associated with the Angola Current (Moroshkin et al., 1970) accounts for the warmer temperatures in autumn (Fig. VIII-1). Stander (1964, p.17) remarks on the persistent upwelling of cool water off the Orange River over the Orange Banks even under the quiescent conditions found in autumn (Fig. VIII-1). He ascribed this to the effect of the shallow and wide Orange shelf, which forces water to well up over it onto the Walvis shelf farther north.

c. Salinity

Salinity has the advantage that it is unaffected by solar heating, which in

PHYSICAL, CHEMICAL AND BIOLOGICAL PARAMETERS OFF ORANGE RIVER AND SYLVIA HILL

(After Hart and Currie, 1960)

SUBDUED UPWELLING AUTUMN

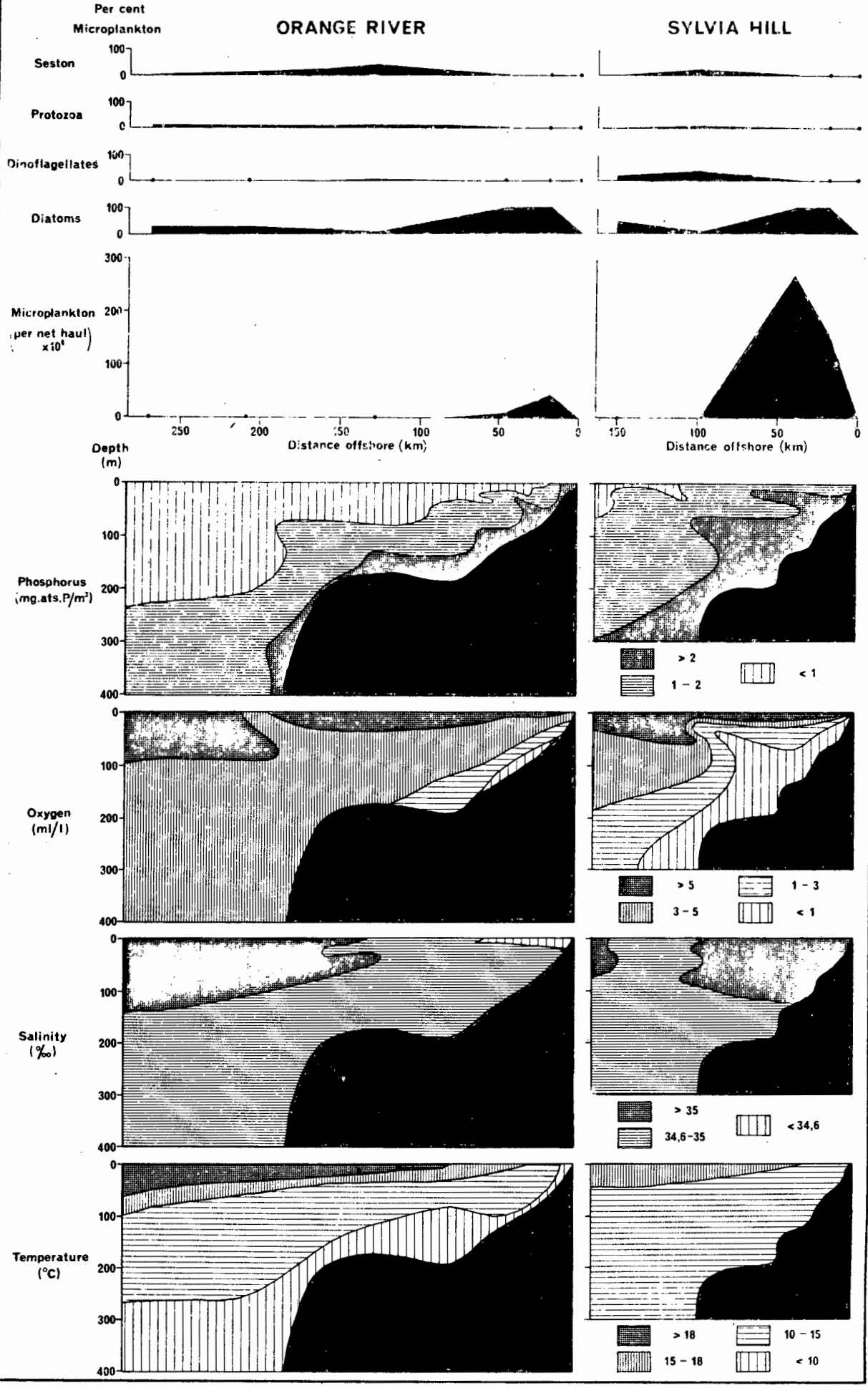

Fig. VIII-1

PHYSICAL, CHEMICAL AND BIOLOGICAL PARAMETERS OFF ORANGE RIVER AND SYLVIA HILL

(After Hart and Currie, 1960)

INTENSE UPWELLING SPRING

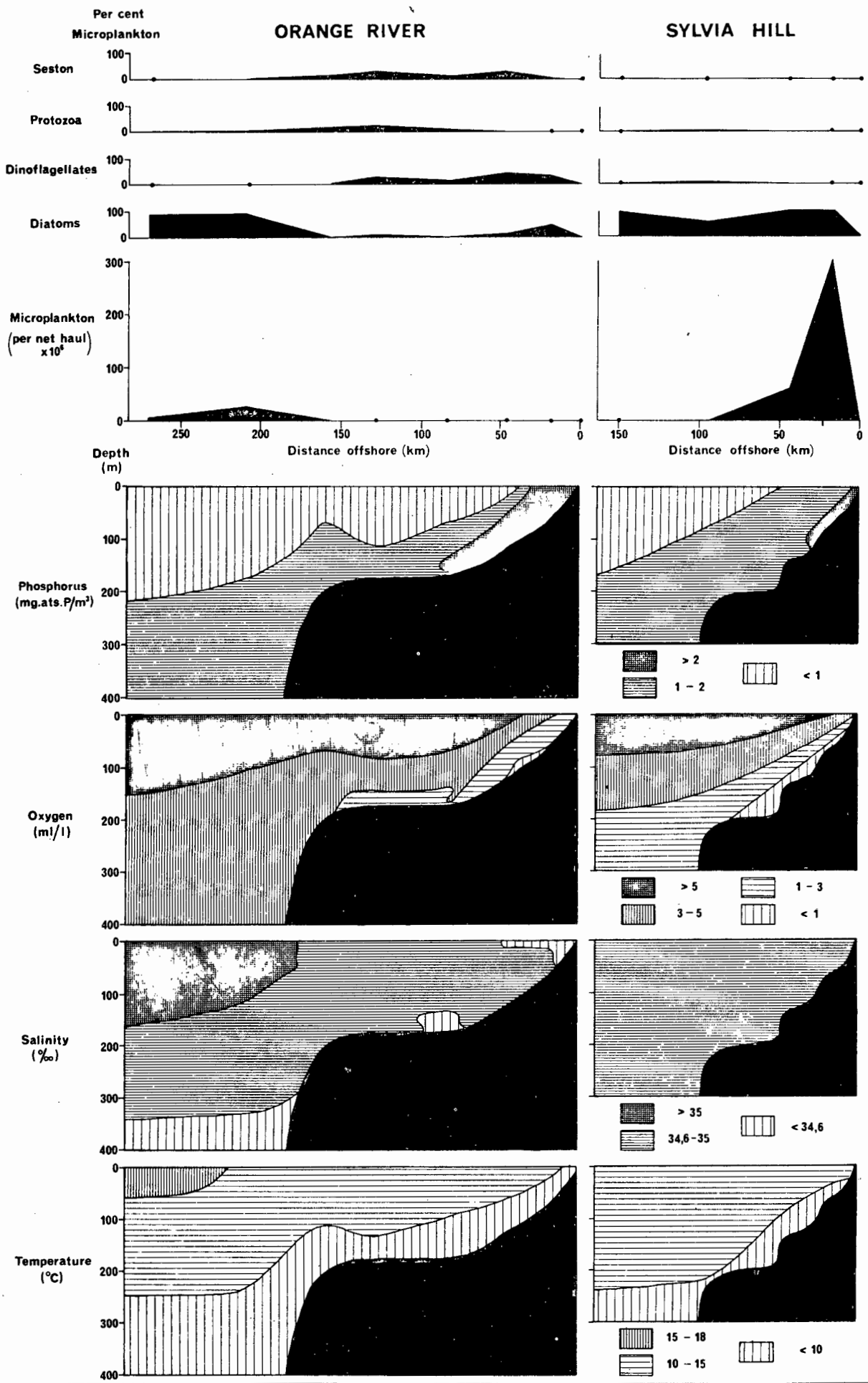

Fig VIII-2

MICROPLANKTON, SURFACE SALINITY AND TEMPERATURE BETWEEN THE ORANGE RIVER AND SYLVIA HILL

(After Hart and Currie,1960)

SUBDUED UPWELLING
Autumn

INTENSE UPWELLING
Spring

Microplankton
(per net haul)
$\times 10^6$

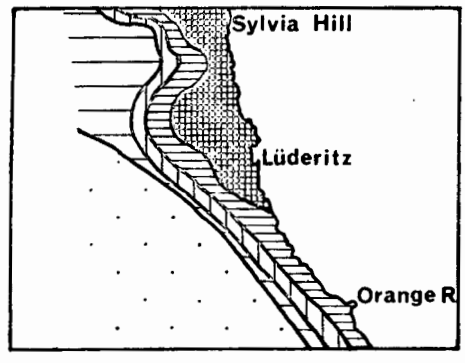

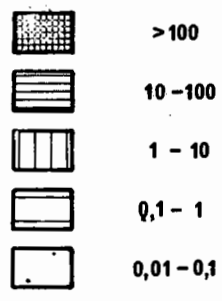

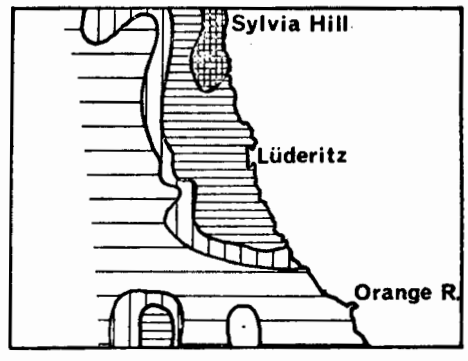

Salinity
(‰)

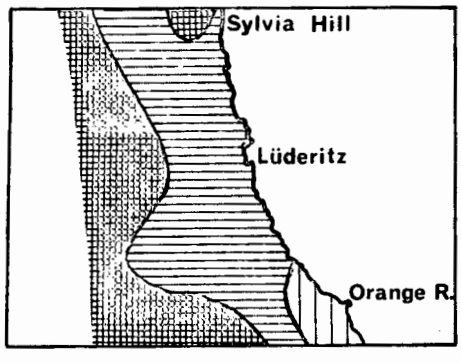

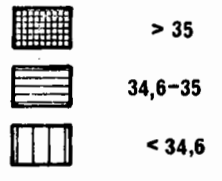

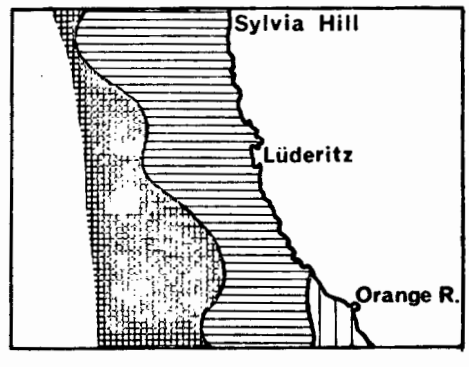

Temperature
(°C)

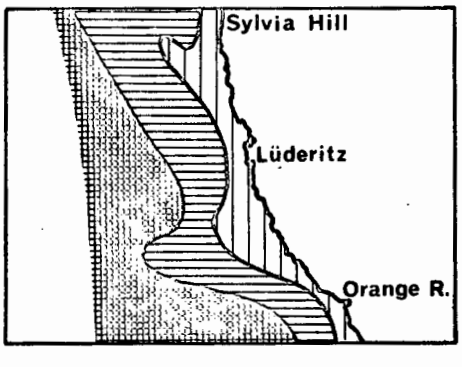

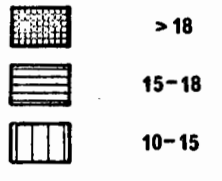

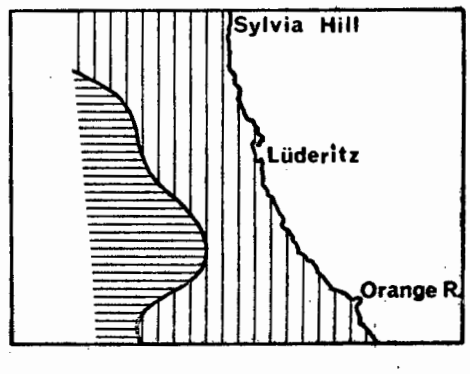

Fig.VIII-3

autumn warms poorly saline upwelled water over the middle shelf off the Orange and over the upper slope off Sylvia Hill. The dilution of the sea by fresh water from the Orange River, particularly after the summer rains, is easily detected (Fig. VIII-1 and VIII-3), along with the poleward intrusion of saline water of the Angola Current near the coast off Sylvia Hill. The persistent tongue of cool, upwelled water leading northwards to the upper slope from Lüderitz (Stander, 1964, p.16) is also well shown in Figures VIII-3 and VIII-1.

4. Non-conservative properties

a. Introduction

Nutrient and oxygen levels fluctuate according to the rates of both consumption by plankton and replenishment by upwelling. They are therefore termed non-conservative properties of sea water. The interplay between nutrient levels, which determine the productivity of the surface water, and oxygen levels which influence the preservation of organic matter is of vital importance in understanding the distribution of bottom sediments on the continental margin.

b. Oxygen

The interface between the oxygen-rich Benguela Current and the oxygen-poor Angola Current fluctuates seasonally with significant consequences for both marine organisms and biogenic sediments. Visser (1970) discusses the formation of an oxygen-minimum layer, which is 850 m thick off the Congo River. Three causes were suggested: 1) oxidation of dead plankton and their excreta (termed "seston" by Hart and Currie, 1960) while sinking through the water column; 2) respiration of oxygen by living plankton; and 3) chemical and bacterial decomposition of organic-rich biogenic sediments.

Oxygen is replenished from the atmosphere at the air-sea interface in the mixed surface layer, and is also produced by phytoplankton via photosynthesis. However plankton-rich water is less transparent to the light required for photosynthesis, thus inhibiting this mode of oxygen replenishment. In addition, the stability of the thermocline helps to conserve the oxygen-poor water within it by hindering vertical mixing (Visser, 1970).

Copenhagen (1953) and Hart and Currie (1960) both correlated periods of calms and of northerly winds with the onset of mass mortalities of marine organisms. Under such conditions both upwelling caused by southerly winds and replenishment of water from the Good Hope Jet (Bang, 1976) cease. The upwelled water contains 5-6 ml O_2/l, whereas the oxygen levels can drop to below 0,5 ml O_2/l in the oxygen-minimum layer (Visser, 1970). Therefore when upwelling ceases to replenish oxygen, and calm conditions inhibit mixing in the surface layer, continuing oxidation of sinking organic detritus, respiration of plankton and decomposition of organic-rich sediments lead to upward expansion of the bottom layer of oxygen-poor

water (Fig. VIII-1). When the layer reaches the surface, mass mortalities of plankton, nekton and birdlife occur. This additional influx of organic detritus accelerates the consumption of oxygen until anaerobic conditions occur, particularly in the interstitial waters of the sediments. Under these circumstances organic matter is not oxidized and accumulates on the sea floor. (The formation of pyrite and gypsum under similar conditions during the Neogene is proposed in Chapter IV.)

Oxygen-deficient water is more extensive off Sylvia Hill than off the Orange River (Figs. VIII-1 and VIII-2) demonstrating the greater influence of the De Decker Current (De Decker, 1970) farther north, and the coastward shift with increasing latitude. The importance of monitoring the De Decker Current is stressed by Bang (1976), who proposed the installation of oxygen-sensing, current-measuring buoys at key positions along the continental margin.

c. Phosphate

The inverse relationship between oxygen and phosphate concentrations is clear in both Figures VIII-1 and VIII-2, but nutrient regeneration in bottom waters over the middle shelf is best illustrated in Figure VIII-2. Both Hart and Currie (1960) and Calvert and Price (1971b) present evidence of recycling of nutrients removed from upwelled water at the surface near the coast and released over the middle shelf on decomposition of the sinking organic detritus. The formation of microsphorite in the organic-rich bottom sediments formed under these conditions is discussed in Chapter V.

C. MICROPLANKTON

Hart and Currie's (1960) data on microplankton have been re-plotted above their respective profiles (Figs. VIII-1 and VIII-2) to facilitate comparison of physical, chemical and biological parameters. The vast numbers of microplankton were plotted on an arithmetic scale to stress the greater importance of the Sylvia Hill region during both seasons (Figs. VIII-1, VIII-2, and VIII-3), and the richness of the coastal waters as opposed to oceanic waters.

Diatoms predominate at most stations (Figs. VIII-1 and VIII-2) particularly towards the coast, whereas dinoflagellates dominate the impoverished flora at a few stations farther offshore. Protozoa, including planktonic foraminifera, occur in relatively small quantities at all stations, particularly off the Orange River, but actual quantities tend to be higher off Sylvia Hill (Hart and Currie, 1960, Tables 14 and 15).

D. SEDIMENT COMPOSITION

1. Calcium carbonate

Birch et al. (1976, Fig. 5) have shown that high concentrations of calcium carbonate blanket the outer shelf and the upper slope off southwestern Africa,

south of 19°S. The 50% isopleth swings towards the coast off Hondeklip Bay (30°S), swings seaward again off Chamais Bay (28°S) and coastwards again at Conception Bay (24°S). Figure VIII-4 illustrates the northward divergence seawards of the carbonate-rich sediments between latitudes 25° and 30°S. On comparing this trend with the surface distribution of temperature, salinity and microplankton (Fig. VIII-3) observed by Hart and Currie (1960) one notes a positive correlation with temperature and salinity and a negative correlation with the abundance of microplankton. The closest correlation, albeit negative, is with the microplankton distribution in autumn after upwelling had subsided. This suggests that the relatively quiescent conditions between periods of active upwelling are most significant in terms of biogenic sedimentation in the study area.

2. Organic carbon

The distribution of organic carbon illustrates better than any other parameter the distinction between organic-rich sediments off southwestern Africa and organic-poor sediments east of Cape Agulhas (Birch et al., 1976, Fig. 6). Within the west-coast sediments there is a general increase in organic carbon towards the north, but the richest patches in a given area tend to lie on the middle shelf. The highest values (>10%) are found on the middle shelf between 21°S (Palgrave Point) and 26°S (Spencer Bay), but most of the sediments are considered organic-rich, other shelf sediments generally containing less than 1% (Emery et al., 1973, p.836).

Between 25° and 30°S (Fig. VIII-5) organic-carbon values are low near the coast, where wave action keeps the water well aerated, thus accelerating the oxidation of organic matter (Marchand, 1928). Inner-shelf sediments are more organic-rich in the north, probably reflecting the quieter wave regime north of Lüderitz (Van Ieperen, 1976). Off the Orange River, values exceed 2% on the middle shelf in a zone midway between wave-agitated waters inshore and the current-swept outer shelf (Bang, 1976). Closer to the coast, but still on the middle shelf, the sediments are diluted by organic-poor terrigenous fines. Lower mud values (Fig. VII-23) on the Orange Banks indicate that the Good Hope Jet (Bang, 1976) may generate a shelf-edge bottom Ekman layer in the region, which helps to concentrate organic detritus on the middle shelf. Below the shelf-break, organic-rich sediments are attributed to shelf-edge upwelling (Bang, 1971). Farther down the slope, sediments are depleted in organic matter due to oxidation while settling through the well-aerated South Atlantic Central Water. Summerhayes (1972) and Birch et al. (1976) also detected downslope reduction in organic-carbon values south of the study area and invoked the same explanation.

The northern half of the region is characterized by anomalously high values of organic carbon, both on the shelf and on the slope (Fig. VIII-5). High values

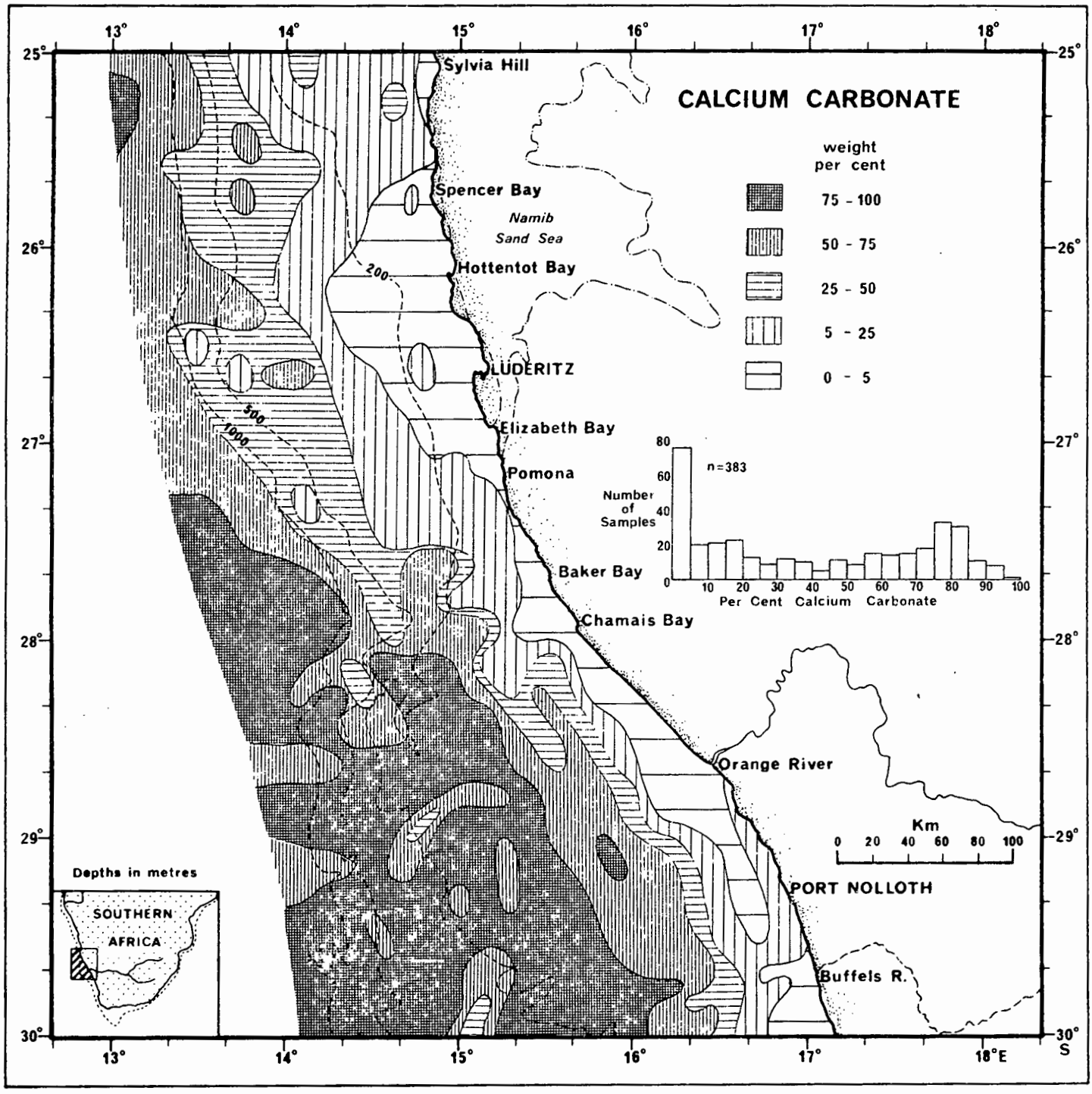
CALCIUM CARBONATE
weight per cent
75 - 100
50 - 75
25 - 50
5 - 25
0 - 5
Sylvia Hill
Spencer Bay
Namib Sand Sea
Hottentot Bay
LÜDERITZ
Elizabeth Bay
Pomona
Baker Bay
Chamais Bay
Orange River
PORT NOLLOTH
Buffels R.
200
500
1000
n=383
Number of Samples
Per Cent Calcium Carbonate
Km
Depths in metres
SOUTHERN AFRICA
13°
14°
15°
16°
17°
18°E
25°
26°
27°
28°
29°
30°S

Fig. VIII-4

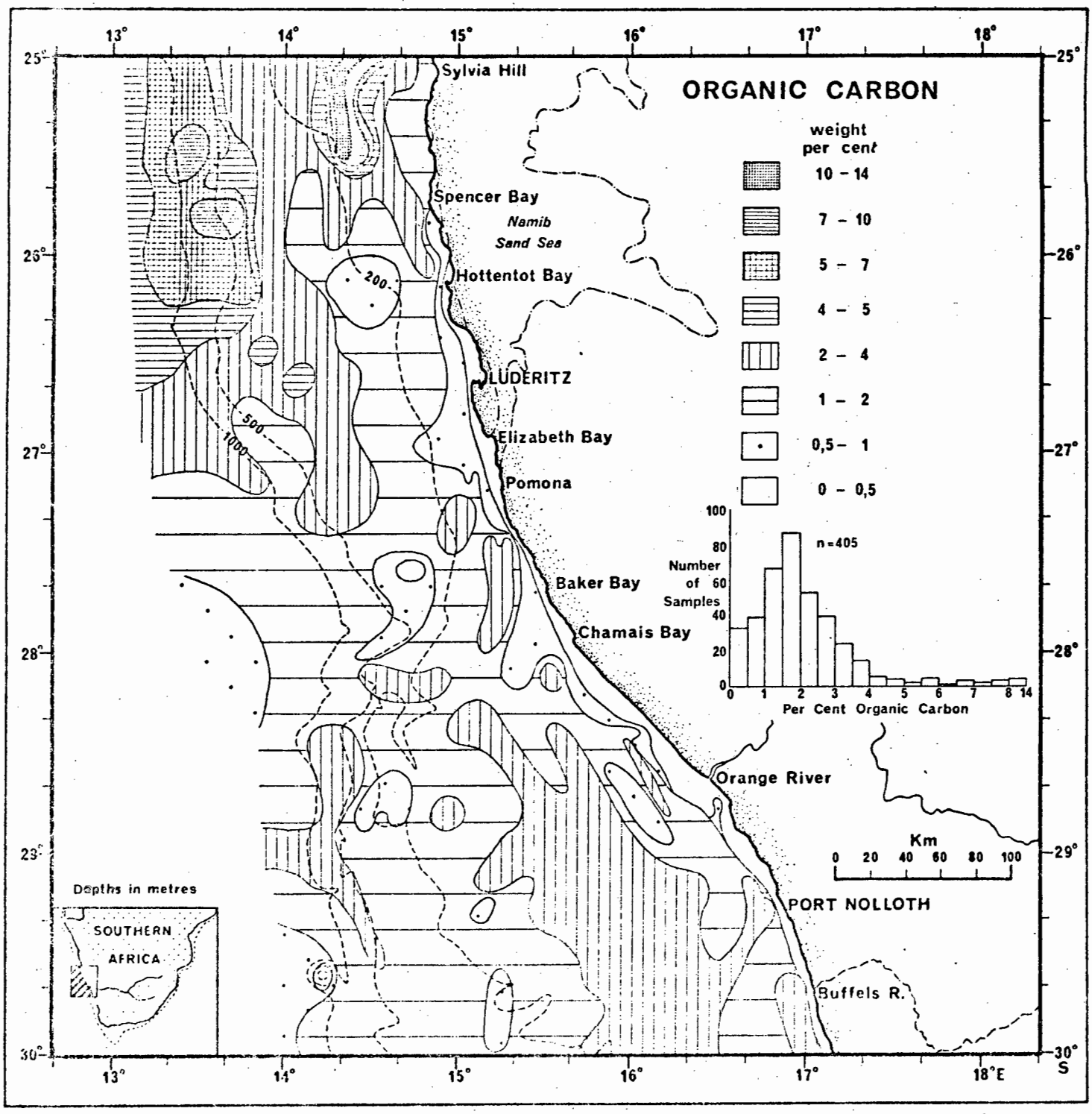
ORGANIC CARBON
weight per cent
10 - 14
7 - 10
5 - 7
4 - 5
2 - 4
1 - 2
0,5 - 1
0 - 0,5
n=405
Number of Samples
Per Cent Organic Carbon
Sylvia Hill
Spencer Bay
Namib Sand Sea
Hottentot Bay
LUDERITZ
Elizabeth Bay
Pomona
Baker Bay
Chamais Bay
Orange River
PORT NOLLOTH
Buffels R.
200
500
1000
Km
0 20 40 60 80 100
Depths in metres
SOUTHERN AFRICA
13° 14° 15° 16° 17° 18°E
25° 26° 27° 28° 29° 30° S

Fig.VIII-5

on the slope are due to the development of oxygen-deficient bottom water as detailed in Section VII-B-3b. Below the shelf break, between latitudes 26°20'S and 24°20'S, there is a zone containing 5-10% organic matter (Bremner, 1974; Birch et al., 1976, Fig. 6). This unusually organic-rich slope deposit is correlated with the periodical development of a major plume of upwelling north of a pivot off the Sperrgebiet Trough Namib (Stander, 1964, p.33), and to vigorous shelf-edge upwelling, illustrated in the salinity profile off Sylvia Hill in autumn (Fig. VIII-1). Relatively low values southwest of Lüderitz across the shelf may be caused by funnelling of the Good Hope Jet's oceanic waters onto the shelf to compensate for upwelling (Bang, 1976).

North of Hottentot Bay (26°S), outer-shelf sediments, although containing 2-4% organic carbon, nevertheless have lower values than those on the slope or the middle shelf, thus continuing the trend observed on the Orange shelf.

The highest values (up to 14%) are found on the middle shelf north of Spencer Bay (Fig. VIII-5) and mark the southern tip of the well-known diatomaceous oozes that extend northwards past Walvis Bay to Palgrave Point (Birch et al., 1976, Fig. 11). The relatively constant upwelling regime off the wind-swept Sperrgebiet Trough Namib continually supplies nutrient-rich water to feed large standing crops of phytoplankton off the Namib Sand Sea, between Lüderitz and Walvis Bay. The phytoplankton are grazed on their seaward edge by zooplankton (Unterüberbacker, 1964; Du Plessis, 1967), and pelagic fish feed over the middle shelf above the boundary between the two plankton zones (Visser et al., 1973). Mass mortalities of both plankton and fish occur, particularly after the spring upwelling season, and are associated with intrusions of warm, saline, oxygen-poor water of the Angola Current (See section VIII-3b).

Restricted suites of mud (<63 micron) and clay (<2 micron) fractions were analysed for organic carbon. Similar patterns were observed to that obtained for the main suite (Fig. VIII-5). The mud data (Fig. VIII-6) emphasized the separation of two zones of organic-rich sediment north of Bogenfels and south of Port Nolloth. The clay data, in contrast, emphasized the lack of organic carbon in both slope- and inner-shelf sediments (Fig. VIII-7). In neither fraction did the fractionation process lead to higher values than those obtained when analyzing the original samples.

Summerhayes (1972, Fig. 71. VIII.4) plotted organic carbon versus silt values for sediments from the Agulhas Bank. He differentiated between terrigenous and biogenic sediments and showed that whereas terrigenous sediments increased their organic carbon content slightly with increasing silt content, biogenic sediments were richest in organic carbon when they contained 30-50% silt. Between latitudes 25° and 30°S on the west coast a similar pattern has been obtained for both clay and silt versus organic carbon (Figs. VIII-8 and VIII-9). The most

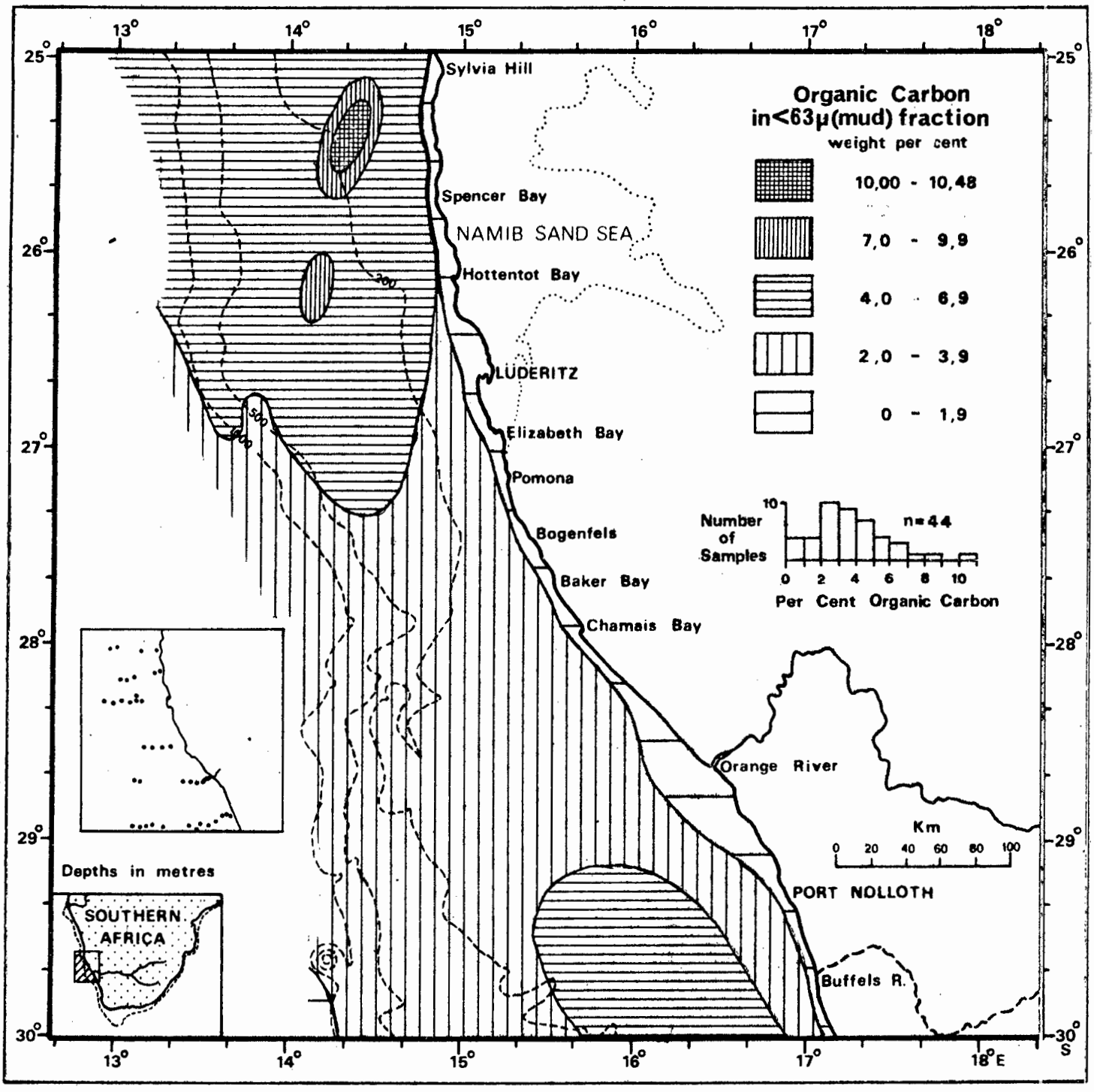
Organic Carbon
in<63μ(mud) fraction
weight per cent
10,00 - 10,48
7,0 - 9,9
4,0 - 6,9
2,0 - 3,9
0 - 1,9
Sylvia Hill
Spencer Bay
NAMIB SAND SEA
Hottentot Bay
LÜDERITZ
Elizabeth Bay
Pomona
Bogenfels
Baker Bay
Chamais Bay
Orange River
PORT NOLLOTH
Buffels R.
Number of Samples
n=44
Per Cent Organic Carbon
Km
Depths in metres
SOUTHERN AFRICA
13°
14°
15°
16°
17°
18°E
25°
26°
27°
28°
29°
30°S

Fig. VIII-6

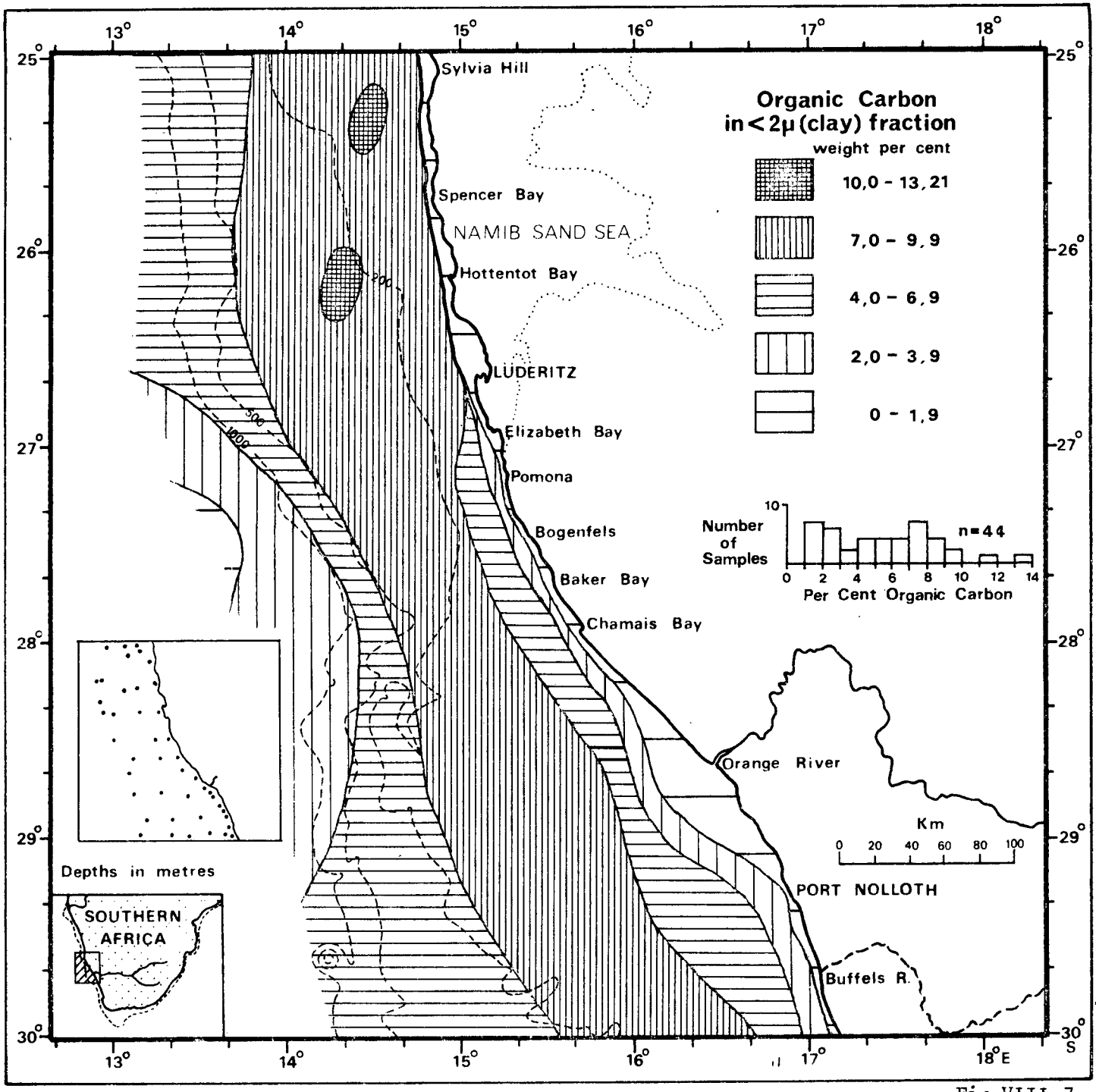
Organic Carbon
in < 2μ (clay) fraction
weight per cent
10,0 - 13,21
7,0 - 9,9
4,0 - 6,9
2,0 - 3,9
0 - 1,9
Sylvia Hill
Spencer Bay
NAMIB SAND SEA
Hottentot Bay
LÜDERITZ
Elizabeth Bay
Pomona
Bogenfels
Baker Bay
Chamais Bay
Orange River
PORT NOLLOTH
Buffels R.
Number of Samples
n=44
Per Cent Organic Carbon
Km
Depths in metres
SOUTHERN AFRICA
13°
14°
15°
16°
17°
18°E
25°
26°
27°
28°
29°
30°S

Fig.VIII-7

ORGANIC CARBON vs SILT

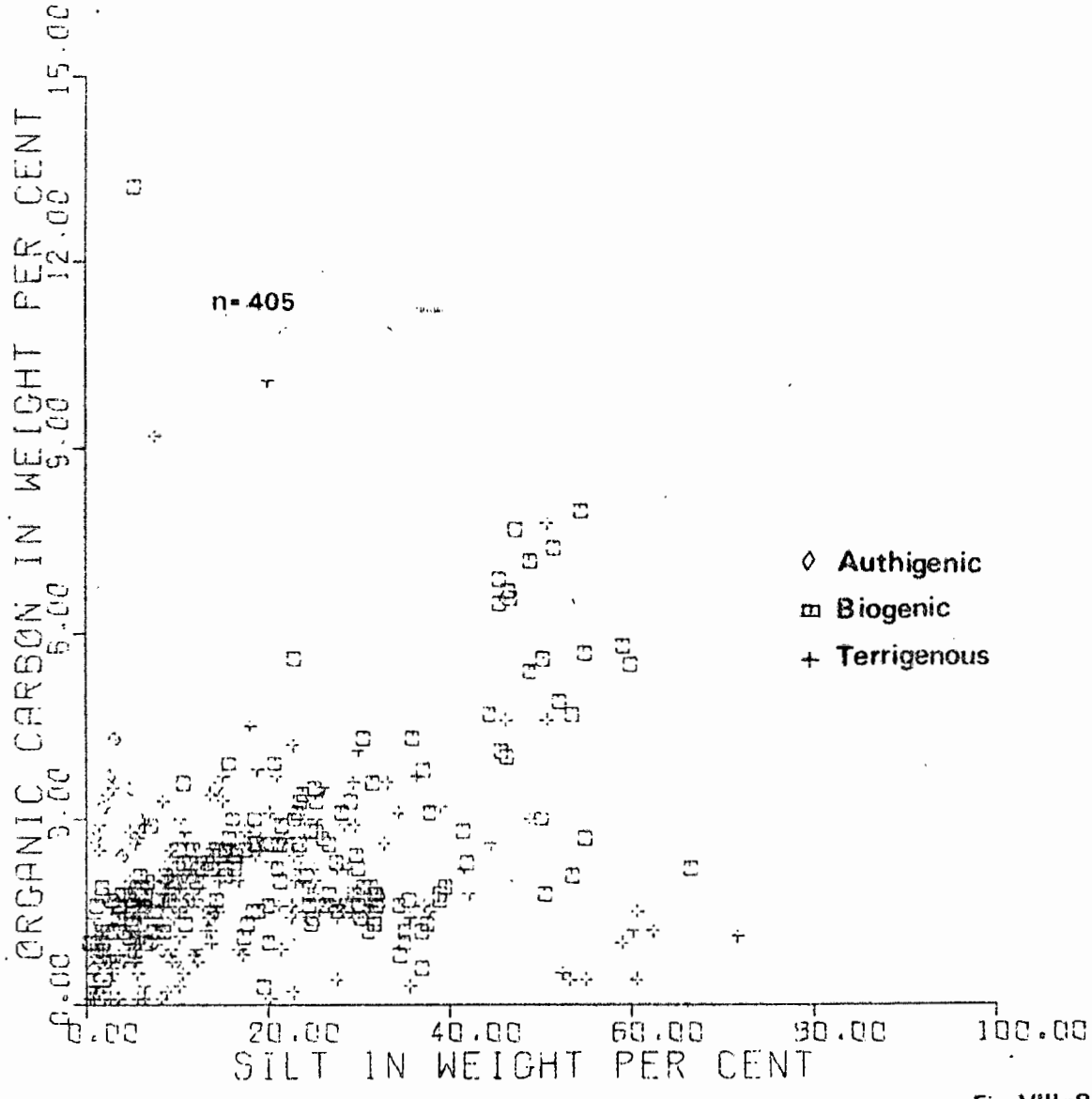

Fig. VIII-8

ORGANIC CARBON vs CLAY

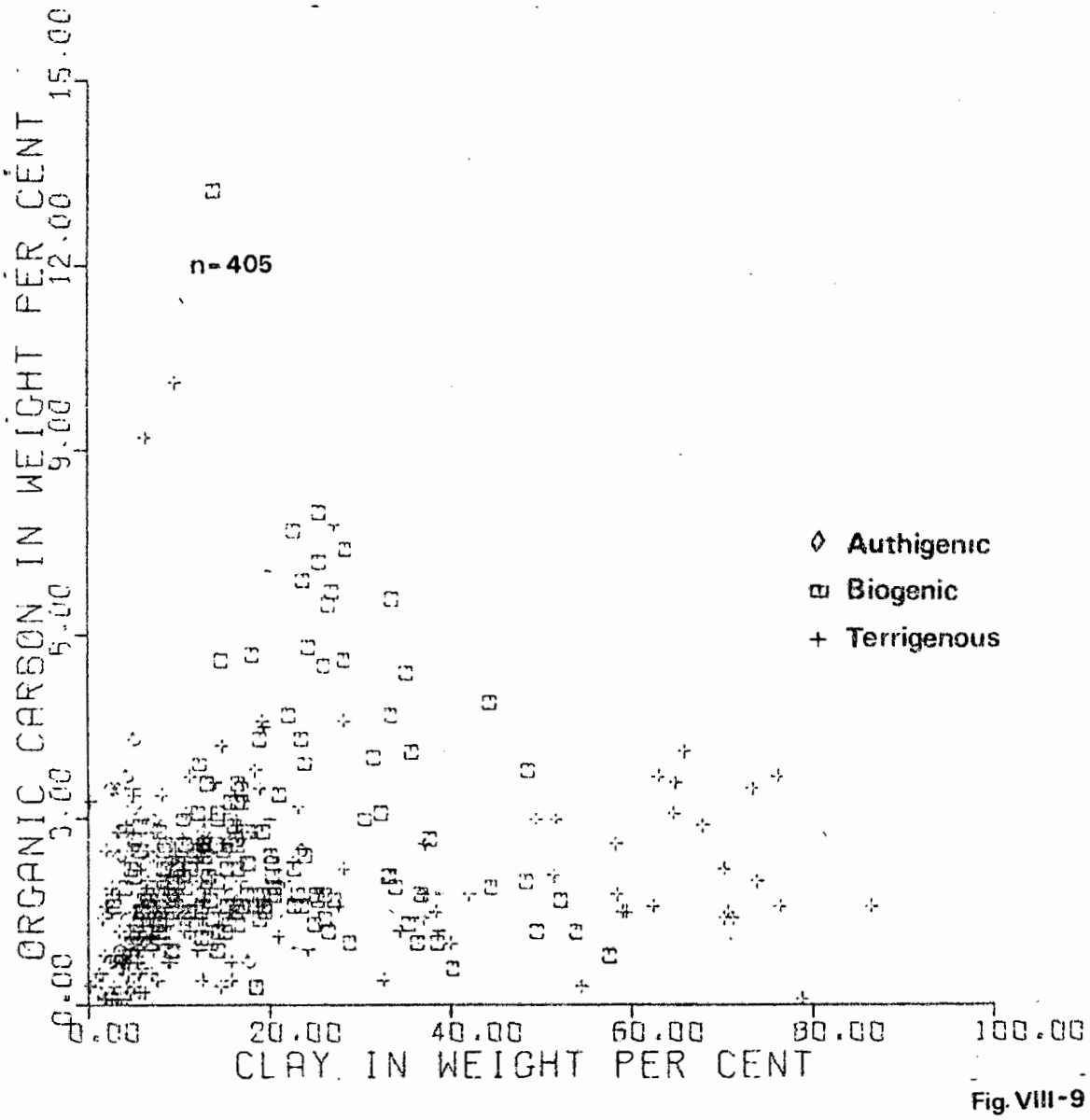

Fig. VIII-9

organic-rich sediments generally contain approximately 50% silt and 25% clay, and are biogenic. The down-slope decrease in organic carbon in biogenic sediments is well illustrated by Fig. VIII-9.

E. BIOGENIC COMPONENTS

1. Introduction

The biogenic components of the sediments have been grouped into plankton, nekton and benthos. Most of the data have been supplied by specialists who have examined representative samples from the area. Only the benthonic foraminifera are being studied intensively (Martin, 1974) and failure to stain subsamples on retrieval has prevented differentiation between the tests of living and dead foraminifera. Only broad trends will therefore be drawn from the present preliminary study of the biogenic components.

2. Plankton

a. Phytoplankton

i). Diatoms. Diatoms were detected in the sand fraction at isolated points in two areas (Fig. VIII-10), in the terrigenous mud belt off the Orange River and in the organic-rich sediments north of Lüderitz. The clay fraction of a sample from the middle-shelf south of Sylvia Hill (25°S) was almost entirely composed of diatom frustules and the silt fraction of both shelf and slope sediments contained frustules.

Eleven samples were sent to Mr. I. Kruger, who is familiar with diatom species encountered in the surface waters off South West Africa. A pilot study was suggested to compare the diatom death-assemblages in the sediments with the known life-assemblages in the water. Five inshore samples ranging in depth from 38 to 110 m, and six offshore samples ranging from 562 to 1495 m were selected for study.

Twelve genera and seventeen species were identified. In general, inshore samples contain more diatoms and a greater variety of species than offshore samples. Sixteen species were identified but only five species are common in inshore samples; three are occasionally abundant.

Actinocyclus ehrenbergii

Coscinodiscus centralis (occasionally abundant)

Coscinodiscus gigas var. praetexta (occasionally abundant)

Fragilaria karsteni

Thalassiosira decipiens (occasionally abundant)

All are known to be indicative of coastal waters (Kruger, 1973, personal communication) and Fragilaria karsteni was also singled out by Hart and Currie (1960, p.248) as such an indicator. Species diversity generally increases south-

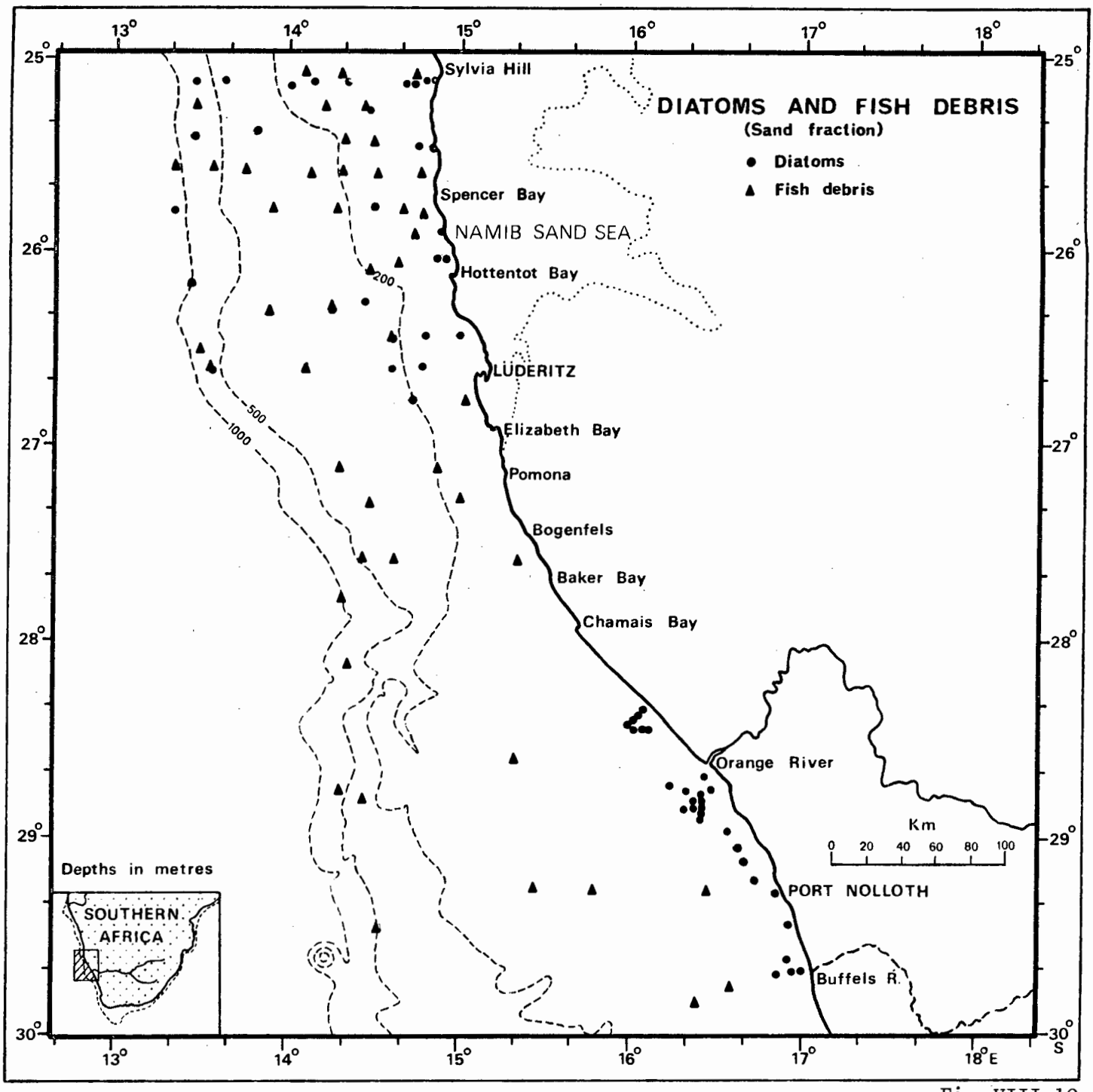
DIATOMS AND FISH DEBRIS
(Sand fraction)
Diatoms
Fish debris
Sylvia Hill
Spencer Bay
NAMIB SAND SEA
Hottentot Bay
LÜDERITZ
Elizabeth Bay
Pomona
Bogenfels
Baker Bay
Chamais Bay
Orange River
PORT NOLLOTH
Buffels R.
200
500
1000
Km
0 20 40 60 80 100
Depths in metres
SOUTHERN AFRICA
13°
14°
15°
16°
17°
18°E
25°
26°
27°
28°
29°
30°S

Fig. VIII-10

wards; six species were found off Sylvia Hill, whereas twelve species were found off the Buffels River.

Offshore samples contained far fewer diatoms than inshore samples, reflecting the relative scarcity of diatoms in the overlying water (Hart and Currie, 1960, p.240). Only six species were identified in the offshore samples; the three most frequently encountered are:

Coscinodiscus centralis

Fragilaria karsteni

Coscinodiscus gigas var. praetexta

These diatoms are commonly found in the inshore samples suggesting that "inshore" conditions extend beyond the shelf break. Hart and Currie (1960, p.240) also suggested that much longer traverses are needed before truly oceanic conditions are reached. In our samples a definitely oceanic species, Rhizosolenia robusta, was found in only one sample. Only four of the seventeen species in the sediments are contained in a list of 95 diatom species published by Hart and Currie (1960, Table 12, p.219). The four species are:

Fragilaria karsteni: Dominant in 11/92 stations. Present in 26/92 stations.

Chaetoceros didymum: Dominant in 9/93 stations. Present in 16/92 stations.

Rhizosolenia robusta: Present in 3/92 stations.

Coscinodiscus gigas: Present in 2/92 stations.

F. karsteni and C. gigas are present in 7/11 sediment samples whereas C. didymum and R. robusta only occur in one sample.

Because so few species are found in the sediments, it is likely that the vast majority of diatoms are dissolved while sinking to the bottom through sea water, which is always undersaturated with respect to amorphous silica (Sverdrup et al., 1942, p.180). Only those diatoms with skeletons robust enough to withstand dissolution are preserved in the sediments. Coscinodiscus gigas var. praetexta is a good example of such a diatom. On the other hand, Hart and Currie (1960, p.246) write of "the outstanding importance of the group Chaetoceraceae in the rich coastal waters during both the seasons studied ..." Despite the fact that the highest concentrations of these diatoms were found beside Sylvia Hill on both surveys of Hart and Currie (Fig. VIII-3), Chaetoceraceae were absent from all sediment samples, except one off the Orange River. The most abundant diatom in the surface water thus appears to be one of the most soluble. Such large-scale solution of silica leads to continual recycling of nutrients in the coastal zone of upwelling as reported by Hart and Currie (1960, p.203) and Calvert and Price (1971, pp.515-520).

ii) Dinoflagellates. Dr. R.J. Davey of ESSO Production Research-European examined eleven samples from two traverses, one off the Orange River and another off Sylvia Hill. His main conclusions (Davey and Rogers, 1975) are that a simple

dinoflagellate-cyst assemblage is dominated by the same two species found on the western Agulhas Bank (Davey, 1971). Spiniferites ramosus var. ramosus found in sediments beneath upwelled water near Cape Hangklip is dominant near the coast off the Orange River and Sylvia Hill. Operculodinium centrocarpum, found beneath the warm Agulhas Current, is dominant beneath warmer offshore water on the west coast. The same two cysts were found by Dr. H. Schalke during pollen analysis of five cores from Rietvlei near Cape Town (Schalke, 1973). The cysts were cited as evidence of a marine transgression in one of the cores.

b. Planktonic foraminifera

Dr. W.G. Siesser undertook a pilot study to compare the species of planktonic foraminifera in surface sediments with the species found in cores from the slope off Cape Town. Sixty-three samples were screened to exclude particles finer than 0,125 mm, i.e. only particles coarser than very fine sand were retained. Counts were made to determine the number of individuals per gram of sediment. Results are shown in Fig. VIII-11. In general, the trends are as expected. Low values ($<10^3$ ind/g) are found in a belt near the coast, the belt widening north of Chamais Bay until it covers the entire shelf off Sylvia Hill. The highest values ($>10^5$ ind/g) lie on the middle Orange shelf seaward of very low values ($<10^3$ ind/g) near the coast and slightly lower values (10^4-10^5 ind/g) offshore. The highest values coincide with foraminiferal sediments rich in organic matter and faecal pellets. Cold upwelled water is rich in nutrients, and a rich crop of phytoplankton is developed. Protozoa, including foraminifera, and radiolaria, are not found near the coast but make their appearance 40 to 50 km offshore in warmer oceanic water (Figs. VIII-1 and VIII-2). Off Walvis Bay it has been established that zooplankton values decrease landwards from a maximum on the middle shelf, whereas phytoplankton values decrease seawards (Unterüberbacker, 1964, Fig. 1; Du Plessis, 1967, Chart 22). The transition zone is where zooplankton graze on phytoplankton (Kruger, 1973, personal communication). Zooplankton faecal pellets (Seston) are common in the water over the Orange middle shelf (Figs. VIII-1 and VIII-2) and can be directly related to abundant grazing zooplankton in a similar transition zone. Because zooplankton faecal pellets accelerate the settling of organic matter (Smayda, 1971) such areas of high surface productivity are underlain by organic-rich foraminiferal sediments.

Semiquantitative counts (Siesser, 1973) of planktonic and benthonic foraminifera were made by Dr. Siesser on sixteen samples from the Orange shelf. All but one sample were from the foraminifera-rich zone. The assemblage comprises four subantarctic, one transitional, seven subtropical, and one tropical species. The subantarctic species Globigerina quinqueloba has the highest mean abundance (about 33%) followed by the two subtropical species Globigerinella aequilateralis (about

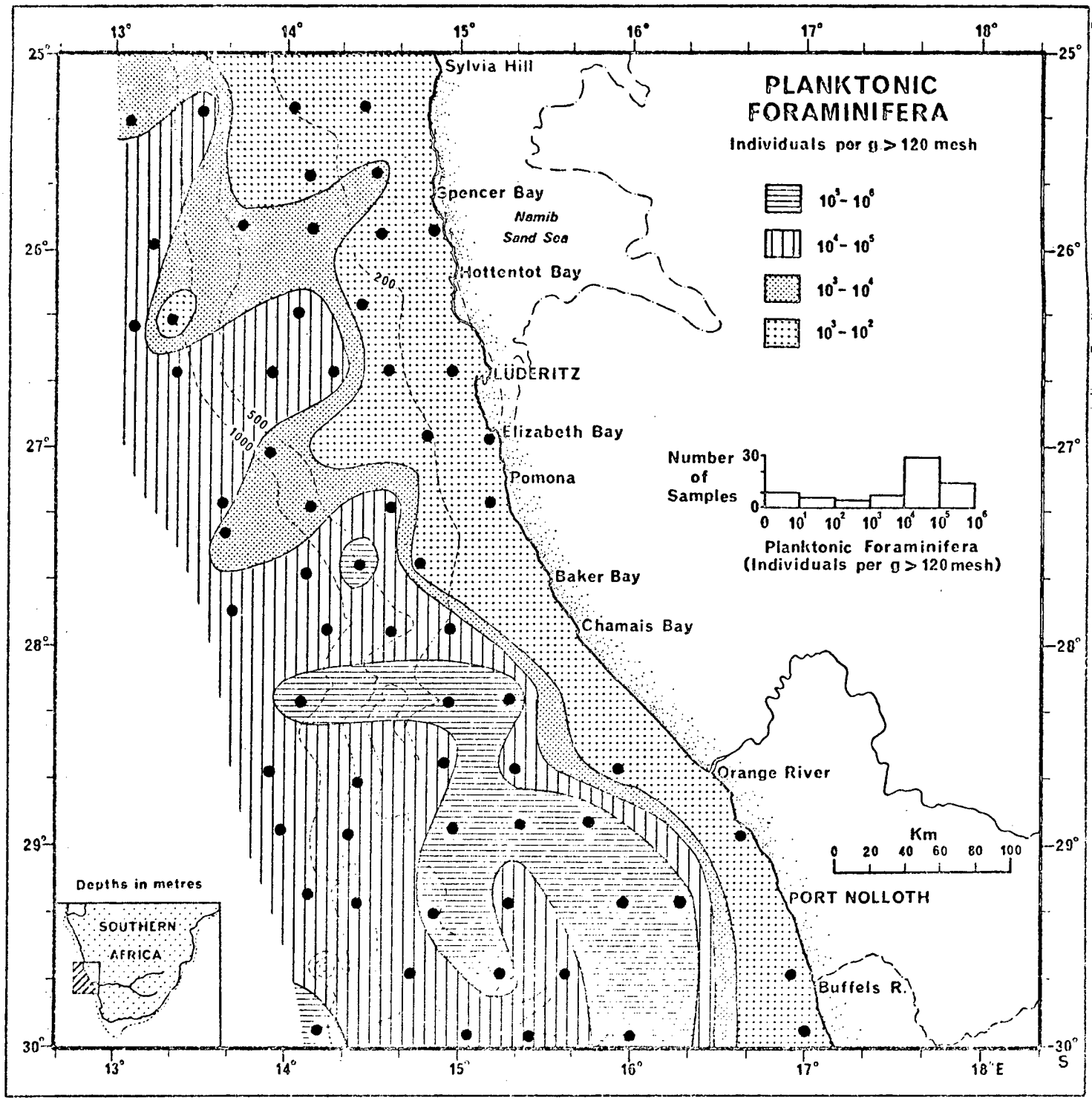
PLANKTONIC FORAMINIFERA
Individuals per g > 120 mesh
10⁵ - 10⁶
10⁴ - 10⁵
10³ - 10⁴
10³ - 10²
Sylvia Hill
Spencer Bay
Namib Sand Sea
Hottentot Bay
LÜDERITZ
Elizabeth Bay
Pomona
Baker Bay
Chamais Bay
Orange River
PORT NOLLOTH
Buffels R.
200
500
1000
Number of Samples
30
0
0 10¹ 10² 10³ 10⁴ 10⁵ 10⁶
Planktonic Foraminifera
(Individuals per g > 120 mesh)
Km
0 20 40 60 80 100
Depths in metres
SOUTHERN AFRICA
13° 14° 15° 16° 17° 18° E
25° 26° 27° 28° 29° 30° S

Fig.VIII-11

16%) and Globoquadrina dutertrei (about 15%), the transitional species Globorotalia inflata (about 13%) and the subantarctic species Globigerina bulloides (about 12%); miscellaneous species made up about 6%.

c. Coccoliths

High mud values on the slope correspond with high carbonate values (Figs. VII-23 and VIII-4). Scanning electron micrographs demonstrate that coccoliths dominate the clay fraction on both the slope and the outer shelf. They are also important constituents of the silt fraction, associated with fragments of foraminiferal tests and occasional coccospheres.

3. Nekton

Swimming organisms in the study area range from pelagic and demersal fish to seabirds, seals and whales. Fish debris is occasionally encountered in the form of rare otoliths on the Orange shelf and more common vertebrae, jawbones, teeth and scales on the Walvis shelf (Fig. VIII-10).

No bird remains were found but the islands of Possession and Ichabo, in particular, are abundantly coated with phosphate-rich guano from birds such as cormorants and gannets. The distribution of seabirds in the study area was mapped by Summerhayes et al. (1974), who found that many species were concentrated up to 150 km out to sea along the shelf break. This distribution was attributed to the offshore divergence belt (Bang, 1971), where shelf-edge upwelling is maintained by the steady, powerful trade winds throughout the year. In contrast, the coastal waters are subject to a seasonally and diurnally variable wind regime and consequently upwelling is a more intermittent process, leading to less reliable food resources for marine avifauna.

A possible seal coprolite was described in Chapter III, but no bones were recovered. No whale bones were found although they are frequently trawled from the shelf off Cape Town and have been dredged from the shelf north of latitude 25°S (Bremner, 1975, personal communication).

4. Benthos

a. Benthonic foraminifera

Visual estimates of the abundance of benthonic foraminifera in the sand fraction of all samples were made and plotted (Fig. VIII-12). Tests were observed in all samples except those from the Orange River delta. South of Port Nolloth (29°20'S) tests were also observed in the terrigenous mud belt, presumably under conditions of slower sedimentation. Highest concentrations were confined to patches on the middle and outer shelf, but this distribution is probably controlled landwards by terrigenous dilution and seawards by deposition of the debris of planktonic foraminifera and coccoliths (cf. Siesser, 1972b for Agulhas Bank components).

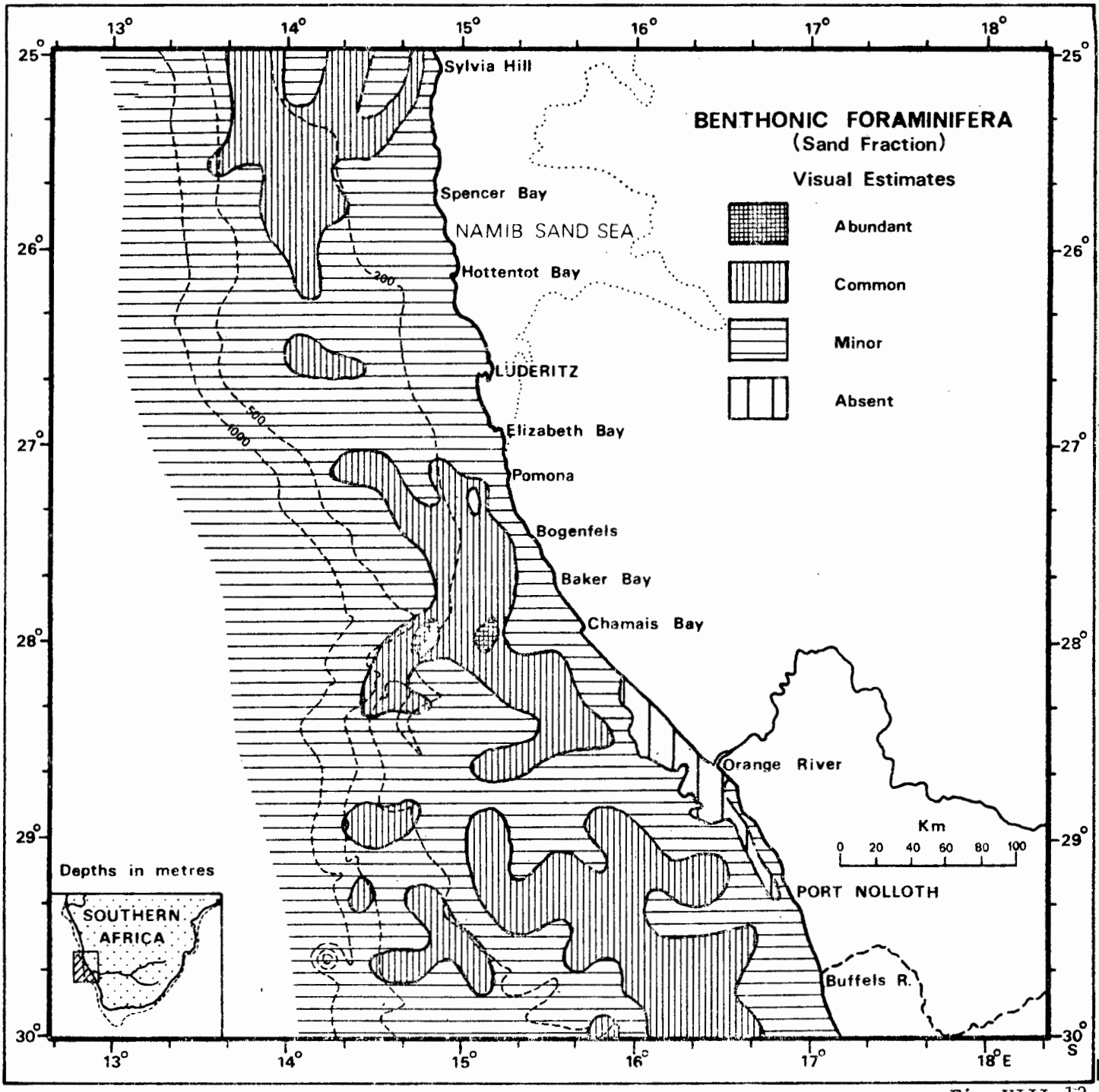
BENTHONIC FORAMINIFERA
(Sand Fraction)
Visual Estimates
Abundant
Common
Minor
Absent
Sylvia Hill
Spencer Bay
NAMIB SAND SEA
Hottentot Bay
LÜDERITZ
Elizabeth Bay
Pomona
Bogenfels
Baker Bay
Chamais Bay
Orange River
PORT NOLLOTH
Buffels R.
200
500
1000
Km
0 20 40 60 80 100
Depths in metres
SOUTHERN AFRICA
13°
14°
15°
16°
17°
18°E
25°
26°
27°
28°
29°
30°S

Fig. VIII-12

During coarse-fraction component analysis benthonic foraminifera were generally most abundant in the medium-sand fraction (Figs. V-3 to V-8) but were commonly found also in the fine and coarse-sand fractions. Only along the Knoll-Point profile ($25^{o}30'S$) were benthonic foraminifera, chiefly Bolivina, abundant in the very-fine-sand fraction of the organic-rich sediments on the middle shelf.

Martin (1974) identified 104 species from 57 genera in 67 samples from the study area. Five depth zones were tentatively proposed (Table VIII-1).

TABLE VIII-1

Depth zones of benthonic foraminifera

(Martin, 1974)

Zone	Depth range (m)	Bathymetric zone
1	0-40/50	Inner shelf
2	40/50-120	Inner shelf
3	120-420	Middle to outer shelf
4	420-900	Upper slope
5	900	Middle slope

In Zone 1 limited numbers of a few species were found on the rocky nearshore part of the inner shelf. Ammonia beccarii, Pararotalia sp. and Discammina sp. were most abundant. Zone 2 occupies the outer section of the inner shelf, which is largely covered with terrigenous mud from the Orange River. Elphidium advenum is abundant throughout the zone, but Florilus boueanum becomes less abundant with depth and may be averse to the mud substrate. Elphidium advenum remains important in Zone 3 across the middle shelf to about 350 m on the outer shelf but Cassidulina laevigata v. carinata and Uvigerina perigrina are the major contributors. In sandy facies Quinqueloculina agglutinans is a major component. The upper slope in Zone 4 is characterized by Bulimina marginata, B. inflata and B. alazanensis, and Brizalina spathulata and Uvigerina canariensis become important. Zone 5, on the middle slope is poor in numbers but rich in large specimens of Dentalina filiformis, Pyrgo serrata, P. murrhina, Martinotiella communis, Vaginulina spinigera and Karreriella bradyii.

The distribution of benthonic foraminifera (Fig. VIII-12) corresponds in broad terms to that for organic carbon (Fig. VIII-5). Wave action hinders the development of benthic communities near the coast. On the other hand, low temperatures, reduced food supply and high pressures limit numbers on the slope, but the stable conditions encourage the growth of numerous species. Enhanced organic-carbon values on the middle and outer shelf combine with favourable physical conditions to stimulate the growth of benthic communities.

Badly abraded foraminifera, particularly the shallow-water Ammonia beccarii, are found well beyond their optimal depth range of 0-50 m. A Late Tertiary regression is suggested to explain their anomalous distribution (Dingle, 1973a).

b. Molluscs

North of Hottentot Bay, gravelly sand and sandy gravel are common on the shelf (Fig. VII-20). Unbroken mollusc shells are the chief components of this gravel (Fig. VIII-13) and identifications have been made by Drs. A.J. Tankard and B.F. Kensley of the South African Museum and by Mr. A.J. Carrington of the Anglo-American Corporation of South Africa.

Ten species of bivalves, eight species of gastropods, and three species of brachiopods were identified. These are listed in separate groups in order of the frequency of their presence in the 53 samples examined e.g. Lucinoma capensis (26) was identified in 26 of the 53 samples. The regional distribution of the four species encountered most frequently is illustrated in Figure VIII-14.

BIVALVES

Lucinoma capensis (26)
Dosinia lupinus (15)
Carditella similis (9)
Limopsis chuni (7)
Tellina cf. gilchristi (4)
Palliolum vitreum (3)
Pitar (lamelliconcha) callicomatus (2)
Aulacomya ater (1)
Macoma ordinaria (1)
Ostrea sp. (1)

GASTROPODS

Nassarius analogica (16)
Turritella declivis (4)
Volutacorbis abyssicola (3)
Argobuccinum argus (2)
Ancilla bulloides (1)
Natica saldontiana (1)
Conus gradatulus (1)

BRACHIOPODS

Discinisca tenuis (3)
Kraussina rubra (3)
Terebratulina cf. abyssicola (1)

Geographically, most of the shells are located on the middle and outer shelf, north of Hottentot Bay. One of the richest assemblages was found in sample 3224 from the shelf break (215 m) off Sylvia Hill. Among the shells were Aulacomya ater, Ostrea sp., and Argobuccinum argus, all extant species which today live in the subtidal zone (Carrington and Tankard, 1973, personal communications). Another shell from the same assemblage was Pitar (lamelliconcha) callicomatus which has

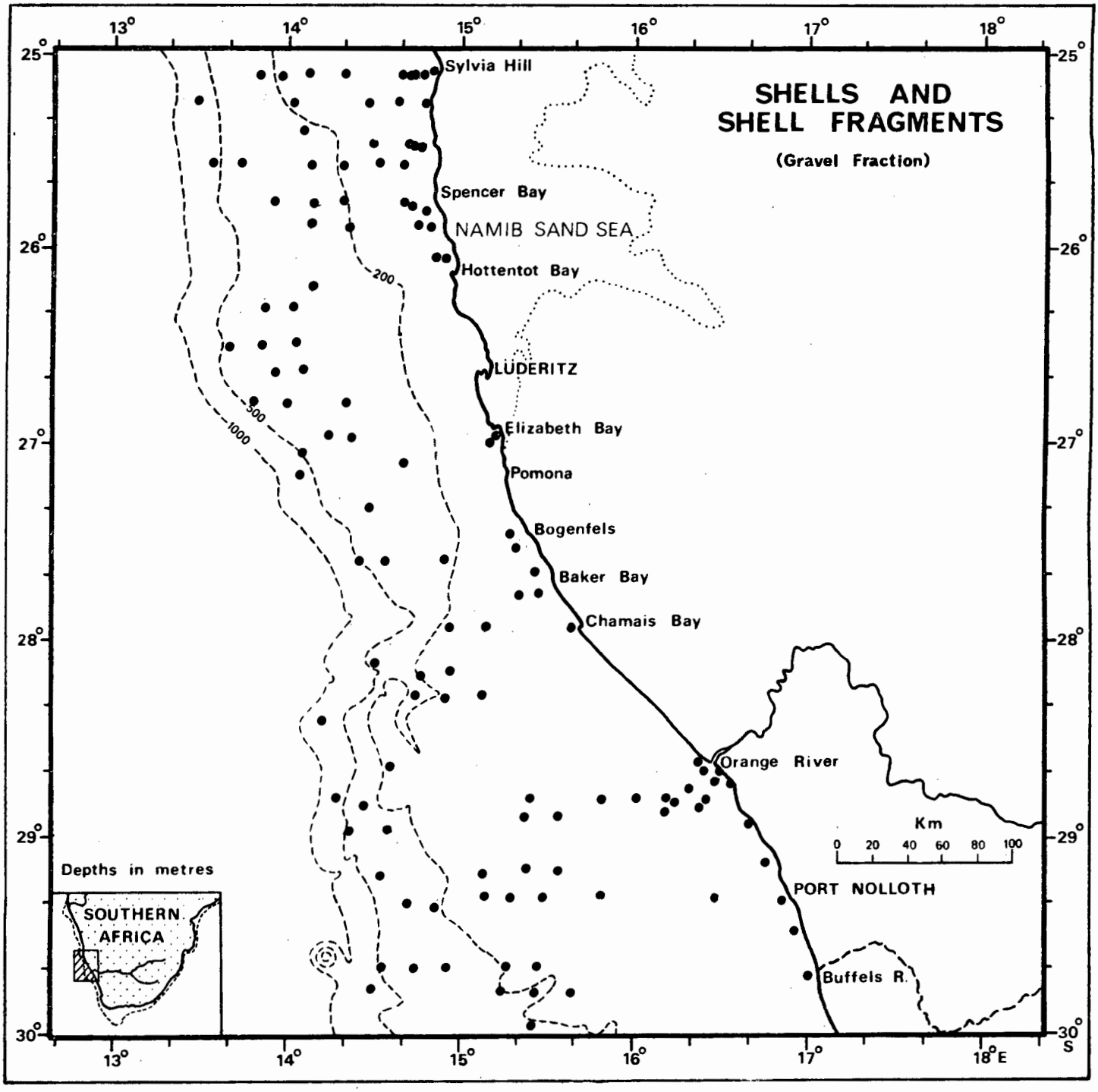
SHELLS AND
SHELL FRAGMENTS
(Gravel Fraction)
Sylvia Hill
Spencer Bay
NAMIB SAND SEA
Hottentot Bay
LÜDERITZ
Elizabeth Bay
Pomona
Bogenfels
Baker Bay
Chamais Bay
Orange River
PORT NOLLOTH
Buffels R.
200
500
1000
Km
0 20 40 60 80 100
Depths in metres
SOUTHERN AFRICA
13°
14°
15°
16°
17°
18°E
25°
26°
27°
28°
29°
30°S

Fig.VIII-13

MOLLUSC SPECIES

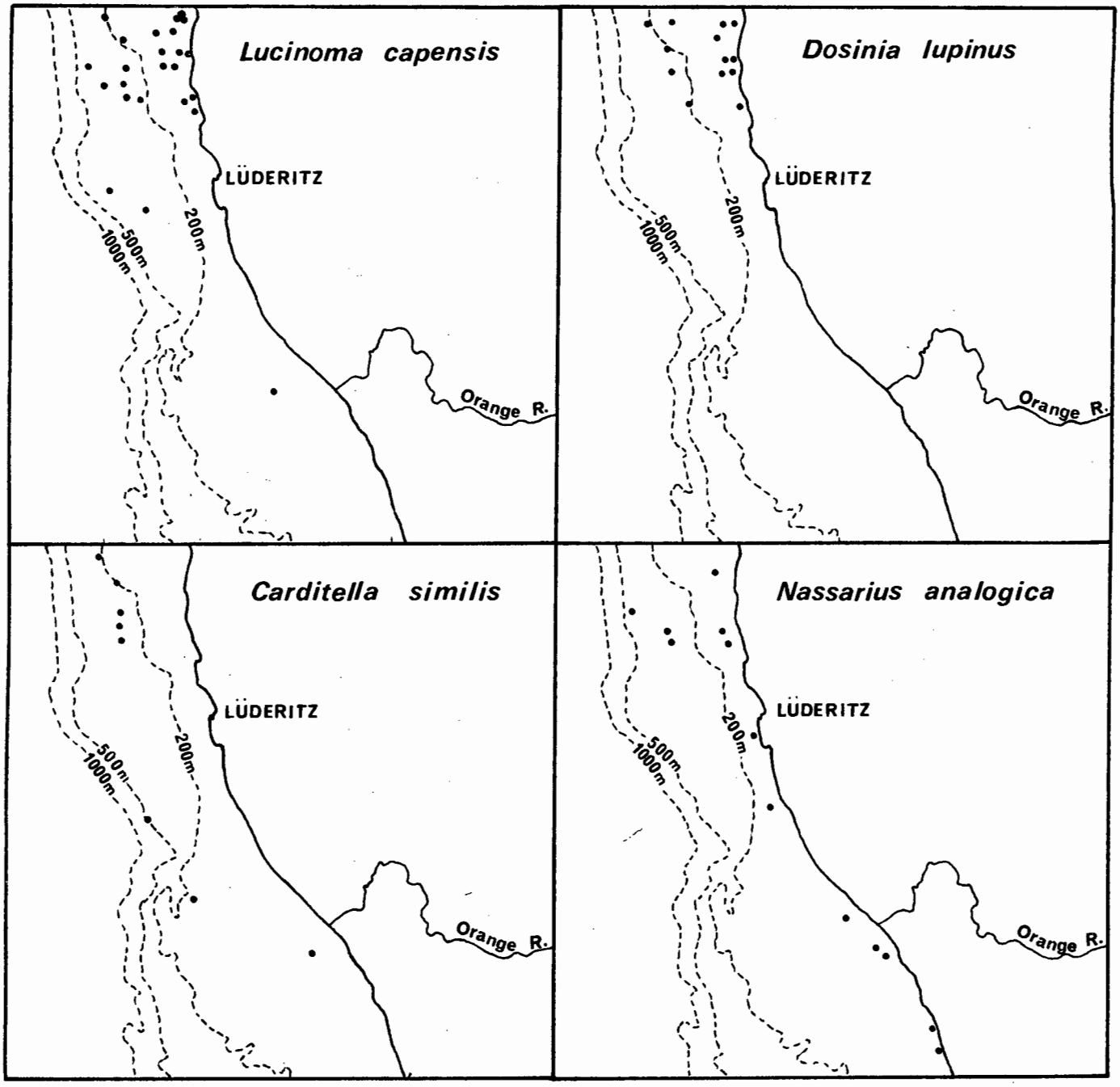

Fig.VIII-14

not previously been recorded from South West African waters. Rare living specimens have only been recorded from the East Pacific coast between Mexico and Ecuador in depths of 26 to 73 m (Kensley, 1973, personal communication). Little is known about the depth ranges, time spans, and environments of some of the listed molluscs. However, Tankard and Carrington are of the opinion that assemblages from outer shelf sediments (e.g. 3224) are of shallow-water origin. Because all the species are extant, and because few are found as far back as the Tertiary, it is suggested that the shell beds on the outer shelf developed during a late Tertiary regression postulated by Dingle (1973a, p.355).

Near the coast, brachiopods attached to dredged rock samples are all Recent as are specimens of the small gastropod Nassarius analogica associated with the mud belt off the Orange River. The delicate, small lamellibranchs Palliolum vitreum and Carditella similis are the only unbroken molluscs found so far on the Orange Banks.

c. Ostracodes

Dingle (1973, personal communication) determined that ostracodes were present in small numbers but no detailed work has been attempted to date.

d. Faecal pellets

The distribution of faecal pellets (Fig. VIII-15) closely parallels that of organic carbon. Structureless, dark brown, ovoid faecal pellets are typically very-fine-sand size on the middle shelf and are relatively rare off the mouth of the Orange River. They increase in concentration south of the Orange River in the belt of terrigenous mud until off the Olifants River over 90% of the sediment is composed of faecal pellets (Birch, 1975). A steady southward decline in sedimentation rate is suggested to account for the steady increase in faecal pellet abundance. As off Cape Agulhas (Rogers, 1971) polychaete worms are invoked to account for the pellets because Christie (1972, personal communication) found large numbers of the worms in terrigenous mud off Lambert's Bay (32^{o}S).

Larger, more friable, medium-sand-size faecal pellets composed of carbonate detritus are distinctive components of the organic-rich sediment below the shelf break north of Lüderitz. Polychaete worms are again suggested to explain the presence of the pellets, which are a feature of the outer shelf and the upper slope as far north as the Walvis Ridge (Bremner, 1975a). The worms are probably confined to this section of the continental margin because nowhere else are slope and upper-shelf sediments so rich in organic detritus.

E. CONCLUSIONS

The data presented above suggest that most of the continental margin seaward of the inner shelf is rich in biogenic detritus, which reflect the periodic occurr-

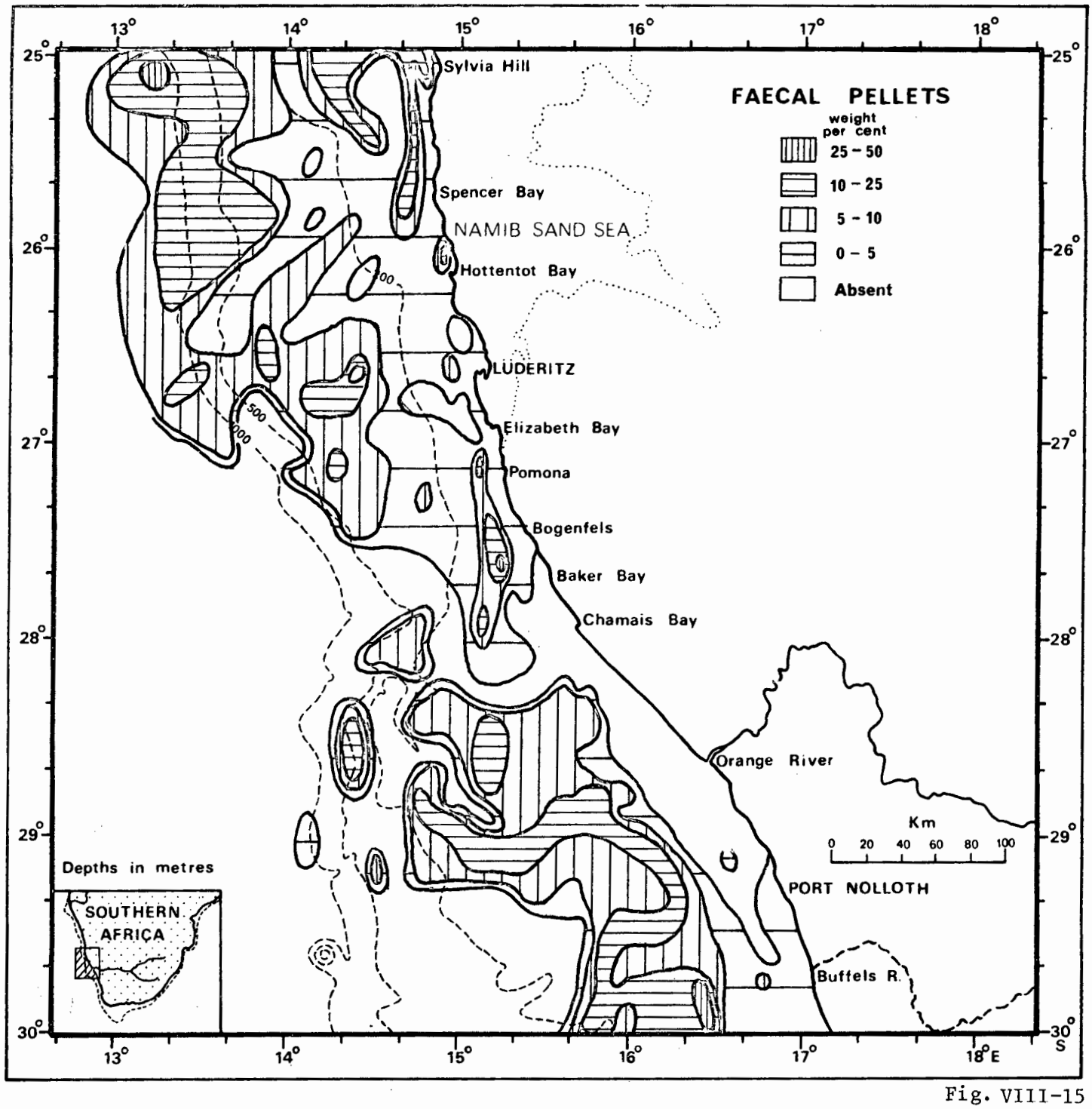
FAECAL PELLETS
weight per cent
25 – 50
10 – 25
5 – 10
0 – 5
Absent
Sylvia Hill
Spencer Bay
NAMIB SAND SEA
Hottentot Bay
LÜDERITZ
Elizabeth Bay
Pomona
Bogenfels
Baker Bay
Chamais Bay
Orange River
PORT NOLLOTH
Buffels R.
Km
0 20 40 60 80 100
Depths in metres
SOUTHERN AFRICA
100
500
1000
13°
14°
15°
16°
17°
18°
18°E
25°
26°
27°
28°
29°
30°
S

Fig. VIII-15

ence of quiescent conditions following intense periods of upwelling. A sharp distinction, however, is drawn between the sediments on the Orange shelf, where nutrient-rich, poorly saline water is warmed by solar insol tion, and the colder waters over the Walvis shelf. According to Sverdrup et al. (1942), solar radiation reaches a world maximum at 30° latitude off Namaqualand, which may explain why planktonic foraminifera can thrive and dominate the sediments seaward of the Orange inner shelf. The surface waters are warm enough but not too low in salinity for these organisms to thrive. This favourable environment is created by a combination, then, of topographically induced upwelling and solar warming of surface waters.

The Walvis shelf is extraordinarily rich in biogenic detritus, but in the study area the intensity of the wind-accelerated upwelling off the Sperrgebiet Trough Namib and the lower intensity of solar radiation maintains much cooler water over most of the shelf, thus forcing the planktonic foraminifera seawards over the continental slope. The decline in intensity of upwelling north of the study area and the increasing influence of the warm Angola Current allows the foraminifera to move back over the shelf, as reflected in the carbonate content of the sediments (Bremner, 1974). The unstable conditions on the fluctuating northern boundary of the Benguela Current System are reflected in a belt of the most organic-rich sediments in the world. The biogenic sediments are therefore considered to be valuable indicators of the long-term oceanographic regime in the region.

CHAPTER IX

CONCLUSIONS

A. MESOZOIC SEDIMENTATION

The study area lies off the Orange River and the Namib Desert, between latitudes 25° and 30°S. The shelf was chiefly constructed during the Cretaceous, when the chief source, presumably the Orange River, was located between latitudes 32° and 33°S, well south of its present position (28°40'S). (Emery et al., 1975). During the Early Cretaceous the depositional basin was restricted to the west by South America and to the south by the Falkland Plateau, so that any wave-driven dispersal system would have been much weaker than that prevailing today. The combination of a wet climate, widespread distribution of Karoo sediments and a newly lowered base-level led to an outpouring of terrigenous sediment into the sea and the creation of a river-dominated, possibly partly subaerial, delta of Mississippian proportions.

B. NEOGENE SEDIMENTATION

By the end of the Cretaceous the Orange River appears to have reached its present position, possibly as a result of crustal warping in its catchment. Its present channel gives evidence of an original meandering course across flat-lying Karoo sediments, such as those underlying the Upper Orange and the Upper Vaal Rivers today. At least two periods of uplift caused the river to incise its meanders through the Karoo sediments in the Middle and Lower Orange to the underlying Precambrian rocks (De Villiers and Söhnge, 1959). In places the river re-excavated valleys in the pre-Karoo topography, but in others it cut across the structural grain of the Precambrian sequences. The gentler slopes of the valley (De Villiers and Söhnge, 1959) cut during the earlier period of uplift indicate a wetter, possibly more tropical climate, probably during the Early Tertiary, after which offshore deposition declined (Emery et al., 1975). Uplift at the end of the Tertiary led to the incision during the Quaternary of the precipitous gorge of the Lower Orange, as well as that of the Fish River Canyon (Haughton, 1927; Simpson and Davies, 1957). The steeper valley slopes are attributed to aridification of the lower reaches of the Orange River system, as a result of the initiation and northward migration of the Benguela Current and the Namib Desert since the Early Tertiary (Van Zinderen Bakker, 1976). During interpluvials, such as that of today, the lower reaches of the Orange River system received little water from tributaries, so that incision progresses intermittently during floods derived from the headwaters, which are far upstream and subject to a wetter climate.

C. BATHYMETRY

The continental margin is divided into the Orange shelf, which is up to 100 km wide and 200 m deep, the Walvis shelf, which is up to 80 km wide and 400 m deep, and a transitional zone off Chamais Bay ($28^{o}S$), which is only 40 km wide. The inner shelf is defined as the area underlain by Precambrian rocks, which is usually within 10 km of the coast and shallower than -100 m. The coastal outline along the edge of the inner shelf is intimately related to lithological variations in Precambrian bedrock. The offshore edge appears to be relatively uniform as far as latitude $26^{o}S$, where Precambrian Damara sediments underlie a wider, more gently sloping inner shelf.

D. PETROGRAPHY OF POST-PALAEOZOIC BEDROCK

The middle shelf, south of the Orange River, is underlain by relatively steeply dipping beds of ferruginous sandstone and mudstone, which form scarps on the sea floor. North of the Orange River, similar scarps on the middle shelf are composed of petrographically homogeneous quartzose lime wackestones. On seismic evidence the unfossiliferous sandstones are thought to be Cretaceous and are tentatively correlated with ferruginous Pomona beds onshore, which are considered to be Cretaceous. The poorly fossiliferous limestones are tentatively dated as Palaeogene by analogy with an identical lithofacies on the Agulhas Bank.

The outer shelf is generally underlain by relatively flat-lying Neogene strata, which cap a much thicker succession of more steeply dipping Cretaceous and Palaeogene strata. Samples of semi-consolidated clay from the Walvis shelf have been dated as Neogene using nannofossils, and nummulitic limestones from the Orange Banks have been assigned an Upper Middle Miocene age. Overlying conglomeratic phosphorites are thus no older than Upper Miocene. Undated quartz-free algal limestones cap the Tripp Seamount and the Orange Banks, in the similar depth ranges of 150-200 m.

E. NEOGENE, AUTHIGENIC GYPSUM AND PYRITE

Two samples of Neogene semi-consolidated clays from the upper slope off Lüderitz contain pyritized worm tubes, sometimes enclosed by euhedral crystals of gypsum. A Late-Pliocene/Early-Pleistocene regression is invoked to shift anaerobic conditions from the middle shelf to the upper slope. Pyrite forms by combining terrigenous adsorbed iron with sulphur released by anaerobic bacteria from the reduction of sea-water sulphate. Gypsum is formed once the solubility product of calcium and sulphate is exceeded. Calcium is provided by the dissolution of planktonic foraminiferal tests, and sulphate is a dissolved constituent of sea water.

F. RESIDUAL PHOSPHORITE PELLETS

The outer shelf north of latitude 26°S is unusual in that the bedrock strata have steeper dips than those underlying the outer shelf farther south. The surficial sediment in the area is phosphorite pellets derived from pelletal phosphorite bedrock. The pellets within the bedrock were probably formed of microsphorite (microcrystalline phosphorite) in unconsolidated laminae in Miocene diatomaceous oozes. Pellet formation occurred during a Late-Miocene regression, which concentrated the pellets as a lag deposit. The succeeding Pliocene transgression deposited matrix material less organic-rich than the original microsphorite. The resultant pelletal phosphorite was then subject to a Late-Pliocene regression, which eroded the pellets out of the bedrock to form, for the second time, a lag deposit of phosphorite pellets.

G. RESIDUAL GLAUCONITE

Although phosphorite and glauconite sands often occur in the same deposits elsewhere on the continental margin, the two minerals are concentrated in separate regions in the study area. Glauconite is concentrated in three main belts cutting diagonally across the Walvis shelf, the richest deposit being located on the Lüderitz Bank on the middle shelf north of Lüderitz.

H. RESIDUAL QUARTZ

Very fine residual quartz sands on the middle and outer Walvis Shelf are derived from semi-consolidated Neogene clays and possibly also from quartzose lime wackestones. Coarse quartz sand on the middle shelf south of the Orange River was eroded from unfossiliferous littoral sandstones of ?Palaeogene age.

I. QUATERNARY CLIMATIC FLUCTUATIONS

The effect of Quaternary climatic fluctuations on sedimentary processes along the west coast and its hinterland is reviewed. There is evidence that the climatic zones on average lay farther south than today, at the beginning of the Pleistocene, so that pluvials were caused by high-intensity summer rainfall during interglacials. By the Late Pleistocene, pluvials were associated with glacials, which brought low-intensity winter-rainfall to the catchment of the Orange River, in particular. The northern edge of the Namib Desert may have oscillated during the same period from an Early Pleistocene interglacial position in the Saldanha region to beyond the mouth of the Congo River during Late Pleistocene glacials. Evidence of Late-Pleistocene glacio-eustatic regressions is supplied by river channels incised to -100 m where submerged beaches have also been found. Transgressions are recorded by infilled river channels, raised beaches, and complex sequences of stabilized coastal dunes.

J. RECENT TERRIGENOUS SEDIMENTATION

The bulk of the terrigenous sediment reaching the coast today is derived from friable Karoo sediments in the catchment of the Upper Orange River. The sediment is delivered, chiefly in suspension, to the coast in summer, where it is fractionated and then dispersed both up and down the coast. A powerful littoral drift carries the river's bedload along the beaches north of the Orange River. Violent gales then deflate a series of south-facing beaches between Chamais Bay (28°S) and Elizabeth Bay (27°S). Various trains of barchan dunes formed from sand blown off the beaches coalesce near Lüderitz (26°40'S) at the southern end of the Namib Sand Sea. The seaward edge of the Sand Sea is eroded by wave action, thereby feeding sand back into the littoral zone to nourish the four cuspate forelands between latitude 25°S and Walvis Bay (23°S).

Back at the mouth of the Orange River, the river's suspended load is deposited on a wave-dominated submarine delta. Very fine sand characterizes the delta front between 0 and approximately -40 m; clayey silt and then silty clay are found on the prodelta between -40 and -120 m. Afternoon southerly gales generate northerly currents, which carry the summer floodwaters north of the mouth until the wind drops in the evening. At night and in the morning a weak counter-current is able to move undeposited sediment back towards the mouth. In winter during periods of low discharge the wind system is weak, thus allowing the counter-current to transport sediment southwards as far as St Helena Bay (33°S). The result is a thick deposit, up to 70 m thick, of clayey silt north of the Orange, and 10 m of silty clay in a long, narrow belt south of the river.

K. RECENT BIOGENIC SEDIMENTATION

The deposition of biogenic sediment is largely controlled by the Benguela Current. Rich deposits of planktonic foraminifera from the slope to the middle shelf indicate that upwelling is an inner-shelf phenomenon off the Orange. In contrast, off Lüderitz, foraminiferal sediments are confined to the slope and the outer Walvis shelf. This distribution coincides with the development of the major plume of upwelling north of the peak-wind region between Pomona and Bogenfels (27-28°S). North of 27°S the winds, although seasonally still powerful, steadily decline in strength. At the same time the well-oxygenated northward-moving, nutrient-rich upwelled water begins to interact with oxygen-depleted, southward-moving water from the Oxygen Minimum Layer extending south from the equator. The interaction causes the death, at intervals, of vast numbers of phytoplankton. Their debris form the most organic-rich belt of diatomaceous oozes in the world, stretching from latitude 26°S in the study area to beyond Walvis Bay, where it forms a deposit over 10 m thick, on the middle shelf.

REFERENCES

ACOCKS,J.P.H. 1953. The veld types of South Africa. Mem.bot.Surv.S.Afr.28:1-192.

ADAMSON,G.D. 1922. Possibilities of irrigation in the lower reaches of the Orange River. S.Afr.Irrigation Mag. 1(3):225-229.

AHMED,A.A-M. 1968. Geochemical and mineralogical studies of sediments from the south-west African shelf. Unpubl.M.Phil. thesis, Univ.London.

ALLEN,J.R.L. 1964. The Nigerian continental margin: bottom sediments, submarine morphology and geological evolution. Mar.Geol. 1: 289-332.

ALLEN,J.R.L. 1965. A review of the origin and characteristics of Recent alluvial sediments. Sedimentology. 5: 89-191.

ALLEN,J.R.L. 1970. Physical processes of sedimentation. London: Allen and Unwin.

AMES,L.L. 1959. The genesis of carbonate apatites. Econ.Geol. 54: 829-841.

ANONYMOUS. 1922. Silt in the Orange River. S.Afr.Irrigation Mag. 1(4): 175-176.

BAGNOLD,R.A. 1941. The physics of blown sand and desert dunes. London: Chapman and Hall.

BANG,N.D. 1971. The southern Benguela Current region in February, 1966: Part II. Bathythermography and air-sea interactions. Deep-Sea Res. 18: 209-224.

BANG,N.D. 1973. Oceanography: Oceanographic environment of southern Africa. In: SPIES,J.J. and DU PLESSIS,P.C. eds. The Standard Encyclopaedia of Southern Africa. 8: 282-286. Cape Town: Nasou.

BANG,N.D. 1976. On estimating the oceanic mass flux budget of lateral and cross circulations of the southern Benguela upwelling system. 1st interdisciplinary Conf.mar. freshwater Res.S.Afr. Fiche 6G4-7 A11.

BARNARD,W.S. 1973. Duinformasies in die Sentrale Namib. Tegnikon. Dec: 1-13.

BATURIN,G.N. 1971. Formation of phosphate sediments and water dynamics. Oceanology 11: 372-376.

BATURIN,G.N. 1972. Phosphorus in interstitial waters of sediments of the south-eastern Atlantic. Oceanology 12: 849-855.

BATURIN,G.N., MERKULOVA,K.I. and CHALOV,P.I. 1972. Radiometric evidence for recent formation of phosphatic nodules in marine shelf sediments. Mar.Geol. 13(3): M37-M41.

BEETZ,W. and KAISER,E. 1926. Die Lagerungsverhältnisse der älteren Schichten in der südlichen Namib. In: KAISER,E. Die Diamantenwüste Südwest-Afrikas. Berlin: Reimer.

BERNER,R.A. 1970. Sedimentary pyrite formation. Am.J.Sci. 268: 1-23.

BEUKES,N.J. 1969. Die sedimentologie van die Etage Holkranssandsteen, Sisteem Karroo. Unpubl.M.Sc. thesis, Univ.Orange Free State, Bloemfontein. 1-138.

BEUKES,N.J. 1970. Stratigraphy and sedimentology of the Cave Sandstone Stage, Karoo System. In: HAUGHTON,S.H. ed. Proc.2nd I.U.G.S. Gondwanaland Symp. Pretoria: C.S.I.R. 321-341.

BIRCH,G.F. 1971. The glauconite deposits on the Agulhas Bank, South Africa. Unpubl.M.Sc. thesis, Geol.Dept., Univ.Cape Town.

BIRCH,G.F. 1974. Phosphorite deposits off the southwestern Cape coast and their relationship to the unconsolidated sediments. Tech.Rep.jt geol.Surv./Univ. Cape Town.mar.Geol.Progm. 6: 16-23.

BIRCH,G.F. 1975. Sediments on the continental margin off the west coast of South Africa. Unpubl.Ph.D. thesis, Geol.Dept, Univ.Cape Town.

BIRCH,G.F. and ROGERS,J. 1973. Nature of the sea floor between Lüderitz and Port Elizabeth. S.A. Shipping News Fishg.Ind.Rev. 28(7): 56-65.

BIRCH,G.F., ROGERS,J., BREMNER,J.M. and MOIR,G.J. 1976. Sedimentation controls on the continental margin of southern Africa. 1st interdisciplinary Conf. mar.freshwater Res.S.Afr. Fiche 20a C1-D12.

BISCAYE,P.E. 1965. Mineralogy and sedimentation of Recent deep-sea clay in the Atlantic Ocean and adjacent seas and oceans. Bull.geol.Soc.Am. 76: 803-832.

BLATT,H., MIDDLETON,G. and MURRAY,R. 1972. Origin of sedimentary rocks. New Jersey: Prentice Hall.

BOGOROV,G.V., VOLOVOV,V.I. and ILYIN,A.V. 1971. Microrelief of the Atlantic bottom. In: Conditions of sedimentation in the Atlantic coean. Oceanol.Res. 21: 247-270. (In Russian : English abstract).

BORNHOLD,B.D. 1973. Late Quaternary sedimentation in the eastern Angola Basin. Woods Hole oceanogr.Inst. WHOI-73-80: 1-213.

BOWMAN,I. 1924. Desert trails of Atacama. Spec.Publ.Am.geogr.Soc. 5: 1-362.

BREED,C.S., FRYBERGER,S.G., McCAULEY,C. and LENNARTZ,F. In press. Chapter N. Namib Sand Sea. In: McKEE,E.D. ed. Studies of global sand seas. Prof.Paper U.S.geol.Surv.

BREMNER,J.M. 1974. Texture and composition of surficial continental margin sediments between the Kunene River and Sylvia Hill, S.W.A. Tech.Rep.jt.geol. Surv./Univ.Cape Town mar.Geol.Progm. 6: 39-43.

BREMNER,J.M. 1975a. Faecal pellets, glauconite, phosphorite and bedrock from the Kunene-Walvis continental margin. Tech.Rep.jt.geol.Surv./Univ.Cape Town mar.Geol.Progm. 7: 59-67.

BREMNER,J.M. 1975b. Physiography of the Kunene-Walvis shelf and adjacent drainage area. Tech.Rep.jt.geol.Surv./Univ.Cape Town mar.Geol.Progm. 7: 5-10.

BREMNER,J.M. 1975c. Mineralogy and distribution of clay minerals on the South West African shelf and adjacent hinterland. Tech.Rep.jt.geol.Surv./Univ. Cape Town mar.Geol.Progm. 7: 46-55.

BREMNER,J.M. In preparation. Sediments on the South West African continental margin between 17°S and 25°S. Ph.D. thesis in preparation.

BRITISH STANDARDS INSTITUTION. 1963. Methods for the determination of particle size of powders. Part 2. Liquid sedimentation methods. Br.Stand.Inst. BS 3406: 1-49.

BRITISH STANDARDS INSTITUTION. 1967. Methods of testing soils for civil engineering purposes. Text 7(c). Standard method for fine-grained soils (pipette method). Br.Stand.Inst. BS 1377: 61-72.

BROECKER,W.S., THURBER,D.L., GODDARD,J., KU,T-L, MATTHEWS,R.K. and MESOLELLA,K.J. 1968. Milankovitch hypothesis supported by precise dating of coral reefs and deep sea sediments. Science 159: 297-300.

BROWN,A.C. 1959. The ecology of South African estuaries. Part IX: Notes on the estuary of the Orange River. Trans.R.Soc.S.Afr. 35: 463-473.

BRUCE,R.W. and KRÜGER,G.P. 1970. Die algemene geologie en geomorfologie van die bo-Oranjeopvanggebied gelëe in die Hoëveldstreek, met spesiale verwysing na die invloed daarvan op gronderosie. Internal Rep.res.Inst.Highveld Region, Potchefstroom. 1-77.

BRYAN,G.M. and SIMPSON,E.S.W. 1971. Seismic refraction measurements on the continental shelf between the Orange River and Cape Town. In: DELANY,F.M. ed. The geology of the East Atlantic continental margin. Rep.Inst.geol.Sci. 70(16): 191-198.

BURCHELL,W.J. 1822. Travels in the interior of southern Africa. London: Longman, Hurst, Rees, Orme and Brown. 2 vols.

BURKE,K., DUROTOYE,A.M., and WHITEMAN,A.J. 1971. A dry phase south of the Sahara 20 000 years ago. W.Afr.J.Archaeol. 1: 1-8.

BURNETT,W.C. 1974. Phosphorite deposits from the sea floor off Peru and Chile : radiochemical and geochemical investigations concerning their origin. Unpubl.Ph.D. thesis, Inst.Geophys., Univ. Hawaii.

BUSHINSKY,G.I. 1966. Old phosphorites of Asia and their genesis. Jerusalem: Israel Programme for Scientific Translations (1968 translation from Russian).

BUTZER,K.W. 1971a. Fine alluvial fills in the Orange and Vaal basins of South Africa. Proc.Ass.Am.Geogr. 3: 41-48.

BUTZER,K.W. 1971b. Environment and archaeology: An ecological approach to prehistory. 2nd ed. London: Methuen.

BUTZER,K.W. 1973a. The geology of Nelson Bay cave, Robberg, South Africa. S.Afr.archaeol.Bull. 28: 97-110.

BUTZER,K.W. 1973b. Pleistocene "periglacial" phenomena in southern Africa. Boreas. 2(1): 1-11.

BUTZER,K.W., FOCK,G.J., STUCKENRATH,R. and ZILCH,A. 1973. Palaeohydrology of Late Pleistocene lake, Alexandersfontein, Kimberley, South Africa. Nature. 243 (5406): 328-330.

BUTZER,K.W., HELGREN,D.M., FOCK,G.J. and STUCKENRATH,R. 1973. Alluvial terraces of the Lower Vaal River, South Africa: a reappraisal and reinvestigation. J.Geol. 81: 341-362.

CALVERT,S.E. and PRICE,N.B. 1970. Minor metal contents of Recent organic-rich sediments off South West Africa. Nature. Lond. 227(5258): 593-595.

CALVERT,S.E. and PRICE,N.B. 1971a. Recent sediments of the South West African shelf. In: DELANY,F.M. ed. The geology of the East Atlantic continental margin. Rep.Inst.geol.Sci. 70(16): 171-185.

CALVERT,S.E. and PRICE,N.B. 1971b. Upwelling and nutrient regeneration in the Benguela Current, October, 1968. Deep-Sea Res. 18: 505-523.

CARRINGTON,A.J. In preparation. Tertiary and Quaternary deposits of the Hondeklip Bay area, Namaqualand. Ph.D. thesis in preparation.

CARRINGTON,A.J. and KENSLEY,B.F. 1969. Pleistocene molluscs from the Namaqualand coast. Ann.S.Afr.Mus. 52(9): 189-223.

CARVER,R.E. 1971. Heavy-mineral separation. In: CARVER,R.E. ed. Procedures in sedimentary petrology. 427-452. New York: Wiley-Interscience.

CHAPPELL,J. 1974. Late Quaternary glacio- and hydro-isostasy, on a layered earth. Quatern.Res. 4(4): 405-428.

CHESTER,R. and ELDERFIELD,H. 1975. Ion-exchange characteristics of Orange River sediments, Namibia. Ann.Rep.res.Inst.afr.Geol.Univ. Leeds 19: 8.

CHRISTIE,N.D. 1975. Relationship between sediment texture, species richness and volume of sediment sampled by a grab. Mar.Biol. 30: 89-96.

COETZEE,J.A. 1967. Pollen analytical studies in East and Southern Africa. In: VAN ZINDEREN BAKKER,E.M. Sr. ed. Palaeoecology of Africa 3: 1-146.

COOKE,H.B.S. 1947. The development of the Vaal River and its deposits. Trans.geol. Soc.S.Afr. 49: 243-260.

COOKE,R.U. and WARREN,A. 1973. Geomorphology in deserts. London: Batsford.

COOPER,W.S. 1967. Coastal dunes of California. Mem.geol.Soc.Am. 104: 1-124.

COPENHAGEN,W.J. 1934. Occurrence of sulphides in certain areas of the sea bottom on the South African coast. Investl Rep.Fish.mar.Biol.Surv.Div.Un.S.Afr. 3: 1-11.

COPENHAGEN,W.J. 1953. The periodic mortality of fish in the Walvis region. A phenomenon within the Benguela Current. Investl Rep.Div.Sea Fish.S.Afr. 14: 1-35.

CREAGER,J.S. and STERNBERG,R.W. 1972. Some specific problems in understanding bottom sediment distribution and dispersal on the continental shelf. In: SWIFT,S.J.P., DUANE,D.B. and PILKEY,O.H. eds. Shelf sediment transport: process and pattern. Stroudsburg: Dowden, Hutchinson and Ross. 347-362.

CURRAY,J.R. 1960. Sediments and history of Holocene transgression, continental shelf, northwest Gulf of Mexico. In: SHEPARD,F.P. et al. eds. Recent sediments, Northwest Gulf of Mexico. Tulsa: Am.Ass.Petroleum.Geol. 221-266.

CURRAY,J.R. 1961. Late Quaternary sea-level: a discussion. Bull.geol.Soc.Am. 72: 1707-1712.

CURRAY,J.R. 1965. Late Quaternary history, continental shelves of the United States. In: WRIGHT,H.E. and FREY,D.G. eds. The Quaternary of the United States. New Jersey: Princeton University Press. 723-735.

D'ANGLEJAN,B.F. 1967. Origin of marine phosphorites off Baja California, Mexico. Mar.Geol. 5: 15-44.

D'ANGLEJAN,B.F. 1968. Phosphate diagenesis of carbonate sediments as a mode of in situ formation of marine phosphorites: observations in a core from the Eastern Pacific. Canad.J.Earth Sci. 5: 81-87.

DARTEVELLE,E. and ROGER,J. 1954. Contribution à la connaissance de la fauna du Miocène de l'Angola. Communicaciones Servico Geologico Portugal. 35: 227-312.

DAVEY,R.J. 1971. Palynology and palaeo-environmental studies, with special reference to the continental shelf sediments of South Africa. In: FARINACCI,A. ed. Proc. 2nd planktonic Conf. Rome. 331-347.

DAVEY,R.J. and ROGERS,J. 1975. Palynomorph distribution in Recent offshore sediments along two traverses off South West Africa. Mar.Geol. 18: 213-225.

DE DECKER,A.H.B. 1970. Notes on an oxygen-depleted subsurface current off the west coast of South Africa. Investl Rep.Div.Sea Fish.S.Afr. 84: 1-24.

DE VILLIERS,J. and SÖHNGE,P.G. 1959. Geology of the Richtersveld. Mem.geol.Surv. S.Afr. 48: 1-295.

DIESTER-HAASS,L., SCHRADER,H.-J. and THIEDE,J. 1973. Sedimentological and palaeoclimatological investigations of two pelagic ooze cores off Cape Barbas, North-West Africa. "Meteor" -Forsch.-Ergebnisse C (16): 19-66.

DINGLE,R.V. 1971. Tertiary sedimentary history of the continental shelf off southern Cape Province. Trans.geol.Soc.S.Afr. 74: 173-186.

DINGLE,R.V. 1973a. The geology of the continental shelf between Lüderitz and Cape Town, (Southwest Africa), with special reference to Tertiary strata. J.geol.Soc.Lond. 129: 337-363.

DINGLE,R.V. 1973b. Regional distribution and thickness of post-Palaeozoic sediments on the continental margin of southern Africa. Geol.Mag. 110(3): 97-102.

DINGLE,R.V. 1973c. Preliminary stratigraphical classification of the Cainozoic succession on the South African continental shelf. Trans.R.Soc.S.Afr. 40(5): 367-372.

DINGLE,R.V. 1975. Agulhas Bank phosphorites : a review of 100 years of investigation. Trans.geol.Soc.S.Afr. 77: 261-264.

DINGLE,R.V., GERRARD,I., GENTLE,R.I. and SIMPSON,E.S.W. 1971. The continental shelf between Cape Town and Cape Agulhas. In: DELANY,R.M. ed. The geology of the East Atlantic continental margin. Rep.Inst.geol.Sci. 70(16): 199-209.

DINGLE,R.V. and SCRUTTON,R.A. 1974. Continental breakup and the development of post-Palaeozoic sedimentary basins around southern Africa. Bull.geol.Soc.Am. 85: 1467-1474.

DRAKE,D.E., KOLPACK,A.L. and FISCHER,P.J. 1972. Sediment transport on the Santa Barbara-Oxnard shelf, Santa Barbara Channel, California. In: SWIFT,D.J.P., DUANE,D.B. and PILKEY,O.H. eds. Shelf sediment transport : process and pattern. Stroudsburg: Dowden, Hutchinson and Ross. 307-331.

DUNHAM,R.J. 1962. Classification of carbonate rocks according to depositional texture. In: HAM,W.E. ed. Classification of carbonate rocks - a symposium. Mem.Am.Ass.Petrol.Geol. 1: 108-121.

DU PLESSIS,A., SCRUTTON,R.A., BARNABY,A.M. and SIMPSON,E.S.W. 1972. Shallow structure of the continental margin of southwestern Africa. Mar.Geol. 13: 77-89.

DU PLESSIS,E. 1967. Seasonal occurrence of thermoclines off Walvis Bay, South West Africa. Investl.Rep.mar.Res.Lab.S.W.Afr. 13: 1-16.

EDWARDS,D. 1974. Vegetation of the Upper Orange River valley and environs. In: VAN ZINDEREN BAKKER,E.M. Sr. ed. The Orange River: Progress Report. Proc. 2nd limn.Conf. on Orange River System Bloemfontein: Inst.env.Sci., Univ. Orange Free State. 13-30.

EINSELE,G. and WERNER,F. 1972. Sedimentary processes at the entrance Gulf of Aden/Red Sea. "Meteor" - Forsch.-Ergebnisse C (10): 39-62.

EKMAN,V.W. 1905. On the influence of the earth's rotation on ocean currents. Ark.Math.Astr.Fys. 2(11): 1-53.

EMERY,K.O. 1968. Relict sediments on continental shelves of world. Bull.Am.Ass. Petrol.Geol. 52(3): 445-464.

EMERY,K.O. 1971. A geophysical and geological study of the Eastern Atlantic continental margin, 1971-1974. Woods Hole: National Science Foundation and Woods Hole Oceanographic Institution.

EMERY,K.O. 1972. Eastern Atlantic continental margin: some results of the 1972 cruise of the R.V. Atlantis II. Science 178: 298-301.

EMERY,K.O. and GARRISON,L.E. 1967. Sea levels 70 000 to 20 000 years ago. Science 157: 684-687.

EMERY,K.O., MILLIMAN,J.D. and UCHUPI,E. 1973. Physical properties and suspended matter of surface waters in the southeastern Atlantic Ocean. J.sedim.Petrol. 43(3): 822-837.

EMERY,K.O., UCHUPI,E., BOWIN,C.O., PHILLIPS,J. and SIMPSON,E.S.W. 1975. Continental margin off western Africa: Cape St Francis (South Africa) to Walvis Bay (South West Africa). Bull.Am.Ass.petrol.Geol. 59: 3-59.

EMILIANOV,E.M. and SENIN,Hu.M. 1969. Peculiarities in the material composition of sediments on the shelf of South-Western Africa. (Lithology and mineral resources) 2: 10-25 (In Russian).

FAYOSE,E.A. 1970. Stratigraphical palaeontology of Afowo 1 well, South Western Nigeria. J.min.Geol. 5(1-2): 1-99.

FINKEL,H.J. 1959. The barchans of southern Peru. J.Geol. 67: 614-647.

FLEMMING,B.W. 1976. Construction and calibration of an automatically recording settling tube system for the hydraulic grain size analysis of sands. Tech.Rep.jt.geol.Surv./Univ. Cape Town mar.Geoscience Group 8: 47-59.

FLEMMING,N.C. 1965. Form and relation to present sea level of Pleistocene marine erosion features. J.Geol. 73: 799-811.

FLINT,R.F. 1971. Glacial and Quaternary geology. New York: Wiley.

FOLK,R.L. 1954. The distinction between grain size and mineral composition in sedimentary rock nomenclature. J.Geol. 62: 344-365.

FOLK,R.L. 1959. Practical petrographic classification of limestones. Bull.Am.Ass. Petrol.Geol. 43(1): 1-38.

FOLK,R.L. 1962. Spectral subdivision of limestone types. Mem.Am.Ass.Petrol.Geol. 1: 62-84.

FOLK,R.L. 1968. Petrology of sandstones. In: Petrology of sedimentary rocks. 102-140. Austin: Hemphill's.

FOSTER,R.W. 1974. Report on vibracore programme March 1972 to January 1974. Internal Rep.Mar.Diamond Corp. 1-35.

FRANCHETEAU,J. and LE PICHON,X. 1972. Marginal fracture zones as structural framework of continental margins in South Atlantic Ocean. Bull.Am.Ass.Petrol.Geol. 56(6): 991-1007.

FREAS,D.H. and RIGGS,S.R. 1968. Environments of phosphorite deposition in the Central Florida phosphate district. In: BROWN,L.F. ed. Proc.Fourth Forum Geology of Industrial Minerals, Bureau of econ.Geol.Univ. Texas, Austin. 117-128.

FRYBERGER,S.G. In press. Chapter F. Dune forms and wind regime. In: McKEE,E.D. ed. Studies of global sand seas. Prof.Paper U.S.geol.Surv.

FULLER,A.O. 1972. Possible fracture zones and rifts in Southern Africa. In: Studies in Earth and Space Sciences. Mem.geol.Soc.Am. 132: 129-172.

GALEHOUSE,J.S. 1971. Point counting. In: CARVER,R.E. ed. Procedures in sedimentary petrology. 385-409. New York: Wiley-Interscience.

GERMOND,R.C. 1967. Chronicles of Basutoland. Morija: Morija Sasuto Book Depot.

GEVERS,T.W., PARTRIDGE,F.C. and JOUBERT,G.K. 1937. The pegmatite area south of the Orange River in Namaqualand. Mem.geol.Surv.S.Afr. 31: 1-172.

GIBBS,R.J. 1967. Amazon River: environmental factors that control its dissolved and suspended load. Science 156: 1734-1737.

GOLDHABER,M.B. and KAPLAN,I.R. 1974. The sulfur cycle. In: GOLDBERG,E.D. ed. The Sea, Volume 5, Marine Chemistry: 569-655. New York: Wiley-Interscience.

GOULD,H.R. 1970. The Mississippi Delta Complex. In: MORGAN,J.P. ed. Deltaic sedimentation: modern and ancient. Spec.Publ.Soc.econ.Palaeont.Miner. 15: 3-30.

GREEN,L.G. 1948. To the River's End. Cape Town: Timmins.

GREENMAN,L. 1969. The Elizabeth Bay Formation, Lüderitz, and its bearing on the genesis of dolomite. Trans.geol.Soc.S.Afr. 72(3): 115-121.

GRIFFIN,J.J., WINDOM,H. and GOLDBERG,E.D. 1968. The distribution of clay minerals in the World Ocean. Deep-Sea Res. 15(4): 433-460.

GROLIER,M.J. ERICKSEN,G.E., McCAULEY,J.F. and MORRIS,E.C. 1974. The desert land forms of Peru: a preliminary photographic atlas. Preliminary interagency Rep.: Astrogeology 57 U.S.Geol.Surv. 1-146.

GROVE,A.T. 1969. Landforms and climatic change in the Kalahari and Ngamiland. Geogr.J. 135: 191-212.

GUILCHER,A. 1969. Pleistocene and Holocene sea level changes. Earth-Sci.Rev. 5: 69-97.

GULBRANDSEN,R.A. 1969. Physical and chemical factors in the formation of marine apatite. Econ.Geol. 64: 365-382.

GULBRANDSEN,R.A. 1970. Relation of carbon dioxide content of apatite of the Phosphoria Formation to regional facies. U.S.geol.Surv.Prof.Paper 700-B: B9-B13.

HALLAM,C.D. 1964. The geology of the coastal diamond deposits of Southern Africa (1959). In: HAUGHTON,S.H. ed. The geology of some ore deposits in Southern Africa. Johannesburg: Geol.Soc.S.Afr. 671-728.

HARGER,H.S. 1913. Some features associated with the denudation of the South African continent. Proc.geol.Soc.S.Afr. 16: xxii-xxxix.

HARMSE,H.J. VON M. 1974. An evaluation of the possible influence of rock and soil on erosion in the catchment area of the Hendrik Verwoerd Dam. In: VAN ZINDEREN BAKKER, E.M. Sr. ed. The Orange River: Progress Report. Proc. 2nd limn.Conf. on Orange River System Bloemfontein: Inst.env.Sci., Univ.Orange Free State. 31-40.

HART,T.J. and CURRIE,R.I. 1960. The Benguela Current. Discovery Reps. 31: 123-298.

HASTENRATH,S.L. 1967. The barchans of the Arequipa region, southern Peru. Z. Geomorph. 11: 300-331.

HAUGHTON,S.H. 1927. Notes on the river-system of south-west Gordonia. Trans.R. Soc.S.Afr. 14: 225-231.

HAUGHTON,S.H. 1931. The Late Tertiary and Recent deposits of the west coast of South Africa. Trans.geol.Soc.S.Afr. 34: 19-57.

HAY,W.W. 1974. Introduction. In: HAY,W.W. ed. Studies in palaeo-oceanography. Spec.Publ.Soc.econ.Palaeontol.Mineral. 20: 1-5.

HAYES,M.O. 1967. Relationship between coastal climate and bottom sediment type on the inner continental shelf. Mar.Geol. 5: 111-132.

HAYS,J.D., LOZANO,J. and IRVING,G. 1974a. -17 000 year map of the Atlantic and western Indian sectors of the Antarctic Ocean (60° to 30° South). Climatic Res.Unit Publ. 2: 52. Norwich: School of Environmental Sciences.

HAYS,J.D., LOZANO,J. and IRVING,G. 1974b. High southern latitude estimated temperature changes of the last 20 000 years. Climatic Res.Unit Publ. 2: 80. Norwich: School of Environmental Sciences.

HEIN,J.R. and GRIGGS,G.B. 1972. Distribution and scanning electron microscope (SEM) observations of authigenic pyrite from a Pacific deep-sea core. Deep-Sea Res. 19: 133-138.

HENDEY,Q.B. 1974. The Cenozoic Carnivora of the south-western Cape Province. Ann.S.Afr.Mus. 1-369.

HOYT,J.H. OOSTDAM,B.L. and SMITH,D.D. 1969. Offshore sediments and valleys of the Orange River (South and South West Africa). Mar.Geol. 7(1): 69-84.

HOYT,J.H., SMITH,D.D. and OOSTDAM,B.L. 1965a. Sediment distribution on the inner continental shelf, west coast of southern Africa. Bull.Am.Assoc.Petrol.Geol. 49: 344-345 (Abstract).

HOYT,J.H., SMITH,D.D. and OOSTDAM,B.L. 1965b. Pleistocene low sea-level stands on the southwest African continental shelf. Abstr. 7th int.Congr., Int.Ass. quatern.Res. 227.

HÜLSEMANN,J. 1966. On the routine analysis of carbonates in unconsolidated sediments. J.sedim.Petrol. 36(2): 622-625.

HUMPHRIES,D.W. 1961. A non-laminated miniature sample splitter. J.sedim.Petrol. 31: 471-473.

ILYIN,A.V. 1971. Main features of geomorphology of Atlantic bottom. In: Conditions of sedimentation in the Atlantic Ocean. Oceanol.Res. 21: 107-246. (In Russian: English abstract).

INMAN,D.L., EWING,G.C. and CORLISS,J.B. 1966. Coastal sand dunes of Guerrero Negro, Baja California, Mexico. Bull.geol.Soc.Am. 77: 787-802.

INMAN,D.L. and NORDSTROM,C.E. 1971. On the tectonic and morphologic classifications of coasts. J.Geol. 74: 1125-1136.

JACOT GUILLARMOD,A. 1962. The bogs and sponges of the Basutoland mountains. S.Afr.J.Sci. 58(6): 179-182.

JACOT GUILLARMOD,A. 1963. Further observations on the bogs of the Basutoland mountains. S.Afr.J.Sci. 59(4): 115-118.

JACOT GUILLARMOD,A. 1969. The effect of land-usage on aquatic and semi-aquatic vegetation at high altitudes in southern Africa. Hydrobiologia 34(1): 3-13.

JACOT GUILLARMOD,A. 1972a. The Caledon River in the early days of European settlement. The Civ.Engr. in S.Afr. Feb. 1972: 93-94.

JACOT GUILLARMOD,A. 1972b. The bogs and sponges of the Orange River catchment within Lesotho. The Civ.Engr. in S.Afr. Feb. 1972: 84-85.

JOHNS,W.D., GRIM,R.E. and BRADLEY,W.F. 1954. Quantitative estimations of clay minerals by diffraction methods. J.sedim.Petrol. 24(4): 242-251.

JOHNSON,D. 1919. Shore processes and shoreline development. New York: Wiley.

JOHNSON,M.R., BOTHA,B.J.V., HUGO,P.J., KEYSER,A.W., TURNER,B.R. and WINTER, H.de la R. In press. Preliminary report on stratigraphic nomenclature in the Karoo sequence. Rep.S.Afr.Comm.strat.Nomenclature.

JOUBERT,P. 1975. The gneisses of Namaqualand and their deformation. Trans.geol. Soc.S.Afr. 27(3): 339-345.

JOUBERT,P. and KRÖNER,A. 1971. The Stinkfontein Formation south of the Richtersveld. Trans.geol.Soc.S.Afr. 75: 47-54.

JOYNT,R.H., GREENSHIELDS,R. and HODGEN,R. 1972. Advances in sea and beach diamond mining techniques. ECOR Symp.Ocean's Challenge to S.Afr.Engrs. C.S.I.R.S71.

KAISER,E. 1926. Die Diamantenwüste Südwestafrikas. Berlin: Reimer.

KAYSER,K. 1973. Beiträge zur geomorphologie der Namib-Küstenwüste. Z.Geomorph. N.F. Suppl. Vol. 17: 156-157.

KEULDER,P.C. 1973. Hidrochemie van die bo-Oranjeopvanggebied met spesiale verwysing na die beskikbaarheid van kleigeadsorbeerde katione. Unpubl.Ph.D. thesis, Univ.Orange Free State, Bloemfontein. 1-185.

KEULDER,P.C. 1974. Hydrochemistry and geochemistry of the catchment area of the Hendrik Verwoerd Dam. In: VAN ZINDEREN BAKKER,E.M. Sr. ed. The Orange River: Progress Report. Proc. 2nd limn.Conf. on Orange River system. Bloemfontein: Inst.env.Sci.Univ. Orange Free State. 41-54.

KEYSER,U. 1972. The occurrence of diamonds along the coast between the Orange River estuary and the Port Nolloth Reserve. Bull.geol.Surv.S.Afr. 54: 1-23.

KING,L.C. 1968. The morphology of the earth, a study and synthesis of world scenery. 2nd ed. New York: Hafner.

KING,L.H. 1967. Use of a conventional echo-sounder and textural analyses in delineating sedimentary facies: Scotian Shelf. Canad. J.Earth Sci. 4: 691-708.

KNETSCH,G. 1937. Beiträge zur Kenntnis der Diamantlagerstätten an der Oranjemündung in Südwestaftrka. Geol.Rdsch. 28: 188-207.

KOKOT,D.F. 1965. Oranjerivier. Tegnikon. 14: 7-9.

KOLODNY,Y. and KAPLAN,I.R. 1970. Uranium isotopes in sea-floor phosphorites. Geochim.et cosmochim.Acta. 34: 3-24.

KORN,H. and MARTIN,H. 1951a. The seismicity of South-West Africa. Trans.geol.Soc. S.Afr. 54: 85-88.

KORN,H. and MARTIN,H. 1951b. The Pleistocene in South West Africa. Proc. 3rd Pan Afr.Cong.Prehistory 14-22.

KRIEL,J.P. 1972. The role of the Hendrik Verwoerd Dam in the Orange River project. The Civ.Engr. in S.Afr. Feb. 1972: 51-61.

KRINSLEY,D.H. and DOORNKAMP,J.C. 1973. Atlas of quartz sand surface textures. Cambridge: Cambridge University Press.

KRÖNER,A. 1975. Late Precambrian formations in the western Richtersveld, Northern Cape Province. Trans.R.Soc.S.Afr. 41(4): 375-433.

KRÖNER,A. and JACKSON,M.P.A. 1974. Geological reconnaissance of the coast between Lüderitz and Marble Point, South West Africa. In: KRÖNER,A. ed. Contributions to the Precambrian geology of Southern Africa: A volume in honour of John de Villiers. Bull.Precambrian Res.Unit. 15: 79-103. Geol.Dept., Univ. Cape Town.

KUENEN,Ph.H. and PERDOK,W.G. 1962. Experimental abrasion 5. Frosting and defrosting of quartz grains. J.Geol. 70: 648-658.

LARSON,R.L. and LADD,J.W. 1973. Evidence for the opening of the South Atlantic in the Early Cretaceous. Nature Lond. 246: 209-212.

LEWIS,A.D. 1936. Sand dunes of the Kalahari within the borders of the Union. S.Afr.geogr.J. 19: 22-32.

LEWIS,K.B. 1971. Slumping on a continental slope inclined at 1^{o}-4^{o}. Sedimentology 16: 97-110.

LISITZIN,A.P. 1972. Sedimentation in the world ocean. Spec.Publ.Soc.econ.Paleont. Miner. 17: 1-218.

LOGAN,R.F. 1960. The Central Namib Desert, South West Africa. Publ.nat.Acad.Sci. - nat.Res.Coun. 758: 1-141.

LOGAN,R.F. 1969. Geography of the Central Namib Desert. In: McGINNIES,W.G. and GOLDMAN,B.J. eds. Arid lands in perspective. Tucson: Am.Assoc.Advancement Sci. 129-143.

LOGAN,R.F. 1972. The geographical divisions of the deserts of South West Africa. Mitt.Basler Afr.Bibliogr. 4-6: 46-65.

LOVE,L.G. 1965. Micro-organic material with diagenetic pyrite from the Lower Proterozoic Mount Isa shale and a carboniferous shale. Proc.Yorkshire geol. Soc. 35: 187-202.

LOW,D.C. 1967. Observations regarding the Orange River effluent. Unpubl.Rep. Anglo Am.oceanogr.Res.Unit. 1-2.

MARCHAND,J.M. 1928. The nature of the sea-floor deposits in certain regions on the west coast. Spec.Rep.Fish.mar.Biol.Surv.S.Afr. 6: 1-11.

MAREE,B.D. 1966. Die voorkoms van diamante op land en onder die see langs die weskus van suidelike Afrika. Tegnikon. 15: 149-159.

MARSH,J.S. 1973. Relationships between transform directions and alkaline igneous rock lineaments in Africa and South America. Earth Planet.Sci.Lett. 18: 317-323.

MARTIN,H. 1965. The Precambrian geology of South West Africa and Namaqualand. Precambrian Res.Unit., Geol.Dept., Univ.Cape Town.

MARTIN,R.A. 1974. Benthonic foraminifera from the western coast of southern Africa. Tech.Rep.jt.geol.Surv./Univ.Cape Town mar.Geol.Progm. 6: 83-87.

McBRIDE,E.F. 1963. A classification of common sandstones. J.sedim.Petrol.33: 664-669.

McCAULEY,J.F. 1973. Mariner 9 evidence for wind erosion in the equatorial and mid-latitude of Mars. J.geophys.Res. 78(20): 4123-4137.

McKEE,E.D. In press. Studies of global sand seas. Prof.Paper.U.S.Geol.Surv.

McKEE,E.D. and BREED,C.S. 1974. An investigation of major sand seas in desert areas throughout the world. In: FREDEN,S.C., MERCANTI,E.P. and BECKER,M.A. eds. Third Earth Resources Technology Satellite - 1 Symposium. NASA. SP-351: 665-679.

McMANUS,D.A. 1970. Criteria of climatic change in the inorganic components of marine sediments. Quatern.Res. 1: 72-102.

MASON,B. 1952. Principles of Geochemistry. 2nd edn. New York: Wiley.

MEADE,R.H. 1969. Errors in using modern stream-load data to estimate natural rates of denudation. Bull.geol.Soc.Am. 80: 1265-1274.

MEADE,R.H. and TRIMBLE,S.W. 1974. Changes in sediment loads in rivers of the Atlantic drainage of the United States since 1900. In: Symposium - Effects of Man on the Interface of the Hydrological Cycle with the Physical Environment - IAHS - Publ. 113: 99-104.

MEIGS,P. 1966. Geography of coastal deserts. UNESCO arid zone Res. 28: 1-140.

MERENSKY,H. 1909. The diamond deposits of Lüderitzland, German South West Africa. Trans.geol.Soc.S.Afr. 12: 13-23.

METEOROLOGICAL SERVICES OF THE ROYAL NAVY AND THE SOUTH AFRICAN AIR FORCE. 1944. Weather on the coasts of southern Africa. Volume 2. Local information. Cape Town: S.Afr.Govt.

MIDGLEY,D.C. and PITMAN,W.V. 1969. Surface water resources of South Africa. Rep.hydrol.res.Unit Univ.Witwatersrand 2/69: 1-54.

MILLIMAN,J.D. and EMERY,K.O. 1968. Sea levels during the past 35 000 years. Science. 162: 1121-1123.

MILLIMAN,J.D., SUMMERHAYES,C.P., and BARRETTO,H.T. 1975. Oceanography and suspended matter off the Amazon River February-March 1973. J.sedim.Petrol. 45(1): 189-206.

MORGANS,J.F.C. 1956. Notes on the analysis of shallow-water soft substrata. J.anim.Ecol. 25: 367-387.

MOROSHKIN,K.V., BUBNOV,V.A. and BULATOV,R.P. 1970. Water circulation in the eastern South Atlantic Ocean. Oceanology. 10: 27-37.

MURRAY,L.G. 1969. Exploration and sampling mathods employed in the offshore diamond industry. In: Ninth Commonw.min.metallurg.Congr.Lond. Paper 14: 1-24.

MURRAY,L.G., JOYNT,R.H., O'SHEA,D.O'C., FOSTER,R.W. and KLEINJAN,L. 1971. The geological environment of some diamond deposits off the coast of South West Africa. In: DELANY,F.M. ed. The geology of the East Atlantic continental margin. Rep.Inst.geol.Sci. 70(13): 119-141.

NAGTEGAAL,P.J.C. 1973. Adhesion-ripple and barchan-dune sands of the Recent Namib (SW Africa) and Permian Rotliegend (NW Europe) Deserts. Madoqua .(Series II). 2(63-68): 5-19.

NELSON,B.W. 1970. Hydrography, sediment dispersal, and Recent historical development of the Po River Delta Complex. In: MORGAN,J.P. ed. Deltaic sedimentation: ancient and modern. Spec.Publ.Soc.econ.Paleont.Miner. 15: 152-184.

O'BRIEN,R.J. 1972. The barchans of the Southern Namib: a grain size analysis. Proc. 4th S.Afr.Univ.geogr.Conf. 22-31.

OOMKENS,E. 1970. Depositional sequences and sand distribution in the postglacial Rhone Delta Complex. In: MORGAN,J.P. ed. Deltaic sedimentation: ancient and modern. Spec.Publ.Soc.econ.Paleont.Miner. 15: 198-212.

O'SHEA,D.O'C. 1971. An outline of the inshore submarine geology of southern South West Africa and Namaqualand. Unpubl.M.Sc. thesis, Geol.Dept., Univ. Cape Town.

PARKER,R.J. 1971. The petrography and major element geochemistry of phosphorite nodule deposits on the Agulhas Bank, South Africa. Bull.S.Afr.nat.Comm. oceanogr.Res.mar.Geol.Prgm. 2: 1-94.

PARKER,R.J. 1975. The petrology and origin of some glauconitic and glauco-conglomeratic phosphorites from the South African continental margin. J. sedim.Petrol. 45(1): 230-242.

PARKER,R.J. and SIESSER,W.G. 1972. Petrology and origin of some phosphorites from the South African continental margin. J.sedim.Petrol. 42(2): 434-440.

PATERSON,W.S.B. 1972. Laurentide ice sheet: estimated volumes during Late Wisconsin. Rev.geophys.Space Physics. 10: 885-912.

PENCK,A. 1914. The shifting of the climatic belts. Scottish geogr.Mag. 30: 281-293.

PRICE,N.B. and CALVERT,S.E. 1973. The geochemistry of iodine in oxidised and reduced Recent marine sediments. Geochim.et cosmochim.Acta 37: 2149-2158.

REUNING,E. 1931. The Pomona-Quartzite and Oyster-Horison on the west coast of the mouth of the Oliphants River. Trans.R.Soc.S.Afr. 19: 205-214.

RICH,J.L. 1942. The face of South America: an aerial traverse. Spec.Publ.Am. geogr.Soc. 26: 1-299.

RICKARD,D.T. 1970. The origin of framboids. Lithos. 3: 269-293.

RIGGS,S.R. and FREAS,D.H. 1965. Stratigraphy and sedimentation of phosphorite in the Central Florida Phosphate District. Am.Inst.min.Metall.petrol.Engrs. Preprint No. 65H84: 1-17.

ROGERS,A.W. 1915a. The geology of part of Namaqualand. Trans.geol.Soc.S.Afr. 18: 72-101.

ROGERS,A.W. 1915b. The occurrence of dinosaurs in Bushmanland. Trans.R.Soc.S.Afr. 5: 265-272.

ROGERS,A.W. 1917. Namaqualand. S.Afr.geogr.J. 1: 23-33.

ROGERS,A.W. 1922. Post-Cretaceous climates of South Africa. S.Afr.J.Sci. 19: 1-31.

ROGERS,J. 1971. Sedimentology of Quaternary deposits on the Agulhas Bank. Bull.S.Afr.nat.Comm.oceanogr.Res.mar.Geol.Progm. 1: 1-117.

ROGERS,J. 1972. Preliminary observations on texture, composition and depositional history of sediments on the Orange-Lüderitz continental margin. Tech.Rep. S.Afr.nat.Comm.oceanogr.Res.mar.Geol.Progm. 4: 44-59.

ROGERS,J. 1973. Texture, composition and depositional history of unconsolidated sediments from the Orange-Lüderitz shelf, and their relationship with Namib Desert sands. Tech.Rep.jt geol.Surv./Univ.Cape Town mar.Geol.Progm. 5: 67-88.

ROGERS,J. 1974. Surficial sediments and Tertiary limestones from the Orange-Lüderitz shelf. Tech.Rep.jt geol.Surv./Univ.Cape Town mar.Geol.Progm. 6: 24-38.

ROGERS,J. 1975a. Sediment flow along the coastal zone of Namaqualand and the Southern Namib. Tech.Rep.jt.geol.Surv./Univ.Cape Town mar.Geol.Progm. 7: 35-36.

ROGERS,J. 1975b. Reconnaissance study of clay minerals and regional distribution of potassium on the Orange-Lüderitz continental margin. Tech.Rep.jt geol. Surv./Univ.Cape Town mar.Geol.Progm. 7: 56-58.

ROGERS,J. 1975c. Surface textures of quartz grains from subaqueous and aeolian environments in the Orange-Lüderitz coastal zone. Tech.Rep.jt geol.Surv./ Univ.Cape Town mar.Geol.Progm. 7: 28-34.

ROGERS,J. and BREMNER,J.M. 1973. Bathymetry of the Lüderitz-Walvis continental margin. Tech.Rep.jt geol.Surv./Univ.Cape Town mar.Geol.Progm. 5: 7-9.

ROGERS,J. and KRINSLEY,D.H. In preparation. Surface textures of quartz grains from subaqueous and aeolian environments of the Orange-Lüderitz coastal zone and middle shelf.

ROGERS,J., SUMMERHAYES,C.P., DINGLE,R.V., BIRCH,G.F., BREMNER,J.M. and SIMPSON, E.S.W. 1972. Distribution of minerals on the seabed around South Africa and problems in their exploration and eventual exploitation. In: ECOR Symp. Ocean's Challenge to S.Afr.Engrs.C.S.I.R. S71.

ROGERS,J. and TANKARD,A.J. 1974. Surface textures of some quartz grains from the west coast of southern Africa. Proc.Electron Microscopy Soc.S.Afr. 4: 55-56.

ROONEY,T.P.and KERR,P.F. 1967. Mineralogic nature and origin of phosphorite, Beaufort County, North Carolina. Bull.geol.Soc.Am. 78: 731-748.

ROOSEBOOM,A. 1974. Meting en analise van sedimentafvoer in riviere. Tech.Rep. Dept Water Affairs S.Afr. 58: 1-43.

ROOSEBOOM,A. and MAAS,N.F. 1974. Sedimentafvoergegewens vir die Oranje-, Tugela- en Pongolariviere. Tech.Rep.Dept Water Affairs S.Afr. 59: 1-48.

ROURKE,J.P. 1972. Taxonomic studies on Leucospermum R. Br. J.S.Afr.Bot.Suppl. Vol. 8: 1-194.

SARNTHEIN,M. 1971. Oberflächensedimente im Persischen Golf und Golf von Oman. II. Quantitative Komponentenanalyse der Grobfraktion. "Meteor"-Forsch.-Ergebnisse C(5): 1-113.

SARNTHEIN,M. and WALGER,E. 1974. Der äolische Sandstrom aus der W-Sahara zur Atlantikküste. Geol.Rdsch. 63(3): 1065-1087.

SCHALKE,H.J.W.G. 1973. The Upper Quaternary of the Cape Flats area (Cape Province, South Africa). Scripta Geologica. 15: 1-57.

SCHULZE,B.R. 1965. Climate of South Africa. Part 8. General Survey. Weather Bur.Dept Transport S.Afr. WB 28: 1-330.

SCRUTON,P.C. 1956. Oceanography of Mississippi delta sedimentary environments. Bull.Am.Ass.petroleum Geol. 40: 2864-2952.

SCRUTTON,R.A. 1973. Gravity results from the continental margin of South-Western Africa. Mar.geophys.Res. 2: 11-21.

SCRUTTON,R.A. and DINGLE,R.V. 1975. Basement control over sedimentation on the continental margin west of southern Africa. Trans.geol.Soc.S.Afr. 77: 253-260.

SEELY,M.K. and SANDELOWSKY,B.H. 1974. Dating the regression of a river's end-point. S.Afr.archaeol.Bull.Goodwin Ser. 2: 61-64.

SELBY,M.J., RAINS,R.B. and PALMER,R.W.P. 1974. Eolian deposits of the ice-free Victoria Valley, Southern Victoria Land, Antarctica. N.Z.Geol.Geophys. 17(3): 543-562.

SENIN,Yu.M. 1969. Phosphorus in bottom sediments of the South West African shelf. (Lithology and mineral resources.) 1: 11-26. (In Russian).

SHACKLETON,N.J. and OPDYKE,N.D. 1973. Oxygen isotope and palaeo-magnetic stratigraphy of Equatorial Pacific core V28-238: oxygen isotope temperatures and ice volumes on a 10^5 year and 10^6 year scale. Quatern.Res. 3(1): 39-55.

SHANNON,L.V. 1966. Hydrology of the south and west coasts of South Africa. Investl.Rep.Div.Sea Fish.S.Afr. 58: 1-62.

SHEPARD,F.P. 1932. Sediments of the continental shelves. Bull.geol.Soc.Am. 43: 1017-1039.

SHEPARD,F.P. 1973. Submarine Geology. New York: Harper and Row.

SIESSER,W.G. 1971. Petrology of some South African coastal and offshore carbonate rocks and sediments. Bull.S.Afr.nat.Comm.oceanogr.Res.mar.Geol.Progm. 3: 1-232.

SIESSER,W.G. 1972a. Limestone lithofacies from the South African continental margin. Sedimentary Geol. 8: 83-112.

SIESSER,W.G. 1972b. Abundance and distribution of carbonate constituents in some South African coastal and offshore sediments. Trans.R.Soc.S.Afr. 40(4): 261-277.

SIESSER,W.G. 1973. Micropalaeontology and palaeoclimatology of some South African continental slope cores. Tech.Rep.jt geol.Surv./Univ.Cape Town mar.Geol. Progm. 5: 94-114.

SIESSER,W.G. 1975. Calcareous nannofossils from the South African continental margin. Bull.jt geol.Surv./Univ.Cape Town mar.Geol.Progm. 5: 1-135.

SIESSER,W.G. and ROGERS,J. 1971. An investigation of the suitability of four methods in routine carbonate analysis of marine sediments. Deep-Sea Res. 18: 135-139.

SIESSER,W.G. and ROGERS,J. 1976. Authigenic pyrite and gypsum in South West African continental slope sediments. Sedimentology. 23(4): 567-578.

SIESSER,W.G., SCRUTTON,R.A. and SIMPSON,E.S.W. 1974. Atlantic and Indian Ocean margins of Southern Africa. In: BURK,C.A. and DRAKE,C.L. eds. The geology of continental margins. New York: Springer-Verlag. 641-654.

SIMPSON,E.S.W. 1966. Die geologie van die vastelandsplat. Tegnikon. 15: 168-176.

SIMPSON,E.S.W. 1968. Marine geology: progress and problems. Proc.geol.Soc.S.Afr. 71: 97-111.

SIMPSON,E.S.W. 1971. The geology of the south-west African continental margin: a review. In: DELANY,F.M. ed. The geology of the East Atlantic continental margin. Rep.Inst.geol.Sci. 70(16): 157-170.

SIMPSON,E.S.W. and DAVIES,D.H. 1957. Observations on the Fish River Canyon in South West Africa. Trans.R.Soc.S.Afr. 35(2): 97-107.

SIMPSON,E.S.W. and DU PLESSIS,A. 1968. Bathymetric, magnetic and gravity data from the continental margin of southwestern Africa. Canad.J.Earth Sci. 5: 1119-1123.

SIMPSON,E.S.W. and NEEDHAM,H.D. 1967. The floor of the southeast Atlantic: a review. In: UNESCO-IUGS Symp.Montevideo, Uruguay : Continental drift emphasizing the history of the South Atlantic area. 39-81.

SIMPSON,E.S.W. and PURSER,S.M.L. 1974. Southeast Atlantic and southwest Indian Oceans. Bathymetry 1:10 000 000 at 33°. Chart 125A. 1st ed. Geol.Dept, Univ.Cape Town.

SIMPSON,G.G. 1973. Tertiary penguins (sphenisciformes, spheniscidae) from Ysterplaats, Cape Town, South Africa. S.Afr.J.Sci. 69: 342-344.

SMAYDA,T.J. 1971. Normal and accelerated sinking of phytoplankton in the sea. Mar.Geol. 11: 105-122.

SMITH,J.D. and HOPKINS,T.S. 1972. Sediment transport on the continental shelf off of Washington and Oregon in light of recent current measurements. In: SWIFT,D.J.P., DUANE,D.B. and PILKEY,O.H. eds. Shelf sediment transport: process and pattern. Stroudsburg: Dowden, Hutchinson and Ross. 143-180.

STANDER,G.H. 1964. The Benguela Current off South West Africa. Investl Rep.mar. Res.Lab.S.W.Afr. 12: 1-43.

STERNBERG,R.W. and McMANUS,D.A. 1972. Implications of sediment dispersal from long-term, bottom-current measurements on the continental shelf of Washington. In: SWIFT,D.J.P., DUANE,D.B. and PILKEY,O.H. eds. Shelf sediment transport: process and pattern. Stroudsburg: Dowden, Hutchinson and Ross. 181-194.

STOCKEN,C.G. 1962. The diamond deposits of the Sperrgebiet, South West Africa. Field excursion guide, 5th Ann.Congr.geol.Soc.S.Afr. 1-16.

SUMMERHAYES,C.P. 1972. Aspects of the mineralogy and geochemistry of Agulhas Bank sediments. Tech.Rep.S.Afr.nat.Comm.oceanogr.Res.mar.Geol.Progm. 4: 64-81.

SUMMERHAYES,C.P., BIRCH,G.F. and ROGERS,J. 1971. Distribution of phosphate in sediments. Tech.Rep.S.Afr.nat.Comm.oceanogr.Res.mar.Geol.Progm. 3: 77-81.

SUMMERHAYES,C.P., BIRCH,G.F., ROGERS,J. and DINGLE,R.V. 1973. Phosphate in sediments off southwestern Africa. Nature Lond. 243: 509-511.

SUMMERHAYES,C.P., HOFMEYR,P.K. and RIOUX,R.H. 1974. Seabirds off the southwestern coast of Africa. Ostrich. 45: 83-110.

SVERDRUP,H.U., JOHNSON,M.W. and FLEMING,R.H. 1942. The oceans, their physics, chemistry and general biology. New York: Prentice-Hall.

SWIFT,D.J.P. 1970. Quaternary shelves and the return to grade. Mar.Geol. 8: 5-30.

SWIFT,D.J.P. 1974. Continental shelf sedimentation. In: BURK,C.A. and CLARKE,C.L. eds. The geology of continental margins. New York: Springer-Verlag. 117-135.

SWIFT,D.J.P., STANLEY,D.J. and CURRAY,J.R. 1971. Relict sediments on continental shelves: a reconsideration. J.Geol. 79(3): 322-346.

TANKARD,A.J. 1974a. Petrology and origin of the phosphorite and aluminium phosphate rock of the Langebaanweg-Saldanha area, South-Western Cape Province, South Africa. Ann.S.Afr.Mus. 65(8): 217-249.

TANKARD,A.J. 1974b. Varswater Formation of the Langebaanweg-Saldanha area, Cape Province. Trans.geol.Soc.S.Afr. 77: 265-283.

TANKARD,A.J. 1975a. The marine Neogene Saldanha Formation. Trans.geol.Soc.S.Afr. 78(2): 257-264.

TANKARD,A.J. 1975b. Late Pleistocene molluscs from the south-western Cape Province, South Africa. Ann.S.Afr.Mus. 69(2): 17-45.

TANKARD,A.J. 1976a. The Late Cenozoic history and palaeoenvironments of the coastal margin of the South-Western Cape Province, South Africa. Unpubl.Ph.D. thesis, Geol.Dept., Rhodes Univ., Grahamstown.

TANKARD,A.J. 1976b. Cenozoic sea level changes: a discussion. Ann.S.Afr.Mus. 71: 1-17.

TANKARD,A.J. 1976c. Pleistocene history and coastal morphology of the Ysterfontein-Elands Bay area, Cape Province. Ann.S.Afr.Mus. 69(5): 73-119.

TANKARD,A.J. and SCHWEITZER,F.R. 1974. The geology of Die Kelders cave and environs: a palaeoenvironmental study. S.Afr.J.Sci. 70: 365-369.

TERRY,R.D. and CHILINGAR,G.V. 1955. Charts for estimating percentage composition of rocks and sediments. J.sedim.Petrol. 25: 229-234.

THERON,J.C. 1970. Some geological aspects of the Beaufort Series in the Orange Free State. Unpubl.Ph.D. thesis, Univ.Orange Free State, Bloemfontein.

THERON,J.C. 1973. Sedimentological evidence for the extension of the African continent southwards during the Late Permian-Early Triassic times. Proc. 3rd I.U.G.S. Gondwanaland Symp. Canberra. 61-71.

TOOMS,J.S., SUMMERHAYES,C.P.and CRONAN,D.S. 1969. Geochemistry of marine phosphate and manganese deposits. Oceanogr.mar.Biol. 7: 48-100.

TRIMBLE,S.W. 1973. A geographic analysis of erosive land use in the Southern Piedmont. Unpubl.Ph.D. thesis, Univ. Georgia.

TRIPP,R.T. 1975. South African Sailing Directions. Volume II. The coasts of South West Africa and the Republic of South Africa from the Kunene River to Cape Hangklip. Kenwyn: Hydrographer, South African Navy. 1-223.

TRUEMAN,N.A. 1971. A petrological study of some sedimentary phosphorite deposits. Bull.Austral.miner.Dev.Labs. 11: 1-65.

TURNER,B.R. 1970. Facies analysis of the Molteno sedimentary cycle. In: HAUGHTON, S.W. ed. Proc. 2nd I.U.G.S. Gondwanaland Symp. Pretoria: C.S.I.R. 313-319.

TURNER,B.R. 1972. Silica diagenesis in the Molteno sandstone. Trans.geol.Soc. S.Afr. 75: 55-66.

TURNER,B.R. 1975. The stratigraphy and sedimentary histories of the Molteno Formation in the main Karroo Basin of South Africa and Lesotho. Unpubl.Ph.D. thesis, Univ. Witwatersrand.

UNTERÜBERBACHER,H.K. 1964. Zooplankton studies in the waters off Walvis Bay with special reference to the copepoda. Investl Rep.mar.Res.Lab.S.W.Afr. 11: 1-42.

VAN ANDEL,Tj.H. 1967. The Orinoco delta. J.sedim.Petrol. 37(2): 297-310.

VAN ANDEL,Tj.H. and CALVERT,S.E. 1971. Evolution of sediment wedge, Walvis shelf, Southwest Africa. J.Geol. 79: 585-602.

VAN DER MERWE,C.R. and HEYSTEK,H. 1955a. Clay minerals of South African soil groups: II. Sub-tropical black clays and related soils. Soil Sci. 79: 147-158.

VAN DER MERWE,C.R. and HEYSTEK,H. 1955b. Clay minerals of South African soil groups. III. Soils of the desert and adjoining semi-arid regions. Soil Sci. 80: 479-494.

VAN DER MERWE,C.R. and HEYSTEK,H. 1956. Clay minerals of South African soil groups. IV. Soils of the temperate regions. Soil Sci. 81: 399-414.

VAN IEPEREN,M.P. 1975. Characteristics of wave fields at Walvis Bay, Lüderitz, Mossel Bay and the weathership: A preliminary survey. Rep.nat.Res.Inst. Oceanol.S.Afr. Sea/75/1: 1-10.

VAN IEPEREN,M.P. 1976. Characteristics of wave fields recorded along the western coast of southern Africa. Proc. 1st interdisciplinary Conf.mar.freshwater Res.S.Afr. Fiche 8 G12-9B9.

VAN SCHAIK,C., HARPER,A. and VAN DER WESTHUIZEN,B. 1970. Wave conditions for the South West Africa coastal area. Rep.Coun.sci.industr.Res.S.Afr. MEG 945, Series MEW/127: 1-47.

VAN STRAATEN,L.M.J.U. 1965. Sedimentation in the northwestern part of the Adriatic Sea. In: WHITTARD,W.F. and BRADSHAW,R. eds. Submarine geology and geophysics - Proc.Symp.Colston Res.Soc. 17: 143-162.

VAN WARMELO,W. 1922. Hydrography of the Orange River. S.Afr.Irrigation Mag. 1(4): 172-174.

VAN ZINDEREN BAKKER,E.M. Sr. 1967. Upper Pleistocene and Holocene stratigraphy and ecology on the basis of vegetation changes in sub-Saharan Africa. In: BISHOP,W.W. et al. eds. Background to evolution in Africa. Chicago: University of Chicago, 125-147.

VAN ZINDEREN BAKKER,E.M. Sr. 1975. The origin and palaeoenvironment of the Namib Desert biome. J.Biogeogr. 2: 65-73.

VAN ZINDEREN BAKKER,E.M. Sr. 1976. The evolution of Late-Quaternary palaeoclimates of Southern Africa. In: VAN ZINDEREN BAKKER,E.M. Sr ed. Palaeoecology of Africa 9: 1-46. Cape Town: Balkema.

VAN ZINDEREN BAKKER,E.M. Sr and BUTZER,K.W. 1973. Quaternary environmental changes in southern Africa. Soil Sci. 116(3): 236-248.

VARIAN TECHTRON. 1973. Instruction manual for model AA-7 atomic absorption spectrophotometer. Melbourne: Varian Techtron.

VEEH,H.H., BURNETT,W.C. and SOUTAR,A. 1973. Contemporary phosphorites on the continental margin of Peru. Science. 844-845.

VEEH,H.H., CALVERT,S.E. and PRICE,N.B. 1974. Accumulation of uranium in sediments and phosphorites on the South West African shelf. Mar.Chem. 2(3): 189-202.

VEEH,H.H. and CHAPPELL,J. 1970. Astronomical theory of climatic change: support from New Guinea. Science. 167: 862-865.

VISSER,G.A. 1970. The oxygen-minimum layer between the surface and 1000 m in the north-eastern South Atlantic. Bull.Div.Sea Fish.S.Afr. 6: 10-22.

VISSER,G.A., KRUGER,I. and COETZEE,D.J. 1973. Environmental studies in South West African waters. Abstr.S.Afr.nat oceanogr.Symp. 25-26.

VON BACKSTRÖM,J.W. 1964. The geology of an area around Keimoes, Cape Province, with special reference to phacoliths of charnockitic adamellite-porphyry. Mem.geol.Surv.S.Afr. 53: 1-218.

VON BACKSTRÖM,J.W. and DE VILLIERS,J. 1972. The geology along the Orange River valley between Onseepkans and the Richtersveld. Expl. sheets 2817D (Vioolsdrif) 2818C and D (Goodhouse) and 2819C (Onseepkans) geol.Surv.S.Afr. 1-101.

WAGNER,P.A. 1914. The Diamond Fields of Southern Africa. Johannesburg: The Transvaal Leader. (1961 reprint: Cape Town: Struik).

WAGNER,P.A. 1916. The geology and mineral industry of South West Africa. Mem.geol. Surv.S.Afr. 7: 1-234.

WAGNER,P.A. and MERENSKY,H. 1928. The diamond deposits on the coast of Little Namaqualand. Trans.geol.Soc.S.Afr. 31: 1-41.

WALCOTT,R.J. 1972. Past sea levels, eustasy, and deformation of the earth. Quatern.Res. 2: 1-14.

WALKER,T.R. and HONEA,R.M. 1969. Iron content of modern deposits in the Sonoran Desert: A contribution to the origin of red beds. Bull.geol.Soc.Am. 80: 535-544.

WATSON,A.C. 1930. The guano islands of southwestern Africa. Geogr.Rev. 20: 631-641.

WELLINGTON,J.H. 1933. The middle course of the Orange River. S.Afr.geogr.J. 16: 58-68.

WELLINGTON,J.H. 1955. Southern Africa - a geographical study. Vol. 1. Physical geography. Cambridge: Cambridge University Press.

WIEGEL,R.L. 1964. Oceanographical Engineering. Englewood Cliffs, N.J.: Prentice-Hall.

WILLIAMS,M.A.J. 1975. Late Pleistocene tropical aridity synchronous in both hemispheres? Nature Lond. 253: 617-618.

WILSON,I.G. 1971. Desert sandflow basins and a model for the development of ergs. Geogr.J. 137(2): 180-199.

WILSON,I.G. 1972. Sand waves. New Scientist. 23 March: 634-637.

WRIGHT,J.A. 1964. Gully pattern and development in wave-cut bedrock shelves north of the Orange River mouth, South West Africa. Trans.geol.Soc.S.Afr. 67: 163-171.

WRIGHT,L.D. and COLEMAN,J.M. 1973. Variations in morphology of major river deltas as functions of ocean wave and river discharge. Bull.Am.Ass.petroleum Geol. 57(2): 370-398.

WRIGHT,L.D. and COLEMAN,J.M. 1974. Mississippi river mouth processes: effluent dynamics and morphologic development. J.Geol. 82: 751-778.

ZOUTENDYK,P. 1973. The biology of the Agulhas sole, Austroglossus pectoralis. Part I. Environment and trawling grounds. Trans.R.Soc.S.Afr. 40(5): 349-366.

APPENDICES

A. SHIPBOARD TECHNIQUES

1. Navigation

Although DECCA navigation was available during the cruises through the study area, it was considered unreliable and erratic during the earlier cruises. As a result celestial and dead-reckoning methods of navigation were employed in the southern half of the area. The accuracy of positions obtained using these methods varies from 2-10 km depending on weather conditions during periods of observation. During the day the accuracy of DECCA is 2 km, but the variations in the layers of the ionosphere after nightfall causes accuracy to deteriorate. The system is considered to be satisfactory within 350 km of a master station during the day, and within 220 km at night. Towards the fringes of its range the hyperbolae's intersections become so oblique that it is difficult to pinpoint one's position.

Within 30 km of the coast radar was used to measure ranges to pairs of coastal landmarks. Most of the coast is rocky with numerous distinctive indentations and promontories, but difficulty was experienced off the low straight coastline between the Orange River and Chamais Bay. A further problem arose north of Lüderitz, where the coast is sometimes formed of high cliffs of dune sand, a poor reflector of radar emissions. This problem was eased by the presence of substantial stretches of rocky cliffs between the sections of dune coast. Generally good weather and weak currents enabled the ship's officers to keep to the planned traverses in most instances.

2. Echo sounding

Echograms were obtained from both the main and daughter set of a 12 kHz ELAC echosounder. A transducer width of 36 cm produced a wide beam of approximately 20^{o}. The echograms are therefore subject to some error in areas of high relief and on steep slopes. However, most of the study area exhibited subdued relief and gentle gradients both on the shelf and on the upper slope. The echograms were routinely annotated at 15-minute intervals, at the beginning and end of each station, and at course and speed alterations.

3. Sampling of unconsolidated sediments

An analysis of sampling operations is given in Table XI-1, where it is seen that 455 sediment samples were recovered by the "Thomas B. Davie" from the continental margin in the study area. Data were used from 91 grab samples recovered from the inner shelf by the Marine Diamond Corporation (O'Shea, 1971, Table 1). In addition 45 beach samples, 42 river samples and 35 dune samples were included in the study. The total number of samples involved therefore numbered 668.

TABLE APPENDIX-1

Analysis of sampling operations

Gear	Stations occupied	Unconsolidated sediments	Semi-consolidated sediments	Rocks	Unsuccessful
Grab	314	286	-	26	19
Small Gravity Corer	156	151	17	6	3
Rock Dredge	29	16	-	10	5
Large Gravity Corer	2	2	-	-	-
All types	501	455	17	41	27

286 samples were taken with a galvanised Van Veen grab, modified in its trip mechanism according to a Kiel-University design. A hinged T-bar fits into a slot and is released on impact with the sea floor. This modification prevented premature closure and was the chief reason that the sample recovery was as high as 91%. The grab was used mainly on the inner and middle shelves. The amount of sample varied according to the texture of the sediment. For example, approximately 2 litres would be obtained from the compact, very fine sand of the Orange delta front, whereas approximately 10 litres of watery silty clay were regularly obtained from the prodelta. The subject of variability in both sample size and depth of penetration is discussed by Christie (1975).

151 samples of unconsolidated sediment were recovered using a small gravity corer. The success rate was 98% proving the corer's reliability in the deep waters of the outer shelf and the upper slope. However, the largest sample was a core less than 0,5 m long, and the smallest samples were inadequate for anything more than microscopic examination. The core tube was made of copper, the cutting edge was made of steel and the core-catcher was made of PVC plastic.

4. Sampling of semi-consolidated sediments

Seventeen samples of semi-consolidated sediments were sampled with the small gravity corer, proving that in some areas of the margin unconsolidated sediment

was either absent or only a few centimetres thick.

5. Sampling of bedrock

Rock samples were recovered using the grab (26), dredge (10) and small gravity corer (5). However, the dredge recovered much larger samples and sometimes a variety of rock types was encountered. This variety was due to the procedure of dredging for at least 10 minutes once uneven bottom was encountered. At a dredging speed of 2 knots approximately 0,5 km of sea floor was thus traversed while dredging.

6. Storage of samples

Samples of unconsolidated and semi-consolidated sediment were stored wet either in air-tight, 2,5-litre plastic tubs or in 200 ml screw-top plastic jars. Rock samples were usually stored in heavy-gauge plastic fertilizer bags.

7. Processing of unconsolidated sediments

Although most samples were analysed in the laboratory some sediments were partially analysed on board during the later cruises. On these cruises each subsample was wet-sieved with a 63µm sieve to remove the silt and clay fractions. The coarse fraction was then examined under a binocular microscope and an estimate of the abundance of the various components noted on a card. A second subsample was dialysed for at least 12 hours and transferred to a 200 ml screw-top plastic jar for chemical analyses in the laboratory. A third subsample was also dialysed and then wet-sieved as above. The fine fraction was retained in a 1-litre plastic bottle for pipette analyses ashore; the coarse fraction was stored in a 200 ml plastic jar and later sieved in the laboratory.

B. LABORATORY TECHNIQUES

1. Bathymetry

A series of base maps was compiled at a scale of 1:150 000 from South African Charts SAN 109-114. Navigational data from the bridge log kept by the ship's officers were transferred to the base maps. The tracks between stations were divided into segments equal to the distance travelled in 5 minutes. Uncorrected depth readings were read from the echograms at 5-minute intervals and then transferred to their positions on the plotted tracks. Two copies of each base map were then made and tracks from one copy pasted over tracks on the other copy after adjusting the tracks to reduce depth differences at track intersections. Because DECCA navigation was only working satisfactorily during later cruises, the latitudinal tracks of the earlier cruises were adjusted to match depths on longitudinal tracks of the later cruises.

Isobaths were drawn at 10-metre intervals to 500 m and at 100 m intervals below 500 m on the upper slope. Although the base maps were all drawn at a natural scale of 1:150 000, the central latitude of each individual chart was used in the scale calculation. As the end-result was to be a 1:1 000 000 map at latitude 33°S, a 15-minute, 1:150 000 grid at latitude 33°S was generated by computer. The contours were transferred to this grid and then reduced photographically to a scale of 1:1 000 000 to fit a computer-generated, 15-minute, 1:1 000 000 grid calculated at latitude 33°S.

Bathymetric profiles along 30 latitudinal traverses were constructed by tracing main-set echograms, omitting periods on station. In tracing and reducing these profiles, significant detail was lost. To record this detail, selected portions of both main-set and daughter-set echograms were traced and presented unreduced.

Slope changes and various morphological features were recognised on the echograms and transferred to the tracks on the 1:150 000 base map. A morphogenetic map was constructed by reducing these data.

Shelf gradients were calculated by measuring the perpendicular distance, in nautical miles, from the coast to the inflexion of the deepest shelf break. The depth of the inflexion in metres below sea level, divided by the distance to the coast in kilometres, gave the gradient in metres per kilometre. When this ratio was multiplied by 10^3 its arc tangent gave the gradient in degrees.

Using the same procedure, the slope gradient was calculated by measuring the horizontal distance between the same shelf-break inflexion and the seaward end of the traverse. In most cases the traverses are perpendicular to the slope contours. In some cases the traverses are oblique and the slope gradient was measured between the inflexion and the seaward end of a neighbouring traverse to make the line normal to the isobaths. The difference in depth between the two points gave the vertical distance in metres.

2. Petrography of bedrock samples

All rock samples were examined qualitatively, but only selected samples were thin-sectioned and examined petrographically. A distinction was drawn between rocks from the Precambrian outcrop beside the coast and post-Palaeozoic sediments farther offshore. It was decided to omit the Precambrian rocks from a reconnaissance petrographic study, because of their insignificance to the sedimentary history of the region, the wide spacing of the samples, the structural and lithological complexity of many of the formations and the narrowness of the outcrop adjacent to a well-exposed hinterland. In contrast, the broad facies of the post-Palaeozoic sediments are persistent over large areas, therefore justifying the study of widely-spaced samples.

Selected post-Palaeozoic samples were thin-sectioned and the abundance of the various rock components estimated using a petrographic microscope and standard comparison charts (Terry and Chilinger, 1955).

3. Micropalaeontology of semi-consolidated Cenozoic sediments

Seventeen samples of semi-consolidated sediments have been examined by one or more of the following specialists: I.G. McMillan of SOEKOR (microfossils); R.P. Stapleton of the Geological Survey (microfossils and nannofossils); and W.G. Siesser of the Joint Geological Survey/University of Cape Town Marine Geoscience Unit (nannofossils). Stapleton (personal communication, 1974) commented on the high degree of mixing of both younger fauna from the overlying unconsolidated sediment and of specimens reworked from older strata. As a result he frequently recorded a Quaternary assemblage of foraminifera associated with a Neogene assemblage of nannofossils.

Except for sample 3387, McMillan (personal communication, 1974) assigned an outer-shelf/slope environment of deposition to all the samples he examined. Sample 3387 contained inner-middle shelf fauna (Ammonia beccarii, Cibicides lobatulus and Elphidium macellum). Samples 3207, 3208, 3257, 3360, 3375 and 3386 contained Ammonia beccarii in otherwise deep-water assemblages, but the reason for its presence in such deep water is not clear.

Each of the specialists concluded that most of the species indicated cool temperatures similar to those prevailing today. McMillan (personal communication, 1974) considered that species such as Globigerinoides trilobus, G. cf. succulifer and ?Globigerina riveroae indicated higher temperatures during deposition of samples 3016D, 3016GC and 3024.

The majority of the sediments have Tertiary, chiefly Neogene ages, thus confirming interpretations of the available seismic profiles that Neogene strata crop out on the outer shelf and on the upper slope (Du Plessis et al., 1972; Dingle, 1973).

4. Sedimentology of all unconsolidated marine sediments

a. Storage and subsampling

The bulk samples were stored wet because the majority are muddy and aggregate severely on drying. The sediments were subsampled with a plastic tube to obtain a vertical core through the sample.

b. Desalting

Two desalting procedures were used. Initially subsamples were diluted with tap water and the excess water removed via a 0,3µm candle filter under vacuum.

Later the simpler and much more effective dialysis method was used to desalt subsamples overnight in cellophane tubes hung in a tub of tap water. Accumulated salt was continuously siphoned from the bottom of the tub while a fresh supply of water maintained the overall volume.

c. Textural and component analysis

A second subsample was desalted and then wet-sieved through a 63µm sieve to separate the coarse and fine fractions. The fine fraction was pipetted according to standard procedures (British Standards Institution, 1963; 1967) to determine the silt and clay contents. The coarse fraction was separated into sand and gravel fractions by hand-sieving. A binocular-microscope examination of the latter fractions produced qualitative data on the regional distribution of coarse-fraction components.

d. Faecal pellet and glauconite determinations

Faecal pellets were removed from the sand fraction by soaking the sediment in sodium hypochlorite and disaggregating the pellets in an ultrasonic bath. The disaggregated pellets were washed through a 63µm sieve. Glauconite was separated magnetically from the remaining material by means of a Franz Isodynamic Separator using settings recommended by Birch (1971).

e. Phosphate and potash analyses

A third subsample was sent to the laboratories of the Phosphate Development Corporation in Phalaborwa, Transvaal, where the phosphate (P_2O_5) content was determined by a standard vanado-molybdate colorimetric method. The potash (K_2O) content was determined by X-Ray fluorescence spectrophotometry. Summerhayes (1971) has ascertained that the P_2O_5 analyses have a standard deviation of 0,1, 0,4 and 0,5% at the 15,0, 5,0 and 0,5% P_2O_5 concentrations, whereas Birch (1975) found a precision of approximately 5% for all concentrations of K_2O. In addition to the routine analyses on all samples of unconsolidated sediment, additional P_2O_5 analyses were performed on sand fractions of the same samples.

f. Analysis for organic carbon and calcium carbonate

One subsample was dried and crushed after desalting and then analysed for organic carbon and calcium carbonate. Organic carbon was determined using wet-oxidation of the sediment by hot chromic acid, followed by titration of the excess acid against ferrous sulphate (Morgans, 1956). Calcium carbonate content was measured by gasometry (Hülsemann, 1966; Siesser and Rogers, 1971).

5. Texture and sand-size components along six traverses across the continental margin

a. Removal of faecal pellets and size analysis

Fresh subsamples were taken from 80 samples along six traverses selected from thirty sampling traverses across the continental margin. Each subsample was wet-sieved and the fine fraction (<63μm) dried and sent to Phalaborwa for phosphate analysis by colorimetry and for potash analysis by atomic absorption spectrophotometry. (The change of analytical method for potash occurred in September, 1974).

Faecal pellets were removed from the coarse fraction by an improved method devised by Bremner (1975a, p.59) and assessed by Birch (1975, p.121). The pellets are disintegrated by oxidizing their organic binding material in warm hydrogen peroxide and then washed through a 63μm sieve. The process was restricted to those samples in which the presence of faecal pellets had been established by binocular-microscope examination. This restricted the recording of false values in sediments free of faecal pellets, determined by Birch (1975) to be as high as 12%. The false values are attributed to the release of organically bound coatings of fines on and in sand-size particles.

The percentage of faecal pellets was calculated from the loss in weight of the coarse fraction after the hydrogen-peroxide treatment. The percentage was then added to the previously determined percentage of mud (silt plus clay). The resultant value is termed "mud plus faecal pellets" and represents the amount of mud in the sediment before a proportion was reworked into sand-size faecal pellets by burrowing polychaete worms such as Diopatra monroi and Lumbrineris heteropoda difficilis (Christie, 1975, p.95).

The treated coarse fractions were then dried and sieved at half-phi intervals for 10 minutes. Size statistics for the coarse fraction and the proportions of sand-size phi fractions in the sediment as a whole were determined by computer. The programme was originally written by R. Lefever of the Department of Geology at the University of California, Los Angeles and was modified by G.J. Moir of the Department of Geology at the University of Cape Town.

b. Coarse-fraction component analysis

Half-phi fractions of the coarse fraction were combined into 329 phi-fractions after sieving and stored in glass vials. Some fractions contained so few grains that each grain was counted. Other fractions were split with a microsplitter (Humphries, 1961) to a subsample of a few thousand grains, which were strewn over a gridded counting tray. A line count of up to 34 components was made of all grains lying on the longer set of parallel grid lines. When such a

procedure produced totals less than 100, grains were counted along the shorter lines perpendicular to the first set, in order to exceed the minimum number.

The number frequencies obtained were converted to number percentages of the phi-fraction concerned, and then plotted along traverses. The sets of component data for each phi-fraction were accompanied by the weight percentages for the individual phi-fractions. This method of presentation was adopted in preference to the illustration of the component data as weight percentages of the entire sediment, in order to cope with the components present in small quantities in the coarse and fine extremes of the sediment. Errors inherent in the number percentage concept were minimized by counting within individual phi-fractions rather than within unsieved sand fractions of widely varying grain size (Galehouse, 1971, p.394).

A minimum grain number of 100 was obtained in 94% of the fractions studied, but the number of grains counted per fraction varied from 1 to 1129. The total number of grains counted was 88 124 in 329 phi-fractions, leading to a mean of 268 grains counted per fraction. The variability in grain numbers per fraction is inherent in the line-counting method, which requires that grains be counted on a grid traversing the entire grainspread (Galehouse, 1971, p.392).

The above method differs from that adopted by Shepard (1973) by usually exceeding the 100 grains recommended and by more rigorous selection of those grains along lines rather than near grid intersections. However, the method is less rigorous than that of Sarnthein (1971) who counted 500-800 grains in each phi-fraction and of Diester-Haass et al. (1973) who counted 800-1000 grains per fraction. In addition the above authors all multiplied the number percentages of each component by the weight percentage of the phi-fraction concerned. Einsele and Werner (1972) refined the process further by determining the weights of 20-50 grains of each component in each phi-fraction before calculating the weight percentages of the components.

The adopted method was chosen as a compromise between the less rigorous "Shepard" method and the extremely rigorous "Sarnthein" or "Kiel" method, to satisfy the requirements of a subsection of this thesis. Thin-sectioning of unsieved, artificially consolidated sand fractions as practised on Agulhas Bank sediments by Siesser (1972b) was rejected, not only because of the difficulty in producing large numbers of thin sections, but also because the method produces poor counting statistics for the extremes of the size distribution. In addition Siesser (1972b) was studying sediments rich in non-foraminiferal skeletal carbonate debris, whereas the writer's samples were relatively poor in such material and most components were readily identifiable under the binocular microscope.

6. Analysis of the clay fraction (<2μm)

a. Separation

Fresh subsamples of 44 marine and of 8 river sediments were dialysed, emptied into 2,5 litre plastic tubs and diluted with 1 litre of distilled water. By a process of repeated settling, siphoning, dilution and agitation, controlled by pipetting tables, the clay fractions (<2μm) were separated from the coarser fractions into a second set of tubs.

b. Concentration

The tubs were sealed and each fraction was allowed to settle for 2-3 weeks, when the supernatant water was siphoned off. Each fraction was further concentrated by homogenizing the suspension and transferring it to a 4-tube centrifuge. Each fraction was then centrifuged and the centrifugate divided into two portions by emptying the contents of opposing pairs of tubes into separate 250 ml plastic, capped bottles.

c. X-ray diffraction (XRD)

i) Removal of carbonate

The XRD fractions were transferred to 250 ml glass beakers and treated with 50 ml of 30% acetic acid overnight to remove carbonate. Excess acid was removed by centrifuging and each sample then washed by centrifuging twice more with distilled water. The leached, washed fractions were each returned to the beakers and made up to 100 ml with tap water.

ii) Removal of organic matter

Organic matter was removed by adding 25 ml of 30% hydrogen peroxide (H_2O_2) dropwise to each fraction, heating gently on a waterbath and swirling continually. Over-vigorous frothing was subdued by reducing the surface tension with a single drop of octanol. A further 25 ml H_2O_2 were added to check the completeness of the reaction and the process repeated. Excess H_2O_2 was then removed by centrifuging as described above. Four drops of dilute (1:1) hydrochloric acid (HCl) were added to flocculate the clay where necessary.

iii) Magnesium saturation

Each fraction was transferred to a 250 ml conical flask and made up to 150 ml with tap water. The pH was adjusted to between 3,5 and 4,0 with the aid of dilute HCl and litmus paper. Fifty millilitres of 3N $MgCl_2$ solution were added to each suspension, thus reducing the normality to 1N. The flasks were then sealed with rubber stoppers, lined with thin plastic and agitated gently in batches of 12 on a shaker for 4 hours. Excess $MgCl_2$ solution was then removed by centrifuging, as described previously, and each prepared fraction stored in capped, glass vials.

iv) Slide preparation

An oriented slide was prepared for each fraction by adding homogenized suspension to the slide with an eye-dropper and drying the clay rapidly at a temperature of 50°C in an oven. Just prior to diffraction each slide was painted with ethylene glycol following a procedure established by Birch (1975, p.138).

Because the aim of the study was merely to establish broad regional trends in the distribution of clay minerals, only glycolated slides were prepared. This eliminated analysis of both heated and unheated unglycolated fractions.

v) X-ray diffraction

Procedures followed by Birch (1975) when diffracting clays from the shelf south of the study area were adopted to facilitate inter-area comparison. A Phillips X-ray diffractometer, fitted with a Geiger counter and using nickel-filtered Cukα radiation was employed to analyse the pre-treated fractions.

Instrument settings were:

Kv: 48

mA: 20

Attenuation: 2

Proportional counter: 45

Rate meter: 4×10^2; 1×10^3

Time constant: 1

Windows: $1^\circ/0$, 1 mm/1°

Each fraction was scanned at a speed of $1^\circ 2\theta$/minute from 2° - $13^\circ 2\theta$.

vi) Identification of clay minerals

The following basal reflections from X-ray diffractograms of glycolated slides were assigned to the various clay minerals:

17Å: Montmorillonite

10Å: Illite

7Å: Kaolinite plus chlorite

Birch (1975, p.139) has described the difficulties of distinguishing kaolinite from chlorite, but found only minor quantities of chlorite in the clays south of the study area. Similarly, Bremner (1975c, p.47) has reported an absence of chlorite in most clays from the shelf north of the study area. For the limited purposes of this section of the study, only the abundance of 7Å material has been recorded, with the strong likelihood that the bulk of such material is, in fact, kaolinite.

vii) Semi-quantitative determination of clay-mineral abundances.

After drawing a base line for each diffractogram, the areas beneath each of the 17Å, 10Å and 7Å peaks were determined and the mineral proportions calculated using the form factors suggested by Johns, Grim and Bradley (1954):

Montmorillonite: X1

Illite: X4

Kaolinite plus chlorite: X2

d. Atomic-absorption spectrophotometry (AAS)

i) Powdering of fraction

Each AAS subsample was dried in an oven at 150°C. A large agate mortar was then cleaned with tap water and dilute HCl using paper towels, and then with double-distilled water and acetone using tissues. After hand-crushing each sample was transferred to a vial using a piece of glossy paper.

ii) Solution preparation

Duplicate solutions of each fraction were prepared employing a technique involving a more powerful combination of acids than that used earlier by Birch (1975, p.143) in his study of sediments south of the study area. The need to adapt the technique arose from the relatively higher content of organic matter in the sediments. Unfortunately the ability of the initial nitric acid/perchloric acid combination to dissolve platinum in the presence of chloride required the use of firstly a glass beaker and then a platinum crucible, with the inevitable errors involved in adding the extra operations of transferring and evaporation. More time was also required for what was already a time-consuming procedure. (Since these analyses have been completed a fully automated X-ray fluorescence spectrophotometer has been installed in the Geochemistry Department at the University of Cape Town. It is felt strongly that such an instrument is much more suitable for clay-fraction analysis by eliminating dissolution problems, by running its own standards, and by being fully computer-compatible. As a result it is less prone to operator error, is much simpler in operation, and is considerably faster.)

For each batch of 6 samples, including one blank, six 50 ml Pyrex glass beakers were boiled in dilute HCl, washed with double-distilled water and dried with ANALAR acetone. Where possible, 0,500 g of crushed clay was weighed into each numbered beaker. (When insufficient clay was available the quantities were halved or quartered to facilitate calculations of the quantities of reagents required). To dissolve calcium carbonate and organic matter 10 ml of a 1:4 solution of concentrated (71-73%) perchloric acid (conc. $HClO_4$) and concentrated (65%) nitric acid (conc. HNO_3) were added to the clay. The sample was then evaporated to dampness on a hot plate in a fume cupboard.

Numbered platinum crucibles were cleaned by boiling in dilute HCl and washing in double-distilled water. Each residue was then transferred quantitatively to a crucible, using a rubber policeman and double-distilled water from a wash bottle to remove all fragments from the beaker. Excess water was then evaporated on a hot plate.

Ten millilitres of 40% hydrogen fluoride (HF) and then 10 ml of conc. $HClO_4$ were added to each crucible. On heating, silicates are dissolved by the HF, and when white fumes appear towards the end of the process, silica volatilizes as silica fluoride which is catalyzed by decomposition products of $HClO_4$. Once fuming ceased, the crucibles were removed from the hot plate to prevent baking of the residues.

After cooling, 10 ml of dilute HCl were added to each crucible and the final residue dissolved by gentle heating and swirling. A batch of 50 ml volumetric flasks and plastic storage bottles was then washed twice with single-distilled water, once in 70% nitric acid and four times with double-distilled water. The final solutions, after cooling if necessary, were then transferred quantitatively from the crucible to the flask and the solutions made up to 50 ml. Each plastic bottle was labelled and then rinsed three times with small amounts of the solution, before the solution was transferred from the volumetric flask. Each bottle was capped tightly to prevent evaporation and stored in a freezer to hinder adsorbtion of ions on the walls of the bottle.

iii) Instrument operation

The concentrations of five elements (Fe, Mn, Cu, Pb and Zn) were measured using a Varian Techtron Model AA-6. Supervision was initially supplied by Dr. M.J. Orren and subsequently by Dr. G.A. Eagle. The numerous technical details are found in the Varian manual (Varian Techtron, 1973) but the chief instrument settings for the 5 elements are:

Element	Wavelength	Slit Width	Lamp Current	Flame
	nm	nm	mA	
Fe	248,3	0,2	5	Air-acetylene
Mn	279,5	0,2	5	Air-acetylene
Cu	324,8	0,5	3	Air-acetylene
Pb	217,0	1,0	5	Air-acetylene
Zn	213,9	0,5	5	Air-acetylene

iv) Calculation of element concentrations

For each element the blanks were low in the majority of cases, erratic high values being ascribed to contamination from a variety of sources, chiefly from dust raised from building operations near the laboratory. An average blank value from the lower set of values was then used to correct the readings obtained for each element. Standards were made up daily and run before and after every 10 samples. Calibration curves were then drawn up to convert absorbances to concentrations. These values were then corrected using regression coefficients obtained for the elements concerned on clays north of the study area by Bremner (in preparation).

v) Accuracy and precision

Birch (1974, p.145) in his study of the shelf south of 30°S has commented in detail on the precision and accuracy of his AAS data for a series of elements including the five studied. Values for the mean percentage deviation of the concentrations of each element in duplicate solutions confirm Birch's (1975, p.145) findings that Fe and Mn, and in this study also Cu, were much more reproducible than were Pb and Zn.

Element	Mean Percentage Deviation
Fe	6,0
Mn	6,6
Cu	8,4
Pb	19,9
Zn	33,2

7. Dispersal and deposition of terrigenous sediments

a. Texture

The texture of a suite of 46 river, 43 beach, 35 dune and 77 inner-shelf sediments was studied to trace the dispersal and deposition of terrigenous sediment, chiefly from the Orange River, along the coast of the study area. The raw data for the inner-shelf samples were supplied by O'Shea (personal communication) and these data are the best because the coarse fractions were sieved at quarter-phi intervals. The river samples were wet-sieved, the fines pipetted and the coarse fraction dried and sieved at half-phi intervals. The beach and dune samples were dry-sieved at half-phi intervals and contained too few fines to justify pipetting.

The data were computed in the same fashion as described in Section XI-4a, but in this case the moment measures of the coarse fraction were utilized because the sediments were all Recent and terrigenous, unlike the shelf samples, which were frequently mixed both in origin and in age. The computer was instructed only to assess the coarse fraction for two reasons. Firstly the movement of this fraction usually takes place by processes of saltation and creep, rather than by suspension, as in the case of the fines. Secondly the data required to compute statistics for the entire sediment would have necessitated detailed pipette analyses of the fine fraction taking up an unwarranted amount of time. However, because the sediment was artificially truncated, only the first two moment measures (mean and standard deviation) were utilized, the remaining two (skewness and kurtosis) being designed to monitor the tails of the distribution.

Towards the end of the study, a settling tube was constructed by Flemming (1976) and the opportunity was taken of analyzing a suite of 6 river, 1 beach and 6 deltaic sediments. Each sample was wet-sieved to obtain a coarse fraction,

which was then dried and then split with a microsplitter (Humphries, 1961) to a split of 2-3 g. As each split settled through the column, a cumulative curve was drawn instantaneously by a chart recorder. Although the coarse sediments from the mouth of the Orange River settled in little more than a minute, the very fine sand of the delta front took up to 20 minutes to settle. Thereafter the cumulative curve was read at 30 points and the data punched for the prepared programme. Comparison of the first and second moments obtained by sieving and settling the same sediments shows that mean values tend to be very similar, regardless of the method, confirming the observations of Flemming (1976, p.49) concerning quartz-dominated sediments. On the other hand, sorting of the coarser sediments seems to improve with settling, whereas it becomes slightly poorer in the finer deltaic sediments. This slight trend may possibly be attributed to the differing hydraulic properties of coarse irregularly shaped quartz particles and of fine equant grains of heavy minerals.

b. Heavy fraction

The coarse fractions of 3 river, 35 beach and 9 dune samples were placed in bromoform in open funnels and the heavy fraction separated according to standard procedures (Carver, 1971, p.439). Due to the abundance of heavy rock fragments in many samples, the term "heavy fraction" has been used in preference to the more normal term, "heavy minerals". The analyses were conducted on the entire sand fraction to obtain data comparable to that of O'Shea (1971), who also used the entire coarse fraction of his inner-shelf samples. However, O'Shea's suite chiefly comprised well-sorted fine and very fine sands, where heavy minerals are concentrated, whereas the writer's suite included much coarser sediments rich in rock fragments.

c. Calcium carbonate

The carbonate content of 31 beach samples was determined by the gasometric method of Hülsemann (1966).

C. STATION LIST: R.V. "THOMAS B. DAVIE"

TYPE 1 : Grab

" 2 : Gravity core

" 3 : Dredge

" 4 : Long gravity core

LAT. : Latitude, degrees south

LONG. : Longitude, degrees east

DEPTH : Metres

DISTANCE: Nautical miles offshore from nearest part of coast

STATION	TYPE	CRUISE	DATE	LAT.	LONG.	DEPTH	DISTANCE
2729 1	2	257	22: 2:71	29 55.0	14 11.0	1057	138.8
2730 1	2	257	22: 2:71	29 55.0	14 22.0	730	132.2
2731 1	2	257	22: 2:71	29 55.0	14 33.0	480	125.3
2732 1	2	257	23: 2:71	29 56.0	14 43.0	428	119.2
2733 1	2	257	23: 2:71	29 56.0	14 54.0	392	110.0
2734 1	1	257	23: 2:71	29 56.0	15 4.0	312	103.3
2735 1	1	257	23: 2:71	29 56.0	15 14.0	209	95.3
2736 1	1	257	23: 2:71	29 57.0	15 25.0	205	87.4
2737 1	1	257	23: 2:71	29 57.0	15 36.0	195	77.9
2738 1	1	257	23: 2:71	29 57.0	15 48.0	190	67.9
2739 1	1	257	23: 2:71	29 57.0	16 .0	190	57.0
2740 1	1	257	23: 2:71	29 54.0	16 10.0	176	47.8
2741 1	1	257	23: 2:71	29 51.0	16 22.0	169	36.9
2742 1	1	257	23: 2:71	29 46.0	16 35.0	150	25.3
2743 1	3	257	23: 2:71	29 43.0	16 47.0	123	14.0
2744 1	1	257	23: 2:71	29 42.0	16 54.0	110	8.0
2745 1	1	257	23: 2:71	29 41.0	17 .0	80	2.6
2746 1	1	257	24: 2:71	29 55.0	17 1.0	110	5.7
2747 1	3	257	24: 2:71	29 55.0	16 51.0	138	13.8
2748 1	1	257	24: 2:71	29 55.0	16 39.0	160	23.3
2749 1	1	257	24: 2:71	29 55.0	16 28.0	183	32.7
2750 1	1	257	24: 2:71	29 46.0	16 24.0	172	34.5
2751 1	1	257	24: 2:71	29 47.0	16 13.0	180	44.0
2752 1	1	257	24: 2:71	29 47.0	16 1.0	170	54.0
2753 1	1	257	24: 2:71	29 47.0	15 50.0	191	63.6
2754 1	1	257	24: 2:71	29 46.0	15 39.0	195	71.6
2755 1	1	257	24: 2:71	29 45.0	15 27.0	202	80.4
2756 1	1	257	24: 2:71	29 45.0	15 15.0	200	89.4
2757 1	2	257	24: 2:71	29 45.0	15 7.0	270	95.2
2844 1	1	261	13: 5:71	29 46.0	14 56.0	408	103.3
2845 1	2	261	13: 5:71	29 46.0	14 44.0	439	112.3
2846 1	2	261	13: 5:71	29 46.0	14 31.0	640	120.5
2847 1	2	261	13: 5:71	29 45.4	14 18.7	956	127.9
2848 1	2	261	13: 5:71	29 37.0	14 2.0	1495	131.5
2849 1	2	261	13: 5:71	29 37.0	14 16.0	250	122.5
2850 1	2	261	13: 5:71	29 37.0	14 22.0	980	118.8
2851 1	2	261	13: 5:71	29 38.0	14 33.0	481	113.9
2852 1	2	261	13: 5:71	29 38.0	14 44.0	420	106.5
2853 1	2	261	13: 5:71	29 38.0	14 55.0	370	99.5
2854 1	2	261	13: 5:71	29 38.0	15 5.0	280	92.7
2855 1	2	261	14: 5:71	29 38.0	15 16.0	183	85.5
2856 1	2	261	14: 5:71	29 38.0	15 26.0	194	77.1
2857 1	2	261	14: 5:71	29 38.0	15 38.0	180	69.0
2858 1	1	261	14: 5:71	29 38.0	15 49.0	190	60.3
2859 1	1	261	14: 5:71	29 38.0	16 1.0	185	50.8
2860 1	1	261	14: 5:71	29 38.0	16 13.0	170	40.5
2861 1	1	261	14: 5:71	29 38.0	16 25.0	165	31.1
2862 1	1	261	14: 5:71	29 38.0	16 36.0	157	22.1
2863 1	1	261	14: 5:71	29 38.0	16 47.0	130	13.0
2864 1	1	261	14: 5:71	29 38.0	16 52.0	125	8.9

STATION	TYPE	CRUISE	DATE	LAT.	LONG.	DEPTH	DISTANCE
2865 1	1	261	14: 5:71	29 38.0	16 56.0	102	5.2
2866 1	1	261	14: 5:71	29 26.9	16 55.4	77	2.6
2867 1	1	261	14: 5:71	29 27.0	16 44.0	113	12.0
2868 1	1	261	14: 5:71	29 27.0	16 41.0	122	14.0
2869 1	1	261	14: 5:71	29 27.0	16 30.0	145	22.5
2870 1	1	261	14: 5:71	29 27.0	16 19.0	154	31.1
2871 1	1	261	15: 5:71	29 27.0	16 8.0	168	40.0
2872 1	1	261	15: 5:71	29 27.0	15 56.0	177	50.0
2873 1	1	261	15: 5:71	29 28.0	15 45.0	178	58.1
2874 1	1	261	15: 5:71	29 28.0	15 32.0	180	67.8
2875 1	1	261	15: 5:71	29 28.0	15 20.0	197	76.6
2876 1	1	261	15: 5:71	29 29.0	15 8.0	170	84.6
2877 1	2	261	15: 5:71	29 29.0	14 56.0	260	92.7
2878 1	2	261	15: 5:71	29 29.0	14 44.0	342	104.0
2879 1	2	261	15: 5:71	29 29.0	14 33.0	530	106.6
2880 1	2	261	15: 5:71	29 27.0	14 20.0	1026	114.5
2881 1	2	261	15: 5:71	29 16.0	14 16.0	1000	107.4
2882 1	2	261	15: 5:71	29 17.0	14 25.0	655	103.1
2883 1	2	261	15: 5:71	29 18.0	14 34.0	386	97.9
2884 1	2	261	15: 5:71	29 19.0	14 43.0	252	93.8
2885 1	2	261	16: 5:71	29 20.0	14 52.0	208	88.9
2886 1	3	261	16: 5:71	29 21.0	15 1.0	166	84.5
2887 1	3	261	16: 5:71	29 22.0	15 10.0	165	78.4
2888 1	3	261	16: 5:71	29 17.0	15 .0	204	81.8
2889 1	2	261	16: 5:71	29 17.0	15 9.0	172	76.0
2890 1	3	261	16: 5:71	29 17.0	15 18.0	180	70.2
2891 1	2	261	16: 5:71	29 17.0	15 28.0	192	63.8
2892 1	3	261	16: 5:71	29 17.0	15 39.0	180	56.5
2893 1	2	261	17: 5:71	29 17.0	15 48.0	178	49.8
2894 1	1	261	17: 5:71	29 17.0	15 58.0	170	41.8
2895 1	1	261	17: 5:71	29 17.0	16 8.0	169	34.5
2896 1	1	261	17: 5:71	29 17.0	16 18.0	155	27.2
2897 1	3	261	17: 5:71	29 17.0	16 27.1	139	20.8
2898 1	1	261	17: 5:71	29 17.0	16 38.9	125	11.1
2899 1	1	261	17: 5:71	29 17.7	16 51.5	62	1.6
2900 1	3	261	17: 5:71	29 6.2	16 44.8	68	3.1
2901 1	1	261	17: 5:71	29 8.0	16 40.0	100	7.8
2902 1	1	261	17: 5:71	29 7.0	16 34.0	124	10.9
2903 1	1	261	17: 5:71	29 7.0	16 23.0	135	19.0
2904 1	3	261	17: 5:71	29 7.0	16 25.0	130	17.5
2905 1	1	261	17: 5:71	29 7.0	16 13.0	148	25.4
2906 1	1	261	17: 5:71	29 7.0	16 5.0	165	31.3
2907 1	1	261	17: 5:71	29 8.0	15 54.0	170	40.5
2908 1	1	261	17: 5:71	29 8.0	15 45.0	175	47.0
2909 1	1	261	17: 5:71	29 9.0	15 34.0	182	54.6
2910 1	1	261	17: 5:71	29 9.0	15 22.0	180	62.7
2911 1	3	261	17: 5:71	29 9.0	15 19.5	172	64.2
2912 1	3	261	18: 5:71	29 10.0	15 9.0	175	71.2
2913 1	3	261	18: 5:71	29 10.0	14 59.0	188	77.1
2914 1	1	261	18: 5:71	29 11.0	14 49.0	205	84.5

STATION	TYPE	CRUISE	DATE	LAT.	LONG.	DEPTH	DISTANCE
2915 1	1	261	18: 5:71	29 11.2	14 39.0	230	90.3
2916 1	1	261	18: 5:71	29 10.0	14 33.0	258	93.2
2917 1	3	261	18: 5:71	29 8.0	14 22.0	432	99.0
2918 1	2	261	18: 5:71	29 6.0	14 10.0	984	105.5
2919 1	2	261	18: 5:71	28 57.0	14 10.0	882	99.5
2920 1	2	261	18: 5:71	28 57.0	14 22.0	440	91.5
2921 1	2	261	18: 5:71	28 56.0	14 35.0	225	82.1
2922 1	1	261	18: 5:71	28 55.0	14 46.0	190	74.5
2923 1	1	261	18: 5:71	28 55.0	14 58.0	179	66.6
2924 1	1	261	18: 5:71	28 54.0	15 10.0	158	59.2
2925 1	1	261	19: 5:71	28 54.0	15 22.0	183	52.0
2926 1	1	261	19: 5:71	28 53.0	15 34.0	182	43.4
2927 1	1	261	19: 5:71	28 53.0	15 46.0	172	36.1
2928 1	1	261	19: 5:71	28 52.0	15 58.0	149	27.4
2929 1	1	261	19: 5:71	28 52.0	16 10.0	125	20.3
2930 1	1	261	19: 5:71	28 52.0	16 23.0	97	11.5
2931 1	1	261	19: 5:71	28 57.0	16 32.0	97	5.9
2932 1	1	261	19: 5:71	28 56.3	16 39.7	34	1.9
2933 1	3	261	19: 5:71	28 47.1	16 32.2	32	1.5
2934 1	1	261	19: 5:71	28 47.0	16 21.0	63	11.0
2935 1	1	261	19: 5:71	28 48.0	16 11.0	126	16.7
2936 1	3	261	19: 5:71	28 48.0	16 6.0	130	19.3
2937 1	3	261	19: 5:71	28 48.5	16 .0	140	23.5
2938 1	1	261	19: 5:71	28 49.0	15 49.5	170	31.0
2939 1	1	261	19: 5:71	28 47.0	15 35.0	186	39.3
2940 1	1	261	19: 5:71	28 48.0	15 24.0	185	46.1
2941 1	2	261	19: 5:71	28 48.0	15 11.0	164	53.8
2942 1	1	261	20: 5:71	28 49.0	14 59.0	169	62.3
2943 1	2	261	20: 5:71	28 49.0	14 47.0	185	70.2
2944 1	3	261	20: 5:71	28 50.0	14 39.0	165	75.4
2945 1	2	261	20: 5:71	28 50.3	14 27.0	265	84.0
2946 1	2	261	20: 5:71	28 47.0	14 18.0	594	88.7
2947 1	2	261	20: 5:71	28 48.0	14 11.0	1004	93.2
2948 1	2	261	20: 5:71	28 40.0	14 13.0	936	88.0
2949 1	2	261	20: 5:71	28 41.0	14 25.0	477	80.0
2950 1	2	261	20: 5:71	28 39.0	14 35.0	178	72.0
2951 1	2	261	20: 5:71	28 36.0	14 45.0	185	63.0
2952 1	2	261	20: 5:71	28 35.5	14 55.0	179	56.1
2953 1	2	261	20: 5:71	28 37.0	15 10.0	167	46.9
2954 1	2	261	20: 5:71	28 37.0	15 20.0	186	40.5
2955 1	2	261	20: 5:71	28 37.0	15 33.0	172	32.9
2956 1	2	261	21: 5:71	28 37.0	15 45.0	146	25.5
2957 1	1	261	21: 5:71	28 37.0	15 56.0	122	18.2
2958 1	1	261	21: 5:71	28 37.0	16 8.0	100	10.4
2959 1	1	261	21: 5:71	28 37.0	16 19.0	19	3.7
2960 1	1	261	21: 5:71	28 39.6	16 21.9	19	4.1
2961 1	1	261	21: 5:71	28 40.2	16 24.6	23	3.3
2962 1	1	261	21: 5:71	28 44.3	16 28.0	30	3.6
2963 1	1	261	21: 5:71	28 44.6	16 33.8	22	.4
2964 1	1	261	21: 5:71	28 41.2	16 29.0	19	1.6

STATION	TYPE	CRUISE	DATE	LAT.	LONG.	DEPTH	DISTANCE
2965 1	1	261	21: 5:71	28 38.8	16 26.7	12	.9
2966 1	1	261	21: 5:71	28 37.0	16 23.4	16	1.3
2967 1	1	261	21: 5:71	28 27.0	16 10.0	36	2.5
2968 1	1	261	21: 5:71	28 27.0	16 .0	90	8.6
2969 1	1	261	21: 5:71	28 27.0	15 49.0	125	16.0
2970 1	3	261	21: 5:71	28 26.0	15 36.0	135	22.6
2971 1	1	261	21: 5:71	28 26.0	15 24.0	162	30.7
2972 1	1	261	21: 5:71	28 26.0	15 12.0	179	38.2
2973 1	1	261	21: 5:71	28 25.0	15 .0	173	45.5
2974 1	1	261	21: 5:71	28 25.0	14 48.0	186	54.9
2975 1	1	261	22: 5:71	28 25.0	14 35.0	180	65.0
2976 1	3	261	22: 5:71	28 25.0	14 23.0	186	73.1
2977 1	2	261	22: 5:71	28 25.0	14 25.0	274	72.0
2978 1	2	261	22: 5:71	28 24.0	14 12.0	736	81.4
2979 1	2	261	22: 5:71	28 24.0	14 5.0	1010	87.2
2980 1	2	261	22: 5:71	28 13.2	13 50.5	1622	95.4
2981 1	2	261	22: 5:71	28 17.0	14 5.0	1291	84.2
2982 1	2	261	22: 5:71	28 17.0	14 17.0	850	75.0
2983 1	2	261	22: 5:71	28 18.0	14 29.0	473	65.8
2984 1	3	261	22: 5:71	28 17.0	14 34.0	280	61.5
2985 1	2	261	22: 5:71	28 17.0	14 44.2	209	54.8
2986 1	2	261	22: 5:71	28 17.0	14 55.8	189	44.9
2987 1	2	261	22: 5:71	28 17.0	15 7.5	182	35.8
2988 1	2	261	22: 5:71	28 16.0	15 18.0	153	27.8
2989 1	2	261	22: 5:71	28 15.8	15 27.7	139	21.1
2990 1	1	261	23: 5:71	28 15.5	15 38.0	120	14.3
2991 1	1	261	23: 5:71	28 15.3	15 47.4	100	8.4
2992 1	1	261	23: 5:71	28 15.0	15 56.8	58	2.2
2993 1	1	261	23: 5:71	28 7.0	15 45.5	77	3.8
2994 1	1	261	23: 5:71	28 7.0	15 34.0	109	10.8
2995 1	1	261	23: 5:71	28 8.0	15 22.0	124	20.4
2996 1	1	261	23: 5:71	28 9.0	15 8.0	158	31.5
2997 1	1	261	23: 5:71	28 10.0	14 56.0	183	41.3
2998 1	1	261	23: 5:71	28 11.0	14 46.0	198	49.0
2999 1	1	261	23: 5:71	28 7.0	14 31.0	280	59.3
3000 1	2	261	23: 5:71	28 7.0	14 21.0	742	67.4
3001 1	2	261	23: 5:71	28 7.0	14 13.0	1006	74.0
3002 1	2	261	23: 5:71	27 56.0	14 14.5	1180	67.8
3003 1	2	261	23: 5:71	27 57.0	14 25.0	815	60.1
3004 1	2	261	23: 5:71	27 56.5	14 36.8	642	50.8
3005 1	2	261	23: 5:71	27 56.3	14 47.6	244	42.0
3006 1	1	261	24: 5:71	27 56.0	14 57.6	189	34.0
3007 1	1	261	24: 5:71	27 55.8	15 9.5	147	23.4
3008 1	3	261	24: 5:71	27 55.5	15 16.4	141	17.8
3009 1	1	261	24: 5:71	27 55.5	15 20.0	130	15.8
3010 1	1	261	24: 5:71	27 55.5	15 31.0	88	8.1
3011 1	1	261	24: 5:71	27 57.0	15 38.2	52	2.6
3012 1	3	261	24: 5:71	27 46.3	15 31.9	42	1.8
3013 1	1	261	24: 5:71	27 47.3	15 20.4	130	11.3
3014 1	1	261	24: 5:71	27 47.0	15 9.0	153	2.8

STATION	TYPE	CRUISE	DATE	LAT.	LONG.	DEPTH	DISTANCE
3015 1	1	261	24: 5:71	27 47.0	14 57.0	195	30.9
3016 1	2	261	24: 5:71	27 47.0	14 48.0	360	38.0
3017 1	2	261	24: 5:71	27 47.0	14 36.0	485	47.0
3018 1	2	261	24: 5:71	27 48.0	14 24.0	860	55.5
3019 1	2	261	24: 5:71	27 48.0	14 19.0	1000	59.5
3020 1	2	261	24: 5:71	27 38.8	14 7.2	1258	65.3
3021 1	2	261	24: 5:71	27 36.0	14 18.0	862	55.7
3022 1	2	261	24: 5:71	27 36.0	14 26.0	463	48.8
3023 1	2	261	24: 5:71	27 36.0	14 36.5	356	40.5
3024 1	2	261	25: 5:71	27 35.8	14 45.5	292	33.2
3025 1	1	261	25: 5:71	27 35.4	14 55.5	185	25.9
3026 1	1	261	25: 5:71	27 35.0	15 5.5	132	17.5
3026 1	3	261	25: 5:71	27 35.0	15 5.5	132	17.5
3027 1	1	261	25: 5:71	27 37.0	15 27.6	50	1.8
3119 1	1	268	18:11:71	29 29.0	14 40.0	315	102.8
3120 1	1	268	18:11:71	28 50.0	14 35.0	180	78.0
3121 1	1	268	18:11:71	28 39.0	14 53.5	188	58.9
3122 1	1	268	18:11:71	28 15.0	15 43.0	108	10.8
3123 1	1	268	18:11:71	28 14.0	15 45.0	99	8.7
3124 1	1	268	18:11:71	28 13.0	15 47.0	93	6.7
3125 1	1	268	18:11:71	28 12.0	15 49.0	85	4.7
3126 1	1	268	19:11:71	27 46.0	15 32.2	43	1.0
3127 1	1	268	19:11:71	27 46.0	15 30.0	61	2.5
3128 1	1	268	19:11:71	27 46.0	15 27.7	82	4.9
3129 1	1	268	19:11:71	27 46.0	15 25.4	113	6.7
3130 1	1	268	19:11:71	27 46.0	15 23.2	120	8.6
3131 1	1	268	19:11:71	27 37.0	15 16.0	120	10.6
3132 1	1	268	19:11:71	27 37.0	15 18.2	118	9.0
3133 1	3	268	19:11:71	27 37.0	15 20.5	118	7.2
3134 1	1	268	19:11:71	27 37.0	15 22.6	115	5.5
3135 1	1	268	19:11:71	27 37.0	15 25.0	72	3.7
3136 1	1	268	19:11:71	27 37.0	15 27.0	50	2.3
3137 1	1	268	19:11:71	27 30.0	15 21.0	70	3.5
3138 1	1	268	19:11:71	27 27.0	15 21.0	55	1.8
3139 1	1	268	19:11:71	27 27.0	15 19.0	92	3.2
3140 1	1	268	19:11:71	27 27.0	15 16.7	112	5.1
3141 1	1	268	19:11:71	27 27.0	15 13.8	126	7.1
3142 1	1	268	19:11:71	27 27.6	15 11.6	125	8.6
3143 1	1	268	19:11:71	27 27.0	15 9.7	130	10.1
3144 1	1	268	19:11:71	27 27.0	14 58.0	228	19.2
3145 1	1	268	19:11:71	27 28.0	14 48.0	303	28.0
3146 1	1	268	19:11:71	27 28.0	14 36.0	352	38.6
3147 1	2	268	19:11:71	27 27.0	14 25.0	421	47.9
3148 1	4	268	19:11:71	27 26.0	14 13.0	725	57.8
3149 1	2	268	19:11:71	27 26.0	14 2.0	1100	67.2
3150 1	2	268	19:11:71	27 26.0	13 39.0	1800	86.3
3151 1	2	268	19:11:71	27 17.5	13 39.0	1730	84.1
3152 1	2	268	20:11:71	27 18.0	13 57.0	995	69.4
3153 1	2	268	20:11:71	27 18.0	14 8.0	632	59.9
3154 1	1	268	20:11:71	27 18.0	14 18.0	423	52.4

STATION	TYPE	CRUISE	DATE	LAT.	LONG.	DEPTH	DISTANCE
3155 1	1	268	20:11:71	27 18.0	14 28.0	374	43.4
3156 1	1	268	20:11:71	27 18.0	14 39.0	315	34.0
3157 1	1	268	20:11:71	27 17.0	14 48.0	270	25.7
3158 1	1	268	20:11:71	27 16.5	15 .0	175	14.8
3159 1	1	268	20:11:71	27 16.5	15 6.0	145	9.9
3160 1	3	268	20:11:71	27 16.0	15 9.0	131	6.7
3161 1	1	268	20:11:71	27 17.0	15 10.6	129	5.5
3162 1	1	268	20:11:71	27 17.5	15 12.8	112	3.5
3163 1	1	268	20:11:71	27 17.0	15 15.2	48	1.7
3164 1	1	268	20:11:71	27 7.0	15 12.0	38	2.5
3165 1	1	268	20:11:71	27 7.0	15 9.8	90	4.5
3166 1	1	268	20:11:71	27 7.0	15 7.6	123	6.6
3167 1	1	268	20:11:71	27 7.0	15 5.5	134	8.2
3168 1	1	268	20:11:71	27 7.0	15 2.5	149	10.8
3169 1	1	268	20:11:71	27 7.0	14 52.0	202	19.9
3170 1	1	268	20:11:71	27 5.0	14 41.0	279	28.0
3171 1	1	268	20:11:71	27 5.0	14 31.0	349	35.9
3172 1	1	268	20:11:71	27 7.0	14 18.0	403	47.9
3173 1	2	268	20:11:71	27 8.5	14 5.0	562	58.5
3174 1	2	268	21:11:71	27 10.5	13 52.0	1050	70.6
3175 1	2	268	21:11:71	27 12.0	13 24.0	2060	95.3
3176 1	2	268	21:11:71	27 3.0	13 22.5	1760	93.9
3177 1	2	268	21:11:71	27 2.0	13 43.0	1000	75.5
3178 1	2	268	21:11:71	27 2.0	13 54.0	650	65.8
3179 1	2	268	21:11:71	27 2.0	14 6.0	437	56.0
3180 1	2	268	21:11:71	26 57.0	14 14.0	392	47.1
3181 1	2	268	21:11:71	26 57.0	14 22.5	364	40.3
3182 1	2	268	21:11:71	26 57.0	14 32.0	322	32.3
3183 1	1	268	21:11:71	26 57.0	14 40.0	270	25.8
3184 1	1	268	21:11:71	26 57.0	14 49.0	208	18.3
3185 1	1	268	21:11:71	26 57.0	15 .0	136	9.0
3186 1	1	268	21:11:71	26 57.0	15 12.5	18	1.1
3187 1	1	268	22:11:71	26 57.8	15 10.9	36	2.1
3188 1	1	268	22:11:71	26 59.2	15 8.9	55	4.2
3189 1	1	268	22:11:71	27 .4	15 7.0	100	6.0
3190 1	1	268	22:11:71	26 57.0	15 3.0	118	7.0
3191 1	1	268	22:11:71	26 47.0	15 4.0	57	2.2
3192 1	1	268	22:11:71	26 47.0	15 1.7	93	4.4
3193 1	1	268	22:11:71	26 47.0	14 59.5	119	6.1
3194 1	1	268	22:11:71	26 47.0	14 57.0	135	8.0
3195 1	1	268	22:11:71	26 47.0	14 55.0	148	9.9
3196 1	1	268	22:11:71	26 47.0	14 43.0	207	20.7
3197 1	2	268	22:11:71	26 47.0	14 31.0	289	31.2
3198 1	2	268	22:11:71	26 47.0	14 21.0	350	39.3
3199 1	2	268	22:11:71	26 47.0	14 10.0	375	49.4
3200 1	2	268	22:11:71	26 47.0	13 59.0	411	58.6
3201 1	2	268	22:11:71	26 47.0	13 47.0	458	70.0
3202 1	2	268	22:11:71	26 47.0	13 37.0	900	78.2
3203 1	2	268	22:11:71	26 47.0	13 22.0	1530	88.8
3204 1	2	268	22:11:71	26 37.0	13 22.0	1480	87.1

STATION	TYPE	CRUISE	DATE	LAT.	LONG.	DEPTH	DISTANCE
3205 1	2	268	22:11:71	26 37.0	13 33.0	995	77.0
3206 1	2	268	22:11:71	26 37.0	13 44.0	453	68.2
3207 1	2	268	22:11:71	26 37.0	13 55.0	418	62.5
3208 1	2	268	23:11:71	26 37.0	14 5.5	390	50.0
3209 1	2	268	23:11:71	26 37.0	14 16.0	352	41.1
3210 1	1	268	23:11:71	26 37.0	14 25.0	305	34.4
3211 1	1	268	23:11:71	26 37.0	14 36.0	240	26.2
3212 1	1	268	23:11:71	26 37.0	14 47.0	165	16.7
3213 1	1	268	23:11:71	26 37.5	14 57.5	115	7.0
3214 1	1	268	23:11:71	26 37.0	15 2.0	40	2.5
3215 1	1	268	26:11:71	25 6.0	14 49.5	27	1.8
3215 1	2	268	26:11:71	25 6.0	14 49.5	27	1.8
3216 1	1	268	26:11:71	25 6.8	14 47.4	38	3.0
3217 1	1	268	26:11:71	25 7.0	14 44.8	50	5.8
3218 1	1	268	26:11:71	25 7.0	14 42.2	62	7.8
3219 1	1	268	26:11:71	25 7.0	14 40.0	75	9.7
3220 1	3	268	26:11:71	25 7.0	14 29.0	110	19.2
3221 1	1	268	26:11:71	25 7.0	14 19.0	155	28.2
3222 1	1	268	26:11:71	25 7.0	14 7.0	181	38.5
3223 1	1	268	26:11:71	25 8.0	13 59.0	198	45.1
3224 1	1	268	23:11:71	25 8.0	13 52.0	215	51.9
3224 1	2	268	26:11:71	25 8.0	13 52.0	215	51.9
3224 1	3	268	26:11:71	25 8.0	13 52.0	215	51.9
3225 1	2	268	26:11:71	25 7.0	13 36.0	530	66.9
3226 1	2	268	27:11:71	25 7.0	13 26.0	970	75.5
3227 1	2	268	27:11:71	25 7.0	13 15.0	1450	84.9
3228 1	2	268	27:11:71	25 25.0	13 25.0	1000	75.5
3229 1	2	268	27:11:71	25 24.0	13 36.0	651	65.6
3230 1	2	268	27:11:71	25 23.0	13 47.0	354	55.5
3231 1	1	268	27:11:71	25 22.0	13 58.0	260	45.8
3232 1	1	268	27:11:71	25 22.0	14 5.0	210	39.1
3233 1	1	268	27:11:71	25 26.0	14 13.0	212	33.0
3234 1	1	268	27:11:71	25 26.5	14 21.0	182	25.5
3254 1	2	268	28:11:71	26 12.0	13 36.0	660	72.0
3235 1	1	268	27:11:71	25 27.5	14 29.0	145	18.5
3236 1	1	268	27:11:71	25 28.0	14 38.0	97	10.5
3237 1	1	268	27:11:71	25 28.0	14 41.0	98	7.9
3238 1	1	268	27:11:71	25 27.6	14 43.8	89	5.1
3239 1	1	268	27:11:71	25 27.7	14 47.4	55	1.5
3240 1	1	268	27:11:71	25 50.0	14 49.5	58	2.2
3241 1	1	268	28:11:71	25 49.0	14 47.1	80	4.0
3242 1	1	268	28:11:71	25 48.2	14 44.8	101	5.0
3243 1	1	268	28:11:71	25 47.6	14 42.5	115	6.8
3244 1	1	268	28:11:71	25 47.0	14 40.0	122	8.6
3245 1	2	268	28:11:71	25 47.0	14 29.0	170	19.1
3246 1	2	268	28:11:71	25 47.0	14 18.0	210	29.2
3247 1	2	268	28:11:71	25 47.0	14 7.0	250	39.0
3248 1	2	268	28:11:71	25 47.0	13 55.5	320	48.9
3249 1	2	268	28:11:71	25 47.0	13 44.0	380	58.9
3250 1	2	268	28:11:71	25 47.0	13 31.0	690	70.7

STATION	TYPE	CRUISE	DATE	LAT.	LONG.	DEPTH	DISTANCE
3251 1	1	268	28:11:71	25 47.5	13 18.5	1200	82.5
3252 1	2	268	28:11:71	25 48.0	13 11.0	1495	89.0
3253 1	2	268	28:11:71	26 11.0	13 25.0	995	81.8
3254 1	2	268	28:11:71	26 12.0	13 36.0	660	72.0
3255 1	2	268	28:11:71	26 13.0	13 47.0	390	61.4
3256 1	2	268	28:11:71	26 13.0	13 57.0	352	53.0
3257 1	2	268	28:11:71	26 11.0	14 8.0	300	42.8
3258 1	1	268	29:11:71	26 9.0	14 18.0	212	33.9
3259 1	1	268	29:11:71	26 7.0	14 28.0	202	24.8
3260 1	1	268	29:11:71	26 5.0	14 37.0	180	17.2
3261 1	1	268	29:11:71	26 1.0	14 46.0	115	9.0
3262 1	1	268	29:11:71	26 3.0	14 49.5	85	7.0
3263 1	1	268	29:11:71	26 3.0	14 51.5	85	5.3
3264 1	1	268	29:11:71	26 3.0	14 54.0	51	3.7
3265 1	1	268	29:11:71	26 3.0	14 56.0	31	2.0
3266 1	1	268	29:11:71	26 26.9	15 5.6	24	1.2
3267 1	1	268	29:11:71	26 26.9	15 3.5	38	2.5
3268 1	1	268	29:11:71	26 27.0	15 1.2	44	4.2
3269 1	1	268	29:11:71	26 26.8	14 53.8	53	5.7
3270 1	1	268	29:11:71	26 26.8	14 57.8	50	5.5
3271 1	1	268	29:11:71	26 27.0	14 47.0	153	12.0
3272 1	1	268	29:11:71	26 27.0	14 36.0	230	20.8
3273 1	1	268	29:11:71	26 28.0	14 25.0	305	30.1
3274 1	1	268	29:11:71	26 29.0	14 14.0	340	39.4
3275 1	2	268	29:11:71	26 29.0	14 3.0	380	50.0
3276 1	2	268	29:11:71	26 30.0	13 52.0	408	59.7
3277 1	2	268	29:11:71	26 30.0	13 41.0	433	69.2
3278 1	2	268	29:11:71	26 31.0	13 30.0	839	78.7
3279 1	2	268	29:11:71	26 31.0	13 15.2	1495	91.9
3280 1	1	268	1:12:71	28 41.1	16 22.8	24	4.9
3281 1	1	268	1:12:71	28 42.0	16 20.8	34	6.5
3282 1	1	268	1:12:71	28 43.2	16 19.0	50	8.5
3283 1	1	268	1:12:71	28 44.3	16 17.2	80	10.4
3284 1	1	268	1:12:71	28 45.7	16 15.5	96	12.4
3285 1	1	268	1:12:71	28 46.8	16 13.6	114	14.2
3286 1	1	268	1:12:71	28 52.4	16 20.4	110	13.6
3287 1	1	268	1:12:71	28 50.2	16 23.8	83	9.8
3288 1	1	268	1:12:71	28 48.7	16 26.0	52	7.5
3289 1	1	268	1:12:71	28 47.6	16 27.8	41	5.6
3290 1	1	268	1:12:71	28 46.3	16 29.2	38	4.1
3291 1	1	268	1:12:71	28 45.3	16 31.4	30	2.1
3292 1	1	268	1:12:71	29 41.3	17 .5	80	2.4
3293 1	1	268	1:12:71	29 41.4	16 58.2	90	4.2
3294 1	1	268	1:12:71	29 41.8	16 56.2	102	6.0
3295 1	1	268	1:12:71	29 42.0	16 52.0	118	9.4
3351 1	3	273	10: 5:72	29 39.6	14 14.0	880	126.0
3352 1	2	273	11: 5:72	29 14.5	14 8.0	1335	112.0
3353 1	2	273	11: 5:72	28 56.0	13 58.5	1665	107.0
3354 1	2	273	11: 5:72	28 38.0	13 54.0	1780	101.1
3355 1	2	273	11: 5:72	27 50.0	13 42.0	2070	90.0

STATION	TYPE	CRUISE	DATE	LAT.	LONG.	DEPTH	DISTANCE
3356 1	2	273	12: 5:72	26 23.0	13 7.0	1430	98.4
3357 1	2	273	12: 5:72	26 21.0	13 20.0	990	86.0
3358 1	2	273	12: 5:72	26 21.0	13 20.0	580	86.5
3359 1	2	273	12: 5:72	26 19.5	13 52.5	385	57.7
3360 1	2	273	12: 5:72	26 19.0	14 4.0	349	47.0
3361 1	2	273	12: 5:72	26 18.0	14 15.0	298	37.7
3362 1	2	273	12: 5:72	26 16.5	14 25.5	215	28.0
3362 2	1	273	12: 5:72	26 16.5	14 25.5	215	28.0
3363 1	1	273	12: 5:72	26 15.5	14 37.0	234	18.2
3364 1	2	273	12: 5:72	26 14.8	14 47.5	135	8.0
3365 1	1	273	12: 5:72	26 14.5	14 49.5	98	4.9
3366 1	1	273	12: 5:72	26 14.0	14 54.0	51	2.5
3367 1	1	273	12: 5:72	25 54.5	14 52.6	33	1.1
3368 1	1	273	12: 5:72	25 54.6	14 50.9	62	2.9
3369 1	1	273	12: 5:72	25 54.7	14 48.6	58	5.1
3370 1	1	273	12: 5:72	25 54.7	14 46.3	82	6.8
3371 1	1	273	12: 5:72	25 55.0	14 44.3	117	8.3
3372 1	1	273	12: 5:72	25 55.0	14 33.0	171	17.8
3373 1	2	273	13: 5:72	25 54.5	14 18.0	220	30.1
3374 1	2	273	13: 5:72	25 53.8	14 9.0	254	37.8
3375 1	2	273	13: 5:72	25 53.0	13 57.0	326	47.7
3376 1	2	273	13: 5:72	25 52.5	13 44.0	408	59.2
3377 1	2	273	13: 5:72	25 52.0	13 32.0	690	70.6
3378 1	2	273	13: 5:72	25 58.0	13 21.0	1120	81.3
3379 1	2	273	13: 5:72	25 38.0	13 13.0	1450	88.1
3380 1	2	273	13: 5:72	25 36.0	13 11.9	1470	88.5
3381 1	2	273	13: 5:72	25 36.0	13 23.1	970	79.0
3382 1	2	273	13: 5:72	25 35.8	13 34.6	555	68.4
3383 1	2	273	13: 5:72	25 36.2	13 45.5	335	58.6
3384 1	2	273	13: 5:72	25 36.0	13 52.0	280	53.9
3385 1	2	273	13: 5:72	25 37.0	13 56.5	275	48.8
3386 1	2	273	13: 5:72	25 36.0	14 8.0	227	38.0
3387 1	2	273	13: 5:72	25 36.0	14 19.0	190	28.8
3388 1	2	273	13: 5:72	25 36.0	14 31.0	158	17.8
3389 1	1	273	14: 5:72	25 36.2	14 38.5	117	11.0
3390 1	1	273	14: 5:72	25 35.8	14 40.4	98	9.7
3391 1	1	273	14: 5:72	25 35.9	14 43.5	84	6.9
3392 1	1	273	14: 5:72	25 36.0	14 45.8	71	5.0
3393 1	1	273	14: 5:72	25 36.0	14 48.2	40	3.0
3394 1	1	273	14: 5:72	25 16.0	14 46.2	33	2.2
3395 1	1	273	14: 5:72	25 16.0	14 44.4	38	3.9
3396 1	1	273	14: 5:72	25 16.0	14 42.4	55	6.0
3397 1	1	273	14: 5:72	25 15.5	14 39.0	61	9.4
3398 1	1	273	14: 5:72	25 15.5	14 37.0	87	11.0
3399 1	1	273	14: 5:72	25 16.0	14 27.0	142	19.5
3400 1	1	273	14: 5:72	25 16.0	14 13.0	182	31.9
3401 1	1	273	14: 5:72	25 16.0	14 3.0	200	41.8
3402 1	1	273	14: 5:72	25 16.0	13 51.0	244	52.2
3403 1	1	273	14: 5:72	25 15.5	13 41.5	332	60.5
3405 1	4	273	14: 5:72	25 17.0	13 16.0	1110	83.3

STATION	TYPE	CRUISE	DATE	LAT.	LONG.	DEPTH	DISTANCE
3404 1	2	273	14: 5:72	25 17.0	13 30.0	690	70.5
3405 1	2	273	14: 5:72	25 17.0	13 16.0	1110	83.3
3406 1	2	273	14: 5:72	25 20.0	13 6.0	1530	92.5
3633 1	1	279	29:11:72	29 .0	16 26.0	129	11.8
3634 1	1	279	29:11:72	28 58.0	16 26.2	123	10.4
3635 1	1	279	29:11:72	28 56.0	16 26.2	117	9.5
3636 1	1	279	29:11:72	28 54.0	16 26.2	106	8.9
3637 1	1	279	29:11:72	28 52.0	16 26.5	89	8.0
3638 1	1	279	29:11:72	28 50.0	16 26.5	70	7.7
3639 1	1	279	29:11:72	28 48.2	16 26.2	50	7.2
3640 1	1	279	29:11:72	28 46.3	16 26.6	37	6.3
3641 1	0	279	29:11:72	28 40.0	16 26.5	0	2.0
3642 1	1	279	29:11:72	28 30.0	16 13.6	27	2.1
3643 1	1	279	29:11:72	28 30.0	16 11.5	31	3.7
3644 1	1	279	29:11:72	28 29.0	16 9.0	33	4.6
3645 1	1	279	29:11:72	28 28.5	16 7.0	40	5.5
3646 1	1	279	29:11:72	28 28.0	16 5.0	50	6.4
3647 1	1	279	29:11:72	28 27.6	16 2.5	60	7.6
3648 1	1	279	29:11:72	28 27.0	16 .0	70	8.6
3649 1	1	279	29:11:72	28 25.2	16 2.5	60	5.9
3650 1	1	279	29:11:72	28 24.0	16 3.6	50	4.4
3651 1	1	279	29:11:72	28 22.0	16 5.0	43	2.0
3652 1	1	279	30:11:72	25 55.0	14 33.0	172	17.8
3653 1	1	279	30:11:72	25 5.8	14 7.7	179	38.4
4644 1	1	300	17: 5:74	29 18.0	16 48.0	89	4.2
4645 1	1	300	17: 5:74	29 13.0	16 45.0	94	4.7
4646 1	1	300	17: 5:74	29 9.0	16 42.0	90	6.5
4647 1	1	300	17: 5:74	29 4.2	16 38.6	94	5.7
4648 1	1	300	17: 5:74	29 .0	16 35.0	90	6.7
4649 1	1	300	17: 5:74	28 55.0	16 33.4	77	3.6
4650 1	1	300	17: 5:74	28 50.7	16 30.0	60	4.6
4651 1	1	300	17: 5:74	28 49.0	16 28.8	51	5.2
4651 2	1	300	17: 5:74	28 49.0	16 28.8	51	5.2
4652 1	1	300	17: 5:74	28 47.0	16 28.2	41	5.1
4652 2	1	300	17: 5:74	28 47.0	16 28.2	41	5.0
4653 1	1	300	17: 5:74	28 45.2	16 28.2	32	4.9
4653 2	1	300	17: 5:74	28 45.2	16 28.2	32	4.9
4654 1	1	300	17: 5:74	28 43.0	16 27.4	28	3.8
4655 1	1	300	17: 5:74	28 41.1	16 26.8	21	2.8
4656 1	1	300	17: 5:74	28 39.3	16 26.0	15	1.7
4657 1	1	300	17: 5:74	28 39.0	16 24.0	20	2.4
4658 1	1	300	17: 5:74	28 38.7	16 21.4	21	3.6
4659 1	1	300	17: 5:74	28 36.8	16 19.2	26	3.4
4660 1	1	300	17: 5:74	28 38.2	16 17.0	48	5.8
4661 1	1	300	17: 5:74	28 38.0	16 14.5	70	7.0
4662 1	1	300	17: 5:74	28 38.0	16 12.2	85	9.5
4663 1	1	300	17: 5:74	28 37.5	16 9.5	95	9.9
4664 1	1	300	17: 5:74	28 37.6	16 7.4	95	10.8
4665 1	1	300	17: 5:74	28 37.0	16 5.0	99	12.4
4666 1	1	300	17: 5:74	28 36.0	16 2.0	106	13.8

STATION	TYPE	CRUISE	DATE	LAT.	LONG.	DEPTH	DISTANCE
4667 1	1	300	17: 5:74	28 34.2	16 1.8	104	12.8
4668 1	1	300	17: 5:74	28 32.2	16 1.6	100	11.4
4669 1	1	300	17: 5:74	28 30.0	16 .0	99	10.9
4670 1	1	300	17: 5:74	28 29.2	15 59.0	89	10.9
4671 1	1	300	17: 5:74	28 21.7	15 58.4	82	6.2
4672 1	1	300	17: 5:74	28 19.4	15 57.6	80	5.1
4673 1	1	300	17: 5:74	28 17.0	15 57.0	78	6.9

D. LOCATION, DEPTH AND COLOUR OF POST-PALEOZOIC ROCKS

Sample Number	Latitude S Deg.	Min.	Longitude E Deg.	Min.	Depth m	Colour	
TERRIGENOUS SANDSTONES AND MUDSTONES(T)							
Ferruginous muddy sandstones							
2747A	29	55,0	16	51,0	138	5YR4/4	Moderate brown
2747B4	29	55,0	16	51,0	138	10YR6/6	Dark yellowish orange
4637	30	16,1	17	04,9	132	10R4/6	Moderate reddish brown
4638	30	00,0	16	47,0	160	10YR4/2	Dark yellowish brown
POINT	31	39,2	18	09,1	+25	5YR2/2	Dusky brown
Phosphatic ferruginous muddy sandstones							
2747B-1	29	55,0	16	51,0	138	10YR4/2	Dark yellowish brown
2747B-2	29	55,0	16	51,0	138	10R5/4	Pale reddish brown
2747B-3	29	55,0	16	51,0	138	10YR5/4	Moderate yellowish brown
2747B-5	29	55,0	16	51,0	138	10YR4/2	Dark yellowish brown
4629D	30	00,0	16	50,0	152	10YR4/2	Dark yellowish brown
4640D	29	59,0	16	54,0	140	10YR4/2	Dark yellowish brown
Ferruginous mudstones							
2743	29	43,0	16	47,0	123	10YR6/4	Moderate yellowish orange
2868A	29	27,0	16	41,0	122	10R4/6	Moderate reddish brown
2868B	29	27,0	16	41,0	122	5YR5/2	Pale brown
4637	30	16,1	17	04,9	132	10R4/6	Moderate reddish brown
Sandy mudstones							
2995C	28	08,0	15	22,0	124	5Y6/1	Light olive gray
2995D	28	08,0	15	22,0	124	5Y8/1	Yellowish gray
1175-46A	28	02,7	15	26,25	95	NF	Light gray
1175-46B	28	02,7	15	26,25	95	5Y8/1	Yellowish gray
Micaceous mudstones							
2868B-1	29	27,0	16	41,0	122	5Y8/2	Pale yellowish gray
1111-44	28	04,1	15	30,05	90	10YR5/4	Moderate yellowish brown
Sandstones							
2936	28	48,0	16	06,0	130	N5	Medium gray
2969E	28	27,0	15	49,0	125	10YR5/2	Moderate yellowish brown
1175-47	28	03,5	15	25,95	99	N8	Very light gray
QUARTZOSE LIMESTONES(Q) AND LIME MUDSTONES(L)							
Quartzose lime wackestones(Q)							
2747C	29	55,0	16	51,0	138	10Y8/2	Pale greenish yellow
2990D	28	15,5	15	38,0	120	5GY7/2	Grayish yellow
2995A	28	08,0	15	22,0	124	N7	Light gray
2995B	28	08,0	15	22,0	124	N4	Medium dark gray
2995E	28	08,0	15	22,0	124	N5	Medium gray
3007-1	27	55,8	15	09,5	147	10YR5/4	Moderate yellowish brown
3007-2	27	55,8	15	09,5	147	N8	Very light gray
3008B	27	55,5	15	16,4	141	N5	Medium gray
3122	28	15,0	15	43,0	108	N6	Medium light gray
3133	27	37,0	15	20,5	118	N5	Medium gray
3141	27	27,0	15	13,8	126	N5	Medium gray
3193	26	47,0	14	49,5	119	N6	Medium light gray
3261	26	01,0	14	46,0	115	N5	Medium gray
3390A	25	35,8	14	40,4	98	5GY7/1	Light greenish gray
3390D	25	35,8	14	40,4	98	5Y8/1	Yellowish gray
3390F	25	35,8	14	40,4	98	N6	Medium light gray
4636	30	18,0	17	05,5	135	5Y6/1	Light olive gray
4638M	30	00,0	16	47,0	160	5B9/1	Bluish white
4638F	30	00,0	16	47,0	160	5B9/1	Bluish white

Sample Number	Latitude S Deg.	Min.	Longitude E Deg.	Min.	Depth m	Colour	
4639D	30	00,0	16	50,0	152	5Y8/1	Yellowish gray
1111-49	28	06,20	15	28,25	117	N5	Medium gray
1111-67	28	14,05	15	21,45	134	N6	Medium light gray
A4923	27	23,0	15	09,0	128	N5	Medium gray
A4923-2	27	23,0	15	09,0	128	5Y8/1	Yellowish gray
GIL 471	26	34,0	14	55,0	128	N5	Medium gray
Phosphatic quartzose lime wackestones/Q)							
3194	26	47,0	14	57,0	135	N5	Medium gray
3390E	25	35,8	14	40,4	98	5Y2/1	Olive black
GIL 469	26	30,0	14	43,0	180	N5	Medium gray
Pyritic lime wackestone(L)							
4639	30	00,0	16	50,0	152	5Y6/2	Light olive gray
Phosphatic pyritic lime wackestones(L)							
2969A	28	27,0	15	49,0	125	N7	Light gray
2969B	28	27,0	15	49,0	125	5Y6/2	Light olive gray
Lime mudstones(L)							
2969D	28	27,0	15	49,0	125	5Y7/2	Yellowish gray
2995B	28	08,0	15	22,0	124	N4	Medium dark gray
2995F	28	08,0	15	22,0	124	N7	Light gray
3027B	27	27,0	15	27,6	50	N3	Dark gray
3027C	27	37,0	15	27,6	50	N4	Medium dark gray
3232A	25	22,0	14	05,0	210	5Y8/1	Yellowish gray
3653D	25	05,8	14	07,7	179	N4	Medium dark gray
4636	30	18,0	17	05,5	135	10YR3/2	Dark yellowish brown
Phosphatic lime mudstones(L)							
3185	26	57,0	15	00,0	136	10Y4/2	Grayish olive
3351A-2	29	39,0	14	14,0	880-152	10YR5/4	Moderate yellowish brown
FORAMINIFERAL LIMESTONES(F)							
Phosphatic nummulitic lime wackestones							
2922	28	55,0	14	46,0	190	10YR2/2	Dusky yellowish brown
2984C	28	17,0	14	34,0	250	5Y7/2	Yellowish gray
Phosphatic planktonic foraminiferal lime wackestones							
2734	29	56,0	15	04,0	312	5Y8/2	Grayish yellow
3005	27	56,3	14	47,6	244	10YR8/2	Very pale orange
ALGAL LIMESTONES(A)							
Algal lime wackestones							
2849B-1	29	37,0	14	16,0	250-152	5Y7/2	Yellowish gray
2849B-4	29	37,0	14	16,0	250-152	10YR8/2	Very pale orange
3351B	29	39,0	14	14,0	880-152	10YR8/4	Pale yellowish orange
Phosphatic algal lime wackestones							
2849A	29	37,0	14	16,0	250-152	10YR5/4	Moderate yellowish brown
2856	29	38,0	15	26,0	194	10YR5/4	Moderate yellowish brown
3351A-1	29	39,0	14	14,0	880-152	10YR7/4	Grayish orange
A5060	29	41,5	15	28,5	183	10YR7/4	Grayish orange
PHOSPHORITES(P)							
Conglomeratic glauconitic phosphate packstones							
2984A	28	17,0	14	34,0	250		
Pebbles	28	17,0	14	34,0	250	10YR6/6	Dark yellowish orange
Matrix	28	17,0	14	34,0	250	5Y8/4	Yellowish gray

Sample	Latitude S Deg.	Min.	Longitude E Deg.	Min.	Depth m	Colour	
2984B	28	17,0	14	34,0	250		
Pebbles	28	17,0	14	34,0	250	10YR6/2	Pale yellowish brown
Matrix	28	17,0	14	34,0	250	5Y7/2	Yellowish gray
2984C	28	17,0	14	34,0	250	5Y7/2	Yellowish gray
3016D	27	47,0	14	48,0	360-393	10YR4/2	Dark yellowish brown
4638G	30	00,0	16	47,0	160	5YR2/1	Brownish black
4639	30	00,0	16	50,0	152	5Y8/1	Yellowish gray
300-80001	28	47,08	15	54,20	157	10YR6/4	Moderate yellowish orange
Pelletal (intraclastic) phosphate wackestone							
3232C	25	22,0	14	05,0	210	10Y7/2	Pale greenish yellow
				MOLLUSCAN LIMESTONES(M)			
Molluscan lime wackestones							
2990	28	15,5	15	38,0	120		
2994	28	07,0	15	34,0	109	5Y6/1	Light olive gray
A4922	27	23,0	15	08,0	138	10Y8/2	Pale greenish yellow
A4923-3	27	23,0	15	09,0	128	N7	Light gray
4638	30	00,0	16	47,0	160		
				MISCELLANEOUS			
Phosphatic silicified wood							
4638	30	00,0	16	47,0	160	N5	Medium gray
4639	30	00,0	16	50,0	152	N5	Medium gray
Coprolite (phosphate mudstone)							
3224D	25	08,0	13	52,0	215	10YR4/2	Dark yellowish brown

E. COMPONENT PROPORTION OF POST-PALAEOZOIC ROCKS

Sample Number	SUMMARY				INTERGRANULAR FABRIC						TERRIGENOUS GRAINS												BIOGENIC GRAINS		AUTHIGENIC GRAINS	
	Intergranular Fabric	Terrigenous Grains	Biogenic Grains	Authigenic Grains	Ferruginous	Phosphatic	Micaceous/Clay	Microspar	Pseudospar	Sparry Calcite	Quartz	Metaquartzite	Feldspar	Chert	Chalcedony	Jasper	Agate	Sedimentary Rock Fragments	Volcanic Rock Fragments	Metamorphic Rock Fragments	Mica	Heavy Minerals	Organic Matter	Bryozoans	Molluscs	Glauconite	Pyrite
TERRIGENOUS SANDSTONES AND MUDSTONES (T)																										
Ferruginous muddy sandstones																										
2747A	50	50	–	–	25	–	–	25	–	–	45	–	tr	5	–	–	–	–	–	–	tr	–	–	–	–	–	–
2747B4	60	40	–	–	60	–	–	–	–	–	35	–	2	2	tr	tr	–	–	–	–	–	–	–	–	–	–	–
4637	60	40	–	–	60	–	–	–	–	–	20	15	–	2	3	–	–	–	–	–	–	–	–	–	–	–	–
4638	50	50	tr	–	50	–	–	–	–	–	40	–	5	tr	–	–	tr	3	–	2	–	–	–	tr	–	–	–
POINT	20	80	–	–	20	–	–	–	–	–	30	10	–	30	–	5	–	5	–	–	–	–	–	–	–	–	–
Phosphatic ferruginous muddy sandstones																										
2747B1	50	50	–	–	35	15	–	–	–	–	50	tr	tr	–	tr	–	–	–	–	–	tr	–	–	–	–	–	–
2747B2	25	75	–	–	10	15	–	–	–	–	70	2	1	2	–	–	–	–	–	–	–	–	–	–	–	–	–
2747B3	50	50	–	–	35	15	–	–	–	–	35	–	tr	15	tr	–	–	–	–	–	–	–	–	–	–	–	–
2747B5	40	60	–	–	15	20	–	–	–	5	40	–	tr	20	tr	tr	–	–	–	–	–	–	–	–	–	–	–
4639D	50	50	–	–	30	20	–	–	–	–	45	–	–	2	–	–	–	2	–	1	–	–	–	–	–	–	–
4640D	60	40	–	–	50	10	–	–	–	–	35	–	1	1	–	–	–	3	–	–	–	–	–	–	–	–	–
Ferruginous mudstones																										
2743	80	20	–	–	80	–	–	–	–	–	10	–	–	–	–	–	–	–	–	–	10	–	–	–	–	–	–
2868A	50	50	–	–	50	–	–	–	–	–	40	–	–	–	–	–	–	–	–	–	10	–	–	–	–	–	–
2868B	20	75	–	5	20	–	–	–	–	–	65	–	–	–	–	–	–	–	–	–	10	–	–	–	–	–	5
4637	80	20	–	–	80	–	–	–	–	–	20	–	–	–	–	–	–	–	–	–	–	–	–	–	–	–	–
Sandy mudstones																										
2995C	90	10	–	–	–	–	80	–	–	10	8	–	tr	–	–	–	–	–	2	–	–	–	–	–	–	–	–
2995D	70	30	–	–	–	–	50	–	–	20	20	–	tr	–	–	–	–	10	–	–	–	tr	–	–	–	–	–
1175-46A	70	30	–	–	–	–	70	–	–	–	30	–	10	–	–	–	–	–	–	–	–	–	–	–	–	–	–
1175-46B	20	80	–	–	–	20	–	–	–	–	75	–	5	tr	–	–	–	–	–	–	–	–	–	–	–	–	–
Micaceous mudstones																										
2868B-1	50	50	–	–	–	–	50	–	–	–	25	–	–	–	–	–	–	–	–	–	20	–	5	–	–	–	–
1111-44	50	50	–	–	–	–	50	–	–	–	20	–	–	–	–	–	–	–	–	–	30	–	–	–	–	–	–

TERRIGENOUS SANDSTONES AND MUDSTONES (T)

Sample Number	SUMMARY				INTERGRANULAR FABRIC							TERRIGENOUS GRAINS										BIOGENIC GRAINS		AUTHIGENIC GRAINS	
	Intergranular Fabric	Terrigenous Grains	Biogenic Grains	Authigenic Grains	Ferruginous	Phosphatic	Micaceous/Clay	Microspar	Pseudospar	Sparry Calcite	Quartz	Metaquartzite	Feldspar	Chert	Chalcedony	Jasper	Agate	Sedimentary Fragments	Volcanic Rock Fragments	Metamorphic Rock Fragments	Mica	Heavy Minerals	Organic Matter	Bryozoans	Molluscs	Glauconite	Pyrite
Sandstones																											
2936	tr	100	-	-	-	-	tr	-	-	-	95	2	2	tr	-	-	-	-	-	-	1	-	-	-	-	-	-
2969E	tr	100	-	-	-	-	tr	-	-	-	85	-	10	-	-	-	-	-	-	-	5	-	-	-	-	-	-
1175-47	20	80	-	-	-	-	-	-	-	20	78	-	1	1	-	-	-	-	-	-	-	-	-	-	-	-	-

Sample Number	SUMMARY			INTERGRANULAR FABRIC							BIOGENIC GRAINS (chiefly carbonate)									TERRIGENOUS GRAINS						AUTHIGENIC GRAINS (chiefly residual)					
	Intergranular Fabric	Biogenic Grains	Terrigenous Grains	Authigenic Grains	Ferruginous	Phosphatic	Glauconitic	Micrite	Microspar	Pseudospar	Sparry Calcite	Molluscs	Bryozoans	Echinoderms	Coralline Algae	Cirripeds	Benthonic Foraminifera	Planktonic Foraminifera	Faecal Pellets	Fish Debris (Phos)	Sponge Spicules (Silfceous)	Rock Fragments	Quartz	Chert	Jasper	Organic Matter	Heavy Minerals	Feldspar	Pyrite	Glauconite	Phos. Fragments	Phos. Infillings	Phos. Pellets
Phosphatic quartzose lime wackestones(Q)																																	
3194	70	tr	26	4	-	10	50	10	-	-	-	tr	-	-	-	-	tr	-	-	-	-	-	25	-	-	-	tr	-	tr	-	-	-
3390E	60	-	35	5	-	35		25	-	-	-	-	-	-	-	-	-	-	-	-	-	-	30	-	-	-	-	5	5	tr	tr	-	-
GIL469	70	-	25	5	-	15		10	45	-	-	tr	-	-	-	-	-	-	-	-	-	-	25	-	-	-	-	tr	5	tr	tr	-	-

Sample Number	SUMMARY				INTERGRANULAR							BIOGENIC GRAINS (chiefly carbonate)															TERRIGENOUS Grains						AUTHIGENIC Grains (chiefly residual				
	Intergranular Fabric	Biogenic Grains	Terrigenous Grains	Authigenic Grains	Ferruginous	Phosphatic	Glauconitic	Micrite	Microspar	Pseudospar	Sparry Calcite	Molluscs	Bryozoans	Echinoderms	Coralline Algae	Cirripeds	Benthonic Foraminifera	Planktonic Foraminifera	Faecal Pellets	Fish Debris (Phos)	Sponge Spicules (Siliceous)	Rock Fragments	Quartz	Chert	Jasper	Organic Matter	Heavy Minerals	Feldspar	Pyrite	Glauconite	Phos. Fragments	Phos. Infillings	Phos. Pellets
LIME MUDSTONES (L)																																			
Pyritic lime wackestones																																			
4639	85	-	5	10	-	-	-	85	-	-	-	-	-	-	-	-	-	-	-	-	-	-	5	-	-	-	-	-	10	-	-	-	
Phosphatic pyritic lime wackestones (L)																																			
2969A	70	-	tr	30	-	15		45	10	-	-	-	-	-	-	-	-	-	-	-	-	-	tr	-	-	-	-		30	-	-	-	-
2969B	75	-	4	21	-	15		55	5	-	-	-	-	-	-	-	-	-	-	-	-	-	4	-	-	-	-		20	1	-	-	-
Lime mudstones																																			
2969D	90	-	5	5	-	-		-	90	-	-	-	-	-	-	-	-	-	-	-	-	-	5	-	-	-	-	-	5	tr	-		-
2995B	90	-	5	5	-	-		50	40	-	-	-	-	-	-	-	-	-	-	-	-	-	5	-	-	-	-	-	5	-	-		-
2995F	95	-	5	-	-	-		75	-	-	20	-	-	-	-	-	-	-	-	-	-	-	5	-	-	-	-	-	-	-	-		-
3027B	100	-	-	-	10	-		-	90	-	-	-	-	-	-	-	-	-	-	-	-	-	-	-	-	-	-	-	-	-	-		-
3027C	100	-	tr	-	30	-		-	70	-	-	-	-	-	-	-	-	-	-	-	-	-	tr	-	-	-	-	-	-	-	-		-
3232A	100	-	-	-	-	-		70	30	-	-	-	-	-	-	-	-	-	-	-	-	-	-	-	-	-	-	-	-	-	-		-
3653D	100	-	-	tr	-	-		80	20	-	-	-	-	-	-	-	-	-	-	-	-	-	-	-	-	-	-	-	tr	-	-		-
4636	100	-	tr	-	-	-		85	10	5	-	-	-	-	-	-	-	-	-	-	-	-	tr	-	-	-	-	-	-	-	-		-
Phosphatic lime mudstones (L)																																			
3185	95	-	3	2	-	30		65	-	-	-	-	-	-	-	-	-	-	-	-	-	-	-	-	-	-	-		-	-	-	-	-
3351A-2	100	-	-	-	10	30		60	-	-	-	-	-	-	-	-	-	-	-	-	-	-	-	-	-	-	-		-	-	-	-	-
FORAMINIFERAL LIMESTONES (F)																																			
Phosphatic nummulitic lime packstones																																			
2922	50	50	-	-	-	30		20	-	-	-	tr	tr	tr	tr	-	45	5	-	-	-	-	-	-	-	-	-	-	-	-	-	-	-	-
2984C	50	50	-	-	-	30		5	15	-	-	tr	tr	tr	tr	-	50	-	-	-	-	-	-	-	-	-	-	-	-	-	-	-	-	-
Phosphatic planktonic foraminiferal lime wackestones																																			
2734	50	40	-	10	-	5		45	-	-	-	-	-	-	-	-	5	35	-	-	-	-	-	-	-	-	-	-	1	1	-	8	-
3005	50	50	-	tr	-	-		25	25	-	-	10	-	5	-	-	15	20	-	-	-	-	-	-	-	-	-	-	-	tr	-	tr	-

Sample Number	SUMMARY				INTERGRANULAR				BIOGENIC GRAINS (chiefly carbonate)										TERRIGENOUS GRAINS							AUTHIGENIC GRAINS (chiefly residual				
	Intergranular Fabric	Biogenic Grains	Terrigenous Grains	Authigenic Grains	Ferruginous	Phosphatic	Glauconitic	Micrite	Microspar	Pseudospar	Sparry Spicules	Molluscs	Bryozoans	Echinoderms	Coralline Algae	Cirripeds	Benthonic Foraminifera	Planktonic Foraminifera	Faecal Pellets	Fish Debris (Phos)	Sponge Spicules (Siliceous)	Rock Fragments	Quartz	Chert	Jasper	Organic Matter	Heavy Minerals	Feldspar	Pyrite	Glauconite	Phos. Fragments	Phos. Infillings	Phos. Pellets
ALGAL LIMESTONES(A)																																	
Algal lime wackestones																																	
2849B-1	50	50	-	-	-	-		45	5	-	-	-	35	-	15	-	-	tr	-	-	-	-	-	-	-	-	-	-	-	-	-	-	-
2849B-4	70	30	-	-	-	-		60	10	-	-	-	5	tr	20	-	3	2	-	-	-	-	-	-	-	-	-	-	-	-	-	-	-
3351B	40	60	-	-	5	10		15	10	-	-	-	tr	tr	30	-	20	10	-	-	-	-	-	-	-	-	-	-	-	-	-		-
Phosphatic algal lime wackestones																																	
2849A	40	60	-	-	-	20		15	5	-	-	-	5	-	55	-	tr	tr	-	-	-	-	-	-	-	-	-	-	-	-	-	-	-
2856	65	35	-	tr	5	50		-	10	-	-	-	-	tr	30	-	tr	5	-	-	-	-	-	-	-	-	-	-	-	tr	-	-	-
3351A-1	50	50	-	-	-	20		25	-	5	-	6	4	-	40	-	tr	tr	-	-	-	-	-	-	-	-	-	-	-	-	-	-	-
A5060	50	50	-	-	-	35		5	10	-	-	-	5	-	45	-	tr	tr	-	-	-	-	-	-	-	-	-	-	-	-	-	-	-

Sample Number	SUMMARY				INTERGRANULAR FABRIC						BIOGENIC GRAINS									TERRIGENOUS GRAINS					AUTHIGENIC GRAINS			
	Intergranular Fabric	Biogenic Grains	Terrigenous Grains	Authigenic Grains	Ferruginous	Phosphatic	Glauconitic	Micrite	Microspar	Sparry Calcite	Bryozoans	Molluscs	Echinoderms	Coralline Algae	Benthonic Foraminifera	Planktonic Foraminifera	Fish Debris	Sponge Spicules		Quartz	Chert	Jasper	Feldspar	Heavy Minerals	Glauconite	Phos. Pellets	Phos. Lithoclasts	Pyrite
PHOSPHORITES (P)																												
Conglomeratic glauconitic phosphate packstones																												
2984A																												
Matrix	40	5	5	50	-	30	-	10	-			-	-	-	-	-	tr	5		5	-	-	-	-	40	tr	10	-
Pebbles	50	50	-	-	-	-	-	40	10			-	-	25	25	-	-	-		-	-	-	-	-	-	-	-	-
Pebbles	40	40	20	-	-	20	-	20	-			-	-	-	-	40	-	-		20	-	-	-	-	-	-	-	-
2984B																												
Matrix	60	5	5	30	-	40	-	20	-			-	-	-	1	1	3	-		5	-	-	-	-	25	tr	5	-
Pebbles	60	40	-	-	-	-	40	20	-			-	tr	35	2	3	-	-		-	-	-	-	-	-	-	-	-
2984C																												
Pebbles	100	-	-	-	-	20	60	20	-			-	-	-	-	-	-	-		-	-	-	-	-	-	-	-	-
Pebbles	60	40	-	-	-	60	-	-	-			-	-	-	40	-	-	-		-	-	-	-	-	-	-	-	-
Pebbles	70	-	-	30	-	70	-	-	-			-	-	-	-	-	-	-		-	-	-	-	-	30	-	-	-
Matrix	50	30	5	15	-	50	-	-	-			-	-	-	5	20	5	-		5	-	-	-	-	15	-	-	-
3016D	75	15	10	25	-	20	25	20	10	-	-	-	-	-	10	5	-	-		10	-	-	-	-	-	-	-	-
4638	50	tr	30	20	-	25	5	20	-	-	-	-	-	-	tr	-	-	-		20	tr	tr	tr	10	20	-	-	-
4639	30	-	20	50	-	30	-	-	-	-	-	-	-	-	-	-	-	-		20	-	-	-	-	45	tr	-	5
300-8001																												
Pebbles	60	-	40	-	20	20	-	20	-	-	-	-	-	-	-	-	-	-		40	-	-	-	-	-	-	-	-
Pebbles	40	40	20	-	20	20	-	-	-	-	5	25	tr	tr	10	-	-	-		20	-	-	-	-	-	-	-	-
Pebbles	60	20	-	20	20	20	-	20	-	-	-	-	-	-	20	-	-	-		-	-	-	-	-	20	-	-	-
Pebbles	60	30	-	10	20	20	-	20	-	-	10	10	tr	-	10	tr	-	-		-	-	-	-	-	10	-	-	-
Matrix	80	10	tr	10	10	40	-	20	-	10	-	5	-	-	2	3	-	-		tr	-	-	-	-	10	-	-	-
Pelletal (intraclastic) phosphate wackestone																												
3232C	40	2	20	38	-	20	-	20	-	-	-	-	-	-	tr	-	2	-		20	-	-	-	-	3	30	5	-

Sample Number	SUMMARY				INTERGRANULAR FABRIC						BIOGENIC GRAINS (chiefly carbonate)												TERRIGENOUS GRAINS							AUTHIGENIC GRAINS (chiefly residual)			
	Intergranular Fabric	Biogenic Grains	Terrigenous Grains	Authigenic Grains	Ferruginous	Phosphatic	Micrite	Microspar	Pseudospar	Sparry Calcite	Molluscs	Bryozoans	Echinoderms	Coralline Algae	Cirripeds	Benthonic Foraminifera	Planktonic Foraminifera	Faecal Pellets	Fish Debris Phos.	Sponge Spicules (Siliceous)	Rock Fragments	Quartz	Chert	Jasper	Organic Matter	Heavy Minerals	Feldspar	Pyrite	Glauconite	Phosphorite Fragments	Phosphorite Pellets
MOLLUSCAN LIMESTONES (M)																																
Molluscan lime wackestones																																
2990	Too friable to section																															
2994	60	20	20	tr	-	-	30	25	5	-	15	tr	tr	-	-	5	tr	-	-	-	-	20	-	-	-	-	-	tr	tr	-	-
A4922	70	25	4	1	-	-	10	50	10	-	20	tr	-	-	-	5	-	-	-	-	-	4	-	-	-	-	-	1	tr	-	-
A4923-3	80	20	tr	tr	-	-	-	-	80	-	10	3	tr	-	5	2	tr	-	-	-	-	tr	-	-	-	-	-	-	tr	-	-
MISCELLANEOUS																																
Coprolite (phosphate mudstone)																																
3224D	95	5	-	-	-	95	-	-	-	-	-	-	-	-	-	-	-	5	-		-	-	-	-	-	-		-	-	-	-

Sample Number	Grain Size: Composition and Texture	P_2O_5 %
	TERRIGENOUS SANDSTONES AND MUDSTONES(T)	
Ferruginous muddy sandstones		
2747A	Muddy fine sandstone: Immature calcitic ferruginous quartzose chert-arenite	0,3
2747B4	Medium sandy mudstone: Immature ferruginous quartzose chert-arenite	3,2
4637	Fine pebbly coarse and fine sandy claystone: Immature ferruginous sublitharenite	0,3
4638	Clayey coarse and fine sandstone: Immature ferruginous sublitharenite	1,5
POINT	Fine sandy fine conglomerate: Mature iron-cemented chert-pebble conglomerate	0,5
Phosphatic ferruginous muddy sandstones		
2747B1	Slightly pebbly muddy fine sandstone: Immature phosphate-rich ferruginous orthoquartzite	6,4
2747B2	Muddy medium sandstone: Immature phosphate-rich ferruginous sublitharenite	6,4
2747B3	Very fine sandy claystone: Immature phosphate-rich ferruginous chert-arenite	7,1
2747B5	Muddy medium sandstone: Immature phosphate-rich ferruginous chert-arenite	8,1
4639D	Coarse and very fine sandstone: Immature phosphate-rich ferruginous sublitharenite	5,1
4640D	Medium sandy claystone: Immature phosphate-rich ferruginous sublitharenite	21,3
Ferruginous mudstones		
2743	Silty claystone: Immature micaceous ferruginous orthoquartzite	0,2
2868A	Silty claystone: Immature mica-rich ferruginous orthoquartzite	0,2
2868B	Clayey siltstone: Immature mica-rich ferruginous orthoquartzite	2,9
4637	Silty claystone: Immature ferruginous orthoquartzite	-
Sandy mudstones		
2995C	Very fine sandy mudstone: Immature quartzose volcanic arenite	0,7
2995D	Fine sandy mudstone: Immature calcitic sedarenite	0,3
1175-46A	Fine sandy mudstone: Immature calcitic arkose	0,5
1175-46B	Muddy fine sandstone: Immature subarkose	3,2
Micaceous mudstones		
2868B-1	Silty claystone: Immature micaceous orthoquartzite	0,8
1111-44	Silty claystone: Immature micaceous orthoquartzite	-
Sandstones		
2936	Fine sandstone: Mature orthoquartzite	0,2
2969E	Very fine sandstone: Mature subarkose	0,3
1175-47	Fine sandstone: Mature calcitic subarkose/sublitharenite	-
	QUARTZOSE LIMESTONES(Q) AND LIME MUDSTONES(L)	
Quartzose lime wackestones(Q)		
2747C	Medium calcarenite: Quartzose lime wackestone	0,5
2990D	Very fine calcarenite: Quartzose lime wackestone	1,0
2995A	Very fine calcarenite: Quartzose lime wackestone	0,1
2995B	Very fine calcarenite: Quartzose lime wackestone	0,4
2995E	Fine calcarenite: Quartz-rich lime wackestone	0,6
3007-1	Very fine calcarenite: Quartz-rich lime wackestone	0,9
3007-2	Very fine calcarenite: Quartz-rich lime wackestone	0,9

Sample Number	Grain Size: Composition and Texture	P_2O_5 %
3008B	Very fine calcarenite: Quartzose lime wackestone	1,4
3122	Very fine calcarenite: Quartzose lime wackestone	1,2
3133	Very fine calcarenite: Quartz-rich lime wackestone	1,8
3141	Very fine calcarenite: Quartzose lime wackestone	1,6
3193	Very fine calcarenite: Quartzose lime wackestone	2,0
3261	Very fine calcarenite: Quartzose lime wackestone	2,9
3390A	Medium calcarenite: Quartz-rich lime wackestone	1,2
3390D	Medium calcarenite: Quartzose lime wackestone	1,5
3390F	Coarse and very fine calcarenite: Quartz-rich lime wackestone	3,9
4636	Very fine calcarenite: Quartzose lime wackestone	0,6
4638M	Coarse and very fine calcarenite: Quartz-rich lime wackestone	-
4638F	Slightly pebbly coarse and very fine calcarenite: Quartz- and glauconite-rich lime wackestone	1,1
4639D	Very fine calcarenite: Quartzose lime wackestone	0,3
1111-49	Fine calcarenite: Lithoclast-rich quartzose lime wackestone	0,6
1111-67	Very fine calcarenite: Quartz-rich lime wackestone	-
A4923-1	Very fine calcarenite: Quartzose lime wackestone	0,8
A4923-2	Very fine calcarenite: Quartzose lime wackestone	0,9
GIL 471	Very fine calcarenite: Pyrite- and quartz-rich lime wackestone	2,5
Phosphatic quartzose lime wackestones(Q)		
3194	Very fine calcarenite: Phosphate-rich quartzose lime wackestone	5,0
3390E	Fine calcarenite: Phosphatic quartzose lime wackestone	15,8
GIL 469	Very fine calcarenite: Phosphate-rich quartzose lime wackestone	6,1
Pyritic lime wackestone(L)		
4639	Calcilutite: Pyrite-rich lime wackestone	-
Phosphatic pyritic lime wackestone(L)		
2969A	Calcilutite: Phosphate-rich pyritic lime wackestone	6,4
2969B	Calcilutite: Phosphate- and pyrite-rich lime wackestone	5,6
Lime mudstones(L)		
2969D	Calcilutite: Lime mudstone	0,5
2995B	Calcilutite: Lime mudstone	0,7
2995F	Calcilutite: Lime mudstone	1,4
3027B	Calcilutite: Lime mudstone	0,1
3027C	Calcilutite: Lime mudstone	0,1
3232A	Calcilutite: Lime mudstone	0,0
4636	Calcilutite: Lime mudstone	0,64
Phosphatic lime mudstones(L)		
3185	Calcilutite: Phosphatic lime mudstone	11,8
3351A-Z	Calcilutite: Ferruginous phosphatic lime mudstone	11,0
3653D	Calcilutite: Phosphatic lime mudstone	8,04
	FORAMINIFERAL LIMESTONES(F)	
Phosphatic nummulitic lime packstones		
2922	Calcirudite: Phosphatic nummulitic lime packstone	13,6
2984C	Calcirudite: Phosphatic nummulitic lime packstone	-
Phosphatic planktonic foraminiferal lime wackestones		
2734	Fine calcarenite: Phosphate-rich planktonic foraminiferal lime wackestone	6,9
3005	Slightly pebbly fine calcarenite: Mollusc- and benthonic foraminifer-rich planktonic foraminiferal lime packstone	1,40

Sample Number	Grain Size: Composition and Texture	P_2O_5 %
	ALGAL LIMESTONES(A)	
Algal lime wackestones		
2849B-7	Calcirudite: Coralline algae-rich bryozoan lime packstone	0,7
2849B-4	Medium calcarenite: Coralline algae-rich lime wackestone	0,7
3351B	Fine calcarenite: Benthonic and planktonic foraminifer-rich coralline algal lime packstone	3,4
Phosphatic algal lime wackestones		
2849A	Medium calcarenite: Phosphate-rich coralline algal lime wackestone	8,6
2856	Fine sandy phosphorudite: Coralline algal phosphate packstone	18,1
3351A-1	Calcirudite: Phosphate-rich coralline algal lime wackestone	8,1
A5060	Coarse calcarenite: Phosphatic coralline algal lime packstone	14,0
	PHOSPHORITES(P)	
Conglomeratic glauconitic phosphate packstones		
2984A	Fine sandy coarse to very fine phosphorudite: Glauconitic calclithic phosphate packstone	21,0
(Pebbles)	Fine calcarenite: Benthonic and planktonic foraminiferal lime wackestone	
(Pebbles)	Very fine calcarenite: Phosphate- and quartz-rich planktonic-foraminiferal lime wackestone	
(Matrix)	Fine to very fine phospharenite: Phosphorite-rich glauconitic phosphate packstone	
2984B	Fine sandy phosphorudite: Glauconitic calclithic phosphate packstone	21,0
(Pebbles)	Coarse calcarenite: Coralline algal lime packstone	
(Matrix)	Medium phospharenite: Glauconitic phosphate packstone	
2984C	Pebbly fine phospharenite: Glauconitic, planktonic foraminiferal calclithic phosphate packstone	21,5
(Pebbles)	Glaucolutite: Phosphate-rich glauconite mudstone	
(Pebbles)	Fine phospharenite: Glauconitic phosphate wackestone	
(Pebbles)	Medium phospharenite: Benthonic foraminiferal phosphate wackestone	
(Matrix)	Fine phospharenite: Glauconite- and planktonic foraminifer-rich phosphate packstone	
3016D	Fine phospharenite: Benthonic foraminifer-, glauconite and quartz-rich phosphate packstone	8,46
4638G	Slightly pebbly coarse and very fine phospharenite: Glauconite- and quartz-rich phosphate packstone/wackestone	
4639	Fine phospharenite: Pyrite-bearing quartz-rich glauconitic phosphate packstone.	-
300-8001	Fine sandy phosphorudite: Mollusc- and glauconite-rich calclithic phosphate packstone	-
(Pebbles)	Medium calcarenite: Mollusc-, benthonic foraminifer-, phosphate- and quartz-rich ferruginous lime wackestone/packstone	
(Pebbles)	Very fine calcarenite: Phosphate-rich ferruginous quartzose lime wackestone	
(Pebbles)	Fine calcarenite: Benthonic foraminifer-, glauconite- and phosphate-rich lime wackestone	
(Pebbles)	Coarse calcarenite: Bryozoa-, mollusc-, benthonic foraminifer-, glauconite-, phosphate- and goethite-rich lime packstone	
(Matrix)	Fine phospharenite: Mollusc- and glauconite-rich phosphate wackestone	
Pelletal (intraclastic) phosphate wackestone		
3232C	Slightly pebbly to medium phospharenite: Quartz-rich pelletal (intraclastic) phsophate wackestone	26,2

Sample Number	Grain Size: Composition and Texture	P_2O_5 %
	MOLLUSCAN LIMESTONES(M)	
Molluscan lime wackestones		
2990	Calcirudite: Molluscan lime wackestone	-
2994	Calcirudite: Mollusc- and quartz-rich lime wackestone	0,4
A4922	Calcirudite: Mollusc-rich lime wackestone	0,7
A4923-3	Calcirudite: Mollusc-rich lime wackestone	0,6
4638	Calcirudite: Molluscan lime wackestone	-
	MISCELLANEOUS	
Phosphatic silicified wood		
4638	Phosphate-veined silicified coniferous wood	4,4
4639	Phosphate-veined silicified coniferous wood	4,4
Coprolite		
3224	Phospholutite: Phosphate mudstone	-

G. LOCATION, DEPTH AND AGE OF SEMI-CONSOLIDATED SEDIMENTS

Sample	Latitude S. Deg. Min.	Longitude E. Deg. Min.	Depth m	Age range	Specialist
2734	29 56,0	15 04,0	312	Tertiary	Stapleton
2945	28 50,3	14 27,0	265	Middle Eocene to Upper Miocene	Siesser
3005	27 56,3	14 47,6	244	Tertiary	Stapleton
3015	27 47,0	14 57,0	195	Tertiary	Stapleton
3016D	27 47,0	14 48,0	360	Upper Pliocene	McMillan
3016GC	27 47,0	14 48,0	360	Middle Eocene to Upper Miocene	Siesser
3024	27 35,8	14 45,5	292	Middle Eocene to Lower Pliocene	Siesser
3153	27 18,0	14 08,0	632	Middle Miocene to Middle Pliocene	Siesser
3202	26 47,0	13 37,0	900	Upper Miocene to Lower Pliocene	Siesser
3205	26 37,0	13 33,0	995	Lower Pleistocene	McMillan
3207	26 37,0	13 55,0	418	Upper Pleistocene	McMillan
3208	26 37,0	14 05,5	390	Middle Miocene to Lower Pliocene	Siesser
3257	26 11,0	14 08,0	300	Miocene	Stapleton
3360	26 19,0	14 04,0	349	Miocene	Stapleton
3375	25 53,0	13 57,0	326	Upper Pliocene to Lower Pleistocene	McMillan
3386	25 36,0	14 08,0	227	Lower Pleistocene	McMillan
3387	25 36,0	14 19,0	190	Quaternary	McMillan

H. BASIC SEDIMENTOLOGICAL DATA FOR UNCONSOLIDATED MARINE SEDIMENTS

P2O5 : Phosphate expressed as P_2O_5

K2O : Potash expressed as K_2O

GLAUC : Glauconite

ORG.C : Organic carbon

FP : Faecal pellets

TERR : Terrigenous detritus

CACO3 : Calcium carbonate : $CaCO_3$

All values expressed as weight per cent of the total sediment

STATION	P2O5	K2O	GLAUC	ORG.C	GRAVEL	SAND	SILT	CLAY	FP	TERR	CACO3
2729	.20	.71	1	1.2	.00	42.4	31.0	26.6	0	13	84.7
2730	.21	.49	1	1.6	.00	53.9	26.5	19.6	0	9	87.6
2731	.39	.56	1	1.8	.00	47.3	32.0	20.6	0	12	82.0
2732	.66	.81	2	1.6	.00	58.3	24.6	16.9	0	11	81.8
2733	1.27	.59	2	1.6	.00	67.4	20.0	12.5	0	8	83.9
2734	6.80	.63	1	1.2	.00	83.5	8.5	7.8	0	29	49.8
2735	8.52	.20	0	.9	.10	84.4	1.2	14.3	0	9	65.5
2736	2.44	.46	1	1.1	.00	82.4	4.6	13.0	0	11	80.2
2737	2.04	.43	0	1.4	.00	76.2	4.9	18.9	0	12	79.4
2738	1.34	.65	1	2.1	.00	60.7	6.0	33.3	18	22	70.0
2739	2.02	.80	1	2.7	.00	68.2	15.7	16.2	10	9	79.6
2740	.68	.50	1	3.4	.00	55.1	23.8	21.1	12	22	67.4
2741	.93	2.20	8	2.8	.05	55.6	24.7	19.2	12	38	46.4
2742	1.29	2.70	49	1.4	.10	75.5	13.6	10.9	5	19	26.2
2743	.32	1.67	6	2.0	.90	60.6	16.7	21.7	5	85	4.9
2744	.20	2.89	0	3.1	.00	.9	34.4	64.7	1	91	2.7
2745	.22	3.55	0	2.9	.00	2.6	29.6	67.9	2	92	2.5
2746	.24	2.82	0	3.6	.00	1.9	33.2	64.9	33	89	3.7
2747	.21	1.96	2	1.4	.00	27.2	35.7	37.0	2	92	3.7
2748	.85	2.49	17	1.4	2.10	63.9	22.6	11.2	5	61	17.8
2749	2.33	1.50	7	2.9	.30	86.8	7.2	5.6	14	28	53.3
2750	.37	.79	1	3.9	.00	60.4	15.6	23.9	43	26	65.6
2751	1.82	.66	1	3.0	.00	65.6	18.4	15.8	29	13	76.2
2752	2.06	.64	1	2.4	.00	65.7	13.9	20.2	23	0	89.3
2753	1.42	.44	1	2.0	.00	80.3	10.4	9.3	13	14	78.3
2754	1.70	.29	1	1.7	.10	85.8	7.9	6.1	0	13	79.5
2755	2.53	.38	1	1.3	2.30	86.9	5.0	5.8	0	11	79.2
2756	8.67	.20	1	1.0	.10	94.6	.6	4.6	0	22	52.5

STATION	P2O5	K2O	GLAUC	ORG.C	GRAVEL	SAND	SILT	CLAY	FP	TERR	CACO3
2844	.92	.37	1	1.4	.00	61.5	24.9	13.7	0	12	82.2
2845	.61	.60	4	1.6	.10	55.7	26.2	17.1	0	8	83.8
2846	.23	.33	1	1.5	.10	55.6	27.7	16.6	0	17	80.0
2847	.16	.35	0	1.6	.00	47.2	30.0	22.8	0	9	87.7
2848	.13	1.51	0	1.0	.00	26.3	35.0	38.6	0	9	88.8
2850	.18	1.55	0	1.8	.00	47.3	29.5	23.1	0	18	82.8
2851	.54	1.49	1	1.8	.01	54.1	26.7	19.2	0	13	80.7
2852	.64	1.68	4	1.8	.00	58.2	24.4	17.5	0	15	76.1
2853	2.42	1.47	1	1.5	.04	70.2	18.8	11.0	0	10	80.1
2854	5.85	1.33	1	1.3	.00	83.8	8.5	7.7	0	6	74.9
2855	7.28	1.00	0	1.0	.00	91.4	1.7	6.8	0	8	69.8
2856	1.40	1.06	0	1.5	3.30	79.9	7.5	9.3	0	6	87.5
2857	1.58	1.18	1	1.6	.70	80.4	3.7	15.2	0	17	75.9
2858	.86	1.30	1	3.0	.00	73.4	16.1	10.5	19	14	77.7
2859	2.19	1.49	2	2.9	.00	62.5	21.5	16.0	8	26	61.2
2860	1.33	1.42	1	2.6	1.00	63.0	20.4	15.7	7	34	56.8
2861	.68	1.93	14	2.7	.40	58.9	26.0	5.0	8	30	50.0
2862	.82	2.29	13	2.3	10.70	46.3	20.4	22.5	4	66	15.0
2863	.18	.93	2	1.5	2.70	67.1	14.5	15.7	0	68	25.2
2865	.24	2.95	1	3.5	.00	.5	26.2	73.4	0	82	11.0
2866	.12	3.02	0	.1	.00	.7	20.3	78.8	0	76	23.6
2867	.23	1.54	1	1.6	.70	42.8	28.0	27.5	1	92	3.7
2868	.34	2.28	3	3.0	.50	22.4	25.4	51.7	0	88	3.0
2869	3.24	3.16	31	1.6	1.20	76.1	14.2	8.5	3	46	10.7
2870	.84	2.55	2	3.0	.00	62.8	23.0	14.3	9	24	65.9
2871	2.02	.97	4	2.4	.00	70.5	16.6	12.9	13	31	55.1
2872	.96	2.26	1	2.6	.00	72.7	18.7	8.6	16	0	98.9
2873	.99	.18	1	2.3	.00	75.2	13.3	11.4	0	14	79.5

STATION	P2O5	K2O	GLAUC	ORG.C	GRAVEL	SAND	SILT	CLAY	FP	TERR	CACO3
2874	4.10	2.35	1	1.4	.00	88.7	3.5	7.8	0	0	88.8
2875	1.24	2.45	1	1.7	.02	81.9	8.8	9.4	0	14	79.8
2876	1.04	2.22	0	1.3	.03	87.0	5.0	8.0	0	5	90.3
2877	3.81	2.22	0	1.2	.00	77.4	7.5	15.1	0	8	79.1
2878	2.20	2.41	1	1.3	.00	74.4	17.7	7.9	0	8	83.2
2879	.46	2.45	0	2.4	.02	46.2	29.8	24.0	0	20	74.3
2880	.22	2.49	0	1.7	.00	37.3	35.6	27.1	0	14	82.3
2881	.22	2.24	0	1.8	.00	42.2	31.7	26.1	0	20	75.9
2882	.24	2.74	0	2.3	.00	37.6	42.0	20.4	0	17	78.3
2883	.92	2.26	0	1.5	.00	69.9	18.2	11.9	0	12	82.3
2884	2.20	2.06	0	1.2	.20	77.8	7.8	14.2	0	1	90.4
2885	4.42	2.22	0	1.2	.00	90.0	2.3	7.7	0	9	76.9
2888	4.32	2.24	0	1.2	.00	90.1	1.7	8.2	0	13	73.3
2889	5.70	2.26	0	.9	.40	88.5	2.0	9.1	0	7	75.5
2890	1.82	2.06	0	1.4	.10	89.8	3.5	6.7	0	18	88.3
2891	1.42	2.30	0	2.2	.80	72.6	10.1	16.4	10	11	81.2
2892	2.18	2.29	1	2.5	.00	74.2	14.2	11.6	5	13	76.6
2893	2.39	1.20	1	2.5	.10	73.2	11.7	14.9	0	12	55.8
2894	1.52	1.01	1	2.3	.00	73.9	16.2	9.9	9	26	65.1
2895	.96	1.35	1	3.1	.03	57.6	28.1	14.3	8	22	69.2
2896	.93	1.35	3	3.3	.04	58.2	25.3	16.5	10	26	63.8
2897	2.09	1.60	7	1.4	.30	83.3	9.6	6.9	2	74	11.2
2898	.45	1.92	2	1.6	.20	41.0	31.3	27.6	0	91	3.0
2899	.28	2.49	1	2.1	4.40	35.3	9.0	51.4	4	85	10.4
2900	.25	1.67	1	.3	1.30	92.6	1.0	5.1	0	92	5.3
2901	.21	3.51	0	2.0	.00	.9	25.2	73.9	0	94	1.4
2902	.34	2.49	1	1.8	.00	15.7	42.2	42.1	1	92	3.3
2903	.93	1.42	2	2.6	1.30	64.4	21.6	12.6	0	72	20.7

STATION	P205	K20	GLAUC	ORG.C	GRAVEL	SAND	SILT	CLAY	FP	TERR	CACO3
2905	.72	2.03	5	3.6	.10	76.0	10.8	13.0	24	31	56.2
2906	2.16	1.89	2	3.3	.00	60.7	23.6	15.7	13	35	52.1
2907	5.20	2.19	6	2.6	.00	70.8	18.5	10.8	10	0	81.7
2908	3.60	1.45	1	2.5	.00	71.9	15.4	12.7	5	21	64.8
2909	1.27	1.57	1	2.5	.03	74.5	17.4	8.2	7	14	77.6
2910	.62	1.57	1	2.0	.04	81.5	9.4	9.1	11	3	92.1
2911	.50	1.62	1	2.3	.00	80.1	10.7	9.2	10	36	58.3
2912	.61	.22	0	2.5	.02	84.3	10.0	5.7	13	12	81.4
2913	.52	1.51	1	1.8	.03	85.2	6.0	8.9	8	10	89.3
2914	.98	1.40	1	1.9	.00	89.7	6.2	4.1	9	9	90.2
2915	3.55	1.40	1	1.5	.00	88.0	6.1	6.0	0	15	72.7
2916	2.98	1.51	1	1.3	10.50	63.1	10.9	15.5	5	9	80.6
2917	1.74	1.76	3	2.0	.10	64.4	21.3	14.3	0	24	64.7
2918	.30	.60	0	2.0	.30	13.0	53.0	33.0	0	2	74.0
2919	.20	1.80	0	3.0	.00	19.0	50.0	30.0	0	1	83.0
2920	.92	.98	4	1.2	.05	84.9	7.4	7.7	0	11	80.8
2921	3.41	.32	1	1.2	1.30	90.5	2.9	5.3	0	6	81.8
2922	.63	.87	0	1.5	.00	87.2	6.6	6.2	6	47	48.5
2923	.43	.87	1	1.9	.00	87.7	1.7	10.6	12	4	91.2
2924	.64	.81	1	1.6	.00	87.0	6.4	6.6	0	11	84.8
2925	1.50	.98	1	2.1	.10	74.0	15.3	10.5	6	13	78.7
2926	3.99	1.04	1	2.6	.04	67.2	18.7	14.1	14	24	60.5
2927	3.13	1.28	2	3.3	.04	53.8	29.2	16.9	11	22	62.9
2928	.53	1.38	1	2.2	.00	61.8	25.0	13.2	5	55	39.4
2929	.54	1.62	4	.9	.00	74.4	12.1	13.5	0	89	4.5
2930	.17	2.68	0	1.4	.00	.1	29.6	70.3	0	96	1.4
2931	.16	2.71	0	1.5	.00	.1	29.2	70.6	0	95	2.1
2932	.15	1.76	1	.3	.04	95.9	1.1	2.9	0	78	20.0

STATION	P2O5	K2O	GLAUC	ORG.C	GRAVEL	SAND	SILT	CLAY	FP	TERR	CACO3
2934	.14	2.20	0	1.6	.00	.4	37.2	62.3	0	96	.6
2935	.41	1.51	3	.7	.03	72.0	12.2	15.8	0	91	3.5
2937	.79	1.11	2	1.9	.00	74.8	12.4	12.8	7	59	33.3
2938	2.72	1.57	2	3.1	.00	64.7	23.2	12.1	17	24	60.5
2939	3.48	.55	1	2.8	.00	66.6	25.4	8.0	6	28	56.9
2940	1.62	.34	1	2.0	.10	78.3	12.1	9.5	8	12	79.5
2941	.60	.70	1	1.6	.60	74.6	.0	.0	12	21	74.3
2942	.32	.28	0	2.1	.00	80.6	6.0	13.4	0	38	57.5
2943	.43	.18	0	1.5	.70	77.2	5.9	16.2	10	12	84.2
2944	.22	.17	0	1.0	.90	62.3	.4	36.4	0	4	94.0
2945	3.79	.19	0	.9	20.70	64.7	5.3	9.3	0	0	93.1
2946	.99	1.77	1	2.1	.00	55.5	24.2	20.3	0	16	76.9
2947	.24	.61	1	1.8	.00	36.1	39.0	25.0	0	19	76.7
2948	.24	.97	1	2.2	22.30	25.1	29.9	22.7	0	36	58.9
2949	.37	.51	1	2.2	.00	63.6	21.0	15.4	13	18	68.6
2950	.20	.23	0	.8	.20	93.8	1.4	4.6	0	8	89.5
2952	.87	.17	1	1.6	2.00	83.1	1.1	2.9	0	14	80.3
2953	2.20	.36	1	1.7	1.70	81.2	9.1	8.1	13	6	83.7
2954	2.76	.23	1	2.2	2.30	71.9	16.2	9.6	8	14	74.3
2955	2.18	1.00	1	1.5	.10	74.0	14.0	11.8	6	52	37.9
2956	1.80	.54	1	2.4	13.30	60.2	14.8	11.6	4	29	52.4
2957	.34	2.20	1	.9	9.20	57.4	21.5	12.1	0	86	10.6
2958	.98	2.99	0	2.2	4.40	47.2	27.7	20.7	0	91	2.4
2959	.16	1.50	0	.1	.00	90.4	6.4	3.2	0	98	1.3
2960	.14	1.30	0	.1	.02	93.3	3.5	3.2	0	98	1.5
2961	.11	1.30	0	.1	.10	90.2	5.7	4.1	0	99	.4
2962	.18	1.30	0	.1	.04	89.0	8.2	2.7	0	99	.4
2963	.40	1.60	3	.1	.30	94.1	2.0	3.6	0	77	18.5

STATION	P2O5	K2O	GLAUC	ORG.C	GRAVEL	SAND	SILT	CLAY	FP	TERR	CACO3
2964	.16	1.20	0	.0	.04	96.2	1.7	2.1	0	99	.8
2965	.12	1.27	0	.1	.00	92.9	3.7	3.1	0	99	1.0
2966	.12	1.40	0	.1	.00	95.3	2.6	2.1	0	93	6.0
2967	.12	1.87	3	.4	.03	29.2	55.0	15.8	0	95	1.4
2968	.16	2.48	0	2.2	.20	.5	41.6	5.8	0	94	1.9
2969	1.36	3.10	0	1.5	11.60	55.5	23.0	9.8	7	82	11.9
2970	1.50	.14	1	2.2	.90	74.3	13.7	11.2	6	33	57.3
2971	1.88	.90	1	1.6	.00	84.8	9.4	5.8	8	52	38.6
2972	1.76	.26	1	2.2	.00	76.5	15.3	8.2	13	11	78.4
2973	1.56	.15	1	2.1	.10	86.3	8.7	5.0	10	8	82.7
2974	1.46	.00	1	1.8	.20	86.1	6.5	7.2	6	13	79.3
2975	.28	.18	0	1.2	.00	90.6	2.3	7.1	0	30	66.8
2976	.40	.38	1	2.6	.00	65.9	21.3	12.8	10	21	72.3
2978	.18	.27	1	2.0	.10	42.0	9.7	48.3	0	28	68.1
2979	.20	1.01	1	1.7	.00	42.6	32.1	25.4	0	16	79.9
2980	.16	.59	0	.8	.00	8.1	34.5	57.4	0	20	78.3
2981	.13	.65	1	1.9	.03	16.0	39.6	44.4	0	26	70.2
2982	.20	.70	1	1.9	.00	49.0	30.5	20.5	0	16	80.1
2983	1.26	2.38	19	1.8	.05	70.8	9.1	20.1	0	26	48.7
2985	.53	.70	0	1.7	.20	83.6	2.7	13.5	0	7	88.3
2986	1.82	.61	1	1.8	1.70	79.8	5.6	12.8	6	14	77.3
2987	1.71	.27	1	2.1	3.70	79.1	11.2	9.7	0	11	80.4
2988	4.20	.22	1	1.6	8.60	75.2	8.5	7.8	0	77	8.0
2989	2.74	.19	3	1.8	3.60	66.9	4.3	25.2	0	21	65.5
2990	.40	.48	4	1.6	.10	60.5	21.2	18.3	11	49	43.0
2991	.69	1.76	2	.5	1.30	86.1	5.6	7.0	0	93	2.2
2992	.16	2.08	0	.1	.00	97.0	.4	2.6	0	88	11.4
2993	2.10	1.24	0	.2	.20	93.7	1.4	4.7	0	94	.0

STATION	P2O5	K2O	GLAUC	ORG.C	GRAVEL	SAND	SILT	CLAY	FP	TERR	CACO3
2994	.32	.57	0	.9	3.80	55.1	16.8	24.3	0	64	33.3
2995	.34	1.19	2	.9	.40	83.2	9.2	7.2	3	85	10.9
2996	4.12	2.37	22	1.1	.40	82.3	10.3	7.0	3	48	16.6
2997	1.78	.37	1	2.2	.20	77.6	12.8	8.7	0	0	93.0
2998	1.50	.21	1	2.0	.20	84.4	6.7	8.7	9	7	84.6
2999	.30	.39	1	2.3	.00	71.1	11.5	17.4	7	11	84.0
3000	.60	3.00	25	1.1	.00	70.2	17.3	12.5	0	24	47.2
3001	.16	.52	1	1.4	.00	41.9	31.8	26.1	0	23	74.3
3002	.12	.59	1	1.3	.00	43.3	31.7	24.9	0	13	84.4
3003	.32	2.29	16	1.3	.00	58.8	24.8	16.4	0	25	55.7
3004	2.64	8.57	58	.7	2.40	70.2	9.8	17.7	0	9	24.1
3005	.66	.59	0	1.8	54.30	32.1	4.0	9.6	8	30	65.0
3006	2.19	.30	1	1.7	4.10	74.7	14.2	7.0	0	23	67.8
3007	1.68	.99	2	2.2	50.20	77.7	12.2	9.9	11	30	58.9
3009	.40	1.98	14	.7	.00	81.3	9.4	9.1	0	82	1.6
3010	.58	1.40	2	.6	.01	91.2	2.9	5.9	0	93	1.6
3011	.32	3.18	0	.1	.10	97.7	.5	1.8	0	84	3.6
3013	.44	1.36	8	3.2	.05	37.6	39.1	23.2	0	70	14.8
3014	1.02	1.33	1	1.4	.40	61.6	27.6	10.3	6	77	16.4
3015	1.45	1.13	2	1.8	1.30	77.0	11.7	9.9	0	68	23.0
3016	1.42	1.08	28	1.0	6.70	44.5	20.0	28.8	0	28	37.8
3017	.20	2.62	13	1.4	4.00	57.2	30.1	8.7	0	37	47.1
3018	.39	.61	2	1.6	.00	52.1	28.6	19.2	0	21	73.5
3019	.18	.35	1	1.6	.00	42.0	34.4	23.6	0	20	76.3
3020	.17	.37	1	1.3	.00	27.2	37.5	35.3	0	22	75.5
3021	.14	.68	1	1.6	.00	49.4	32.0	18.6	0	34	62.3
3022	.36	3.18	17	1.2	.70	75.2	13.6	10.6	0	43	36.8
3023	.40	1.75	7	1.0	.30	85.2	5.8	8.7	0	58	31.9

STATION	P2O5	K2O	GLAUC	ORG.C	GRAVEL	SAND	SILT	CLAY	FP	TERR	CACO3
3024	.29	.40	1	.3	1.50	60.2	19.6	18.6	0	15	82.9
3025	.84	1.64	2	1.0	.50	87.3	6.5	5.6	4	9	84.6
3026	.97	1.75	1	1.6	.10	63.2	26.6	11.1	2	81	11.8
3119	2.89	.30	1	1.5	.00	83.1	5.7	11.2	0	5	84.7
3120	.36	.12	0	1.2	.00	88.3	4.1	7.6	0	3	94.0
3121	1.01	.15	1	1.8	.00	91.8	1.7	6.5	9	25	69.3
3123	.32	1.87	2	.7	.40	85.5	5.4	8.7	0	93	2.8
3124	.24	1.41	4	.7	.00	94.5	4.0	5.5	3	90	4.2
3125	.25	1.46	3	.4	.00	96.8	2.5	.8	0	94	.7
3126	.18	1.47	1	.3	58.00	35.6	1.3	5.1	0	86	11.9
3127	.28	1.38	4	.3	.00	78.9	6.4	14.7	0	94	1.4
3128	.72	1.34	11	.7	.00	90.1	5.5	4.4	0	84	1.2
3129	.60	2.94	15	.5	.00	85.0	10.6	4.5	0	82	.6
3130	1.09	5.47	47	.9	.00	86.0	8.2	5.8	6	45	3.5
3131	.61	1.66	6	2.4	.00	80.7	12.1	7.2	28	65	23.6
3132	.34	1.53	5	2.5	.00	85.8	9.3	4.9	9	68	21.6
3134	1.00	1.11	59	1.0	.00	88.6	7.1	4.3	2	32	3.7
3137	.12	1.79	1	.0	7.80	88.0	3.8	.4	0	0	.0
3139	.33	1.86	1	2.6	.00	8.9	32.8	58.3	0	85	9.4
3140	.36	1.68	4	2.0	.50	59.5	23.1	16.9	7	74	17.5
3141	.43	2.02	7	2.6	.00	62.1	22.6	15.3	18	69	18.5
3142	.56	1.51	4	2.5	1.00	73.3	19.0	6.7	23	69	20.6
3143	.44	1.49	2	1.9	2.90	78.3	10.3	8.5	21	75	19.0
3144	1.44	2.50	13	3.0	.80	55.1	24.0	20.1	2	61	16.3
3145	.68	3.86	10	1.6	.00	79.2	10.2	10.5	5	73	12.2
3146	.47	3.32	33	1.6	.00	79.4	11.0	9.6	2	49	14.7
3147	.32	1.42	6	1.6	.00	94.7	2.8	2.0	7	58	31.7
3149	.14	.77	1	1.5	.00	49.5	31.0	19.5	0	23	73.0

STATION	P205	K20	GLAUC	ORG.C	GRAVEL	SAND	SILT	CLAY	FP	TERR	CACO3
3150	.12	.53	0	1.2	.00	15.4	35.0	49.6	0	19	78.7
3151	.12	.52	1	1.8	.00	12.8	50.5	36.7	0	21	75.2
3152	.17	1.38	2	1.7	32.20	60.3	4.8	2.7	0	36	59.2
3153	.27	2.64	1	3.7	.00	2.9	20.9	76.2	0	78	14.0
3154	.30	1.72	9	2.9	.00	55.2	28.4	16.4	5	47	38.4
3155	.35	1.97	9	3.1	.00	62.9	20.2	10.9	5	60	24.6
3156	.32	1.72	4	1.7	.00	79.1	11.3	9.6	3	80	12.8
3157	1.13	2.93	17	1.6	.00	86.3	6.2	7.5	6	67	10.9
3158	.71	3.02	17	2.8	2.90	61.6	17.4	18.1	3	52	24.2
3159	.96	1.65	5	3.8	.00	62.8	18.8	18.4	5	52	34.3
3161	.43	2.88	2	.9	2.00	86.9	5.4	5.7	0	89	6.1
3165	.39	1.55	2	.7	.00	91.0	5.2	3.8	0	93	2.6
3166	.41	2.53	5	1.7	.00	80.7	11.9	7.4	11	85	6.5
3167	.32	3.60	2	1.0	7.80	82.0	5.2	5.0	2	92	3.4
3168	.36	3.59	9	1.1	5.40	82.9	5.9	5.8	3	82	5.3
3169	1.04	5.96	50	1.5	4.30	82.8	7.1	5.8	5	38	7.1
3170	.48	1.60	3	1.0	.00	88.9	4.8	6.2	4	88	5.5
3171	1.91	1.43	2	2.7	.00	68.5	21.9	9.7	8	70	18.5
3172	.69	3.21	27	3.3	.00	67.7	15.1	17.2	11	38	27.1
3173	.31	1.58	4	1.2	.00	75.6	13.1	11.3	7	64	29.1
3174	.21	.98	2	2.3	.00	54.7	27.5	17.8	0	31	61.5
3175	.14	.55	0	1.7	.00	8.8	38.9	52.2	0	29	67.2
3176	.15	.56	1	2.7	.00	7.4	54.9	37.7	0	20	75.0
3177	.21	1.26	6	2.6	.00	56.6	26.8	16.6	7	37	51.8
3178	.30	1.99	12	1.0	.00	78.4	13.7	7.9	0	57	28.2
3179	.32	1.46	4	2.0	1.60	62.2	23.8	12.4	0	49	42.8
3180	.32	1.50	3	2.4	.00	67.4	22.9	9.7	8	62	30.0
3181	.34	1.45	3	2.4	.00	68.8	18.6	12.6	5	67	24.8

STATION	P205	K20	GLAUC	ORG.C	GRAVEL	SAND	SILT	CLAY	FP	TERR	CACO3
3182	.40	1.39	1	1.5	.00	81.8	10.2	8.0	5	83	11.1
3183	.40	4.45	2	1.2	.00	88.7	5.7	5.6	4	72	22.4
3184	.56	1.87	6	.8	.00	92.0	3.3	4.7	2	90	1.7
3186	.28	1.67	0	.5	.80	96.8	.8	1.6	0	94	4.0
3187	.40	1.39	0	.0	.00	92.4	4.1	3.5	0	0	.0
3188	.22	1.93	5	.1	.10	97.2	.9	1.8	0	0	1.8
3189	.39	1.90	3	.7	.00	93.5	2.6	4.0	0	94	1.1
3192	.40	2.45	17	.8	.00	92.3	3.6	4.1	0	76	4.3
3194	.56	1.36	41	.9	.00	91.2	4.2	4.6	3	56	.4
3195	.36	5.59	55	1.1	.00	89.1	5.9	5.1	0	41	.8
3196	1.15	1.18	3	1.2	.10	90.5	4.9	4.6	0	90	1.5
3197	.77	1.54	3	1.7	8.80	73.2	9.1	8.9	7	78	13.7
3198	.51	2.12	7	3.0	.20	65.8	21.2	12.9	10	67	19.2
3199	.35	1.34	2	3.6	.00	56.4	29.5	14.1	16	52	38.8
3200	.34	1.24	3	3.5	.40	57.4	25.2	17.0	9	43	46.3
3201	.44	2.24	12	1.4	.70	73.4	13.5	12.3	0	52	32.6
3202	.35	2.76	19	2.2	.00	48.2	23.6	28.2	7	46	30.1
3203	.16	.70	1	3.1	.00	29.8	37.8	32.3	12	26	67.0
3204	.17	.67	1	4.0	.00	22.1	46.4	31.5	7	33	59.4
3205	.27	4.71	30	2.6	.00	63.4	23.6	12.9	10	30	34.7
3206	.50	2.72	21	2.0	.00	74.5	14.7	10.7	9	55	18.7
3207	.33	1.10	4	3.6	.00	51.9	31.5	16.6	16	38	50.6
3208	.32	1.33	2	4.3	1.40	39.2	35.9	23.5	10	34	54.6
3209	.58	5.74	41	2.6	.00	67.6	19.8	12.7	6	29	23.5
3210	.78	2.86	15	3.7	.00	73.7	15.0	11.3	20	61	14.3
3211	.89	1.32	7	1.6	.00	88.1	4.3	7.6	3	86	1.7
3212	1.09	1.28	2	1.3	28.10	60.1	4.3	7.6	4	86	6.9
3213	.30	2.07	7	1.2	.00	87.2	5.0	7.8	5	90	.2

STATION	P2O5	K2O	GLAUC	ORG.C	GRAVEL	SAND	SILT	CLAY	FP	TERR	CACO3
3215	.76	1.68	3	1.5	.00	89.2	5.8	5.0	11	89	.3
3216	4.73	1.53	5	2.0	.20	85.8	4.9	9.1	7	76	2.2
3217	1.98	1.57	2	3.4	21.60	56.6	13.6	8.1	3	79	7.0
3218	.88	1.67	4	2.7	5.10	78.8	5.6	10.5	16	83	5.7
3219	.60	1.80	13	2.8	6.90	80.7	4.9	7.5	4	72	8.4
3221	1.65	1.01	1	13.2	36.90	43.9	5.3	13.8	25	46	23.3
3222	21.50	.40	2	3.2	23.40	69.5	2.0	5.1	0	0	42.6
3223	26.40	.55	1	2.7	.00	94.3	.9	4.8	3	20	1.2
3224	.21	.49	1	2.9	1.00	93.2	1.5	4.3	0	0	.0
3225	2.93	1.22	4	4.2	.00	62.4	22.8	14.8	11	61	27.1
3226	1.61	.75	0	6.7	.00	26.5	46.6	26.9	0	19	64.9
3227	.56	.66	0	5.6	.00	62.4	23.0	14.6	50	19	69.4
3228	.55	.75	1	7.4	.00	20.0	51.6	28.4	10	26	59.2
3229	.52	.91	1	6.5	.00	27.8	45.6	26.5	13	35	49.5
3230	.89	.82	1	2.8	.00	40.8	41.5	17.7	5	38	53.2
3231	22.70	.64	1	3.5	.00	82.2	14.3	3.5	7	20	10.1
3232	13.00	.56	1	2.5	53.80	42.7	1.5	2.0	2	52	7.7
3234	6.82	1.82	12	10.1	.00	70.2	20.1	9.7	2	35	15.1
3235	4.38	1.57	4	9.2	21.50	64.4	7.7	6.4	18	47	20.0
3237	.85	1.48	3	1.2	29.40	65.3	1.8	3.5	2	75	17.7
3238	.91	1.91	6	2.8	.00	85.6	10.9	3.5	12	77	9.4
3239	.62	1.64	2	1.9	60.60	32.5	4.3	2.6	6	62	31.0
3241	.44	1.49	5	2.0	.00	86.1	7.4	6.5	0	89	1.3
3242	.41	1.70	5	2.6	.00	89.7	5.4	4.9	0	87	2.4
3243	.60	1.87	5	3.3	4.00	87.2	8.5	.3	0	81	6.3
3244	.63	2.18	7	3.4	7.80	84.9	2.3	5.0	0	82	3.5
3245	1.67	6.01	57	1.8	.00	73.9	10.3	15.8	0	32	2.9
3246	4.59	3.92	36	2.1	.00	78.7	10.6	10.7	0	42	5.5

STATION	P2O5	K2O	GLAUC	ORG.C	GRAVEL	SAND	SILT	CLAY	FP	TERR	CACO3
3247	7.72	4.06	19	1.5	28.40	59.6	4.5	7.5	0	39	18.3
3248	7.49	1.19	5	2.8	21.30	69.6	5.9	3.3	0	40	29.2
3249	3.45	.64	1	7.7	.00	30.0	47.3	22.7	0	24	52.3
3250	1.94	.75	1	8.0	.00	20.0	54.5	25.5	0	33	45.8
3251	1.14	.89	1	6.6	.00	19.7	46.7	33.6	0	28	56.4
3252	.34	2.03	0	4.9	.00	3.6	52.1	44.3	0	25	64.9
3253	.35	1.69	2	6.9	.00	30.7	45.6	23.7	0	24	60.8
3255	.84	1.56	6	5.8	.00	16.6	59.1	24.3	0	28	54.0
3256	2.14	3.04	16	3.5	.00	55.0	26.1	18.9	0	53	18.8
3257	2.19	7.00	51	2.1	.00	74.4	12.0	13.5	0	22	16.6
3258	.81	8.43	89	.6	.00	95.4	.9	3.6	0	5	2.4
3259	.70	8.53	93	.7	.00	96.1	1.5	2.3	0	4	.3
3260	.50	8.11	88	.9	.00	95.1	1.3	3.6	0	8	.4
3263	3.12	1.63	1	2.6	.00	18.2	44.6	37.2	0	85	1.4
3264	3.88	1.62	3	1.8	.00	81.9	9.0	9.0	0	81	1.0
3265	.38	1.80	4	.8	.00	84.3	11.9	3.8	0	89	4.7
3266	.31	1.72	3	.7	.00	92.7	4.3	3.0	0	92	3.0
3267	.20	1.75	2	.3	.00	98.0	1.8	.2	0	95	2.4
3269	.28	1.97	2	.8	.00	94.5	2.6	2.9	0	94	1.4
3271	1.56	1.61	4	1.4	.00	81.5	6.0	12.5	3	86	3.1
3272	3.18	1.38	11	1.2	.30	92.1	1.9	5.7	2	77	1.1
3273	3.54	3.25	23	2.0	.00	84.4	8.9	6.7	6	61	2.5
3275	.20	5.96	46	2.8	.00	68.7	18.5	12.8	5	18	30.8
3276	.85	1.78	14	4.3	.00	50.5	30.6	18.9	11	30	45.5
3277	.80	2.80	7	2.2	.00	28.8	66.5	4.7	3	43	43.8
3278	.41	6.64	47	2.5	1.40	58.5	16.5	23.6	1	31	16.9
3279	.28	.67	1	4.1	.00	18.6	45.7	35.7	7	26	65.5
3280	.14	1.30	0	.0	.00	92.9	4.1	3.1	0	99	.5

STATION	P205	K20	GLAUC	ORG.C	GRAVEL	SAND	SILT	CLAY	FP	TERR	CACO3
3281	.12	1.49	0	.3	.00	85.6	10.2	4.2	4	99	.5
3282	.43	1.67	0	.4	.90	30.8	60.6	7.7	8	95	3.1
3283	.80	2.22	0	1.5	.00	1.0	60.7	38.3	0	84	11.6
3284	.25	2.78	0	1.6	.00	.7	12.8	86.5	0	95	1.3
3285	.16	2.50	0	2.2	.00	1.1	28.7	70.2	0	95	.7
3286	.28	2.84	0	1.6	.00	1.1	22.5	76.4	0	94	2.2
3287	.16	2.02	0	1.0	.00	1.0	59.0	40.1	0	97	1.2
3288	.15	2.28	0	1.2	1.60	1.8	62.3	34.3	0	96	2.0
3289	.12	1.72	0	.4	.00	14.1	53.3	32.6	0	98	1.1
3290	.12	1.65	0	.5	.40	41.7	52.3	5.6	0	98	.8
3291	.27	1.78	0	.8	2.10	67.2	17.2	3.5	0	92	5.8
3292	.20	2.58	0	.3	.40	9.4	35.7	54.5	0	88	5.1
3293	.20	2.79	0	4.1	.00	4.2	29.9	65.9	0	89	3.6
3294	.29	2.49	0	3.7	.00	.4	36.5	63.0	0	90	3.1
3295	.23	2.26	0	3.0	.00	1.6	48.9	49.5	0	89	5.2
3352	.25	.60	1	1.9	.00	34.6	31.4	34.0	0	26	69.9
3353	.20	.67	0	3.8	.00	14.3	37.2	48.6	0	18	74.2
3354	.18	.61	0	1.2	.00	9.4	37.0	53.8	0	26	71.7
3355	.15	.53	1	.6	.00	22.8	37.0	40.2	0	23	75.6
3356	.20	.74	1	4.7	.00	22.2	44.4	33.4	0	25	65.0
3359	.73	5.09	37	3.9	1.70	65.2	20.8	12.3	8	0	65.0
3360	1.17	4.03	53	2.5	.10	71.3	15.3	13.3	0	0	.0
3361	.94	7.78	73	3.0	.00	86.4	6.3	7.4	0	15	4.1
3362	.30	8.79	96	.2	.00	97.4	1.1	1.5	0	2	.9
3367	.27	1.49	4	.5	.00	95.9	2.8	1.3	3	94	.8
3368	.60	1.81	1	.8	10.90	85.4	1.8	1.9	0	89	7.2
3371	.82	1.93	8	2.9	.00	89.3	6.5	4.2	9	82	2.9
3372	1.08	7.34	1	1.5	.00	93.6	3.7	2.7	0	92	1.0

STATION	P2O5	K2O	GLAUC	ORG.C	GRAVEL	SAND	SILT	CLAY	FP	TERR	CACO3
3373	2.55	5.77	43	2.3	11.20	73.5	9.2	6.1	10	25	20.7
3374	5.72	3.60	26	1.4	41.90	50.6	3.2	4.3	0	36	19.6
3375	3.40	2.75	16	3.0	.00	83.5	10.4	6.1	25	38	31.0
3376	1.90	.76	0	7.2	.00	25.6	48.9	25.5	0	0	47.2
3377	.88	.71	0	.0	.00	15.1	59.6	25.3	0	0	42.2
3378	.50	.92	1	5.6	.00	21.4	50.4	28.2	16	28	61.0
3379	.29	.69	0	5.4	.00	16.0	48.8	35.2	6	22	68.2
3380	.27	.49	0	5.5	.00	14.1	59.9	26.0	9	20	69.6
3381	.28	.60	0	7.8	.00	25.0	50.8	27.2	24	49	39.1
3382	.70	1.50	2	4.6	.00	25.3	46.3	28.3	0	49	38.2
3383	5.83	.63	1	4.6	.00	30.1	50.8	19.2	3	38	37.5
3386	2.31	1.54	12	2.0	30.60	56.8	4.9	7.7	0	47	31.2
3387	12.00	1.53	0	.0	.00	.0	.0	.0	0	0	.0
3388	2.24	5.18	50	2.4	4.30	88.3	4.0	3.4	2	34	6.5
3389	1.38	2.20	2	3.5	10.10	81.8	3.0	5.0	3	57	30.2
3398	1.32	2.07	1	1.4	62.80	34.6	.8	1.7	2	65	27.8
3399	1.29	1.22	4	4.5	4.20	58.3	18.0	19.5	0	61	18.7
3400	18.12	.77	4	4.3	10.00	91.7	3.2	5.1	10	26	12.8
3401	20.80	.64	1	3.5	1.90	90.6	4.9	2.6	4	29	6.0
3402	20.84	.64	1	3.7	.00	93.3	2.5	4.3	10	23	12.0
3403	3.75	.79	3	2.5	.00	66.5	23.8	9.7	11	43	39.7
3404	1.72	.81	0	5.7	.00	27.0	54.8	18.1	0	0	71.5
3406	.93	.60	1	4.7	.00	24.3	53.6	22.1	15	0	89.0
3633	.00	.00	0	1.8	1.33	36.7	25.0	37.0	0	0	.0
3634	.00	.00	0	1.8	.00	12.2	29.4	58.4	0	0	.0
3635	.00	.00	0	1.5	.00	12.8	28.2	59.0	0	0	.0
3636	.00	.00	0	1.4	.00	4.4	24.5	71.1	0	0	.0
3637	.00	.00	0	1.5	.00	2.6	37.9	59.4	0	0	.0

STATION	P2O5	K2O	GLAUC	ORG.C	GRAVEL	SAND	SILT	CLAY	FP	TERR	CACO3
3638	.00	.00	0	1.2	.00	1.0	60.2	38.7	0	0	.0
3639	.00	.00	0	1.1	.06	7.4	71.6	21.0	0	0	.0
3640	.00	.00	0	.2	.40	71.1	22.8	5.6	0	0	.0
3642	.00	.00	0	.2	.00	85.1	8.7	6.2	0	0	.0
3643	.00	.00	0	.4	.00	59.9	27.5	12.6	0	0	.0
3644	.00	.00	0	.0	.00	64.7	22.8	12.5	0	0	.0
3645	.00	.00	0	.0	.00	17.3	53.8	28.8	0	0	.0
3646	.00	.00	0	.0	.00	9.2	63.8	27.0	0	0	.0
3647	.00	.00	0	.0	.63	5.2	65.3	29.5	0	0	.0
3648	.00	.00	0	.0	.00	5.0	52.1	42.8	0	0	.0
3649	.00	.00	0	.0	.00	2.9	58.9	38.2	0	0	.0
3650	.00	.00	0	.0	.00	6.5	57.5	36.0	0	0	.0
3651	.00	.00	0	.0	.12	11.8	62.8	25.3	0	0	.0
4644	.00	.00	0	.0	.00	.3	72.6	27.0	0	0	.0
4645	.00	.00	0	.0	.00	14.2	29.8	56.0	0	0	.0
4646	.00	.00	0	.0	.00	.5	45.1	74.5	0	0	.0
4647	.00	.00	0	.0	.00	.9	25.2	73.9	0	0	.0
4648	.00	.00	0	.0	.00	1.6	27.4	71.0	0	0	.0
4649	.00	.00	0	.0	.00	.5	33.7	65.8	0	0	.0
4650	.00	.00	0	.0	.00	2.3	55.6	42.1	0	0	.0
4651	.00	.00	0	.0	.00	1.7	71.6	26.8	0	0	.0
4652	.00	.00	0	.0	.00	35.9	53.1	11.0	0	0	.0
4653	.00	.00	0	.0	.00	71.4	60.4	12.3	0	0	.0
4654	.00	.00	0	.0	.00	.6	43.5	56.0	0	0	.0
4655	.00	.00	0	.0	.00	1.7	67.8	30.5	0	0	.0
4656	.00	.00	0	.0	.00	68.5	4.4	27.1	0	0	.0
4657	.00	.00	0	.0	.00	36.2	52.2	11.7	0	0	.0
4658	.00	.00	0	.0	.00	2.6	36.8	60.7	0	0	.0

STATION	P2O5	K2O	GLAUC	ORG.C	GRAVEL	SAND	SILT	CLAY	FP	TERR	CACO3
4659	.00	.00	0	.0	.00	26.0	29.1	44.9	0	0	.0
4660	.00	.00	0	.0	.00	34.3	46.6	19.1	0	0	.0
4661	.00	.00	0	.0	.00	.9	51.0	48.1	0	0	.0
4662	.00	.00	0	.0	.00	1.7	24.7	73.6	0	0	.0
4663	.00	.00	0	.0	.00	.9	59.1	39.9	0	0	.0
4664	.00	.00	0	.0	.00	58.3	12.2	29.5	0	0	.0
4665	.00	.00	0	.0	.00	39.2	32.6	28.3	0	0	.0
4666	.00	.00	0	.0	.00	30.6	38.5	30.8	0	0	.0
4667	.00	.00	0	.0	.00	62.2	23.0	14.8	0	0	.0
4668	.00	.00	0	.0	.00	46.5	43.2	10.3	0	0	.0
4669	.00	.00	0	.0	.00	63.7	23.6	12.7	0	0	.0
4670	.00	.00	0	.0	.00	.9	35.8	63.3	0	0	.0
4671	.00	.00	0	.0	.00	64.4	13.9	21.7	0	0	.0
4672	.00	.00	0	.0	.00	80.4	7.6	12.0	0	0	.0
4673	.00	.00	0	.0	.00	49.2	20.9	29.8	0	0	.0

I. CLAY-MINERAL DATA FROM 8 RIVER AND 44 MARINE SEDIMENTS

SAMPLE	7Å(Kaolin and chlorite) %	10Å(Illite) %	14Å(Montmorillonite) %
RS-29 (Upper Orange)	5,1	63,3	31,6
RS-27 (Middle Orange)	13,0	57,8	29,7
RS-36 (Lower Orange)	9,4	69,8	20,8
RS-25 (Fish)	14,1	78,1	7,8
RS-47 (Orange estuary)	13,3	66,1	20,6
RS-51 (Orange estuary)	8,6	77,8	13,6
RS-24 (Buffels)	19,0	79,2	1,8
RS-31 (Kaukausib)	8,0	86,4	5,7
2730	10,7	49,5	39,8
2735	15,4	80,6	4,0
2738	18,2	52,5	29,3
2741	11,2	61,8	27,0
2745	30,1	68,1	18,8
2746	11,1	69,8	19,1
2866	10,1	66,5	23,4
2871	12,9	55,5	31,6
2875	11,7	73,9	14,4
2879	6,3	47,9	45,9
2899	9,9	75,2	14,9
2901	10,3	64,5	25,2
2930	8,0	72,9	19,1
2938	19,9	62,2	17,8
2942	12,9	87,1	0,0
2947	23,2	39,9	37,0
2968	12,2	62,6	25,2
2981	12,5	54,8	32,7
2990	10,1	55,8	34,1
3002	12,7	36,0	51,3
3006	19,5	70,7	9,8
3010	10,6	71,5	17,9
3140	16,4	66,6	17,0
3145	16,5	65,9	17,6
3150	18,1	55,2	26,7
3195	14,3	74,7	11,0
3198	8,0	80,2	11,8

SAMPLE	7Å(Kaolin and chlorite) %	10Å(Illite) %	14Å(Montmorillonite) %
3202	12,8	76,1	11,0
3203	17,2	66,4	16,4
3221	7,1	75,8	17,2
3226	10,0	71,3	18,7
3228	18,1	67,0	14,9
3231	20,7	73,9	5,4
3235	5,8	91,5	2,7
3238	14,1	64,7	21,2
3256	14,8	60,5	24,6
3258	9,4	70,8	19,8
3263	15,8	70,2	14,0
3279	16,4	54,4	29,2
3284	12,2	70,8	17,0
3378	7,3	69,4	23,3
3379	9,0	72,8	18,1
3399	7,9	85,4	6,7
3636	6,4	71,8	21,8

J. GEOCHEMICAL DATA ON <2-MICRON FRACTION

Sample Number	Copper	Lead	Zinc	Manganese	Iron	Organic Carbon
	p.p.m.	p.p.m.	p.p.m.	p.p.m.	%	%
RS-24	363	74	212	1108	12,5	1,47
RS-36	72	33	246	971	12,8	0,51
RS-47	63	37	228	475	12,0	0,77
RS-51	63	42	423	1070	11,1	1,18
RS-62	94	36	834	1178	14,5	2,09
2730	86	44	94	104	3,7	4,09
2735	63	66	404	68	1,2	6,74
2738	79	65	333	119	3,3	7,10
2741	78	44	97	159	5,4	7,58
2745	74	42	100	264	10,2	2,40
2746	57	25	102	208	9,5	2,97
2866	52	28	91	211	11,3	1,90
2871	68	51	341	169	5,8	5,64
2875	73	59	294	141	3,3	7,07
2879	92	59	277	117	3,6	4,18
2899	51	27	91	214	9,5	2,14
2901	55	46	178	239	12,7	1,48
2930	62	31	96	358	10,7	1,09
2938	67	34	152	124	3,5	7,40
2947	70	44	85	93	3,0	3,57
2968	59	42	192	241	11,6	2,04
2981	81	47	87	105	3,5	2,31
2990	64	23	108	229	6,9	6,01
3002	81	59	290	111	3,7	2,36
3006	80	42	73	120	4,1	9,46
3010	75	25	97	205	10,2	6,19
3140	50	44	112	214	9,4	5,33
3145	84	29	105	154	4,9	8,99
3150	61	50	74	109	2,9	1,28
3195	68	23	165	178	9,4	7,45
3198	88	34	91	130	5,0	8,27
3203	85	45	264	97	2,8	3,81
3221	99	25	99	121	3,6	7,23
3226	83	45	102	70	2,2	6,77
3228	87	54	112	98	2,7	-

Sample Number	Copper p.p.m.	Lead p.p.m.	Zinc p.p.m.	Manganese p.p.m.	Iron %	Organic Carbon %
3231	107	40	103	72	2,0	-
3235	94	23	349	98	3,3	-
3238	62	25	113	148	6,4	9,52
3256	95	47	303	145	5,7	7,75
3258	92	23	604	138	7,6	13,21
3263	58	25	151	188	7,0	8,30
3279	77	49	115	92	3,0	4,45
3284	64	35	93	308	11,7	1,19
3378	72	50	82	98	3,0	5,15
3379	90	62	116	79	2,4	4,55
3399	101	41	151	105	3,4	11,45
3636	42	32	97	273	10,7	1,10

K. COMPARISON OF MOMENT MEASURES OBTAINED BY SETTLING AND BY SIEVING COARSE FRACTIONS OF FLUVIAL AND DELTAIC SEDIMENTS

Sample Number	Mean Size Settling phi	Mean Size Sieving phi	Sorting Settling phi	Sorting Sieving phi	Gravel %	Sand %	Mud %
RS 29	2,68-fS	2,80-fS	0,32-vws	0,47-ws	-	94,32	5,68
RS 27	2,84-fS	2,86-fS	0,26-vws	0,40-ws	-	95,00	5,00
RS 35	3,65-vfS	3,64-vfS	0,22-vws	0,31-vws	-	56,50	43,50
RS 45	-	2,64-fS	-	0,76-ms	-	0,82	99,18
RS 44	-0,28-vcS	-0,56-vcS	0,41-ws	0,48-ws	13,59	86,41	-
RS 43	0,47-cS	0,11-cS	0,50-mws	0,48-ws	1,80	98,20	-
BS112	1,12-mS	1,07-mS	0,61-mws	0,70-mws	0,96	99,04	-
2965	3,13-vfS	3,19-vfS	0,27-vws	0,39-ws	-	92,31	7,69
2961	3,26-vfS	3,41-vfS	0,39-ws	0,31-vws	-	62,73	37,27
3280	3,38-vfS	3,45-vfS	0,31-vws	0,29-vws	-	83,14	16,86
3281	3,63-vfS	3,60-vfS	0,30-vws	0,24-vws	-	73,54	26,46
3282	3,91-vfS	3,70-vfS	0,32-vws	0,26-vws	-	31,65	68,35
3283	-	3,75-vfS	-	0,05-vws	-	0,10	99,90
3284	-	2,47-fS	-	1,04-ps	-	0,25	99,75
3285	-	3,19-vfS	-	0,63-mws	-	0,18	99,82
2935	3,41-vfS	3,51-vfS	0,26-vws	0,28-vws	-	71,99	28,01